

UNIVERSITY OF KWAZULU-NATAL



**NOVEL SERIES OF DEHYDROZINGERONE INSPIRED
POTENTIAL ANTIMYCOBACTERIAL AGENTS: DESIGN,
SYNTHESIS, SPECTRAL STUDIES AND *IN VITRO*
BIOLOGICAL EVALUATION**

By

GIRISH A. HAMPANNAVAR M. Pharm

214584499

2016

**NOVEL SERIES OF DEHYDROZINGERONE INSPIRED
POTENTIAL ANTIMYCOBACTERIAL AGENTS: DESIGN,
SYNTHESIS, SPECTRAL STUDIES AND *IN VITRO*
BIOLOGICAL EVALUATION**

GIRISH A. HAMPANAVAR

214584499

2016

A thesis submitted to the School of Health Science, Discipline of Pharmaceutical science, Department of Pharmaceutical Chemistry, University of KwaZulu-Natal, Westville, for the degree of Doctor of Philosophy.

This thesis has been prepared according to **Format 4** (Thesis by publications) as outlined in the guidelines of College of Health Sciences, University of KwaZulu-Natal. The chapters consist of an overall introduction, chapters in discrete research papers and a final discussion. Two chapters have been published and the remaining chapters have been submitted in peer-reviewed internationally accepted journals.

As the candidate's supervisor, I have approved this thesis for examination/submission.

Supervisor: _____

Signed: _____

Date: _____

ABSTRACT

Tuberculosis (TB) is a key health burden globally. With the emergence of resistance issue, the antitubercular research has been challenging. Novel effective drugs are immediately required to treat this serious epidemic disease. Innovative potential antitubercular drug candidates are momentarily required to combat the disadvantages linked with existing drugs or line of treatments. Synthetic manipulations of natural sources are being extensively investigated worldwide for developing potent and efficient drugs. Besides, these manipulations also offer effective leads for further optimization. Therefore, this project is an effort in identifying a novel and effective antitubercular leads based on natural product model dehydrozingerone (DZG), a curcumin degradant.

In this project we have performed an extensive literature survey of DZG for its known biological activities. And further, we have synthesized some novel series of DZG fused heterocyclic compounds with three different 5 membered heterocyclic scaffolds namely, thiazole, thiazolidon-4-one and pyrazole. A total of 53 compounds comprising of styryl hydrazine thiazole hybrids (**6a-o**, Chapter 3), styryl hydrazine thiazolidin-4-one hybrids (**7a-d**, **10a-l** and **13a-b**, Chapter 4) and lastly styryl fused pyrazole derivatives of acid hydrazides, semicarbazone and thiosemicarbazones (**8a-i**, **11a-h** and **14a-c**, Chapter 5) have been synthesized by versatile synthetic routes as outlined in schemes of respective chapters. The completion of reaction and the purity of synthesized compounds were established by chromatographic analysis. All the newly synthesized compounds displayed acceptable analysis for their anticipated structures, which were established based on physicochemical and spectral data (IR, ^1H NMR, ^{13}C NMR and HRMS).

These newly synthesized compounds were primarily evaluated for their *in vitro* antimycobacterial activities at Infectious Disease Research Institute (IDRI) within the National Institute of Allergy and Infectious Diseases (NIAID) screening program, Bethesda, USA or Department of Microbiology, Inkosi Albert Luthuli Hospital, Durban, South Africa.

From the systematic analysis of antimycobacterial activity results obtained following key observations were made.

- i. Degradants of curcumin have been looked upon for molecular variations in developing diverse scaffolds. DZG is an imperative scaffold and its numerous analogs have emerged as a promising leads in the design and development of some novel medicinally active compounds with improved metabolic, pharmacokinetic and pharmacological profiles, indicating that there is much scope for considering DZG as a structural framework for developing effective leads.

- ii. Chapter 3: Of the fifteen novel styryl hydrazine thiazole derivatives synthesized and tested, compound **6o** exhibited significant antimycobacterial activity ($H_{37}Rv$; MIC = 1.5 μM ; IC_{50} = 0.48 μM) along with bactericidal (MBC = 12 μM) and intracellular antimycobacterial activities (IC_{50} = < 0.098 μM). Furthermore, **6o** displayed prominent antimycobacterial activity under hypoxic (MIC = 46 μM) and normal oxygen (MIC = 0.28 μM) conditions along with anti-mycobacterial efficiency against isoniazid (MIC = 3.2 μM for INH-R1; 1.5 μM for INH-R2) and rifampicin (MIC = 2.2 μM for RIF-R1; 6.3 μM for RIF-R2) resistant strains of *Mycobacterium tuberculosis*. Presence of electron donating groups on the phenyl ring of thiazole moiety had positive correlation for antimycobacterial activity.
- iii. Chapter 4: From the eighteen novel styryl hydrazine thiazolidin-4-one hybrids derivatives synthesized and tested, Compounds **7a** (MIC = 110 μM ; IC_{50} = 67 μM), **7c** (MIC = 120 μM ; IC_{50} = 66 μM) and **10g** (MIC = 100 μM ; IC_{50} = 100 μM) exhibited noteworthy antimycobacterial activity. Further, the title compounds displayed least cytotoxic effects against a mammalian Vero cell determined using MTT assay.
- iv. Chapter 5: Among the twenty novel styryl pyrazolo carbazone derivatives synthesized and tested, Compounds **8a**, **8c**, **8d**, **8g**, **8h**, **8i** and **11f** showed reasonable antibacterial activity (MIC = 50 $\mu g/mL$) against *B. subtilis*, compound **11a** demonstrated noteworthy activity towards *P. aeruginosa* (MIC = 25 $\mu g/mL$). Further, compounds **8a**, **8d**, **8e**, **8f**, **8i**, and **11h** showed good to moderate antifungal activity ranging from 25 to 50 $\mu g/mL$ towards *C. neoformans* (MIC = 25 $\mu g/mL$) and *C. albicans* (MIC = 50 $\mu g/mL$). Besides, compound **8a**, comprising of isonicotinoyl hydrazide portion displayed remarkable antitubercular activity (MIC = 0.78 $\mu g/mL$) against $H_{37}Rv$. Substituted urea derivatives, **14a-c** and **11d** also exhibited encouraging activity (MIC = 12.5 and 25 $\mu g/mL$, respectively) whereas, derivative with carbothioamide portion **11a**, (MIC = 0.78 $\mu g/mL$) illustrated significant activity against $H_{37}Rv$. Moreover, some of the tested compounds showed reasonable activity against MDR (multi drug resistant) and MOTT (mycobacteria other than tuberculosis) strains.

DECLARATION 1: PLAGIARISM

I, **Girish A. Hampannavar**, declare that

- i. The research reported in this dissertation, except where otherwise indicated, is my original work.
- ii. This dissertation has not been submitted for any degree or examination at any other university.
- iii. This dissertation does not contain other persons' data, pictures, graphs or other information, unless specifically acknowledged as being sourced from other persons.
- iv. This dissertation does not contain other persons' writing, unless specifically acknowledged as being sourced from other researchers. Where other written sources have been quoted, then:
 - a. their words have been re-written but the general information attributed to them has been referenced;
 - b. where their exact words have been used, their writing has been placed inside quotation marks, and referenced.
- v. Where I have reproduced a publication of which I am an author, co-author or editor, I have indicated in detail which part of the publication was actually written by myself alone and have fully referenced such publications.
- vi. This dissertation does not contain text, graphics or tables copied and pasted from the Internet, unless specifically acknowledged, and the source being detailed in the dissertation and in the References sections.

Signed:  _____

Date: _____

DECLARATION 2: PUBLICATIONS

DETAILS OF CONTRIBUTION TO PUBLICATIONS that form part and/or include research presented in this thesis (include publications in preparation, submitted, *in press* and published and give details of the contributions of each author to the experimental work and writing of each publication).

Publications

1. Hampannavar, G. A.; Karpoormath, R.; Palkar, M. B.; Shaikh, M. S. An Appraisal on Recent Medicinal Perspective of Curcumin Degradant: Dehydrozingerone (DZG). *Bioorganic & Medicinal Chemistry* **2016**, *24* (4), 501–520.
Contributions: I did the literature review and wrote the entire manuscript under the supervision of Dr. Rajshekhar Karpoormath. Rest all the co-authors assisted me in improvisation, writing up and summarizing the literature review (conclusion).
2. Hampannavar, G. A.; Karpoormath, R.; Palkar, M. B.; Shaikh, M. S.; Chandrasekaran, B. Dehydrozingerone Inspired Styryl Hydrazine Thiazole Hybrids as Promising Class of Antimycobacterial Agents. *ACS Medicinal Chemistry Letters* **2016**, *7* (7), 686–691.
Contributions: I generated the rationale and did all the experimental and characterization as well as writing up of manuscript under the guidance of Dr. Rajshekhar Karpoormath (Supervisor). The co-authors assisted me in writing up of results and discussion and designing of the target molecules.
3. Hampannavar, G. A.; Palkar, M. B.; Shaikh, M. S.; Cherukupalli S.; Karpoormath, R.; Design and synthesis of novel styryl hydrazine thiazolidin-4-one hybrids impelled from Dehydrozingerone as potential antimycobacterial agents. *Submitted to RSC Advances*.
Contributions: I did all the experimental work, characterization and writing up of the manuscript under supervision of Dr. Rajshekhar Karpoormath. Rest all co-authors assisted me in writing up of results and discussion.

4. Hampannavar, G. A.; Palkar, M. B.; Kajee, A.; Shaikh, M. S.; Mlisana, K. P.; Karpoornath, R.; Dehydrozingerone encouraged novel styryl pyrazolo carbazone hybrids as potential antimicrobial and antimycobacterial agents. *Manuscript*.

Contributions: I generated the rationale, did all the experimental work, characterization, antimicrobial and antimycobacterial screening and writing up of manuscript with the directions of Dr. Rajshekhar Karpoornath (Supervisor). Rest all the co-authors assisted me in writing up of results and discussion. Koleka P. Mlisana facilitated the microbiology laboratory and Ms. Afsana assisted me in carrying out antimicrobial and antimycobacterial activity.

Conference contributions

1. **Poster presentation**: In Search of Selective 11 β -HSD Type 1 Inhibitors without Nephrotoxicity by Virtual Based Screening Approach to Resolve the Metabolic Syndrome. CHPC National Meeting, held at Kruger National Park, Mpumalanga, South Africa, from 1st to 5th December **2014**.
2. **Poster presentation**: Dehydrozingerone Inspired Styryl Hydrazine Thiazole Hybrids as Promising Class of Antimycobacterial Agents. College of Health Sciences Research Symposium, held at Nelson R Mandela School of Medicine Campus, Durban, South Africa, from 8th to 9th September **2016**.
3. **Poster presentation**: Design and synthesis of novel carbazolo–thiazoles as potential antimycobacterial agents using a molecular hybridization approach. All Africa Congress on Pharmacology and Pharmacy, held at Misty Hills Hotel and Conference Centre, Muldersdrift, Gauteng, South Africa, from 5th to 8th October **2016**.
4. **Oral presentation**: Dehydrozingerone Inspired Styryl Hydrazine Thiazole Hybrids as Promising Class of Antimycobacterial Agents. All Africa Congress on Pharmacology and Pharmacy, held at Misty Hills Hotel and Conference Centre, Muldersdrift, Gauteng, South Africa, from 5th to 8th October **2016**.

Other publications

1. Cherukupalli, S.; Karpoormath, R.; Chandrasekaran, B.; **Hampannavar, G. A.**; Thapliyal, N.; Palakollu, V. N. An Insight on Synthetic and Medicinal Aspects of pyrazolo[1,5-*a*]pyrimidine Scaffold. *Eur. J. Med. Chem.* **2017**, *126*, 298–352
2. Palkar, M. B.; Rane, R. A.; Thapliyal, N.; Shaikh, M. S.; Alwan, W. S.; Jain, K. S.; Karunanidhi, S.; Patel, H. M.; **Hampannavar, G. A.**; Karpoormath, R. An Insight into Purine, Tyrosine and Tryptophan Derived Marine Antineoplastic Alkaloids. *Anticancer. Agents Med. Chem.* **2016**, *15* (8).
3. Rane, R. A.; Karunanidhi, S.; Jain, K.; Shaikh, M. H.; **Hampannavar, G. A.**; Karpoormath, R. A Recent Perspective on Discovery and Development of Diverse Therapeutic Agents Inspired from Isatin Alkaloids. *Curr. Top. Med. Chem.* **2016**, *16* (11), 1262–1289.
4. Rane, R. A.; Karunanidhi, S.; Jain, K.; Shaikh, M. H.; **Hampannavar, G. A.**; Karpoormath, R. A Recent Perspective on Discovery and Development of Diverse Therapeutic Agents Inspired from Isatin Alkaloids. *Curr. Top. Med. Chem.* **2015**
5. Palkar, M. B.; Praveen, D. M.; Ronad, P. M.; Viswanathswamy, A. H. M.; Rane, R. A.; Patel, H. M.; Shaikh, M. S.; **Hampannavar, G. A.**; Jain, K. S.; Karpoormath, R. Novel Series of Phenylalanine Analogs Endowed with Promising Anti-Inflammatory Activity: Synthesis, Pharmacological Evaluation, and Computational Insights. *Med. Chem. Res.* **2015**, *24* (5), 1988–2004.
6. Palkar, M. B.; Jalalpure, S. S.; Rane, R. A.; Patel, H. M.; Shaikh, M. S.; **Hampannavar, G. A.**; Alwan, W. S.; Bolakatti, G. S.; Karpoormath, R. Novel Series of Coumarinyl Substituted-Thiazolidin-2,4-Dione Analogs as Anticancer Agents: Design, Synthesis, Spectral Studies and Cytotoxicity Evaluation. *Anticancer. Agents Med. Chem.* **2015**, *15* (8), 970–979.
7. Rane, R. A.; Karpoormath, R.; Naphade, S. S.; Bangalore, P.; Shaikh, M.; **Hampannavar, G. A.** Novel Synthetic Organic Compounds Inspired from Antifeedant Marine Alkaloids as Potent Bacterial Biofilm Inhibitors. *Bioorg. Chem.* **2015**, *61*, 66–73.
8. Shaikh, M. S.; Thapliyal, N.; Rane, R. A.; Pal, M. B.; Faya, A. M.; Patel, H. M.; Alwan, W. S.; Jain, K.; **Hampannavar, G. A.** Current Perspective of Natural

Alkaloid Carbazole and Its Derivatives as Antitumor Agents. *Anticancer. Agents Med. Chem.* **2015**, 27 (0), 1049–1065.

9. Shaikh, M. S.; Palkar, M. B.; Patel, H. M.; Rane, R. A.; Alwan, W. S.; Shaikh, M. M.; Shaikh, I. M.; **Hampannavar, G. A.**; Karpoomath, R. Design and Synthesis of Novel Carbazolo–thiazoles as Potential Anti-Mycobacterial Agents Using a Molecular Hybridization Approach. *RSC Adv.* **2014**, 4 (107), 62308–62320.

Signed:  _____

Date: _____

Dedicated

to

*My Mother, a strong and gentle soul, who have raised me to be the
person I am today*

*My Father for his unconditional care, unceasing support and
encouragement*

*My Wife for her solace and love all the way, without whom none
of my success would be possible*

ACKNOWLEDGEMENT

I bow to almighty and my parents, to whom I owe the successful completion of my thesis. I would also like to express my deepest gratitude and heartfelt thanks to all those who helped me directly or indirectly in the completion of my research work.

I am deeply indebted to my supervisor Dr. Rajshekhar Karpoornath, for his valuable guidance, patience and stimulating suggestions in all the times of research and writing of this thesis. Your kindness and enthusiasm and faith in me energized me all throughout. Thank you, Dr. for your generosity and commitment to excellence.

Special thanks to Dr. Mahesh B. Palkar, for his precious scientific contributions all throughout the research, you're an inspiration and I'm blessed to have you. I am beholden for your constant encouragement and moral support in tough times. I feel short of words to thank you.

I would like to take a moment to remember Late. Dr. Veeresh Maddi, my previous supervisor for his integral vision on research.

I honestly thank Dr. Jim P. Boyce, Program Officer, Division of Microbiology and Infectious Diseases, NIAID, National Institutes of Health, Bethesda, USA for his cooperation and assistance in carrying out antimycobacterial screening studies.

My sincere thanks to Prof. Koleka Mlisana, Ms. Afsana Kajee and other staff of department of microbiology, Inkosi Albert Luthuli hospital, Durban for their assistance in performing antimicrobial and antimycobacterial screening studies.

I would like to thank the technical staff Mr. Dilip Jagjivan, School of Physics and Chemistry and Ms. Caryl Janse van Rensburg, Mass Spectrometry Laboratory, School of Chemistry, UKZN-Pietermaritzburg for their assistance in spectroscopic experiments. I also thank Ms. Unathi Bongoza and Michael Pillay, School of Physics and Chemistry for their assistance in X-ray crystal structure analysis.

My special thanks to all the past and present group members of Synthetic and Medicinal Chemistry Research Group, for their support and contributions. The blissful days spent with you all will be cherished forever.

My humble gratitude to University of KwaZulu-Natal, South Africa, for granting approval for my research proposal and providing all the necessary facilities to carrying it out successfully. My sincere

thanks and appreciations for all the supporting staff at Discipline of Pharmaceutical Sciences College of Health Sciences.

I am also thankful to my teachers at K.L.E's College of Pharmacy, Hubballi helping me to keep my spirits high in my profession.

A special word of thanks to Dr. Naren Rana and his family, whose spiritual wisdom and divine perceptions has enlightened me. Uncle, you are one of the most generous people I know.

Words aren't enough to express how lucky I'm to have Ashwini as my dearest wife, who always stands by my side during my hard times. Dear Ashwini, you are the precious gift bestowed upon me to reconcile the loss of paradise.

I extend my gratitude to my Father-in-law Shri. Chandrashekhhar and Mother-in-law Smt. Shivalela whose support and encouragement has seen me through tumultuous times.

I owe deep honor and love to my Parents Shri. Appasaheb and Late Smt. Shakuntala, for my existence and I am indebted to you both for inculcating in me the dedication and discipline to do whatever I undertake well. Thank you both for pushing me to reach for the stars there by raising my spirits to achieve the same which could never be accomplished without the support of this wonderful family. I have to specially mention my deep gratitude and love to my elder sisters Manjula and Bharathi for being with me all the times with their constant encouragement and co-operation. Cheers to my nephew Mallikarjun, whose friendliness always brightens up my day. Warm blessings and love to all my niblings Siddhalinges, Dhaksha, Spoorthi and Arpita.

Finally, I would like to take the opportunity to thank all my relatives and teachers. I ask for forgiveness for any inadvertent exclusions.

LIST OF ABBREVIATIONS

^{13}C NMR	: Carbon-13 nuclear magnetic resonance
^{19}F NMR	: fluorine-19 nuclear magnetic resonance spectroscopy
^1H NMR	: Proton nuclear magnetic resonance
3D-QSAR	: three dimensional quantitative structure activity relationship
3D-QSPR	: three dimensional quantitative structure property relationship
AAPH	: 2,2 ¹ -azobis(2-amidinopropanehydrochloride)
ABTS	: (2,2 ¹ -azinobis (3-ethylbenzothiazoline-6-sulfonic acid)
AcOH/HOAc	: Acetic acid
AD	: Alzheimer's disease
ADC	: Albumin, dextrose, and catalase
AIDS	: Acquired immune deficiency syndrome
AMPK	: AMP-activated protein kinase
ATCC	: American type culture collection
ATP	: Adenosine triphosphate
BHT	: 2,6-di- <i>tert</i> -butyl-4-methylphenol
CDCl_3	: Deuterated chloroform
CH_3I	: Methyl iodide
CH_3OH	: Methanol
CHCl_3	: Chloroform
COSY	: correlated nuclear magnetic resonance spectroscopy
DCM	: Dichloromethane
DMEM	: Dulbecco modified eagle medium
DMF	: Dimethylformamide
$\text{DMSO-}d_6$: Deuterated DMSO
DNA	: Deoxyribonucleic acid
DPPH	: 2,2-diphenyl-1-picrylhydrazyl
DZG	: Dehydrozingerone
EBV-EA	: Epstein-Barr virus early antigen
ED_{50}	: the concentration causing 50% of maximum effect for any measured biological effect of interest
EDTA	: Ethylenediaminetetraacetic acid
EIMS	: Electron Ionization Mass Spectroscopy
ESI	: Electrospray ionization
Et_3N	: Triethylamine
EtOAc	: Ethyl acetate
FBS	: Fetal bovine serum
FST	: Forced swim test
FTIR	: Fourier transform infrared spectroscopy
GA	: Glycyrrhetic acid
GLUT4	: Insulin-regulated glucose transporter
GSH	: Glutathione
HBSS	: Hanks' balanced salt solution
HCl	: Hydrochloric acid
HFD	: High-fat diet
HIV	: Human immunodeficiency virus

HMBC	: heteronuclear multiple bond coherence
HRMS	: High-resolution mass spectrometry
HSQC	: heteronuclear single quantum coherence
IC ₅₀	: the drug concentration causing 50% inhibition
IC ₉₀	: a measure of the concentration of drug needed to inhibit 90% growth
IDRI	: Infectious disease research institute
IGR	: insect growth regulatory
INH	: Isoniazid
J _{CF}	: Carbon-Fluorine coupling
K ₂ CO ₃	: Potassium carbonate
LO	: Lysyl oxidase
LORA	: Low oxygen recovery assay
MABA	: Microplate alamar blue assay
MAC	: <i>M. avium</i> complex
MAPK	: Mitogen-activated protein kinase
MBC	: Minimum bactericidal concentration
MCA	: Mono-carbonyl analogs
MDR-TB	: Multi drug resistant tuberculosis
MHB	: Muller-Hinton Broth
MIC	: Minimum inhibitory concentration
MOPS	: (3-(<i>N</i> -morpholino)propanesulfonic acid)
MOTT	: Mycobacteria other than tuberculosis
mp	: Melting point
Mtb	: <i>Mycobacterium tuberculosis</i>
MTT	: [3-(4,5-Dimethylthiazol-2-yl)-2,5-Diphenyltetrazolium Bromide]
NaOH	: Sodium hydroxide
ND	: Not determined
NHCEs	: New hybrid chemical entities
NIAID	: National institute of allergy and infectious diseases
NOESY	: nuclear overhauser effect spectroscopy
NRP	: Non-replicating persistent
OA	: Oleoic acid
OD	: Optical density
OHP	: Hydroxyproline
PDB	: protein data bank
PDGF	: Platelet-derived growth factor
PET	: Positron emission tomography
PMA	: phorbol 12-myristate 13-acetate
POCl ₃	: Phosphoryl chloride
ppm	: Parts per million
PTPs	: Protein tyrosine phosphatases
QSAR	: Quantitative structure–activity relationship
RFU	: Relative fluorescence unit
RIF	: Rifampicin
RLU	: Relative luminescent units

ROS	: Reactive oxygen species
RPMI	: Roswell Park Memorial Institute medium
RT	: Room temperature
SAR	: Structure activity-relationships
SPECT	: Single photon emission computed tomography
TB	: Tuberculosis
TBE	: Tryphan blue exclusion
TDR-TB	: Totally drug resistant tuberculosis
THF	: Tetrahydrofuran
TLC	: Thin layer chromatography
TMS	: Tetramethylsilane
TOH	: α -tocopherol
TPA	: 12- <i>O</i> -tetradecanoylphorbol-13-acetate
TST	: Tail suspension test
UA	: Ursolic acid
US-FDA	: U S Food and Drug Administration
VSMC	: Vascular smooth muscle cells
WHO	: World Health Organization
XDR-TB	: Extensively drug resistant tuberculosis
XO	: Xanthine oxidase

TABLE OF CONTENTS

Abstract	ii
Declaration 1: Plagiarism	iv
Declaration 2: Publications	v
Dedication	ix
Acknowledgement.....	x
List of abbreviations.....	xii
Table of contents	xv
List of figures	xvii
List of tables.....	xviii

Chapter 1:

1	General introduction.....	1
1.1	Background	1
1.2	Microbial infections	1
1.3	Treating microbial infections	2
1.4	Antimicrobial agents	2
1.5	Classification of antimicrobial agents	3
1.6	Antimicrobial resistance.....	3
1.7	Tuberculosis	6
1.8	Management of tuberculosis	6
1.9	Antitubercular drugs: Mechanism of action.....	9
1.10	Antitubercular drug development.....	10
2	Genesis of our research	17
3	Objectives of the present research work.....	19

Chapter 2:

1	Introduction	25
2	Dehydrozingerone identified for manifold pharmacological activities.....	29
2.1	Dehydrozingerone as antioxidant.....	29
2.2	Dehydrozingerone as antimutagen	37
2.3	Dehydrozingerone as anti-inflammatory.....	51
2.4	Dehydrozingerone as anti-depressant.....	53
2.5	Dehydrozingerone against Alzheimer's disease.....	53
2.6	Dehydrozingerone as anti-malarial	54
2.7	Dehydrozingerone as antifungal/antifeedant.....	56
2.8	Dehydrozingerone as Antiplatelet	57
2.9	Dehydrozingerone as β -adrenoceptor antagonist	57
2.10	Dehydrozingerone: <i>in silico</i> studies	58
2.11	Dehydrozingerone reported for miscellaneous activities	60
3	Conclusion and future perspective	62
4	Conflicts of interest	62
5	Acknowledgments.....	62

Chapter 3:

1	Introduction	71
2	Chemistry	74
3	Results and discussion.....	75
3.1	Synthesis and spectral studies	75
3.2	Antimycobacterial activity	80
4	Conclusion.....	87
5	Experimental	87
5.1	Chemistry protocols	87
5.2	Biological protocols (<i>In vitro</i> anti-mycobacterial activity characterization).....	100

Chapter 4:

1	Introduction	111
2	Chemistry	113
3	Results and discussion.....	116
3.1	Synthesis and spectral studies	116
3.2	Antimycobacterial activity	120
3.3	Cytotoxic activity	125
4	Conclusion.....	125
5	Experimental	126
5.1	Chemistry protocols	126
5.2	<i>In vitro</i> antimycobacterial evaluation.....	135
5.3	Cytotoxicity studies: MTT assay.....	136
5.4	X-ray crystallographic data of compound 4.	136

Chapter 5:

1	Introduction	142
2	Chemistry	145
3	Results and discussion.....	148
3.1	Synthesis and spectral studies	148
3.2	<i>In vitro</i> antimicrobial activity.....	150
3.3	Antimycobacterial activity	152
4	Conclusion.....	154
5	Experimental	154
5.1	Chemistry protocols	154
5.2	Biological activity protocols	165

Chapter 6:

1	Summary and conclusion	171
2	Future work	173

APPENDIX – I	(Supplementary Information- Chapter 3).....	175
APPENDIX – II	(Supplementary Information- Chapter 4)	220
APPENDIX – III	(Supplementary Information- Chapter 5).....	261
APPENDIX – IV	(Published papers).....	301

LIST OF FIGURES

Chapter 1:

Figure 1: Representation of Prokaryotic cell and Eukaryotic cell.....	2
Figure 2: Various antibiotic classes along with and their associated resistant mechanisms with respective examples	5
Figure 3: Progression of TB infection in humans	6
Figure 4: Structures of first and second-line antitubercular drugs.	9
Figure 5: Mechanism of action of various approved antitubercular drugs.....	10
Figure 6: Global status showing MDR-TB incidences	10
Figure 7: END TB strategy by WHO in 2015.....	11
Figure 8: TB drug development pipeline.	14

Chapter 2:

Figure 1: Structure of Dehydrozingerone (DZG).....	25
Figure 2: Degradation products of curcumin.	26
Figure 3: DZG as active scaffold with manifold pharmacological activities.....	27
Figure 4: Imperative structural features of Dehydrozingerone (DZG) and effects of substitutions over various biological activities.....	28
Figure 5: Naturally occurring antioxidants.	29

Chapter 3:

Figure 1: Cinnamoyl-rifamycin derivative.....	71
Figure 2: Compounds with styryl portion reported against <i>M. tuberculosis</i> H ₃₇ RV	72
Figure 3: The literature reported derivatives containing styryl and thiazoles moieties and their anti-mycobacterial activities along with the designed compounds	73
Figure 4: A section of the ¹³ C NMR spectrum (150.89 MHz) of compound 6k, illustrating C-F coupling.....	77
Figure 5: A section of the ¹³ C NMR spectrum (150.89 MHz) of compound 6m, illustrating C-F coupling.....	79
Figure 6: Illustration of anti-TB results against <i>M. tuberculosis</i> H ₃₇ Rv: Compounds with MIC values and varying substitution patterns.	81
Figure 7: Anti-TB activity profile of most active compounds	86

Chapter 4:

Figure 1: Thiazolidin-4-one scaffold and its various bioactive compounds.	111
Figure 2: Molecular hybridization assisted design of thiazolidin-4-one analogues impelled from DZG scaffold as possible antimycobacterial agents.....	113
Figure 3: X-ray crystallographic image of compound 5.	118
Figure 4: Compound 5 depicting styryl and hydrazono-thiazolidone portions.	118
Figure 5: 2D correlations of compound 5.	120

Chapter 5:

Figure 1: Approved drugs containing pyrazole core.	143
Figure 2: Semicarbazone and thiosemicarbazones bearing biologically active compounds.	144
Figure 3: Design strategy for synthesis of styryl pyrazolo carbazones.	145

LIST OF TABLES

Chapter 1:

Table 1: First and second-line antitubercular drugs with their associated adverse effects.....	8
Table 2: Antitubercular drugs currently in lead optimization stages along with their associated mechanism of actions.....	12
Table 3: Natural secondary metabolites as antitubercular drugs.....	15
Table 4: Naturally inspired semisynthetic antitubercular drugs.....	16

Chapter 2:

Table 1: Structures of asymmetrical mono-carbonyl ferrocenylidene curcumin and their dihydropyrazole compounds from dehydrozingerone derivatives.....	36
Table 2: Structures of DZG and chalcone analogs.....	40
Table 3: Structures of C-4'-alkylated DZG and Isoeugenol analogs.....	41
Table 4: Data for GA-DZG conjugates against human tumor cell replication.....	42
Table 5: Structures of DZG analogs.....	46
Table 6: Structures of DZG and isoeugenol analogs.....	47
Table 7: Automated Docking Analysis through Scigress Explorer 7.7.0.47.....	59

Chapter 3:

Table 1: Depiction of C-F coupling values for compound 6k.....	76
Table 2: Depiction of C-F coupling values for compound 6m.....	78
Table 3: Level I results under aerobic conditions for newly synthesized title compounds against <i>M. tuberculosis</i> H ₃₇ Rv strain.....	80
Table 4: Anti-mycobacterial activity data of newly synthesized compounds against five drug-resistant isolates of <i>M. tuberculosis</i> H ₃₇ Rv.....	83
Table 5: Bactericidal, cytotoxicity, intracellular and anti-mycobacterial activity of selected title compounds against <i>M. tuberculosis</i> H ₃₇ Rv grown under various conditions.....	85
Table 6: Anti-mycobacterial activity of selected title compounds against other disease-relevant Mycobacterial species.....	86

Chapter 4:

Table 1: Antimycobacterial and cytotoxic activity data of title compounds against <i>M. tuberculosis</i> H ₃₇ Rv strain under aerobic conditions.....	122
Table 2: Sample and crystal data for compound 4.....	136
Table 3: Data collection and structure refinement for compound 4.....	137

Chapter 5:

Table 1: The antibacterial and antifungal activity data of a novel series of styryl pyrazolo carbazone derivatives.....	151
Table 2: The antimycobacterial activity data of a novel series of styryl pyrazolo carbazone derivatives.....	153

Note: Referencing styles of individual chapters are as per guidelines of communicated journals.

CHAPTER 1

1 GENERAL INTRODUCTION

1.1 Background

In context of drug discovery, medicinal chemistry holds a stake that emphasize on design and synthesis of small organic compounds with a foremost focus on a given biological activity in question. Medicinal chemistry borders various arenas of research and employs strategies such as design, synthesis, and screening (by *in vitro* and *in vivo* assays) of drugs along with insightful structure activity relationship studies. In the past, medicinal chemists primarily explored medicines from natural sources like plants, fungi, bacteria, soil, marine, insects, reptiles etc. which were rich with pharmacologically active chemical substances. By early 18th century, with emerging understandings of basic chemistry and physics principles, chemists had begun to synthesize the chemical compounds. Discovery of volatile liquid chloroform, as a general anesthetic by Justus von Liebig (1803-1872) was the first inception of synthetic drugs. Later, these profusely ascending synthetic and natural drugs were classified based on their pharmacological responses. Eventually, these empirical findings found their place in monographs. In spite of accessible resources, computational tools and well-equipped laboratories, modern day medicinal chemists are facing a cumulative challenge to deliver safer and more effective medicines. Drug likeliness, stability, solubility, permeability, metabolic stability, efficacy, toxicity, emergence of resistance by microorganisms, and cost-effective treatment are some of the critical considerations in drug development process.

1.2 Microbial infections

Humans have always suffered outbursts of diseases and epidemics ever since the beginning of civilization. The eruptions of infectious and communicable diseases had devastating effect on the structure of society and its economy. The inexplicable appearance, be it the most feared plagues of the past to the Ebola in the present, have put the mankind in serious health crisis.

Disease causing microorganisms are called as pathogens. Although all of the microorganisms are not pathogens, some have defending mechanisms against the growing injurious pathogens. Any susceptible host with weak immune system may effortlessly heap an infectious agent compared to healthy individuals. Pathogens also find their place in patients with sinking (elderly patients) or compromised (HIV patents) immunity and receiving chemotherapy (cancer patents). Infectious agents may be one among the bacteria, virus, fungi or protozoa. The mode of transmission of these infectious agents maybe through either direct or indirect contact [1]. Touching, inhaling the

discharged droplets (by sneezing or coughing) or sexual contact with an infected patient are some among the direct means for transmission. Several diseases namely, ringworm, tuberculosis, HIV-AIDS, trichinosis, influenza, rabies etc. are blown out by direct transmission. Indirect transmission occurs when the pathogen stays outside the host, survives for a period of time before affecting the fresh individual. For example, used tissues, clothing, toys, drinking contaminated water are some of indirect means of transmission. Another category, a vector borne, are the diseases transmitted by vectors (disease transmitting biological agents) that carry the disease without infecting themselves. For example, malaria is a vector borne disease where female anopheles mosquitos are the vectors. Similarly, these mosquitos are the vectors for several detrimental diseases namely dengue, yellow fever, St Louis Encephalitis etc.[2]

1.3 Treating microbial infections

In order to control or eradicate the pathogenicity associated with a diverse range of pathogens, it becomes most important to discern about the mode of transmission and the lifecycle of causative organisms and its interaction with the host. This strategy helps in identifying the accessible drug targets like enzymes, enzyme precursors or substrates that may assist reasonably in altering, control or preventing the growth of pathogens. Fortunately, the bacteria are prokaryotes, making its treatment informal with least side effects. Prokaryotes are considerably different from eukaryotes in terms of structural features and metabolic characteristics. (Fig. 1)

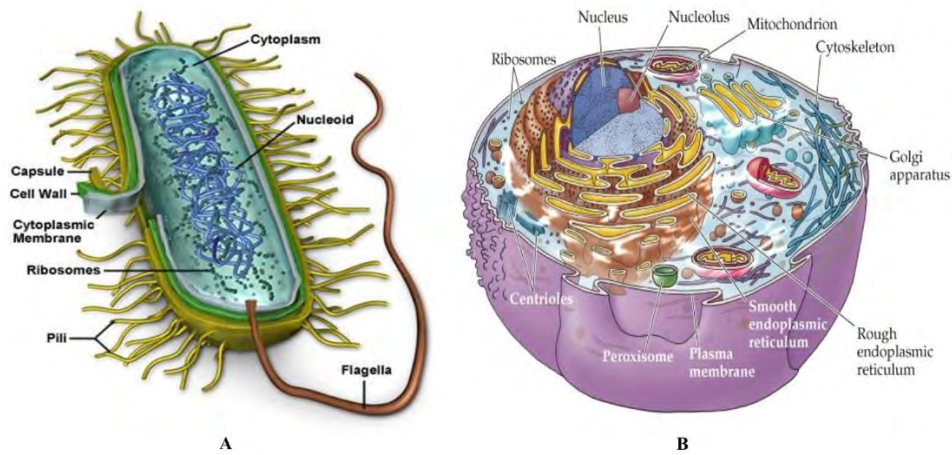


Figure 1: Representation of Prokaryotic cell (A) and Eukaryotic cell (B) (*Image courtesy: Biochemanics*)

1.4 Antimicrobial agents

Any substance of natural, semisynthetic or synthetic origin used to kill or inhibit the growth of microorganisms are known as antimicrobial agents. These agents may be sourced naturally, like

antibiotics or else can be obtained by chemical synthesis, known as chemotherapeutic agents. Introduction of sulphonamides (in 1936) and penicillin (in 1941) were the starting point of modern era in chemotherapy and the golden age of antimicrobial therapy.[3] In the present day, antimicrobial agents are the most widely and often indiscreetly used drugs.[4] For effective antimicrobial chemotherapy, a given antimicrobial agent should possess *in vivo* as well as *in vitro* effectiveness, absence of toxicity, and most importantly reasonable cost.[5] Ideally, any antimicrobial agent should be nontoxic to the host and toxic to the microbe (selective toxicity), microbicidal rather than microbistatic, fairly soluble, long acting, metabolically stable during and after administration, must not develop microbial resistance and not produce allergic responses by interfering with the host cells. The terms antimicrobial, antibiotic and anti-infective, often encompass a wide range of pharmaceutical agents that include antibacterial, antifungal, antiviral, and antiparasitic drugs.

1.5 Classification of antimicrobial agents

The antimicrobial agents are classified in several ways namely, based on activity spectrum, effect on bacteria or depending upon mode of action. Based on the spectrum of activity they are further sub classified as broad and narrow spectrum antimicrobials. Broad spectrum antimicrobials are usually active against both gram positive and gram negative bacteria. Examples tetracyclines, fluoroquinolones, cephalosporins, etc.[6] Narrow spectrum antimicrobials have limited action on a particular species of microorganisms. For example, glycopeptides and bacitracin against gram positive, polymyxins against gram negative [7], aminoglycosides, sulfonamides against aerobic and nitroimidazole against anaerobes. Further, upon effect on bacteria, they are classified as bactericidal and bacteriostatic. Bactericidal agents kill the target microorganisms, for example penicillins, cephalosporins, aminoglycosides, etc. Bacteriostatic agents arrest the growth or replication of microorganisms, for example sulfonamides, tetracyclines, macrolides, etc. Depending on mode of action antimicrobials are classified as inhibitors of cell wall synthesis examples penicillins, cephalosporins, bacitracin and vancomycin, inhibitors of cell membrane function example polymixin B, colistin, etc., inhibitors of protein synthesis example tetracyclines, macrolides, chloramphenicol, aminoglycosides, etc., inhibitors of nucleic acid synthesis examples, rifampin, metronidazole, and quinolones, lastly, inhibitors of other metabolic processes example, sulfonamides and trimethoprim.[8]

1.6 Antimicrobial resistance

In the course of prolonged antimicrobial chemotherapy, the microorganisms undergo mutations in their genes making them insensitive from the further action of antimicrobial agents, thus attaining resistance. Subsequently, the formerly effective antimicrobial agent will no longer be

beneficial. This ability of microorganisms to attain resistance to antimicrobial agents has further exceeded our imagination. These adaptive resistance mechanisms are achieved in various ways namely [9]

- a. by enzymatic degradation of antibacterial drugs.
- b. by alteration of bacterial proteins that are antimicrobial targets, and
- c. by modifications in membrane permeability to antibiotics, thus actively pumping out the drug from the cell.

Figure 2 presents a list of resistant mechanisms associated with various antibiotic classes with examples. Eventually, this transformation in resistance brought by mutation is transmitted to the other members of identical species and also transverse through the species by diverse genetic exchange mechanisms. Currently, the resistance has widely spread and posing difficulties in treatment. Appearance of multidrug resistant organisms in the last few decades has created a grave concern. Lack in antimicrobial stewardship, slack in antimicrobial drug development and more limited options for treating resistant infections [10] has finally caught the attention of medicinal chemists and drug discovery scientists. According to World Health Organization (WHO), globally about 480 000 people develop multidrug resistant TB each year and is creating complications in fighting some deadly diseases namely HIV and malaria. This resistance is also a serious concern in treating infections during cancer chemotherapy, diabetes, organ transplantation and major surgery (for example, caesarean sections or hip replacements).[11] Therefore, this situation warrants the need of curative steps in minimizing the emergence and spread of antimicrobial resistance.

Antibiotic class	Resistance Mechanism	Examples
Aminoglycosides	Changes in outer membrane permeability	<i>P. aeruginosa</i>
β -lactams	Alterations in plasma binding proteins	<i>S. pneumoniae</i>
Chloramphenicol	Chloramphenicol acetyltransferase degradation	<i>S. pneumoniae</i>
Glycopeptides	Altered peptidoglycan cross linking	<i>E. faecium</i> and <i>E. faecalis</i>
Fosfomycin	Thioltransferase enzyme degradation	<i>P. aeruginosa</i> and <i>B. subtilis</i>
Fusidic acid	Mutation leading to reduced binding to active site	<i>S. aureus</i>
Macrolides	Alter in efflux of Mef type pump	<i>S. pneumoniae</i> and <i>S. pyogenes</i>
Quinolones	Mutation leading to reduced binding to active site	<i>S. aureus</i> and <i>S. pneumoniae</i>
Tetracyclines	New membrane transporters	gram-positive and gram-negative bacteria
Sulfonamides	Mutation or recombination of genes encoding DHPS	<i>E. coli</i> , <i>S. aureus</i> , and <i>S. pneumoniae</i>
Trimethoprim	Mutations in gene encoding DHFR	<i>H. influenzae</i> , <i>S. aureus</i> , and <i>S. pneumoniae</i>

Figure 2: Various antibiotic classes along with and their associated resistant mechanisms with respective examples. [12,13]

1.7 Tuberculosis

In the current era of microbial infections, tuberculosis (TB) predominantly remains as one of the life-threatening disease world-wide. TB is the second foremost reason of death from an infectious disease globally. According to 2015 WHO report, 10.4 million new cases were reported globally. Among these cases, 60% of them were from six countries namely, India, Indonesia, China, Nigeria, Pakistan and South Africa.[14] It is caused by tubercle bacilli *Mycobacterium tuberculosis* belonging to family Mycobacteriaceae and the order Actinomycetales, is one of the leading causes for death by an infectious bacterial pathogen. It appears across a spectrum in humans, from latent infection to active tuberculosis (Fig. 3). This chronic disease commonly affects lungs and gets transmitted by direct mode of transmission. The property of bacilli to stay dormant, its nature to survive in adverse environmental conditions, and unusual cell wall makes its treatment challenging.

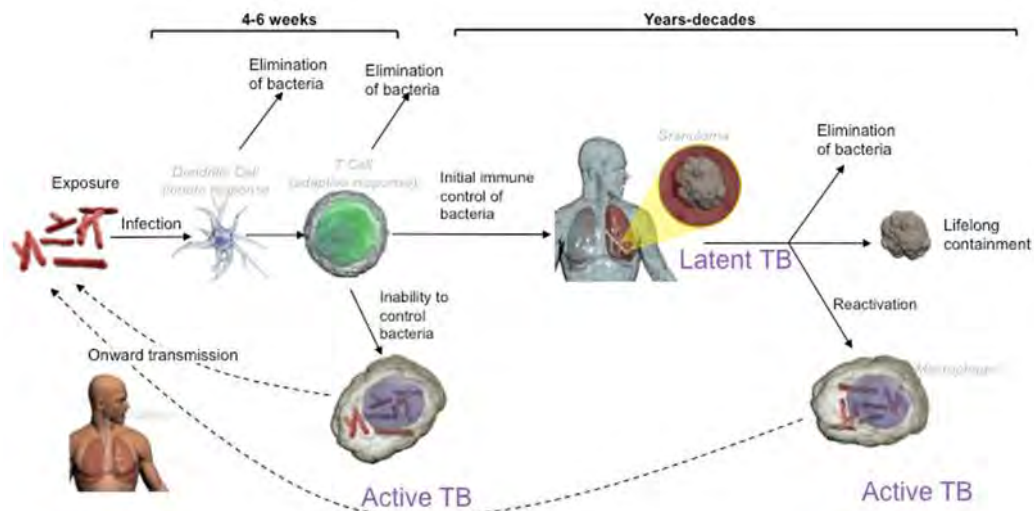


Figure 3: Progression of TB infection in humans. (*Image courtesy:* Infection Landscapes)

1.8 Management of tuberculosis

TB together with acquired immune deficiency syndrome (AIDS) is the highest cause of mortality. Further, emergence of drug-resistant mycobacterial strains like multidrug resistant TB (MDR-TB), extensively drug resistant TB (XDR-TB) and totally drug resistant TB (TDR-TB), are often attributed to failures in TB control programs. Presently available antitubercular drugs have often been associated with some limitations namely, long treatment duration, resistance, severe side effects, lack of selectivity, ineffective drug delivery systems leading to inadequate drug concentrations at the site of infection, frequency of dosing and poor patient compliance. Table 1 elaborates the available first-line and second-line antitubercular drugs with their associated

adverse effects. Figure 4 depicts the structures first and second-line antitubercular drugs. Thus, there is an imperative and urgent need for an effective treatment strategy for TB. Drug resistant TB can be effectively managed by following points[15]

- a. Setting up of specialized units having second line reserve drugs that could be regulated in order to prevent the emergence of incurable tuberculosis.
- b. Designing an appropriate regimen for the individual patient.
- c. Reliable susceptibility testing.
- d. Reliable supplies of second line drugs.
- e. Priority is prevention (priority for MDR-TB).
- f. Using WHO standard regimens for new cases and retreatment.
- g. MDR-TB as a consequence of poor treatment.
- h. Long-term involvement of staff and financial resources.

Table 1: First and second-line antitubercular drugs with their associated adverse effects.[16]

Class of drugs	Drug name	Adverse effects
First-line drugs	Isoniazid	Asymptomatic elevation of aminotransferases, clinical hepatitis, peripheral neurotoxicity, lupus-like syndrome, and monoamine (histamine/tyramine) poisoning.
	Rifampin	Cutaneous reactions, gastrointestinal reactions (nausea, anorexia, abdominal pain), flulike syndrome, hepatotoxicity, orange discoloration of bodily fluids (sputum, urine, sweat, tears), and drug interactions due to induction of hepatic microsomal enzymes.
	Rifabutin	Hematologic toxicity, uveitis, gastrointestinal symptoms, polyarthralgias, hepatotoxicity, pseudojaundice (skin discoloration with normal bilirubin), rashes, flulike syndrome, and orange discoloration of bodily fluids (sputum, urine, sweat, tears).
	Rifapentine	Same as Rifampin
	Pyrazinamide	Hepatotoxicity, gastrointestinal symptoms (nausea, vomiting), Nongouty polyarthralgia, asymptomatic hyperuricemia, acute gouty arthritis, transient morbilliform rash, and dermatitis.
Second-line drugs	Ethambutol	Retrolbulbar neuritis and cutaneous reactions.
	Cycloserine	Headache, psychosis, seizures and peripheral neuritis.
	Ethionamide	Gastrointestinal side effects, hepatotoxicity, neurotoxicity, gynecomastia, alopecia, hypothyroidism, and impotence.
	Streptomycin	Ototoxicity, neurotoxicity, and nephrotoxicity.
	Amikacin/kanamycin	Ototoxicity, and nephrotoxicity.
	Capreomycin	Ototoxicity, and nephrotoxicity.
	<i>p</i> -Aminosalicylic acid	Hepatotoxicity, gastrointestinal distress, malabsorption syndrome, hypothyroidism, and coagulopathy.
	Levofloxacin, Moxifloxacin and Gatifloxacin.	Nausea, bloating, dizziness, insomnia, tremulousness, headache rash, pruritis, and photosensitivity.

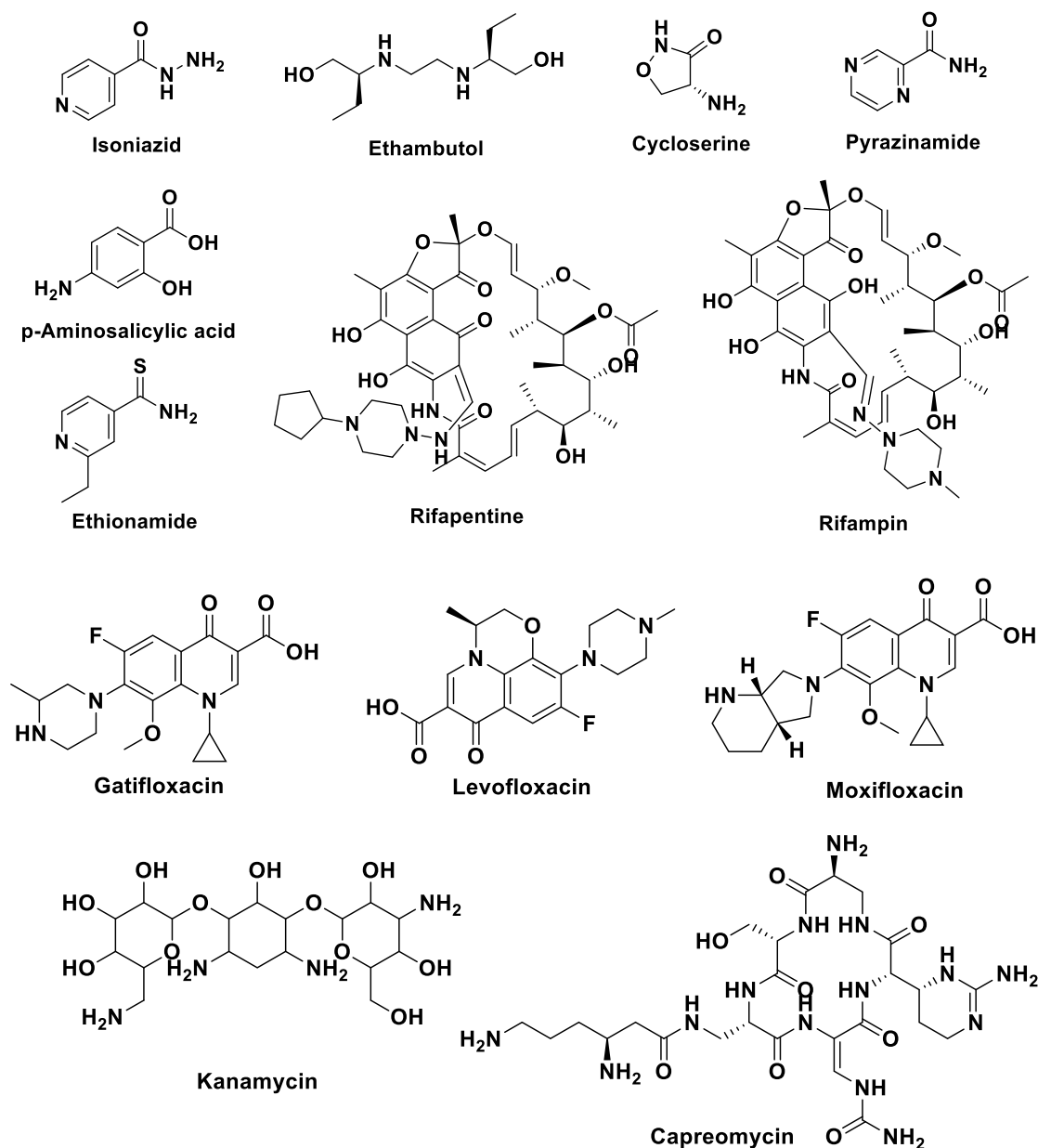


Figure 4: Structures of first and second-line antitubercular drugs.

1.9 Antitubercular drugs: Mechanism of action

Recent advances in elementary microbial genetics, has helped us in understanding the biochemical process involved in microbes. This cognizance has considerably helped in treatment of TB. The molecular targets targeted by antitubercular drugs have received much of the attention of medicinal chemists in the recent past. Targeting on or more sites of action simultaneously, has been advantageous in managing drug resistant TB. Figure 5 elaborates the mechanism of action of various approved antitubercular drugs.

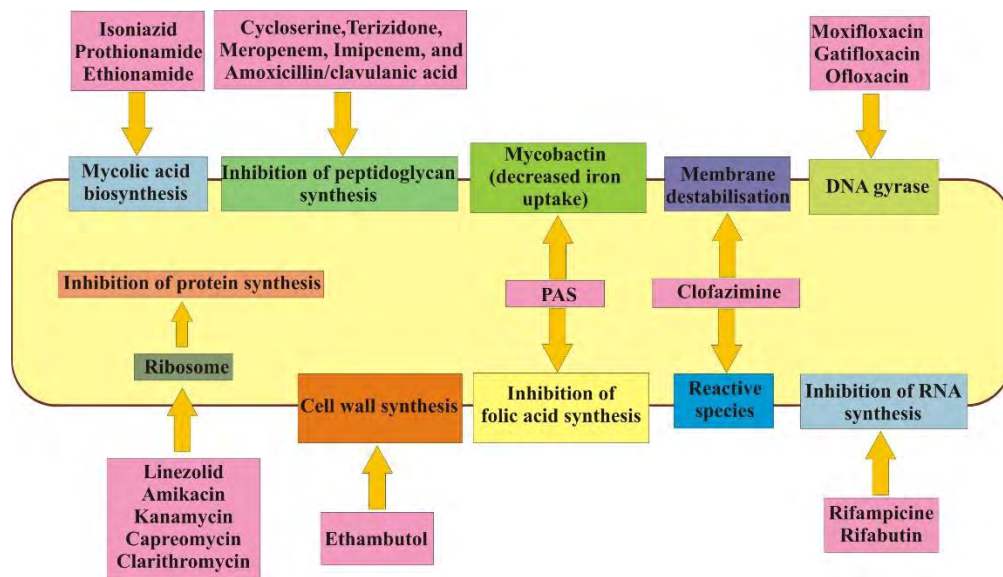


Figure 5: Mechanism of action of various approved antitubercular drugs.[17]

1.10 Antitubercular drug development

Globally over 480000 cases of MDR-TB occur annually (Fig. 6), 9% of them are being affected by XDR-TB. The management of MDR/XDR-TB is unfortunately lengthy, toxic and more expensive,[18] with success rate extremely disappointing (<20% among cases with resistance patterns beyond XDR). With the launch of “END TB Strategy”, WHO has supported universal access to high quality MDR diagnosis and treatment.[19] (Fig. 7)

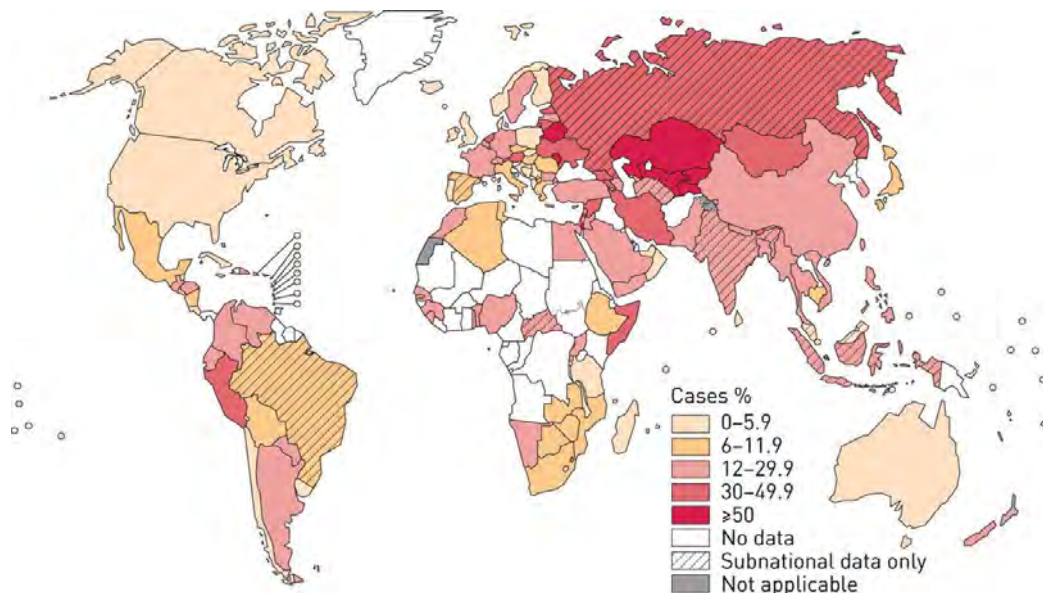


Figure 6: Global status showing MDR-TB incidences. (Image courtesy: WHO)

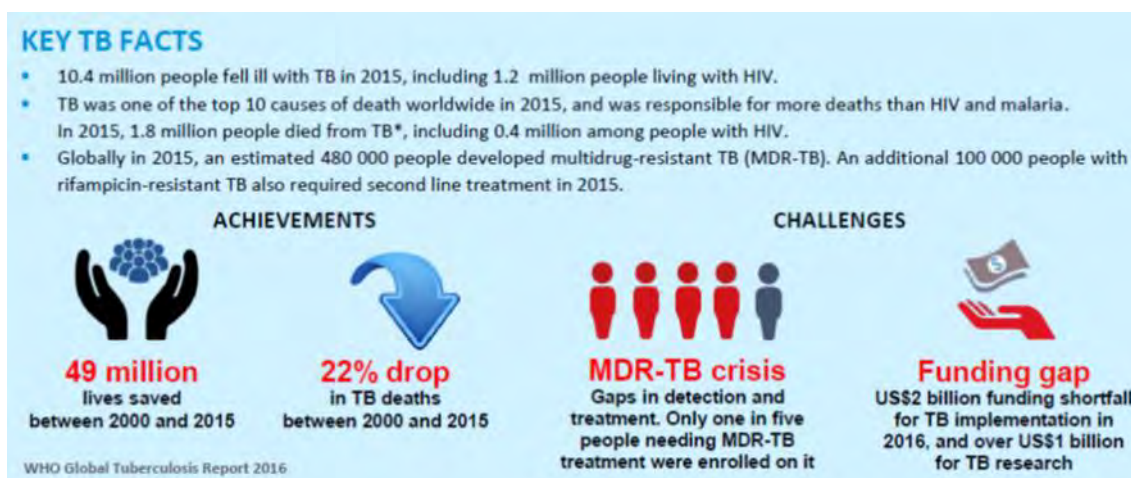


Figure 7: END TB strategy by WHO in 2015.

With the current first-line regimen being persistently followed since last 40 years, non-compliance of patient, adverse effects, and long treatment duration has led to emergence of resistant forms. All these facts are compelling for the need for new anti-TB drugs at an alarming rate. Numerous drugs are being investigated that regulate, cure or check further transmission of TB. Current drug development programmes focus on finding novel mechanism of action acting on vast biological pathways namely protein synthesis, cell wall synthesis, membrane energy production etc.[20] and are in late stages of development (Table 2).

Table 2: Antitubercular drugs currently in lead optimization stages along with their associated mechanism of actions.

Drug	Chemical class	Development stage	Mechanism of action/target
CPZEN-45	Caprazamycin derivative (Nucleoside antibiotic)	Early stage	Inhibition of cell-wall biosynthesis
SQ-609	Dipiperidine	Early stage	Inhibition of cell-wall biosynthesis
TBI-166	Riminophenazine	Early stage	Accumulation of lysophospholipids,
Spectinamide 1599	Spectinomycin analogues	Early stage	Inhibits protein synthesis
BTZ-043	Benzothiazinone	GLP Toxicity	Inhibits Mtb cell wall synthesis
PBTZ-169	Benzothiazine	GLP Toxicity	Inhibits cell-wall biosynthesis
TBA-7371	Benzothiazinone	GLP Toxicity	Disruption of cell-wall biosynthesis
GSK-070	Oxaborole	GLP Toxicity	Leucyl-tRNA synthetase inhibitor
Moxifloxacin and gatifloxacin	Quinolones	Phase III	DNA-gyrase inhibitor
PA824, OPC67683	Nitroimidazoles	Phase II	mycolic acid biosynthesis inhibition
TMC207 (Bedaquiline)	Diarylquinolines	Phase II	ATP-synthase inhibitor
SQ109	Diamine	Phase I	Unknown
Rifamycins	Rifamycins	Phase III	RNA polymerase inhibitor
Linezolid	Oxazolidinones	Phase II	50S ribosomal subunit
PNU-100480	Oxazolidinones	Phase I	50S ribosomal subunit
AZD5847	Oxazolidinones	Phase I	50S ribosomal subunit
Benzothiazinone	Benzothiazinones	Pre-clinical	DprE1 epimerase
Dinitrobenzamide	Dinitrobenzamides	Pre-clinical	DprE1 epimerase
VI-9376	Nitro-bromoquinoxaline	Pre-clinical	DprE1 epimerase
Q203	Imidazopyridine	Phase I	Inhibits mycobacterial growth

In 2012, the TB treatment reached a historic land mark with the approval of bedaquiline by the U.S. Food and Drug Administration (US-FDA), thus paying off for the efforts over last 40 years.[21] Yet the journey of discovering and developing new drugs to combat TB is still persistent. The TB drug pipeline (Fig. 8). is still however inadequate compared to what is desirable.

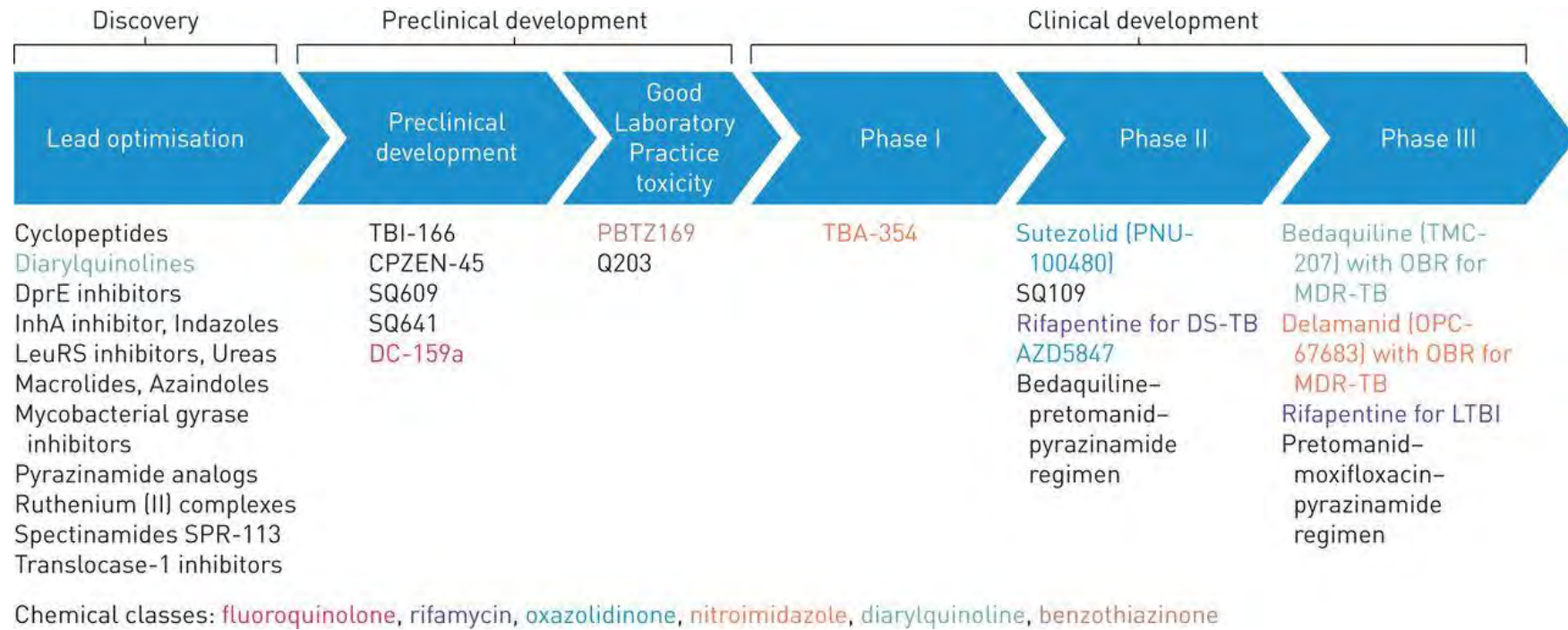


Figure 8: TB drug development pipeline.

Antitubercular drug research is shifting its horizon towards naturally obtained sources, in a hope to discover new safe and effective leads. Interestingly, these compounds have portrayed remarkable activity towards sensitive and Multi drug resistant strains of TB. The drugs from natural origin have been categorized as natural products, semisynthetic compounds resultant from natural products, and synthetic compounds based on natural product models.[22] Natural product chemistry and organic synthesis are potential tools for optimizing leads and generate new diverse entities from natural scaffolds. Unification of these two branches has been a vital foundation for modern day ration drug design. Antitubercular secondary metabolites have been isolated from plants, bacteria, fungi, algae and marine organisms. Some of them have been categorized under various chemical classes (Table 3).

Table 3: Natural secondary metabolites as antitubercular drugs.[23]

Class of compounds	Examples	Source
Terpenes	Salasol A & Celahin C	<i>Microtropis japonica</i>
Steroids	Ergosterol peroxide and β -sitostenone	<i>R. boniana</i>
Alkaloids	Ambiguine K, L, M & N	<i>Fischerella ambigua</i> (a cynobacterium)
Flavonoids	Khonklonginol A, B & H, Eriosemaone A and Lupinifolin	<i>Eriosema chinense</i>
Coumarins	Scopoletin	<i>Fatoua pilosa</i>
Chalcones	Isobavachalcone	<i>Fatoua pilosa</i>
Lignans	Beilschmin A	<i>Beilschmiedia tsangii</i>
Xanthones	α -mangostin	<i>Garcinia mangosta</i>
Anthracenes	Mollicellin K	<i>Chaetomium brasiliense</i> (an fungus)
Peptides	Trichoderin A, A1 & B	Trichoderma sp. 05FI48 strain (an fungus)

Additionally, several semisynthetic and synthetic derivatives based on natural product models have been successfully explored for their antitubercular properties. (Table 4). Chemical diversity, more number of chiral centres, steric convolution, and biochemical specificities have made these natural scaffolds as indispensable. Therefore, all these facts remarkably portray the significance of natural products as a stand point in the contemporary drug discovery and development. Therefore, our work is one such effort in identifying synthetic antitubercular lead compounds based on natural product model.

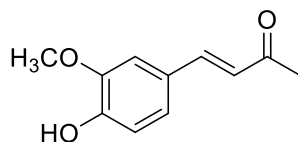
Table 4: Naturally inspired semisynthetic antitubercular drugs.

Natural compound	Inspired semisynthetic derivatives
Streptomycin (<i>Streptomyces griseus</i>)	Kanamycin and Amikacin
Capreomycin 1A & 1B (<i>Streptomyces capreolus</i>)	Viomycin
Rifamycin (<i>Amycolatopsis rifamycinica</i>)	Rifampicin, Rifabutin, Rifalazil, Rifametane and Rifapentine [23]
Spectinomycin (<i>Streptomyces spectabilis</i>)	Spectinamides (semisynthetic derivative)[24]
Capuramycin	SQ641[25]

2 GENESIS OF OUR RESEARCH

Our literature review suggested that countries like India, Indonesia, China, Nigeria, Pakistan and South Africa carry massive burden of TB. Further, 60% of globally estimated MDR-TB cases were reported from TB-endemic countries namely China, India, the Russian Federation and South Africa alone.[26] Clinicians managing the TB cases frequently encounter significant challenges such as lack of clinical experience, adverse events, lack of patients adherence, inadequate availability diagnostics or second line drugs, thus augmenting the risk of drug resistance. Therefore, after considering all these solemn facts, we should tactically accelerate a robust and diverse drug discovery and development programs to fill the pipeline with potential leads. In parallel, we need to develop and improve techniques in understanding the pathogenesis and host-pathogen interactions of TB in order to discover novel valid TB targets. We should also look on to an angle for extensive exploitation of chemical space and optimize lead hits for effective TB drugs for future. Naturally available antitubercular drugs should be explored which usually have least or devoid of side effects. Drugs from natural sources have enormous potential in modulating the immune response and inhibit the mechanism of resistance in disease stricken state. Several naturally derived drugs like pyridomycin, cyclomarin A, lassomycin, and ecumicin have shown potent activity against MDR and XDR-TB.[27] Also, streptomycin, kanamycin, rifampicin, capreomycin 1A and clarithromycin are some of the significant antimycobacterial drugs obtained from natural products.[28] Hence, it is considerably important to focus our attention in developing natural products as hits for generating leads derived from them.

Therefore, in order to identify new lead inspired from natural source, we came across a natural chalcone, Dehydrozingerone (DZG). DZG is isolated from rhizomes of ginger (*Zingiber officinale* Roscoe, family Zingiberaceae) and is famously identified as a half structural analog of curcumin. DGZ is known for its variety of pharmacological activities namely antibacterial, anticancer, antifungal, antimalarial, anti-inflammatory, antidepressant, antioxidant etc.



Structure of Dehydrozingerone

Our extensive literature survey revealed no reports on its antitubercular properties. Therefore, our research was focused in modifying the structural core of DZG with various antitubercular heterocycles by molecular hybridization to attain novel antitubercular leads. The following paragraphs enlighten about the work planned and executed in succeeding chapters.

- During our comprehensive literature review, we witnessed there was no review published on DZG. Hence we envisioned to write a review on the medicinal perspectives of DZG covering its entire array of pharmacological properties.
- Thiazole is an essential heterocyclic scaffold in drug discovery. Its derivatives are known to possess a varied range of activities such as antihypertensive, anti-inflammatory, anti-HIV, antibacterial, and antimycobacterial. However, there were no reports on styryl thiazoles as antimycobacterials. Therefore, we have envisaged to synthesize DZG inspired styryl hydrazine thiazole hybrids as antimycobacterial agents. The outcome of this work uplifted the importance of incorporating the styryl portion for antimycobacterial activity. Because of the outstanding contribution by the styryl portion on the thiazole heterocycle core, the subsequent chapters have retained this portion.
- Thiazolidin-4-one ring systems are biologically active 5-membered heterocycles that contain nitrogen and sulphur heteroatoms. This vital core structure has extensively been investigated for numerous biological properties, namely antimicrobial, antiviral, anticonvulsant, anti-inflammatory, anticancer, and antitubercular. With the findings on the importance of the styryl portion, in this chapter we have foreseen to synthesize styryl thiazolidin-4-one derivatives as potential antimycobacterial agents.
- Pyrazole is a well-known 5-membered heterocycle that has been known to exhibit a significant range of biological activities, namely antibacterial, antifungal, anticancer, antiviral, antidiabetic, anti-inflammatory, anti-atherosclerosis, and antimycobacterial. Further, semicarbazone and thiosemicarbazones are versatile chemical intermediates that are employed in the synthesis of several key heterocyclic compounds. These semicarbazone and thiosemicarbazones are themselves known to be biologically active and possess assorted pharmacological responses, namely antibacterial, antiproliferative, antifungal, anticancer, anticonvulsant, and antitubercular. Therefore, in this chapter we anticipated the synthesis of carbazones, semicarbazone, and thiosemicarbazone derivatives of styryl fused pyrazole as potential antibacterial, antifungal, and antimycobacterial agents.

3 OBJECTIVES OF THE PRESENT RESEARCH WORK

Microbial infections are erupting at an alarming rate. Appearance of drug resistance is a serious concern in modern day chemotherapy. New drugs with an ability to overcome the drawbacks of existing antimicrobial chemotherapy are at high priority. The field of medicinal chemistry is contributing implicitly to the process of drug discovery and development. Synthesis of novel chemical entities, modification in existing scaffolds, combining two or more bioactive molecules (hybridization), replacing groups with bioisosteres, and optimization of natural compounds to identify promising leads are some of the interesting themes in the field of medicinal chemistry. Heterocyclic scaffolds having one or more hetero atoms have become indispensable in drug discovery, which is evident from the fact that more than 95% of the marketed drugs are built on heterocyclic scaffolds

In observation of all these above facts, the present research project work was planned. The aims and objectives of the present research work are

1. To carry out extensive literature survey for identification of new chemical entities as antimicrobial/antitubercular activity (Identification of a research gap and defining the scope of proposed work).
2. To synthesize a novel series of DZG fused hybrid chemical entities containing the following heterocyclic scaffolds
 - a. Styryl hydrazine thiazole derivatives.
 - b. Styryl hydrazine thiazolidin-4-one derivatives and
 - c. Styryl pyrazolo carbazone derivatives.
3. To purify the synthesized compounds by chromatographic techniques namely column (flash) chromatography.
4. To establish the structure of synthesized compounds by physicochemical and spectral analysis (IR, ^1H NMR, ^{13}C NMR and High resolution mass spectrometry).
5. To carry out the preliminary biological evaluation of the synthesized compounds for their antitubercular and antibacterial activity.

The subsequent chapter unveils the extensive investigations on literature about DZG and its semisynthetic derivatives acknowledged for its diverse pharmacological properties.

References

- [1] National Institutes of Health, (2007).
- [2] H.M. Wei, X.Z. Li, M. Martcheva, *J. Math. Anal. Appl.* 342 (2008) 895–908.
- [3] S. Seth, *Textbook of Pharmacology*, 2009.
- [4] S. Leekha, C.L. Terrell, R.S. Edson, *Mayo Clin. Proc.* 86 (2011) 156–67.
- [5] J.R. Moellering Jr, *Clin. Ther.* 4 (1980) 1–7.
- [6] K.M. Overbye, J.F. Barrett, *Drug Discov. Today* 10 (2005) 45–52.
- [7] M.E. Falagas, S.K. Kasiakou, L.D. Saravolatz, *Clin. Infect. Dis.* 40 (2005) 1333–1341.
- [8] R.I. Aminov, *Front. Microbiol.* 1 (2010) 134.
- [9] L.A. Dever, T.S. Dermody, *Arch. Intern. Med.* 151 (1991) 886–95.
- [10] S. Doron, L.E. Davidson, *Mayo Clin. Proc.* 86 (2011) 1113–23.
- [11] WHO, WHO | Antimicrobial Resistance, World Health Organization, 2016.
- [12] A. Giedraitienė, A. Vitkauskienė, R. Naginienė, A. Pavilionis, *Medicina (Kaunas)*. 47 (2011) 137–46.
- [13] S. Dzidic, J. Suskovic, B. Kos, *Food Technol. Biotechnol.* 46 (2008) 11–21.
- [14] WHO, WHO | Global Tuberculosis Report 2016, World Health Organization, 2016.
- [15] J. Crofton, P. Chaulet, D. Maher, J. Grosset, W. Harris, N. Horne, M. Iseman, B. Watt, *Guidelines for the Management of Drug-Resistant Tuberculosis*, 1997.
- [16] American Thoracic Society/Centers for Disease Control/Infectious Diseases Society of America, *Treatment of Tuberculosis*, 2003.
- [17] I.D. Olaru, F. Von Groote-Bidlingmaier, J. Heyckendorf, W.W. Yew, C. Lange, K.C. Chang, *Eur. Respir. J.* 45 (2015) 1119–1131.
- [18] G.L. Dean, S.G. Edwards, N.J. Ives, G. Matthews, E.F. Fox, L. Navaratne, M. Fisher, G.P. Taylor, R. Miller, C.B. Taylor, A. de Ruiter, A.L. Pozniak, *AIDS* 16 (2002) 75–83.
- [19] World Health Organization, WHO End TB Strategy, World Health Organization, 2015.
- [20] Y. Zhang, *Annu. Rev. Pharmacol. Toxicol.* 45 (2005) 529–564.
- [21] R. Mahajan, *Int. J. Appl. Basic Med. Res.* 3 (2013) 1–2.
- [22] G.M. Cragg, D.J. Newman, K.M. Snader, *J. Nat. Prod.* 60 (1997) 52–60.
- [23] B.R. Copp, *Nat. Prod. Rep.* 20 (2003) 535–557.
- [24] R.E. Lee, J.G. Hurdle, J. Liu, D.F. Bruhn, T. Matt, M.S. Scherman, P.K. Vaddady, Z. Zheng, J. Qi, R. Akbergenov, S. Das, D.B. Madhura, C. Rathi, A. Trivedi, C. Villellas, R.B. Lee, Rakesh, S.L. Waidyarachchi, D. Sun, M.R. McNeil, J.A. Ainsa, H.I. Boshoff, M. Gonzalez-Juarrero, B. Meibohm, E.C. Bottger, A.J. Lenaerts, *Nat Med* 20 (2014) 152–158.
- [25] B. Nikonenko, V.M. Reddy, E. Bogatcheva, M. Protopopova, L. Einck, C.A. Nacy,

- Antimicrob. Agents Chemother. 58 (2014) 587–589.
- [26] World Health Organization, in: Bugs, Drugs Smoke Stories from Public Heal., World Health Organization, 2011, pp. 99–117.
- [27] H. Lee, J.W. Suh, J. Ind. Microbiol. Biotechnol. 43 (2016) 205–212.
- [28] J.D. Guzman, A. Gupta, F. Bucar, S. Gibbons, S. Bhakta, Front. Biosci. (Landmark Ed. 17 (2012) 1861–81.

CHAPTER 2

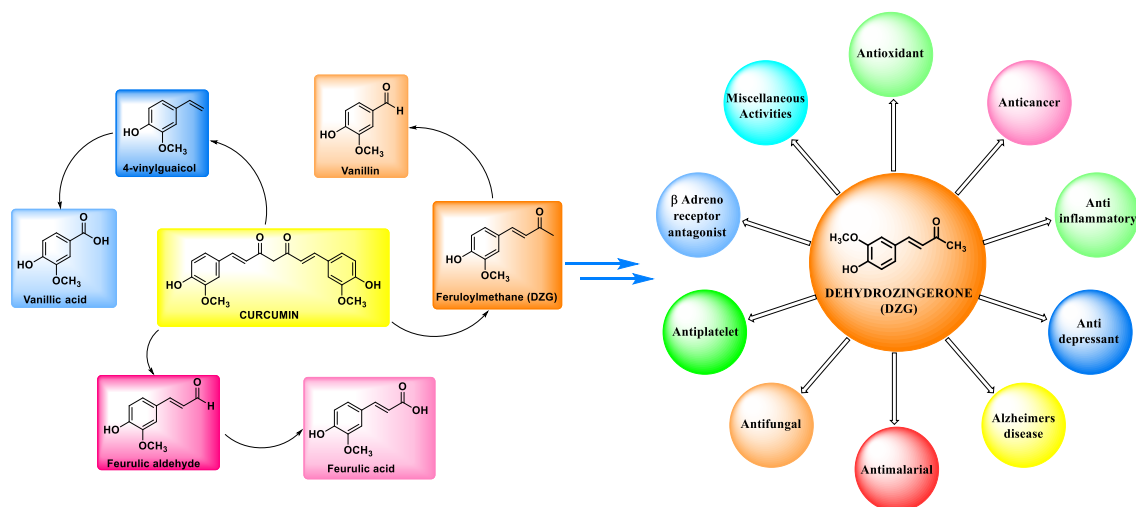
An Appraisal on Recent Medicinal Perspective of Curcumin degradant: Dehydrozingerone (DZG)

Girish A. Hampannavar¹, Rajshekhar Karpoormath¹, Mahesh B. Palkar^{1,2} and Mahamadhanif S. Shaikh¹

¹Department of Pharmaceutical Chemistry, Discipline of Pharmaceutical Sciences, College of Health Sciences, University of KwaZulu-Natal, Westville Campus, Durban – 4000, South Africa

²Department of Pharmaceutical Chemistry, K.L.E. University College of Pharmacy, Vidyanagar, Hubballi – 580031, Karnataka, India

Graphical Abstract



*Corresponding author

E-mail: karpoormath@ukzn.ac.za, rvk2006@gmail.com

Tel no.: +27(0)312607179, +27721107207; Fax No.: +27(0)312607792



Contents lists available at ScienceDirect

Bioorganic & Medicinal Chemistry

journal homepage: www.elsevier.com/locate/bmc

Review article

An appraisal on recent medicinal perspective of curcumin degradant: Dehydrozingerone (DZG)

Girish A. Hampannavar^a, Rajshekhar Karpoomath^{a,*}, Mahesh B. Palkar^{a,b}, Mahamadhanif S. Shaikh^a^a Department of Pharmaceutical Chemistry, Discipline of Pharmaceutical Sciences, College of Health Sciences, University of KwaZulu-Natal, Westville Campus, Durban 4000, South Africa^b Department of Pharmaceutical Chemistry, K.L.E. University College of Pharmacy, Vidyanagar, Hubballi 580031, Karnataka, India

ARTICLE INFO

Article history:

Received 20 October 2015

Revised 23 December 2015

Accepted 31 December 2015

Available online 2 January 2016

Keywords:

Review

Dehydrozingerone (DZG)

Zingiber officinale

Curcumin degradants

Feruloyl/methane

ABSTRACT

Natural products serve as a key source for the design, discovery and development of potentially novel drug like candidates for life threatening diseases. Curcumin is one such medicinally important molecule reported for an array of biological activities. However, it has major drawbacks of very poor bioavailability and solubility. Alternatively, structural analogs and degradants of curcumin have been investigated, which have emerged as promising scaffolds with diverse biological activities. Dehydrozingerone (DZG) also known as feruloylmethane, is one such recognized degradant which is a half structural analog of curcumin. It exists as a natural phenolic compound obtained from rhizomes of *Zingiber officinale*, which has attracted much attention of medicinal chemists. DZG is known to have a broad range of biological activities like antioxidant, anticancer, anti-inflammatory, anti-depressant, anti-malarial, antifungal, anti-platelet and many others. DZG has also been studied in resolving issues pertaining to curcumin since it shares many structural similarities with curcumin. Considering this, in the present review we have put forward an effort to revise and systematically discuss the research involving DZG with its biological diversity. From literature, it is quite clear that DZG and its structural analogs have exhibited significant potential in facilitating design and development of novel medicinally active lead compounds with improved metabolic and pharmacokinetic profiles.

© 2016 Elsevier Ltd. All rights reserved.

Abstract

Natural products serve as a key source for the design, discovery and development of potentially novel drug like candidates for life threatening diseases. Curcumin is one such medicinally important molecule reported for an array of biological activities. However, it has major drawbacks of very poor bioavailability and solubility. Alternatively, structural analogs and degradants of curcumin have been investigated, which have emerged as promising scaffolds with diverse biological activities. Dehydrozingerone (DZG) also known as feruloylmethane, is one such recognized degradant which is a half structural analog of curcumin. It exists as a natural phenolic compound obtained from rhizomes of *Zingerber officinalae*, which has attracted much attention of medicinal chemists. DZG is known to have a broad range of biological activities like antioxidant, anticancer, anti-inflammatory, anti-depressant, anti-malarial, antifungal, anti-platelet and many others. DZG has also been studied in resolving issues pertaining to curcumin since it shares many structural similarities with curcumin. Considering this, in the present review we have put forward an effort to revise and systematically discuss the research involving DZG with its biological diversity. From literature, it is quite clear that DZG and its structural analogs have exhibited significant potential in facilitating design and development of novel medicinally active lead compounds with improved metabolic and pharmacokinetic profiles.

Keywords

Review, dehydrozingerone (DZG), *Zingerber officinalae*, curcumin degradants, feruloylmethane.

1 Introduction

From time immemorial natural products sourced from plants, animals, marines and minerals have been the basis of treatment for variety of diseases. Plants in particular have been the basis of many traditional medicine systems throughout the world for thousands of years and they still continue to offer humankind with new remedies. The foundation of the modern pharmaceutical industry was primarily based on the techniques developed to identify and synthesize active ingredients from the traditional medicines obtained from natural sources. Plant-based medicines were initially dispensed as crude medicines such as tinctures, teas, poultices, powders and other herbal formulations,¹ which now serve as the basis of novel drug discovery. For example, plant based compounds like quinine, reserpine, curcumin, vincristine, vinblastine, pilocarpine, atropine, morphine, taxol, etc., have been investigated and exploited as important pharmaceutical drugs for the treatment of vital diseases or disorders. Hence, natural products have been proven templates for the development of new scaffolds for drugs.²⁻⁵

Dehydrozingerone (DZG; Fig. 1) also known as feruloylmethane and vanillylidene acetone, isolated from rhizomes of ginger (*Zingiber officinale* Roscoe, family: Zingiberaceae)⁶⁻⁸ and can be synthesized in laboratory by simple aldol condensation of vanillin and acetone.⁹ It is famously identified as a half structural analog of curcumin and is a classic example of a natural chalcone. DZG [(*E*)-4-(4-hydroxy-3-methoxyphenyl)but-3-en-2-one] is a remarkable scaffold comprising of a phenyl ring bearing methoxy group *ortho* to the phenolic OH and an α,β -unsaturated carbonyl group with terminal methyl group. Besides, DZG is an unsaturated derivative of the natural product zingerone and resembles segment of curcumin as well as share many structural and pharmacological similarities with curcumin.

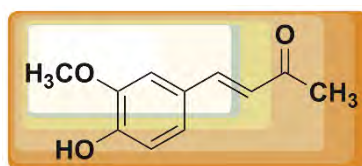


Figure 1: Structure of Dehydrozingerone (DZG).

DZG and curcumin also claim mutual chemical resemblances as both bear styryl ketone moieties with similar substitutions on the phenyl ring.^{10,11} It is a recognized biosynthetic intermediate¹² and also an identified degradant of curcumin¹³ (Fig. 2).¹³⁻¹⁶ DZG is a known metabolic product of curcumin that has a larger biological half-life than curcumin itself.¹⁷ In spite of versatile applications of Curcumin (*diferuloylmethane*), a polyphenol extract of *Curcuma longa*,¹⁸ is still known to have weak bioavailability and suffers from premature degradation on oral

administration that holds back its use as a successful therapeutic agent.¹⁹ These pharmacokinetic instabilities of curcumin may be due to following reasons,

- Liability of β -diketone moiety in the structure of curcumin (as substrates) to several aldo-keto reductases in vivo.²⁰⁻²²
- Enzymatic cleavage at the benzylic position.²³
- Instability of reactive β -diketone moiety at neutral-basic pH conditions in vitro.^{13,24}
- Instability of active methylene group at a pH above 6.5.²⁵

However, the curcuminoids, degradants and biosynthetic intermediates of curcumin also exhibit many exceptional pharmacological effects. These emerging new class of compounds have been termed as mono-carbonyl analogs (MCA's) or mono-carbonyl enones or dienones.²⁶ These enone analogs emanate in 5, 3 and 7 carbon spacers (7 carbon spacers as in curcumin) and have explicable biological activities on comparison with curcumin.²⁷ Furthermore several studies involving MCA's have proven improved bioactivities and enhanced pharmacokinetic profiles compared to curcumin.²⁸⁻³⁰

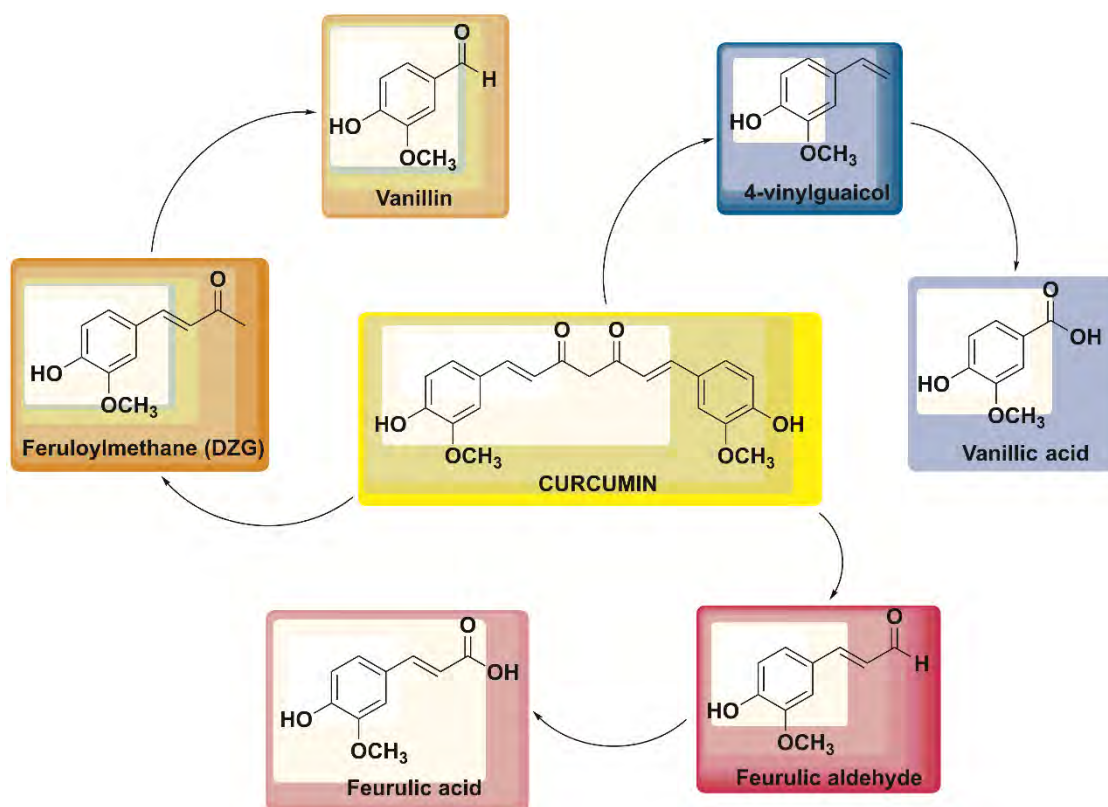


Figure 2: Degradation products of curcumin.

In recent times, scientists have shown enormous interest towards exploring the medicinal potentials especially for their antioxidant and anticancer activity. The degradation products as well as curcuminoids have played a key role in understanding the mechanism of action of curcumin. Recent studies have shown that degradation products such as ferulic acid and vanillic acid as human metabolites of curcumin, have contributed towards the antioxidant effects of curcumin.³¹ Hence, the structural analogs or degradants have emerged as promising scaffolds that have contributed towards designing valuable impending drugs. With these distinguishing structural features DZG as an active scaffold has been exploited for diverse medicinal properties (Fig. 3) as discussed in this review.

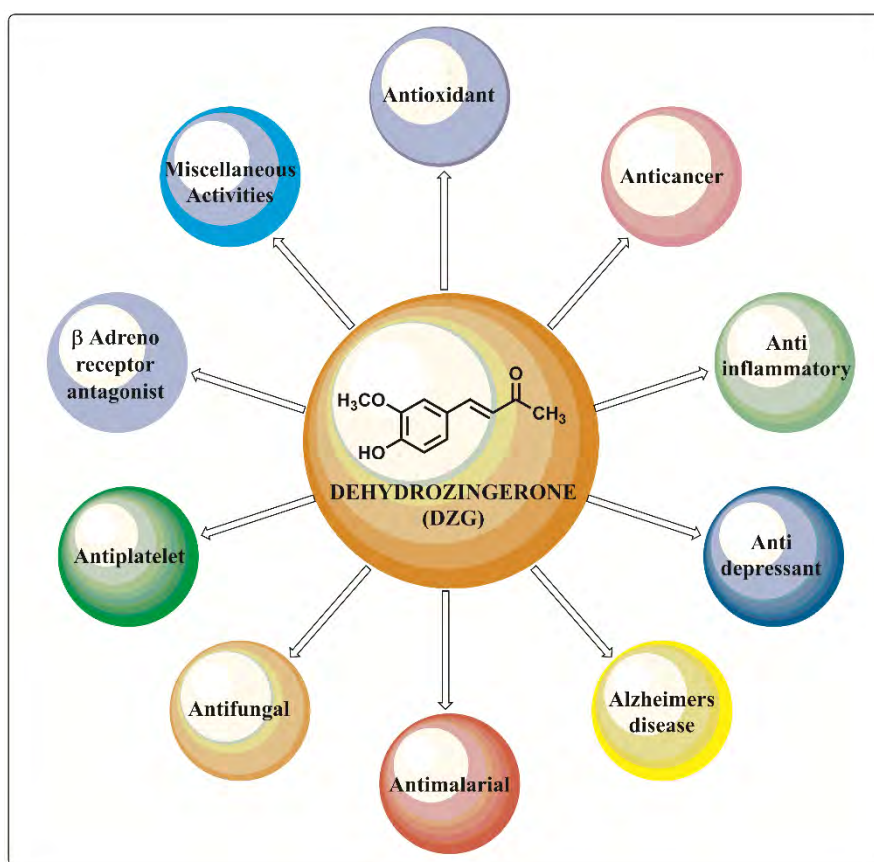


Figure 3: DZG as active scaffold with manifold pharmacological activities

The variations in the biological activity of DZG as a result of its structural manipulations are precisely highlighted in Figure 4. In this mini review we have recapitulated the progress of research involving DZG and its derivatives and discussed its diverse application in the field of medicinal chemistry emphasizing on their brief structure activity-relationships (SAR).

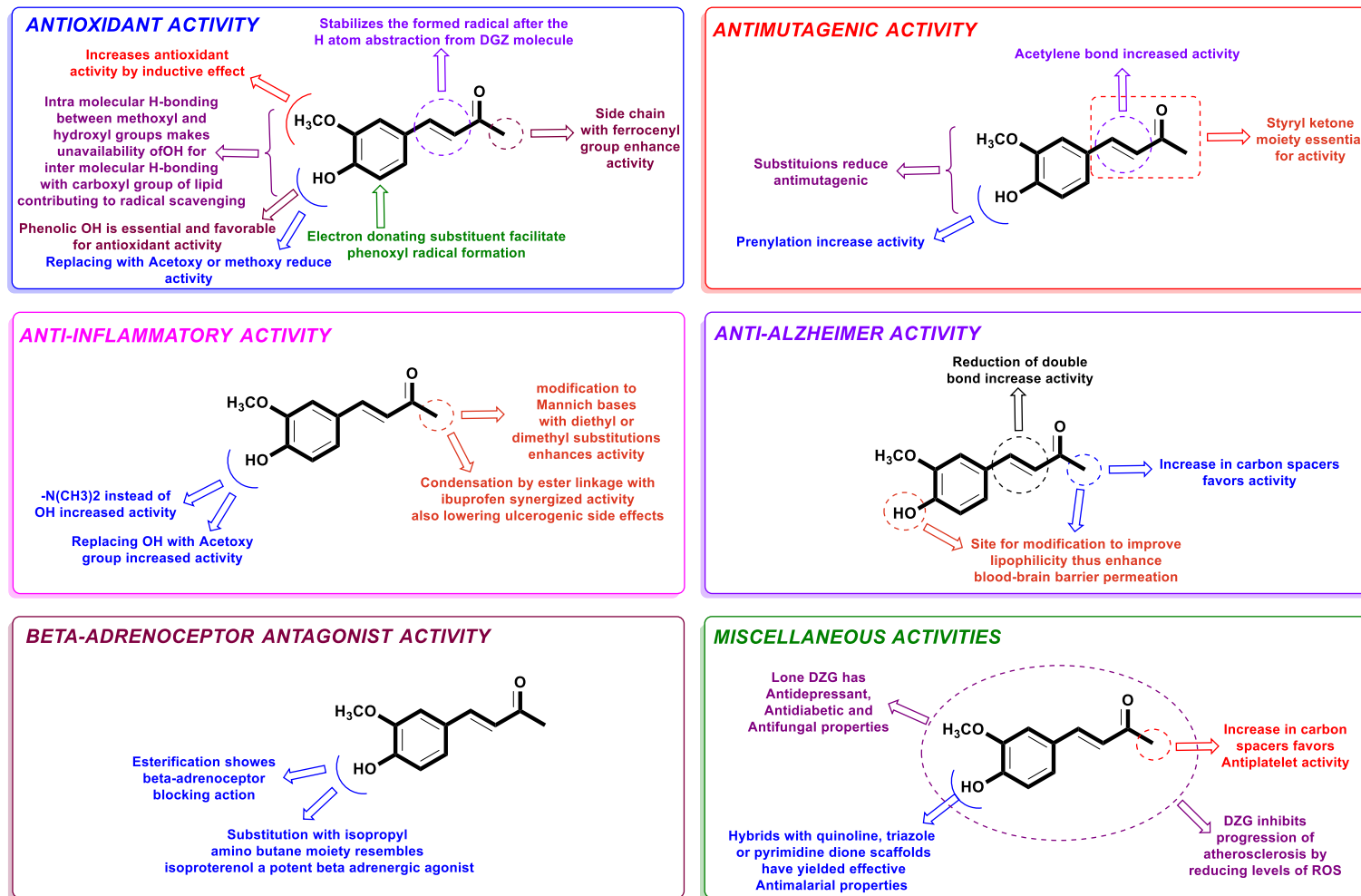


Figure 4: Imperative structural features of Dehydrozingerone (DZG) and effects of substitutions over various biological activities.

2 Dehydrozingerone identified for manifold pharmacological activities

2.1 Dehydrozingerone as antioxidant

Reactive oxygen species (ROS) are produced during aerobic respiration. Regardless of multiple preserved redox modulating systems, a part of ROS constantly flee from the mitochondrial respiratory sequence which is sufficient to damage cells in a variety of ways that include DNA mutations,³² lipid peroxidation,³³ ATP depletion,³⁴ and apoptosis.³⁵ Antioxidants are the key negotiators that prevent the reaction of ROS with biomolecules and have immense potential against pathophysiology of numerous diseases including cancer, heart disease, aging and different neurological disorders. Ranges of naturally occurring antioxidants have been isolated from plants and have been further tailored structurally to give in newer derivatives. Some of the naturally occurring antioxidants usually phenols and poly phenols³⁶ have been depicted in the Figure 5.³⁷

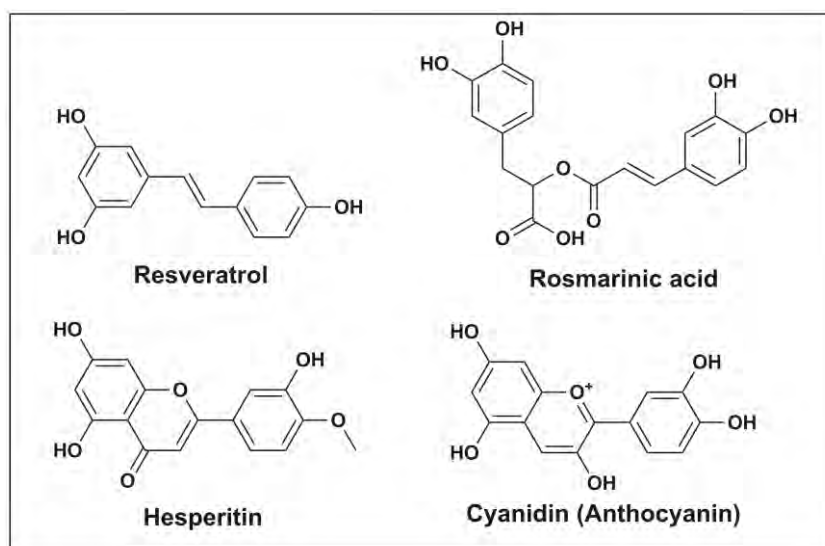
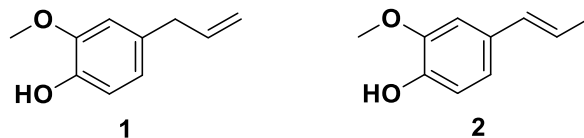


Figure 5: Naturally occurring antioxidants.

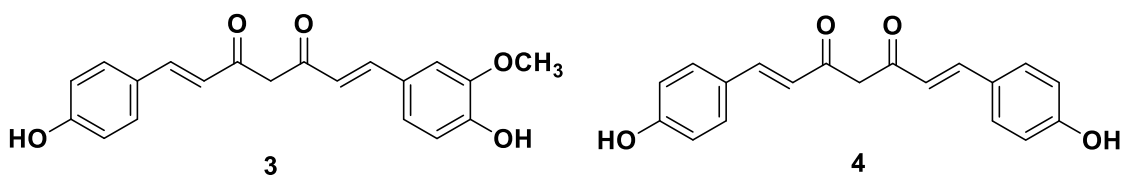
Rajakumar *et al.*, have reported the antioxidant properties of three structurally related compounds namely DZG, eugenol (**1**) and isoeugenol (**2**) by means of various experimental models. In this study compound **2** was found to be the highly active in restraining ferrous-ion, ferric-ion and cumene-hydroperoxide-induced lipid peroxidation in rat brain homogenates. All the tested compounds displayed considerable hydroxyl radical scavenging activity. Compound **2** was found as a powerful scavenging superoxide anion produced by the xanthine-xanthine oxidase system, whereas compound **1** was observed to inhibit xanthine oxidase. The high antioxidant activity of **2** was due to the existence of a conjugated double bond, which augments the stability of the

phenoxy radical by electron delocalization. Such electron delocalization is not possible with **1**. In DZG, the stability was diminished by an electron withdrawing keto group at the para position to hydroxyl group. Over all, this study evidently demonstrated the essential structural features and the antioxidant potential of naturally occurring phenols, of which compound **2** emerged as a potential antioxidant as compared to DZG.¹⁰

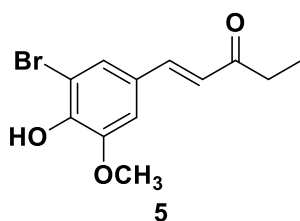


In order to understand the antioxidant properties of DZG and curcumin, Rajakumar *et al.*, have reported the inhibition of lipid peroxidation by both DZG and curcumin in rat brain homogenates. Interestingly both compounds inhibited the formation of conjugated dienes and spontaneous lipid peroxidation. These two compounds also inhibited lipid peroxidation induced by ferrous ions, ferric-ascorbate and ferric-ADP-ascorbate. In each of these cases curcumin was found to be more active than DZG and α -tocopherol. This study established that 1,3-diketone structure was not necessary for inhibiting lipid peroxidation by curcumin because DZG, which is devoid of this system was also capable of inhibiting lipid peroxidation. The phenolic groups in both of these compounds were found to favor considerably for the antioxidant properties, since they react with free radicals to form phenoxy radical. Methoxy group at *ortho*-position to the phenolic group in both DZG and curcumin were known to increase the antioxidant activity due to inductive effect. This study demonstrated that DZG like curcumin inhibits lipid peroxidation although to a lesser extent and additionally the antioxidant activity of curcumin was refereed by its two phenolic groups, which accounts for its superior activity.¹¹

Subramanian *et al.*, have reported the shielding potential of natural antioxidants against oxidative damage of DNA by excited species of oxygen that is, ¹O₂, a singlet molecular oxygen, known to induce single strand breaks in plasmid DNA. Natural antioxidants namely curcumin, DZG besides two other desmethoxycurcumin (**3**) and bisdemethoxycurcumin (**4**) were examined in this study. The results showed that curcumin and its derivatives and to a smaller degree other natural antioxidants tender noteworthy protection to DNA against ¹O₂. Curcumin was found to be most effective followed by DZG then **3** and **4**. At higher concentration DZG, **3** and **4** were found to be equally active. Thus this study fairly highlighted an explanation regarding probable mechanism of antimutagenic properties of these tested natural antioxidants.⁵



Priyadarsini *et al.*, have reported structurally allied phenols namely DZG, bromopentenone (5), eugenol (1) and isoeugenol (2) for antioxidant properties by inhibiting lipid peroxidation in membrane models. Additionally, the physicochemical properties of the transient intermediates of these antioxidants produced by the scavenging of several oxidizing free radicals were computed using pulse radiolysis technique.³⁸

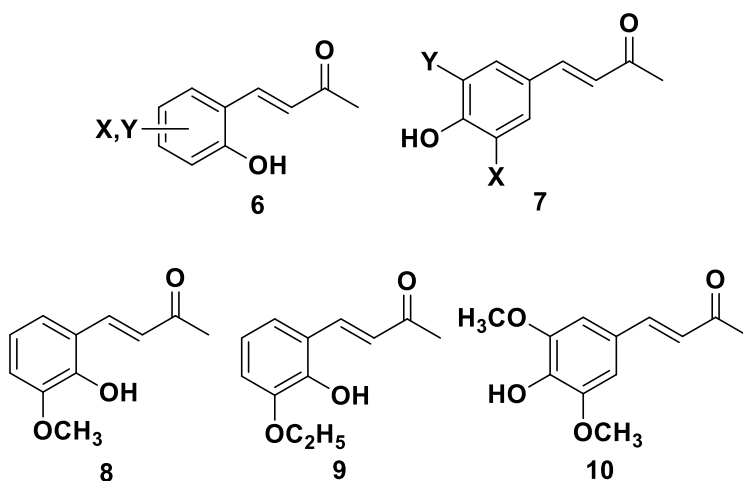


Jovanovic *et al.*, have reported antioxidant mechanisms of curcumin by laser flash photolysis and pulse radiolysis. This study revealed that the apparent site of reaction is the central CH₂ group in the heptadienone link of curcumin, which has two labile hydrogens. This was supported by comparing the reaction patterns of curcumin and DZG. DZG did not react with the methyl radical, indicating that the presence of the labile hydrogens is crucial for the H-atom donating ability of curcumin. Thus the electron donating ability of curcumin is assessed from the measurements of one-electron-transfer equilibria of DZG radicals. The major conclusion of this study was that the H-atom transfer plays a crucial role in the antioxidant action of curcumin.³⁹

Priyadarsini *et al.*, have reported the free radical reactions of DZG studied at different pH using a range of oxidants by means of nanosecond pulse radiolysis procedure. This study employed several free radicals both primary and secondary to access the antioxidant potential of DZG. Several specific free radicals were generated namely N₃[•], Br[•], Br₂[•], and TI(II) that were employed with DZG giving rise to the phenoxyl radical across the total pH range. Observations at pH 6 suggest that there is formation of OH-adduct which absorbs at 460 nm along with another small oxidation product confirmed by HPLC analysis. And at pH 10 there was only one oxidation product that is, phenoxyl radical absorbing at 360 nm. This study demonstrated that the phenoxyl radical from DZG is deficient to abstract hydrogen because of delocalization of the unpaired electron into an aromatic ring structure. The phenoxyl radical was recognized to have a lifetime of a few milliseconds. The thermodynamic parameter and one-electron reduction potential of DZG was considerably high thus not making DZG as a perfect candidate for an antioxidant

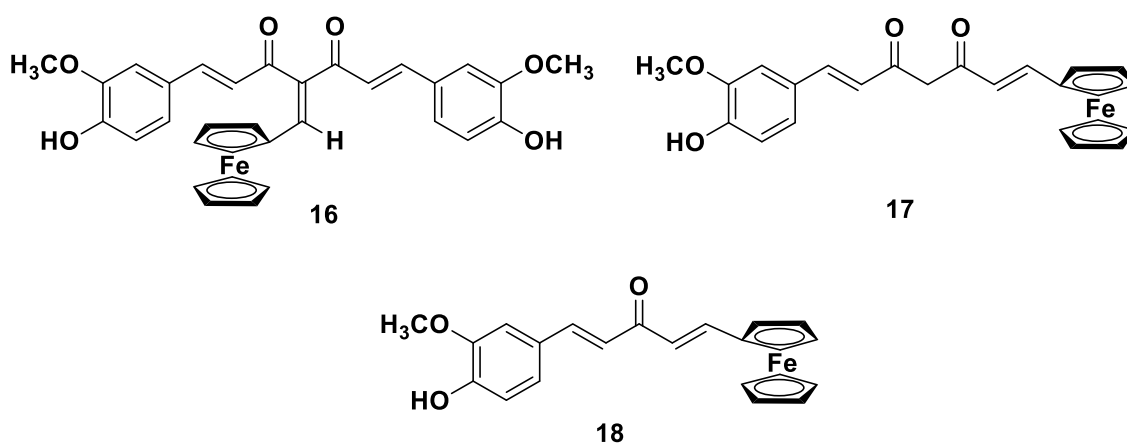
property, but the rapid kinetic parameters might be accountable for its antioxidant activity. In lack of any other substrate, the phenoxyl radicals might vanish by several mechanisms, for example, radical-radical reactions with alkoxy and peroxy radicals, thus averting the spread of the chain reaction of lipid peroxidation. These results put forward that DZG like many other phenolic antioxidants can counter both primary and secondary radicals.¹⁷

Yamagami *et al.*, have reported antioxidant activities against lipid peroxidation induced by *tert*-butylhydroperoxide or γ -irradiation for a series of hydroxybenzalacetones derivatives **6** and **7**. Authors have also reported relationship between the structure and activity by using free-energy related substituent parameters. Further in order to interpret the resultant correlations, authors have further measured DPPH (1,1-diphenyl-2-picrylhydrazil) free radical scavenging activities of synthesized compounds and later performed the QSAR analysis. In this study it was concluded that the inhibitory potencies were primarily due to the formation of phenoxy radicals as well as from the electron-donating substituents, which further contributed to ease phenoxy radical formations. Similarly, the ortho substituents were effective in stabilizing the generated phenoxy radicals. The results indicated a remarkable enhancement of activity for compounds **8**, **9**, and **10**.⁴⁰

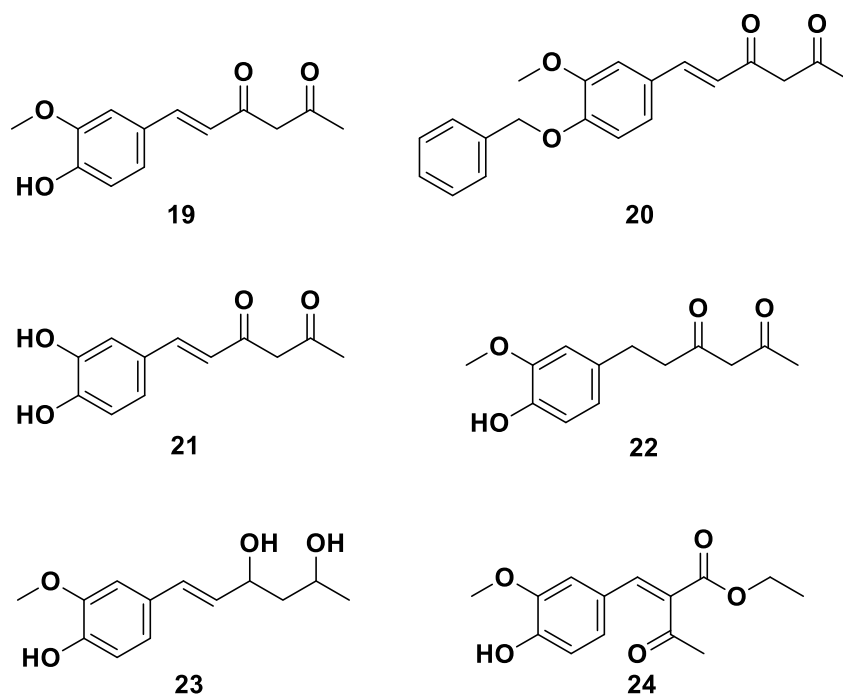


Kuo *et al.*, have synthesized a novel series of DZG derivatives and evaluated them as potential antioxidants. Amongst the series, compound **11** displayed significant inhibition of Fe²⁺-induced lipid peroxidation (to elucidate antioxidant activity) in rat brain homogenate with an IC₅₀ of 6.3 ± 0.4 μM as compared to the standard antioxidant, α -tocopherol (TOH) with IC₅₀ = 2.5 ± 0.1 μM. In addition, the tested compounds did not form complex with ferrous ion in the iron chelation study performed by authors as addition of ferrous ion did not source any spectral shift or absorbance variation. Thus the authors expected that the test compounds might have exerted their effects on lipid peroxidation primarily by scavenging free radicals rather than functioning as iron chelators. This belief was further supported by reassessing DPPH test that gave information about

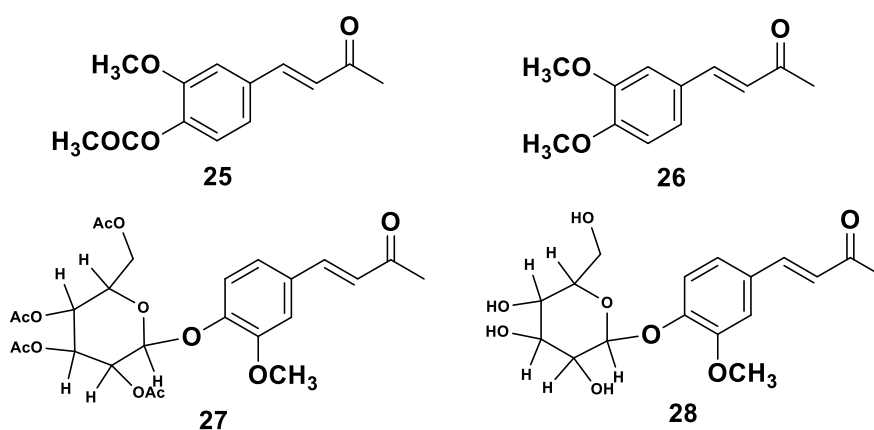
DPPH, ABTS⁺ and galvinoxyl radicals. Results revealed that all compounds protected DNA against Cu²⁺/GSH-induced oxidation, but promoted ·OH-induced oxidation of DNA. Compounds **16**, **17** and **18** scavenged the radicals with *n* values (*n* is a stoichiometric factor that implies the number of radicals trapped by one molecule of the antioxidant and can be used as a quantitative index to express the antioxidant capacity) 9.5, 5.7 and 4.7, respectively thus protecting DNA against AAPH-induced oxidation. Further compound **16** could trap more DPPH and ABTS⁺ than compounds **17** and **18**. All the compounds could not react with galvinoxyl radical. This study conclude that phenolic hydroxyl groups and iron atom in ferrocenylidene curcumin derivatives play an important role for antioxidant activity.⁴³



In order to clarify the contribution of phenolic and enolic hydroxyl group to the antioxidant capacity of feruloylacetone Feng *et al.*, have reported derivatives of DZG (**19-24**), which was taken as a model compound of half-curcumin. The synthesized compounds were evaluated for their antioxidant properties by trapping ABTS⁺, DPPH and galvinoxyl radicals. The reductive capacities were also screened by quenching singlet oxygen and by inhibiting the oxidation of linoleic acid. Oxidation of DNA mediated by hydroxyl radical and AAPH were also studied with the synthesized compounds. In addition, compounds were applied to protect erythrocytes against AAPH and hemin-induced hemolysis. The results suggest that the antioxidant capacity of half-curcumin was derived from the phenolic-OH and the conjugated linkage between phenolic and enolic-OH. The enolic-OH itself could not trap radicals.⁴⁴

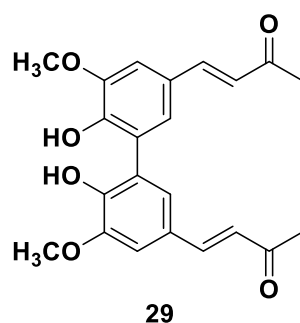


Kubra *et al.*, have reported synthesis and antioxidant properties of DZG derivatives by scavenging the stable DPPH radical. The reduction capability of the DPPH radical was established by its absorbance decrease at 517 nm, as induced by natural antioxidants. The IC_{50} value of DZG was found to be 0.3 mM comparable to Trolox (0.26 mM), whereas the IC_{50} value of **25**, **26**, **27** and **28** were found to be 40, 20, 10 and 7.5 mM respectively. Antioxidant activity assays of derivatives with varied substituents inferred that the existence of hydroxyl substituents on the phenyl nucleus enhanced activity, whereas substitutions like methoxyl and acetoxy groups reduced antioxidant activity remarkably. DZG, which hold an extended conjugated system was found to be active.⁴⁵



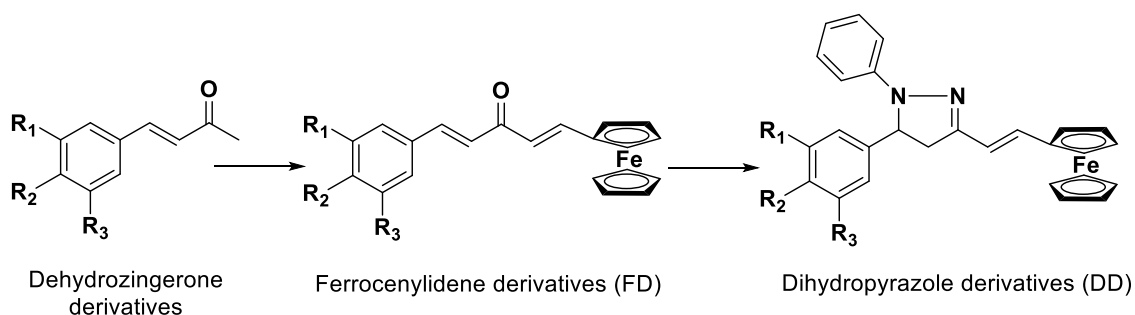
Kancheva *et al.*, synthesized DZG and dimer of DZG **29** and screened their antioxidant activity by bulk lipid autoxidation method, which involved DZG and compound **29** as individual compounds (1 mM), as equimolar binary (1:1) and ternary (1:1:1) mixtures with TOH and/or

ascorbyl palmitate (AscPH). The highest oxidation stability of lipid substrate in the presence of individual compounds was found for TOH, followed by **29** and DZG, which was established from the main kinetic parameters (antioxidant efficiency, reactivity and capacity). AscPH did not demonstrate any protective effect. Synergism was achieved for the binary mixtures of (TOH + AscPH) [42.4%], (DZG + TOH) [32.4%] and (DZG + AscPH) [35.6%] and for the ternary combination of (DZG + TOH + AscPH) [28.7%]. Unusual protective effects observed were explained on the basis (of results) of TOH regeneration and its content determined by HPLC.⁴⁶



Li *et al.*, have reported a new series of asymmetrical mono-carbonyl ferrocenylidene curcumin and their dihydropyrazole compounds from dehydrozingerone derivatives (**30-44**, Table 1) and investigated their antioxidant abilities in protecting DNA against AAPH induced oxidation and scavenging ABTS cationic radical. Compound **40** possessed the highest scavenging of ABTS⁺, whereas compound **33** had higher protecting property of DNA against AAPH induced oxidation. These results suggest that the antioxidant abilities of compounds would increase when the ferrocenyl group was introduced along with other substituent groups in the molecule.⁴⁷

Table 1: Structures of asymmetrical mono-carbonyl ferrocenylidene curcumin and their dihydropyrazole compounds from dehydrozingerone derivatives.



Ferrocenylidene derivatives				Dihydropyrazole derivatives			
	R ₁	R ₂	R ₃		R ₁	R ₂	R ₃
30	H	H	H	38	H	H	H
31	H	OH	H	39	H	H	H
32	H	H	H	40	H	N(CH ₃) ₂	H
33	H	N(CH ₃) ₂	H	41	H	OH	H
34	H	OH	H	42	H	H	OH
35	H	H	OH	43	H	OH	OCH ₃
36	H	OH	OC ₂ H ₅	44	H	OH	OC ₂ H ₅
37	NO ₂	OH	OCH ₃				

(Note: It is phenyl instead of ferrocenyl for structures **30**, **31** and **38** only)

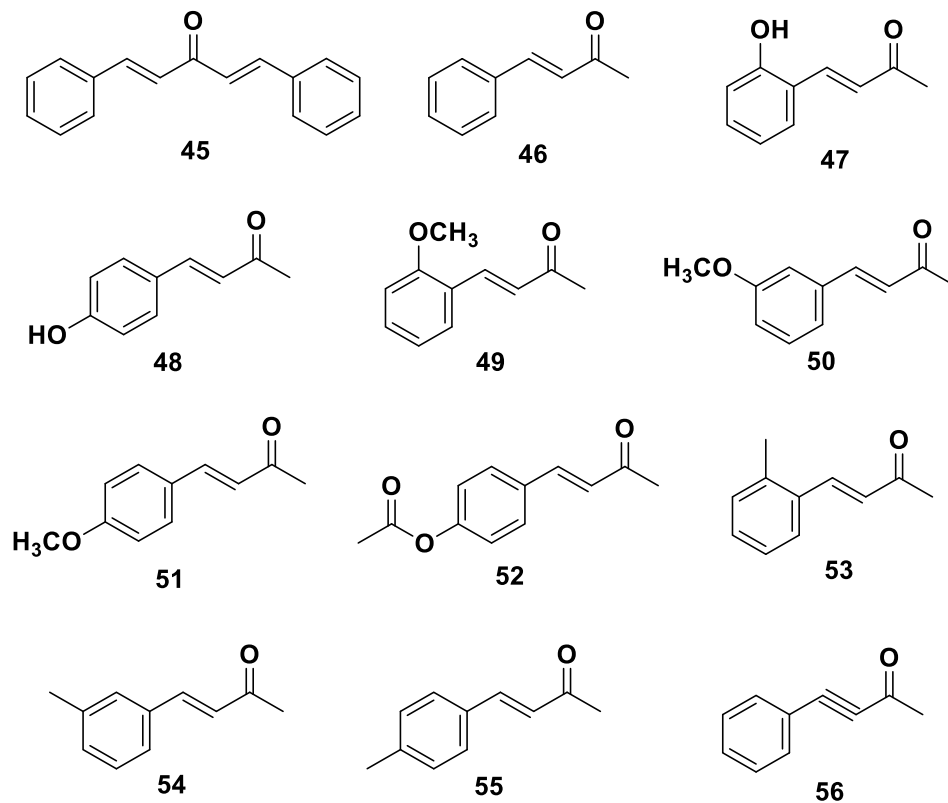
2.2 Dehydrozingerone as antimutagen

The phyto-constituents are vital and important part of our routine diet providing protective effects from mutagens. Numerous phyto-constituents namely coumarin, xanthenes, terpenoid, pigments, anthraquinone, tannin, phenolic, cymopol, halogenated flavonoids, dibenzoate diterpenes, organosulfur, nitrogenous compounds and curcuminoids from various plant species have been reported to have antimutagenic properties.⁴⁸

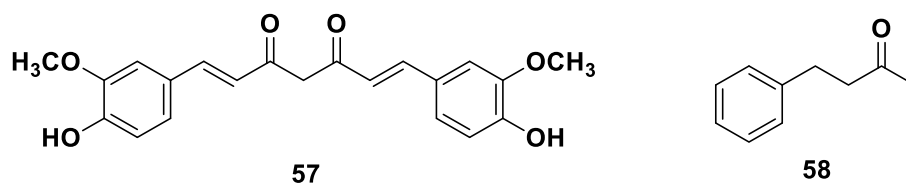
Synthetic curcuminoid derivatives have been reported to have antimutagenic properties.⁴⁹⁻⁵² Monocarbonyl analogs of curcumin are widely explored as they have better pharmacokinetic and pharmacodynamic properties than curcumin and are emerging as a new class of anticancer agents.^{53,54} Dehydrozingerone, isolated from ginger (*Zingiber officinale*) has the structure corresponding to half analog of curcumin and also monocarbonyl analog of curcumin have been reported to have antimutagenic properties. Following discussion reviews about DZG as an antimutagen.

Motohashi *et al.*, have investigated antimutagenic activities of DZG and their synthetic analogs (**45-56**) against UV-induced mutagenesis in *Escherichia coli*. Studies suggest that the effect of DZG against the UV-induced mutagenesis was poor, but benzalacetone (**46**), a dehydroxy-demethoxy product of DZG revealed the strongest antimutagenic activity among the ring-substituted analogs except for 2-hydroxybenzalacetone (**47**). Results also disclosed that the ring-substitution with a group such as 4-hydroxyl, methoxyl or methyl reduced the antimutagenic activity, while α,β -unsaturated (double bond) carbonyl functionality was essential for the

antimutagenicity. Compounds **46**, **47** and **56** decreased both the UV- and γ -induced mutagenesis. This clearly suggests that ring-substitution was not effective and a double- or triple-bonded carbonyl system was required for the antimutagenic activity.⁷



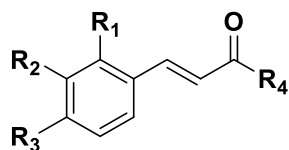
Motohashi *et al.*, have evaluated anti-tumor activity of DZG and its related compounds (**57**, **26**, **8**, **47**, **48**, **50**, **51**, **2**, **56**, **46** and **58**) by determining the inhibitory effect on Epstein-Barr virus early antigen (EBV-EA) activation induced by 12-*O*-tetradecanoylphorbol-13-acetate (TPA). The IC_{50} of DZG was found to be 95 mol ratio/TPA, which was almost similar to curcumin (**57**) 97 mol ratio/TPA. Isoeugenol (**2**) that lacks carbonyl group in the side chain, exhibited 50% inhibition with 38 mol ratio/TPA, thus accounting for one-third antioxidant activity of DZG. Compounds **26**, **8** and monosubstituted compounds were also tested for the EBV-EA activation. Compound **26**, IC_{50} = 107 mol ratio/TPA was less effective than DZG while compound **8** (IC_{50} = 50) exhibited more potent activity than DZG. Compounds **47**, **48** and **51** were found to be more active whereas compound **50** was less active as compared to DZG. The influence of the carbon-carbon bond attached to the benzene ring was also assessed with compound **56** having a triple bond, **46** with a double bond and **58** with a single bond. The inhibitory effect was significant and highest in **56** (IC_{50} = 48 mol ratio/TPA) followed by **46** (IC_{50} = 129 mol ratio/TPA) and then **58** (IC_{50} = 222 mol ratio/TPA).⁵⁵



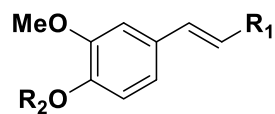
Rao *et al.*, have reported the cyto-protective effects of DZG and two other structurally related phenolic compounds Eugenol (**1**) and Isoeugenol (**2**) against cisplatin-induced toxicity in *vero* (African Green Monkey Kidney) cells by observing variation in percentage trypan blue exclusion (TBE), percentage release of lactate dehydrogenase (LDH), and glutathione (GSH) content. Cisplatin is known to cause cytotoxicity in kidney cells due to oxidative injury, involvement of hydrogen peroxide in outer medullary cortical tubule cells and peroxidation of cell membranes. Several literature reports reveal that various antioxidants are known to prevent cisplatin induced cytotoxicity. Among the tested series, compound **2** was the most active followed by **1** and then DZG in preventing cell death induced by cisplatin, while none of the compounds were able to prevent the reduction of the GSH content.⁵⁶

Motohashi *et al.*, in conjunction with previous studies, have further reported the structure activity relationship of benzalacetone derivatives as potential anti-tumor agents by assaying in EBV-EA activation model. The results of benzalacetone derivatives were in agreement with the previous findings.⁵⁷

Tatsuzaki *et al.*, have synthesized twenty-eight new compounds (summarized in Table 2 and Table 3) related to DZG, isoeugenol and 2-hydroxychalcone, which were evaluated for their *in vitro* activity against a panel of human tumor cells viz. Human epidermoid carcinoma of the nasopharynx (KB), multidrug-resistant expression P-glycoprotein (KB-VCR) and human lung carcinoma (A549). From results it was clear that other than isoeugenol analogs **76-84**, most compounds exhibited moderate to strong cytotoxic activity against the cell lines tested. Particularly, compound **65** displayed significant cytotoxic activity against the A549 ($IC_{50} = 0.6 \mu\text{g/mL}$), while compounds **9**, **66** and **67** showed comparable cytotoxic activity against both KB ($IC_{50} = 2.0, 1.0, \text{ and } 2.0 \mu\text{g/mL}$) and KB-VCR ($IC_{50} = 1.9, 1.0, \text{ and } 2.0 \mu\text{g/mL}$) respectively, suggesting that they are not substrates for the P-glycoprotein drug efflux pump.⁵⁸

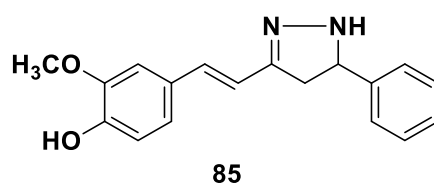
Table 2: Structures of DZG and chalcone analogs (**8**, **59**, **60**, **46**, **61**, **9**, **62**, **63**, **64**, **65**, **66** and **67**)

	R ₁	R ₂	R ₃	R ₄
DZG	H	OMe	OH	Me
8	OH	OMe	H	Me
59	H	OH	OMe	Me
60	OH	H	OMe	Me
46	H	H	H	Me
61	H	OEt	OH	Me
9	OH	OEt	H	Me
62	OH	F	H	Me
63	H	F	OMe	Me
64	H	OMe	OH	Ph
65	OH	OMe	H	Ph
66	H	OH	OMe	Ph
67	OH	H	OMe	Ph

Table 3: Structures of C-4¹-alkylated DZG (**26, 68-75**) and Isoeugenol (**76-84**) analogs

DZG R ₁ = COMe	Isoeugenol R ₁ = Me	R ₂
68	76	
69	77	
70	78	
71	79	
72	80	
26	81	Me
73	82	
74	83	
75	84	

In 2006, Ex-Elixis INC reported pyrazole derivatives as tyrosine kinase modulators in treatment of cancer. This study reports anticancer potential of compound **85**, which is analogous to DGZ derivative.⁵⁹



Conjugation of two bioactive compounds/scaffolds has been effective strategy in designing pharmacophores as ligands, inhibitors and other class of drugs. Tatsuzaki *et al.*, have synthesized some novel conjugates of DZG with triterpenoids as promising cytotoxic agents. In this work, triterpenoids namely glycyrrhetic acid (GA, **86**), oleanolic acid (OA, **87**) and ursolic acid (UA, **88**) were esterified with DGZ (**89-91**) to yield eleven different novel DZG analogs **92-102**. These synthesized compounds were screened for their *in vitro* anti-cancer activity against nine different human cancer cell lines as depicted in Table 4.

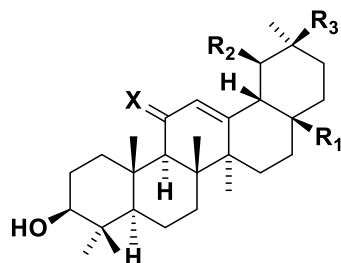
Table 4: Data for GA-DZG conjugates against human tumor cell replication.

Compound	ED ₅₀ (μM)/cell line ^a								
	KB	KB-VIN	A549	1A9	HCT-8	ZR-751	PC-3	DU-145	LN-Cap
92	1.6	2.5	2.0	0.9	1.7	2.8	1.4	3.1	0.6
93	0.8	2.8	2.2	0.8	1.9	3.0	1.1	3.6	2.8
94	0.9	1.9	2.8	1.6	2.0	1.9	2.8	9.9	6.5
95	6.2	>15	15.5	5.9	2.6	>15	7.4	>15	1.9
96	1.8	1.7	1.7	1.1	2.7	5.2	3.3	5.8	1.1
97	2.9	13.2	3.0	1.8	4.9	8.8	3.5	>15	6.8
98	3.0	8.7	3.2	1.3	2.2	2.7	1.6	2.7	4.4
99	NA ^b	NA	>14	>14	>14	NA	>14	>14	>14
100	9.9	NA	>14	13.3	>14	>14	14.1	>14	14.1
101	NA	NA	NA	>14	>14	NA	14.1	>14	14.1
102	>14	>14	NA	NA	>14	NA	>14	13.0	>14
GA, 86	>21	>21	NA	>21	19.5	NA	>21	>21	>21
DZG	NA	NA	>52	33.9	>52	>52	>52	>52	51.0
DOX^c	0.1	4.97	0.18	0.02	1.20	0.04	0.26	0.15	0.04

^aHuman epidermoid carcinoma of the lung (A549), ovarian (1A9), colon (HCT-8), breast (ZR-751), prostate (PC-3, DU-145, LN-Cap); ^bNot active; ^cDoxorubicin

Compounds **92**, **93** and **94** exhibited significant cytotoxic activity against LN-Cap, 1A9, and KB cells lines with ED₅₀ values of 0.6, 0.8 and 0.9 μM respectively. Conjugates of DZG and OA or UA were inactive, suggesting that the GA component was critical for activity. In general, this

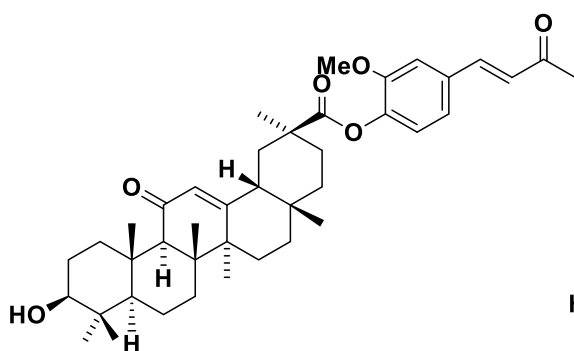
study unearths that GA and DZG as individual components were inactive whereas their conjugates GA-DZG displayed potent cytotoxic activity. Thus GA-DZG conjugates were established as new chemical entities in anti-cancer drug discovery and development.⁶⁰



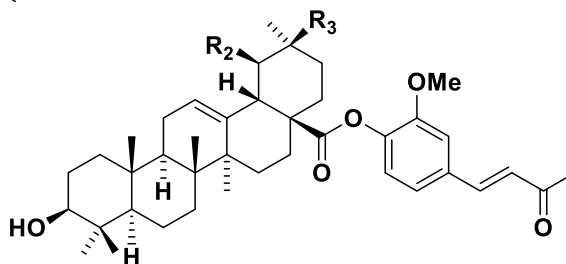
86: GA, X=O, R₁=Me, R₂=H, R₃=COOH

87: OA, X=H, R₁=COOH, R₂=H, R₃=Me

88: UA, X=H, R₁=COOH, R₂=Me, R₃=H

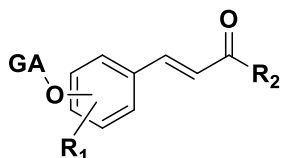


89: GA-DZG



90: OA-DZG, R₂=H, R₃=Me

91: UA-DZG, R₂=Me, R₃=H



92: 4-OGA, R₁=3-OMe, R₂=Me

93: 2-OGA, R₁=3-OMe, R₂=Me

94: 3-OGA, R₁=4-OMe, R₂=Me

95: 2-OGA, R₁=4-OMe, R₂=Me

96: 4-OGA, R₁=3-OEt, R₂=Me

97: 2-OGA, R₁=3-OEt, R₂=Me

98: 2-OGA, R₁=3-F, R₂=Me

99: 4-OGA, R₁=3-OMe, R₂=Ph

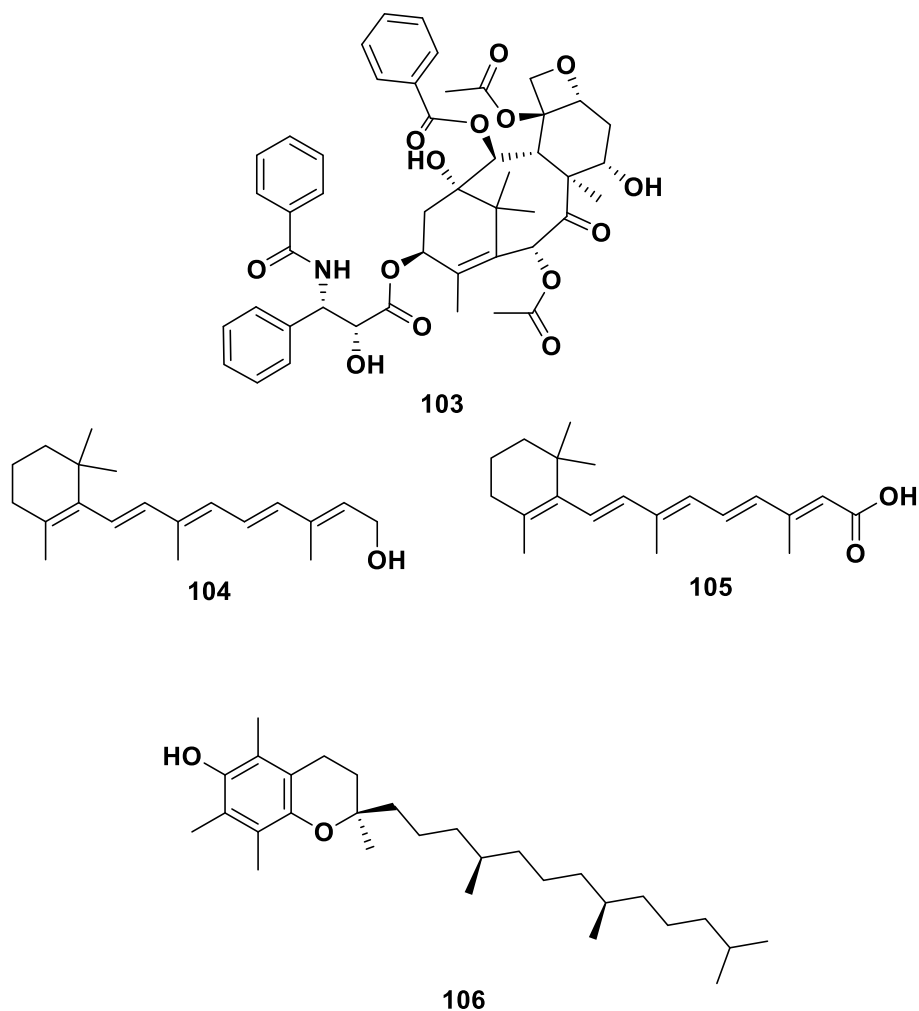
100: 2-OGA, R₁=3-OMe, R₂=Ph

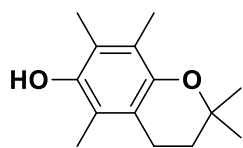
101: 3-OGA, R₁=4-OMe, R₂=Ph

102: 2-OGA, R₁=4-OMe, R₂=Ph

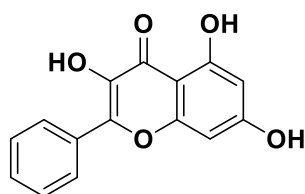
Nakagawa-Goto and co-others have reported newer conjugates of cytotoxic drug, paclitaxel (**103**) and various dietary antioxidants as new class of antitumor drugs. Dietary antioxidants namely retinol (**104**, Vitamin A), retinoic acid (**105**, Vitamin A acid), α -tocopherol (**106**, Vitamin E),

2,2,5,7,8-pentamethyl-6-chromanol (**107**, Vitamin E analog), curcumin (**57**), DZG and its analog (**8**). In addition, certain antioxidant flavonoids such as galangin (**108**) and coumarins, chrysin (**109**) and 4-methylumbelliferone (**110**) were also conjugated with paclitaxel through an ester linkage. All these novel conjugates were tested against various multi-drug resistant human cancer cell lines. These tested conjugates showed selective inhibition towards ovarian carcinoma (1A9) and nasopharynx carcinoma (KB) cells. However, little or no activity was observed against other tested cell lines. Paclitaxel conjugates with DZG (**111**) and 4-methylumbelliferone (**112**) were found to be highly active against 1A9 ($ED_{50} = 0.005 \mu\text{g/mL}$) and KB ($ED_{50} = 0.005$ and $0.14 \mu\text{g/mL}$) cells respectively. The glycinate ester salt of vitamin E **113**, conjugated with **103** showed strong inhibitory activity against human pancreatic cancer cell (Panc-1) with less effect on the normal ovarian epithelial cell line (E6E7) and emerged as a promising lead candidate in anticancer drug discovery.⁶¹

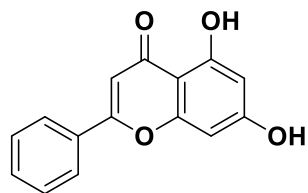




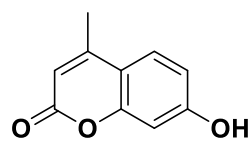
107



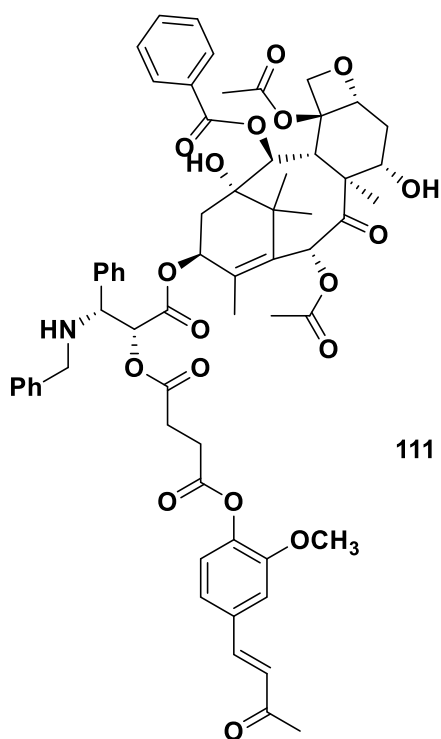
108



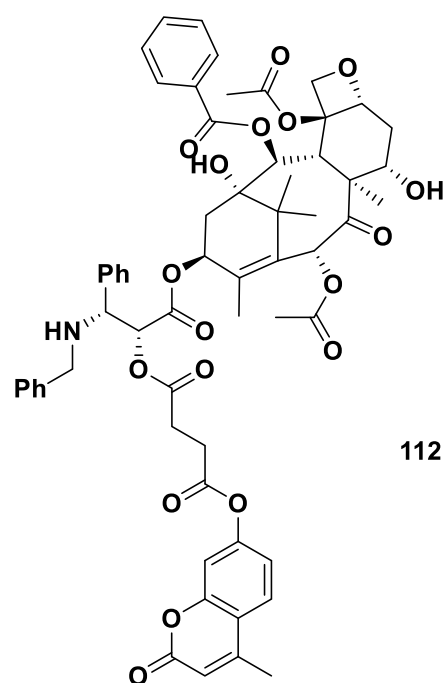
109



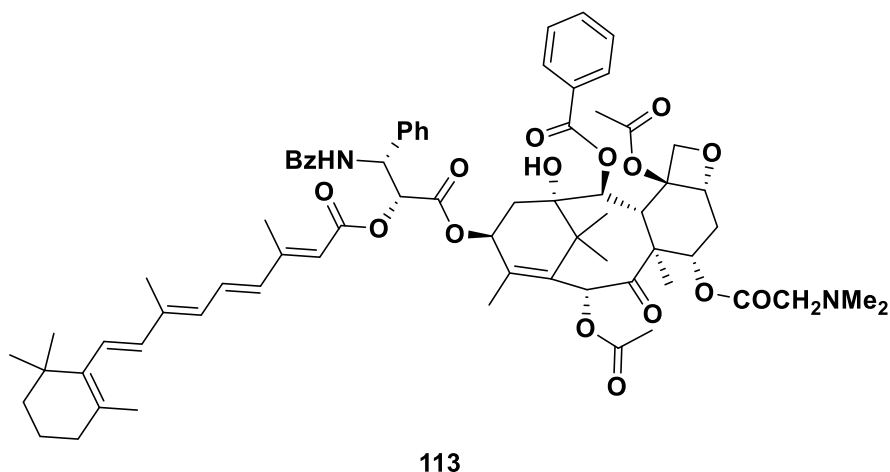
110



111

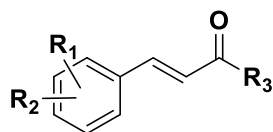


112

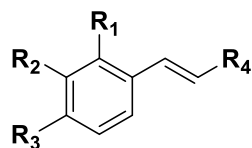


Tatsuzaki *et al.*, have synthesized a series of forty new DZG analogs (Table 5 and 6) and *in vitro* anticancer activity was evaluated against TPA-induced EBV-EA activation assay. Among the synthesized compounds, the prenylated analogs **114** and **123–125** exhibited the most significant and promising activity (100% inhibition of activation at 1×10^3 mol ratio/TPA and 82–80%, 37–35% and 13–11% inhibition at 5×10^2 , 1×10^2 and 1×10 mol ratio/TPA, respectively).⁶²

Table 5: Structures of DZG analogs (**8**, **9**, **46**, **59-67**).



	R ₁	R ₂	R ₃
DGZ	3-OMe	4-OH	Me
8	2-OH	3-OMe	Me
9	2-OH	3-OEt	Me
46	H	H	Me
59	3-OH	4-OMe	Me
60	2-OH	4-OMe	Me
61	3-OEt	4-OH	Me
62	2-OH	3-F	Me
63	3-F	4-OMe	Me
64	3-OMe	4-OH	Ph
65	2-OH	3-OMe	Ph
66	3-OH	4-OMe	Ph
67	2-OH	4-OMe	Ph

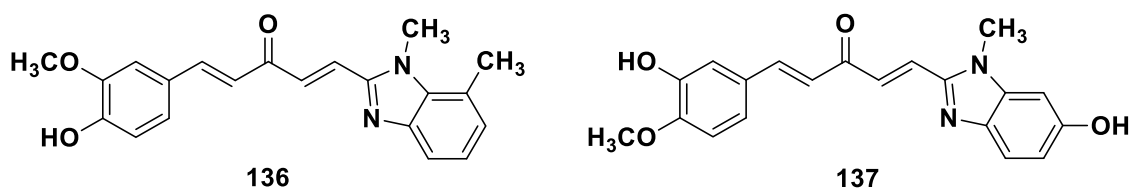
Table 6: Structures of DZG (114-126) and isoeugenol (127-135) analogs.

DZG R ₄ = COM e	R ₁	R ₂	R ₃	Isoeugenol R ₄ = Me
114	H	OMe		127
115	H	OMe		128
116	H	OMe		129
117	H	OMe		130
118	H	OMe		131
119	H	OMe		132
120	H	OMe		133
121	H	OMe		134
122	H	OMe		135
123		OMe	H	-
124	H			-
125		H		-
126		F	H	-

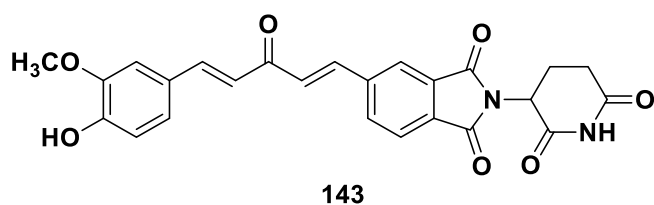
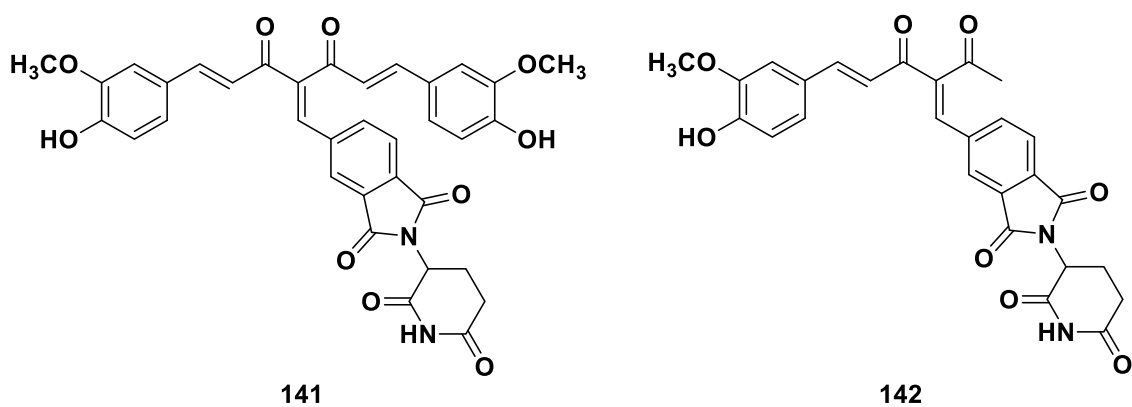
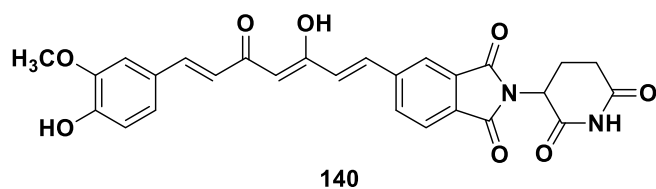
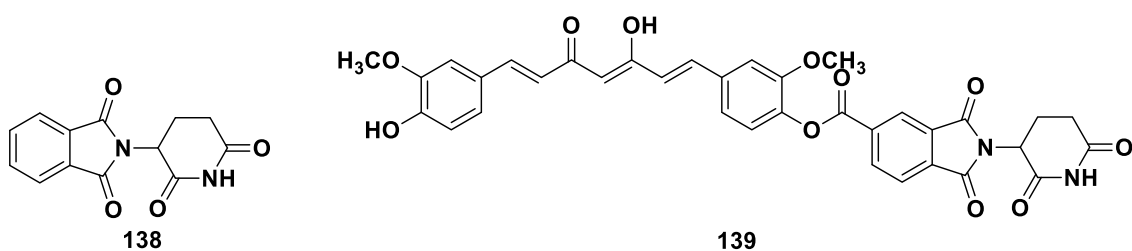
Yogosawa *et al.*, were the first to elucidate the growth-inhibitory mechanisms of DZG and its structural isomers (**8** and **59**) in human colon cancer cells (HT-29), thus providing some insights into the molecular mechanism of action of DZG. This study suggested that DZG inhibits the cell growth by inducing cell-cycle arrest at the G₂/M phase by up-regulation of p21 in a dose dependent manner. It is quite evident from this study that accumulation of ROS was interrelated

with growth-inhibitory effects, thus suggesting DZG analogs as potential chemotherapeutic agents for colon cancer.⁶³

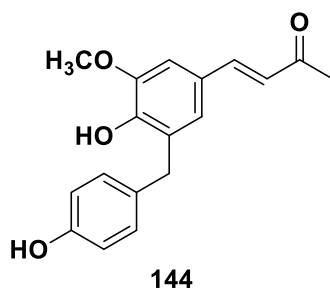
Woo *et al.*, have reported the synthesis of a new library of some benzimidazolyl curcumin mimics by aldol condensation of DZG and DZG analogs with substituted benzimidazolyl-2-carbaldehyde. The *in vitro* anticancer activity was performed by colorimetrically using MTT (3-[4,5-dimethylthiazol-2-yl]-2,5-diphenyltetrazolium bromide) assay model against various human cancer cells viz. breast adenocarcinoma (MCF-7), neuroblastoma (SH-SY5Y), hepatocellular carcinoma (HEPG2) and Lung carcinoma (H460). Among the tested series, compound **136** ($IC_{50} = 1.0$ and $1.9 \mu M$) displayed most promising cytotoxicity against SH-SY5Y and Hep-G2 cells respectively, while compound **137** ($IC_{50} = 1.9 \mu M$) presented significant activity against MCF-7 cancer cells.⁶⁴



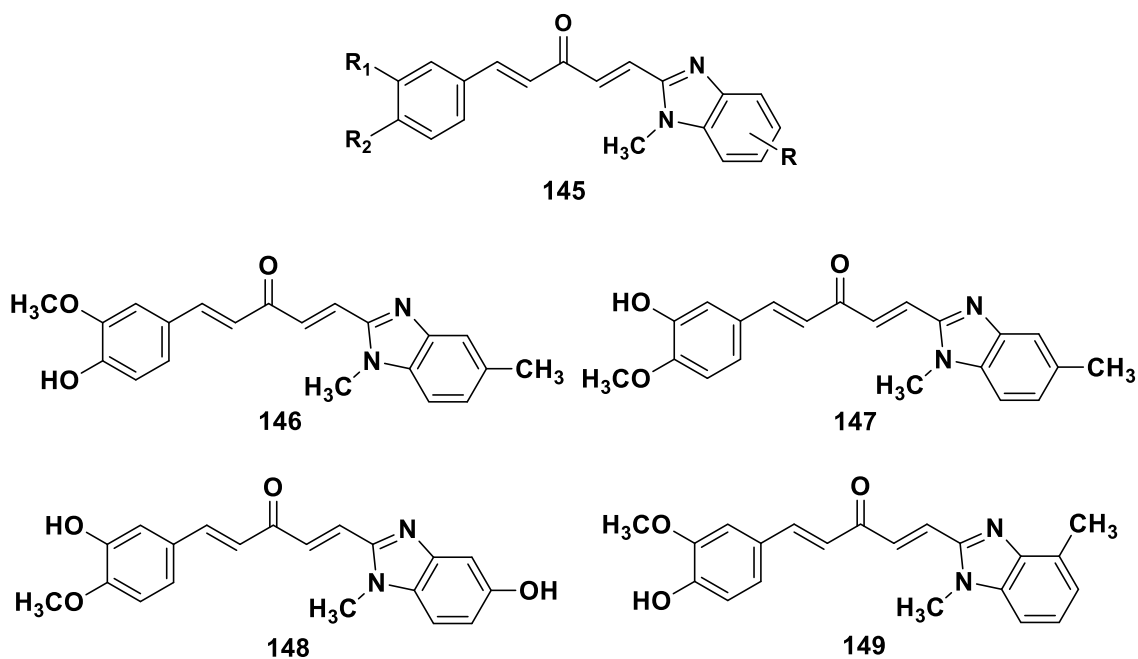
Liu *et al.*, in an effort to develop agents for treating human multiple myeloma (MM), have reported the synthesis of a series of novel hybrid molecules of thalidomide (**138**) and curcumin (**139-142**) along with DZG (**143**). The anticancer activity of these synthesized hybrids was evaluated against various human multiple myeloma cells (MM1S, RPMI8226, U266) and human lung carcinoma cells (A549). Perusal of results, it was found that compound **141** (di-ketone) and **143** (mono-ketone) significantly inhibited the cell growth of all three cell lines by $\geq 90\%$ at $10 \mu M$, while compound **142** was inactive, thus suggesting that the 4-hydroxy-3-methoxy benzylidene moiety may be an essential scaffold for antiproliferative activity. Further, there was an attempt to study whether these active compounds produce cytotoxic effects through the modulation of ROS. Interestingly, compounds **141** and **143** increased the production of ROS in U266 cells at both 3 and $10 \mu M$ concentrations, leading to G1/S arrest, apoptosis and cell death. These findings suggest that the hybrid compounds could be a new leads against human multiple myeloma.⁶⁵



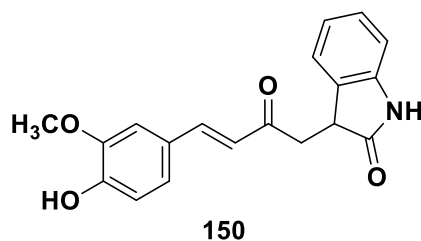
In 2013, Uha Mikakuto Co. Ltd., reported the synthesis of novel DZG derivative (**144**) having potent anticancer activity, particularly against oral cavity cancer than DZG.⁶⁶



Eom *et al.*, have synthesized a library of curcumin derivatives mainly DZG mimics (**145**) having benzimidazole functionalities and evaluated them against multidrug resistant (MDR) ovarian cancer cell lines (NCI/ADR-RES). The cytotoxicity assay was carried out by MTT assay against both MDR strains with over-expressed P-glycoprotein (P-gp) and non-MDR strains (OVCAR-8) without P-gp. The cytotoxicity results against non-MDR cancer cells demonstrated reasonably strong to moderate potency suggesting comprehensive increase in activity after addition of the benzimidazole group to feruloyl structure. The inhibitory effect on MDR was found to be weaker in contrast to non-MDR cancer cells. However, after taking into consideration the resistance factor (RF), that is, the ratio of the IC₅₀ values of MDR cells to that of non-MDR, the library illustrated a small RF values, which explains that the divergence of the inhibitory potency between MDR ovarian cancer cell (NCI/ADR-RES) and non-MDR ovarian cancer cell (OVCAR-8). Compounds **146**, **147** and **148** displayed strong cytotoxic effect on both type of cancer cells with the RF values 1.7, 1.7 and 1.4, respectively. Compound **149** showed inhibition with IC₅₀ value of 23.2 μM on MDR and 0.7 μM on non-MDR with high RF value of 33.1. This suggests the incapability of compound **149** to differentiate MDR cancer cells from non-MDR cells⁶⁷.



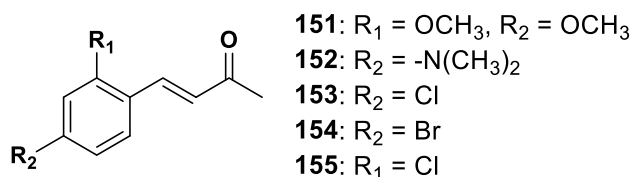
Bode *et al.*, have disclosed the synthesis of novel DZG analog (**150**) and reported them for Aurora B kinase inhibition activity in cancer therapy⁶⁸.



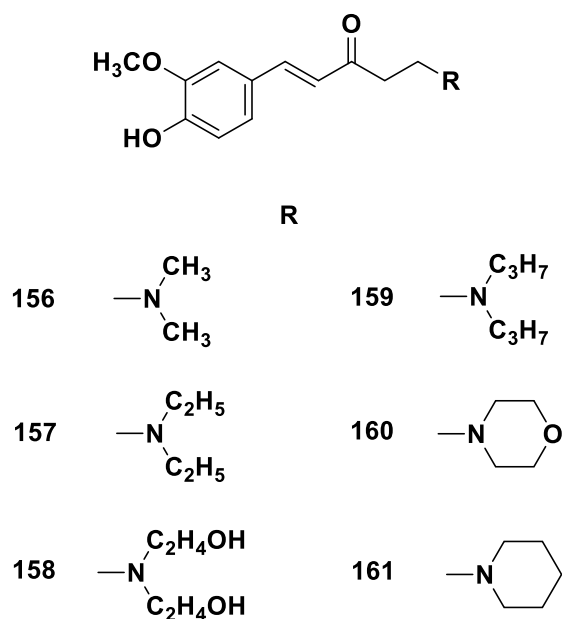
2.3 Dehydrozingerone as anti-inflammatory

Curcuminoids have been reported as anti-inflammatory agents⁶⁹. Many of the curcuminoids are synthetically tailored and studied for anti-inflammatory properties⁷⁰⁻⁷². Following discussion elaborates research employing DZG as anti-inflammatory agents.

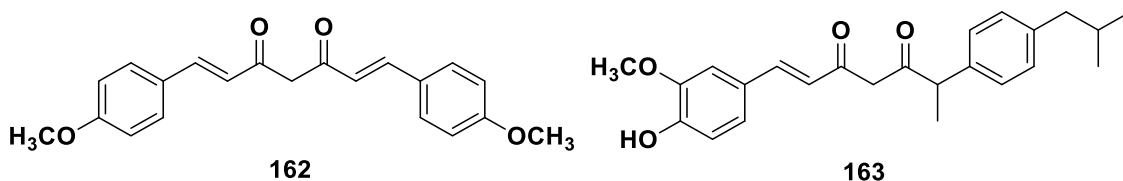
Elias *et al.*, have reported the synthesis of a novel series of substituted 4-phenyl-3-buten-2-ones (**151-155**) and screened them for *in vivo* anti-inflammatory activity by carrageenan-induced paw edema in rats. Among the tested series, most of the compounds exhibited a comparable activity with DZG. In particular, compounds **25** and **152** displayed significant anti-inflammatory activity, while compounds **151** and **51** revealed little or no activity.⁹



Jayasekhar *et al.*, have reported the synthesis of DZG Mannich bases by two methods. The first method involved the treatment of DZG with secondary alkyl amine hydrochlorides and paraformaldehydes, whereas the second method was direct aldol condensation of vanillin with 4-alkylaminobutan-2-one. All the synthesized compounds were evaluated for anti-inflammatory, analgesic and antipyretic activities. Perusal of results it was found that most of the compounds showed superior anti-inflammatory activity compared to DZG. In particular, compounds **156**, **157** and **160** exhibited significant anti-inflammatory activity. Compounds **158** and **160** displayed the most promising analgesic activity whereas **156** and **158** presented excellent antipyretic activity.⁷³



Santhakumari *et al.*, have reported novel method for synthesis of newer curcuminoids (**3**, **162** and **163**) by Claisen-Dieckmann condensation of α,β -unsaturated ketones (both DZG and 4-(4-methoxyphenyl)but-3-en-2-one) along with various esters in presence of sodium ethoxide and dimethyl sulphoxide. Further employing the same reaction procedure, authors have reported DGZ-Ibuprofen derivative (**163**) where the α,β -unsaturated moiety of DZG and the ester group of ibuprofen was condensed. The synthesized compound **163** was screened for analgesic activity by acetic acid-induced writhing in albino mice. Although compound **163** demonstrated analgesic activity (59% at 1.0 mmol/kg), it was less compared to Ibuprofen (69% at 1.0 mmol/kg). Compound **163** was also screened for anti-inflammatory activity for acute, sub-acute and chronic models using reported methods. Results of this study suggested that **163** displayed significant activity (76%) compared to ibuprofen (73%) in equimole dose. Compound **163**, also showed predominant activity against formaldehyde induced arthritis at 0.5 mmol/kg dose level. However even the compound **163** did not induce gastrointestinal ulceration at dose level of 1 mmol/kg suggesting it to be a potent anti-inflammatory compound without any ulcerogenic side effects. These overall findings suggest that compound **163** emerged as the most promising anti-inflammatory agent with less gastrointestinal side effects.⁷⁴



2.4 Dehydrozingerone as anti-depressant

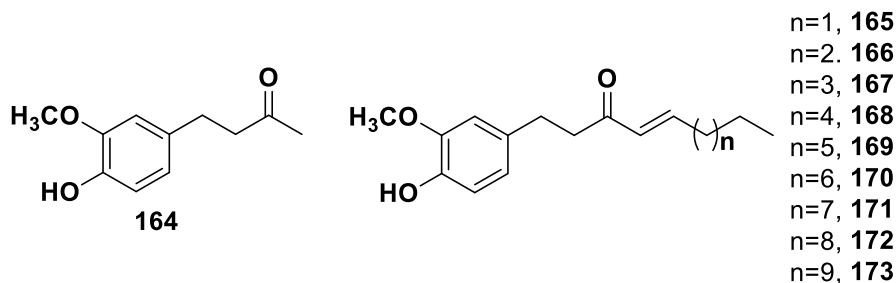
Various natural products have been explored as herbal medicines for treating depression.⁷⁵⁻⁷⁷ Numerous classes of phytoconstituents especially curcuminoids, flavonoids and poly phenols have been reported to possess antidepressant properties.⁷⁸ A brief account from literature explains the use of DZG as antidepressant.

Martinez *et al.*, have assessed the antidepressant property of DZG and the involvement of serotonergic and noradrenergic systems. Authors have also established the *in vitro* antioxidant activity of DZG by evaluating peroxidation in the hippocampus, cortex and cerebellum of mice. The participation of serotonergic and noradrenergic systems was verified by the tail suspension test (TST), forced swim test (FST) and yohimbine lethality test in mice models. DZG significantly reduced the period of immobility in the TST and FST, suggesting an antidepressant-like profile. Thus signifying that DZG could be a natural stand-in for development of antidepressants having little or no adverse effects.⁷⁹

2.5 Dehydrozingerone against Alzheimer's disease

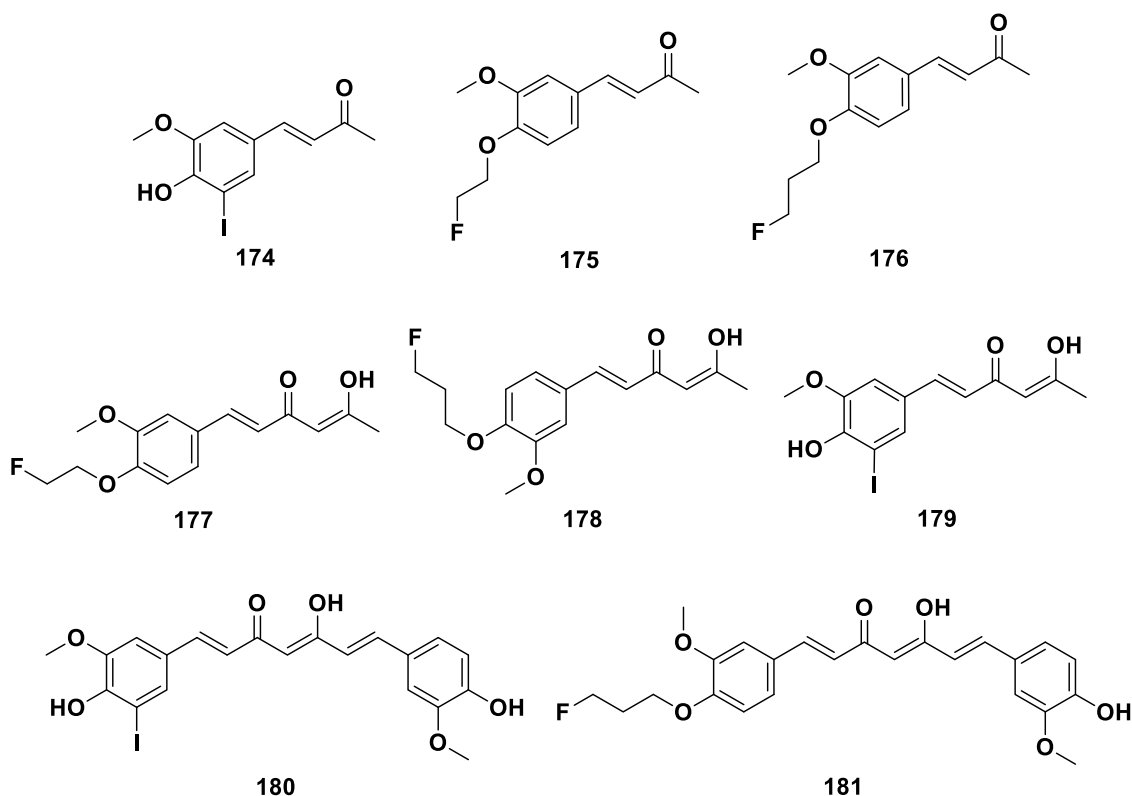
Alzheimer's disease (AD) is a neurodegenerative disorder and pathologically illustrated by gradual loss of memory, way of thinking and other cognitive functions along with dementia.

Kim *et al.*, reported the synthesis of novel shogaols derivatives (**164-173**) prepared by the reduction of DZG. In this work authors evaluated the significance of the side-chain length connected to DZG in defending cells from β A insult using PC12 rat pheochromocytoma and IMR-32 human neuroblastoma cells. The cytoprotective property of synthesized compounds against β A insult was established using MTT assay. Results suggested that the efficacy of cell protection from β A insult increased with the increase in side chain. From this series compound (**173**) exhibited the best results.⁸⁰



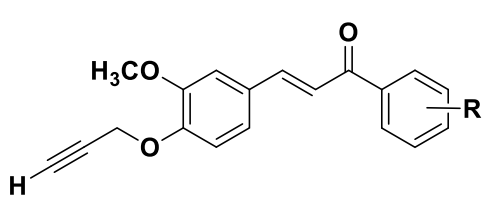
AD is characterized by the buildup of amyloid plaques and neurofibrillary tangles in the brain and thus the *in vivo* imaging of plaques and tangles would be of great assistance for the early finding of AD. Ryu *et al.*, reported the synthesis of a series of newer DZG (**174-179**) and curcumin (**180-**

181) derivatives and evaluated them for *in vitro* and *in vivo* as β -amyloid (β A) plaque imaging probes by positron emission tomography (PET) or single photon emission computed tomography (SPECT). The curcumin analogs exhibited superior binding affinities for β A aggregates than DZG derivatives. In particular, compound **181** was found to be most potent ligand having suitable lipophilicity, realistic initial brain uptake and metabolic firmness in the normal mouse brain. These outcomes suggest that compound **181** emerged as a potential candidate for β A plaque imaging.⁸¹

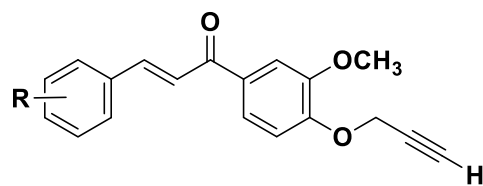


2.6 Dehydrozingerone as anti-malarial

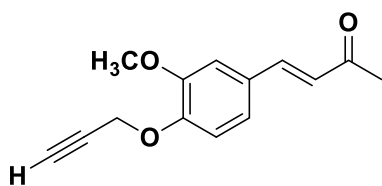
Molecular hybridization-based drug design approach⁸² has been exploited by many researchers in order to develop new hybrid chemical entities (NHCEs) as promising drug candidates. It is well known that more efficacious drug candidates with synergistic activity can be designed by joining two or more biologically active pharmacophores or heterocyclic systems in a single molecular framework. Recently Guantai *et al.*, have reported the synthesis of some series of novel DZG derived chalcones and dienone hybrid derivatives containing aminoquinoline and other nucleoside templates as potential antimalarial agents (**182-229**). Amongst all, compound **202** exhibited most promising antimalarial activity against three strains of *Plasmodium falciparum*.⁸³



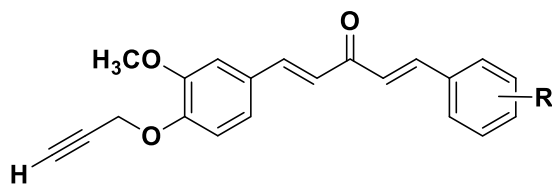
- 182: R= 4-OCH₃
 183: R= 2,4-OCH₃
 184: R=2,3,4-OCH₃



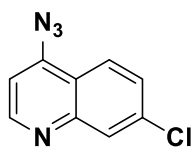
- 185: R=2,4-OCH₃
 186: R=2,3,4-OCH₃
 187: R=2,4-Cl
 188: R=4-F
 189: R=2,4-F



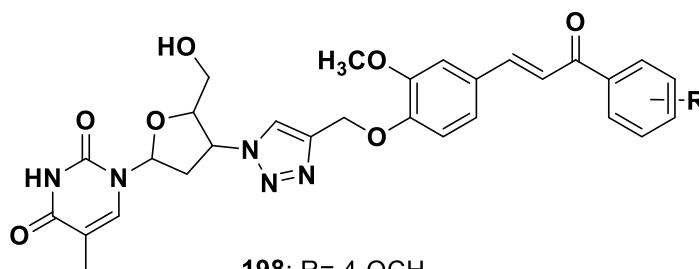
190



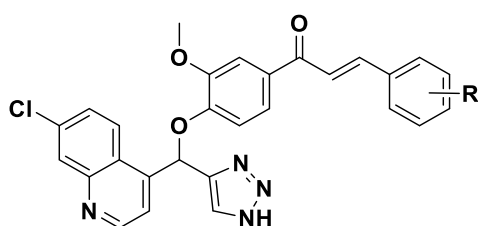
- 191: R= 4-OCH₃
 192: R= 2,4-OCH₃
 193: R=2,3,4-OCH₃
 194: R=2,4-Cl
 195: R=4-F
 196: R=2,4-F



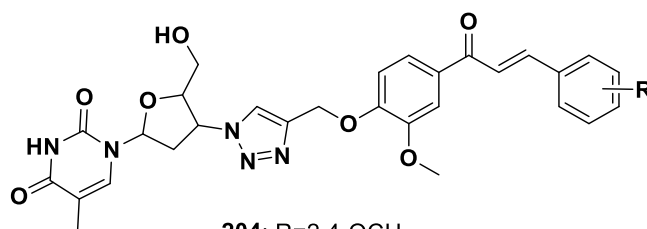
197



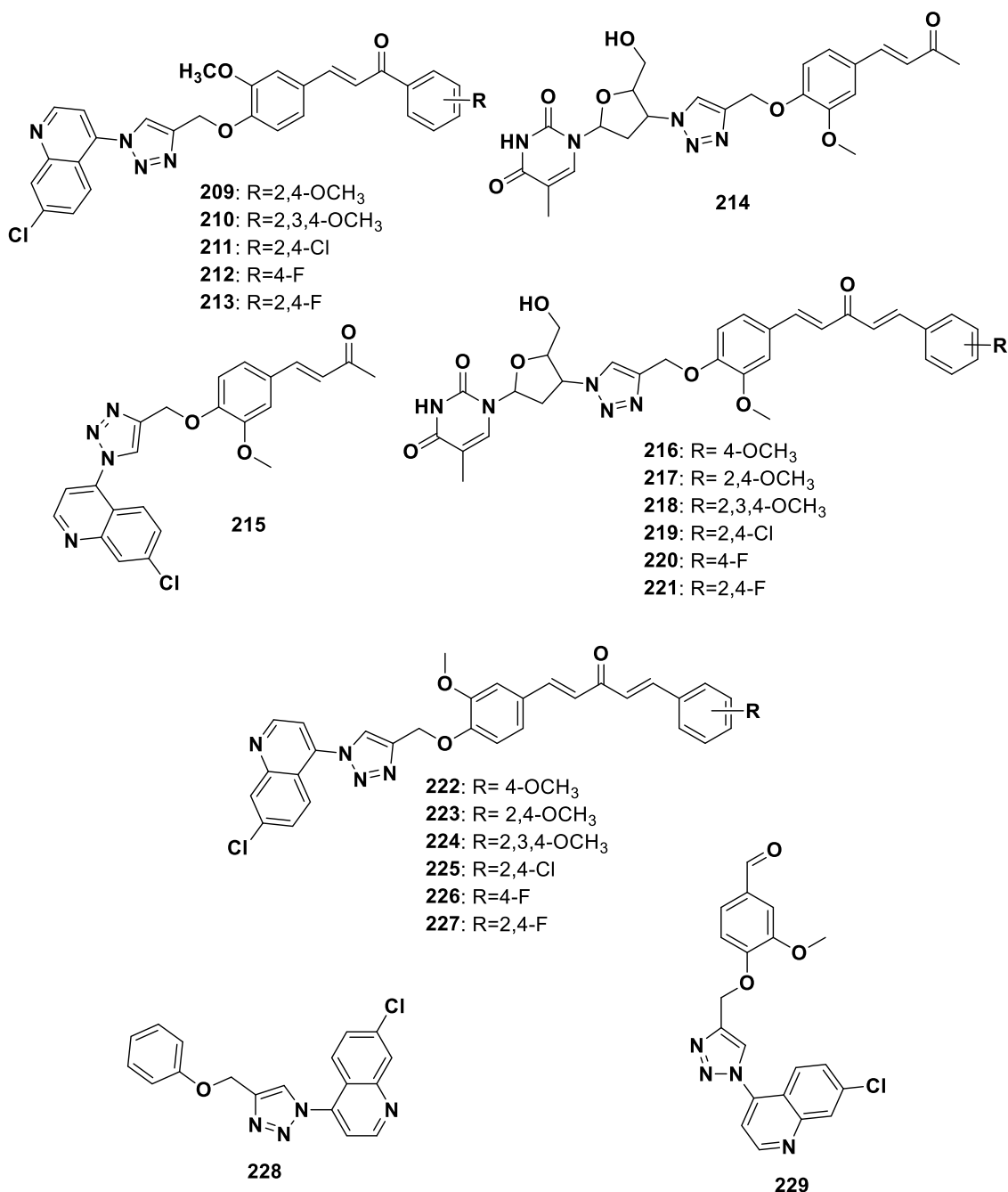
- 198: R= 4-OCH₃
 199: R= 2,4-OCH₃
 200: R=2,3,4-OCH₃



- 201: R= 4-OCH₃
 202: R= 2,4-OCH₃
 203: R=2,3,4-OCH₃



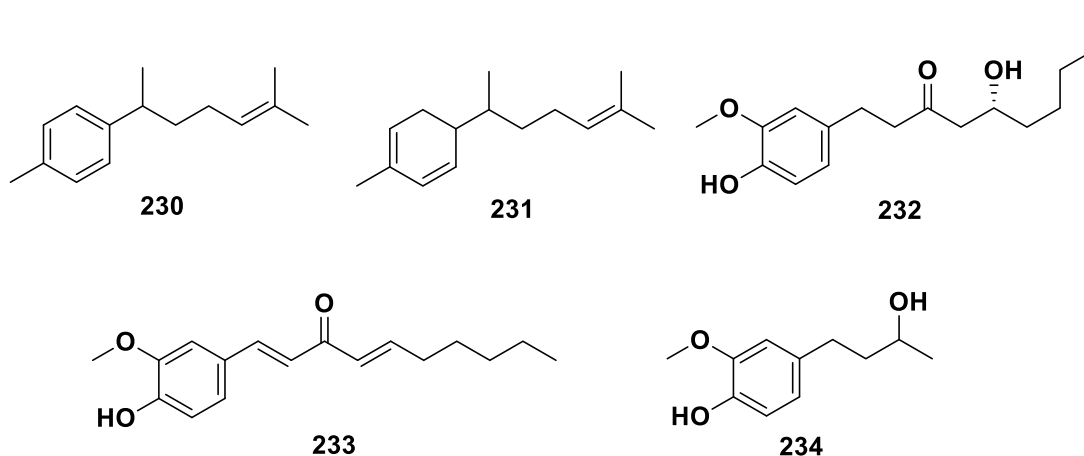
- 204: R=2,4-OCH₃
 205: R=2,3,4-OCH₃
 206: R=2,4-Cl
 207: R=4-F
 208: R=2,4-F



2.7 Dehydrozingerone as antifungal/antifeedant

Agarwal *et al.*, have reported the isolation of various natural compounds like curcumene (**230**), zingiberene (**231**) and 6-gingerol (**232**, ginger oleoresin) from fresh rhizomes of *Zingiber officinale*. Authors have also reported the synthesis of DZG derivatives [6]-dehydroshogaol (**233**), zingerone (**164**) and dihydrozingerone (**234**). These tested compounds displayed modest insect growth regulatory (IGR) and antifeedant activity against *Spilosoma obliqua* and substantial antifungal activity against *Rhizoctonia solani*. Amongst the series tested, compound **233** exhibited

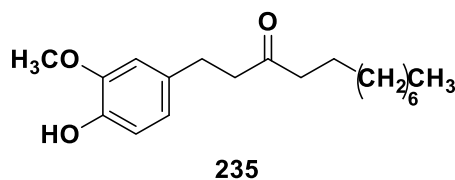
maximum IGR activity ($EC_{50} = 3.55$ mg/ml) while its DZG portion has imparted maximum antifungal activity ($EC_{50} 86.49$ mg l⁻¹).⁸⁴



Kubra et al., have evaluated the antifungal effectiveness of DZG against *Aspergillus oryzae*, *Aspergillus flavus*, *Aspergillus niger*, *Aspergillus ochraceus*, *Fusarium oxysporum* and *Penicillium chrysogenum*. The MIC and fungicidal concentration was ranging from 755 to 911 μ M and 880 to 1041 μ M respectively, which suggests that these fungal species were found vulnerable to DZG. Authors have also studied scanning electron microscopy to monitor morphological changes such as cell lysis, inhibition and morphological alterations in hyphae and sporulation in *A. ochraceus* on treatment with DZG. This study provides an insight for exploiting DZG as a potential antifungal scaffold with the presence of α,β -unsaturated carbonyl (C = O) group (conjugation system) on the aromatic ring with methoxyl and phenolic hydroxyl groups.⁸⁵

2.8 Dehydrozingerone as Antiplatelet

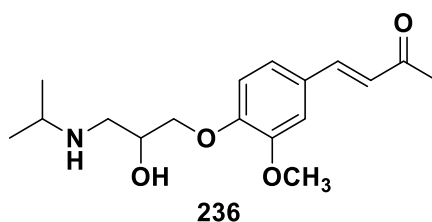
Shih *et al.*, have reported the synthesis of some novel DZG derivatives derived from shogaol and gingerol and evaluated them for anti-platelet aggregation activity. Amongst the synthesized compounds, [6]-paradol **235** displayed the most significant inhibition of platelet aggregation induced by arachidonic acid.⁸⁶



2.9 Dehydrozingerone as β -adrenoceptor antagonist

Wu *et al.*, have reported the synthesis of a novel dehydrozingeronolol (**236**) derived from DZG, and evaluated it for cardioselectivity, β -adrenoceptor antagonist and intrinsic sympathomimetic

activity. Results suggested that compound **236** blocked (-) isoproterenol-induced tachycardia effects, thus signifying its bradycardia effect along with β -adrenoceptor blocking activities.⁸⁷



2.10 Dehydrozingerone: *in silico* studies

Singh *et al.*, have reported *in silico* model to study the binding mode of curcumin and DZG with Human papilloma virus protein (HPV16 E6), a key protein dynamically participating in oral and cervical cancers and a model target for restoring the tumor suppressor role of p53. The binding interactions of the compounds have been studied by molecular docking using Autodock4. In this work, curcumin was found to have best binding interactions at the target site as compared to other curcuminoids, demethoxy and bis-demethoxy curcumin, which have lower but similar potential. Eighteen other naturally occurring congeners of curcumin were also docked in order to find the best candidate. However, only chlorogenic acid (**237**) was found to have considerable binding energy than curcumin itself (Table 7). This study has provided an insight for the design and development of drugs against both oral and cervical cancers from natural origin.⁸⁸

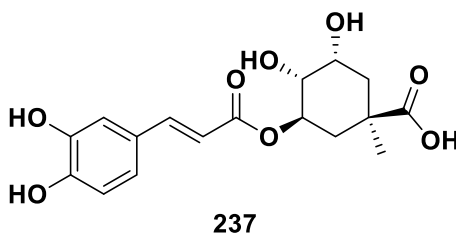


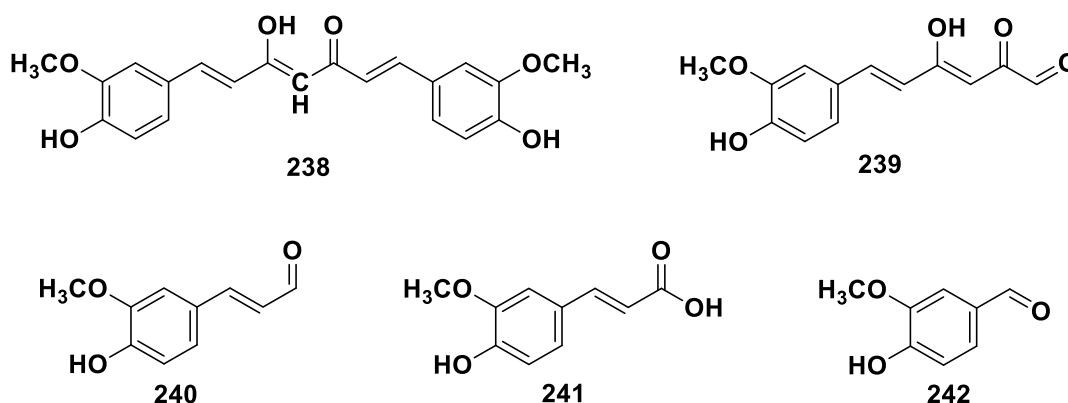
Table 7: Automated Docking Analysis through Scigress Explorer 7.7.0.47.

Ligands	PMF score dock flexible ligand in rigid active site (kcal/mol) through Scigress 7.7.0.47
Bis demethoxy curcumin	-51.503
Caffeic acid	-62.267
Capsaicin	-50.654
Cholorogenic acid	-99.782*
Cassumunins A	-44.556
Cassumunins B	-55.462
Curcumin	-85.699*
Curcumin dipiperoyl ester	-74.859
Cyclocurcmin	-54.515
Demethoxy curcumin	-78.974*
Dehydrozingerone	-41.759 [#]
Diaryl pentanoids	-61.251
Diaryl pentanoids II	-54.224
Dihydro guarietic acid	-65.578
Eugenol	-37.275
Ferulic acid	-46.627
Piperic acid	-60.454
Quercetin	-67.679
Yakuchinone A	-45.20
Yakuchinone B	-53.811
Zingerone	-40.826

*Inhibitors showing significant docking results; [#] DZG

Shen *et al.*, have reported the molecular docking simulation studies of curcumin (**57**) and tautomer of curcumin (**238**) and its degradation products (**239-242**) over Xanthine oxidase (XO), an

enzyme capable of generating reactive oxygen species and having roles in pathogenesis of many diseases. As such curcumin did not display any inhibitory activity against XO because of its twisted steric bulkiness. However, degradation products of curcumin were found to fit efficiently into the binding pocket of XO, which was built by using salicylate as reference ligand. Two natural polyphenols, quercetin and luteolin known to possess high inhibitory activities against XO were chosen to validate the model. Quercetin displayed six binding interactions with amino acid residues namely Arg880, Arg912, Phe914, Phe1009, Thr1010 and Glu1261, while luteolin showed interactions with residues Asn768, Arg880, Phe914, Phe1009, Thr1010 and Ala1079 of XO. It was observed that both quercetin and luteolin have common binding region with four amino acid residues. Compound **239**, a major degradation product of curcumin, showed comparable binding affinity that is, 4.57 μM with that of quercetin (1.12 μM) and luteolin (1.45 μM). DZG a minor degradation product was seen to bind with Phe914, Phe1009, Thr1010 and Ser876 residues of XO with a binding affinity of 91.2 μM . Thus this study highlighted the mechanisms underlying inhibition of XO.⁸⁹



2.11 Dehydrozingerone reported for miscellaneous activities

Transfer of vascular smooth muscle cells (VSMC) is known to be linked with development of atherosclerosis. Growth factors and ROS produced during vascular injury are considered to play a major role in pathogenesis of atherosclerosis. Therefore, inhibition of growth factor or ROS-mediated signaling may signify a potential therapeutic approach for interference with the progression of atherosclerosis. Liu *et al.*, have explored the effect of DZG on platelet-derived growth factor (PDGF) stimulated VSMC movement, proliferation, and collagen synthesis. In an effort to understand the mechanism, authors have studied the effect of DZG on hydrogen peroxide (H_2O_2)-stimulated PDGF receptor signaling. Further, growth factor-mediated cell proliferation is negatively regulated by protein tyrosine phosphatases (PTPs); therefore, authors have also assessed the effect of DZG on PTP activity in cells treated with H_2O_2 . In this study the efficacy of DZG with curcumin and isoeugenol (structural analogs of DZG) was compared in order to

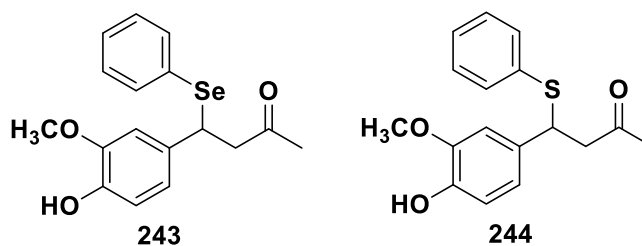
understand the structural necessities for activity and DZG emerged as an effective inhibitor of growth factor/H₂O₂-stimulated VSMC functions by inhibiting the oxidation of cellular phosphatases.⁹⁰

Oxidative stress is one of the interfering factors in wound healing course. This stress once triggered by the wound results in the production of ROS, thereby delaying usual wound repair. So reducing the level of ROS would be an important approach to improve healing process. Rao *et al.*, have demonstrated the influence of DZG as a ROS scavenger on both normal and dexamethasone delayed wound healing in albino rats. It was found that DGZ privileged the healing of re-sutured incision wounds as compared to control. Further, there was significant improvement in granulation breaking strength and the rise in the hydroxyproline (OHP) and lysyl oxidase (LO) levels in the granulation tissue was also observed clearly suggesting that the DZG was influential and supportive in hastening the healing process in both normal and dexamethasone-suppressed wounds in rat models.⁹¹

Soo *et al.*, have reported the blood sugar lowering property of DZG. In this study authors have revealed that DZG increases phosphorylation or activation of AMK kinase to bring about a drop in blood sugar levels and boost insulin sensitivity as well as reduce body fat. Thus DZG could be an ideal molecule for drug discovery in the treatment of Type II diabetes mellitus and obesity.⁹²

Kim *et al.*, have investigated the effects of DZG on metabolic profiles in mice. It was evidently found that DZG suppressed high-fat diet (HFD)-induced increase in glucose and cholesterol through a mechanism involving AMP-activated protein kinase (AMPK). This was due to increased phosphorylation of AMPK in skeletal muscles. Maximum AMPK activation by DZG was found at the concentration of 30 μ M for 10 min. In addition, DGZ was also found to activate p38 mitogen-activated protein kinase (MAPK) signaling in an AMPK-dependent manner and also increase in GLUT4 (major transporter for glucose uptake) expression in skeletal muscles. These all findings thus explain the possible molecular mechanism of AMPK pathway activation in skeletal muscle by DZG.⁹³

Martinez *et al.*, have synthesized two new organochalcogen-containing zingerone derivatives and evaluated for their antioxidant properties by ABTS⁺ assay. Novel compounds, **243** and **244** exhibited improved activity over DZG (IC₅₀ 8.0 \pm 1.0 μ M) with IC₅₀ values of 8.0 \pm 1.0 μ M and 6.5 \pm 0.5 μ M, respectively, with two-fold increase in activity as compared to phenolic antioxidants. The enhancement in activity was mainly attributed to a mechanism that eliminates phenylselenyl or phenylthiyl radicals.⁹⁴



3 Conclusion and future perspective

A great deal of time has been taken to prove that the time-honored medicinal plants have the power to cure. Drugs derived from natural sources have always been precious precursors for modern medicines. Taking a step one day at a time, in the near future, the nature's enormity and diversity would provide us the solutions to fight even the most fearsome diseases. To overcome the problems associated with curcumin, curcuminoids and the degradants of curcumin have been looked upon for molecular variations in developing diverse scaffolds with least side effects and improved bioavailability. These curcuminoids and degradation products of curcumin have also helped towards improving its metabolic profile in humans as well as mechanism leading to pharmacological responses^{15,95}. Therefore, over the course of years several studies have come up with compounds or structural analogs of curcumin (mono-carbonyl analogs or mono-carbonyl enones) that have excluded β -diketone moiety to restrain stability and improve metabolic profiles. One such distinguished degradant of curcumin is DZG, which is endowed with a broad range of biological activities like antioxidant, anticancer, anti-inflammatory, anti-depressant, anti-malarial, antifungal, anti-platelet and many others. Therefore, in this review we have put forward an extensive effort to revise and systematically discuss the research involving DZG with its biological diversity. In conclusion, it is quite evident that DZG is an imperative scaffold and its numerous analogs have emerged as a promising leads in the design and development of some novel medicinally active compounds with improved metabolic, pharmacokinetic and pharmacological profiles, indicating that there is much scope for further investigation.

4 Conflicts of interest

The authors declare that they have no conflict of interest. The funding agency had no role in manuscript contents or in the decision to publish the present manuscript.

5 Acknowledgments

The authors are thankful to the College of Health Sciences, University of KwaZulu-Natal, Durban, South Africa for the facilities and financial support.

References

1. Samuelsson, G. *Drugs of Natural Origin: a Textbook of Pharmacognosy, 5th Swedish Pharma Press*; 5th ed.; Swedish Pharmaceutical Press, **2004**.
2. Newman, D. J.; Cragg, G. M.; Snader, K. M. *Nat. Prod. Rep.* **2000**, *17*, 215–234.
3. Newman, D. J.; Cragg, G. M.; Snader, K. M. Natural products as sources of new drugs over the period 1981-2002. *J. Nat. Prod.* **2003**, *66*, 1022–1037.
4. Cragg, G. M.; Newman, D. J.; Snader, K. M. *J. Nat. Prod.* **1997**, *60*, 52–60.
5. Subramanian, M.; Sreejayan; Rao, M. N. a.; Devasagayam, T. P. a.; Singh, B. B. *Fundam. Mol. Mech. Mutagen.* **1994**, *311*, 249–255.
6. de Bernardi, M.; Vidari, G.; Vita-Finzi, P. *Phytochemistry* **1976**, *15*, 1785–1786.
7. Motohashi, N.; Ashihara, Y.; Yamagami, C.; Saito, Y. *Mutat. Res. - Fundam. Mol. Mech. Mutagen.* **1997**, *377*, 17–25.
8. Kuo, P.-C.; Damu, A. G.; Cherng, C.-Y.; Jeng, J.-F.; Teng, C.-M.; Lee, E.-J.; Wu, T.-S. *Arch. Pharm. Res.* **2005**, *28*, 518–528.
9. Elias, G.; Rao, M. N. a *Eur. J. Med. Chem.* **1988**, *23*, 379–380.
10. Rajakumar, D. V; Rao, M. N. *Biochem. Pharmacol.* **1993**, *46*, 2067–2072.
11. Rajakumar, D. V.; Rao, M. N. a. *Mol. Cell. Biochem.* **1994**, *140*, 73–79.
12. Roughley, P.; Whiting, D. *J. Chem. Soc.* **1973**, *20*, 2379–2388.
13. Wang, Y. J.; Pan, M. H.; Cheng, A. L.; Lin, L. I.; Ho, Y. S.; Hsieh, C. Y.; Lin, J. K. *J. Pharm. Biomed. Anal.* **1997**, *15*, 1867–1876.
14. Suresh, D.; Gurudutt, K. N.; Srinivasan, K. *Eur. Food Res. Technol.* **2009**, *228*, 807–812.
15. Shen, L.; Ji, H.-F. *Trends Mol. Med.* **2012**, *18*, 138–144.
16. Esatbeyoglu, T.; Ulbrich, K.; Rehberg, C.; Rohn, S.; Rimbach, G. *Food Funct.* **2015**, *6*, 887–893.
17. Priyadarsini, K. I.; Devasagayam, T. P. a; Rao, M. N. a; Guha, S. N. *Radiat. Phys. Chem.* **1999**, *54*, 551–558.
18. Anderson, A. M.; Mitchell, M. S.; Mohan, R. S. *J. Chem. Educ.* **2000**, *77*, 359.
19. Anand, P.; Kunnumakkara, A. B.; Newman, R. a.; Aggarwal, B. B. *Mol. Pharm.* **2007**, *4*, 807–818.
20. Rosemond, M. J. C.; St. John-Williams, L.; Yamaguchi, T.; Fujishita, T.; Walsh, J. S. *Chem. Biol. Interact.* **2004**, *147*, 129–139.
21. Straganz, G. D.; Glieder, A.; Brecker, L.; Ribbons, D. W.; Steiner, W. *Biochem. J.* **2003**, *369*, 573–81.
22. Grogan, G. *Biochem. J.* **2005**, *388*, 721–30.

-
23. Nagpure, B. A. a L.; Gupta, R. K. *Indian J. Chem. - Sect. B Org. Med. Chem.* **2011**, *50*, 1119–1122.
 24. Tomren, M. A.; Másson, M.; Loftsson, T.; Tønnesen, H. H. *Int. J. Pharm.* **2007**, *338*, 27–34.
 25. Sardjiman, S.; Reksohadiprodjo, M. *Eur. J. Med. Chem.* **1997**, *32*, 625–630.
 26. Mosley, C. A.; Liotta, D. C.; Snyder, J. P. In *The Molecular Targets and Therapeutic Uses of Curcumin in Health and Disease*; **2007**; Vol. 595, pp. 77–103.
 27. Weber, W. M.; Hunsaker, L. a.; Roybal, C. N.; Bobrovnikova-Marjon, E. V.; Abcouwer, S. F.; Royer, R. E.; Deck, L. M.; Vander Jagt, D. L. *Bioorganic Med. Chem.* **2006**, *14*, 2450–2461.
 28. Liang, G.; Shao, L.; Wang, Y.; Zhao, C.; Chu, Y.; Xiao, J.; Zhao, Y.; Li, X.; Yang, S. *Bioorg. Med. Chem.* **2009**, *17*, 2623–31.
 29. Zhao, C.; Liu, Z.; Liang, G. *Curr. Pharm. Des.* **2013**, *19*, 2114–2135.
 30. Shetty, D.; Kim, Y.; Shim, H.; Snyder, J. *Molecules* **2014**, *20*, 249–292.
 31. Shen, L.; Ji, H.-F. *Trends Mol. Med.* **2012**, *18*, 363–364.
 32. Fuchs-Tarlovsky, V.; Calderon-Cuevas, J. Nova Science Publishers, Inc., **2014**; pp. 273–285.
 33. El-Beltagi, H. S.; Mohamed, H. I. *Not. Bot. Horti Agrobot. Cluj-Napoca* **2013**, *41*, 44–57.
 34. Jeong, J. I.; Lee, Y. W.; Kim, Y. K. *Neurochem. Res.* **2003**, *28*, 1201–11.
 35. Wang, X.; Zhang, P.; Zhao, L.; Tu, Y.; Dai, K. *Zhonghua Xueyexue Zazhi* **2014**, *35*, 511–514.
 36. Kelsey, N. a.; Wilkins, H. M.; Linseman, D. a. *Molecules* **2010**, *15*, 7792–7814.
 37. Brewer, M. S. *Compr. Rev. Food Sci. Food Saf.* **2011**, *10*, 221–247.
 38. Priyadarsini.K.I, Guha.S.N, R. M. N. A. *Free Radic. Biol. Med.* **1998**, *24*, 933–941.
 39. Jovanovic, S. V; Steenken, S.; Boone, C. W.; Simic, M. G. *J. Am. Chem. Soc.* **1999**, *121*, 9677–9681.
 40. Yamagami, C.; Motohashi, N.; Emoto, T.; Hamasaki, a; Tanahashi, T.; Nagakura, N.; Takeuchi, Y. *Bioorganic Med. Chem. Lett.* **2004**, *14*, 5629–5633.
 41. Parihar, V. K.; Dhawan, J.; Kumar, S.; Manjula, S. N.; Subramanian, G.; Unnikrishnan, M. K.; Rao, C. M. *Chem. Biol. Interact.* **2007**, *170*, 49–58.
 42. Musialik, M.; Litwinienko, G. *J. Therm. Anal. Calorim.* **2007**, *88*, 781–785.
 43. Li, P.-Z.; Liu, Z.-Q. *Eur. J. Med. Chem.* **2011**, *46*, 1821–6.
 44. Feng, J.-Y.; Liu, Z.-Q. *Eur. J. Med. Chem.* **2011**, *46*, 1198–206.
 45. Kubra, I. R.; Bettadaiah, B. K.; Murthy, P. S.; Rao, L. J. M. *J. Food Sci. Technol.* **2014**, *51*, 245–255.
-

-
46. Kancheva, V.; Slavova-Kazakova, A.; Fabbri, D.; Dettori, M. A.; Delogu, G.; Janiak, M.; Amarowicz, R. *Food Chem.* **2014**, *157*, 263–274.
 47. Li, P.-Z.; Liu, Z.-Q. *Med. Chem. Res.* **2014**, *23*, 3478–3490.
 48. Sangwan, N. S.; Shanker, S.; Sangwan, R. S.; Kumar, S. *Phyther. Res.* **1998**, *12*, 389–399.
 49. Anto, R. J.; George, J.; Dinesh Babu, K. V.; Rajasekharan, K. N.; Kuttan, R. *Mutat. Res. - Genet. Toxicol.* **1996**, *370*, 127–131.
 50. Anto, R. J.; Kuttan, G.; Babu, K. V. D.; Rajasekharan, K. N.; Kuttan, R. *Int. J. Pharm.* **1996**, *131*, 1–7.
 51. Ramsewak, R. S.; DeWitt, D. L.; Nair, M. G. *Phytomedicine* **2000**, *7*, 303–308.
 52. Ruby, a J.; Kuttan, G.; Babu, K. D.; Rajasekharan, K. N.; Kuttan, R. *Cancer Lett.* **1995**, *94*, 79–83.
 53. Yin, S.; Zheng, X.; Yao, X.; Wang, Y.; Liao, D. *J. Cancer Ther.* **2013**, *4*, 113–123.
 54. Liu, Z.; Sun, Y.; Ren, L.; Huang, Y.; Cai, Y.; Weng, Q.; Shen, X.; Li, X.; Liang, G.; Wang, Y. *BMC Cancer* **2013**, *13*, 494.
 55. Motohashi, N.; Yamagami, C.; Tokuda, H.; Konoshima, T.; Okuda, Y.; Okuda, M.; Mukainaka, T.; Nishino, H.; Saito, Y. *Cancer Lett.* **1998**, *134*, 37–42.
 56. Rao, M. A. M.; Kumar, M. M.; Rao, M. A. M. *J. Biochem.* **1999**, *125*, 383–390.
 57. Motohashi, N.; Yamagami, C.; Tokuda, H.; Okuda, Y.; Ichiishi, E.; Mukainaka, T.; Nishino, H.; Saito, Y. *Mutat. Res.* **2000**, *464*, 247–54.
 58. Tatsuzaki, J.; Bastow, K. F.; Nakagawa-Goto, K.; Nakamura, S.; Itokawa, H.; Lee, K. H. *J. Nat. Prod.* **2006**, *69*, 1445–1449.
 59. Exelixis, Inc., Patent WO2006033943(A2), 2006.
 60. Tatsuzaki, J.; Taniguchi, M.; Bastow, K. F.; Nakagawa-Goto, K.; Morris-Natschke, S. L.; Itokawa, H.; Baba, K.; Lee, K.-H. *Bioorg. Med. Chem.* **2007**, *15*, 6193–6199.
 61. Nakagawa-Goto, K.; Yamada, K.; Nakamura, S.; Chen, T.-H.; Chiang, P.-C.; Bastow, K. F.; Wang, S.-C.; Spohn, B.; Hung, M.-C.; Lee, F.-Y.; Lee, F.-C.; Lee, K.-H. *Bioorg. Med. Chem. Lett.* **2007**, *17*, 5204–5209.
 62. Tatsuzaki, J.; Nakagawa-Goto, K.; Tokuda, H.; Lee, K.-H. *J. Asian Nat. Prod. Res.* **2010**, *12*, 227–232.
 63. Yogosawa, S.; Yamada, Y.; Yasuda, S.; Sun, Q.; Takizawa, K.; Sakai, T. *J. Nat. Prod.* **2012**, *75*, 2088–2093.
 64. Woo, H. B.; Eom, Y. W.; Park, K.-S.; Ham, J.; Ahn, C. M.; Lee, S. *Bioorg. Med. Chem. Lett.* **2012**, *22*, 933–936.
 65. Liu, K.; Zhang, D.; Chojnacki, J.; Du, Y.; Fu, H.; Grant, S.; Zhang, S. *Org Biomol Chem* **2013**, *11*, 4757–4763.
-

-
66. Uha Mikakuto Company Limited. Patent JP2013010720A, 2013.
 67. Eom, Y. W.; Oh, S.; Woo, B.; Ham, J.; Ahn, C. M.; Lee, S. *Bull. Korean Chem. Soc.* **2013**, *34*, 1272–1274.
 68. University of Minnesota. Patent WO2014066840A1, 2014.
 69. Bagad, A. S.; Joseph, J. A.; Bhaskaran, N.; Agarwal, A. *Adv. Pharmacol. Sci.* **2013**, *2013*, 538–544.
 70. Liu, Z.; Tang, L.; Zou, P.; Zhang, Y.; Wang, Z.; Fang, Q.; Jiang, L.; Chen, G.; Xu, Z.; Zhang, H.; Liang, G. *Eur. J. Med. Chem.* **2014**, *74*, 671–682.
 71. Claramunt, R. M.; Bouissane, L.; Cabildo, M. P.; Cornago, M. P.; Elguero, J.; Radziwon, a.; Medina, C. *Bioorg. Med. Chem.* **2009**, *17*, 1290–1296.
 72. Wu, J.; Zhang, Y.; Cai, Y.; Wang, J.; Weng, B.; Tang, Q.; Chen, X.; Pan, Z.; Liang, G.; Yang, S. *Bioorg. Med. Chem.* **2013**, *21*, 3058–3065.
 73. Jayasekhar, P.; Rao, S. B.; Santhakumari, G. *Indian J. Pharm. Sci.* **1998**, *60*, 191.
 74. Santhakumari, G.; Jayasekhar, P.; Rao, S. B. *Indian J. Pharm. Sci.* **2002**, *64*, 82–87.
 75. Abbas, G.; Rauf, K.; Mahmood, W. *Nat. Prod. Res.* **2014**, *29*, 302–307.
 76. Fajemiroye, J. O.; Galdino, P. M.; Marciano De Paula, J. A.; Rocha, F. F.; Akanmu, M. a; Vanderlinde, F. A.; Zjawiony, J. K.; Costa, E. A. *Food Funct.* **2014**, *5*, 1819–1828.
 77. Liao, J.-C.; Tsai, J.-C.; Liu, C.-Y.; Huang, H.-C.; Wu, L.-Y.; Peng, W.-H. *BMC Complement. Altern. Med.* **2013**, *13*, 299.
 78. Bhutani, M. K.; Bishnoi, M.; Kulkarni, S. K. *Pharmacol. Biochem. Behav.* **2009**, *92*, 39–43.
 79. Martinez, D. M.; Barcellos, A.; Casaril, A. M.; Savegnago, L.; Lernardão, E. J. *Pharmacol. Biochem. Behav.* **2014**, *127*, 111–117.
 80. Kim, D. S. H. ; Kim, J. Y. *Bioorg. Med. Chem. Lett.* **2004**, *14*, 1287–1289.
 81. Ryu, E. K.; Choe, Y. S.; Lee, K.-H.; Choi, Y.; Kim, B.-T. *J. Med. Chem.* **2006**, *49*, 6111–6119.
 82. Claudio Viegas-Junior, B. S. P.; Amanda Danuello, B. S. P.; Vanderlan da Silva Bolzani, B. S. P.; Eliezer J. Barreiro, B. S. P.; Carlos Alberto Manssour Fraga, B. S. P. *Curr. Med. Chem.* **2007**, *14*, 1829–1852.
 83. Guantai, E. M.; Ncokazi, K.; Egan, T. J.; Gut, J.; Rosenthal, P. J.; Smith, P. J.; Chibale, K. *Bioorg. Med. Chem.* **2010**, *18*, 8243–8256.
 84. Agarwal, M.; Walia, S.; Dhingra, S.; Khambay, B. P. *Pest Manag. Sci.* **2001**, *57*, 289–300.
 85. Kubra, I. R.; Murthy, P. S.; Rao, L. J. M. *J. Food Sci.* **2013**, *78*, M64–M69.
 86. Shih, H.-C.; Chern, C.-Y.; Kuo, P.-C.; Wu, Y.-C.; Chan, Y.-Y.; Liao, Y.-R.; Teng, C.-M.; Wu, T.-S. *Int. J. Mol. Sci.* **2014**, *15*, 3926–3951.
-

87. Wu, B.-N.; Yang, C.-R.; Yang, J.-M.; Chen, I.-J. *Gen. Pharmacol. Vasc. Syst.* **1994**, *25*, 651–659.
88. Singh, A. K.; Misra, K. *Interdiscip. Sci. Comput. Life Sci.* **2013**, *5*, 112–118.
89. Shen, L.; Ji, H.-F. *Bioorg. Med. Chem. Lett.* **2009**, *19*, 5990–5993.
90. Liu, Y.; Dolence, J.; Ren, J.; Rao, M.; Sreejayan, N. *J. Cardiovasc. Pharmacol.* **2008**, *52*, 422–429.
91. Rao, M. C.; Sudheendra, A. T.; Nayak, P. G.; Paul, P.; Kutty, G. N.; Shenoy, R. R. *Mol. Cell. Biochem.* **2011**, *355*, 249–256.
92. Korea University Research and Business Foundation. Patent WO2014112763A1, 2014.
93. Kim, S. J.; Kim, H. M.; Lee, E. S.; Kim, N.; Lee, J. O.; Lee, H. J.; Park, N. Y.; Jo, J. Y.; Ham, B. Y.; Han, S. H.; Park, S. H.; Chung, C. H.; Kim, H. S. *J. Cell. Mol. Med.* **2015**, *19*, 620–629.
94. Martinez, D. M.; Barcellos, A. M.; Casaril, A. M.; Savegnago, L.; Perin, G.; Schiesser, C. H.; Callaghan, K. L.; Lenardão, E. J. *Tetrahedron Lett.* **2015**, *56*, 2243–2246.
95. Aggarwal, B. B.; Sung, B. *Trends Pharmacol. Sci.* **2009**, *30*, 85–94.

CHAPTER 3

Dehydrozingerone inspired styryl hydrazine thiazole hybrids as promising class of anti-mycobacterial agents.

Girish A. Hampannavar,[†] Rajshekhar Karpoormath,^{*,†} Mahesh B. Palkar,^{§,†} Mahamadhanif S. Shaikh[†] and Balakumar Chandrasekaran[†]

[†]Department of Pharmaceutical Chemistry, Discipline of Pharmaceutical Sciences, College of Health Sciences, University of KwaZulu-Natal, Westville Campus, Durban – 4000, South Africa

[§]Department of Pharmaceutical Chemistry, K.L.E. University College of Pharmacy, Vidyanagar, Hubballi – 580031, Karnataka, India

Graphical Abstract



*Corresponding author

E-mail: karpoormath@ukzn.ac.za, rvk2006@gmail.com

Tel no.: +27(0)312607179, +2721107207; Fax No.: +27(0)312607792

Dehydrozingerone Inspired Styryl Hydrazine Thiazole Hybrids as Promising Class of Antimycobacterial Agents

Girish A. Hampannavar,[†] Rajshekhkar Karpoornath,^{*†} Mahesh B. Palkar,^{§,†} Mahamadhanif S. Shaikh,[†] and Balakumar Chandrasekaran[†][†]Department of Pharmaceutical Chemistry, Discipline of Pharmaceutical Sciences, College of Health Sciences, University of KwaZulu-Natal, Westville Campus, Durban 4000, South Africa[§]Department of Pharmaceutical Chemistry, K.L.E. University College of Pharmacy, Vidyanagar, Hubballi 580031, Karnataka, India

Supporting Information

ABSTRACT: Series of styryl hydrazine thiazole hybrids inspired from dehydrozingerone (DZG) scaffold were designed and synthesized by molecular hybridization approach. *In vitro* antimycobacterial activity of synthesized compounds was evaluated against *Mycobacterium tuberculosis* H₃₇Rv strain. Among the series, compound **60** exhibited significant activity (MIC = 1.5 μM; IC₅₀ = 0.48 μM) along with bactericidal (MBC = 12 μM) and intracellular antimycobacterial activities (IC₅₀ = <0.098 μM). Furthermore, **60** displayed prominent antimycobacterial activity under hypoxic (MIC = 46 μM) and normal oxygen (MIC = 0.28 μM) conditions along with antimycobacterial efficiency against isoniazid (MIC = 3.2 μM for INH-R1; 1.5 μM for INH-R2) and rifampicin (MIC = 2.2 μM for RIF-R1; 6.3 μM for RIF-R2) resistant strains of Mtb. Presence of electron donating groups on the phenyl ring of thiazole moiety had positive correlation for biological activity, suggesting the importance of molecular hybridization approach for the development of newer DZG clubbed hydrazine thiazole hybrids as potential antimycobacterial agents.

KEYWORDS: Antimycobacterial activity, bactericidal, dehydrozingerone, NLAID, thiazole



Abstract

Series of styryl hydrazine thiazole hybrids inspired from dehydrozingerone (DZG) scaffold were designed and synthesized by molecular hybridization approach. *In vitro* anti-mycobacterial activity of synthesized compounds was evaluated against *Mycobacterium tuberculosis* (Mtb) H₃₇Rv strain. Among the series, compound **60** exhibited significant activity (MIC = 1.5 μM; IC₅₀ = 0.48 μM) along with bactericidal (MBC = 12 μM) and intracellular anti-mycobacterial activities (IC₅₀ = < 0.098 μM). Furthermore, **60** displayed prominent anti-mycobacterial activity under hypoxic (MIC = 46 μM) and normal oxygen (MIC = 0.28 μM) conditions along with anti-mycobacterial efficiency against isoniazid (MIC = 3.2 μM for INH-R1; 1.5 μM for INH-R2) and rifampicin (MIC = 2.2 μM for RIF-R1; 6.3 μM for RIF-R2) resistant strains of Mtb. Presence of electron donating groups on the phenyl ring of thiazole moiety had positive correlation for biological activity, suggesting the importance of molecular hybridization approach for the development of newer DZG clubbed hydrazine thiazole hybrids as potential anti-mycobacterial agents.

Keywords

Anti-mycobacterial activity, Bactericidal, Dehydrozingerone, NIAID, Thiazole.

1 Introduction

Tuberculosis (TB) is a chronic necrotizing bacterial infection caused by *Mycobacterium tuberculosis* (Mtb), which has been a bane of humanity for thousands of years and remains as one of the rampant health problems in the world. TB is an ancient enemy and current threat that has been ranked among the foremost killers of the 21st century.¹ According to World Health Organization (WHO) report, around 9 million people were found infected and around 1.5 million casualties occurred because of TB. Besides the life threatening strains of MDR-TB (Multi Drug Resistance Tuberculosis) are appearing, some of which can lead to high mortality rate (e.g., 72-89%) with death occurring in short period (4-16 weeks).² In 2013 around 480,000 affirmative cases of MDR-TB were witnessed.³ India, China, the Russian Federation and South Africa have almost 60% of the world's cases of MDR-TB. In addition, the risk becomes even greater if the person is co-infected with the HIV (human immunodeficiency virus).⁴ The global resurgence of TB and development of drug resistance necessitates for an imperative attention of medicinal chemists to develop innovative anti-mycobacterial agents as no new classes of anti-TB agents have been developed since the introduction of rifampin in to clinical practice in 1960s.

It is well known fact that *trans*-cinnamic acid analogs have recently drawn back the intentness of medicinal chemists due to their admirable pharmacological properties like antioxidant,⁵ antibacterial⁶ and antitumor.⁷ Rastogi et al. have demonstrated the synergistic activity of *trans*-cinnamic acid in amalgamation with INH, rifamycin and other recognized antimicrobial agents against Mtb.⁸ Further, Reddy et al. have reported the superior intracellular and *in vivo* activity of a cinnamoyl-rifamycin derivative (**Figure 1**) in contrast with rifamycin when tested against susceptible and MDR strains of Mtb along with *M. avium* complex (MAC).⁹ Several compounds resembling cinnamic acid and bearing styryl group or α,β -unsaturated carbonyl groups are reported for anti-mycobacterial activities (**Figure 2**).¹⁰

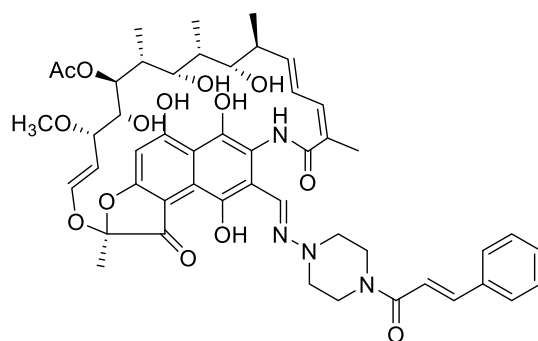


Figure 1: Cinnamoyl-rifamycin derivative.

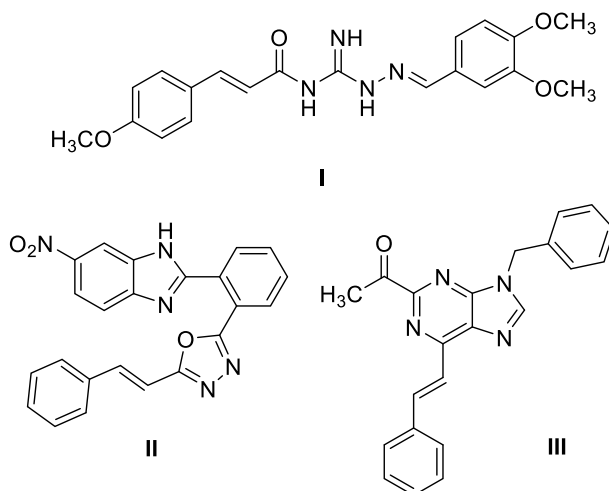


Figure 2: Compounds with styryl portion reported against *M. tuberculosis* H₃₇RV. (I: MIC 6.49 μ M)¹¹; (II: MIC 12.5 μ g/mL)¹²; (III: MIC 6.25 μ M)¹³

From literature, it was also found that derivatives resulting by combining cinnamoyl portion with various chemical classes of compounds have been reported to possess promising anti-mycobacterial activity.¹⁴⁻¹⁶ Besides, various drug-like heterocycles namely benzimidazoles¹⁷ and quinazolinones¹⁸ were integrated with cinnamoyl or aryl styryl groups have also been reported to augment the anti-mycobacterial properties.

Dehydrozingerone (DZG), also known as feruloylmethane, a half structural analog of curcumin, is isolated from *Curcuma longa*. Chemically DZG is (*E*)-4-(4-hydroxy-3-methoxyphenyl)but-3-en-2-one and possess an α,β -unsaturated carbonyl (styryl ketone) group that resembles the *trans*-cinnamic acid structure. DZG analogs have been reported to possess broad range of biological activities like antioxidant, anticancer, anti-inflammatory, antidepressant, antimalarial, antifungal etc.¹⁹

The thiazole nucleus is a common motif presently found in several FDA-approved drugs, such as the nonsteroidal anti-inflammatory drug meloxicam²⁰ and the tyrosine kinase inhibitor dasatinib.²¹ Recently, Meissner et al., have demonstrated the structure-activity relationships (SAR) of novel series of 2-aminothiazole analogs as effective anti-mycobacterial agents²² and Carradori et al., have reported microwave assisted method for the synthesis of substituted-thiazolyl hydrazines.²³ Therefore, thiazole is an essential scaffold in drug discovery since its derivatives known to possess wide spectrum of activities such as anti-hypertensive, anti-inflammatory, anti-HIV, anti-bacterial and anti-mycobacterial,^{24,25} which have tremendously captivated attention of medicinal chemists. **Figure 3** highlights the molecular manipulation of DZG-thiazole moiety and their resultant anti-mycobacterial activities.

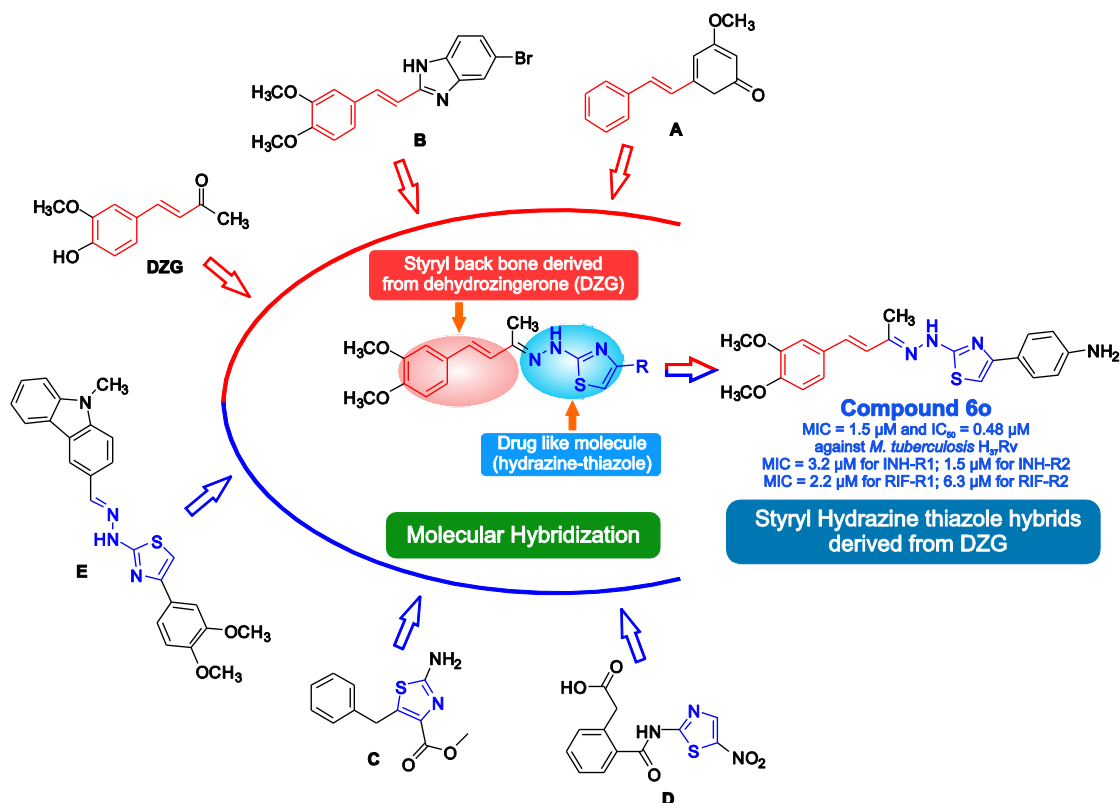


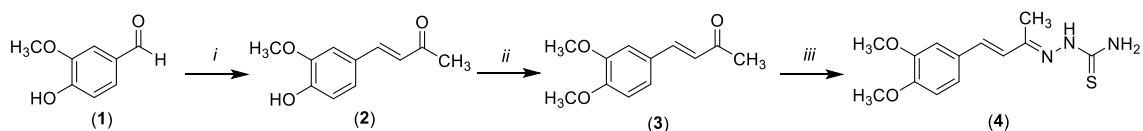
Figure 3: The literature reported derivatives containing styryl and thiazoles moieties and their anti-mycobacterial activities along with the designed compounds. Compound **60** exhibited most promising anti-mycobacterial activity among the synthesized compounds. A: (*E*)-3-methoxy-5-styrylcyclohexa-2,4-dien-1-one (MIC against H₃₇Rv = 32 µg/mL)²⁶; B: (*E*)-5-bromo-2-(3,4-dimethoxystyryl)-1*H*-benzo[*d*]imidazole (MIC against H₃₇Rv = > 7.25 µg/mL)¹⁷; C: 2-amino-5-benzylthiazole-4-carboxylate (MIC against H₃₇Rv = 0.06 µg/mL)²⁷; D: Nitazoxanide (MIC against H₃₇Rv = 16 µg/mL)²⁸; E: Carbazolo-thiazole analog (MIC against H₃₇Rv = 21 µM)²⁴

In view of the above facts and in continuation of our research program on the design and development of new anti-mycobacterial agents^{19,24,29} it was foreseen to amalgamate two biologically active pharmacophores (styryl portion of DZG and thiazole) in one molecular platform to engender a new scaffold for anti-mycobacterial evaluation. As shown in **Figure 3**, the designed hybrid analogs possess both DZG (comprising styryl) and thiazole motifs connected with each other via a hydrazine linker. These unifications were suggested as an effort to explore the possible synergistic influence of such structural hybridizations on the anticipated activity, hoping to discover a new lead structure that would have a promising anti-mycobacterial activity.

2 Chemistry

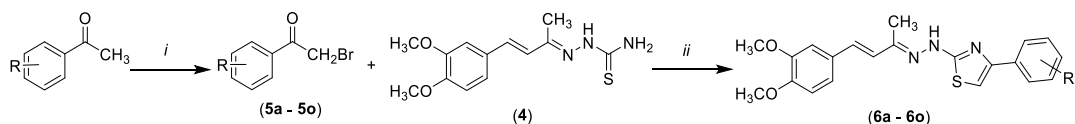
The synthesis of a novel series of styryl hydrazine thiazole hybrids derived from DZG (**6a-6o**) was achieved through efficient and versatile synthetic routes. The starting material DZG (**2**) was prepared by using commercially available vanillin (**1**) by simple Aldol condensation with acetone in presence of base. Methylation of **2** was done with methyl iodide in presence of potassium carbonate in *N,N*-Dimethylformamide to yield (*E*)-4-(3,4-dimethoxyphenyl)but-3-en-2-one (**3**). Further, Schiff base of compound **3** was formed with thiosemicarbazide to yield **4** (Scheme 1). The various appropriately substituted 2-bromo-1-phenylethanones (**5c-5o**) were synthesized from their respective acetophenones. Compound (**4**) was then condensed with various freshly synthesized 2-bromo-1-(substituted phenyl)-ethanones (**5a-5o**) to yield corresponding final compounds i.e., 2-(2-((2*E*,3*E*)-4-(3,4-dimethoxyphenyl)but-3-en-2-ylidene)hydrazinyl)-4-(substituted phenyl)thiazoles (**6a-6o**; Scheme 2). The anticipated structures of the final compounds were in agreement with the spectral (IR, ¹H NMR and ¹³C NMR) data obtained and were further substantiated by HRMS data, which is summarized in supporting information.

Scheme 1[‡]



[‡]Reaction conditions: (i) Acetone, NaOH; (ii) CH₃I, K₂CO₃, DMF, reflux, 1.5 h; (iii) Thiosemicarbazide, AcOH, CH₃OH, reflux, 3 h.

Scheme 2[§]



[§]Reaction conditions: (i) Br₂, Ether, 0-5 °C for **5c**; Br₂, CHCl₃, reflux, 3 h for **5d** and **5g**; Br₂, CHCl₃, 0-5 °C for **5e** and **5f**; CuBr₂, EtOAc, CHCl₃, reflux, 12 h for **5h-5o**; (ii) methanol, reflux, 3 h.

3 Results and discussion

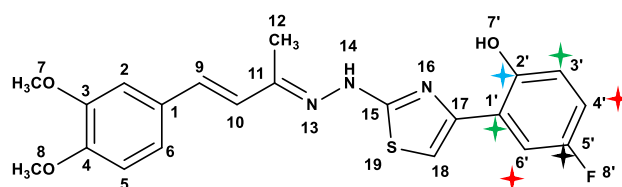
3.1 Synthesis and spectral studies

The entire newly synthesized final compounds showed satisfactory analysis of their anticipated structures, which are summarized in experimental section. In general, the IR spectrum of compound (**4**) evidently displayed characteristic absorption bands around 3422.9 cm^{-1} for N-H (of NH_2 group), 1552.69 cm^{-1} for C = N and 1159.88 cm^{-1} for C = S groups. These observations were further confirmed from ^1H NMR spectrum of compound **4** exhibited the presence of distinctive singlet signals at around δ 10.22, 8.22-7.76, 7.154-7.150, 3.79-3.76 and 2.11 for the N-H proton, NH_2 proton, 2nd proton of phenyl ring, methoxyl (OCH_3) protons and methyl (CH_3) protons indicating its formation by a process of simple carbon-nitrogen bond creation with thiosemicarbazide in the presence of acetic acid as catalyst. In addition, the appearance of most informative doublet signals around δ 6.81-6.77 ppm ($J = 16.53\text{ Hz}$) and 7.06-7.01 ($J = 16.84\text{ Hz}$) confirms the presence of olefinic protons.

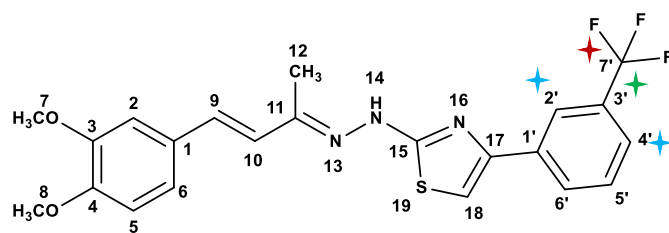
From the IR spectrum of the compounds **6a-6o**, it was observed that the disappearance of the characteristic bands due to NH_2 (N-H Str.) and C = S groups while the appearance of moderately strong peaks around $3332.78\text{-}3128.29\text{ cm}^{-1}$ and $1597.2\text{-}1551.13\text{ cm}^{-1}$, are attributed to the N-H and C = N groups respectively, indicating the formation of thiazole nucleus by Hantzsch cyclo-condensation reaction. The ^1H NMR spectrum (400 and 600 MHz, $\text{DMSO-}d_6$) of the final compounds (**6a-6o**) displayed some distinctive singlet signals at around δ 11.42-10.22 ppm for N-H proton, δ 7.21-7.20 for 2nd and δ 7.12-7.08 for 6th aromatic protons of DZG scaffold and δ 2.17-2.08 ppm for methyl ($\text{N} = \text{C-CH}_3$) protons respectively. In addition, the most informative singlet signal resonated around δ 7.70-7.31 ppm, which was attributed to the aromatic proton at H-5 of thiazole ring, thus indicating its formation through cyclo-condensation process. Whereas most characteristic doublet signals around δ 6.83-6.64 ppm ($J = 16.52\text{-}16.24\text{ Hz}$, $\text{Ph-HC}=\underline{\text{C}}\text{H-}$) and δ 7.57-6.91 ppm ($J = 16.52\text{-}14.76\text{ Hz}$, $\text{Ph-}\underline{\text{H}}\text{C}=\text{CH-}$) evidently indicated the presence of olefinic protons. This observation was found in consistent with previously reported similar type of compounds.³⁰ Further, the unique singlet signals resonating around δ 3.82-3.77 ppm indicated the presence of methoxyl protons (OCH_3) on the 3rd and 4th position of the DZG scaffold, while the hydroxyl (OH) protons on aromatic ring resonated as singlet signals around δ 11.24-10.86 ppm. The various signals appeared as either doublets or multiplets around δ 8.29-6.77 ppm accounted for aromatic protons. The *E*-configuration was ascertained for all final derivatives on the basis of 2D NMR studies. These findings were further corroborated from their respective ^{13}C NMR spectra of the title compounds. The characteristic signals resonated at around δ 169.53-156.50 and 108.52-102.10 ppm were assigned to carbons of C-2 and C-5 of thiazole ring. The

most prominent carbon signals observed around δ 149.27-148.91 and 132.56-126.23 ppm accounted for aromatic carbons having methoxyl groups and olefinic (Ph-H $\underline{C}=\underline{C}$ H-) carbons respectively. Further, the characteristic carbon signals appeared around δ 55.49-55.47 and 12.35-12.15 ppm indicated the presence of methoxyl and methyl groups in the title compounds, while the various aromatic carbons resonated around δ 140.78-108.03 ppm. Further, the fluorine containing compounds **6k** and **6m** have been discussed, which results in a very characteristic NMR spectra and the J_{CF} values are represented in **Table 1** (**Figure 4**) and **2** (**Figure 5**) In addition, the formation of title compounds (**6a-6o**) was also confirmed from their respective mass spectra (HRMS), which were in agreement with their anticipated molecular weights.

Table 1: Depiction of C-F coupling values for compound **6k**.³¹



Carbon number	J_{CF} values (in Hz)
5'	233.29
6'	24.76
4'	23.14
1'	7.74
3'	7.90
2'	1.99

Table 2: Depiction of C-F coupling values for compound **6m**.

Carbon number	J_{CF} values (in Hz)
7'	272.35
3'	31.13
2'	3.50
4'	3.96

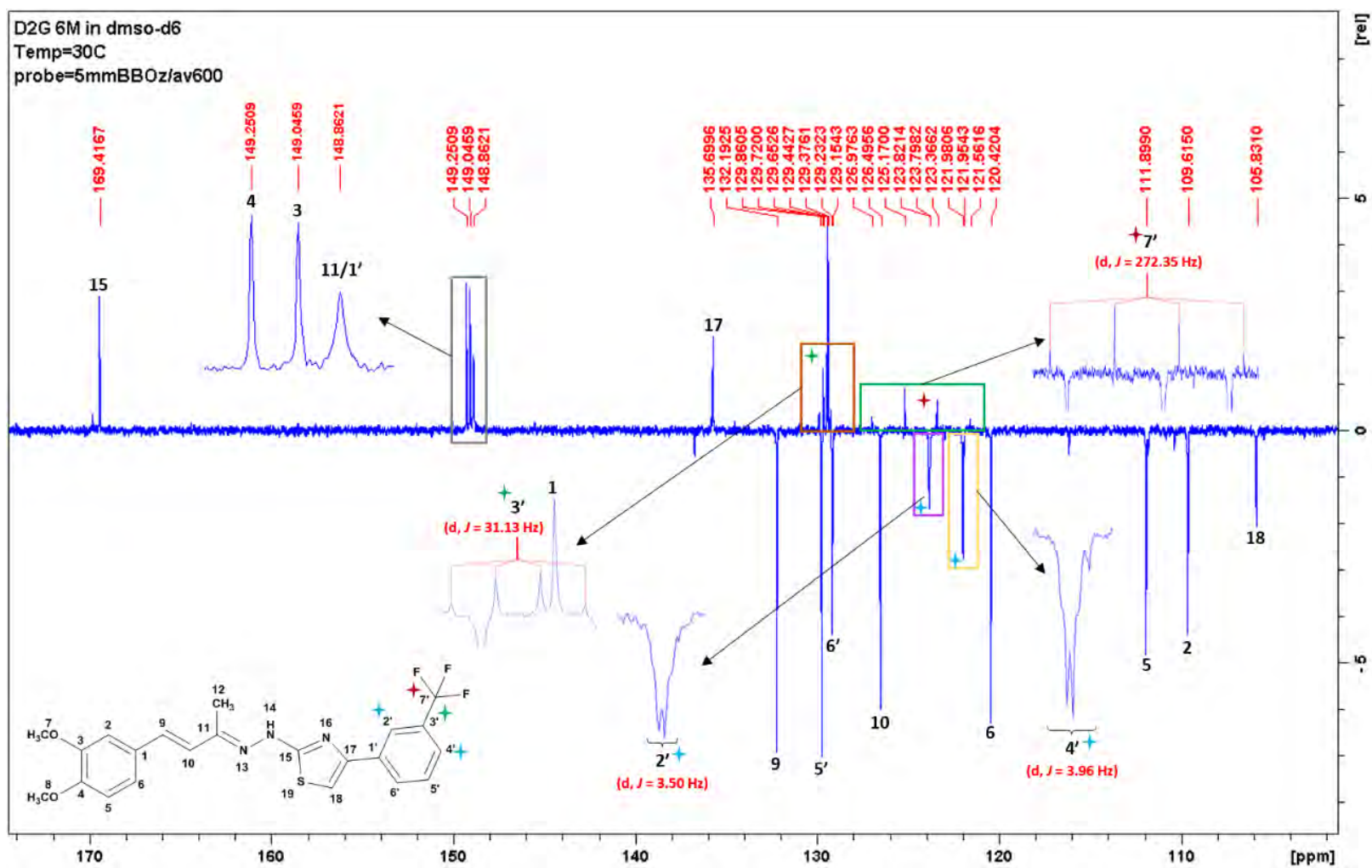


Figure 5: A section of the ^{13}C NMR spectrum (150.89 MHz) of compound 6m, illustrating C-F coupling.

3.2 Antimycobacterial activity

Both level I and II (*in vitro*) characterization of anti-mycobacterial activity of newly synthesized title compounds (**4**, **6a-6o**) was carried out at Infectious Disease Research Institute (IDRI) within the National Institute of Allergy and Infectious Diseases (NIAID) screening program, Bethesda, MD, USA. In the initial studies (level I), minimum inhibitory concentration (MIC) was established against Mtb strain H₃₇Rv grown under aerobic conditions by using a dual read-out (OD₅₉₀ and fluorescence) assay procedure. All the synthesized compounds exhibited an interesting and noteworthy activity profiles with MIC ranging from 1.5 to > 200 μ M against the tested mycobacterial strain (**Table 3**).

Table 3: Level I results under aerobic conditions for newly synthesized title compounds (**4** and **6a-6o**) against *M. tuberculosis* H₃₇Rv strain.

Compound	MIC (μ M) ^a	IC ₅₀ (μ M) ^b	IC ₉₀ (μ M) ^c
4	2.1	0.98	2.4
6a	> 200	> 25	> 25
6b	> 200	55	> 100
6c	> 200	> 200	> 200
6d	15	8.4	16
6e	> 50	20	> 50
6f	> 200	> 100	> 100
6g	16	7.4	16
6h	> 200	50	> 100
6i	28	6.6	13
6j	40	24	46
6k	> 200	66	> 200
6l	88	23	99
6m	> 200	> 200	> 200
6n	> 200	> 200	> 200
6o	1.5	0.48	1.5
Rifampicin	0.0067	0.0037	0.007

^aMIC is minimum inhibitory concentration at which *M. tuberculosis* H₃₇Rv growth was completely inhibited; ^bIC₅₀ value is the concentration at which growth is inhibited by 50%; ^cIC₉₀ value is the concentration at which growth is inhibited by 90%.

Interestingly, it was observed that compound **4** (MIC = 2.1 μ M) having thiourea group (without thiazole moiety) displayed encouraging anti-mycobacterial activity with an IC₅₀ value of 0.98 μ M. This evidently indicated that the DZG structural core has greatly contributed for anti-mycobacterial activity. This finding instigated us to explore brief SAR investigations in order to

study the biological effects of various substituents on aromatic ring at 4th position of the thiazole moiety, which was in turn attached to DZG scaffold through a hydrazine linkage. Amongst tested series, compound **6o** (MIC = 1.5 μ M) with *p*-amino (NH₂) group on phenyl ring at 4th position of thiazole moiety exhibited excellent anti-mycobacterial activity with IC₅₀ value of 0.48 μ M, whereas compounds **6d** (MIC = 15 μ M), **6g** (MIC = 16 μ M) and **6i** (MIC = 28 μ M) substituted with one or two methoxyl (OCH₃) groups on thiazolylphenyl ring exhibited good inhibitory activity with IC₅₀ value of 8.4, 7.4 and 6.6 μ M respectively. In the case of compounds **6j** (MIC = 40 μ M) and **6l** (MIC = 88 μ M) with hydroxyl (OH) group on phenyl ring displayed considerable anti-mycobacterial activity with IC₅₀ value of 24 μ M and 23 μ M respectively. These findings demonstrate that the thiazole core contributed for enhanced activity and plays significant role in the action against Mtb. The activity was also considerably affected by nature of substituent on phenyl ring at 4th position of the thiazole nucleus. Consistent with our prior report,²⁴ we found that the presence of electron donating (NH₂, OCH₃ and OH) groups on phenyl ring have greatly influenced and conferred good anti-mycobacterial activity while the electron withdrawing (CF₃, NO₂, F and Br) substituents have caused decrease in activity. Thus, compounds **6a**, **6c**, **6h** and **6m** having either nitro or halogen groups on phenyl ring were found to exhibit poor activity with MIC value > 200 μ M. (Figure 6). Compounds with promising anti-mycobacterial activity profile were further subjected for level II screening in order to evaluate their broad spectrum efficiency under assorted conditions against relevant drug resistant isolates of Mtb and other disease causing mycobacterial species.

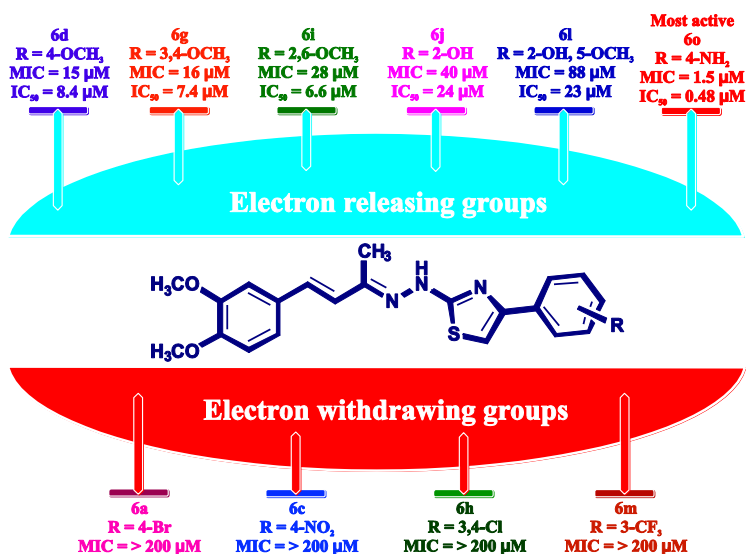


Figure 6: Illustration of anti-TB results against *M. tuberculosis* H₃₇Rv: Compounds with MIC values and varying substitution patterns.

The MIC of test compounds (**4**, **6d**, **6g**, **6i** and **6o**) was assessed against five drug resistant isolates (INH-R1, INH-R2, RIF-R1, RIF-R2 and FQ-R1) of Mtb strains under aerobic conditions. The anti-mycobacterial activity results are summarized in **Table 4**. Perusal of the data, we observed that all tested compounds showed excellent anti-mycobacterial activity against INH-R1 and INH-R2, while two compounds (**4** and **6o**) exhibited the most promising anti-mycobacterial activity against the tested organisms. In particular, both resistant strains (R1 and R2) of INH and RIF were found to be extremely susceptible to compounds **4** and **6o**, while these two compounds had an almost comparable activity with that of Levofloxacin against FQ-R1. As compared to reference drug INH (MIC = > 200 μ M; IC₅₀ = > 200 μ M), Compound **4** (MIC = 5.3 and 2.5 μ M; IC₅₀ = 1.3 and 0.79 μ M) and **6o** (MIC = 3.2 and 1.5 μ M; IC₅₀ = 0.68 and 0.38 μ M) displayed highest anti-mycobacterial activity against INH-R1 and INH-R2 respectively. In the case of RIF-R1 and RIF-R2, compound **6o** (MIC = 2.2 and 6.3 μ M; IC₅₀ = 0.54 and 0.76 μ M) exhibited significant antibacterial activity, whereas compounds **4** (MIC = 4 and 4.8 μ M; IC₅₀ = 1.1 and 1.2 μ M) showed moderate activity when compared to reference drug RIF (MIC = 2 and > 50 μ M; IC₅₀ = > 50 μ M). Nevertheless, the fluoroquinolone-resistant strain (FQ-R1) was found to be less susceptible to these compounds.

Table 4: Anti-mycobacterial activity data of newly synthesized compounds (**4**, **6d**, **6g**, **6i** and **6o**) against five drug-resistant isolates of *M. tuberculosis* H₃₇Rv.

Compound	INH-R1 ^a			INH-R2 ^b			RIF-R1 ^c			RIF-R2 ^d			FQ-R1 ^e		
	MIC (μM)	IC ₅₀ (μM)	IC ₉₀ (μM)	MIC (μM)	IC ₅₀ (μM)	IC ₉₀ (μM)	MIC (μM)	IC ₅₀ (μM)	IC ₉₀ (μM)	MIC (μM)	IC ₅₀ (μM)	IC ₉₀ (μM)	MIC (μM)	IC ₅₀ (μM)	IC ₉₀ (μM)
4	5.3	1.3	6.6	2.5	0.79	2.9	4	1.1	4.6	4.8	1.2	5.9	17	2.8	16
6d	15	12	> 50	12	8	> 50	25	11	> 50	31	8.7	> 50	22	23	> 50
6g	24	12	> 200	13	7.1	12	28	9.2	27	46	19	> 200	30	18	> 200
6i	32	9.1	> 25	19	5.6	> 25	17	7	19	41	10	> 25	33	13	> 25
6o	3.2	0.68	3.8	1.5	0.38	1.7	2.2	0.54	2.6	6.3	0.76	9.2	21	2.3	33
Rifampicin	0.018	0.0084	0.022	0.0065	0.0047	0.012	2	1.2	2.3	> 50	> 50	> 50	0.027	0.013	0.039
Isoniazid	> 200	> 200	> 200	> 200	> 200	> 200	0.17	0.15	0.21	0.62	0.54	0.6	0.35	0.36	0.47
Levofloxacin	1.2	0.64	1.4	1.4	0.84	1.4	0.76	0.59	0.91	1.1	0.6	1.2	20	12	22

^aINH-R1 was derived from H₃₇Rv and is a *katG* mutant (Y155* = truncation). ^bINH-R2 is strain ATCC35822. ^cRIF-R1 was derived from H₃₇Rv and is a *nrpoB* mutant (S522L). ^dRIF-R2 is strain ATCC35828. ^eFQ-R1 is a fluoroquinolone-resistant strain derived from H₃₇Rv and is a *gyrB* mutant (D94N). (INH – Isoniazid, RIF – Rifampicin and FQ – Fluoroquinolone)

In addition, these five promising compounds (**4**, **6d**, **6g**, **6i** and **6o**) were systematically assessed against Mtb H₃₇Rv grown under varied conditions. The antimicrobial activity of these compounds under hypoxic conditions was assessed using the low oxygen recovery assay (LORA). Further, the bactericidal (MBC: Minimum Bactericidal Concentration) activity of these compounds was assessed against Mtb H₃₇Rv grown in aerobic conditions in 7H9-Tw-OADC medium. The cytotoxicity and intracellular anti-mycobacterial activity of compounds was also determined using the THP-1 human monocytic cell line, and THP1 cells infected with Mtb respectively. The results of all these investigations are represented in **Table 5**. A systematic analysis of the data revealed that compound **4** and **6o** exhibited an interesting and potent anti-mycobacterial activity profile as depicted in **Figure 7**. All the five title compounds displayed an interesting cytotoxicity profile with IC₅₀ values ranging from 11 to > 50 µM. Among the series tested, compounds **6o** (IC₅₀ = 11 µM) and **6g** (IC₅₀ = 38 µM) showed moderate cytotoxicity, while other compounds did not show cytotoxic effect upto concentration > 50 µM. The existence of virulent intracellular Mtb in primary human macrophages compromise it's functioning and arrest phagosome maturation thus coping up with various host threats. The aptitude of the bacteria to assault and survive inside cells may be implicated for the persistence of TB. Therefore, it is of greater corollary for an effective tuberculosis management that these compounds should also be capable of killing intracellular TB in human macrophages, apart from their *in vitro* activity against TB strains. Accordingly, two compounds (**4** and **6o**) also displayed effective intracellular anti-mycobacterial activity with IC₅₀ value of < 0.098 µM. However, oxygen restriction also affects adaptive immune responses and triggers antimicrobial effector mechanisms in macrophages and restricts growth of intracellular Mtb.

Table 5: Bactericidal, cytotoxicity, intracellular and anti-mycobacterial activity of selected title compounds (**4**, **6d**, **6g**, **6i** and **6o**) against *M. tuberculosis* H₃₇Rv grown under various conditions.

Compound	Anti-mycobacterial activity						Minimum Bactericidal Concentration ^b (MBC, μ M)	Cytotoxicity ^c IC ₅₀ (μ M)	Intracellular Activity (against <i>M. tuberculosis</i>) ^d	
	Under Low Oxygen ^a			Under Normal Oxygen					IC ₅₀ (μ M)	IC ₉₀ (μ M)
	MIC (μ M)	IC ₅₀ (μ M)	IC ₉₀ (μ M)	MIC (μ M)	IC ₅₀ (μ M)	IC ₉₀ (μ M)				
4	29	0.19	2.1	0.50	0.15	0.27	8	> 50	< 0.098	< 0.098
6d	> 200	59	190	15	2.5	5.8	> 200	> 50	0.60	2.4
6g	> 200	52	> 200	17	2.2	5.9	85	38 [^]	0.47	1.3
6i	> 100	1.5	25	51	2.8	11	150	> 25	0.34	0.95
6o	46	0.063	1.5	0.28	0.097	0.16	12	11 [^]	< 0.098	< 0.098
Rifampicin	0.13 [#]	0.00041 [#]	0.0065 [#]	0.0096 [#]	0.00072 [#]	0.0025 [#]	ND	ND	ND	ND
Metronidazole	200 ^{\$}	29 ^{\$}	110 ^{\$}	> 200 ^{\$}	> 200 ^{\$}	> 200 ^{\$}	ND	ND	ND	ND
Staurosporine	ND	ND	ND	ND	ND	ND	ND	0.018	ND	ND
Isoniazid	ND	ND	ND	ND	ND	ND	ND	ND	0.23	0.29

^aOrganisms grown under hypoxic conditions were assessed using LORA assay; ^bOrganisms were grown under aerobic conditions in 7H9-Tw-OADC medium; ^cCytotoxicity was determined using the human monocytic (THP-1) cell line; ^dIntracellular activity was determined using THP1 infected with *M. tuberculosis*; [#]Calculated averages for rifampicin for each run (number of replicates 6); ^{\$}Metronidazole was run as a control once in each run; [^]compounds found to be cytotoxic; ND: Not determined.

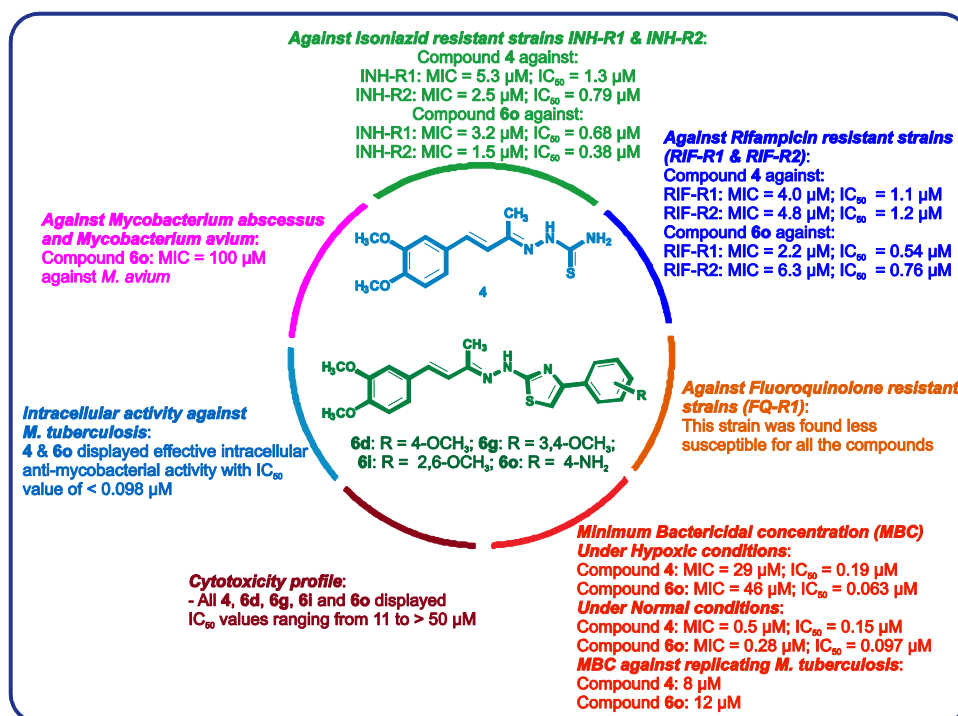


Figure 7: Anti-TB activity profile of most active compounds; **6d**: R = 4-OCH₃; **6g**: R = 3,4-OCH₃; **6i**: R = 2,6-OCH₃ and **6o**: 4-NH₂. The title compounds (**4**, **6d**, **6g**, **6i** and **6o**) were also evaluated for their *in vitro* anti-mycobacterial activity against other disease-relevant Mycobacterial species like *Mycobacterium abscessus* and *Mycobacterium avium* by using MABA method. (Table 6). The results reveal that compound **6o** (MIC = 100 μ M) demonstrated a moderate activity especially against *M. avium* as compared to the reference drug RIF (MIC = 0.1 μ M), while compound **6i** displayed a MIC of > 100 μ M against *M. abscessus* and *M. avium*. However, the remaining compounds showed little or poor activity (MIC = > 200 μ M) against tested organisms.

Table 6: Anti-mycobacterial activity of selected title compounds (**4**, **6d**, **6g**, **6i** and **6o**) against other disease-relevant Mycobacterial species.

Compound	<i>M. abscessus</i> ^a			<i>M. avium</i> ^b
	MIC (μ M)	IC ₅₀ (μ M)	IC ₉₀ (μ M)	MIC (μ M)
4	> 200	> 200	> 200	> 200
6d	> 200	> 200	> 200	> 200
6g	> 200	> 200	> 200	> 200
6i	> 100	> 100	> 100	> 100
6o	> 200	> 200	> 200	100
Rifampicin	3.3	2.1	3.1	0.1

^a*M. abscessus* subsp. *bollettii* 103; ^b*M. avium* subsp. *avium* 2285 (S)

4 Conclusion

In summary, in this work we established the synthesis of a series of styryl hydrazine thiazole hybrids derived from dehydrozingerone and their *in vitro* anti-TB activity. The ease, simply obtainable reactants and reagents, and practically good yields (51–74%) make this synthetic method more attractive and efficient. Moreover, compound **60** emerged as most promising anti-mycobacterial agent since it has demonstrated most prominent activity under hypoxic condition along with its potential efficiency against drug resistant isolates of Mtb strains and displayed significant bactericidal and intracellular anti-mycobacterial activity. These findings suggest that the designed compounds highlighted the benefit of incorporating a hydrazine linkage to combine styryl portion of DZG and thiazole core, thus providing a good starting point for further lead optimization. The possible enhancement in the anti-mycobacterial activity can be further accomplished by slender variation in the ring substituents and/or extensive additional functionalization warrants further investigations.

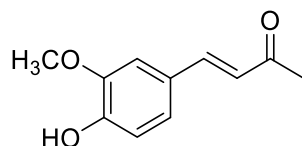
5 Experimental

5.1 Chemistry protocol

All the chemicals used in this research work were purchased from Sigma-Aldrich and Merck Millipore, South Africa. The commercially available chemicals 4-bromo-phenacyl bromide (**5a**) and phenacyl bromide (**5b**) were purchased from Sigma-Aldrich (South Africa). All the solvents, except those of laboratory-reagent grade, were dried and purified when necessary according to previously published methods. The progress of the reactions and the purity of the compounds were monitored by thin-layer chromatography (TLC) on pre-coated silica gel plates procured from E. Merck and Co. (Darmstadt, Germany) using 36% ethyl acetate in n-hexane as the mobile phase and iodine vapor as the visualizing agent.

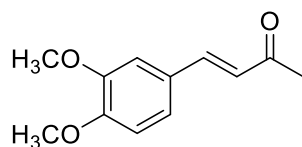
The melting points of the synthesized compounds were determined using a Thermo Fisher Scientific (IA9000, UK) digital melting point apparatus and are uncorrected. The IR spectra were recorded on a Bruker Alpha FT-IR spectrometer (Billerica, MA, USA) using the ATR technique. The ^1H NMR and ^{13}C NMR spectra were recorded on a Bruker AVANCE 400 and 600 MHz (Bruker, Rheinstetten/Karlsruhe, Germany) spectrometers using CDCl_3 and $\text{DMSO-}d_6$. The chemical shifts are reported in δ ppm units with respect to TMS as an internal standard. HRMS spectra were recorded on an Autospec mass spectrometer with electron impact at 70 eV.

5.1.1 Synthesis of (E)-4-(4-hydroxy-3-methoxyphenyl)but-3-en-2-one (2)³²



Vanillin (5 g, 0.033 mol) was dissolved in acetone (80 mL) to which, 50 mL NaOH (2.0 g, 0.25 mol) was slowly added with continuous stirring for 2-3 h. Excess acetone was removed under reduced pressure. Upon acidification with 0.1 N HCl, a yellow precipitate was obtained, which was extracted with CHCl₃ and the organic layer was dried over anhydrous sodium sulphate. Excess solvent was removed under reduced pressure and the yellow solid obtained was recrystallized from ethanol. Yield: 62%, mp: 127-129 °C; FTIR (ATR, V_{max} , cm⁻¹): 3280.90 (O-H Str.), 3052.25 (Ar-H Str.), 1672.37 (C=O Str.); ¹H NMR (400 MHz, DMSO-*d*₆, δ ppm): 9.61 (s, 1H, OH), 7.53-7.49 (d, J = 16.24 Hz, 1H, Ph-HC=CH-), 7.298-7.294 (d, J = 1.88 Hz, 1H, ArH), 7.14-7.11 (dd, J = 8.14, 1.90 Hz, 1H, ArH), 6.81-6.79 (d, J = 8.12 Hz, 1H, ArH), 6.68-6.64 (d, J = 16.28 Hz, 1H, Ph-HC=CH-), 3.81 (s, 3H, OCH₃), 2.28 (s, 3H, CH₃); ¹³C NMR (100 MHz, DMSO, δ ppm): 197.76 (C=O), 149.35, 147.91, 143.89, 125.81, 124.29, 123.20, 115.58, 111.23, 55.63 (OCH₃), 27.11 (CH₃).

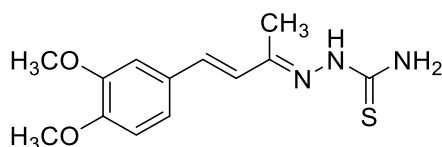
5.1.2 Synthesis of (E)-4-(3,4-dimethoxyphenyl)but-3-en-2-one (3)



To a stirred solution of compound **2** (2.0g, 0.010 mol, 1.0 Eq.) in *N,N*-dimethyl formamide (10 mL), K₂CO₃ (2.297 g, 0.017 mol, 1.6 Eq.) was added and refluxed at 80 °C for 90 min. To this reaction mass, methyl iodide (2.66 g, 0.019 mol, 1.8 Eq.) was slowly added and refluxed for 4-5 h. After completion of reaction (monitored on TLC), the reaction mixture was poured into ice cold water, and neutralized with dil. HCl. The solid precipitated was extracted with ethyl acetate (3 times X 15 mL) and the combined extract was dried over anhydrous sodium sulphate and concentrated under reduced pressure to obtain brown solid, which was recrystallized from ethanol to afford the desired compound (**3**), as light brown solid. Yield: 89%, mp: 81-82 °C; FTIR (ATR, V_{max} , cm⁻¹): 3046.27 (Ar-H Str.), 2935.28 (C-H Str. of CH₃), 1663.91 (C=O Str.); ¹H NMR (400 MHz, DMSO-*d*₆, δ ppm): 7.57-7.53 (d, J = 16.28 Hz, 1H, Ph-HC=CH-), 7.327-7.32 (d, J = 1.92 Hz, 1H, ArH), 7.26-7.23 (dd, J = 10.25, 1.92 Hz, 1H, ArH), 7.01-6.99 (d, J = 8.28 Hz, 1H, ArH), 6.75-6.71 (d, J = 16.24 Hz, 1H, Ph-HC=CH-), 3.80 (s, 3H, OCH₃), 3.79 (s, 3H, OCH₃), 2.30 (s,

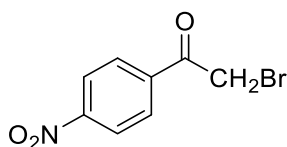
3H, CH₃); ¹³C NMR (100 MHz, DMSO, δ ppm): 197.86 (C=O), 150.98, 148.95, 143.50, 127.11, 125.17, 123.02, 111.56, 110.34, 55.53 (OCH₃), 27.16 (CH₃).

5.1.3 Synthesis of (E)-2-((E)-4-(3,4-dimethoxyphenyl)but-3-en-2-ylidene)hydrazine-1-carbothioamide (**4**)³³



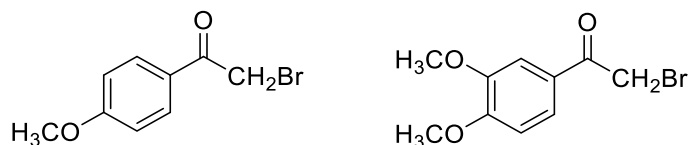
To a constantly stirred solution of compound **3** (2.0 g, 0.0097 mol, 1.0 Eq.) and thiosemicarbazide (0.972 g, 0.011 mol, 1.1 Eq.) in anhydrous methanol (20 mL), was added a catalytic quantity of glacial acetic acid (0.1 Eq.) and refluxed for 3-4 h. After completion of reaction (monitored on TLC), the reaction mass was allowed to cool to room temperature and the solid separated was filtered under suction. The residue was thoroughly washed with cold methanol to afford compound **4** as yellow crystalline solid. Yield: 85%, mp: 223-224 °C; FTIR (ATR, V_{max} , cm⁻¹): 3422.90 (N-H Str. of NH₂), 3212.08 (N-H Str. of NH), 3080.98 (Ar C-H Str.), 2943.75 (C-H Str. of CH₃), 1618.11 (C = N Str.), 1159.88 (C = S); ¹H NMR (400 MHz, DMSO-*d*₆, δ , ppm): 10.22 (s, 1H, NH), 8.22 (s, 1H, NH₂), 7.76 (s, 1H, NH₂), 7.154-7.150 (d, J = 1.80 Hz, 1H, ArH), 7.08-7.01 (m, 2H, ArH), 6.97-6.94 (d, J = 8.28 Hz, 1H, ArH), 6.81-6.77 (d, J = 16.52 Hz, 1H, Ph-HC=C $\underline{\text{H}}$ -), 3.79 (s, 3H, OCH₃), 3.76 (s, 3H, OCH₃), 2.11 (s, 3H, CH₃); ¹³C NMR (100 MHz, DMSO, δ , ppm): 178.47 (C = S), 150.05, 148.89, 146.04, 137.87, 129.11, 128.97, 121.81, 116.04, 111.74, 110.87, 55.47 (OCH₃), 19.97, 12.13 (CH₃); HRMS (ESI, m/z) [M-H]⁻; calculated for C₁₃H₁₆N₃O₂S, 278.0963; found 278.0965.

5.1.4 Synthesis of 2-bromo-1-(4-nitrophenyl)ethanone (**5c**)³⁴



To a stirring solution of 1-(4-nitrophenyl)ethanone (1.0 g, 0.0061 mol, 1.0 Eq.) in dry diethyl ether (20 mL) over ice bath, bromine (1.2 g, 0.372 mL, 0.0073 mol, 1.2 Eq.) dissolved in 10 mL of dry diethyl ether was slowly added in a drop-wise manner. The reaction mixture was further stirred for 2 h at room temperature. The mixture was evaporated under reduced pressure and the residue was washed with aqueous sodium bicarbonate to afford compound **5c** as yellow solid which was used without further purification. Yield: 68%; ¹H NMR (400 MHz, CDCl₃, δ , ppm): 8.35-8.33 (d, J = 8.80 Hz, 2H, ArH), 8.16-8.14 (d, J = 8.80 Hz, 2H, ArH), 4.45 (s, 2H, CH₂).

5.1.5 General procedure for synthesis of 2-bromo-1-(4-methoxyphenyl)ethanone (5d) and 2-bromo-1-(3,4-dimethoxyphenyl)ethanone (5g)³⁵



To a stirred solution of appropriately substituted acetophenones (1.0 g, 1.0 Eq.) in 10 mL of chloroform, bromine (1.2 Eq.) dissolved in 5 mL of chloroform was slowly added in a drop-wise manner. The mixture was stirred for additional 30 min, and then refluxed for 3h until TLC shows full consumption of starting materials. The mixture was evaporated under reduced pressure and the residue was washed with aqueous sodium bicarbonate and extracted with DCM which was further evaporated under reduced pressure to get desired products.

5.1.5.1 2-bromo-1-(4-methoxyphenyl)ethanone (5d):

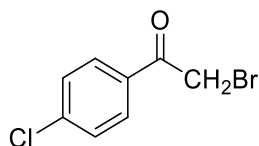
Dark brown solid, Yield: 62%; ¹H NMR (400 MHz, CDCl₃, δ, ppm): 7.97-7.95 (d, *J* = 8.88 Hz, 2H, ArH), 6.96-6.94 (d, *J* = 8.88 Hz, 2H, ArH), 4.39 (s, 2H, CH₂), 3.88 (s, 3H, OCH₃).

5.1.5.2 2-bromo-1-(3,4-dimethoxyphenyl)ethanone (5g):

Brown solid, Yield: 58%; ¹H NMR (400 MHz, CDCl₃, δ, ppm): 7.61-7.58 (dd, *J* = 8.22, 1.94 Hz, 1H, ArH), 7.53-7.52 (d, *J* = 1.84 Hz, 1H, ArH), 6.90-6.88 (d, *J* = 8.44 Hz, 1H, ArH), 4.39 (s, 2H, CH₂), 3.95 (s, 3H, OCH₃), 3.92 (s, 3H, OCH₃).

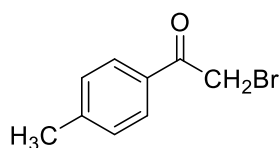
5.1.6 General procedure for synthesis of 2-bromo-1-(4-chlorophenyl)ethanone (5e) and 2-bromo-1-*p*-tolylethanone (5f)³⁶

To a stirred solution of appropriately substituted acetophenone (1.0 g, 1.0 Eq.) in 10 mL chloroform, bromine (1.0 Eq.) dissolved in 5 mL of chloroform was slowly added at 0 °C for a period of 15 minutes. The reaction mixture was further stirred at room temperature for 2 h. After completion of reaction (monitored on TLC), the mixture was evaporated under reduced pressure to obtain desired residue, which were used without further purification.



5.1.6.1 2-bromo-1-(4-chlorophenyl)ethanone (5e):

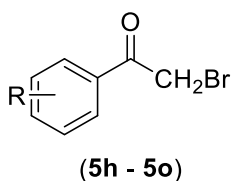
Light yellow solid, Yield: 73%; ¹H NMR (400 MHz, CDCl₃, δ, ppm): 7.93-7.91 (d, *J* = 8.52 Hz, 2H, ArH), 7.47-7.45 (d, *J* = 8.64 Hz, 2H, ArH), 4.40 (s, 2H, CH₂).



5.1.6.2 2-bromo-1-*p*-tolylethanone (**5f**):

Dark brown solid, Yield: 66%; $^1\text{H NMR}$ (400 MHz, CDCl_3 , δ , ppm): 7.94-7.92 (d, $J = 8.20$ Hz, 2H, ArH), 7.34-7.32 (d, $J = 8.04$ Hz, 2H, ArH), 4.47 (s, 2H, CH_2), 2.47 (s, 3H, CH_3).

5.1.7 General procedure for synthesis of substituted 2-bromo-1-phenylethanones (**5h-5o**)³⁷



5h: R = 3,4-Cl

5l: R = 2-OH, 5-OCH₃

5i: R = 2,6-OCH₃

5m: R = 3-CF₃

5j: R = 2-OH

5n: R = 2-OH, 5-Br

5k: R = 2-OH, 5-F

5o: R = 4-NH₂

To a hot solution of copper(II) bromide (1.07 g, 0.007 mol, 2 equiv.) in ethyl acetate (10 mL) was added a solution of appropriately substituted acetophenones (0.003 mol, 1 equiv.) in chloroform (10 mL) drop wise over 30 min. The reaction mixture was then refluxed for 12 h and cooled to room temperature; cuprous bromide (which turned to white indicating conversion of CuBr_2 into CuBr) was filtered through Celite bed. The filtrate was washed with saturated NaHCO_3 /brine solution and dried over anhydrous Na_2SO_4 . The resultant solution was concentrated under reduced pressure to afford the desired compounds (**5h-5o**).

5.1.7.1 2-bromo-1-(3,4-dichlorophenyl)ethanone (**5h**):

Brown liquid, Yield: 61%; $^1\text{H NMR}$ (400 MHz, CDCl_3 , δ , ppm): 8.06 (s, 1H, ArH), 7.81-7.79 (d, $J = 8.45$ Hz, 1H, ArH), 7.59-7.56 (d, $J = 8.32$ Hz, 1H, ArH), 4.38 (s, 2H, CH_2).

5.1.7.2 2-bromo-1-(2,6-dimethoxyphenyl)ethanone (**5i**):

Greenish yellow solid, Yield: 57%; $^1\text{H NMR}$ (400 MHz, CDCl_3 , δ , ppm): 7.32-7.28 (t, $J = 8.40$ Hz, 1H, ArH), 6.57 (s, 1H, ArH), 6.55 (s, 1H, ArH), 4.36 (s, 2H, CH_2), 3.80 (s, 6H, di-OCH₃).

5.1.7.3 2-bromo-1-(2-hydroxyphenyl)ethanone (**5j**):

Brown liquid, Yield: 54%; $^1\text{H NMR}$ (400 MHz, CDCl_3 , δ , ppm): 11.72 (s, 1H, OH), 7.54-7.52 (t, $J = 7.30$ Hz, 1H, ArH), 7.49-7.45 (t, $J = 7.20$ Hz, 1H, ArH), 7.03-7.01 (d, $J = 8.48$ Hz, 1H, ArH), 6.93-6.92 (d, $J = 7.32$, 1H, ArH), 4.44 (s, 2H, CH_2).

5.1.7.4 2-bromo-1-(5-fluoro-2-hydroxyphenyl)ethanone (5k):

Yellow crystalline solid, Yield: 66%; ¹H NMR (400 MHz, CDCl₃, δ, ppm): 11.40 (s, 1H, OH), 7.35-7.32 (d, *J* = 8.75 Hz, 1H, ArH), 7.20-7.18 (d, *J* = 8.48 Hz, 1H, ArH), 6.94-6.91 (m, 1H, ArH), 4.31 (s, 2H, CH₂).

5.1.7.5 2-bromo-1-(2-hydroxy-5-methoxyphenyl)ethanone (5l):

Yellowish brown solid, Yield: 58%; ¹H NMR (400 MHz, CDCl₃, δ, ppm): 11.36 (s, 1H, OH), 7.16 (s, 2H, ArH), 6.96-6.94 (d, *J* = 9.97 Hz, 1H, ArH), 4.44 (s, 2H, CH₂), 3.80 (s, 3H, OCH₃).

5.1.7.6 2-bromo-1-(3-(trifluoromethyl)phenyl)ethanone (5m):

Yellow liquid, Yield: 54%; ¹H NMR (400 MHz, CDCl₃, δ, ppm): 8.24 (s, 1H, ArH), 8.18-8.16 (d, *J* = 7.88 Hz, 1H, ArH), 7.88-7.86 (d, *J* = 7.92 Hz, 1H, ArH), 7.67-7.63 (t, *J* = 7.78 Hz, 1H, ArH), 4.45 (s, 2H, CH₂).

5.1.7.7 2-bromo-1-(5-bromo-2-hydroxyphenyl)ethanone (5n):

Yellowish brown solid, Yield: 61%; ¹H NMR (400 MHz, CDCl₃, δ, ppm): 11.63 (s, 1H, OH), 7.847-7.841 (d, *J* = 2.24 Hz, 1H, ArH), 7.60-7.57 (dd, *J* = 8.92, 2.24 Hz, 1H, ArH), 6.94-6.92 (d, *J* = 8.96 Hz, 1H, ArH), 4.40 (s, 2H, CH₂).

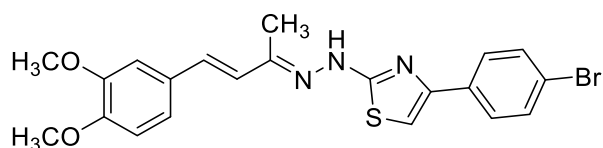
5.1.7.8 1-(4-aminophenyl)-2-bromoethanone (5o):

Light green liquid, Yield: 46%; ¹H NMR (400 MHz, CDCl₃, δ, ppm): 8.09-8.05 (m, 1H, ArH), 7.77-7.74 (m, 1H, ArH), 6.76-6.72 (m, 2H, ArH), 4.75 (s, 2H, NH₂), 4.32 (s, 2H, CH₂).

5.1.8 General procedure for synthesis of substituted 2-(2-((2*E*,3*E*)-4-(3,4-dimethoxyphenyl)but-3-en-2-ylidene)hydrazinyl)-4-phenylthiazoles (6a-6o)

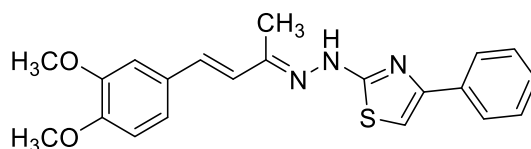
To a stirred solution of compound **4** (0.5 g, 0.0018 mol, 1.0 Eq.) in 10 mL anhydrous methanol, was added an appropriate 2-bromo-1-(substituted phenyl)-ethanones (**5a-5o**, 1.1 Eq.), and the reaction mixture was refluxed for 4-7 h until TLC showed full consumption of starting materials. The reaction mass was cooled to room temperature, thus formed residue was collected by filtration and was stirred in saturated NaHCO₃ solution for 15-30 min. This mixture was further extracted with dichloromethane (10 mL X 3 times). The combined organic layer was dried over anhydrous Na₂SO₄ and excess of solvent was evaporated under reduced pressure to yield the crude solids, which were further purified by recrystallization with ethanol to afford the desired title compounds (**6a-6o**).

5.1.8.1 2-(2-((2E,3E)-4-(3,4-dimethoxyphenyl)but-3-en-2-ylidene)hydrazinyl)-4-(4-bromophenyl)-thiazole (**6a**):



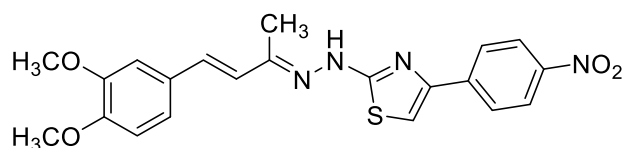
Off white solid, Yield: 74%, mp: 211-212 °C; FTIR (ATR, ν_{max} , cm^{-1}): 3266.13 (N-H Str.), 3110.36 (Ar-H Str.), 2969.62 (C-H Str. of CH_3), 1552.69 (C = N Str.); ^1H NMR (400 MHz, $\text{DMSO}-d_6$, δ , ppm): 11.16 (s, 1H, NH), 7.83-7.80 (d, $J = 8.52$ Hz, 2H, ArH), 7.60-7.58 (d, $J = 8.52$ Hz, 2H, ArH), 7.38 (s, 1H, H-5 of thiazole), 7.20 (s, 1H, H-2 of DZG), 7.11-7.08 (dd, $J = 8.34, 1.74$ Hz, 1H, ArH), 6.96-6.92 (m, $J = 7.36$ Hz, 2H, ArH), 6.81-6.77 (d, $J = 16.44$ Hz, 1H, Ph-HC=CH-), 3.82 (s, 3H, OCH_3), 3.77 (s, 3H, OCH_3), 2.15 (s, 3H, CH_3); ^{13}C NMR (100 MHz, DMSO , δ , ppm): 169.23 (C-2 of thiazole), 149.12, 148.93, 132.13, 131.49, 129.28, 127.52, 126.43, 120.43, 111.69, 109.31, 104.81 (C-5 of thiazole), 55.47 (OCH_3), 12.24 (CH_3); HRMS (ESI, m/z) [$\text{M}-\text{H}$]; calculated for $\text{C}_{21}\text{H}_{19}\text{BrN}_3\text{O}_2\text{S}$, 456.0381; found 456.0386.

5.1.8.2 2-(2-((2E,3E)-4-(3,4-dimethoxyphenyl)but-3-en-2-ylidene)hydrazinyl)-4-phenylthiazole (**6b**):



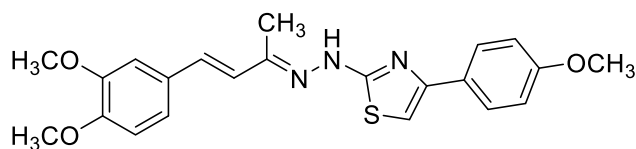
Brown solid, Yield: 69%, mp: 185-186 °C; FTIR (ATR, ν_{max} , cm^{-1}): 3270.64 (N-H Str.), 3078.43 (Ar-H Str.), 2932.94 (C-H Str. of CH_3), 1551.53 69 (C = N Str.); ^1H NMR (400 MHz, $\text{DMSO}-d_6$, δ , ppm): 11.13 (s, 1H, NH), 7.87-7.86 (d, $J = 7.32$ Hz, 2H, ArH), 7.41 (t, $J = 7.66$ Hz, 2H), 7.31 (s, 1H, H-5 of thiazole), 7.30-7.27 (m, 1H, ArH), 7.21 (s, 1H, H-2 of DZG), 7.11-7.08 (dd, $J = 8.30, 1.74$ Hz, 1H, ArH), 6.96-6.92 (m, 2H, ArH), 6.82-6.78 (d, $J = 16.41$ Hz, 1H, Ph-HC=CH-), 3.82 (s, 3H, OCH_3), 3.77 (s, 3H, OCH_3), 2.15 (s, 3H, CH_3); ^{13}C NMR (100 MHz, DMSO , δ , ppm): 169.11 (C-2 of thiazole), 149.10, 148.94, 131.96, 128.54, 127.42, 126.52, 125.49, 120.40, 111.68, 109.29, 103.92 (C-5 of thiazole), 55.47 (OCH_3), 54.85 (OCH_3), 48.56, 30.63, 12.23 (CH_3); HRMS (ESI, m/z) [$\text{M}-\text{H}$]; calculated for $\text{C}_{21}\text{H}_{20}\text{N}_3\text{O}_2\text{S}$, 378.1276; found 378.1288.

5.1.8.3 2-(2-((2E,3E)-4-(3,4-dimethoxyphenyl)but-3-en-2-ylidene)hydrazinyl)-4-(4-nitrophenyl)thiazole (**6c**):



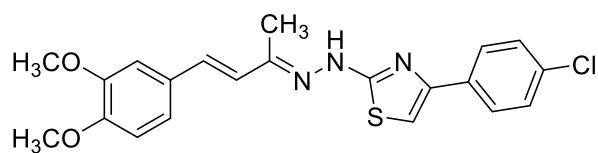
Yellowish brown solid, Yield: 64%, mp: 219-221 °C; FTIR (ATR, ν_{max} , cm^{-1}): 3332.78 (N-H Str.), 3056.92 (Ar-H Str.), 2960.57 (C-H Str. of CH_3), 1562.05 (C = N Str.); ^1H NMR (400 MHz, $\text{DMSO}-d_6$, δ , ppm): 11.28 (s, 1H, NH), 8.29-8.26 (d, $J = 8.84$ Hz, 2H, ArH), 8.13-8.11 (d, $J = 8.76$ Hz, 2H, ArH), 7.70 (s, 1H, H-5 of thiazole), 7.20 (s, 1H, H-2 of DZG), 7.11-7.09 (d, $J = 8.28$ Hz, 1H, ArH), 6.95-6.91 (m, 2H, ArH), 6.82-6.78 (d, $J = 16.40$ Hz, 1H, Ph-HC=C $\underline{\text{H}}$ -), 3.82 (s, 3H, OCH_3), 3.77 (s, 3H, OCH_3), 2.16 (s, 3H, CH_3); ^{13}C NMR (100 MHz, DMSO , δ , ppm): 169.53 (C-2 of thiazole), 149.16, 148.94, 140.79, 132.33, 129.24, 126.33, 126.28, 126.18, 124.07, 123.91, 120.46, 118.75, 111.67, 109.32, 108.52 (C-5 of thiazole), 55.47 (OCH_3), 54.85 (OCH_3), 48.56, 12.28 (CH_3).

5.1.8.4 2-(2-((2E,3E)-4-(3,4-dimethoxyphenyl)but-3-en-2-ylidene)hydrazinyl)-4-(4-methoxyphenyl)thiazole (**6d**):



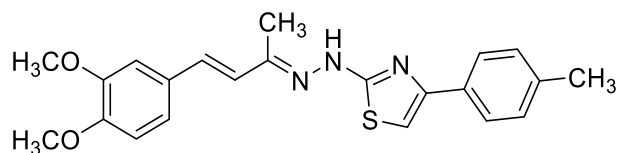
Brick red solid, Yield: 60%, mp: 211-212 °C; FTIR (ATR, ν_{max} , cm^{-1}): 3338.11 (N-H Str.), 3128.29 (Ar-H Str.), 2989.29 (C-H Str. of CH_3), 1573.83 (C = N Str.); ^1H NMR (400 MHz, $\text{DMSO}-d_6$, δ ppm): 11.12 (s, 1H, NH), 7.79-7.77 (d, $J = 8.76$ Hz, 1H, ArH), 7.52 (s, 1H, H-5 of thiazole), 7.20 (s, 1H, H-2 of DZG), 7.13-7.09 (m, 2H, ArH), 6.99-6.93 (m, 4H, ArH), 6.82-6.78 (d, $J = 16.41$ Hz, 1H, Ph-HC=C $\underline{\text{H}}$ -), 3.81 (s, 3H, OCH_3), 3.78 (s, 3H, OCH_3), 3.77 (s, 3H, OCH_3), 2.16 (s, 3H, CH_3); ^{13}C NMR (100 MHz, DMSO , δ , ppm): 168.87 (C-2 of thiazole), 149.10, 148.91, 148.63, 148.37, 131.89, 129.32, 126.51, 120.37, 117.97, 111.74, 111.71, 109.24, 55.43 (OCH_3), 54.86 (OCH_3), 12.20 (CH_3); HRMS (ESI, m/z) [$\text{M}-\text{H}$]; calculated for $\text{C}_{22}\text{H}_{22}\text{N}_3\text{O}_3\text{S}$, 408.1382; found 408.1387.

5.1.8.5 2-(2-((2*E*,3*E*)-4-(3,4-dimethoxyphenyl)but-3-en-2-ylidene)hydrazinyl)-4-(4-chlorophenyl)thiazole (**6e**):



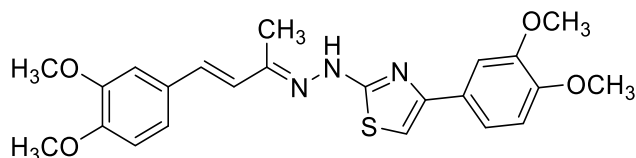
Yellow solid, Yield: 57%, mp: 217-220 °C; FTIR (ATR, ν_{max} , cm^{-1}): 3260.81 (N-H Str.), 3107.14 (Ar-H Str.), 2970.15 (C-H Str. of CH_3), 1551.13 (C = N Str.); ^1H NMR (400 MHz, $\text{DMSO-}d_6$, δ , ppm): 11.16 (s, 1H, NH), 7.89-7.87 (d, $J = 8.52$ Hz, 2H, ArH), 7.47-7.45 (d, $J = 8.52$ Hz, 2H, ArH), 7.37 (s, 1H, H-5 of thiazole), 7.20 (s, 1H, H-2 of DZG), 7.11-7.08 (dd, $J = 8.34, 1.50$ Hz, 1H, ArH), 6.96-6.92 (m, 2H, ArH), 6.81-6.77 (d, $J = 16.45$ Hz, 1H, Ph-HC=CH-), 3.82 (s, 3H, OCH_3), 3.77 (s, 3H, OCH_3), 2.15 (s, 3H, CH_3); ^{13}C NMR (100 MHz, DMSO , δ , ppm): 169.23 (C-2 of thiazole), 149.12, 148.94, 148.64, 133.67, 132.11, 131.82, 129.29, 128.58, 127.20, 126.44, 120.43, 111.69, 109.31, 104.74 (C-5 of thiazole), 55.47 (OCH_3), 54.87 (OCH_3), 30.65, 12.24 (CH_3); HRMS (ESI, m/z) [M-H]; calculated for $\text{C}_{21}\text{H}_{19}\text{ClN}_3\text{O}_2\text{S}$, 412.0887; found 412.0891.

5.1.8.6 2-(2-((2*E*,3*E*)-4-(3,4-dimethoxyphenyl)but-3-en-2-ylidene)hydrazinyl)-4-(*p*-tolyl)thiazole (**6f**):



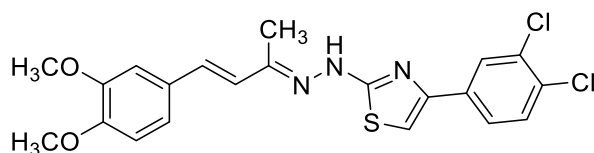
Yellow solid, Yield: 61%, mp: 223-225 °C; FTIR (ATR, ν_{max} , cm^{-1}): 3262.88 (N-H Str.), 3108.13 (Ar-H Str.), 2968.25 (C-H Str. of CH_3), 1552.29 (C = N Str.). ^1H NMR (400 MHz, $\text{DMSO-}d_6$, δ , ppm): 11.10 (s, 1H, NH), 7.76 (s, 1H, ArH), 7.74 (s, 1H, H-5 of thiazole), 7.21-7.20 (m, 4H, ArH), 7.11-7.09 (d, $J = 8.20$ Hz, 1H, ArH), 6.95-6.91 (m, 2H, ArH), 6.81-6.77 (d, $J = 16.45$ Hz, 1H, Ph-HC=CH-), 3.82 (s, 3H, OCH_3), 3.77 (s, 3H, OCH_3), 2.31 (s, 3H, CH_3), 2.15 (s, 3H, CH_3); ^{13}C NMR (100 MHz, DMSO , δ , ppm): 168.99 (C-2 of thiazole), 149.09, 148.94, 136.69, 131.93, 129.33, 129.12, 126.53, 125.45, 120.39, 111.69, 109.29, 103.00 (C-5 of thiazole), 55.47 (OCH_3), 54.87 (OCH_3), 30.65, 20.76 (CH_3), 12.21 (CH_3).

5.1.8.7 2-(2-((2E,3E)-4-(3,4-dimethoxyphenyl)but-3-en-2-ylidene)hydrazinyl)-4-(3,4-dimethoxyphenyl)thiazole (**6g**):



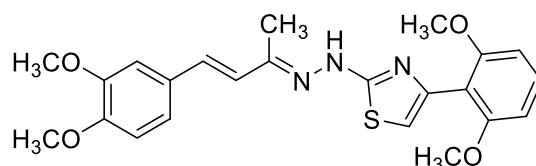
Brown solid, Yield: 54%, mp: 196-198 °C; FTIR (ATR, ν_{max} , cm^{-1}): 3266.42 (N-H Str.), 3112.80 (Ar-H Str.), 2963.85 (C-H Str. of CH_3), 1554.06 (C = N Str.); ^1H NMR (400 MHz, $\text{DMSO-}d_6$, δ , ppm): 11.10 (s, 1H, NH), 7.43 (s, 1H, ArH), 7.40 (s, 1H, H-5 of thiazole), 7.20 (s, 1H, H-2 of DZG), 7.17 (s, 1H, ArH), 7.11-7.08 (d, $J = 8.20$ Hz, 1H, ArH), 6.98-6.91 (m, 3H, ArH), 6.81-6.77 (d, $J = 16.49$ Hz, 1H, Ph-HC=CH-), 3.82 (s, 3H, OCH_3), 3.80 (s, 3H, OCH_3), 3.78 (s, 3H, OCH_3), 3.77 (s, 3H, OCH_3), 2.15 (s, 3H, CH_3); ^{13}C NMR (100 MHz, DMSO , δ , ppm): 168.91 (C-2 of thiazole), 149.09, 148.94, 148.68, 148.38, 131.88, 129.34, 126.56, 120.38, 117.95, 111.79, 111.70, 109.30, 102.10 (C-5 of thiazole), 55.47 (OCH_3), 54.88 (OCH_3), 12.22 (CH_3); HRMS (ESI, m/z) [M-H] $^-$; calculated for $\text{C}_{23}\text{H}_{24}\text{N}_3\text{O}_4\text{S}$, 438.1488; found 438.1494.

5.1.8.8 2-(2-((2E,3E)-4-(3,4-dimethoxyphenyl)but-3-en-2-ylidene)hydrazinyl)-4-(3,4-dichlorophenyl)thiazole (**6h**):



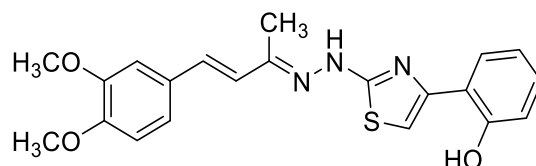
Off white solid, Yield: 63%, mp: 195-197 °C; FTIR (ATR, ν_{max} , cm^{-1}): 3255.29 (N-H Str.), 3113.15 (Ar-H Str.), 2963.17 (C-H Str. of CH_3), 1552.24 (C=N Str.); ^1H NMR (400 MHz, $\text{DMSO-}d_6$, δ , ppm): 11.18 (s, 1H, NH), 8.10 (s, 1H, ArH), 7.86-7.83 (dd, $J = 8.44, 1.80$ Hz, 1H, ArH), 7.67-7.65 (d, $J = 8.44$ Hz, 1H, ArH), 7.52 (s, 1H, H-5 of thiazole), 7.20 (s, 1H, H-2 of DZG), 7.11-7.09 (dd, $J = 8.22, 1.22$ Hz, 1H, ArH), 6.97-6.93 (m, 2H, ArH), 6.81-6.77 (d, $J = 16.45$ Hz, 1H, Ph-HC=CH-), 3.82 (s, 3H, OCH_3), 3.77 (s, 3H, OCH_3), 2.15 (s, 3H, CH_3); ^{13}C NMR (100 MHz, DMSO , δ , ppm): 169.30 (C-2 of thiazole), 149.15, 148.94, 132.26, 131.39, 130.83, 129.57, 129.26, 127.17, 126.36, 125.50, 120.46, 111.69, 109.32, 106.16 (C-5 of thiazole), 55.47 (OCH_3), 30.65, 12.25 (CH_3).

5.1.8.9 2-(2-((2E,3E)-4-(3,4-dimethoxyphenyl)but-3-en-2-ylidene)hydrazinyl)-4-(2,6-dimethoxyphenyl)thiazole (**6i**):



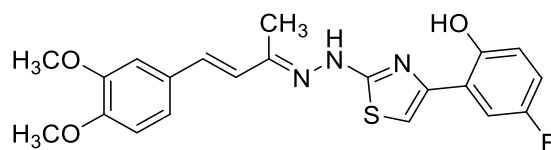
Yellow solid, Yield: 61%, mp: 158-160 °C; FTIR (ATR, ν_{max} , cm^{-1}): 3348.27 (N-H Str.), 3027.82 (Ar-H Str.), 2996.52 (C-H Str. of CH_3), 1556.20 (C = N Str.); ^1H NMR (400 MHz, $\text{DMSO-}d_6$, δ , ppm): 10.39 (s, 1H, NH), 7.48-7.44 (d, $J = 8.50$ Hz, 2H, ArH), 7.43 (s, 1H, H-5 of thiazole), 7.35-7.28 (m, 1H, ArH), 7.20 (s, 1H, H-2 of DZG), 7.11-7.08 (d, $J = 8.32$ Hz, 1H, ArH), 6.97-6.91 (m, 2H, ArH), 6.82-6.78 (d, $J = 16.49$ Hz, 1H, Ph-HC=C $\underline{\text{H}}$ -), 3.82 (s, 3H, OCH_3), 3.77 (s, 3H, OCH_3), 3.69 (s, 6H, 2 OCH_3), 2.13 (s, 3H, CH_3); ^{13}C NMR (100 MHz, DMSO , δ , ppm): 158.27 (C-2 of thiazole), 149.06, 148.94, 129.39, 126.72, 120.41, 111.69, 109.21, 104.40, 104.04 (C-5 of thiazole), 55.63 (OCH_3), 55.47 (OCH_3), 19.76, 12.24 (CH_3); HRMS (ESI, m/z) [M-H] $^-$; calculated for $\text{C}_{23}\text{H}_{24}\text{N}_3\text{O}_4\text{S}$, 438.1488; found 438.1503.

5.1.8.10 2-(2-((2E,3E)-4-(3,4-dimethoxyphenyl)but-3-en-2-ylidene)hydrazinyl)-4-(2-hydroxyphenyl)thiazole (**6j**):



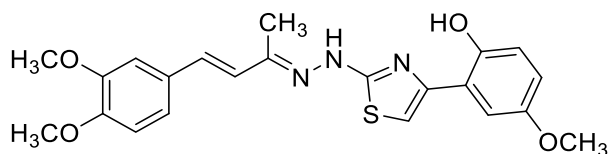
Yellow solid, Yield: 71%, mp: 200-202 °C; FTIR (ATR, ν_{max} , cm^{-1}): 3232.04 (N-H Str.), 3116.11 (Ar-H Str.), 2970.12 (C-H Str. of CH_3), 1555.60 (C = N Str.); ^1H NMR (400 MHz, $\text{DMSO-}d_6$, δ , ppm): 11.42 (s, 1H, NH), 11.24 (s, 1H, OH), 7.81-7.79 (d, $J = 7.20$ Hz, 1H, ArH), 7.38 (s, 1H, H-5 of thiazole), 7.21 (s, 1H, H-2 of DZG), 7.17-7.09 (m, 2H, ArH), 7.00-6.93 (m, 2H, ArH), 6.89-6.87 (d, $J = 8.08$, 1H, ArH), 6.86-6.79 (m, 2H, ArH), 3.82 (s, 3H, OCH_3), 3.77 (s, 3H, OCH_3), 2.17 (s, 3H, CH_3); ^{13}C NMR (100 MHz, DMSO , δ , ppm): 168.37 (C-2 of thiazole), 155.23, 149.20, 148.95, 132.53, 129.22, 128.95, 126.79, 126.26, 120.56, 119.01, 118.68, 116.86, 111.68, 109.31, 103.79 (C-5 of thiazole), 55.49 (OCH_3), 12.35 (CH_3); HRMS (ESI, m/z) [M-H] $^-$; calculated for $\text{C}_{21}\text{H}_{20}\text{N}_3\text{O}_3\text{S}$, 394.1225; found 394.1235.

5.1.8.11 2-(2-((2E,3E)-4-(3,4-dimethoxyphenyl)but-3-en-2-ylidene)hydrazinyl)-4-(2-hydroxy-5-fluorophenyl)thiazole (**6k**):



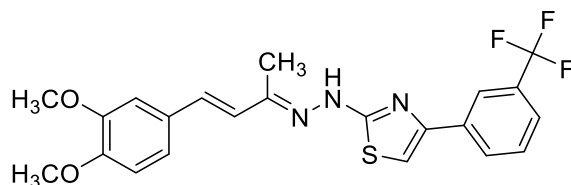
Off white solid, Yield: 69%, mp: 206-208 °C. FTIR (ATR, ν_{max} , cm^{-1}): 3234.72 (N-H Str.), 3118.93 (Ar-H Str.), 2994.14 (C-H Str. of CH_3), 1557.87 (C = N Str.). ^1H NMR (400 MHz, $\text{DMSO-}d_6$, δ , ppm): 11.24 (s, 1H, NH), 11.19 (s, 1H, OH), 7.68-7.64 (dd, $J = 10.20, 3.04$ Hz, 1H, ArH), 7.51 (s, 1H, H-5 of thiazole), 7.21 (s, 1H, H-2 of DZG), 7.12-7.09 (dd, $J = 8.22, 1.26$ Hz, 1H, ArH), 7.01-6.93 (m, 3H, ArH), 6.90-6.87 (m, 1H, ArH), 6.83-6.79 (d, $J = 16.44$ Hz, 1H, -HC=CH-), 3.82 (s, 3H, OCH_3), 3.77 (s, 3H, OCH_3), 2.16 (s, 3H, CH_3); ^{13}C NMR (100 MHz, DMSO , δ , ppm): 156.50 (C-2 of thiazole), 154.19, 151.49, 149.27, 149.20, 148.94, 146.85, 132.56, 129.21, 126.23, 120.55, 119.77, 119.69, 117.80, 117.71, 115.12, 112.75, 112.51, 111.68, 109.31, 105.66 (C-5 of thiazole), 55.48 (OCH_3), 12.34 (CH_3).

5.1.8.12 2-(2-((2E,3E)-4-(3,4-dimethoxyphenyl)but-3-en-2-ylidene)hydrazinyl)-4-(2-hydroxy-5-methoxyphenyl)thiazole (**6l**):



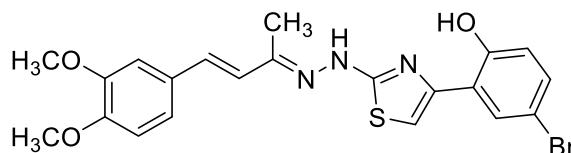
Light green solid, Yield: 66%, mp: 194-196 °C; FTIR (ATR, ν_{max} , cm^{-1}): 3212.30 (N-H Str.), 3118.69 (Ar-H Str.), 2952.72 (C-H Str. of CH_3), 1560.30 (C = N Str.); ^1H NMR (400 MHz, $\text{DMSO-}d_6$, δ , ppm): 11.21 (s, 1H, NH), 10.86 (s, 1H, OH), 7.45 (s, 1H, H-5 of thiazole), 7.38-7.37 (d, $J = 2.80$ Hz, 1H, ArH), 7.21 (s, 1H, H-2 of DZG), 7.12-7.09 (dd, $J = 8.36, 1.68$ Hz, 1H, ArH), 6.99-6.95 (d, $J = 16.32$ Hz, 1H, -HC=CH-), 6.93 (s, 1H, ArH), 6.83-6.77 (m, 3H, ArH), 3.82 (s, 3H, OCH_3), 3.77 (s, 3H, OCH_3), 3.72 (s, 3H, OCH_3), 2.16 (s, 3H, CH_3); ^{13}C NMR (100 MHz, DMSO , δ , ppm): 168.70 (C-2 of thiazole), 168.30, 151.99, 149.98, 149.27, 149.18, 148.94, 132.45, 129.23, 126.29, 120.53, 118.95, 117.47, 115.31, 111.69, 111.10, 109.29, 104.54 (C-5 of thiazole), 55.48 (OCH_3), 12.34 (CH_3); HRMS (ESI, m/z) $[\text{M-H}]^-$; calculated for $\text{C}_{22}\text{H}_{22}\text{N}_3\text{O}_4\text{S}$, 424.1331; found 424.1335.

5.1.8.13 2-(2-((2E,3E)-4-(3,4-dimethoxyphenyl)but-3-en-2-ylidene)hydrazinyl)-4-(3-(trifluoromethyl)phenyl)thiazole (**6m**):



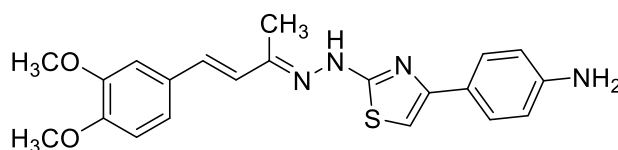
Light brown solid, Yield: 63%, mp: 200-202 °C; FTIR (ATR, ν_{max} , cm^{-1}): 3253.43 (N-H Str.), 3112.11 (Ar-H Str.), 2958.90 (C-H Str. of CH_3), 1556.72 (C = N Str.); ^1H NMR (400 MHz, $\text{DMSO-}d_6$, δ , ppm): 11.20 (s, 1H, NH), 8.22 (s, 1H, ArH), 8.17-8.15 (t, $J = 3.74$ Hz, 1H, ArH), 7.65-7.64 (d, $J = 5.04$ Hz, 1H, ArH), 7.56 (s, 1H, H-5 of thiazole), 7.21 (s, 1H, H-2 of DZG), 7.11-7.09 (dd, $J = 1.70, 8.34$ Hz, 1H, ArH), 6.97-6.93 (m, $J = 8.52$ Hz, 2H, ArH), 6.82-6.78 (d, $J = 16.41$ Hz, 1H, -HC=CH-), 3.82 (s, 3H, OCH_3), 3.77 (s, 3H, OCH_3), 2.16 (s, 3H, CH_3); ^{13}C NMR (100 MHz, $\text{DMSO-}d_6$, δ , ppm): 169.36 (C-2 of thiazole), 149.14, 148.94, 135.66, 132.22, 129.73, 129.63, 129.32, 129.27, 129.14, 126.39, 125.60, 123.80, 121.91, 120.45(CF_3), 111.69, 109.32, 105.87 (C-5 of thiazole), 55.48 (OCH_3), 30.64, 12.25 (CH_3).

5.1.8.14 2-(2-((2E,3E)-4-(3,4-dimethoxyphenyl)but-3-en-2-ylidene)hydrazinyl)-4-(2-hydroxy-5-bromophenyl)thiazole (**6n**):



Yellow solid, Yield: 72%, mp: 201-203 °C; FTIR (ATR, ν_{max} , cm^{-1}): 3229.53 (N-H Str.), 3118.13 (Ar-H Str.), 2957.03 (C-H Str. of CH_3), 1560.50 (C = N Str.); ^1H NMR (400 MHz, $\text{DMSO-}d_6$, δ , ppm): 11.33 (s, 1H, NH), 11.21 (s, 1H, OH), 8.06-8.05 (d, $J = 2.56$ Hz, 1H, ArH), 7.53 (s, 1H, H-5 of thiazole), 7.29-7.26 (dd, $J = 8.62, 2.54$ Hz, 1H, ArH), 7.21 (s, 1H, H-2 of DZG), 7.12-7.09 (dd, $J = 8.28, 1.72$ Hz, 1H, ArH), 6.99-6.95 (d, $J = 15.97$ Hz, 1H, -HC=CH-), 6.93 (s, 1H, ArH), 6.88-6.86 (d, $J = 8.60$, 1H, ArH), 6.82-6.78 (d, $J = 16.40$ Hz, 1H, -HC=CH-), 3.82 (s, 3H, OCH_3), 3.77 (s, 3H, OCH_3), 2.16 (s, 3H, CH_3); ^{13}C NMR (100 MHz, DMSO , δ , ppm): 168.18 (C-2 of thiazole), 154.42, 149.19, 149.10, 148.94, 132.48, 129.44, 129.23, 126.26, 121.50, 120.54, 118.84, 111.69, 110.25, 109.31, 106.17 (C-5 of thiazole), 55.49 (OCH_3), 30.65, 12.30 (CH_3).

5.1.8.15 2-(2-((2E,3E)-4-(3,4-dimethoxyphenyl)but-3-en-2-ylidene)hydrazinyl)-4-(4-aminophenyl)thiazole (**6o**):



Brown solid, Yield: 51%, mp: 200-202 °C; FTIR (ATR, ν_{max} , cm^{-1}): 3406.31 ((N-H Str. of NH_2), 3260.19 (N-H Str.), 3154.51 (Ar-H Str.), 2964.45 (C-H Str. of CH_3), 1597.20 (C=N Str.); ^1H NMR (400 MHz, $\text{DMSO-}d_6$, δ , ppm): 10.22 (s, 1H, NH), 8.22 (s, 1H, ArH), 7.75 (s, 2H, NH_2), 7.15-6.94 (m, 7H, ArH), 6.81-6.77 (d, $J = 16.52$ Hz, 2H, $-\text{HC}=\text{CH}-$), 3.79 (s, 3H, OCH_3), 3.77 (s, 3H, OCH_3), 2.08 (s, 3H, CH_3); ^{13}C NMR (100 MHz, DMSO , δ , ppm): 149.10, 148.91, 126.80, 120.44, 111.74, 109.23, 79.26, 78.93, 78.60, 55.49 (OCH_3), 12.15 (CH_3).

5.2 Biological protocols (*In vitro* anti-mycobacterial activity characterization)

5.2.1 MIC under aerobic conditions³⁸⁻⁴⁰

The *in vitro* anti-mycobacterial activity of synthesized title compounds (**6a-6o**) was carried out at Infectious Disease Research Institute (IDRI) within the National Institute of Allergy and Infectious Diseases (NIAID) screening program, Bethesda, MD, USA. The activity was assessed against *Mycobacterium tuberculosis* H₃₇Rv grown under aerobic conditions by using a dual read-out (OD_{590} and fluorescence) assay procedure. Test compounds (**4** and **6a-6o**) were prepared as 20-point two-fold serial dilutions in DMSO and diluted into 7H9-Tw-OADC medium in 96-well plates with a final DMSO concentration of 2%. The highest concentration of compound was 200 μM where compounds were soluble in DMSO at 10 mM. For compounds with limited solubility, the highest concentration was 50X less than the stock concentration e.g. 100 μM for 5 mM DMSO stock, 20 μM for 1 mM DMSO stock. Each plate included assay controls for background (medium/DMSO only, no bacterial cells), zero growth (100 μM rifampicin) and maximum growth (DMSO only), as well as a rifampicin dose response curve. Plates were inoculated with *Mycobacterium tuberculosis* (Mtb) and incubated for 5 days. Growth was measured by OD_{590} and fluorescence (Ex 560/Em 590) using a BioTek™ Synergy 4 plate reader. Growth was calculated separately for OD_{590} and RFU. To calculate the MIC, the dose response curve was plotted as % growth and fitted to the Gompertz model using GraphPad Prism 5. The MIC was defined as the minimum concentration at which growth was completely inhibited and was calculated from the inflection point of the fitted curve to the lower asymptote (zero growth). In addition, dose response curves were generated using the Levenberg-Marquardt algorithm and the concentrations that

resulted in 50% and 90% inhibition of growth were determined (IC₅₀ and IC₉₀ respectively). (Table 3)

5.2.2 MIC under hypoxic (low) oxygen condition⁴¹

Test compounds (**4**, **6d**, **6g**, **6i** and **6o**) were prepared as 20-point two-fold serial dilutions in DMSO and diluted into DTA medium in 96-well plates with a final DMSO concentration of 2%. The highest concentration of compound was 200 µM where compounds were soluble in DMSO at 10 mM. For compounds with limited solubility, the highest concentration was 50X less than the stock concentration e.g. 100 µM for 5 mM DMSO stock, 20 µM for 1 mM DMSO stock. Control compounds were prepared as two-fold serial dilutions in DMSO and diluted into DTA medium in 96-well plates with a final DMSO concentration of 2%. Mtb constitutively expressing the *luxABCDE* operon was inoculated into DTA medium in gas-impermeable glass tubes and incubated for 18 days to generate hypoxic conditions (Wayne model of hypoxia). At this point, bacteria are in a non-replicating state (NRP stage 2) induced by oxygen depletion. Oxygen-deprived bacteria were inoculated into compound assay plates and incubated under anaerobic conditions for 10 days followed by incubation under aerobic conditions (outgrowth) for 28 h. Growth was measured by luminescence. Oxygen-deprived bacteria were also inoculated into compound assay plates and incubated under aerobic conditions for 5 days. Growth was measured by luminescence. Rifampicin was included in each plate and metronidazole was included in each run as positive controls for aerobic and anaerobic killing of Mtb, respectively.

5.2.3 Minimum Bactericidal Concentration (MBC) determination

Mtb was grown aerobically to logarithmic phase and inoculated into liquid medium containing four different compound concentrations with a final maximum concentration of 2% DMSO. For test compounds (**4**, **6d**, **6g**, **6i** and **6o**) with MIC < 20 µM, the concentration selected were 10X MIC, 5X MIC, 1X MIC and 0.25X MIC. Cultures were exposed to compounds for 21 days and cell viability measured by enumerating colony forming units on agar plates on day 0, 7, 14 and 21. MBC was defined as the minimum concentration required to achieve a 2-log kill in 21 days. For compounds with > 1-log kill, an assessment of time and/or concentration-dependence was determined from the kill kinetics. DMSO was used as a positive control for growth.

5.2.4 Intracellular activity assay⁴²

The intracellular activity of compounds was measured using THP1 human monocytic cell line infected with Mtb. THP-1 cells were differentiated into macrophage-like cells using PMA and infected with bacteria. Infected cells were exposed to compounds for 72 hours. Viable bacterial counts were measured using luminescence as a measure of growth.

The activity of compounds against intracellular bacteria was determined by measuring viability in infected THP-1 cell after 3 days in the presence of test compounds. Test compounds (**4**, **6d**, **6g**, **6i** and **6o**) were prepared as 10-point three-fold serial dilutions in DMSO. The highest concentration of compound tested was 50 μ M where compounds were soluble in DMSO at 10 mM. For compounds with limited solubility, the highest concentration was 200X less than the stock concentration e.g. 25 μ M for 5 mM DMSO stock, 5 μ M for 1 mM DMSO stock. THP-1 cells were cultured in incomplete RPMI and differentiated into macrophage-like cells using 80 nM PMA overnight at 37 °C, 5% CO₂. THP-1 cells were infected with a luminescent strain of H₃₇Rv (which constitutively expresses *luxABCDE*) at a multiplicity of infection of 1 and incubated overnight at 37 °C, 5% CO₂. Infected cells were recovered using Accutase/EDTA solution, washed twice with PBS to remove extracellular bacteria and seeded into assay plates. Compound dilutions were added to a final DMSO concentration of 0.5%. Assay plates were incubated for 72 h at 37 °C, 5% CO₂. Each run included isoniazid as a control. Relative luminescent units (RLU) were measured using a Biotek Synergy 2 plate reader. The dose response curve was fitted using the Levenberg–Marquardt algorithm. The IC₅₀ and IC₉₀ were defined as the compound concentrations that produced 50% and 90% inhibition of growth respectively.

5.2.5 Cytotoxicity assay⁴²

The cytotoxicity of compounds towards eukaryotic cells was determined using the THP-1 human monocytic cell line. THP-1 cells were differentiated into macrophage-like cells using PMA and incubated with compounds for 3 days and cell viability was measured. The IC₅₀ was determined as the concentration of compound causing a 50% loss in viability.

The cytotoxicity of compounds was determined by measuring THP-1 cell viability after 3 days in the presence of test compounds. Test compounds (**4**, **6d**, **6g**, **6i** and **6o**) were prepared as 10-point three-fold serial dilutions in DMSO. The highest concentration of compound tested was 50 μ M where compounds were soluble in DMSO at 10 mM. For compounds with limited solubility, the highest concentration was 200X less than the stock concentration e.g. 25 μ M for 5 mM DMSO stock, 5 μ M for 1 mM DMSO stock. Each plate included staurosporine as a control. THP-1 cells were cultured in incomplete RPMI and differentiated into macrophage-like cells using 80 nM PMA overnight at 37 °C, 5% CO₂. Cells were inoculated into assay plates and cultured for 24 h before compound dilutions were added to a final DMSO concentration of 0.5%. Each run included staurosporine as a control. Assay plates were incubated for 3 days at 37 °C, 5% CO₂; growth was measured using the CellTiter-Glo[®] Luminescent Cell Viability Assay (Promega) which uses ATP as an indicator of cell viability. Relative luminescent units (RLU) were measured using a Biotek Synergy 4 plate reader. The dose response curve was fitted using the Levenberg–Marquardt

algorithm. The IC₅₀ was defined as the compound concentration that produced 50% inhibition of growth.

5.2.6 MIC against drug resistant isolates of *M. tuberculosis*⁴⁰

The MIC of compound was determined by measuring bacterial growth after 5 days in the presence of test compounds. Test compounds (**4**, **6d**, **6g**, **6i** and **6o**) were prepared as 10-point two-fold serial dilutions in DMSO and diluted into 7H9-Tw-OADC medium in 96-well plates with a final DMSO concentration of 2%. The highest concentration of compound was 200 µM where compounds were soluble in DMSO at 10 mM. For compounds with limited solubility, the highest concentration was 50X less than the stock concentration e.g. 100 µM for 5 mM DMSO stock, 20 µM for 1 mM DMSO stock. Each plate included assay controls for background (medium/DMSO only, no bacterial cells), zero growth (100 µM rifampicin) and maximum growth (DMSO only), as well as a rifampicin dose response curve. Plates were inoculated with drug resistant isolates of Mtb and incubated for 5 days; growth was measured by OD₅₉₀. To calculate the MIC, the 10-point dose response curve was plotted as % growth and fitted to the Gompertz model using GraphPad Prism 5. The MIC was defined as the minimum concentration at which growth was completely inhibited and was calculated from the inflection point of the fitted curve to the lower asymptote (zero growth). In addition, dose response curves were generated using the Levenberg-Marquardt algorithm and the concentrations that resulted in 50% and 90% inhibition of growth were determined (IC₅₀ and IC₉₀ respectively). (Table 5)

5.2.7 MIC against other disease-relevant *Mycobacteria* species^{40,43}

The MIC of compound was determined by measuring bacterial growth in the presence of test compounds. Test compounds (**4**, **6d**, **6g**, **6i** and **6o**) were prepared as 20-point two-fold serial dilutions in DMSO and diluted into 7H9-Tw-OADC medium in 96-well plates with a final DMSO concentration of 2%. The highest concentration of compound was 200 µM where compounds were soluble in DMSO at 10 mM. For compounds with limited solubility, the highest concentration was 50X less than the stock concentration e.g. 100 µM for 5 mM DMSO stock, 20 µM for 1 mM DMSO stock. Each plate included assay controls for background (medium/DMSO only, no bacterial cells), zero growth (100 µM rifampicin) and maximum growth (DMSO only), as well as a rifampicin dose response curve. (Table 6)

Mycobacterium abscessus

Plates were inoculated with *M. abscessus* and incubated for 3 days at 37 °C; growth was measured by OD₅₉₀. To dose response curve was plotted as % growth and fitted to the Gompertz model. The MIC was defined as the minimum concentration at which growth was completely inhibited and

was calculated from the inflection point of the fitted curve to the lower asymptote (zero growth). In addition, dose response curves were generated using the Levenberg-Marquardt algorithm and the concentrations that resulted in 50% and 90% inhibition of growth were determined (IC₅₀ and IC₉₀ respectively). Rifampicin was included once in each run.

Mycobacterium avium

Plates were inoculated with *M. avium*, incubated for 5 days at 37 °C and Alamar blue was added to each well (10 µL of Alamar blue to 100 µL culture) and incubated for 24 h at 37 °C. Plates were visually inspected and the color recorded for each well. MIC was defined as the lowest concentration at which no metabolic activity was seen (blue well).

References

- (1) Herzog, H. History of Tuberculosis. *Respiration* **1998**, *65* (1), 5–15.
- (2) Collins, F. M. Mycobacterial Pathogenesis: A Historical Perspective. *Front. Biosci.* **1998**, *3*, e123-132.
- (3) World Health Organization. *Global Tuberculosis Report 2014 (WHO/HTM/TB/2014.08)*; 2014.
- (4) Bloom, B. R. *Tuberculosis: Pathogenesis, Protection, and Control*; Bloom, B. R., Ed.; ASM Press, 1994, 1994.
- (5) Chung, H. S.; Shin, J. C. Characterization of Antioxidant Alkaloids and Phenolic Acids from Anthocyanin-Pigmented Rice (*Oryza Sativa* Cv. Heugjinjubyeo). *Food Chem.* **2007**, *104* (4), 1670–1677.
- (6) Guzman, J. Natural Cinnamic Acids, Synthetic Derivatives and Hybrids with Antimicrobial Activity. *Molecules* **2014**, *19* (12), 19292–19349.
- (7) Bezerra, D. P.; Castro, F. O.; Alves, a. P. N. N.; Pessoa, C.; Moraes, M. O.; Silveira, E. R.; Lima, M. a S.; Elmiro, F. J. M.; Costa-Lotufo, L. V. In Vivo Growth-Inhibition of Sarcoma 180 by Piplartine and Piperine, Two Alkaloid Amides from Piper. *Brazilian J. Med. Biol. Res.* **2006**, *39* (6), 801–807.
- (8) Rastogi, N.; Goh, K. S.; Wright, E. L.; Barrow, W. W. Potential Drug Targets for Mycobacterium Avium Defined by Radiometric Drug-Inhibitor Combination Techniques. *Antimicrob. Agents Chemother.* **1994**, *38* (10), 2287–2295.
- (9) Reddy, V. M.; Nadadhur, G.; Daneluzzi, D.; Dimova, V.; Gangadharam, P. R. Antimycobacterial Activity of a New Rifamycin Derivative, 3-(4-Cinnamylpiperazinyl Iminomethyl) Rifamycin SV (T9). *Antimicrob. Agents Chemother.* **1995**, *39* (10), 2320–2324.
- (10) Prithwiraj De, Damien Veau, Florence Bedos-Belval, S. C. and M. B. *Cinnamic Derivatives in Tuberculosis, Understanding Tuberculosis - New Approaches to Fighting Against Drug Resistance*; Cardona, P.-J., Ed.; InTech, 2012.
- (11) Bairwa, R.; Kakwani, M.; Tawari, N. R.; Lalchandani, J.; Ray, M. K.; Rajan, M. G. R.; Degani, M. S. Novel Molecular Hybrids of Cinnamic Acids and Guanylhydrazones as Potential Antitubercular Agents. *Bioorg. Med. Chem. Lett.* **2010**, *20* (5), 1623–1625.
- (12) Joshi, D. G.; Oza, H. B.; Parekh, H. H. Synthesis of Some Novel 1,3,4-Oxadlazoles and 5-Oxo-Imidazolines as Potent Biologically Active Agents. *Heterocycl. Commun.* **1997**, *3* (2), 169–174.
- (13) Bakkestuen, A. K.; Gundersen, L.-L.; Langli, G.; Liu, F.; Nolsøe, J. M. . 9-Benzylpurines with Inhibitory Activity against Mycobacterium Tuberculosis. *Bioorg. Med. Chem. Lett.*

- 2000, *10* (11), 1207–1210.
- (14) Carvalho, S. A.; da Silva, E. F.; de Souza, M. V. N.; Lourenço, M. C. S.; Vicente, F. R. Synthesis and Antimycobacterial Evaluation of New Trans-Cinnamic Acid Hydrazone Derivatives. *Bioorg. Med. Chem. Lett.* **2008**, *18* (2), 538–541.
- (15) De, P.; Koumba Yoya, G.; Constant, P.; Bedos-Belval, F.; Duran, H.; Saffon, N.; Daffé, M.; Baltas, M. Design, Synthesis, and Biological Evaluation of New Cinnamic Derivatives as Antituberculosis Agents. *J. Med. Chem.* **2011**, *54* (5), 1449–1461.
- (16) Rastogi, N.; Goh, K. S.; Horgen, L.; Barrow, W. W. Synergistic Activities of Antituberculous Drugs with Cerulenin and Trans -Cinnamic Acid against Mycobacterium Tuberculosis. *FEMS Immunol. Med. Microbiol.* **1998**, *21* (2), 149–157.
- (17) Shingalapur, R. V.; Hosamani, K. M.; Keri, R. S. Synthesis and Evaluation of in Vitro Anti-Microbial and Anti-Tubercular Activity of 2-Styryl Benzimidazoles. *Eur. J. Med. Chem.* **2009**, *44* (10), 4244–4248.
- (18) Babu, R. R.; Naresh, K.; Ravi, A.; Madhava Reddy, B.; Harinadha Babu, V. Synthesis of Novel Isoniazid Incorporated Styryl Quinazolinones as Anti-Tubercular Agents against INH Sensitive and MDR M. Tuberculosis Strains. *Med. Chem. Res.* **2014**, *23* (10), 4414–4419.
- (19) Hampannavar, G. A.; Karpoormath, R.; Palkar, M. B.; Shaikh, M. S. An Appraisal on Recent Medicinal Perspective of Curcumin Degradant: Dehydrozingerone (DZG). *Bioorg. Med. Chem.* **2016**, *24* (4), 501–520.
- (20) Luger, P.; Daneck, K.; Engel, W.; Trummlitz, G.; Wagner, K. Structure and Physicochemical Properties of Meloxicam, a New NSAID. *Eur. J. Pharm. Sci.* **1996**, *4*, 175–187.
- (21) Das, J.; Chen, P.; Norris, D.; Padmanabha, R.; Lin, J.; Moquin, R. V.; Shen, Z.; Cook, L. S.; Doweiko, A. M.; Pitt, S.; Pang, S.; Shen, D. R.; Fang, Q.; De Fex, H. F.; McIntyre, K. W.; Shuster, D. J.; Gillooly, K. M.; Behnia, K.; Schieven, G. L.; Wityak, J.; Barrish, J. C. 2-Aminothiazole as a Novel Kinase Inhibitor Template. Structure-Activity Relationship Studies toward the Discovery of N-(2-Chloro-6-Methylphenyl)-2-[[6-[4-(2-Hydroxyethyl)-1-Piperazinyl]-2-Methyl-4-Pyrimidinyl]amino]-1, 3-Thiazole-5-Carboxamide (Dasatinin). *J. Med. Chem.* **2006**, *49* (23), 6819–6832.
- (22) Meissner, A.; Boshoff, H. I.; Vasan, M.; Duckworth, B. P.; Barry, C. E.; Aldrich, C. C. Structure-Activity Relationships of 2-Aminothiazoles Effective against Mycobacterium Tuberculosis. *Bioorganic Med. Chem.* **2013**, *21* (21), 6385–6397.
- (23) Carradori, S.; Secci, D.; D'Ascenzio, M.; Chimenti, P.; Bolasco, A. Microwave and Ultrasound-Assisted Synthesis of Thiosemicarbazones and Their Corresponding (4,5-

-
- Substituted-Thiazol-2-Yl)hydrazines. *J. Heterocycl. Chem.* **2014**, *51* (6), 1856–1861.
- (24) Shaikh, M. S.; Palkar, M. B.; Patel, H. M.; Rane, R. A.; Alwan, W. S.; Shaikh, M. M.; Shaikh, I. M.; Hampannavar, G. A.; Karpoornath, R. Design and Synthesis of Novel Carbazolo-thiazoles as Potential Anti-Mycobacterial Agents Using a Molecular Hybridization Approach. *RSC Adv.* **2014**, *4* (107), 62308–62320.
- (25) Villemagne, B.; Flipo, M.; Blondiaux, N.; Crauste, C.; Malaquin, S.; Leroux, F.; Piveteau, C.; Villeret, V.; Brodin, P.; Villoutreix, B. O.; Sperandio, O.; Soror, S. H.; Wohlkönig, A.; Wintjens, R.; Deprez, B.; Baulard, A. R.; Willand, N. Ligand Efficiency Driven Design of New Inhibitors of *Mycobacterium Tuberculosis* Transcriptional Repressor EthR Using Fragment Growing, Merging, and Linking Approaches. *J. Med. Chem.* **2014**, *57* (11), 4876–4888.
- (26) Mata, R.; Morales, I.; Pérez, O.; Rivero-Cruz, I.; Acevedo, L.; Enriquez-Mendoza, I.; Bye, R.; Franzblau, S.; Timmermann, B. Antimycobacterial Compounds from *Piper S Anctum* †. *J. Nat. Prod.* **2004**, *67* (12), 1961–1968.
- (27) Al-Balas, Q.; Anthony, N. G.; Al-Jaidi, B.; Alnimr, A.; Abbott, G.; Brown, A. K.; Taylor, R. C.; Besra, G. S.; McHugh, T. D.; Gillespie, S. H.; Johnston, B. F.; Mackay, S. P.; Coxon, G. D. Identification of 2-Aminothiazole-4-Carboxylate Derivatives Active against *Mycobacterium Tuberculosis* H37Rv and the β -Ketoacyl-ACP Synthase mtFabH. *PLoS One* **2009**, *4* (5), e5617.
- (28) de Carvalho, L. P. S.; Lin, G.; Jiang, X.; Nathan, C. Nitazoxanide Kills Replicating and Nonreplicating *Mycobacterium Tuberculosis* and Evades Resistance. *J. Med. Chem.* **2009**, *52* (19), 5789–5792.
- (29) Palkar, M. B.; Noolvi, M. N.; Maddi, V. S.; Ghatole, M.; Nargund, L. G. Synthesis, Spectral Studies and Biological Evaluation of a Novel Series of 2-Substituted-5,6-Diarylsubstituted imidazo(2,1-B)-1,3,4-Thiadiazole Derivatives as Possible Anti-Tubercular Agents. *Med. Chem. Res.* **2011**, *21* (7), 1313–1321.
- (30) Kubra, I. R.; Bettadaiah, B. K.; Murthy, P. S.; Rao, L. J. M. Structure-Function Activity of Dehydrozingerone and Its Derivatives as Antioxidant and Antimicrobial Compounds. *J. Food Sci. Technol.* **2014**, *51* (2), 245–255.
- (31) Newmark, R. A.; Hill, J. R. Carbon-13-Fluorine-19 Coupling Constants in Benzotrifluorides. *Org. Magn. Reson.* **1977**, *9* (10), 589–592.
- (32) Elias, G.; Rao, M. N. a. Synthesis and Anti-Inflammatory Activity of Substituted (E)-4-Phenyl-3-Buten-2-Ones. *Eur. J. Med. Chem.* **1988**, *23* (4), 379–380.
- (33) Arshad, A.; Osman, H.; Bagley, M. C.; Lam, C. K.; Mohamad, S.; Zahariluddin, A. S. M. Synthesis and Antimicrobial Properties of Some New Thiazolyl Coumarin Derivatives.
-

-
- Eur. J. Med. Chem.* **2011**, *46* (9), 3788–3794.
- (34) Cui, M.; Ono, M.; Kimura, H.; Liu, B.; Saji, H. Synthesis and Evaluation of Benzofuran-2-Yl(phenyl)methanone Derivatives as Ligands for β -Amyloid Plaques. *Bioorg. Med. Chem.* **2011**, *19* (13), 4148–4153.
- (35) Skoumbourdis, A. P.; Huang, R.; Southall, N.; Leister, W.; Guo, V.; Cho, M.-H.; Inglese, J.; Nirenberg, M.; Austin, C. P.; Xia, M.; Thomas, C. J. Identification of a Potent New Chemotype for the Selective Inhibition of PDE4. *Bioorg. Med. Chem. Lett.* **2008**, *18* (4), 1297–1303.
- (36) Siddiqui, N.; Ahsan, W. Triazole Incorporated Thiazoles as a New Class of Anticonvulsants: Design, Synthesis and in Vivo Screening. *Eur. J. Med. Chem.* **2010**, *45* (4), 1536–1543.
- (37) Kaila, N.; Janz, K.; DeBernardo, S.; Bedard, P. W.; Camphausen, R. T.; Tam, S.; Tsao, D. H. H.; Keith, J. C.; Nickerson-Nutter, C.; Shilling, A.; Young-Sciame, R.; Wang, Q. Synthesis and Biological Evaluation of Quinoline Salicylic Acids As P-Selectin Antagonists. *J. Med. Chem.* **2007**, *50* (1), 21–39.
- (38) Lambert, R. J. W.; Pearson, J. Susceptibility Testing: Accurate and Reproducible Minimum Inhibitory Concentration (MIC) and Non-Inhibitory Concentration (NIC) Values. *J. Appl. Microbiol.* **2000**, *88* (5), 784–790.
- (39) Zelmer, A.; Carroll, P.; Andreu, N.; Hagens, K.; Mahlo, J.; Redinger, N.; Robertson, B. D.; Wiles, S.; Ward, T. H.; Parish, T.; Ripoll, J.; Bancroft, G. J.; Schaible, U. E. A New in Vivo Model to Test Anti-Tuberculosis Drugs Using Fluorescence Imaging. *J. Antimicrob. Chemother.* **2012**, *67* (8), 1948–1960.
- (40) Ollinger, J.; Bailey, M. A.; Moraski, G. C.; Casey, A.; Florio, S.; Alling, T.; Miller, M. J.; Parish, T. A Dual Read-Out Assay to Evaluate the Potency of Compounds Active against Mycobacterium Tuberculosis. *PLoS One* **2013**, *8* (4), 1–9.
- (41) Cho, S. H.; Warit, S.; Wan, B.; Hwang, C. H.; Pauli, G. F.; Franzblau, S. G. Low-Oxygen-Recovery Assay for High-Throughput Screening of Compounds against Nonreplicating Mycobacterium Tuberculosis. *Antimicrob Agents Chemother* **2007**, *51* (4), 1380–1385.
- (42) Andreu, N.; Zelmer, A.; Fletcher, T.; Elkington, P. T.; Ward, T. H.; Ripoll, J.; Parish, T.; Bancroft, G. J.; Schaible, U.; Robertson, B. D.; Wiles, S. Optimisation of Bioluminescent Reporters for Use with Mycobacteria. *PLoS One* **2010**, *5* (5), e10777.
- (43) Franzblau, S. G.; Witzig, R. S.; Mclaughlin, J. C.; Torres, P.; Madico, G.; Hernandez, A.; Degnan, M. T.; Cook, M. B.; Quenzer, V. K.; Ferguson, R. M.; Gilman, R. H. Rapid, Low-Technology MIC Determination with Clinical Mycobacterium Tuberculosis Isolates by Using the Microplate Alamar Blue Assay. *J. Clin. Microbiol.* **1998**, *36* (2), 362–366.
-

CHAPTER 4

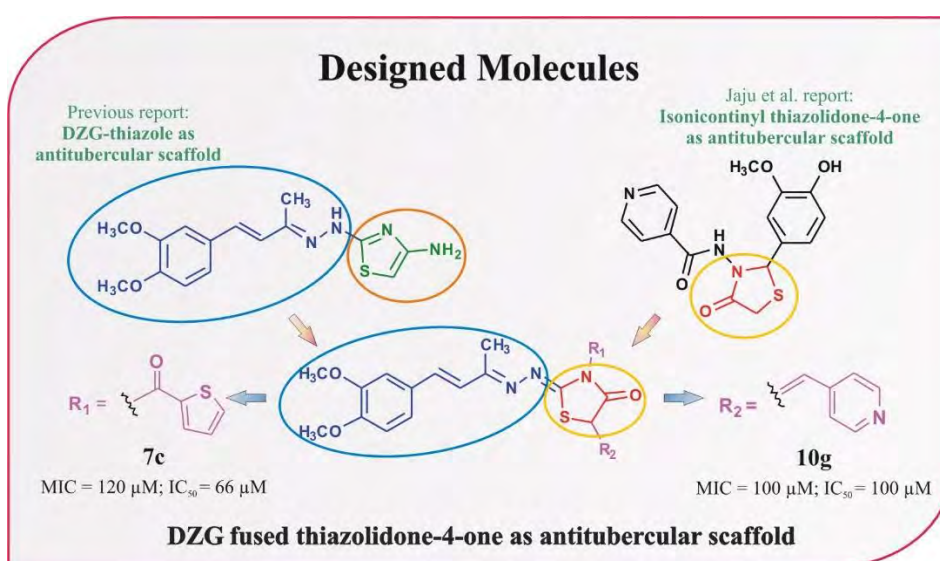
Design and synthesis of novel styryl hydrazine thiazolidin-4-one hybrids impelled from Dehydrozingerone as potential antimycobacterial agents

Girish A. Hampannavar^a, Mahesh B. Palkar^{b,a}, Mahamadhanif S. Shaikh^a, Srinivasulu Cherukupalli^a, Rajshekhar V. Karpoormath^{a*}

^a Department of Pharmaceutical Chemistry, Discipline of Pharmaceutical Sciences, College of Health Sciences, University of KwaZulu-Natal (Westville), Durban-4000, South Africa.

^b Department of Pharmaceutical Chemistry, K.L.E. University College of Pharmacy, Vidyanagar, Hubballi-580031, Karnataka, India.

Graphical Abstract



*Corresponding author

E-mail: karpoomath@ukzn.ac.za, rvk2006@gmail.com

Tel no.: +27(0)312607179, +27721107207; Fax No.: +27(0)312607792

Abstract

A novel series of styryl hydrazine thiazolidin-4-one hybrids (compounds **7a-d**, **10a-l** and **13a-b**) motivated from Dehydrozingerone (DZG) scaffold were designed and synthesized in good yields using a rational hybridization approach. The synthesized compounds were screened for their *in vitro* antimycobacterial activity against *Mycobacterium tuberculosis* H₃₇Rv strain at the National Institute of Allergy and Infectious Diseases (Bethesda, MD, USA). From the tested series, Compounds **7a** (MIC = 110 μ M; IC₅₀ = 67 μ M), **7c** (MIC = 120 μ M; IC₅₀ = 66 μ M) and **10g** (MIC = 100 μ M; IC₅₀ = 100 μ M) exhibited noteworthy antimycobacterial activity. Furthermore, these title compounds displayed diminutive cytotoxic effect against a mammalian Vero cell line using the MTT assay, suggesting for a good therapeutic index. Besides, these research findings on the styryl hydrazine thiazolidin-4-one hybrids derived from DZG scaffold stipulated the prospective magnitude of molecular hybridization and strongly encouraged us for further lead optimization with an aim to develop potential antimycobacterial agents.

Keywords

Antimycobacterial activity; Cytotoxicity; Dehydrozingerone; Thiazolidin-4-one; *Mycobacterium tuberculosis* H₃₇Rv

1 Introduction

Tuberculosis (TB), one of the world's dreadful communicable diseases, is a chronic infectious disease caused by facultative intracellular respiratory pathogen, *Mycobacterium tuberculosis*. It continues to be an utmost prodigious health issue after acquired immune deficiency syndrome (AIDS). According to 2015 WHO report, about 9.6 million people were estimated to have fallen ill because of this dreadful disease.¹ China, India, Russian Federation, and South Africa have almost ~63% of the world's active cases of TB. Apart from Lesotho, South Africa tops the list of incident rates with 834 cases per 100,000 people. TB together with human immunodeficiency virus (HIV) infection has become a lethal combination and covers the principal ascent of the diseases responsible for the highest mortality in Africa. Efforts to eliminate TB have remained as a major challenge because of limitations with existing treatments, poor patient compliance, co-infections, inadequate therapeutic regimen and prolonged treatment. Drug resistance crises due to the emergence of drug-resistant mycobacterial strains like multidrug-resistant TB (MDR-TB), extensively drug-resistant TB (XDR-TB) and totally drug-resistant TB (TDR-TB) to almost marketed frontline drugs, has seriously necessitated the need for effective drug in treating TB.²

From way back, heterocyclic compounds have emerged as imperial small-molecule therapeutics and continued to be explored for their curative medicinal properties. Thiazolidin-4-one ring system is one of the many biologically active 5 membered heterocycles that contain nitrogen and sulphur hetero atoms, is a vital core structure that has extensively been investigated for numerous biological properties. Thiazolidin-4-one (**I**), a saturated five membered heterocyclic compound containing one nitrogen, one sulphur and three carbon atoms including a carbonyl group at 4th position. The thriving introduction of etozoline (**II**) as an antihypertensive, pioglitazone (**III**) as a hypoglycemic agent and ralitoline (**IV**) as a potent anti-convulsant, in clinical practice, has undoubtedly proved the therapeutic potential of thiazolidin-4-one moiety (See Figure 1).

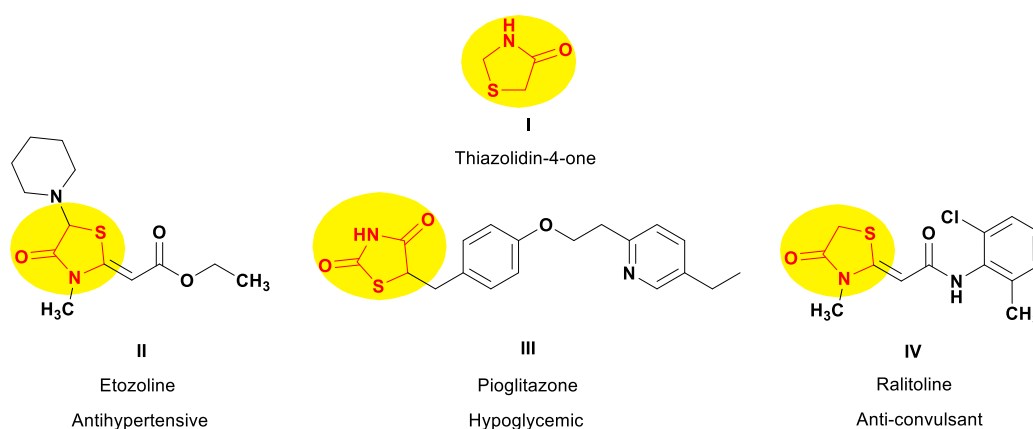


Figure 1: Thiazolidin-4-one scaffold and its various bioactive compounds.

Jaju et al., reported the synthesis and biological evaluation of a series of thiazolidin-4-one derivatives (**X**) fused with isoniazid scaffold, which displayed potent antitubercular activity.³ Besides, thiazolidin-4-one is an acclaimed scaffold in drug discovery as it possesses copious pharmacological activities viz. antimicrobial⁴, antiviral⁵, anticonvulsant, antiinflammatory⁶, antitubercular^{7,8} and anticancer activities.

From primordial times, natural products have been considered as vital cradle for the design, discovery and development of innovative drug like leads for life threatening diseases. Dehydrozingerone (DZG; feruloylmethane), a half structural analog (natural chalcone) of curcumin isolated from rhizomes of *Zingerber officinalae* (Family: Zingiberaceae), is one such medicinally valuable molecule in drug discovery. Chemically DZG is (*E*)-4-(4-hydroxy-3-methoxyphenyl)but-3-en-2-one and possess an α,β -unsaturated carbonyl (styryl ketone) group. Several DZG analogs were synthesized that have been reported to portrait broad range of biological activities like antioxidant, anticancer, anti-inflammatory, antidepressant, antimalarial, antifungal etc.⁹ From reports, it was also established that the derivatives bearing styryl or α,β -unsaturated carbonyl groups are reported to possess antimycobacterial activities.^{10,11}

Our previous reports demonstrate the successful implementation of molecular hybridization-based drug design approach in order to develop new hybrid chemical entities (NHCEs) as promising lead compounds against *Mycobacterium tuberculosis*.^{12,13} It is widely acknowledged that more efficacious NHCEs with synergistic activity can be designed by amalgamation of two or more bioactive pharmacophores or heterocyclic systems in a singular molecular skeleton. In view of these annotations and owing to the fact that there are only few reports on antimycobacterial activity of DZG analogs, we therefore envisaged to explore the design of unique DZG analogs by unification of two bioactive scaffolds (styryl portion of DZG and thiazolidin-4-one) to construct a new pharmacophore for biological evaluation with the anticipation of prospective antimycobacterial activity. Figure 2, illustrates that the newly designed hybrid analogs encompass both DZG (including styryl) and thiazolidin-4-one motifs attached with each other via a hydrazine linker. Herein, we report the design, synthesis and biological evaluation of some novel thiazolidin-4-one analogs derived from DZG as promising antimycobacterial agents.

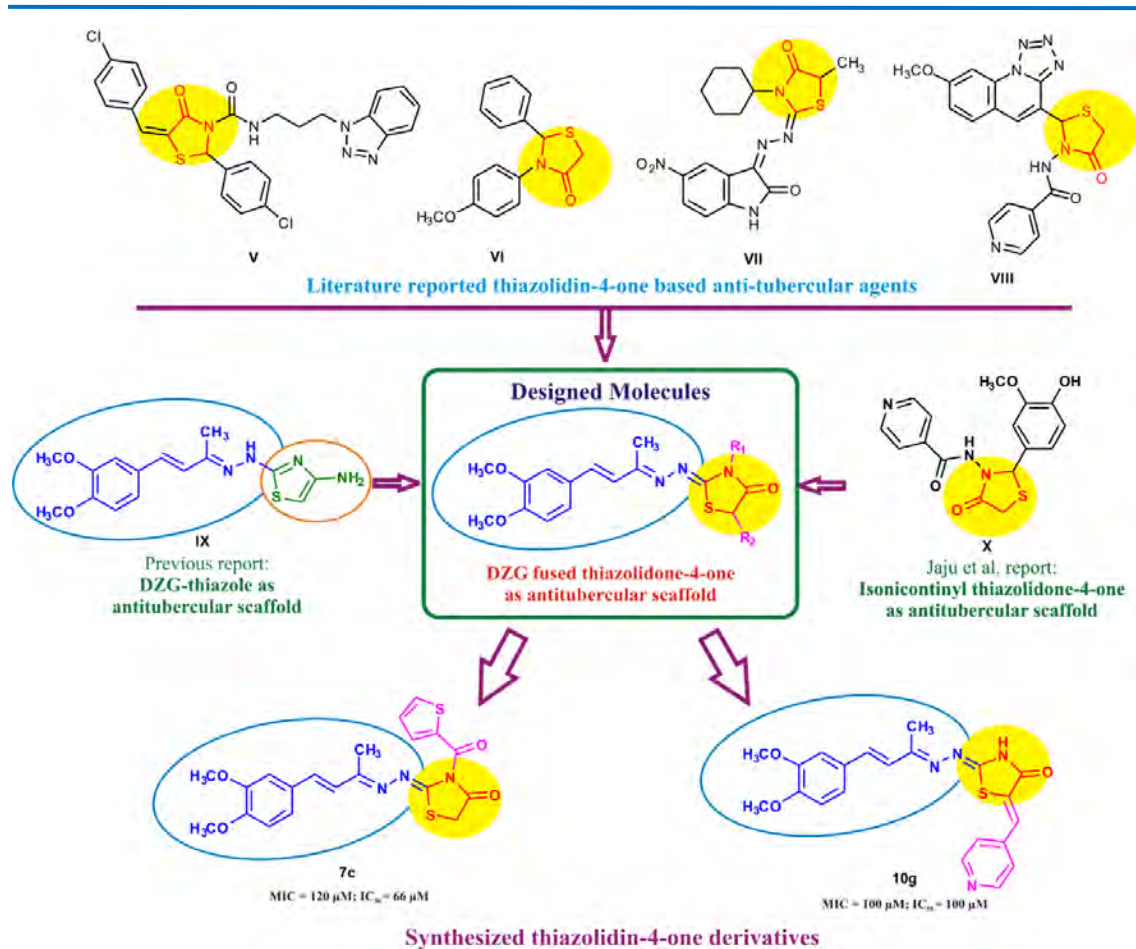


Figure 2: Molecular hybridization assisted design of thiazolidin-4-one analogues impelled from DZG scaffold as possible antimycobacterial agents. The reported thiazolidin-4-one derivatives with promising antimycobacterial activity (**V**: 2.50 µg/mL¹⁴; **VI**: 2.2 µg/mL¹⁵; **VII**: 6.25 µg/mL¹⁶; **VIII**: 1.66 ± 0.5 µM¹⁷; **IX**: 0.48 µM¹² and **X**: 0.31 µg/mL³)

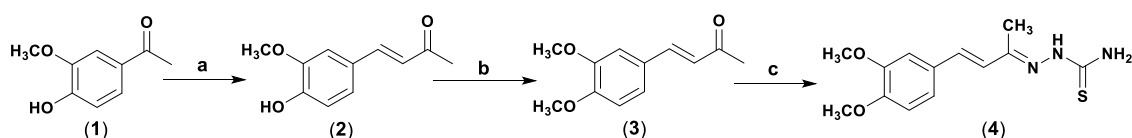
2 Chemistry

The synthesis of some novel series of new substituted 2-((4-(3,4-dimethoxyphenyl) but-3-en-2-ylidene)hydrazono)thiazolidin-4-one derivatives (**7a-d**, **10a-l** and **13a-b**) derived from DZG was attained through efficient and adaptable synthetic routes as depicted in **Schemes I** to **IV**. The starting material, compound **4**, was synthesized as per our previous report¹² (**Scheme I**), was refluxed with methyl bromoacetate in the presence of sodium acetate in absolute ethanol to yield 2-((4-(3,4-dimethoxyphenyl)but-3-en-2-ylidene)hydrazono)thiazolidin-4-one (**5**). Further, a series of title compounds 3-(substituted benzoyl)-2-((4-(3,4-dimethoxyphenyl)but-3-en-2-ylidene)hydrazono)thiazolidin-4-one (**7a-d**) were synthesized by reacting compound (**5**) with various appropriately substituted acid chlorides (**6a-d**) in the presence of pyridine as illustrated in **Scheme II**. Besides, the various substituted arylidene malononitriles (**9a-l**) were prepared by

Knoevenagel condensation¹⁸ reaction of malononitrile with appropriately substituted aromatic/heteroaromatic aldehydes (**8a-l**). Consequently, the active methylene in the thiazolidin-4-one of compound **5** underwent nucleophilic addition reaction to the double bond of a variety of arylidene malononitriles (**9a-l**) via a Michael type addition reaction¹⁹ by refluxing in ethanol containing few drops of piperidine to afford the desired compounds i.e. 5-(substituted benzylidene)-2-((4-(3,4-dimethoxyphenyl)but-3-en-2-ylidene)hydrazono)thiazolidin-4-ones (**10a-l**) as highlighted in **Scheme III**. Similarly, **Scheme IV** represents the reaction of malanonitrile with substituted isatins (**11a-b**) in the presence of pyridine yielded the respective isatin malononitriles (**12a-b**), which were further condensed with compound **5** in the presence of ethanol and catalytic amount of piperdine to obtain final compounds i.e. 5-(5-substituted-2-oxo-indolin-3-ylidene)-2-((4-(3,4-dimethoxyphenyl)but-3-en-2-ylidene)hydrazono)thiazolidin-4-ones (**13a-b**) in good yields. The structural confirmation of key intermediates and all synthesized final derivatives was established by their physico-chemical and spectral (IR, ¹H-NMR and ¹³C-NMR) analysis and their further structural identity were substantiated by HRMS data.

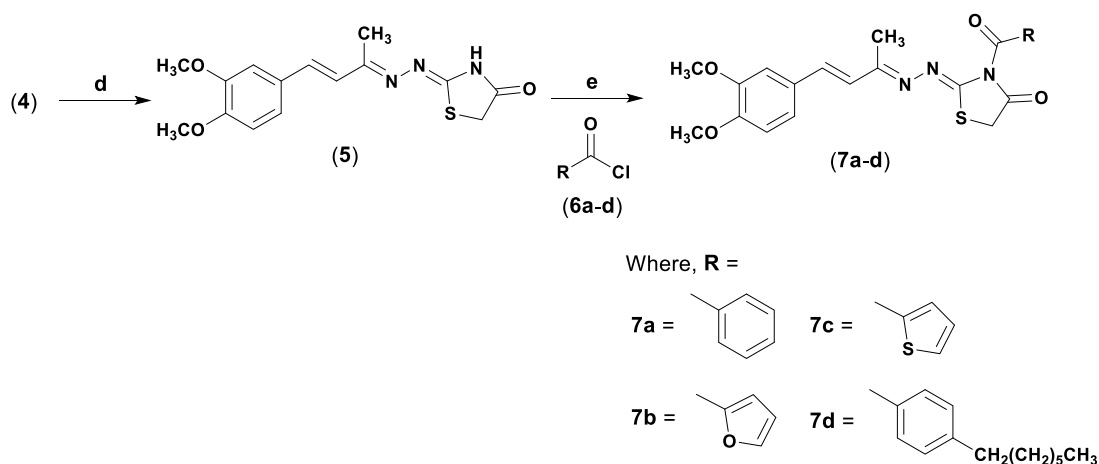
Synthetic Schemes describing synthesis of title compounds **7a-d**, **10a-l** and **13a-b**.

Scheme I*



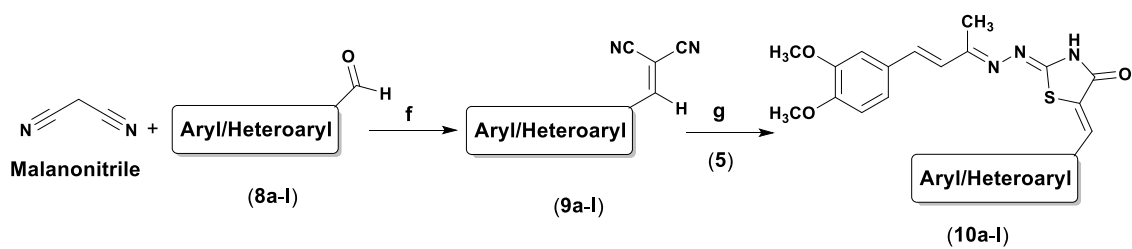
*Reagents and conditions: **a**: acetone, NaOH; **b**: CH₃I, K₂CO₃, DMF, reflux, 1.5 h; **c**: thiosemicarbazide, AcOH, MeOH, reflux, 3 h.

Scheme II*

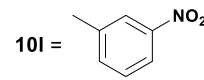
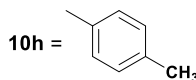
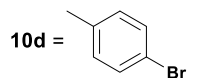
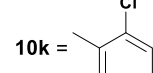
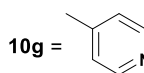
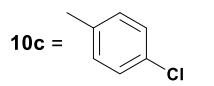
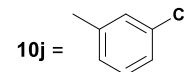
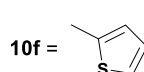
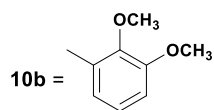
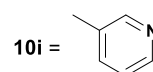
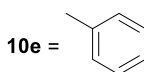
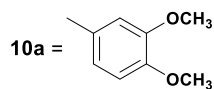


*Reagents and conditions: **d**: BrCH₂COOCH₃, EtOH/NaOAc, reflux 4.30 h; **e**: pyridine, RT.

Scheme III*

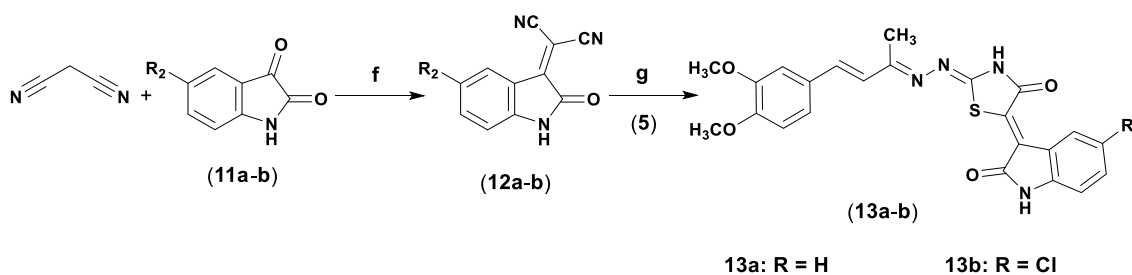


Where, Aryl/Heteroaryl



*Reagents and conditions: f: ethanol, piperidine, reflux 1 h; g: EtOH, piperidine, reflux, 3 h.

Scheme IV*



*Reagents and conditions: f: ethanol, piperidine, reflux 1 h; g: EtOH, piperidine, reflux, 3 h.

3 Results and discussion

3.1 Synthesis and spectral studies

All the newly synthesized final title compounds showed satisfactory analytical data, which were in agreement with their respective anticipated structures, are summarized in experimental section. In general, the IR spectrum of key intermediate compound (**5**) clearly displayed characteristic absorption bands around 3074.82 cm^{-1} for N-H, 1709.23 cm^{-1} for carbonyl (C=O), 1617.92 cm^{-1} for C=C and 1597.49 cm^{-1} for C=N groups, thus confirming the formation of thiazolidin-4-one nucleus. These observations were further substantiated from $^1\text{H-NMR}$ spectrum of compound (**5**), which exhibited the prominent singlet signals around $\delta 11.87$ ppm accounting for the N-H proton of thiazolidin-4-one, 7.23 ppm for an aromatic proton at 2nd position of DZG scaffold, 3.85 ppm for methylene (CH_2) protons of thiazolidin-4-one, $3.81\text{-}3.77$ ppm for methoxyl (OCH_3) protons and 2.18 ppm for methyl (CH_3) protons, thus indicating the formation of thiazolidin-4-one ring from the respective thiosemicarbazide (**4**) by simple cyclo-condensation process. In addition, the appearance of most distinctive doublet signal ($J = 16.49$) around $\delta 6.86\text{-}6.82$ ppm authenticates the presence of vicinal vinyl protons.

From the IR spectrum of the compounds (**7a-d**), it was observed that the disappearance of the characteristic band due to N-H group while the appearance of an additional fairly strong peak around $1760.05\text{-}1737.13\text{ cm}^{-1}$, which is attributed to the benzoyl carbonyl (C=O) group, indicating the formation of title compounds (**7a-d**). This is further evidenced from the $^1\text{H-NMR}$ spectrum (400 MHz) of these compounds recorded in $\text{DMSO-}d_6$, which displayed some distinguishing singlet signals at around $\delta 7.24\text{-}7.22$ ppm for an aromatic proton at 2nd position of DZG scaffold, $\delta 4.22\text{-}4.18$ ppm for methylene (CH_2) protons of thiazolidin-4-one ring, $\delta 3.81\text{-}3.76$ ppm for methoxyl (OCH_3) protons and $\delta 1.96\text{-}1.78$ ppm for methyl ($\text{N}=\text{C-CH}_3$) protons respectively. The most informative doublet signals ($J = 16.57\text{-}16.45$ Hz) resonated around $\delta 7.09\text{-}6.79$ ppm evidently indicated the presence of vicinal vinyl ($-\text{CH}=\text{CH}-$) protons. This observation was found consistent with previously reported similar compounds.¹² Further, the various signals resonated as either doublets or multiplets at around $\delta 8.31\text{-}6.88$ ppm were accounted for aromatic or heteroaromatic protons of compounds (**7a-d**). These findings were further supported from their respective $^{13}\text{C-NMR}$ spectra of the title compounds. The characteristic $^{13}\text{C-NMR}$ signals resonated at around $\delta 171.00\text{-}170.88$ and $168.24\text{-}156.11$ ppm were assigned to carbonyl carbons ($\text{C}=\text{O}$) of thiazolidin-4-one and aromoyl/heteroaromoyl moieties respectively. The prominent carbon signals observed around $\delta 164.39\text{-}164.24$ and $159.02\text{-}158.76$ ppm due to carbons containing arylidine and thiazolidine ($\text{C}=\text{N}$) groups respectively. Further, the informative carbon signals around $\delta 149.73\text{-}148.92$ and $131.01\text{-}128.72$ ppm were accounted for aromatic carbons

having methoxyl groups and vinyl (-HC=CH-) carbons respectively. The carbon signals resonated around δ 121.31-121.26, 111.59-111.58 and 109.55-109.52 ppm were assigned to C-6, C-5 and C-2 carbons of DZG scaffold respectively, while the typical carbon signals appeared around δ 55.50-55.46, 33.23-33.09 and 12.94-12.77 ppm indicated the presence of methoxyl (OCH₃), methylene (-CH₂ of thiazolidin-4-one) and methyl (N=C-CH₃) groups respectively in the title compounds.

From IR spectrum of the title compounds (**10a-l** and **13a-b**), it was observed that the appearance of typical absorption bands around 3118.74-2999.21 cm⁻¹ for N-H, 1729.20-1684.50 cm⁻¹ for carbonyl (C=O of thiazolidin-4-one), 1633.77-1590.52 cm⁻¹ for C=C, and 1599.95-1509.36 cm⁻¹ for C=N groups. The ¹H-NMR spectrum (400 MHz) of these title compounds revealed the most informative singlet signals at around δ 12.88-12.38 and 7.30-7.14 ppm attributing to N-H proton of thiazolidin-4-one and an aromatic proton at 2nd position of DZG scaffold respectively. An apparent structural insight was obtained from the appearance of a prominent singlet signal around δ 7.86-7.52 ppm accounting for the arylidine (HC=C) proton at 5th position of the thiazolidin-4-one nucleus. In particular, it was noticed that the disappearance of a distinct singlet signal at around δ 3.85 ppm for methylene (CH₂) protons of thiazolidin-4-one ring, which evidently confirms the formation of desired final compounds via Knoevenagel condensation. All synthesized compounds displayed singlet signals resonating around δ 3.85-3.76 and 2.27-2.25 ppm indicated the presence of methoxyl protons (OCH₃) on the 3rd and 4th position of the DZG scaffold and methyl (N=C-CH₃) protons respectively. Further, the most attributable doublet signals (J = 16.61-15.13 Hz) resonated around δ 7.21-6.88 ppm evidently confirmed the presence of vicinal vinyl protons (CH=CH), whereas the various signals resonated as either singlet or multiplets between δ 8.84-6.88 ppm accounted for aromatic protons. In case of compounds **13a** and **13b**, the distinct singlet signals appeared at around δ 11.2-11.1 ppm assigned for N-H protons of isatin ring. These elucidations were further authenticated from their respective ¹³C-NMR spectra (100 MHz) of the title compounds. In ¹³C-NMR spectrum, the characteristic carbon signals resonated around δ 167.42-166.74 ppm for carbonyl (C=O) carbon, 129.84-127.01 ppm for arylidine (=CH-C) carbon and 135.71-120.98 ppm for C-5 carbon of thiazolidin-4-one ring, thus confirming the formation of desired title compounds containing thiazolidinone nucleus. The characteristic carbon signals resonated around δ 164.59-160.99 and 159.02-155.76 ppm were assigned to carbons containing arylidine and thiazolidine (C=N) groups respectively. Further, the most informative ¹³C-NMR signals resonated at around δ 152.72-148.21 and 131.97-128.87 ppm were assigned for aromatic carbons having methoxyl groups and vinyl carbons respectively, while the carbon signals appeared around δ 121.84-120.94, 112.76-111.32 and 110.96-109.39 ppm were due to C-6, C-5 and C-2 carbons of DZG scaffold. The prominent carbon signals observed around

δ 56.34-55.43 ppm and δ 13.93-13.09 ppm, suggested the presence of methoxyl (OCH_3) and methyl ($\text{N}=\text{C}-\underline{\text{C}}\text{H}_3$) carbons respectively in the title compounds. In case of compounds **13a** and **13b**, the characteristic signals appeared around δ 168.69-168.42 ppm due to the presence of carbonyl carbon ($\text{C}=\text{O}$) of isatin ring. In addition, the formation of desired final compounds (**7a-d**, **10a-l** and **13a-b**) was also established by recording their respective mass spectra (HRMS), which displayed accurate molecular ion peaks that were in agreement with their expected molecular weights.

Single crystal X-ray diffraction analysis:

A crystal of **5** was solved in the monoclinic space group P 1 21/c 1. Vinyl protons (H9-H10) are antiperiplanar with a dihedral angle of -179.76° , which is consistent with the large coupling constant ($J = 16.49$ Hz) between two vinyl protons. The imine bond ($\text{C13}=\text{N2}$) was also antiperiplanar with a dihedral angle of 178.68° . The core skeleton of compound **5** is evidently planar and also confirms that the molecule is in E configuration. Figure 3 depicts X-ray crystallographic image of compound **5**.

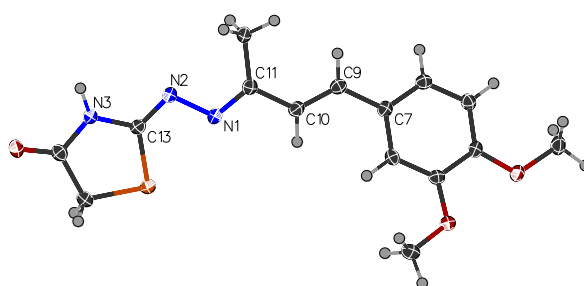


Figure 3: X-ray crystallographic image of compound **5**.

2D NMR Studies

Characterization and assignment of J values for compound **5** was done using 2D NMR studies. The following discussion explains the assignment of ^1H -NMR and ^{13}C -NMR values for the compound **5**, (common scaffold for all the title compounds) with the aid of 2D techniques (COSY, NOESY, HSQC and HMBC). The structure **5** comprises of two portions namely aryl styryl and hydrazono-thiazolidone portion (Figure 4).

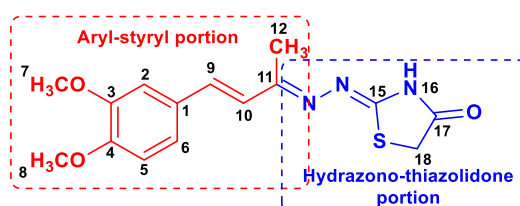


Figure 4: Compound **5** depicting styryl and hydrazono-thiazolidone portions.

Aryl-styryl portion*:

The HMBC correlation from H-12 proton signal at δ 2.17 to C-10 at δ 126.77 (primary carbon) and C-11 at δ 162.30 (quaternary carbon) indicated that methyl group is attached to a quaternary carbon C-11. HSQC correlation of C-10 to a doublet signal at δ 6.83 with a characteristic J value (16.48 Hz) indicated the presence of *trans* proton (H-10) on C-10. Further, HMBC correlation of H-10 to aromatic quaternary carbon, C-1 (δ 129.08) signifies presence of a phenyl carbon. NOESY and COSY correlation of H-10 to a doublet, H-9 at δ 7.10 with large coupling constant value of 16.48 Hz confirms the presence of another *trans* proton. Carbon assignment by HSQC for H-9 was at δ 135.55 (C-9). Appearance of H-9 down field compared to H-10, signifies the deshielding effect which would possibly because of presence of electron releasing groups on phenyl ring. HMBC correlation of C-1 to a doublet aromatic proton at δ 6.94 ($J = 8.40$ Hz) indicated the presence of aromatic proton, H-5. A HSQC signal from H-5 correlated it to its corresponding carbon signal C-5 at δ 111.76. A downfield HMBC signal from H-5 to δ 149.05 corresponded to C-3 bearing $-\text{OCH}_3$ group. An $-\text{OCH}_3$ signal (H-7) at δ 3.08 group also had HMBC correlation to C-3. In addition, another $-\text{OCH}_3$ signal (H-8) at δ 3.76 had HMBC correlation to C-4 at δ 149.06 signifying two methoxy groups on phenyl ring. Further to this C-4 had HMBC correlation with two aromatic protons at δ 7.12 (as doublet of doublet) and δ 7.22 (as doublet) corresponding to H-6 and H-2 respectively. The brief shift of H-2 to down field would possibly have attributed by $-\text{OCH}_3$ adjacent to it. The *ortho* coupled doublet at δ 6.94 (H-5) illustrated cross peak to the doublet of doublets at δ 7.12 (H-6) which consecutively was linked to a small doublet at δ 7.22 (H-2) and was in agreement with reports.²⁰ HSQC correlations of H-6, H-2, H-7 and H-8 to their respective carbons were at δ 121.13, δ 109.59, δ 55.62 and δ 55.60 respectively.

Hydrazono-thiazolidone portion*:

A methylene proton at H-18 at δ 3.84 had HMBC correlation to the most down field resonance in ^{13}C spectrum at δ 173.94 (C-17) and δ 162.30 (C-15). Further, a broad singlet at far down field δ 11.87 corresponded to NH proton (H-16).

(*see Appendix II, Chapter 4 for HMBC, NOESY, COSY and HSQC spectrums)

2D Correlations:

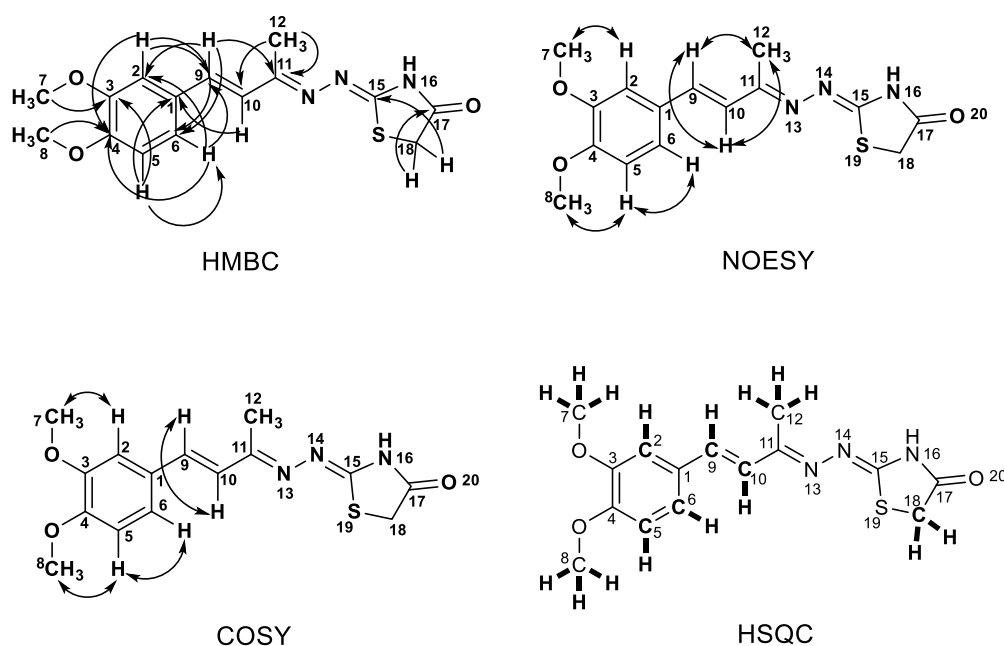


Figure 5: 2D correlations of compound 5.

3.2 Antimycobacterial activity

All the newly synthesized title compounds (**5**, **7a-d**, **10a-l** and **13a-b**) were evaluated for their *in vitro* antimycobacterial activity, which was carried out at Infectious Disease Research Institute (IDRI) within the National Institute of Allergy and Infectious Diseases (NIAID) screening program, Bethesda, MD, USA. In this study, Minimum Inhibitory Concentration (MIC) was established against *M. tuberculosis* strain H₃₇Rv grown under aerobic conditions by using a dual read-out (OD₅₉₀ and fluorescence) assay procedure to minimize problems caused by compound precipitation or autofluorescence.²¹⁻²³ This specific assay mainly analyses the growth in liquid medium of a fluorescent reporter strain of H₃₇Rv, where the readout was either optical density (OD) or fluorescence. The purpose of the screening program was to offer a resource whereby new experimental compounds could be tested for their capacity to inhibit the growth of virulent *M. tuberculosis*. The result of antimycobacterial activity is presented in **Table 1**. All the synthesized compounds exhibited an inspiring activity profile with MIC ranging from 100 to 200 μ M against the tested mycobacterial strain. We studied the effects of aromatic/heteroaromatic substituents at 3rd and 5th position of thiazolidin-4-one ring, which was, in turn connected to DZG scaffold through a hydrazine bridge. Interestingly, it was observed that the compounds (**7a-d**) containing aroyl/heteroaroyle group at 3rd position of thiazolidin-4-one ring displayed greatest encouraging

antimycobacterial activity as compared to other compounds (**10a-l** and **13a-b**). From the tested series, compound **7a** (MIC = 110 μ M) having an unsubstituted aromatic nucleus displayed most promising antimycobacterial activity with an IC₅₀ value of 67 μ M, while compound **7c** (MIC = 120 μ M) substituted with thiophene moiety on thiazolidin-4-one ring exhibited notable inhibitory activity with an IC₅₀ value of 66 μ M. Further, from the series of compounds (**10a-l** and **13a-b**), one compound **10g** (MIC = 100 μ M) with pyridin-4-yl moiety on thiazolidin-4-one ring showed commendable inhibitory activity with an IC₅₀ value of 100 μ M, while the remaining compounds of the series were found to be least active with MIC value >200 μ M.

Table 1: Antimycobacterial and cytotoxic activity data of title compounds (**5**, **7a-d**, **10a-l** and **13a-b**) against *M. tuberculosis* H₃₇Rv strain under aerobic conditions.

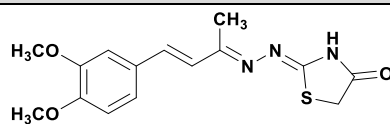
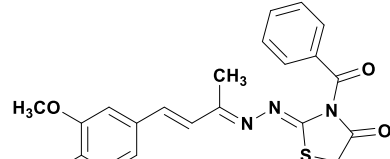
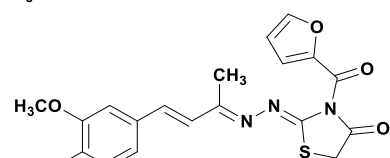
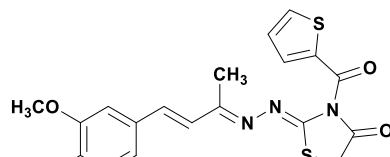
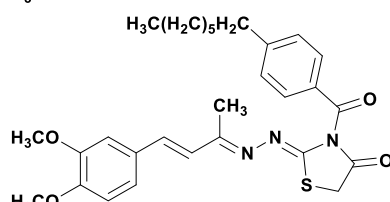
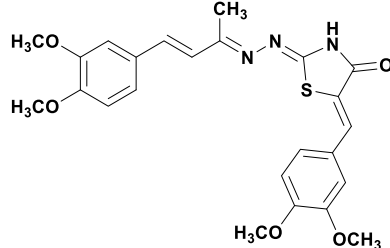
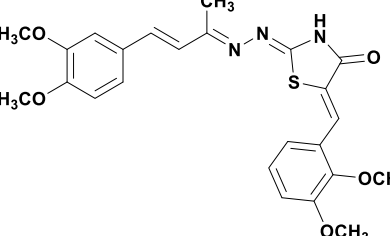
Compound	Structure	MIC ^a (μ M)	IC ₅₀ ^b (μ M)	IC ₉₀ ^c (μ M)	Cytotoxicity IC ₅₀ ^d (μ M)
5		>200	140	>200	263.5
7a		110	67	110	370.5
7b		>200	82	170	346.7
7c		120	66	120	395.2
7d		>200	99	>200	318.4
10a		>200	>200	>200	ND
10b		>200	>200	>200	271.2

Table 1: (Contd.)

Compound	Structure	MIC ^a (μ M)	IC ₅₀ ^b (μ M)	IC ₉₀ ^c (μ M)	Cytotoxicity IC ₅₀ ^d (μ M)
10c		>200	>200	>200	287.1
10d		>200	>200	>200	273.3
10e		>200	>200	>200	ND
10f		>200	>200	>200	302.8
10g		100	100	>100	311.3
10h		>200	>200	>200	ND

Table 1: (Contd.)

Compound	Structure	MIC ^a (μ M)	IC ₅₀ ^b (μ M)	IC ₉₀ ^c (μ M)	Cytotoxicity y IC ₅₀ ^d (μ M)
10i		>200	>200	>200	299.4
10j		>100	>100	>100	242.5
10k		>200	>200	>200	ND
10l		>200	>200	>200	213.5
13a		>200	>200	>200	220.9
13b		>200	>200	>200	238.1
Rifampicin	—	0.006 7	0.003 7	0.00 7	—

^aMIC = Minimum Inhibitory Concentration at which *M. tuberculosis* H₃₇Rv was completely inhibited. ^bIC₅₀ value = Concentration at which growth is inhibited by 50%. ^cIC₉₀ value = Concentration at which growth is inhibited by 90%. ^dCytotoxic activity was determined on mammalian Vero cell line; ND = Not Determined.

In general, a brief structure activity relationship (SAR) studies indicated that the antimycobacterial activity was considerably affected by the nature of substituents present at 3rd position on the thiazolidin-4-one nucleus. It was also observed that the presence of dicarbonyl motif along with benzoyl group in compound **7a** and its bio-isosteric thiophene ring in compound **7c** have greatly influenced for antimycobacterial activity. However, replacing the substituted benzyldine group at 5th position on the thiazolidin-4-one ring with heteroarylidine groups such as thiophene (**10f**), pyridin-3-yl (**10i**) and isatin (**13a-b**) resulted in no significant change in the antimycobacterial activity, with MIC values >200 μ M.

3.3 Cytotoxic activity

The newly synthesized final derivatives (**7a-d**, **10a-l** and **13a-b**) were further assessed for *in vitro* cytotoxic activity (IC₅₀) in a mammalian Vero cell line by following MTT assay protocol. After 72 h of exposure, the cell viability was determined on the basis of the cellular conversion of MTT into a formazan product using a Promega Cell Titre 96 non-radioactive cell proliferation assay. The results presented in **Table 1** reveal that the IC₅₀ values were ranging from 213.5 to 395.2 μ M for the 15 tested derivatives. These synthesized compounds did not produce significant activity against mammalian Vero cell line at concentrations <100 μ M. Within the analogs tested, compounds **7a-d**, **10f** and **10g** display a lower toxicity with IC₅₀ values >300 μ M.

4 Conclusion

In this communication, we report the synthesis, spectral studies and preliminary *in vitro* antimycobacterial activity of some novel series of styryl hydrazine tethered thiazolidin-4-one analogs (**7a-d**, **10a-l** and **13a-b**) derived from an imperative scaffold (i.e. DZG) using a rational hybridization approach. The structures of the desired title compounds were confirmed by their respective spectral (IR, ¹H-NMR and ¹³C-NMR) and HRMS data. From the newly synthesized analogs, compounds **7a**, **7c** and **10g** exhibited the most encouraging antimycobacterial activity against *M. tuberculosis* H₃₇Rv strain. A brief SAR study emphasized that the antimycobacterial effect of compounds was indeed sensitive to the presence of specific substituents at 3rd and 5th position of thiazolidin-4-one nucleus. Further, the title compounds were screened for their *in vitro* cytotoxicity (IC₅₀) against the mammalian Vero cell line by using MTT assay. The results revealed that these compounds displayed antimycobacterial activity at non-cytotoxic concentrations. These results are encouraging due to the fact that compounds with increased cytotoxicity are attractive in the development of new chemical entities for the treatment of TB. This research outcome advocates the advantage of integrating a hydrazine linkage to unite styryl

portion of DZG and thiazolidin-4-one core, thus offers a worthy initial idea for further compound optimization. Thus emerged lead candidates (**7a**, **7c** and **10g**) can be further exploited for additional functionalization to improve the antimycobacterial activity profile, which deserves further investigation.

5 Experimental

5.1 Chemistry Protocol

All the chemicals used in this research work were purchased from Sigma-Aldrich and Merck Millipore, South Africa. All the solvents, except those of laboratory-reagent grade, were dried and purified when necessary according to previously published methods. The progress of the reactions and the purity of the compounds were monitored by thin-layer chromatography (TLC) on pre-coated silica gel plates procured from E. Merck and Co. (Darmstadt, Germany).

The melting points of the synthesized compounds were determined using a Thermo Fisher Scientific (IA9000, UK) digital melting point apparatus and are uncorrected. The IR spectra were recorded on a Bruker Alpha FT-IR spectrometer (Billerica, MA, USA) using the ATR technique. The ¹H-NMR and ¹³C-NMR spectra were recorded on a Bruker AVANCE 400 and 600 MHz (Bruker, Rheinstetten/Karlsruhe, Germany) spectrometer using DMSO-*d*₆. The chemical shifts (δ) reported are given in parts per million (ppm) and the coupling constants (*J*) are in Hertz (Hz) with respect to TMS as the internal standard. The spin multiplicities are reported as s = singlet, d = doublet, t = triplet, dd = doublet of doublet and m = multiplet. HRMS spectra were recorded on an Autospec mass spectrometer with electron impact at 70 eV. Compounds **2**, **3** and **4**, were synthesized in good yields according to our previous report.¹²

5.1.1 Synthesis of 2-((4-(3,4-dimethoxyphenyl)but-3-en-2-ylidene)hydrazono)thiazolidin-4-one (**5**)^{24,25}:

Compound **4** (5 gm, 0.01790 mol.) and sodium acetate (1.46 g, 0.01790 mol.) were refluxed in ethanol for 30 minutes and then methyl bromoacetate (3.012 g, 0.01969 mol.) was added. The resulting mixture was refluxed for 4.30 h until the starting material was consumed. After completion, the mixture was poured in a beaker containing ice and stirred for few minutes. The separated solid was filtered under reduced pressure. Further, recrystallization in ethanol yielded yellow coloured crystalline solid of **5**. TLC was monitored by using solvent system DCM: MeOH (99:1).

Yield: 83%, mp: 197-198 °C; FTIR (ATR, ν_{max} , cm⁻¹): 3074.82 (N-H Str.), 2967.45 (Ar-H Str.), 2928.97 (C-H Str. of CH₃), 1709.23 (C=O Str.), 1617.92 (C=C Str.), 1597.49 (C=N Str.); ¹H-NMR (400 MHz, DMSO-*d*₆, δ , ppm): 11.87 (s, 1H, NH), 7.23 (s, 1H), 7.14-7.09 (m, 2H), 6.96-

6.94 (d, 1H, $J = 8.40$ Hz), 6.86-6.82 (d, 1H, $J = 16.49$ Hz, HC = CH), 3.85 (s, 2H, -CH₂ of thiazolidone), 3.81 (s, 3H, -OCH₃), 3.77 (s, 3H, -OCH₃), 2.18 (s, 3H, -CH₃); ¹³C-NMR (100 MHz, DMSO, δ ppm): 173.72 (C=O, thiazolidin-4-one), 162.11 (C=N of thiazolidone and 2-ylidene carbon), 149.53, 148.94, 135.41, 128.97, 126.66, 121.03 (C-6 of DZG), 111.62 (C-5 of DZG), 109.46 (C-2 of DZG), 55.50 (-OCH₃), 55.47 (-OCH₃), 32.80 (-CH₂ of thiazolidone), 13.06 (-CH₃); HRMS (ESI, m/z) [M-H]⁻; calculated for C₁₅H₁₇N₃O₃S, 318.0912; found 318.0905.

5.1.2 General procedure for synthesis of substituted 3-benzoyl-2-((4-(3,4-dimethoxyphenyl)but-3-en-2-ylidene)hydrazono)thiazolidin-4-one (7a-d)

Compound **5** (0.3 g, 0.00094 mol) was taken in 3.0 mL of pyridine and stirred for 15 minutes. To this was added 1.5 equivalent (0.00141 mol) of appropriately substituted acid chlorides (**6a-d**) with constant stirring for 3 h (till consumption of starting material) at room temperature. Few drops of cold dil. HCl (0.1 N) was added whilst stirring to quench the pyridine. The obtained solid was filtered and washed with water. The solid was recrystallized in ethanol to yield desired title compounds (**7a-d**).

5.1.2.1 3-benzoyl-2-((4-(3,4-dimethoxyphenyl)but-3-en-2-ylidene)hydrazono)thiazolidin-4-one (7a):

Yellow solid, Yield: 39%, mp: 154-156 °C; FTIR (ATR, ν_{max} , cm⁻¹): 3076.01 (Ar-H Str.), 2994.68 (C-H Str. of CH₃), 1705.90 (C=O Str.), 1621.59 (C=C Str.), 1583.66 (C=N Str.), 1760.05 (Acyclic C=O Str.); ¹H-NMR (400 MHz, DMSO-*d*₆, δ , ppm): 8.05 (s, 1H), 8.03 (s, 1H), 7.81-7.77 (t, 1H, $J = 7.44$), 7.64-7.60 (t, 2H, $J = 7.82$ Hz), 7.22 (s, 1H), 7.12-7.10 (m, 1H), 7.09-7.05 (d, 1H, $J = 16.57$ Hz), 6.95-6.93 (d, 1H, $J = 8.40$ Hz), 6.83-6.79 (d, 1H, $J = 16.49$ Hz, HC = CH), 4.22 (s, 2H, -CH₂ of thiazolidone), 3.80 (s, 3H, -OCH₃), 3.76 (s, 3H, -OCH₃), 1.78 (s, 3H, -CH₃); ¹³C-NMR (100 MHz, DMSO, δ ppm): 170.96 (C=O, thiazolidin-4-one), 168.24 (C=O, benzoyl carbon), 164.35 (C=N, 2-ylidene carbon), 158.94 (C=N of thiazolidone), 149.72, 148.92, 136.59, 135.41, 131.01, 130.51, 129.31, 128.71, 125.92, 121.29 (C-6 of DZG), 111.58 (C-5 of DZG), 109.53 (C-2 of DZG), 55.50 (-OCH₃), 55.46 (-OCH₃), 33.23 (-CH₂ of thiazolidone), 12.79 (-CH₃); HRMS (ESI, m/z) [M+Na]⁺; calculated for C₂₂H₂₁N₃O₄S, 446.1150; found 446.1150.

5.1.2.2 2-((4-(3,4-dimethoxyphenyl)but-3-en-2-ylidene)hydrazono)-3-(furan-2-carbonyl) thiazolidin-4-one (7b):

Yellow solid, Yield: 26%, mp: 168-170 °C; FTIR (ATR, ν_{max} , cm⁻¹): 3005.50 (Ar-H Str.), 2958.20 (C-H Str. of CH₃), 1703.06 (C=O Str.), 1621.50 (C=C Str.), 1585.56 (C=N Str.), 1755.04 (Acyclic C=O Str.); ¹H-NMR (400 MHz, DMSO-*d*₆, δ , ppm): 8.24 (s, 1H), 7.87-7.86 (d, 1H, $J = 3.68$ Hz), 7.24 (s, 1H), 7.14-7.10 (m, 2H), 6.96-6.94 (d, 1H, $J = 8.40$ Hz), 6.89-6.88 (dd, 1H, $J = 3.78$, 1.62

Hz), 6.86-6.82 (d, 1H, $J = 16.49$ Hz), 4.18 (s, 2H, $-\text{CH}_2$ of thiazolidone), 3.81 (s, 3H, $-\text{OCH}_3$), 3.77 (s, 3H, $-\text{OCH}_3$), 1.96 (s, 3H, $-\text{CH}_3$); ^{13}C -NMR (100 MHz, DMSO, δ ppm): 170.88 (C=O, thiazolidin-4-one), 164.39 (C=N, 2-ylidene carbon), 158.76 (C=N of thiazolidone), 156.11 (C=O, of furan-2-carbonyl), 151.49, 149.73, 148.93, 146.22, 136.61, 128.72, 125.97, 125.39, 121.31 (C-6 of DZG), 113.96, 111.59 (C-5 of DZG), 109.55 (C-2 of DZG), 55.50 ($-\text{OCH}_3$), 55.47 ($-\text{OCH}_3$), 33.09 ($-\text{CH}_2$ of thiazolidone), 12.94 ($-\text{CH}_3$); HRMS (ESI, m/z) $[\text{M}+\text{Na}]^+$; calculated for $\text{C}_{20}\text{H}_{19}\text{N}_3\text{O}_5\text{S}$, 436.0943; found 436.0945.

5.1.2.3 2-((4-(3,4-dimethoxyphenyl)but-3-en-2-ylidene)hydrazono)-3-(thiophene-2-carbonyl)thiazolidin-4-one (7c):

Yellow solid, Yield: 34%, mp: 212-214 °C; FTIR (ATR, ν_{max} , cm^{-1}): 2995.91 (Ar-H Str.), 2958.38 (C-H Str. of CH_3), 1699.53 (C=O Str.), 1620.69 (C=C Str.), 1581.63 (C=N Str.), 1753.05 (Acyclic C=O Str.); ^1H -NMR (400 MHz, DMSO- d_6 , δ , ppm): 8.31-8.30 (m, 1H), 8.15-8.13 (m, 1H), 7.36-7.34 (t, 1H, $J = 4.38$ Hz), 7.24 (s, 1H), 7.14-7.09 (m, 2H), 6.95-6.93 (d, 1H, $J = 8.40$ Hz), 6.86-6.82 (d, 1H, $J = 16.49$ Hz), 4.19 (s, 2H, $-\text{CH}_2$ of thiazolidone), 3.81 (s, 3H, $-\text{OCH}_3$), 3.77 (s, 3H, $-\text{OCH}_3$), 1.94 (s, 3H, $-\text{CH}_3$); ^{13}C -NMR (100 MHz, DMSO, δ ppm): 170.90 (C=O, thiazolidin-4-one), 164.37 (C=N, 2-ylidene carbon), 161.50 (C=O, thiophene-2-carbonyl), 158.95 (C=N of thiazolidone), 149.72, 148.93, 139.78, 138.95, 136.57, 135.80, 129.50, 128.72, 125.98, 121.29 (C-6 of DZG), 111.59 (C-5 of DZG), 109.55 (C-2 of DZG), 55.47 ($-\text{OCH}_3$), 33.14 ($-\text{CH}_2$ of thiazolidone), 12.93 ($-\text{CH}_3$).

5.1.2.4 2-((4-(3,4-dimethoxyphenyl)but-3-en-2-ylidene)hydrazono)-3-(4-heptylbenzoyl)thiazolidin-4-one (7d):

Yellow solid, Yield: 28%, mp: 121-123 °C; FTIR (ATR, ν_{max} , cm^{-1}): 3043.04 (Ar-H Str.), 2925.12 (C-H Str. of CH_3), 1705.58 (C=O Str.), 1624.73 (C=C Str.), 1597.52 (C=N Str.), 1737.13 (Acyclic C=O Str.); ^1H -NMR (400 MHz, DMSO- d_6 , δ , ppm): 7.95-7.93 (d, 2H, $J = 8.20$ Hz), 7.44 (d, 2H, $J = 8.28$ Hz), 7.22 (s, 1H), 7.12-7.09 (m, 1H), 7.08-7.04 (d, 1H, $J = 16.45$ Hz), 6.95-6.93 (d, 1H, $J = 8.44$ Hz), 6.83-6.79 (d, 1H, $J = 16.45$ Hz), 4.21 (s, 2H, $-\text{CH}_2$ of thiazolidone), 3.80 (s, 3H, $-\text{OCH}_3$), 3.76 (s, 3H, $-\text{OCH}_3$), 2.70-2.67 (t, 2H, $J = 7.56$ Hz), 1.79 (s, 3H, $-\text{CH}_3$), 1.28-1.20 (m, 10H), 0.85-0.82 (t, 3H, $J = 6.84$ Hz); ^{13}C -NMR (100 MHz, DMSO, δ ppm): 171.00 (C=O, thiazolidin-4-one), 167.90 (C=O, benzoyl carbon), 164.24 (C=N, 2-ylidene carbon), 159.02 (C=N of thiazolidone), 151.10, 149.72, 148.92, 136.50, 130.75, 129.27, 128.70, 128.56, 125.94, 121.26 (C-6 of DZG), 121.02, 111.58 (C-5 of DZG), 109.52 (C-2 of DZG), 55.49 ($-\text{OCH}_3$), 35.18, 33.19 ($-\text{CH}_2$ of thiazolidone), 31.19, 30.40, 28.46, 28.44, 22.02, 13.90 ($-\text{CH}_3$), 12.77 ($-\text{CH}_3$); HRMS (ESI, m/z) $[\text{M}+\text{Na}]^+$; calculated for $\text{C}_{29}\text{H}_{35}\text{N}_3\text{O}_4\text{S}$, 544.2246; found 544.2247.

5.1.3 General procedure for synthesis of substituted arylidene malononitriles (**9a-l**)²⁶

To a constantly stirred solution of malononitrile (0.5 g, 0.00757 mol.) in 10.0 mL of ethanol, an appropriately substituted aromatic/heteroaromatic aldehyde (**8a-l**; 0.00757 mol) and 2-4 drops of pyridine was slowly added. The reaction mixture was then either refluxed for 1-2 h (for substituted benzaldehydes) or was stirred at room temperature for 2-3 h (for substituted heteroaromatic aldehydes). The precipitate formed after cooling was filtered to get respective arylidene malononitriles (**9a-l**). The compounds so obtained were fairly pure to carry out the next step.

5.1.4 General procedure for synthesis of substituted 5-(benzylidene)-2-((4-(3,4-dimethoxyphenyl)but-3-en-2-ylidene)hydrazono)thiazolidin-4-one (**10a-l**)²⁷:

To a continuously stirred mixture of compound **5** (0.35 g, 0.00110 mol) and appropriate arylidene malononitriles (**9a-l**; 0.00110 mol) in ethanol (8 mL), few drops of piperidine were added. The reaction mass was refluxed for 3-5 h. The progress of the reaction was constantly monitored by TLC. After cooling, the separated solid or residue was filtered, washed with hot ethanol. All the compounds were further purified by recrystallized in ethanol in order to get the desired title compounds (**10a-l**).

5.1.4.1 5-(3,4-dimethoxybenzylidene)-2-((4-(3,4-dimethoxyphenyl)but-3-en-2-ylidene)hydrazono)thiazolidin-4-one (**10a**):

Yellow solid, Yield: 35%, mp: 227-229 °C; FTIR (ATR, ν_{max} , cm^{-1}): 3115.99 (N-H Str.), 3001.46 (Ar-H Str.), 2957.65 (C-H Str. of CH_3), 1687.41 (C=O Str.), 1624.30 (C=C Str.), 1591.71 (C=N Str.); ¹H-NMR (400 MHz, DMSO-*d*₆, δ , ppm): 12.43 (s, 1H, NH), 7.55 (s, 1H, C=C-H), 7.28 (s, 1H), 7.25 (s, 1H), 7.22-7.20 (m, 1H), 7.18-7.12 (m, 3H), 6.98-6.95 (d, 1H, $J = 8.44$ Hz), 6.95-6.91 (d, 1H $J = 16.49$ Hz, HC = CH), 3.83 (s, 3H, -OCH₃), 3.83 (s, 3H, -OCH₃), 3.82 (s, 3H, -OCH₃), 3.78 (s, 3H, -OCH₃), 2.25 (s, 3H, -CH₃); ¹³C-NMR (100 MHz, DMSO, δ ppm): 167.25 (C=O, thiazolidin-4-one), 163.38 (C=N, 2-ylidene carbon), 156.96 (C=N of thiazolidone), 151.39, 150.24, 149.69, 148.95, 148.86, 136.31, 129.24, 128.88 (C-H, benzylidene carbon), 126.42, 126.36, 122.55, 121.31 (C-6 of DZG), 120.46, 114.14, 112.03, 111.59 (C-5 of DZG), 109.52 (C-2 of DZG), 55.63 (-OCH₃), 55.51 (-OCH₃), 55.47 (-OCH₃), 13.30 (-CH₃); HRMS (ESI, m/z) [$M-H$]; calculated for C₂₄H₂₅N₃O₅S, 466.1437; found 466.1448.

5.1.4.2 5-(2,3-dimethoxybenzylidene)-2-((4-(3,4-dimethoxyphenyl)but-3-en-2-ylidene)hydrazono) thiazolidin-4-one (**10b**):

Yellow solid, Yield: 26%, mp: 195-197 °C; FTIR (ATR, ν_{max} , cm^{-1}): 3109.88 (N-H Str.), 3040.73 (Ar-H Str.), 2948.43 (C-H Str. of CH_3), 1696.80 (C=O Str.), 1623.69 (C=C Str.), 1595.01 (C=N Str.); ¹H-NMR (400 MHz, DMSO-*d*₆, δ , ppm): 12.55 (s, 1H, NH), 7.75 (s, 1H, C=C-H), 7.27 (s,

1H), 7.25-7.23 (d, 1H, $J = 7.88$ Hz), 7.20-7.15 (m, 4H), 6.97-6.95 (d, 1H, $J = 8.40$ Hz), 6.93-6.89 (d, 1H, $J = 16.49$ Hz, HC = CH), 3.84 (s, 3H, -OCH₃), 3.83 (s, 3H, -OCH₃), 3.78 (s, 6H, 2',3'-OCH₃), 2.25 (s, 3H, -CH₃); ¹³C-NMR (100 MHz, DMSO, δ ppm): 167.18 (C=O, thiazolidin-4-one), 163.68 (C=N, 2-ylidene carbon), 156.78 (C=N of thiazolidone), 152.72, 149.73, 148.97, 147.86, 136.49, 128.87, 127.39, 126.26, 124.61, 124.41 (C-5 of thiazolidone), 123.08 (C-H, benzylidene carbon), 121.37 (C-6 of DZG), 119.66, 114.69, 111.61 (C-5 of DZG), 109.53 (C-2 of DZG), 60.97, 56.00 (-OCH₃), 55.84 (-OCH₃), 55.54 (-OCH₃), 55.48 (-OCH₃), 13.28 (-CH₃); HRMS (ESI, m/z) [M-H]⁻; calculated for C₂₄H₂₅N₃O₅S, 466.1437; found 466.1432.

5.1.4.3 5-(4-chlorobenzylidene)-2-((4-(3,4-dimethoxyphenyl)but-3-en-2-ylidene)hydrazono) thiazolidin-4-one (**10c**):

Yellow solid, Yield: 40%, mp: 251-253 °C; FTIR (ATR, ν_{max} , cm⁻¹): 3077.23 (N-H Str.), 3052.86 (Ar-H Str.), 2932.41 (C-H Str. of CH₃), 1729.20 (C=O Str.), 1629.90 (C=C Str.), 1518.99 (C=N Str.); ¹H-NMR (400 MHz, DMSO-*d*₆, δ , ppm): 12.59 (s, 1H, NH), 7.67-7.65 (d, 2H, $J = 8.60$ Hz), 7.60-7.58 (m, 3H), 7.27 (s, 1H), 7.22-7.15 (m, 2H), 6.98-6.96 (d, 1H, $J = 8.40$ Hz), 6.94-6.90 (d, 1H, $J = 16.49$ Hz, HC = CH), 3.83 (s, 3H, -OCH₃), 3.78 (s, 3H, -OCH₃), 2.26 (s, 3H, -CH₃); ¹³C-NMR (100 MHz, DMSO, δ ppm): 166.99 (C=O, thiazolidin-4-one), 163.84 (C=N, 2-ylidene carbon), 156.38 (C=N of thiazolidone), 149.76, 148.97, 136.60, 134.17, 132.58, 131.40, 129.24, 128.84, 127.41 (C-H, benzylidene carbon), 126.19, 124.11 (C-5 of thiazolidone), 121.35 (C-6 of DZG), 111.62 (C-5 of DZG), 109.55 (C-2 of DZG), 55.49 (-OCH₃), 13.35 (-CH₃); HRMS (ESI, m/z) [M-H]⁻; calculated for C₂₂H₂₀ClN₃O₃S, 440.0836; found 440.0839.

5.1.4.4 5-(4-bromobenzylidene)-2-((4-(3,4-dimethoxyphenyl)but-3-en-2-ylidene)hydrazono) thiazolidin-4-one (**10d**):

Yellow solid, Yield: 32%, mp: 255-257 °C; FTIR (ATR, ν_{max} , cm⁻¹): 3049.65 (N-H Str.), 3020.56 (Ar-H Str.), 2930.54 (C-H Str. of CH₃), 1728.47 (C=O Str.), 1628.72 (C=C Str.), 1518.65 (C=N Str.); ¹H-NMR (600 MHz, DMSO-*d*₆, δ , ppm): 12.38 (s, 1H, NH), 7.72-7.70 (d, 2H, $J = 8.28$ Hz), 7.58-7.56 (d, 2H, $J = 8.34$ Hz), 7.54 (s, 1H, C=C-H), 7.25 (s, 1H), 7.19-7.15 (m, 2H), 6.98-6.97 (d, 1H, $J = 8.28$ Hz), 6.90-6.88 (d, 1H, $J = 16.44$ Hz, HC = CH), 3.85 (s, 3H, -OCH₃), 3.80 (s, 3H, -OCH₃), 2.26 (s, 3H, -CH₃); ¹³C-NMR (150 MHz, DMSO, δ ppm): 167.42 (C=O, thiazolidin-4-one), 164.13 (C=N, 2-ylidene carbon), 156.62 (C=N of thiazolidone), 150.57, 149.80, 136.82, 133.56, 132.62, 131.97, 129.65, 127.94 (C-H, benzylidene carbon), 126.97, 125.04 (C-5 of thiazolidone), 123.41, 121.72 (C-6 of DZG), 112.76 (C-5 of DZG), 110.96 (C-2 of DZG), 79.64, 79.41, 79.19, 56.34 (-OCH₃), 56.26 (-OCH₃), 13.90 (-CH₃); HRMS (ESI, m/z) [M-H]⁻; calculated for C₂₂H₂₀BrN₃O₃S, 484.0330; found 484.0349.

5.1.4.5 5-((4-(3,4-dimethoxyphenyl)but-3-en-2-ylidene)hydrazono)thiazolidin-4-one (**10e**):

Yellow solid, Yield: 31%, mp: 205-206 °C; FTIR (ATR, ν_{max} , cm^{-1}): 3112.43 (N-H Str.), 3013.70 (Ar-H Str.), 2959.85 (C-H Str. of CH_3), 1693.90 (C=O Str.), 1590.71 (C=C Str.), 1510.87 (C=N Str.); $^1\text{H-NMR}$ (400 MHz, $\text{DMSO-}d_6$, δ , ppm): 12.56 (s, 1H, NH), 7.66-7.64 (d, 2H, $J = 7.56$ Hz), 7.59 (s, 1H, C=C-H), 7.56-7.52 (t, 2H, $J = 7.58$ Hz), 7.47-7.43 (m, 1H), 7.29 (s, 1H), 7.21-7.16 (m, 2H), 6.98-6.96 (d, 1H, $J = 6.88$ Hz), 6.96-6.92 (d, 1H, $J = 15.13$ Hz, HC = CH), 3.84 (s, 3H, -OCH₃), 3.78 (s, 3H, -OCH₃), 2.26 (s, 3H, -CH₃); $^{13}\text{C-NMR}$ (100 MHz, DMSO , δ ppm): 167.13 (C=O, thiazolidin-4-one), 163.72 (C=N, 2-ylidene carbon), 156.70 (C=N of thiazolidone), 149.73, 148.96, 136.54, 133.65, 129.79, 129.71 (C-H, benzylidene carbon), 129.19, 128.58, 128.76, 126.25, 123.29 (C-5 of thiazolidone), 121.40 (C-6 of DZG), 111.57 (C-5 of DZG), 109.47 (C-2 of DZG), 55.99, 55.54 (-OCH₃), 55.47 (-OCH₃), 18.52, 13.31 (-CH₃); HRMS (ESI, m/z) [M-H]⁻; calculated for $\text{C}_{22}\text{H}_{21}\text{N}_3\text{O}_3\text{S}$, 406.1225; found 406.1223.

5.1.4.6 2-((4-(3,4-dimethoxyphenyl)but-3-en-2-ylidene)hydrazono)-5-(thiophen-2-yl-methylene)thiazolidin-4-one (**10f**):

Yellow orange solid, Yield: 37%, mp: 226-228 °C; FTIR (ATR, ν_{max} , cm^{-1}): 3115.27 (N-H Str.), 3060.27 (Ar-H Str.), 2963.89 (C-H Str. of CH_3), 1694.20 (C=O Str.), 1590.52 (C=C Str.), 1514.47 (C=N Str.); $^1\text{H-NMR}$ (400 MHz, $\text{DMSO-}d_6$, δ , ppm): 12.51 (s, 1H, NH), 7.97-7.96 (d, 1H, $J = 5.00$ Hz), 7.86 (s, 1H, C=C-H), 7.62-7.61 (d, 1H, $J = 3.44$ Hz), 7.30 (s, 1H), 7.28-7.26 (m, 1H), 7.22-7.16 (m, 2H), 6.97-6.92 (m, 2H), 3.84 (s, 3H, -OCH₃), 3.78 (s, 3H, -OCH₃), 2.26 (s, 3H, -CH₃); $^{13}\text{C-NMR}$ (100 MHz, DMSO , δ ppm): 166.91 (C=O, thiazolidin-4-one), 163.70 (C=N, 2-ylidene carbon), 156.30 (C=N of thiazolidone), 149.75, 148.99, 137.82, 136.59, 133.23, 131.82, 128.87, 128.68, 126.24, 122.18 (C-H, benzylidene carbon), 121.48 (C-6 of DZG), 120.98 (C-5 of thiazolidone), 111.58 (C-5 of DZG), 109.49 (C-2 of DZG), 55.54 (-OCH₃), 13.37 (-CH₃); HRMS (ESI, m/z) [M-H]⁻; calculated for $\text{C}_{20}\text{H}_{19}\text{N}_3\text{O}_3\text{S}_2$, 412.0790; found 412.0779.

5.1.4.7 2-((4-(3,4-dimethoxyphenyl)but-3-en-2-ylidene)hydrazono)-5-(pyridin-4-yl-methylene)thiazolidin-4-one (**10g**):

Yellow solid, Yield: 29%, mp: 258-260 °C; FTIR (ATR, ν_{max} , cm^{-1}): 3011.90 (N-H Str.), 2935.45 (Ar-H Str.), 2837.61 (C-H Str. of CH_3), 1719.49 (C=O Str.), 1633.77 (C=C Str.), 1598.56 (C=N Str.); $^1\text{H-NMR}$ (600 MHz, $\text{DMSO-}d_6$, δ , ppm): 12.61 (s, 1H, NH), 8.72-8.71 (d, 2H, $J = 5.04$ Hz), 7.57-7.56 (d, 2H, $J = 5.10$ Hz), 7.53 (s, 1H, C=C-H), 7.27 (s, 1H), 7.2-7.19 (d, 1H, $J = 16.50$ Hz), 7.18-7.17 (d, 1H, $J = 8.28$ Hz), 6.99-6.97 (d, 1H, $J = 8.22$ Hz), 6.93-6.90 (d, 1H, $J = 16.50$ Hz, HC = CH), 3.84 (s, 3H, -OCH₃), 3.80 (s, 3H, -OCH₃), 2.27 (s, 3H, -CH₃); $^{13}\text{C-NMR}$ (150 MHz,

DMSO, δ ppm); 167.20 (C=O, thiazolidin-4-one), 164.59 (C=N, 2-ylidene carbon), 156.53 (C=N of thiazolidone), 150.97, 150.52, 149.71, 141.31, 137.19, 129.51, 129.18 (C-5 of thiazolidone), 126.79, 126.18 (C-H, benzylidene carbon), 123.70, 121.84 (C-6 of DZG), 112.55 (C-5 of DZG), 110.69 (C-2 of DZG), 65.31, 56.27 (-OCH₃), 56.18 (-OCH₃), 31.07, 15.59, 13.93 (-CH₃); HRMS (ESI, m/z) [M-H]⁻; calculated for C₂₁H₂₀N₄O₃S, 407.1178; found 407.1164.

5.1.4.8 2-((4-(3,4-dimethoxyphenyl)but-3-en-2-ylidene)hydrazono)-5-(4-methyl benzylidene)thiazolidin-4-one (**10h**):

Yellow solid, Yield: 40%, mp: 236-238 °C; FTIR (ATR, ν_{max} , cm⁻¹): 3118.74 (N-H Str.), 3019.85 (Ar-H Str.), 2964.49 (C-H Str. of CH₃), 1697.55 (C=O Str.), 1592.59 (C=C Str.), 1514.23 (C=N Str.); ¹H-NMR (400 MHz, DMSO-*d*₆, δ , ppm): 12.50 (s, 1H, NH), 7.55 (s, 2H), 7.52 (s, 1H, C=C-H), 7.36-7.34 (d, 2H, *J* = 8.04 Hz), 7.29 (s, 1H), 7.21-7.15 (m, 2H), 6.98-6.92 (m, 2H), 3.84 (s, 3H, -OCH₃), 3.78 (s, 3H, -OCH₃), 2.36 (s, 3H, -CH₃), 2.26 (s, 3H, -CH₃); ¹³C-NMR (100 MHz, DMSO, δ ppm): 167.22 (C=O, thiazolidin-4-one), 163.59 (C=N, 2-ylidene carbon), 156.80 (C=N of thiazolidone), 149.71, 148.96, 139.84, 136.46, 135.41, 130.88, 129.84 (C-H, benzylidene carbon), 129.80, 128.87, 128.75, 126.29, 122.06 (C-5 of thiazolidone), 121.38 (C-6 of DZG), 111.58 (C-5 of DZG), 109.47 (C-2 of DZG), 55.53 (-OCH₃), 55.47 (-OCH₃), 21.04 (-CH₃), 13.30 (-CH₃); HRMS (ESI, m/z) [M-H]⁻; calculated for C₂₃H₂₃N₃O₃S, 420.1382; found 420.1392.

5.1.4.9 2-((4-(3,4-dimethoxyphenyl)but-3-en-2-ylidene)hydrazono)-5-(pyridin-3-yl-methylene)thiazolidin-4-one (**10i**):

Yellow solid, Yield: 25%, mp: 235-237 °C; FTIR (ATR, ν_{max} , cm⁻¹): 2999.21 (N-H Str.), 2929.09 (Ar-H Str.), 2833.81 (C-H Str. of CH₃), 1713.41 (C=O Str.), 1625.05 (C=C Str.), 1514.55 (C=N Str.); ¹H-NMR (400 MHz, DMSO-*d*₆, δ , ppm): 12.66 (s, 1H, NH), 8.85 (s, 1H), 8.60-8.59 (d, 1H, *J* = 4.76 Hz), 8.02-8.01 (d, 1H, *J* = 8.00 Hz), 7.62 (s, 1H, C=C-H), 7.58-7.55 (dd, 1H, *J* = 7.89, 4.24 Hz), 7.28 (s, 1H), 7.22-7.15 (m, 2H), 6.97-6.91 (m, 2H), 3.83 (s, 3H, -OCH₃), 3.78 (s, 3H, -OCH₃), 2.26 (s, 3H, -CH₃); ¹³C-NMR (100 MHz, DMSO, δ ppm): 166.85 (C=O, thiazolidin-4-one), 163.93 (C=N, 2-ylidene carbon), 156.39 (C=N of thiazolidone), 151.05, 149.84, 149.76, 148.96, 136.69, 135.79, 129.81, 128.82, 126.16, 125.70 (C-5 of thiazolidone), 125.30 (C-H, benzylidene carbon), 124.09, 121.43 (C-6 of DZG), 111.58 (C-5 of DZG), 109.48 (C-2 of DZG), 55.54 (-OCH₃), 55.47 (-OCH₃), 18.52, 13.35 (-CH₃); HRMS (ESI, m/z) [M-H]⁻; calculated for C₂₁H₂₀N₄O₃S, 407.1178; found 407.1172.

5.1.4.10 5-(3-chlorobenzylidene)-2-((4-(3,4-dimethoxyphenyl)but-3-en-2-ylidene)hydrazono)thiazolidin-4-one (**10j**):

Yellow solid, Yield: 28%, mp: 217-219 °C; FTIR (ATR, ν_{max} , cm^{-1}): 3063.62 (N-H Str.), 2917.80 (Ar-H Str.), 2831.79 (C-H Str. of CH_3), 1720.58 (C=O Str.), 1628.09 (C=C Str.), 1599.95 (C=N Str.); $^1\text{H-NMR}$ (400 MHz, $\text{DMSO-}d_6$, δ , ppm): 12.54 (s, 1H, NH), 7.68 (s, 1H, C=C-H), 7.56-7.48 (m, 5H), 7.21-7.16 (d, 1H, $J = 16.61$ Hz, HC = CH), 7.14 (s, 2H), 7.02-7.00 (d, 1H, $J = 8.76$ Hz), 3.80 (s, 3H, -OCH₃), 3.79 (s, 3H, -OCH₃), 2.26 (s, 3H, -CH₃); $^{13}\text{C-NMR}$ (100 MHz, DMSO, δ ppm): 167.06 (C=O, thiazolidin-4-one), 160.99 (C=N, 2-ylidene carbon), 155.76 (C=N of thiazolidone), 150.12, 148.95, 148.87, 137.97, 135.87, 133.77, 131.01, 129.50, 129.23, 128.71, 127.73, 127.01 (C-H, benzylidene carbon), 125.14 (C-5 of thiazolidone), 120.94 (C-6 of DZG), 117.39, 111.83 (C-5 of DZG), 110.35 (C-2 of DZG), 55.51 (-OCH₃), 55.43 (-OCH₃), 19.69, 13.35 (-CH₃).

5.1.4.11 5-(2-chlorobenzylidene)-2-((4-(3,4-dimethoxyphenyl)but-3-en-2-ylidene)hydrazono)thiazolidin-4-one (**10k**):

Yellow solid, Yield: 23%, mp: 213-215 °C; FTIR (ATR, ν_{max} , cm^{-1}): 3029.50 (N-H Str.), 2937.75 (Ar-H Str.), 2838.67 (C-H Str. of CH_3), 1714.87 (C=O Str.), 1619.95 (C=C Str.), 1598.06 (C=N Str.); $^1\text{H-NMR}$ (400 MHz, $\text{DMSO-}d_6$, δ , ppm): 12.70 (s, 1H, NH), 7.75 (s, 1H, C=C-H), 7.71-7.69 (d, 1H, $J = 7.68$ Hz), 7.63-7.61 (d, 1H, $J = 7.96$ Hz), 7.56-7.52 (t, 1H, $J = 7.38$ Hz), 7.49-7.44 (m, 1H), 7.26 (s, 1H), 7.21-7.14 (m, 2H), 6.96-6.94 (d, 1H, $J = 8.40$ Hz), 6.92-6.88 (d, 1H, $J = 16.49$ Hz, HC = CH), 3.82 (s, 3H, -OCH₃), 3.77 (s, 3H, OCH₃), 2.25 (s, 3H, -CH₃); $^{13}\text{C-NMR}$ (100 MHz, DMSO, δ ppm): 166.75 (C=O, thiazolidin-4-one), 164.00 (C=N, 2-ylidene carbon), 156.33 (C=N of thiazolidone), 149.75, 148.95, 136.71, 134.09, 131.54, 131.13, 130.23, 128.90, 128.80, 127.95, 126.86 (C-5 of thiazolidone), 126.13, 123.69 (C-H, benzylidenecarbon), 121.41 (C-6 of DZG), 111.56 (C-5 of DZG), 109.48 (C-2 of DZG), 55.52 (-OCH₃), 55.46 (-OCH₃), 13.34 (-CH₃).

5.1.4.12 2-((4-(3,4-dimethoxyphenyl)but-3-en-2-ylidene)hydrazono)-5-(3-nitrobenzylidene)thiazolidin-4-one (**10l**):

Yellow solid, Yield: 22%, mp: 249-251 °C; FTIR (ATR, ν_{max} , cm^{-1}): 3106.33 (N-H Str.), 3039.40 (Ar-H Str.), 2957.11 (C-H Str. of CH_3), 1693.10 (C=O Str.), 1619.19 (C=C Str.), 1598.60 (C=N Str.); $^1\text{H-NMR}$ (400 MHz, $\text{DMSO-}d_6$, δ , ppm): 12.70 (s, 1H, NH), 8.45 (s, 1H), 8.26-8.24 (d, 1H, $J = 8.20$ Hz), 8.06-8.04 (d, 1H, $J = 7.92$ Hz), 7.84-7.80 (t, 1H, $J = 8.02$ Hz), 7.72 (s, 1H, C=C-H), 7.27 (s, 1H), 7.22-7.15 (m, 2H), 6.97-6.95 (d, 1H, $J = 8.36$ Hz), 6.93-6.89 (d, 1H, $J = 16.45$ Hz, HC = CH), 3.83 (s, 3H, -OCH₃), 3.78 (s, 3H, -OCH₃), 2.26 (s, 3H, -CH₃); $^{13}\text{C-NMR}$ (100 MHz,

DMSO, δ ppm): 166.74 (C=O, thiazolidin-4-one), 164.18 (C=N, 2-ylidene carbon), 155.86 (C=N of thiazolidone), 149.78, 148.95, 148.21, 136.83, 135.38, 135.25, 130.71, 128.79, 126.40 (C-5 of thiazolidone), 126.35 (C-H, benzylidene carbon), 126.05, 124.06, 123.76, 121.36 (C-6 of DZG), 111.60 (C-5 of DZG), 109.64 (C-2 of DZG), 55.52 (-OCH₃), 30.64, 13.41 (-CH₃); HRMS (ESI, m/z) [M-H]⁻; calculated for C₂₂H₂₀N₄O₅S, 451.1076; found 451.1089.

5.1.5 General procedure for synthesis of substituted isatin malononitriles (12a-b)

To a constantly stirred solution of malononitrile (0.5 g, 0.00757 mol) in 10.0 mL of ethanol, substituted isatins (11a-b; 0.00757 mol) and 2-4 drops of pyridine was slowly added. The reaction mixture was then either refluxed for 1 h. The precipitate formed was filtered and washed with ethanol to get respective isatin malononitriles (12a-b). The compounds so obtained were fairly pure to carry out the next step.

5.1.6 General procedure for synthesis of substituted 2-((4-(3,4-dimethoxyphenyl)but-3-en-2-ylidene)hydrazono)-5-(2-oxindolin-3-ylidene)thiazolidin-4-one (13a-b)

To a continuously stirred mixture of compound 5 (0.35 g, 0.00110 mol) and an appropriate isatin malononitriles (12a-b; 0.00110 mol) in ethanol (8 mL), few drops of piperidine was added. The reaction mass was refluxed for 4 h. The progress of the reaction was constantly monitored by TLC. After cooling, the separated solid or residue was filtered, washed with hot ethanol. All the compounds were further purified by recrystallized in ethanol in order to get the desired title compounds (**13a-b**).

5.1.6.1 2-((4-(3,4-dimethoxyphenyl)but-3-en-2-ylidene)hydrazono)-5-(2-oxindolin-3-ylidene)thiazolidin-4-one (**13a**):

Brown solid, Yield: 65%, mp: 273-275 °C; FTIR (ATR, ν_{max} , cm⁻¹): 3108.78 (N-H Str.), 3050.10 (Ar-H Str.), 2960.57 (C-H Str. of CH₃), 1684.50 (C=O Str.), 1606.20 (C=C Str.), 1509.36 (C=N Str.); ¹H-NMR (400 MHz, DMSO-*d*₆, δ , ppm): 12.79 (s, 1H, NH), 11.10 (s, 1H, NH of Isatin ring), 8.83-8.81 (d, 1H, *J* = 7.92 Hz), 7.34-7.30 (t, 1H, *J* = 7.66 Hz), 7.28 (s, 1H), 7.21-7.16 (m, 2H), 7.05-7.01 (t, 1H, *J* = 7.70 Hz), 6.96-6.90 (m, 3H), 3.84 (s, 3H, -OCH₃), 3.77 (s, 3H, -OCH₃), 2.26 (s, 3H, -CH₃); ¹³C-NMR (100 MHz, DMSO, δ ppm): 168.69, 167.14 (C=O, thiazolidin-4-one), 164.13 (C=N, 2-ylidene carbon), 159.00 (C=N of thiazolidone), 149.75, 148.97, 142.86, 136.69, 133.61 (C-5 of thiazolidone), 131.31, 128.83, 127.83, 126.29, 124.20, 121.67, 121.49 (C-6 of DZG), 120.33, 111.55 (C-5 of DZG), 110.06, 109.45 (C-2 of DZG), 55.45 (-OCH₃), 13.10 (-CH₃); HRMS (ESI, m/z) [M-H]⁻; calculated for C₂₃H₂₀N₄O₄S, 447.1127; found 447.1138.

5.1.6.2 5-(5-chloro-2-oxoindolin-3-ylidene)-2-((4-(3,4-dimethoxyphenyl)but-3-en-2-ylidene)hydrazono)thiazolidin-4-one (**13b**):

Brown solid, Yield: 46%, mp: 282-284 °C; FTIR (ATR, ν_{max} , cm^{-1}): 3111.15 (N-H Str.), 3046.29 (Ar-H Str.), 2964.87 (C-H Str. of CH_3), 1685.42 (C=O Str.), 1607.75 (C=C Str.), 1509.51 (C=N Str.); $^1\text{H-NMR}$ (400 MHz, $\text{DMSO-}d_6$, δ , ppm): 12.88 (s, 1H, NH), 11.20 (s, 1H, NH of Isatin ring), 8.84-8.83 (d, 1H, $J = 2.00$ Hz), 7.35-7.32 (q, 1H, $J = 8.32$ Hz), 7.27 (s, 1H), 7.20-7.14 (m, 2H), 6.94-6.93 (d, 1H, $J = 2.92$ Hz), 6.91-6.88 (m, 2H), 3.83 (s, 3H, $-\text{OCH}_3$), 3.76 (s, 3H, $-\text{OCH}_3$), 2.25 (s, 3H, $-\text{CH}_3$); $^{13}\text{C-NMR}$ (100 MHz, DMSO , δ ppm): 168.42, 167.13 (C=O, thiazolidin-4-one), 164.39 (C=N, 2-ylidene carbon), 158.49 (C=N of thiazolidone), 149.76, 148.95, 141.48, 136.81, 135.71 (C-5 of thiazolidone), 130.44, 128.79, 127.12, 126.21, 125.47, 122.89, 121.61, 121.54 (C-6 of DZG), 111.48, 111.32 (C-5 of DZG), 109.39 (C-2 of DZG), 55.99 ($-\text{OCH}_3$), 55.43 ($-\text{OCH}_3$), 18.52, 13.09 ($-\text{CH}_3$).

5.2 *In vitro* antimycobacterial evaluation

All the newly synthesized compounds (**5**, **7a-d**, **10a-l** and **13a, b**) were screened for their *in vitro* antimycobacterial activity against *M. tuberculosis* H₃₇Rv grown under aerobic conditions by using a dual read-out (OD₅₉₀ and fluorescence) assay procedure.²¹⁻²³ The activity was carried out at Infectious Disease Research Institute (IDRI) within the National Institute of Allergy and Infectious Diseases (NIAID) screening program, Bethesda, MD, USA. Test compounds were prepared as 10-point two-fold serial dilutions in DMSO and diluted into 7H9-Tw-OADC medium in 96-well plates with a final DMSO concentration of 2%. The highest concentration of compound was 200 μM and compounds were soluble in DMSO at 10 mM. For compounds with limited solubility, the highest concentration was 50X less than the stock concentration e.g. 100 μM for 5 mM DMSO stock, 20 μM for 1 mM DMSO stock. For potent compounds, assays were repeated at lower starting concentrations. Each plate included assay controls for background (medium/DMSO only, no bacterial cells), zero growth (100 μM Rifampicin) and maximum growth (DMSO only), as well as a rifampicin dose response curve. Plates were inoculated with *M. tuberculosis* and incubated for 5 days: growth was measured by OD₅₉₀ and fluorescence (Ex₅₆₀/Em₅₉₀) using a BioTek™ Synergy4 plate reader. Growth was calculated separately for OD₅₉₀ and RFU. MIC was calculated on the basis of 10-point dose response curve which was plotted as % growth. The MIC was defined as the minimum concentration at which growth was completely inhibited and was calculated from the inflection point of the fitted curve to the lower asymptote (zero growth). In addition, dose response curves were generated using the Levenberg-Marquardt algorithm and the concentrations that resulted in 50% and 90% inhibition of growth were determined (IC₅₀ and IC₉₀ respectively).

5.3 Cytotoxicity studies: MTT assay

The cellular conversion of MTT [3-(4,5-dimethylthiazo-2-yl)-2,5-diphenyl-tetrazolium bromide] into a formazan product was used to evaluate cytotoxic activity (IC_{50}) of some selected compounds (**5**, **7a-d**, **10b-d**, **10f**, **10g**, **10i**, **10j**, **10l**, **13a** and **13b**) against mammalian VERO cells, which were cultured in Dulbecco Modified Eagle Medium (DMEM) containing 2 mM Na_2CO_3 supplemented with 10% (v/v) fetal bovine serum (FBS). The cells were incubated at 37 °C under 5% CO_2 and 95% air in a humidified atmosphere until confluent and then diluted with phosphate-buffered saline. Stock solutions were prepared in dimethyl sulfoxide (DMSO) and further dilutions were made with fresh culture medium. The concentration of DMSO in the final culture medium was 1%, which had no effect on the cell viability. In a transparent 96-well plate, serially diluted stock solutions were placed at 37 °C for 72 h then the medium was removed and monolayer was washed twice with 100 μ L of warm Hanks' balanced salt solution (HBSS). After 72 h of exposure, cell viability was assessed on the basis of MTT into a formazan product using the Promega cell Titre 96 non-radioactive cell proliferation assay.²⁸ The same experimental conditions were maintained for all the compounds.

5.4 X-ray crystallographic data of compound 5.

Table 2: Sample and crystal data for compound 5.

Identification code	Compound 5	
Chemical formula	$C_{15}H_{17}N_3O_3S$	
Formula weight	306.27	
Temperature	296(2) K	
Wavelength	0.71073 Å	
Crystal size	0.190 x 0.290 x 0.530 mm	
Crystal habit	light yellow plate	
Crystal system	monoclinic	
Space group	P 1 21/c 1	
Unit cell dimensions	a = 20.8194(12) Å	$\alpha = 90^\circ$
	b = 7.8281(6) Å	$\beta = 95.764(3)^\circ$
	c = 9.5454(6) Å	$\gamma = 90^\circ$
Volume	1547.81(18) Å ³	
Z	20	
Density (calculated)	6.572 Mg/cm ³	
Absorption coefficient	1.116 mm ⁻¹	
F(000)	3100	

Table 3: Data collection and structure refinement for compound 5.

Theta range for data collection	1.97 to 25.64°
Index ranges	-25 ≤ h ≤ 25, -7 ≤ k ≤ 9, -11 ≤ l ≤ 11
Reflections collected	14169
Independent reflections	2918 [R(int) = 0.0175]
Coverage of independent reflections	99.9%
Absorption correction	multi-scan
Max. and min. transmission	0.8160 and 0.5904
Structure solution technique	direct methods
Structure solution program	SHELXS-97 (Sheldrick, 2008)
Refinement method	Full-matrix least-squares on F ²
Refinement program	SHELXL-97 (Sheldrick, 2008)
Function minimized	$\Sigma w(F_o^2 - F_c^2)^2$
Data / restraints / parameters	2918 / 0 / 202
Goodness-of-fit on F ²	1.039
Final R indices	2656 data; I > 2σ(I) R1 = 0.0290, wR2 = 0.0735 all data R1 = 0.0329, wR2 = 0.0766
Weighting scheme	w = 1/[σ ² (F _o ²) + (0.0354P) ² + 0.8713P] where P = (F _o ² + 2F _c ²)/3
Largest diff. peak and hole	0.258 and -0.236 eÅ ⁻³
R.M.S. deviation from mean	0.041 eÅ ⁻³

Acknowledgments:

Authors are thankful to Discipline of Pharmaceutical Sciences, College of Health Sciences, University of KwaZulu-Natal (UKZN), South Africa, for their constant support, encouragement and financial assistance. Authors also sincerely thank National Institutes of Health and the National Institute of Allergy and Infectious Diseases (NIAID), Bethesda, MD, USA (Contract No. HHSN272201100009I/HHSN27200004 A19) for antimycobacterial screening. Authors express heartfelt thanks to Mr. Dilip Jagjivan and Dr. Caryl Janse Van Rensburg (UKZN, South Africa) for their assistance in the NMR and EIMS experiments.

Conflict of Interest:

Authors hereby declare that there are no financial/commercial conflicts of interest.

References:

- 1 WHO TB report, *WHO | Global tuberculosis report 2015*, World Health Organization, 2015.
- 2 A. Pablos-Méndez, M. C. Raviglione, A. Laszlo, N. Binkin, H. L. Rieder, F. Bustreo, D. L. Cohn, C. S. B. Lambregts-van Weezenbeek, S. J. Kim, P. Chaulet and P. Nunn, *N. Engl. J. Med.*, 1998, **338**, 1641–1649.
- 3 S. Jaju, M. Palkar, V. S. Maddi, P. Ronad, S. Mamledesai, D. Satyanarayana and M. Ghatole, *Arch. Pharm. (Weinheim)*, 2009, **342**, 723–731.
- 4 A. Upadhyay, S. K. Srivastava and S. D. Srivastava, *Eur. J. Med. Chem.*, 2010, **45**, 3541–3548.
- 5 A. Verma and S. K. Saraf, *Eur. J. Med. Chem.*, 2008, **43**, 897–905.
- 6 A. C. Tripathi, S. J. Gupta, G. N. Fatima, P. K. Sonar, A. Verma and S. K. Saraf, *Eur. J. Med. Chem.*, 2014, **72**, 52–77.
- 7 G. Küçükgülzel, A. Kocatepe, E. De Clercq, F. Şahin and M. Güllüce, *Eur. J. Med. Chem.*, 2006, **41**, 353–359.
- 8 A. M. Rana, P. Trivedi, K. R. Desai and S. Jauhari, *Med. Chem. Res.*, 2014, **23**, 4320–4336.
- 9 G. A. Hampannavar, R. Karpoormath, M. B. Palkar and M. S. Shaikh, *Bioorg. Med. Chem.*, 2016, **24**, 501–520.
- 10 A. K. Bakkestuen, L.-L. Gundersen, G. Langli, F. Liu and J. M. . Nolsøe, *Bioorg. Med. Chem. Lett.*, 2000, **10**, 1207–1210.
- 11 D. G. Joshi, H. B. Oza and H. H. Parekh, *Heterocycl. Commun.*, 1997, **3**, 169–174.
- 12 G. A. Hampannavar, R. Karpoormath, M. B. Palkar, M. S. Shaikh and B. Chandrasekaran, *ACS Med. Chem. Lett.*, 2016, **7**, 686–691.
- 13 M. S. Shaikh, M. B. Palkar, H. M. Patel, R. A. Rane, W. S. Alwan, M. M. Shaikh, I. M. Shaikh, G. A. Hampannavar and R. Karpoormath, *RSC Adv.*, 2014, **4**, 62308–62320.
- 14 P. Samadhiya, R. Sharma, S. D. Srivastava and S. K. Srivastava, *Acta Chim Slov*, 2012, **59**, 632–640.
- 15 D. D. Subhedar, M. H. Shaikh, M. A. Arkile, A. Yeware, D. Sarkar and B. B. Shingate, *Bioorganic Med. Chem. Lett.*, 2016, **26**, 1704–1708.
- 16 N. Karali, A. Gürsoy, F. Kandemirli, N. Shvets, F. B. Kaynak, S. Özbey, V. Kovalishyn and A. Dimoglo, *Bioorganic Med. Chem.*, 2007, **15**, 5888–5904.
- 17 D. D. Subhedar, M. H. Shaikh, B. B. Shingate, L. Nawale, D. Sarkar and V. M. Khedkar, *Med. Chem. Commun.*, 2016, **7**, 1832–1848.
- 18 X. Lu, Z. Lu and X. Zhang, *Tetrahedron*, 2006, **62**, 457–460.

- 19 H. Behbehani, H. M. Ibrahim, S. Makhseed, M. H. Elnagdi and H. Mahmoud, *Eur. J. Med. Chem.*, 2012, **52**, 51–65.
- 20 S. Chimichi, B. Cosimelli, M. Bambagiotti-Alberti, S. A. Coran and F. F. Vincieri, *Magn. Reson. Chem.*, 1993, **31**, 1044–1047.
- 21 A. Zelmer, P. Carroll, N. Andreu, K. Hagens, J. Mahlo, N. Redinger, B. D. Robertson, S. Wiles, T. H. Ward, T. Parish, J. Ripoll, G. J. Bancroft and U. E. Schaible, *J. Antimicrob. Chemother.*, 2012, **67**, 1948–60.
- 22 J. Ollinger, M. A. Bailey, G. C. Moraski, A. Casey, S. Florio, T. Alling, M. J. Miller and T. Parish, *PLoS One*, 2013, **8**, 1–9.
- 23 R. J. Lambert and J. Pearson, *J. Appl. Microbiol.*, 2000, **88**, 784–790.
- 24 M. E. Haiba, S. S. Abd El-Karim, R. S. Gouhar, M. I. El-Zahar and S. A. El-Awdan, *Med. Chem. Res.*, 2014, **23**, 3418–3435.
- 25 M. A. Metwally, S. Bondock, H. El-Azap and E.-E. M. Kandeel, *J. Sulfur Chem.*, 2011, **32**, 489–519.
- 26 M. Mantri, O. de Graaf, J. van Veldhoven, A. Göblyös, J. K. von Frijtag Drabbe Künzel, T. Mulder-Krieger, R. Link, H. de Vries, M. W. Beukers, J. Brussee and A. P. Ijzerman, *J. Med. Chem.*, 2008, **51**, 4449–4455.
- 27 H. Behbehani and H. M. Ibrahim, *Molecules*, 2012, **17**, 6362–6385.
- 28 T. Mosmann, *J. Immunol. Methods*, 1983, **65**, 55–63.

CHAPTER 5

Dehydrozingerone encouraged novel styryl pyrazolo carbazone hybrids as potential antimicrobial and antimycobacterial agents.

Girish A. Hampannavar^a, Mahesh B. Palkar^{b,a}, Afsana Kajee^a, Mahamadhanif S. Shaikh^a, Koleka P. Mlisana^c, Rajshekhar V. Karpoormath^{a*}

^a Department of Pharmaceutical Chemistry, Discipline of Pharmaceutical Sciences, College of Health Sciences, University of KwaZulu-Natal (Westville), Durban-4000, South Africa.

^b Department of Pharmaceutical Chemistry, K.L.E. University College of Pharmacy, Vidyanagar, Hubballi-580031, Karnataka, India.

^c Department of Microbiology, National Health Laboratory Services (NHLS), Inkosi Albert Luthuli Central Hospital, Durban, South Africa

Graphical Abstract



*Corresponding author

E-mail: karpoormath@ukzn.ac.za, rvk2006@gmail.com

Tel no.: +27(0)312607179, +27721107207; Fax No.: +27(0)312607792

Abstract

A novel series of Dehydrozingerone (DZG) inspired styryl pyrazolo carbazones (**8a-i**, **11a-h** and **14a-c**) were designed and synthesized in good yields by means of a hybridization approach. The synthesized compounds were screened for their *in vitro* antibacterial and antimycobacterial activities. From the series tested, compounds **8a**, **8c**, **8d**, **8g**, **8h**, **8i** and **11f** showed reasonable antibacterial activity (MIC = 50 µg/mL) against *B. subtilis* and also compound **11a** demonstrated decent activity towards *P. aeruginosa* (MIC = 25 µg/mL). Compounds **8a**, **8d**, **8e**, **8f**, **8i**, and **11h** demonstrated good to moderate antifungal activity ranging from 25 to 50 µg/mL towards *C. neoformans* (MIC = 25 µg/mL) and *C. albicans* (MIC = 50 µg/mL). Besides, compound **8a**, comprising of isonicotinoyl hydrazide portion displayed remarkable antitubercular activity (MIC = 0.78 µg/mL) against H₃₇Rv. Substituted urea derivatives, **14a-c** and **11d** also exhibited encouraging activity (MIC = 12.5 and 25 µg/mL, respectively) whereas, derivative with thiourea portion **11a**, (MIC = 0.78 µg/mL) illustrated significant activity against H₃₇Rv. Moreover, some of the tested compounds showed reasonable activity against MDR (multi drug resistant) and MOTT (mycobacteria other than tuberculosis) strains. Suggesting the importance of styryl pyrazole carbazones for effective antibacterial and antimycobacterial activity.

Keywords

Antibacterial activity, Antimycobacterial activity; Dehydrozingerone; pyrazole; *Mycobacterium tuberculosis* H₃₇Rv.

1 Introduction

Bacterial infections still persist as an important cause of morbidity and mortality. It's one of the serious issues that is threatening and burdening mankind. Further, dearth in response to the drug, which it was originally sensitive to has led to antimicrobial resistance. This resistance has ancillary exacerbated the situation making it nearly impossible to treat. According to WHO, emerging new resistance mechanisms are challenging our capabilities in treating these common infectious diseases, eventually leading to persistent illness of patient followed by disability and death.[1] Furthermore, resistance issues in ailments like tuberculosis, malaria, and HIV have aroused a serious concern in disease management and its mitigation. In particular, tuberculosis is a most dangerous disease affecting one third of the world's population. In spite of several drugs namely, isoniazid, rifampicin, pyrazinamide and ethambutol, existing for its treatment, the resistance issue has left us to look for new drug leads that may possibly overcome this problem. Therefore, much focus is being payed towards generating a new libraries of molecules with a hope to obtain a potential antimicrobial or antitubercular leads. These leads may certainly overcome the existing issues mainly multiple drug dosing regimens, resistance, long treatment duration and toxicity.

In a pursuit to develop novel antibacterial [2] and antitubercular libraries [3,4] we have come across several privileged heterocyclic scaffolds. Pyrazole, a renowned heterocycle have been known to exhibit a significant range of biological activities namely, antibacterial, antifungal [5], anticancer [6], antiviral [7], antidiabetic [8], anti-inflammatory [9], antiatherosclerosis [10], antimycobacterial [11] and several others. Conversely, several pyrazole derivatives have been in clinical use since periods. Some of the drugs having this distinguished motif like celecoxib, eprizole, lonazolac, tepoxalin, rimonabant etc. (Figure 1) have proven efficacy.

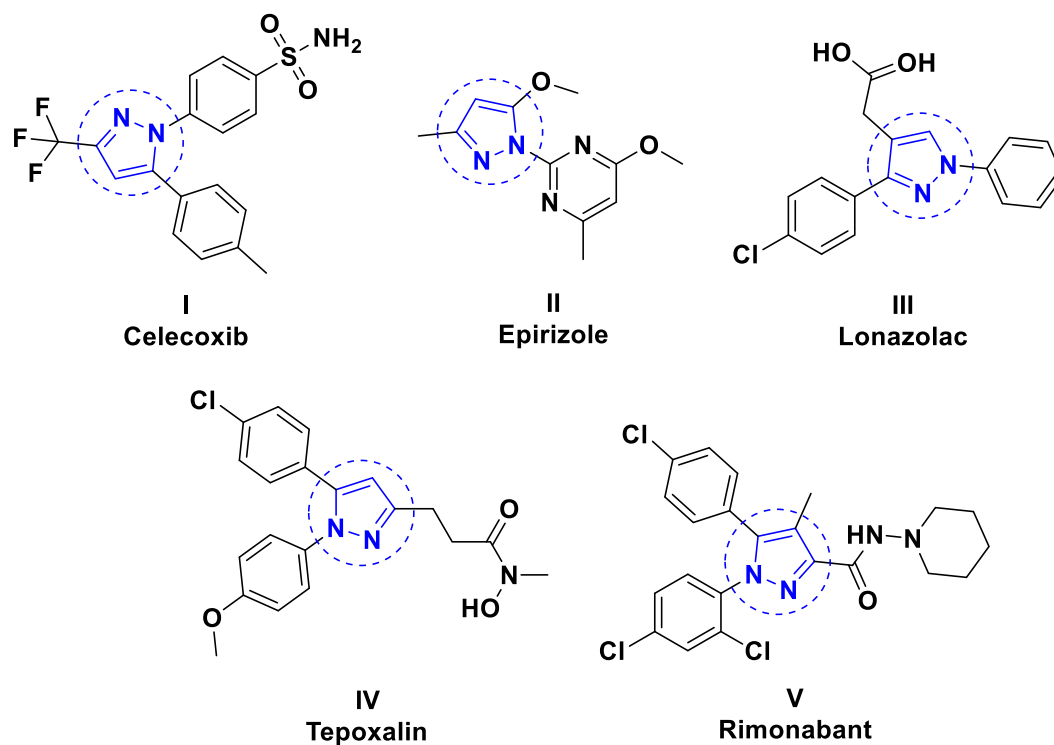


Figure 1: Approved drugs containing pyrazole core.

Further, semicarbazone and thiosemicarbazones are versatile chemical intermediates that are employed in synthesis of several key heterocyclic compounds. Comprised of N, O and S hetero atoms, these semicarbazone and thiosemicarbazones are known to be biologically active and possess assorted pharmacological responses. The activity spectrum of these semicarbazone and thiosemicarbazones range into various categories namely antibacterial, antiproliferative [12], antifungal [13], anticancer [14], anticonvulsant [15], antitubercular [16] etc. (Figure 2)

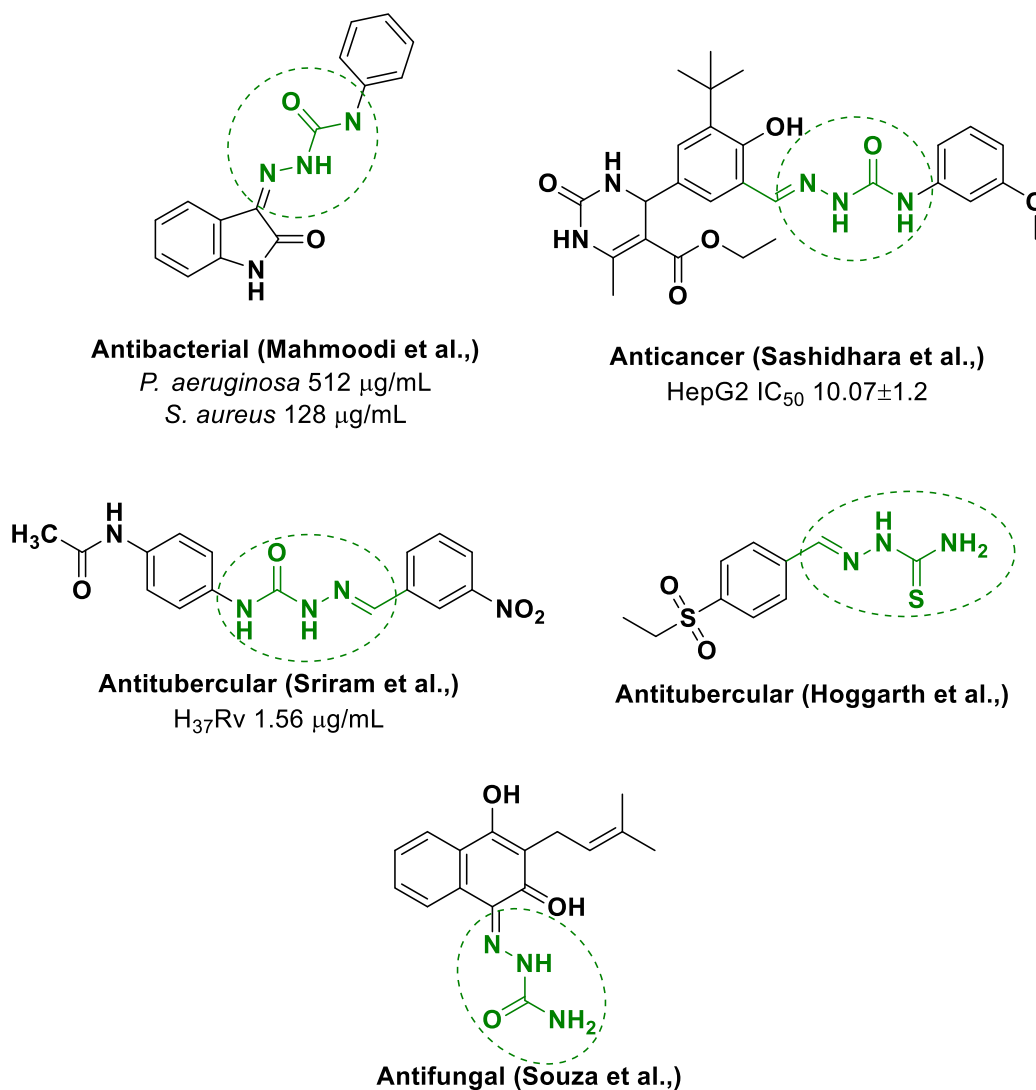


Figure 2: Semicarbazone and thiosemicarbazones bearing biologically active compounds.

From past, the natural products have been a key source for the design, discovery and development of new drug for several deadly diseases. Dehydrozingerone (DZG; feruloylmethane), a half structural analog (natural chalcone) of curcumin isolated from rhizomes of *Zingiber officinale* (Family: Zingiberaceae), is one such medicinally valuable molecule in drug discovery. Chemically, DZG is (*E*)-4-(4-hydroxy-3-methoxyphenyl)but-3-en-2-one and possess an α,β -unsaturated carbonyl (styryl ketone) group. Several DZG analogs have been synthesized and reported for a diverse range of biological activities like antioxidant, anticancer, anti-inflammatory, antidepressant, antimalarial, antifungal etc.[17] Our recent report has emphasized the significance of integrating this DZG on to a thiazole core by molecular hybridization strategy for an effective antitubercular activity.

Thus inspired by these findings, we in this report have anticipated design and synthesis of carbazones, semicarbazone and thiosemicarbazones derivatives of styryl fused pyrazole as potential antibacterial, antifungal and antimycobacterial agents. (Fig. 3)

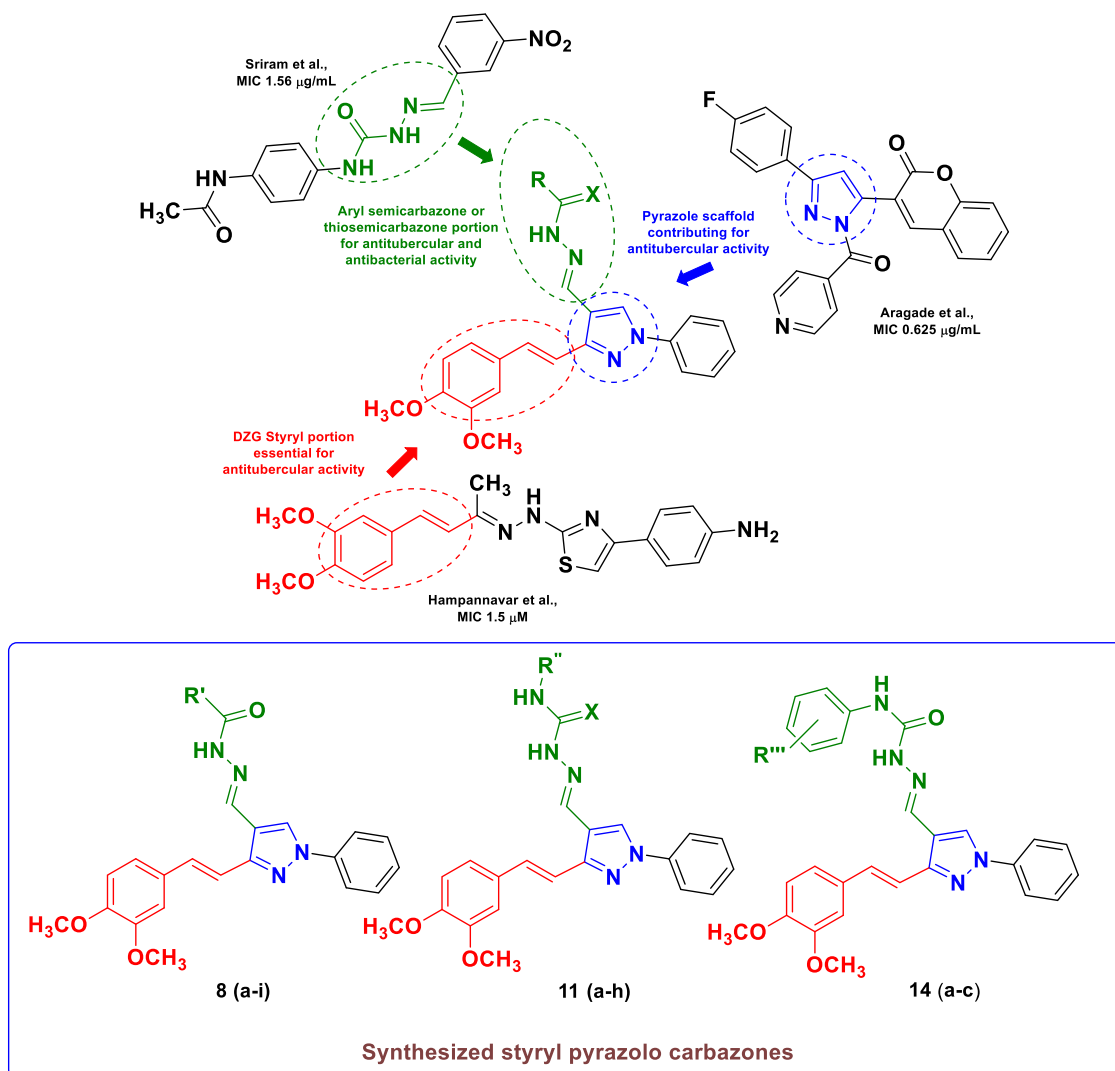


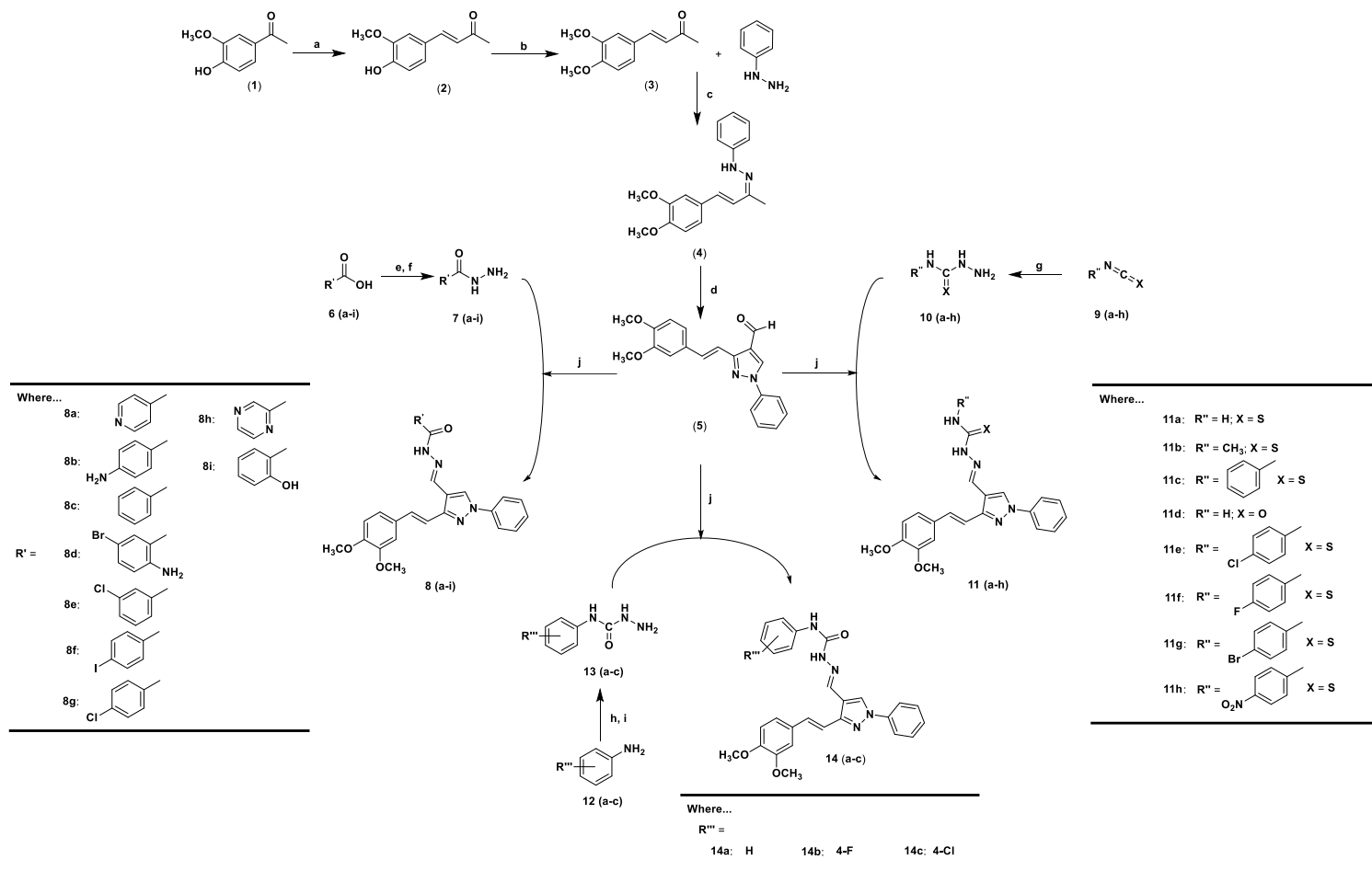
Figure 3: Design strategy for synthesis of styryl pyrazolo carbazones.

2 Chemistry

The synthesis of some novel series of new substituted ((3-(3,4-dimethoxystyryl)-1-phenyl-1*H*-pyrazol-4-yl)methylene)benzohydrazides (**8a-i**), 2-((3-(3,4-dimethoxystyryl)-1-phenyl-1*H*-pyrazol-4-yl)methylene)-*N*-phenylhydrazine-1-carbothioamides and carboxamides derivatives (**11a-h** and **14a-c**) derived from DZG was attained through effective and adaptable synthetic methods as depicted in **Scheme I**. The starting material, compound **3**, synthesized as per our previous report [3], was refluxed with phenylhydrazine in the presence of sodium acetate in methanol to form 1-(4-(3,4-dimethoxyphenyl)but-3-en-2-ylidene)-2-phenylhydrazine (**4**).

Subsequently, compound **4** underwent cyclization followed by formylation with the Vilsmeier–Haack reagent to yield 3-(3,4-dimethoxystyryl)-1-phenyl-1*H*-pyrazole-4-carbaldehyde (**5**). A set of substituted aromatic acid hydrazides **7(a-i)** were prepared from corresponding aromatic acids **6(a-i)**. Further, hydrazinecarbothioamides **10(e-h)**, except **10(a-d)** that were obtained readymade, were synthesized by treating respective isothiocyanates, **9(e-h)** with hydrazine hydrate in ethanol to yield corresponding hydrazinecarbothioamides **10(e-h)**. Besides, aryl hydrazinecarboxamide **13(a-c)** were prepared by from a reported method[18] using aromatic amines **12(a-c)** and by treating them with ethyl chloroformate and triethylamine in anhydrous THF. Finally, the title compounds **8(a-i)**, **11(a-h)** and **14(a-c)** were synthesized by refluxing compound **5** with acid hydrazides **7(a-i)**, hydrazinecarboxamide and carbothioamides (**10a-h**) and aryl hydrazinecarboxamide **13(a-c)** respectively in ethanol in presence of catalytic amount of acetic acid. The compounds obtained were in appreciably good yields and were confirmed by their physico-chemical and spectral (IR, ¹H-NMR and ¹³C-NMR) analysis followed by HRMS.

Scheme I* elaborating synthesis of title compounds 8(a-i), 11(a-h) and 14(a-c).



*Reagents and Conditions: **a**: acetone, NaOH; **b**: CH₃I, K₂CO₃, DMF, reflux, 1.5 h; **c**: NaOAc, MeOH, reflux, 3 h; **d**: POCl₃, DMF, 70-80 °C, 28 h; **e**: H₂SO₄, MeOH, reflux, overnight; **f**: NH₂NH₂.H₂O, EtOH, reflux, overnight; **g**: NH₂NH₂.H₂O, EtOH, Stir, RT, 30 minutes; **h**: Ethyl chloroformate, Et₃N, THF, RT, 1 h; **i**: NH₂NH₂.H₂O, EtOH, reflux, overnight; **j**: EtOH, HOAc 2-3 drops, reflux, 3 h.

3 Results and discussion

3.1 Synthesis and spectral studies

Structures of a key intermediate compounds **4** and **5** as well as their corresponding final derivatives (**8a-i**, **11a-h** and **14a-c**) were established on the basis of their physicochemical and spectral data (IR, $^1\text{H-NMR}$, $^{13}\text{C-NMR}$ and EIMS). All the newly synthesized compounds showed acceptable analysis of their anticipated structures, which are summarized in experimental section. In general, the IR spectrum of first intermediate compound **4**, clearly displayed characteristic absorption bands around 3325.09 cm^{-1} for N-H, 2925.96 cm^{-1} for C-H and 1596.05 cm^{-1} for C=N groups, thus confirming the formation of phenylhydrazine nucleus. Whereas, the IR spectrum of key intermediate compound **5** showed the most informative band around 1661.01 cm^{-1} due to the presence of carbonyl (C=O) group. Further, the disappearance of band 3325.09 cm^{-1} for N-H evidently indicated the formation of pyrazole nucleus. These observations were further substantiated from $^1\text{H-NMR}$ spectrum of compounds **4** and **5**. Compound **4** showed the prominent singlet signals around $\delta 7.34\text{ ppm}$ accounting for the N-H proton of phenylhydrazine, $3.93\text{-}3.89\text{ ppm}$ for methoxyl (OCH_3) protons and 2.08 ppm for methyl (CH_3) protons, thus indicating the formation of compound **4**. In the case of compound **5**, which displayed the most characteristic singlet signals $\delta 10.10\text{ ppm}$ accounting for the CHO (formyl) proton and $\delta 8.39\text{ ppm}$ for aromatic proton at 5th position of pyrazole ring, evidently suggested the formation of pyrazole nucleus from the respective phenylhydrazine (**4**) by simple cyclo-condensation process. In addition, the appearance of most distinctive doublet signal ($J = 16.41\text{-}16.33$) around $\delta 7.70\text{-}6.69\text{ ppm}$ authenticates the presence of vicinal vinyl protons in both key intermediates.

From the IR spectrum of the title compounds **8a-i**, it was observed that the appearance of the characteristic bands around $3197.68\text{-}3057.52\text{ cm}^{-1}$ for N-H, $3007.28\text{-}2925.97\text{ cm}^{-1}$ for C-H and $1599.73\text{-}1505.38\text{ cm}^{-1}$ for C=N groups, respectively. Further, the appearance of an additional fairly strong peak around $1675.95\text{-}1597.18\text{ cm}^{-1}$, which is attributed to the benzohydrazide carbonyl (C=O) group, indicating the formation of title compounds **8a-i**. This is further supported from the $^1\text{H-NMR}$ spectrum (400 MHz) of these compounds recorded in $\text{DMSO-}d_6$, which displayed some distinguishing singlet signals at around $\delta 12.29\text{-}11.43\text{ ppm}$ for N-H proton of benzohydrazide moiety, $\delta 8.58\text{-}8.40\text{ ppm}$ for CH=N protons and $\delta 3.91\text{-}3.78\text{ ppm}$ for methoxyl (OCH_3) protons. In addition, the appearance of characteristic singlet signal at $\delta 8.92\text{-}8.83\text{ ppm}$ attributed to the 5th aromatic (H-5) proton of pyrazole ring, which confirms the formation of title compounds **8a-i** by simple cyclo-condensation reaction. The most instructive doublet signals ($J = 16.53\text{-}16.09$) resonated around $\delta 7.76\text{-}7.63\text{ ppm}$ clearly pointed out the presence of vicinal vinyl

(-CH=CH-) protons. This observation was found consistent with previously reported similar compounds.[3] Furthermore, the various signals resonated as either doublets or multiplets at around δ 8.24-6.88 ppm were accounted for aromatic or heteroaromatic protons of compounds **8a-i**. In the case of compounds **8b**, **8d** and **8i**, the singlet signals resonated at around δ 11.87 and 6.58-5.76 ppm accounted for the amine (NH₂) and hydroxyl (OH) protons respectively. These findings were further substantiated from ¹³C-NMR spectra of these title compounds that the characteristic signals appeared at around δ 163.91-161.63 ppm for carbonyl carbon (C=O) of benzohydrazide moiety and δ 55.70-55.35 ppm for methoxyl carbon (OCH₃) group attached to 3rd and 4th position of DZG scaffold respectively. The prominent ¹³C-NMR signals resonated at around δ 159.30-149.11 and 148.87-147.77 ppm were assigned to (C=N) carbon of benzohydrazide and C-4 carbon of pyrazole moiety respectively. Further, the informative carbon signals around δ 134.63-130.15 ppm were accounted for vinyl (-HC=CH-) carbons. The carbon signals resonated around δ 120.62-120.30, 111.96-111.77 and 109.70-108.81 ppm were assigned to C-6, C-5 and C-2 carbons of DZG scaffold respectively, while the typical carbon signals appeared between δ 140.5-105.6 ppm were accounted for aromatic carbons.

From IR spectrum of the title compounds (**11a-h** and **14a-c**), it was observed that the appearance of typical absorption bands around 3369.49-3276.93 cm⁻¹ for N-H, 2933.89-2828.11 cm⁻¹ for C-H, 1673.67-1662.25 cm⁻¹ for carbonyl (C=O of urea), 1637.46-1577.16 cm⁻¹ for C=C, 1597.12-1547.77 cm⁻¹ for C=N, and 1136.62-1133.46 cm⁻¹ for C=S groups, respectively, thus indicating the formation of these title compounds. This was further corroborated from ¹H-NMR spectrum of compounds **11a-h** and **14a-c**, which exhibited the presence of a very distinct singlet signals resonating at δ 12.11-10.12 ppm due to hydrazine (-N=NH-) protons, δ 9.23-8.89 ppm for aromatic proton at 5th position of pyrazole ring and δ 3.84-3.68 for methoxyl (OCH₃) protons. A decisive structural insight was obtained from the presence of a prominent singlet signal around δ 10.32-9.91 ppm accounting for the -R'-NH-C=X- protons, whereas the CH=N protons were resonated around δ 10.1-10.09 and 8.45-8.05 ppm for compounds **14a-c** and **11a-h** respectively. Further, the most attributable doublet signals (J = 16.92-16.13) resonated around δ 7.66-7.31 ppm concretely confirmed the presence of vicinal vinyl protons (CH=CH), whereas the various signals resonated as either singlet or multiplet between δ 8.75-6.60 ppm accounted for aromatic protons. These interpretations were further authenticated from their respective ¹³C-NMR spectra of the title compounds. In ¹³C-NMR spectrum, the characteristic carbon signals appeared around δ 185.21-185.20 ppm for -CH=N- carbons, δ 177.60-174.70 ppm for thioxo (C=S) carbon and δ 158.44-152.33 ppm for carbonyl (C=O) carbons, thus confirming the formation of title compounds. The various aromatic/hetero-aromatic carbons resonated between δ 145.0-105.0 ppm. The prominent carbon signals observed around δ 55.55-55.30 ppm indicated the presence

of methoxyl (OCH₃) carbons and whereas C-6, C-5 and C-2 carbons of DZG scaffold were resonated δ 120.65-120.36, 111.84-111.64 and 109.69-108.96 ppm respectively in the title compounds. Furthermore, the formation of desired final derivatives (**8a-i**, **11a-h** and **14a-c**) were also confirmed by recording their respective mass spectra (HRMS), which displayed accurate molecular ion peaks that were in agreement with their expected molecular weights.

3.2 *In vitro* antimicrobial activity

All the newly synthesized compounds (**8a-i**, **11a-h** and **14a-c**) were evaluated for their *in vitro* antibacterial and antifungal activity against a panel of pathogenic antibacterial and antifungal microorganisms. This antibacterial and antifungal screening were carried out at the Department of Microbiology, Inkosi Albert Luthuli Hospital, Durban, South Africa. Antibacterial activity was performed on two Gram positive; *Staphylococcus aureus* (ATCC 25923), *Bacillus subtilis* (ATCC 6051) and two Gram negative; *Escherichia coli* (ATCC 35218), *Pseudomonas aeruginosa* (ATCC 27853) bacterial strains. The antibacterial activity was carried out in MH medium (Mueller-Hinton medium: casein hydrolysate 17.5 g, soluble starch 1.5 g, beef extract 1000 mL) using Moxcillin as a reference standard. Antifungal activity was performed against *Candida albicans* (ATCC 90028), *Cryptococcus neoformans* (ATCC 66031), *Aspergillus niger* (ATCC 16404), and *Aspergillus fumigatus* (UKQC strain) using Amphotericin B as a reference drug. Dimethyl sulfoxide was used as solvent control. The results (MIC values) of *in vitro* antibacterial and antifungal screening of the title compounds are summarized in **Table 1**. A systematic examination of the data represented in **Table 1** revealed that the seven compounds **8a**, **8c**, **8d**, **8g**, **8h**, **8i** and **11f** displayed moderate antibacterial activity (MIC = 50 μ g/mL) against *B. subtilis*. Whereas, compound **11a** demonstrated good activity towards *P. aeruginosa* (MIC = 25 μ g/mL) as compared to standard Moxcillin (MIC = 0.39 μ g/mL). Suggesting the spectrum of activity of synthesized compounds towards gram positive and gram negative organisms. However, rest of the compounds in the series revealed little or poor activity against the tested bacterial strains. Further analysis of results suggested that five compounds **8a**, **8d**, **8e**, **8f**, **8i**, and **11h** revealed good to moderate antifungal activity ranging from 25 to 50 μ g/mL towards *C. neoformans* (MIC = 25 μ g/mL) and *C. albicans* (MIC = 50 μ g/mL), respectively compared to standard Amphotericin B (MIC = 0.39 μ g/mL). Further, rest of the compounds were least active with MIC value > 200 μ g/mL against all of the tested fungal strains. Observation of results suggest the benefit of incorporating hydrazide, semicarbazide and thiosemicarbazide portions on the styryl pyrazole scaffold on both antibacterial and antifungal activities.

Table 1: The antibacterial and antifungal activity data (MIC in $\mu\text{g/mL}$) of a novel series of styryl pyrazolo carbazone derivatives (**8a-i**, **11a-h** and **14a-c**).

Compound	Antibacterial				Antifungal			
	MIC values ($\mu\text{g/mL}$)*				MIC values ($\mu\text{g/mL}$)*			
	Gram positive		Gram negative					
<i>S. aureus</i> (ATCC 25923)	<i>B. subtilis</i> (ATCC 6051)	<i>E. coli</i> (ATCC 35218)	<i>P. aeruginosa</i> (ATCC 27853)	<i>C. albicans</i> (ATCC 90028)	<i>C. neoformans</i> (ATCC 66031)	<i>A. niger</i> (ATCC 16404)	<i>A. fumigatus</i> (UKQC strain)	
8a	> 200	50	> 200	> 200	50	25	> 200	> 200
8b	> 200	100	> 200	> 200	> 200	>200	> 200	> 200
8c	> 200	50	> 200	> 200	> 200	>200	> 200	> 200
8d	> 200	50	> 200	> 200	50	25	> 200	> 200
8e	> 200	100	> 200	> 200	50	25	> 200	> 200
8f	> 200	100	> 200	> 200	50	25	> 200	> 200
8g	> 200	50	> 200	> 200	> 200	>200	> 200	> 200
8h	> 200	50	> 200	> 200	> 200	>200	> 200	> 200
8i	> 200	50	> 200	> 200	50	25	> 200	> 200
11a	> 200	100	> 200	25	> 200	>200	> 200	> 200
11b	> 200	100	> 200	> 200	> 200	>200	> 200	> 200
11c	> 200	100	> 200	> 200	> 200	>200	> 200	> 200
11d	> 200	100	> 200	> 200	> 200	>200	> 200	> 200
11e	> 200	100	> 200	> 200	> 200	>200	> 200	> 200
11f	> 200	50	> 200	> 200	> 200	>200	> 200	> 200
11g	> 200	100	> 200	> 200	> 200	>200	> 200	> 200
11h	> 200	100	> 200	> 200	> 200	25	> 200	> 200
14a	> 200	100	> 200	> 200	> 200	>200	> 200	> 200
14b	> 200	100	> 200	> 200	> 200	>200	> 200	> 200
14c	> 200	100	> 200	> 200	> 200	>200	> 200	> 200
Moxicillin	< 0.39	< 0.39	< 0.39	< 0.39	-	-	-	-
Amphotericin B	-	-	-	-	< 0.39	<0.39	<0.39	<0.39

*The bold figures indicate the good activity exhibited by the respective compounds.

3.3 Antimycobacterial activity

The title compounds (**8a-i**, **11a-h** and **14a-c**) were evaluated for *in vitro* antimycobacterial activity against *M. tuberculosis* H₃₇Rv, multi drug resistant strain (UKQC strain), and three strains of MOTT (mycobacteria other than tuberculosis). The culturing was done in Middlebrook 7H9 broth, supplemented with 10% ADC (albumin, dextrose, and catalase) and 0.04% Tween 80 to avoid clump formation and incubated at 37°C in 5% CO₂. The antimycobacterial results (MIC values) of the tested title compounds have been summarized in **Table 2**. Analysis of results showed interesting and noteworthy antimycobacterial activity of synthesized compounds towards *M. tuberculosis* H₃₇Rv with the value ranging from 0.78 to > 200 µg/mL. However, compounds **8a**, comprising isonicotinoyl hydrazide and **11a** encompassing carbothioamide portions showed excellent antitubercular activity (0.78 µg/mL) comparable with standard isoniazid (0.4 µg/mL) and were found much active than standard drug rifampicin (1 µg/mL). Further, compounds **14a-c** and **11d** bearing substituted urea derivatives, showed significant activity of 12.5 µg/mL and 25 µg/mL respectively. Compounds **11d**, **14a**, **14b** and **14c** displayed moderated activity against MDR (UKQC strain) as compared to standard isoniazid (0.4 µg/mL) and rifampicin (1 µg/mL). Furthermore, All the compounds were also tested against three strains of MOTT and all the title compounds showed moderate activity as compared to standard (Table 2). Inclusion of isonicotinoyl (**8a**, MIC = 0.78 µg/mL) and carbothioamide (**11a**, MIC = 0.78 µg/mL) portion on styryl pyrazole scaffold has benefited enormously for antimycobacterial activity. The overall findings suggest a remarkable high activity on *Mycobacterium tuberculosis* H₃₇Rv than the reference drug rifampicin and almost comparable activity with isoniazid. Additionally, the moderate activity of compounds (**11d** and **14a-c**) towards multi drug resistant strain suggest a good starting point for developing the compounds as effective antimycobacterial agents.

Table 2: The antimycobacterial activity data* (MIC in µg/mL) of a novel series of styryl pyrazolo carbazone derivatives (**8a-i**, **11a-h** and **14a-c**).

Compounds	<i>M. tuberculosis</i> (ATCC H ₃₇ RV)	MDR (UKQC strain)	<i>M. kansasii</i> (ATCC 12478)	<i>M. peregrinum</i> (ATCC 14467)	<i>M. fortuitum</i> (ATCC 6841)
8a	0.78	ND	>200	>200	>200
8b	>200	>200	>200	>200	>200
8c	>200	>200	>200	>200	>200
8d	>200	>200	>200	>200	>200
8e	>200	>200	>200	>200	>200
8f	>200	>200	>200	>200	>200
8g	>200	>200	>200	>200	>200
8h	>200	>200	>200	>200	>200
8i	>200	>200	>200	>200	>200
11a	0.78	ND	>200	>200	>200
11b	>200	>200	>200	>200	>200
11c	>200	>200	>200	>200	>200
11d	25	50	>200	>200	>200
11e	>200	>200	>200	>200	>200
11f	>200	>200	>200	>200	>200
11g	>200	>200	>200	>200	>200
11h	>200	>200	>200	>200	>200
14a	12.5	50	>200	>200	>200
14b	12.5	50	>200	>200	>200
14c	12.5	50	>200	>200	>200
Isoniazid	0.4	0.4	>250	>250	>250
Rifampicin	1	1	<0.5	2	64

*The bold figures indicate the good activity exhibited by the respective compounds.

4 Conclusion

In summary, we hereby report the synthesis, spectral studies and *in vitro* antibacterial and antimycobacterial activity of some novel series of styryl pyrazolo carbazone hybrids (**8a-i**, **11a-h** and **14a-c**) inspired from dehydrozingerone based on hybridization approach. The synthesized title compounds were confirmed for their structures by spectral (IR, ¹H-NMR, ¹³C-NMR and HRMS) studies. It is interesting to note that some of the synthesized compounds showed best antimicrobial and antimycobacterial activities. Compounds **8a**, **8c**, **8d**, **8g**, **8h**, **8i** and **11f** showed reasonable antibacterial activity (MIC = 50 µg/mL) against *B. subtilis*. Whereas, compound **11a** demonstrated decent activity towards *P. aeruginosa* (MIC = 25 µg/mL). Further, compounds **8a**, **8d**, **8e**, **8f**, **8i**, and **11h** presented good to moderate antifungal activity ranging from 25 to 50 µg/mL towards *C. neoformans* (MIC = 25 µg/mL) and *C. albicans* (MIC = 50 µg/mL). Additionally, compounds **8a** and **11a** showed excellent antitubercular activity (0.78 µg/mL) and compounds **11d** and **14a-c** showed significant activity (MIC = 25 µg/mL and 12.5 µg/mL respectively) against H₃₇Rv. Compounds **11d** and **14a-c** also showed moderate activity against MDR strains. A brief SAR study emphasizes that the antimicrobial and antimycobacterial was contributed by hydrazine, semicarbazone and thiosemicarbazone portions with varying substitutions on styryl pyrazole motif. The overall results stipulate the benefit of incorporating carbazones on a styryl pyrazole scaffold for effective antimicrobial and antimycobacterial activity. This incorporation could be of potential in further development of effective antimicrobial and antimycobacterial leads.

5 Experimental

5.1 Chemistry protocols

All the chemicals used in this research work were purchased from Sigma-Aldrich and Merck Millipore, South Africa. All the solvents, except those of laboratory-reagent grade, were dried and purified when necessary according to previously published methods. The progress of the reactions and the purity of the compounds were monitored by thin-layer chromatography (TLC) on pre-coated silica gel plates procured from E. Merck and Co. (Darmstadt, Germany).

The melting points of the synthesized compounds were determined using a Bibby Scientific Ltd (Stuart SMP10) digital melting point apparatus and are uncorrected. The IR spectra were recorded on a Bruker Alpha FT-IR spectrometer (Billerica, MA, USA) using the ATR technique. The ¹H-NMR and ¹³C-NMR spectra were recorded on a Bruker AVANCE 400 MHz (Bruker, Rheinstetten/Karlsruhe, Germany) spectrometer using CDCl₃ and/or DMSO-*d*₆. The chemical shifts (δ) reported are given in parts per million (ppm) and the coupling constants (*J*) are in Hertz

(Hz) with respect to TMS as the internal standard. The spin multiplicities are reported as s = singlet, d = doublet, t = triplet, dd = doublet of doublet and m = multiplet. HRMS spectra were recorded on an Autospec mass spectrometer with electron impact at 70 eV. Compounds **2** and **3**, were synthesized in good yields according to our previous report.[3]

5.1.1 Synthesis of 1-(4-(3,4-dimethoxyphenyl)but-3-en-2-ylidene)-2-phenylhydrazine (4)[19]:

Anhydrous sodium acetate (1.1 Eq., 1.1 g, 0.01067 mol.) was added to a stirred solution of phenylhydrazine (1.8 Eq., 1.88 g, 0.01746 mol.) in 15 mL of methanol. The resulting mixture was stirred at RT for about 15 to 20 minutes until all of the sodium acetate dissolved. Subsequently, compound **3** (2.0 g, 0.0097 mol.) was added and the resulting reaction mixture was refluxed for about 3 h. Yellow solid separates out which was filtered and washed with cold methanol followed by cold water. The resulting solid was recrystallized in ethanol to yield compound **4**.

Crystalline yellow solid, Yield: 73%, mp: 162-164 °C; FTIR (ATR, ν_{max} , cm^{-1}): 3325.09 (N-H Str.), 2925.96 (Ar-H Str.), 2828.45 (C-H Str. of CH_3), 1596.05 (C=N Str.); $^1\text{H-NMR}$ (400 MHz, CDCl_3 , δ , ppm): 7.34 (s, 1H, -NH), 7.29-7.25 (m, 2H), 7.14-7.12 (m, 2H), 7.07 (d, 1H, $J = 1.92$ Hz), 7.00 (dd, 1H, $J = 8.30, 1.94$ Hz), 6.91 (d, 1H, $J = 16.33$ Hz, -HC=CH-), 6.85 (t, 2H, $J = 8.80$ Hz), 6.69 (d, 1H, $J = 16.41$ Hz, -HC=CH-), 3.93 (s, 3H, -OCH₃), 3.89 (s, 3H, -OCH₃), 2.08 (s, 3H, -CH₃); $^{13}\text{C-NMR}$ (100 MHz, CDCl_3 , δ ppm): 149.39, 149.21, 144.93, 143.56, 130.46, 129.49, 129.30, 129.08, 129.00, 128.33, 120.50 (C-6 of DZG), 120.42, 113.65, 111.39 (C-5 of DZG), 108.64 (C-2 of DZG), 56.13 (-OCH₃), 56.07 (-OCH₃), 10.30 (-CH₃); HRMS (ESI, m/z) [M-H]; calculated for $\text{C}_{18}\text{H}_{20}\text{N}_2\text{O}_2$, 295.1447; found 295.1454.

5.1.2 Synthesis of 3-(3,4-dimethoxystyryl)-1-phenyl-1H-pyrazole-4-carbaldehyde (5):

POCl_3 (2.0 Eq., 2.07 g, 0.01350 mol.) was added dropwise to anhydrous *N,N*-Dimethylformamide (12.0 mL) contained in round bottom flask at 0 °C. The resulting reaction mixture was stirred for 30-45 minutes until the formation of Vilsmeiers complex. Compound **4** (2.0 g, 0.00675 mol.) was dissolved in a minimum amount of *N,N*-Dimethylformamide and added to Vilsmeiers complex. The resulting reaction mixture was stirred at RT for about 30 minutes and then refluxed at 70-80 °C for 28 h. The reaction mixture was allowed to cool and was poured dropwise into ice with vigorous stirring for about 1 h. Further, 2.0 N NaOH was added to neutralize reaction mixture and further stirred for around 2 h. A brick red solid was obtained which was filtered under suction. Further, the obtained solid was purified on a silica column using n-hexane: EtOAc (80:20) as a mobile phase.

Crystalline yellow solid, Yield: 78%, mp: 125-127 °C; FTIR (ATR, ν_{max} , cm^{-1}): 3116.16 (CHO), 2914.17 (Ar-H Str.), 2832.42 (C-H Str. of CH_3), 1661.01 (C=C Str.), 1590.32 (C=N Str.); $^1\text{H-NMR}$ (400 MHz, CDCl_3 , δ , ppm): 10.10 (s, 1H, -CHO), 8.39 (d, 1H, $J = 0.56$ Hz), 7.76 (d, 2H, $J = 8.28$ Hz), 7.70 (d, 1H, $J = 16.33$ Hz, -HC=CH-), 7.50 (t, 2H, $J = 7.72$ Hz), 7.40-7.36 (m, 1H), 7.37 (d, 1H, $J = 16.36$ Hz, -HC=CH-), 7.16-7.14 (m, 2H), 6.87 (d, 1H, $J = 8.76$ Hz), 3.94 (s, 3H, -OCH₃), 3.90 (s, 3H, -OCH₃); $^{13}\text{C-NMR}$ (100 MHz, CDCl_3 , δ ppm): 184.26 (C=O), 151.78, 149.86, 149.35, 139.25, 134.53, 133.00, 129.91, 129.88, 128.07, 122.76, 121.05, 119.89 (C-6 of DZG), 115.67, 111.37 (C-5 of DZG), 109.41 (C-2 of DZG), 56.13 (-OCH₃); HRMS (ESI, m/z) $[\text{M}+\text{Na}]^+$; calculated for $\text{C}_{20}\text{H}_{18}\text{N}_2\text{O}_3$, 357.1215; found 357.1216.

5.1.3 General procedure for synthesis of substituted acid hydrazides 7a-i:

Substituted aromatic acids, **6a-i** (1.0 g) were dissolved in 10 mL of methanol and about 1.0 mL of H_2SO_4 was added. The resulting mixture was refluxed overnight. After cooling, the reaction mixture was added in water and extracted with dichloromethane. The dichloromethane fraction was washed with saturated NaHCO_3 solution and further filtered through sodium sulfate. The obtained filtrate was evaporated to get respective acid ester. Subsequently, the resulting acid ester was taken in 10 mL of ethanol and 2.0 equivalent of hydrazine hydrate was added. The resulting mixture was refluxed overnight at 80-90 °C to yield respective acid hydrazides. The obtained acid hydrazides were fairly pure and were used without any further purification.

5.1.4 General procedure for synthesis of substituted hydrazinecarbothioamides and hydrazinecarboxamide 10a-h:

Hydrazinecarbothioamides **10a-c** and hydrazinecarboxamide **10d** were obtained readymade. For hydrazinecarbothioamides **10e-h**, 1.0 g of respective substituted aromatic isothiocyanates, **9e-h** were dissolved in ethanol and stirred at RT for 15 minutes. About 2.0 mL of hydrazine hydrate was added to the mixture and stirred further at RT for 30 minutes. The solid obtained was filtered to yield fairly pure hydrazinecarbothioamides **10e-h**.

5.1.5 General procedure for synthesis of substituted aryl hydrazinecarboxamides 13a-c [18]:

A mixture of substituted aromatic amines, **12a-c**, (0.0010 mol.), ethyl chloroformate (0.0020 mol.), and triethylamine (0.0020 mol.) were taken in anhydrous THF (15 mL) and stirred at RT for 1 h. The obtained solid was filtered off and the solution was evaporated under reduced pressure. The residue obtained was dissolved in EtOAc (25 mL) and the organic phase was washed with water (3 x 100 mL). The organic phase was evaporated under reduced pressure to yield respective carbamates. These obtained carbamates were further refluxed overnight with

hydrazine hydrate (2.0 Eq.) in ethanol. The reaction mixture thus attained was evaporated under reduced pressure to yield correspond aryl hydrazinecarboxamides **13a-c** as solid compounds.

5.1.6 General procedure for synthesis of substituted ((3-(3,4-dimethoxystyryl)-1-phenyl-1H-pyrazol-4-yl)methylene)benzohydrazides (8a-i), 2-((3-(3,4-dimethoxystyryl)-1-phenyl-1H-pyrazol-4-yl)methylene)-N-phenylhydrazine-1-carbothioamides and carboxamides (11a-h and 14a-c):

Dissolve compound **5** (0.275 g, 0.00082 mol.) in 8.0 mL of ethanol and add 1.1 Eq., of respective acid hydrazides **7(a-i)**, phenylhydrazine-1-carbothioamides and carboxamides (**11a-h** and **14a-c**). Add 2-3 drops of glacial acetic acid and reflux for about 3-4 h by monitoring TLC. After completion, the reaction mass was allowed to cool to obtain solid. Further purification was achieved by recrystallization in ethanol or by performing column chromatography on silica column with n-hexane and EtOAc (80:20) a mobile phase. For compounds **8b**, **8d** and **11a** neutral alumina was taken as a stationary phase.

5.1.6.1 ((3-(3,4-dimethoxystyryl)-1-phenyl-1H-pyrazol-4-yl)methylene)isonicotinohydrazide (8a):

Yellow solid, Yield: 44%, mp: 192-194 °C; FTIR (ATR, ν_{max} , cm^{-1}): 3141.51 (N-H Str.), 2939.27 (Ar-H Str.), 2831.29 (C-H Str. of CH_3), 1643.38 (C=O Str.), 1595.31 (C=C Str.), 1544.36 (C=N Str.); $^1\text{H-NMR}$ (400 MHz, $\text{DMSO-}d_6$, δ , ppm): 12.06 (s, 1H, =N-NH-), 8.89 (s, 1H, pyrazole CH), 8.78 (dd, 2H, $J = 4.60, 1.32$ Hz), 8.57 (s, 1H, -CH=N), 7.92 (d, 2H, $J = 7.80$ Hz), 7.84 (dd, 2H, $J = 4.56, 1.44$ Hz), 7.71 (d, 1H, $J = 16.52$ Hz, -HC=CH-), 7.63 (d, 1H, $J = 16.45$ Hz, -HC=CH-), 7.54 (t, 2H, $J = 7.94$ Hz), 7.38-7.34 (m, 2H), 7.18 (dd, 1H, $J = 8.28, 1.64$ Hz), 6.98 (d, 1H, $J = 8.32$ Hz), 3.88 (s, 3H, -OCH₃), 3.78 (s, 3H, -OCH₃); $^{13}\text{C-NMR}$ (100 MHz, $\text{DMSO-}d_6$, δ ppm): 161.70 (C=O), 150.50, 149.33, 149.22, 149.17, 142.19, 140.76, 139.12, 131.95, 130.00, 129.86, 129.83, 127.06, 121.72, 120.62 (C-6 of DZG), 118.70, 117.31, 117.06, 111.96 (C-5 of DZG), 109.17 (C-2 of DZG), 55.70 (-OCH₃), 55.65 (-OCH₃); HRMS (ESI, m/z) $[\text{M}+\text{Na}]^+$; calculated for $\text{C}_{26}\text{H}_{23}\text{N}_5\text{O}_3$, 476.1699; found 476.1717.

5.1.6.2 4-amino-((3-(3,4-dimethoxystyryl)-1-phenyl-1H-pyrazol-4-yl)methylene)benzohydrazide (8b):

Off white, Yield: 91%, mp: 257-259 °C; FTIR (ATR, ν_{max} , cm^{-1}): 3444.14, 3345.01 (N-H Str. primary), 3130.78 (N-H Str.), 2959.71 (Ar-H Str.), 2834.41 (C-H Str. of CH_3), 1597.18 (C=O Str.), 1550.66 (C=C Str.), 1505.38 (C=N Str.); $^1\text{H-NMR}$ (400 MHz, $\text{DMSO-}d_6$, δ , ppm): 11.43 (s, 1H, =N-NH-), 8.83 (s, 1H, pyrazole CH), 8.51 (s, 1H, -CH=N), 7.93 (d, 2H, $J = 7.72$ Hz), 7.72 (d, 1H, $J = 16.09$ Hz, -HC=CH-), 7.69 (d, 2H, $J = 8.56$ Hz), 7.63 (d, 1H, $J = 16.37$ Hz, -HC=CH-

), 7.53 (t, 2H, $J = 7.92$ Hz), 7.35 (t, 2H, $J = 7.38$ Hz), 7.18 (d, 1H, $J = 6.52$ Hz), 6.98 (d, 1H, $J = 8.40$ Hz), 6.61 (d, 2H, $J = 8.64$ Hz), 5.76 (s, 2H, -NH₂), 3.89 (s, 3H, -OCH₃), 3.79 (s, 3H, -OCH₃); ¹³C-NMR (100 MHz, DMSO-*d*₆, δ ppm): 162.87 (C=O), 152.24, 149.10, 148.76, 139.10, 133.42, 131.46, 129.86, 129.62, 129.35, 129.08, 126.68, 120.30 (C-6 of DZG), 119.67, 118.44, 117.82, 117.19, 112.68, 111.85 (C-5 of DZG), 109.7 (C-2 of DZG), 55.55 (-OCH₃); HRMS (ESI, m/z) [M+Na]⁺; calculated for C₂₇H₂₅N₅O₃, 490.1855; found 490.1876.

5.1.6.3 ((3-(3,4-dimethoxystyryl)-1-phenyl-1H-pyrazol-4-yl)methylene)benzohydrazide (**8c**):

Yellow solid, Yield: 23%, mp: 212-215 °C; FTIR (ATR, ν_{max} , cm⁻¹): 3197.68 (N-H Str.), 2925.97 (Ar-H Str.), 2850.87 (C-H Str. of CH₃), 1636.31 (C=O Str.), 1597.22 (C=C Str.), 1555.16 (C=N Str.); ¹H-NMR (400 MHz, DMSO-*d*₆, δ , ppm): 11.83 (s, 1H, =N-NH-), 8.90 (s, 1H, pyrazole CH), 8.58 (s, 1H, -CH=N), 7.96-7.93 (m, 4H), 7.76 (d, 1H, $J = 16.49$ Hz, -HC=CH-), 7.66 (d, 1H, $J = 16.45$ Hz, -HC=CH-), 7.56-7.52 (m, 5H), 7.39-7.36 (m, 2H), 7.19 (d, 1H, $J = 8.44$ Hz), 6.99 (d, 1H, $J = 8.24$ Hz), 3.90 (s, 3H, -OCH₃), 3.80 (s, 3H, -OCH₃); ¹³C-NMR (100 MHz, DMSO-*d*₆, δ ppm): 162.92 (C=O), 149.11, 149.07, 148.87, 140.60, 139.03, 133.56, 131.66, 131.58, 129.79, 129.59, 128.48, 127.57, 126.70, 120.38 (C-6 of DZG), 118.45, 117.44, 117.10, 111.79 (C-5 of DZG), 109.03 (C-2 of DZG), 55.52 (-OCH₃), 55.48 (-OCH₃); HRMS (ESI, m/z) [M+Na]⁺; calculated for C₂₇H₂₄N₄O₃, 475.1746; found 475.1763.

5.1.6.4 2-amino-5-bromo-((3-(3,4-dimethoxystyryl)-1-phenyl-1H-pyrazol-4-yl)methylene)benzohydrazide (**8d**):

Yellow solid, Yield: 14%, mp: 212-215 °C; FTIR (ATR, ν_{max} , cm⁻¹): 3453.42, 3358.00 (N-H Str. primary), 3195.73 (N-H Str.), 3007.28 (Ar-H Str.), 2960.67 (C-H Str. of CH₃), 1640.29 (C=O Str.), 1618.80 (C=C Str.), 1579.80 (C=N Str.); ¹H-NMR (400 MHz, DMSO-*d*₆, δ , ppm): 11.68 (s, 1H, =N-NH-), 8.88 (s, 1H, pyrazole CH), 8.51 (s, 1H, -CH=N), 7.95 (d, 2H, $J = 7.88$ Hz), 7.76 (d, 1H, $J = 16.29$ Hz, -HC=CH-), 7.75 (s, 1H), 7.64 (d, 1H, $J = 16.41$ Hz, -HC=CH-), 7.54 (t, 2H, $J = 7.96$ Hz), 7.38-7.32 (m, 3H), 7.17 (d, 1H, $J = 6.72$ Hz), 6.98 (d, 1H, $J = 8.32$ Hz), 6.74 (d, 1H, $J = 8.88$ Hz), 6.58 (s, 2H, -NH₂), 3.88 (s, 3H, -OCH₃), 3.79 (s, 3H, -OCH₃); ¹³C-NMR (100 MHz, DMSO-*d*₆, δ ppm): 163.91 (C=O), 149.26, 149.09, 149.02, 148.78, 140.30, 139.03, 134.63, 131.49, 130.15, 129.78, 129.59, 126.69, 120.47 (C-6 of DZG), 118.44, 117.50, 117.11, 115.01, 111.77 (C-5 of DZG), 108.86 (C-2 of DZG), 105.01, 55.52 (-OCH₃), 55.35 (-OCH₃).

5.1.6.5 3-chloro-((3-(3,4-dimethoxystyryl)-1-phenyl-1H-pyrazol-4-yl)methylene)benzohydrazide (**8e**):

Yellow crystals, Yield: 43%, mp: 191-193 °C; FTIR (ATR, ν_{max} , cm^{-1}): 3143.72 (N-H Str.), 2996.27 (Ar-H Str.), 2957.62 (C-H Str. of CH_3), 1642.06 (C=O Str.), 1593.66 (C=C Str.), 1555.42 (C=N Str.); $^1\text{H-NMR}$ (400 MHz, $\text{DMSO-}d_6$, δ , ppm): 11.92 (s, 1H, =N-NH-), 8.90 (s, 1H, pyrazole CH), 8.57 (s, 1H, -CH=N), 7.97 (s, 1H), 7.94 (d, 2H, $J = 7.88$ Hz), 7.90 (d, 1H, $J = 7.76$ Hz), 7.73 (d, 1H, $J = 16.45$ Hz, -HC=CH-), 7.67 (d, 1H, $J = 8.08$ Hz), 7.64 (d, 1H, $J = 16.45$ Hz, -HC=CH-), 7.60-7.52 (m, 1H), 7.55 (d, 2H, $J = 7.76$ Hz), 7.37-7.34 (m, 2H), 7.19 (dd, 1H, $J = 8.18, 1.30$ Hz), 6.98 (d, 1H, $J = 8.36$ Hz), 3.89 (s, 3H, -OCH₃), 3.79 (s, 3H, -OCH₃); $^{13}\text{C-NMR}$ (100 MHz, $\text{DMSO-}d_6$, δ , ppm): 161.63 (C=O), 149.22, 149.14, 149.01, 141.34, 139.07, 135.57, 133.38, 131.76, 131.61, 130.65, 129.82, 129.70, 127.33, 126.87, 126.51, 120.50 (C-6 of DZG), 118.57, 117.36, 117.06, 111.86 (C-5 of DZG), 109.09 (C-2 of DZG), 55.60 (-OCH₃), 55.55 (-OCH₃).

5.1.6.6 ((3-(3,4-dimethoxystyryl)-1-phenyl-1H-pyrazol-4-yl)methylene)-4-iodobenzohydrazide (**8f**):

Off white solid, Yield: 58%, mp: 251-253 °C; FTIR (ATR, ν_{max} , cm^{-1}): 3183.28 (N-H Str.), 2943.39 (Ar-H Str.), 2832.59 (C-H Str. of CH_3), 1636.73 (C=O Str.), 1593.75 (C=C Str.), 1558.60 (C=N Str.); $^1\text{H-NMR}$ (400 MHz, $\text{DMSO-}d_6$, δ , ppm): 11.87 (s, 1H, =N-NH-), 8.90 (s, 1H, pyrazole CH), 8.57 (s, 1H, -CH=N), 7.96-7.93 (m, 4H), 7.74 (d, 1H, $J = 16.52$ Hz, -HC=CH-), 7.73 (d, 2H, $J = 7.16$ Hz), 7.65 (d, 1H, $J = 16.44$ Hz, -HC=CH-), 7.54 (t, 2H, $J = 7.82$ Hz), 7.38-7.34 (m, 2H, $J = 7.56$ Hz), 7.19 (d, 1H, $J = 7.96$ Hz), 6.98 (d, 1H, $J = 8.28$ Hz), 3.89 (s, 3H, -OCH₃), 3.79 (s, 3H, -OCH₃); $^{13}\text{C-NMR}$ (100 MHz, $\text{DMSO-}d_6$, δ , ppm): 162.17 (C=O), 149.11, 149.05, 148.87, 140.92, 139.00, 137.35, 132.87, 131.62, 129.76, 129.64, 129.57, 129.47, 126.71, 120.37 (C-6 of DZG), 118.45, 117.35, 117.04, 111.78 (C-5 of DZG), 109.01 (C-2 of DZG), 99.36, 55.52 (-OCH₃), 55.46 (-OCH₃); HRMS (ESI, m/z) [$\text{M}+\text{H}+\text{Na}$]⁺; calculated for $\text{C}_{27}\text{H}_{24}\text{N}_4\text{O}_3$, 601.0713; found 601.0730.

5.1.6.7 4-chloro-((3-(3,4-dimethoxystyryl)-1-phenyl-1H-pyrazol-4-yl)methylene)benzohydrazide (**8g**):

Yellow solid, Yield: 32%, mp: 221-223 °C; FTIR (ATR, ν_{max} , cm^{-1}): 3057.52 (N-H Str.), 2934.61 (Ar-H Str.), 2833.51 (C-H Str. of CH_3), 1675.95 (C=O Str.), 1637.46 (C=C Str.), 1595.94 (C=N Str.); $^1\text{H-NMR}$ (400 MHz, $\text{DMSO-}d_6$, δ , ppm): 11.89 (s, 1H, =N-NH-), 8.91 (s, 1H, pyrazole CH), 8.57 (s, 1H, -CH=N), 7.96 (t, 4H, $J = 7.60$ Hz), 7.75 (d, 1H, $J = 16.49$ Hz, -HC=CH-), 7.66 (d, 1H, $J = 16.53$ Hz, -HC=CH-), 7.63 (d, 2H, $J = 8.36$ Hz), 7.54 (t, 2H, $J = 7.88$ Hz), 7.38-7.34 (m,

2H), 7.19 (dd, 1H, $J = 8.20, 1.12$ Hz), 6.99 (d, 1H, $J = 8.28$ Hz), 3.90 (s, 3H, -OCH₃), 3.79 (s, 3H, -OCH₃); ¹³C-NMR (100 MHz, DMSO-*d*₆, δ ppm): 161.81 (C=O), 149.12, 149.06, 148.88, 140.95, 139.01, 136.47, 132.24, 131.62, 129.77, 129.57, 129.50, 128.58, 126.71, 120.39 (C-6 of DZG), 118.45, 117.33, 117.05, 111.78 (C-5 of DZG), 109.00 (C-2 of DZG), 55.51 (-OCH₃), 55.46 (-OCH₃); HRMS (ESI, *m/z*) [M+Na]⁺; calculated for C₂₇H₂₃ClN₄O₃, 509.1356; found 509.1372.

5.1.6.8 ((3-(3,4-dimethoxystyryl)-1-phenyl-1H-pyrazol-4-yl)methylene)pyrazine-2-carbohydrazide (**8h**):

Off white solid, Yield: 17%, mp: 232-234 °C; FTIR (ATR, ν_{max} , cm⁻¹): 3186.88 (N-H Str.), 2926.26 (Ar-H Str.), 2852.57 (C-H Str. of CH₃), 1663.75 (C=O Str.), 1632.57 (C=C Str.), 1599.73 (C=N Str.); ¹H-NMR (400 MHz, DMSO-*d*₆, δ , ppm): 12.29 (s, 1H, =N-NH-), 9.29 (d, 1H, $J = 0.84$ Hz), 8.94 (d, 1H, $J = 2.36$ Hz), 8.92 (s, 1H, pyrazole CH), 8.80 (s, 2H), 7.97 (d, 2H, $J = 7.92$ Hz), 7.72 (d, 1H, $J = 16.48$ Hz, -HC=CH-), 7.63 (d, 1H, $J = 16.48$ Hz, -HC=CH-), 7.54 (t, 2H, $J = 7.88$ Hz), 7.38-7.34 (m, 2H), 7.20 (dd, 1H, $J = 8.14, 1.22$ Hz), 6.99 (d, 1H, $J = 8.32$ Hz), 3.91 (s, 3H, -OCH₃), 3.80 (s, 3H, -OCH₃); ¹³C-NMR (100 MHz, DMSO-*d*₆, δ ppm): 162.65 (C=O), 159.30, 149.16, 149.06, 147.77, 144.74, 144.11, 143.29, 142.68, 139.01, 131.65, 129.75, 129.58, 129.50, 126.76, 120.34 (C-6 of DZG), 118.51, 117.28, 116.88, 111.80 (C-5 of DZG), 109.15 (C-2 of DZG), 55.54 (-OCH₃), 55.53 (-OCH₃).

5.1.6.9 ((3-(3,4-dimethoxystyryl)-1-phenyl-1H-pyrazol-4-yl)methylene)-2-hydroxybenzohydrazide (**8i**):

White solid, Yield: 33%, mp: 230-232 °C; FTIR (ATR, ν_{max} , cm⁻¹): 3170.53 (N-H Str.), 2927.15 (Ar-H Str.), 2835.23 (C-H Str. of CH₃), 1642.48 (C=O Str.), 1598.33 (C=C Str.), 1550.30 (C=N Str.); ¹H-NMR (400 MHz, DMSO-*d*₆, δ , ppm): 11.87 (s, 1H, -OH), 11.86 (s, 1H, =N-NH-), 8.91 (s, 1H, pyrazole CH), 8.40 (s, 1H, -CH=N), 7.94 (d, 2H, $J = 7.80$ Hz), 7.74 (d, 1H, $J = 16.44$ Hz, -HC=CH-), 7.64 (d, 1H, $J = 16.44$ Hz, -HC=CH-), 7.56-7.51 (m, 5H), 7.38-7.36 (m, 2H), 7.17 (dd, 1H, $J = 8.28, 1.64$ Hz), 6.98 (d, 2H, $J = 8.32$ Hz), 3.86 (s, 3H, -OCH₃), 3.78 (s, 3H, -OCH₃); ¹³C-NMR (100 MHz, DMSO-*d*₆, δ ppm): 162.24 (C=O), 149.14, 149.06, 148.83, 147.79, 140.83, 139.00, 138.92, 135.98, 135.33, 131.58, 131.38, 130.60, 130.46, 129.88, 129.76, 129.71, 129.61, 129.57, 129.39, 129.26, 129.12, 128.72, 127.29, 127.00, 126.74, 120.48 (C-6 of DZG), 118.43, 117.94, 117.14, 117.04, 112.45, 112.12, 111.77 (C-5 of DZG), 108.81 (C-2 of DZG), 55.52 (-OCH₃), 55.42 (-OCH₃).

5.1.6.10 2-((3-(3,4-dimethoxystyryl)-1-phenyl-1H-pyrazol-4-yl)methylene)hydrazine-1-carbothioamide (**11a**):

Yellow solid, Yield: 49%, mp: 178-180 °C; FTIR (ATR, ν_{max} , cm^{-1}): 3502.65, 3342.74 (N-H Str. primary), 3136.13 (N-H Str.), 2920.84 (Ar-H Str.), 2850.86 (C-H Str. of CH_3), 1577.16 (C=C Str.), 1544.77 (C=N Str.), 1133.96 (C=S Str.); $^1\text{H-NMR}$ (400 MHz, $\text{DMSO-}d_6$, δ , ppm): 11.34 (s, 1H, =N-NH-), 9.01 (s, 1H, pyrazole CH), 8.30 (s, 1H, -CH=N), 8.26 (s, 1H, -NH₂), 7.88 (d, 2H, $J = 8.32$ Hz), 7.76 (s, 1H, -NH₂), 7.54 (t, 2H, $J = 7.96$ Hz), 7.36 (t, 1H, $J = 7.42$ Hz), 7.31 (s, 2H, -HC=CH-), 7.29 (d, 1H, $J = 1.76$ Hz), 7.13 (dd, 1H, $J = 8.34, 1.86$ Hz), 6.97 (d, 1H, $J = 8.32$ Hz), 3.83 (s, 3H, -OCH₃), 3.78 (s, 3H, -OCH₃); $^{13}\text{C-NMR}$ (100 MHz, $\text{DMSO-}d_6$, δ ppm): 177.60 (C=S), 149.20, 149.02, 148.93, 138.99, 135.52, 131.81, 129.65, 129.45, 128.39, 126.81, 120.52 (C-6 of DZG), 118.34, 117.43, 116.29, 111.72 (C-5 of DZG), 109.02 (C-2 of DZG), 55.53 (-OCH₃).

5.1.6.11 2-((3-(3,4-dimethoxystyryl)-1-phenyl-1H-pyrazol-4-yl)methylene)-N-methylhydrazine-1-carbothioamide (**11b**):

Yellow solid, Yield: 24%, mp: 213-215 °C; FTIR (ATR, ν_{max} , cm^{-1}): 3367.49, 3125.37 (N-H Str.), 2927.24 (Ar-H Str.), 2828.11 (C-H Str. of CH_3), 1623.42 (C=C Str.), 1596.48 (C=N Str.), 1133.46 (C=S Str.); $^1\text{H-NMR}$ (400 MHz, $\text{DMSO-}d_6$, δ , ppm): 11.37 (s, 1H, =N-NH-), 8.92 (s, 1H, pyrazole CH), 8.33 (d, 1H, $J = 4.64$ Hz), 8.30 (s, 1H, -CH=N), 7.90-7.87 (m, 2H), 7.55 (t, 2H, $J = 7.98$ Hz), 7.37 (t, 1H, $J = 5.06$ Hz), 7.35 (d, 1H, $J = 3.60$ Hz), 7.33 (s, 2H, -HC=CH-), 7.14 (dd, 1H, $J = 8.22, 1.86$ Hz), 6.97 (d, 1H, $J = 8.40$ Hz), 3.84 (s, 3H, -OCH₃), 3.78 (s, 3H, -OCH₃), 3.05 (d, 3H, $J = 4.56$ Hz, -CH₃); $^{13}\text{C-NMR}$ (100 MHz, $\text{DMSO-}d_6$, δ ppm): 177.48 (C=S), 149.20, 148.99, 148.89, 138.98, 135.26, 131.86, 129.66, 129.46, 128.30, 126.84, 120.65 (C-6 of DZG), 118.41, 117.42, 116.33, 111.71 (C-5 of DZG), 109.19 (C-2 of DZG), 55.53 (-OCH₃), 55.45 (-OCH₃), 30.76 (-CH₃); HRMS (ESI, m/z) [M-H]⁻; calculated for $\text{C}_{22}\text{H}_{23}\text{N}_5\text{O}_2\text{S}$, 420.1494; found 420.1502.

5.1.6.12 2-((3-(3,4-dimethoxystyryl)-1-phenyl-1H-pyrazol-4-yl)methylene)-N-phenylhydrazine-1-carbothioamide (**11c**):

Off white solid, Yield: 24%, mp: 215-217 °C; FTIR (ATR, ν_{max} , cm^{-1}): 3329.46, 3135.84 (N-H Str.), 2933.89 (Ar-H Str.), 2831.87 (C-H Str. of CH_3), 1618.44 (C=C Str.), 1595.53 (C=N Str.), 1134.65 (C=S Str.); $^1\text{H-NMR}$ (400 MHz, $\text{DMSO-}d_6$, δ , ppm): 11.75 (s, 1H, =N-NH-), 9.91 (s, 1H, -NH), 9.07 (s, 1H, pyrazole CH), 8.41 (s, 1H, -CH=N), 7.90 (d, 2H, $J = 7.76$ Hz), 7.61 (d, 2H, $J = 7.56$ Hz), 7.55 (t, 2H, $J = 7.96$ Hz), 7.39 (d, 2H, $J = 3.32$ Hz), 7.37 (s, 2H, -HC=CH-), 7.36-7.35 (m, 1H), 7.29 (d, 1H, $J = 1.80$ Hz), 7.21 (t, 1H, $J = 7.34$ Hz), 7.14 (dd, 1H, $J = 8.34, 1.82$ Hz), 6.91 (d, 1H, $J = 8.32$ Hz), 3.77 (s, 3H, -OCH₃), 3.68 (s, 3H, -OCH₃); $^{13}\text{C-NMR}$ (100 MHz, $\text{DMSO-}d_6$, δ ppm): 175.38 (C=S), 149.18, 149.10, 148.96, 139.02, 138.96, 136.24, 131.94,

129.65, 129.47, 128.84, 128.15, 126.88, 125.18, 120.45 (C-6 of DZG), 118.45, 117.19, 116.46, 111.68 (C-5 of DZG), 109.26 (C-2 of DZG), 55.50 (-OCH₃), 55.30 (-OCH₃).

5.1.6.13 2-((3-(3,4-dimethoxystyryl)-1-phenyl-1H-pyrazol-4-yl)methylene)hydrazine-1-carboxamide (11d):

Off white solid, Yield: 45%, mp: 183-185 °C; FTIR (ATR, ν_{max} , cm⁻¹): 3449.01, 3369.49 (N-H Str. primary), 3154.90 (N-H Str.), 2910.52 (Ar-H Str.), 2831.62 (C-H Str. of CH₃), 1673.67 (C=O Str.), 1596.05 (C=C Str.), 1546.12 (C=N Str.); ¹H-NMR (400 MHz, DMSO-*d*₆, δ , ppm): 10.12 (s, 1H, =N-NH-), 8.89 (s, 1H, pyrazole CH), 8.05 (s, 1H, -CH=N), 7.89 (d, 2H, *J* = 7.88 Hz), 7.53 (t, 2H, *J* = 7.96 Hz), 7.35 (t, 1H, *J* = 7.38 Hz), 7.34 (s, 2H, -HC=CH-), 7.28 (d, 1H, *J* = 1.80 Hz), 7.12 (dd, 1H, *J* = 8.24, 1.84 Hz), 6.96 (d, 1H, *J* = 8.32 Hz), 6.42 (bs, 2H, -NH₂), 3.82 (s, 3H, -OCH₃), 3.78 (s, 3H, -OCH₃); ¹³C-NMR (100 MHz, DMSO-*d*₆, δ ppm): 156.75 (C=O), 149.11, 149.02, 148.28, 139.09, 132.39, 131.27, 129.60, 129.55, 127.79, 126.61, 120.42 (C-6 of DZG), 118.25, 118.03, 116.46, 111.74 (C-5 of DZG), 108.96 (C-2 of DZG), 55.50 (-OCH₃).

5.1.6.14 (4-chlorophenyl)-2-((3-(3,4-dimethoxystyryl)-1-phenyl-1H-pyrazol-4-yl)methylene)hydrazine-1-carbothioamide (11e):

Yellow solid, Yield: 64%, mp: 214-216 °C; FTIR (ATR, ν_{max} , cm⁻¹): 3307.53, 3146.01 (N-H Str.), 2930.45 (Ar-H Str.), 2831.72 (C-H Str. of CH₃), 1621.05 (C=C Str.), 1591.70 (C=N Str.), 1134.03 (C=S Str.); ¹H-NMR (400 MHz, DMSO-*d*₆, δ , ppm): 11.83 (s, 1H, =N-NH-), 9.97 (s, 1H, NH-C-), 9.05 (s, 1H, pyrazole CH), 8.41 (s, 1H, -CH=N), 7.90 (d, 2H, *J* = 7.88 Hz), 7.67-7.64 (m, 2H), 7.55 (t, 2H, *J* = 7.90 Hz), 7.44-7.35 (m, 5H), 7.29 (d, 1H, *J* = 1.76 Hz), 7.14 (dd, 1H, *J* = 8.32, 1.76 Hz), 6.90 (d, 1H, *J* = 8.32 Hz), 3.77 (s, 3H, -OCH₃), 3.68 (s, 3H, -OCH₃); ¹³C-NMR (100 MHz, DMSO-*d*₆, δ ppm): 175.42 (C=S), 149.20, 149.15, 148.96, 138.96, 138.08, 136.61, 131.96, 129.68, 129.48, 129.13, 128.92, 128.05, 126.93, 126.81, 120.49 (C-6 of DZG), 118.75, 118.48, 117.13, 116.48, 111.68 (C-5 of DZG), 109.32 (C-2 of DZG), 55.50 (-OCH₃), 55.33 (-OCH₃).

5.1.6.15 2-((3-(3,4-dimethoxystyryl)-1-phenyl-1H-pyrazol-4-yl)methylene)-N-(4-fluorophenyl)hydrazine-1-carbothioamide (11f):

Off white solid, Yield: 59%, mp: 206-208 °C; FTIR (ATR, ν_{max} , cm⁻¹): 3322.64, 3139.55 (N-H Str.), 2931.29 (Ar-H Str.), 2830.34 (C-H Str. of CH₃), 1618.91 (C=C Str.), 1597.12 (C=N Str.), 1134.38 (C=S Str.); ¹H-NMR (400 MHz, DMSO-*d*₆, δ , ppm): 11.77 (s, 1H, =N-NH-), 9.92 (s, 1H, NH-C-), 9.05 (s, 1H, pyrazole CH), 8.41 (s, 1H, -CH=N), 7.89 (d, 2H, *J* = 7.92 Hz), 7.60-7.53 (m, 4H), 7.39 (d, 1H, *J* = 16.56 Hz, -HC=CH-), 7.37 (t, 1H, *J* = 7.28 Hz), 7.34 (d, 1H, 16.44 Hz, -HC=CH-), 7.29 (d, 1H, *J* = 1.72 Hz), 7.21 (t, 2H, *J* = 8.84 Hz), 7.14 (dd, 1H, *J* = 8.32, 1.76 Hz), 6.91 (d, 1H, *J* = 8.32 Hz), 3.77 (s, 3H, -OCH₃), 3.69 (s, 3H, -OCH₃); ¹³C-NMR (100 MHz,

DMSO-*d*₆, δ ppm): 175.85 (C=S), 160.82, 158.41, 149.20, 149.13, 148.97, 138.97, 136.35, 135.44, 135.41, 131.96, 129.68, 129.48, 128.81, 127.68, 127.60, 126.92, 120.55 (C-6 of DZG), 118.47, 117.22, 116.43, 114.93, 114.70, 111.68 (C-5 of DZG), 109.22 (C-2 of DZG), 55.51 (-OCH₃), 55.32 (-OCH₃); HRMS (ESI, *m/z*) [M-H]⁻; calculated for C₂₇H₂₄FN₅O₂S, 500.1332; found 500.1343.

5.1.6.16 *N*-(4-bromophenyl)-2-((3-(3,4-dimethoxystyryl)-1-phenyl-1*H*-pyrazol-4-yl)methylene)hydrazine-1-carbothioamide (**11g**):

Yellow solid, Yield: 71%, mp: 217-219 °C; FTIR (ATR, ν_{max} , cm⁻¹): 3308.20, 3145.65 (N-H Str.), 2931.26 (Ar-H Str.), 2832.00 (C-H Str. of CH₃), 1621.11 (C=C Str.), 1587.62 (C=N Str.), 1134.02 (C=S Str.); ¹H-NMR (400 MHz, DMSO-*d*₆, δ , ppm): 11.84 (s, 1H, =N-NH-), 9.96 (s, 1H, NH-C-), 9.05 (s, 1H, pyrazole CH), 8.41 (s, 1H, -CH=N), 7.90 (d, 2H, *J* = 7.80 Hz), 7.62-7.53 (m, 6H), 7.40 (d, 1H, *J* = 16.24 Hz, -HC=CH-), 7.36 (d, 1H, *J* = 7.20 Hz), 7.34 (d, 1H, *J* = 16.36 Hz, -HC=CH-), 7.28 (d, 1H, *J* = 1.68 Hz), 7.13 (dd, 1H, *J* = 8.32, 1.68 Hz), 6.90 (d, 1H, *J* = 8.36 Hz), 3.77 (s, 3H, -OCH₃), 3.68 (s, 3H, -OCH₃); ¹³C-NMR (100 MHz, DMSO-*d*₆, δ ppm): 175.33 (C=S), 149.19, 149.15, 148.96, 138.96, 138.52, 136.64, 131.96, 130.98, 129.68, 129.49, 128.95, 127.10, 126.93, 120.48 (C-6 of DZG), 118.48, 117.32, 117.13, 116.50, 111.68 (C-5 of DZG), 109.34 (C-2 of DZG), 55.51 (-OCH₃), 55.33 (-OCH₃); HRMS (ESI, *m/z*) [M-H]⁻; calculated for C₂₇H₂₄BrN₅O₂S, 560.0756; found 560.0758.

5.1.6.17 2-((3-(3,4-dimethoxystyryl)-1-phenyl-1*H*-pyrazol-4-yl)methylene)-*N*-(4-nitrophenyl)hydrazine-1-carbothioamide (**11h**):

Yellow solid, Yield: 56%, mp: 219-221 °C; FTIR (ATR, ν_{max} , cm⁻¹): 3289.83, 3148.42 (N-H Str.), 2928.49 (Ar-H Str.), 2835.15 (C-H Str. of CH₃), 1643.08 (C=C Str.), 1597.52 (C=N Str.), 1136.62 (C=S Str.); ¹H-NMR (400 MHz, DMSO-*d*₆, δ , ppm): 12.11 (s, 1H, =N-NH-), 10.32 (s, 1H, NH-C-), 9.07 (s, 1H, pyrazole CH), 8.45 (s, 1H, -CH=N), 8.23 (d, 2H, *J* = 9.20 Hz), 8.08 (d, 2H, *J* = 9.12 Hz), 7.91 (d, 2H, *J* = 7.68 Hz), 7.56 (t, 2H, *J* = 7.96 Hz), 7.44 (d, 1H, *J* = 16.92 Hz, -HC=CH-), 7.38 (t, 1H, *J* = 7.38 Hz), 7.36 (d, 1H, *J* = 15.97 Hz, -HC=CH-), 7.28 (d, 1H, *J* = 1.68 Hz), 7.15 (dd, 1H, *J* = 8.36, 1.80 Hz), 6.90 (d, 1H, *J* = 8.36 Hz), 3.76 (s, 3H, -OCH₃), 3.69 (s, 3H, -OCH₃); ¹³C-NMR (100 MHz, DMSO-*d*₆, δ ppm): 174.70 (C=S), 149.23, 149.21, 148.95, 145.47, 143.21, 138.92, 137.62, 132.03, 129.67, 129.49, 129.31, 126.95, 123.88, 123.47, 120.36 (C-6 of DZG), 118.50, 116.87, 116.55, 111.72 (C-5 of DZG), 109.57 (C-2 of DZG), 55.47 (-OCH₃), 55.38 (-OCH₃); HRMS (ESI, *m/z*) [M-H]⁻; calculated for C₂₇H₂₄N₆O₄S, 527.1503; found 527.1502.

5.1.6.18 2-((3-(3,4-dimethoxystyryl)-1-phenyl-1H-pyrazol-4-yl)methylene)-N-phenylhydrazine-1-carboxamide (**14a**):

Off white solid, Yield: 47%, mp: 140-142 °C; FTIR (ATR, ν_{max} , cm^{-1}): 3295.04, 3121.62 (N-H Str.), 2926.73 (Ar-H Str.), 2832.25 (C-H Str. of CH_3), 1673.01 (C=O Str.), 1630.29 (C=C Str.), 1592.39 (C=N Str.); $^1\text{H-NMR}$ (400 MHz, $\text{DMSO-}d_6$, δ , ppm): 10.09 (s, 1H, -CH=N), 9.23 (s, 1H, pyrazole CH), 8.63 (s, 2H, 2-NH), 7.96 (d, 2H, $J = 7.84$ Hz), 7.66 (d, 1H, $J = 16.37$ Hz, -HC=CH-), 7.57 (t, 2H, $J = 7.92$ Hz), 7.44 (d, 1H, $J = 16.13$ Hz, -HC=CH-), 7.45-7.42 (m, 3H), 7.28-7.27 (m, 3H), 7.19 (dd, 1H, $J = 8.30, 1.86$ Hz), 6.99 (d, 1H, $J = 8.44$ Hz), 6.95 (d, 1H, $J = 7.36$ Hz), 3.84 (s, 3H, -OCH₃), 3.79 (s, 3H, -OCH₃); $^{13}\text{C-NMR}$ (100 MHz, $\text{DMSO-}d_6$, δ ppm): 185.21 (-CH=N), 152.53 (C=O), 150.55, 149.48, 149.01, 139.69, 138.64, 134.61, 133.57, 129.70, 129.14, 128.78, 127.61, 122.25, 121.81, 120.53 (C-6 of DZG), 119.13, 118.18, 115.31, 111.84 (C-5 of DZG), 109.69 (C-2 of DZG), 55.55 (-OCH₃).

5.1.6.19 2-((3-(3,4-dimethoxystyryl)-1-phenyl-1H-pyrazol-4-yl)methylene)-N-(4-fluorophenyl)hydrazine-1-carboxamide (**14b**):

Yellow crystalline solid, Yield: 14%, mp: 117-119 °C; FTIR (ATR, ν_{max} , cm^{-1}): 3276.93, 3119.35 (N-H Str.), 2932.54 (Ar-H Str.), 2832.39 (C-H Str. of CH_3), 1665.37 (C=O Str.), 1629.68 (C=C Str.), 1597.48 (C=N Str.); $^1\text{H-NMR}$ (400 MHz, $\text{DMSO-}d_6$, δ , ppm): 10.10 (s, 1H, -CH=N), 9.23 (s, 1H, pyrazole CH), 8.97 (s, 1H, NH), 7.96 (d, 2H, $J = 7.68$ Hz), 7.66 (d, 1H, $J = 16.33$ Hz, -HC=CH-), 7.57 (t, 2H, $J = 7.94$ Hz), 7.47-7.40 (m, 4H), 7.44 (d, 1H, $J = 16.40$ Hz, -HC=CH-), 7.28 (d, 1H, $J = 1.84$ Hz), 7.20-7.17 (dd, 1H, $J = 8.26, 1.94$ Hz), 7.10 (t, 2H, $J = 8.92$ Hz), 6.99 (d, 1H, $J = 8.32$ Hz), 3.84 (s, 3H, -OCH₃), 3.79 (s, 3H, -OCH₃); $^{13}\text{C-NMR}$ (100 MHz, $\text{DMSO-}d_6$, δ ppm): 185.20 (-CH=N), 158.44 (C=O), 156.08, 152.81, 150.55, 149.46, 148.99, 138.63, 136.14, 134.58, 133.55, 129.69, 129.51, 129.12, 127.59, 122.24, 120.52 (C-6 of DZG), 119.92, 119.85, 119.11, 115.32, 115.29, 115.10, 111.81 (C-5 of DZG), 109.66 (C-2 of DZG), 55.53 (-OCH₃).

5.1.6.20 N-(4-chlorophenyl)-2-((3-(3,4-dimethoxystyryl)-1-phenyl-1H-pyrazol-4-yl)methylene)hydrazine-1-carboxamide (**14c**):

Yellow crystalline solid, Yield: 20%, mp: 124-126 °C; FTIR (ATR, ν_{max} , cm^{-1}): 3118.68 (N-H Str.), 2914.96 (Ar-H Str.), 2834.1 (C-H Str. of CH_3), 1662.25 (C=O Str.), 1631.12 (C=C Str.), 1594.35 (C=N Str.); $^1\text{H-NMR}$ (400 MHz, $\text{DMSO-}d_6$, δ , ppm): 10.09 (s, 1H, -CH=N), 9.23 (s, 1H, pyrazole CH), 8.83 (s, 1H, NH), 7.96 (d, 2H, $J = 7.64$ Hz), 7.66 (d, 1H, $J = 16.33$ Hz, -HC=CH-), 7.57 (t, 2H, $J = 7.96$ Hz), 7.47-7.40 (m, 3H), 7.46 (s, 1H, NH), 7.44 (d, 1H, $J = 16.45$ Hz, -HC=CH-), 7.32 (d, 2H, $J = 8.88$ Hz), 7.28 (d, 1H, $J = 1.84$ Hz), 7.19 (dd, 1H, $J = 8.28, 1.84$ Hz), 6.99 (d, 1H, $J = 8.36$ Hz), 3.84 (s, 3H, -OCH₃), 3.79 (s, 3H, -OCH₃); $^{13}\text{C-NMR}$ (100 MHz, DMSO-

d_6 , δ ppm): 185.20 (-CH=N), 152.33 (C=O), 150.55, 149.46, 148.99, 138.63, 138.53, 134.58, 133.55, 129.69, 129.12, 128.61, 127.59, 125.48, 122.24, 120.52 (C-6 of DZG), 119.82, 119.11, 115.29, 111.81 (C-5 of DZG), 109.66 (C-2 of DZG), 55.53 (-OCH₃).

5.2 Biological activity protocols

5.2.1 *In vitro* evaluation of antimicrobial activity:

The synthesized title compounds (**8a-i**, **11a-h** and **14a-c**) were further assessed for antimicrobial activity against panel of bacterial and fungal strains by following earlier reported MIC assay method using resazurin dye.[20]

5.2.1.1 *Microorganisms used:*

Standard cultures of two Gram positive [*S. aureus* (ATCC 25923), *B. subtilis* (ATCC 6051)], two Gram negative [*E. coli* (ATCC 35218), *P. aeruginosa* (ATCC 27853)], four fungal strains [*C. albicans* (ATCC 90028), *C. neoformans* (ATCC 66031), *A. niger* (ATCC 16404)] and *A. fumigatus* were used for the antibacterial and antifungal activity respectively. Culturing and sub-culturing (one day prior to testing) of these microorganisms was carried out at the Department of Microbiology, Inkosi Albert Luthuli Hospital, Durban, South Africa.

5.2.1.2 *Preparation of medium:*

The nutrient medium was prepared by dissolving 22 g of Muller-Hinton Broth (MHB) containing (Acid Hydrolysate of Casein, Beef Extract and Starch) in 1 L of double distilled water. The pH of this medium was adjusted to 7.4 ± 0.1 and sterilized by autoclave for 15 min at 121 °C. The solution was allowed to cool and stored at a temp of 4 °C. Sterility check was performed by incubating un-inoculated media in an aerobic incubator at 37 °C for 18-24 h. For antifungal activity, RPMI 1640 medium with L-glutamine and 0.165 M MOPS and without sodium bicarbonate (Lonza) was used.

5.2.1.3 *Preparation of test compounds (stock solution and working standard):*

An accurately weighed quantity (4.000 mg) of the synthesized compounds and standard drugs were dissolved in 1 mL of DMSO to give stock solution (4000 µg/mL). Further, 100 µL of stock solution was diluted with 900 µL of DMSO to afford working standard solution (400 µg/mL).

5.2.1.4 *Preparation of inoculums:*

One day prior to testing one or more identical colonies of microorganisms were suspended in 4.5 mL sterile double distilled water. Inoculates were adjusted to 0.5 McFarland standard (1.5×10^8 cfu/mL) [21]. A density check turbidimeter was used to ensure that the inoculum was a 0.5 McFarland standard.

5.2.1.5 Broth micro-dilution method:

The preliminary *in vitro* antimicrobial activity for the newly synthesized title compounds (**8a-i**, **11a-h** and **14a-c**) was evaluated using the broth micro-dilution method. 100 μ L of sterile double distilled water was added to all outer-perimeter wells of a 96-well microliter plates to minimize evaporation of the medium in the test wells during incubation. To the remaining test wells 100 μ L of MHB was added. Two fold serial dilutions of the test compounds and standard drugs (Moxicillin and Amphotericin B) were made directly on the microplate using MHB. The compounds were tested at final concentration of (200, 100, 50, 25, 12.5, 6.25, 3.125, 1.56, 0.78, 0.39 μ g/mL). Finally, 10 μ L of the freshly prepared bacterial or fungal inoculum was added to the wells. The microliter plates were covered and sealed with parafilm and incubated at 37 ± 1 °C for 24 h. After this, 10 μ L of freshly prepared resazurin (0.4 mg/mL) was added to the test wells and incubated further for 5h. MIC was determined as a blue color in the test well was interpreted as no bacterial growth and a pink color was scored as growth. The MIC was thus defined at the lowest drug concentration that prevented a color change from blue to pink. Thus the MIC values in μ g/mL were determined.

5.2.1 In vitro evaluation of antimycobacterial activity:

M. tuberculosis (ATCC H₃₇RV), MDR (UKQC strain), *M. kansasii* (ATCC 12478), *M. peregrinum* (ATCC 14467) and *M. fortuitum* (ATCC 6841) were maintained on 7H11 agar plates at 37 °C in an atmosphere of 5% CO₂. Inoculums of strains were prepared by scraping and resuspending a loopful of colonies into Middlebrook 7H9 broth, supplemented with 10% ADC and 0.04% tween 80 to avoid clump formation and incubated at 37 °C in 5% CO₂. The inoculum turbidity was adjusted to a McFarland number 1 standard and further diluted 1:10 in Middlebrook 7H9 broth prior to addition (100 μ L) to each of the test samples and drug-free wells. A growth control and a sterile control were also included for each isolate. Each of the synthesized test compounds and standard drugs were weighed accordingly, dissolved in the appropriate solvent and filter and sterilized using a 0.2-micron polycarbonate filter. Further, an amount, 100 μ L from the stock solution was diluted with 900 μ L of DMSO (some protocols used broth, we in order to overcome solubility concern have used DMSO with the final well on the plate having a concentration of less than 1% of DMSO) to afford working standard solution (400 μ g/mL). A serially diluted drug free control (DMSO) was used to check the activity on each strain. The preliminary *in vitro* antimycobacterial activity for the newly synthesized test compounds (**8a-i**, **11a-h** and **14a-c**) was evaluated using the colorimetric resazurin microplate assay plate method.[22] The outer-perimeter wells of a 96-well microliter plates was filled with 200 uL of sterile double distilled water to minimize evaporation of the medium in the test wells during

incubation. In the remaining test wells, an amount of 100 μL of Middlebrook 7H9 broth with ADC 10%, 100 μL of the test compounds and 100 μL of the mycobacteria was added to get at final concentration of 200, 100, 50, 25, 12.5, 6.25, 3.125, 1.56, 0.78, and 0.39 $\mu\text{g}/\mu\text{L}$. The plates were incubated at 37 $^{\circ}\text{C}$ for 7 days. After incubation, 30 μL of resazurin solution prepared at 0.01% (wt/vol) in distilled water, filter sterilized and stored at 4 $^{\circ}\text{C}$, and was added to each well. The plates were then incubated overnight at 37 $^{\circ}\text{C}$, and assessed for color development. A positive reaction results in a color change from blue to pink indicates bacterial growth, which confirms drug resistance. Therefore, the minimum inhibitory concentration was attributed to the lower concentration of the test compound to inhibit the color change of resazurin. Isoniazid and rifampicin were used as reference standards.

Acknowledgments:

Authors are thankful to Discipline of Pharmaceutical Sciences, College of Health Sciences, University of KwaZulu-Natal (UKZN), South Africa, for their constant support, encouragement and financial assistance. Authors also express heartfelt thanks to Mr. Dilip Jagjivan and Dr. Caryl Janse Van Rensburg (UKZN, South Africa) for their assistance in the NMR and EIMS experiments.

Conflict of Interest:

Authors hereby declare that there are no financial/commercial conflicts of interest.

References:

- [1] WHO | Antimicrobial resistance, WHO. (2016). <http://www.who.int/mediacentre/factsheets/fs194/en/> (accessed December 7, 2016).
- [2] W.S. Alwan, R. Karpoormath, M.B. Palkar, H.M. Patel, R.A. Rane, M.S. Shaikh, A. Kajee, K.P. Mlisana, Novel imidazo[2,1-b]-1,3,4-thiadiazoles as promising antifungal agents against clinical isolate of *Cryptococcus neoformans*, *Eur. J. Med. Chem.* 95 (2015) 514–525. doi:10.1016/j.ejmech.2015.03.021.
- [3] G.A. Hampannavar, R. Karpoormath, M.B. Palkar, M.S. Shaikh, B. Chandrasekaran, Dehydrozingerone Inspired Styryl Hydrazine Thiazole Hybrids as Promising Class of Antimycobacterial Agents, *ACS Med. Chem. Lett.* 7 (2016) 686–691. doi:10.1021/acsmchemlett.6b00088.
- [4] M.S. Shaikh, M.B. Palkar, H.M. Patel, R.A. Rane, W.S. Alwan, M.M. Shaikh, I.M. Shaikh, G.A. Hampannavar, R. Karpoormath, Design and synthesis of novel carbazolo-thiazoles as potential anti-mycobacterial agents using a molecular hybridization approach, *RSC Adv.* 4 (2014) 62308–62320. doi:10.1039/C4RA11752B.
- [5] Z. Wu, S. Wu, Y. Ye, X. Zhou, P. Wang, W. Xue, D. Hu, Synthesis and Bioactivities of Novel 1-(3-Chloropyridin-2-yl)-*N*-Substituted-5-(Trifluoromethyl)-Pyrazole Carboxamide Derivatives, *J. Heterocycl. Chem.* (2015). doi:10.1002/jhet.2587.
- [6] H. Kumar, D. Saini, S. Jain, N. Jain, Pyrazole scaffold: A remarkable tool in the development of anticancer agents, *Eur. J. Med. Chem.* 70 (2013) 248–258. doi:10.1016/j.ejmech.2013.10.004.
- [7] S.-R. Shih, T.-Y. Chu, G.R. Reddy, S.-N. Tseng, H.-L. Chen, W.-F. Tang, M. Wu, J.-Y. Yeh, Y.-S. Chao, J.T. Hsu, H.-P. Hsieh, J.-T. Horng, Pyrazole compound BPR1P0034 with potent and selective anti-influenza virus activity., *J. Biomed. Sci.* 17 (2010) 13. doi:10.1186/1423-0127-17-13.
- [8] D.-M. Shen, E.J. Brady, M.R. Candelore, Q. Dallas-Yang, V.D.-H. Ding, W.P. Feeney, G. Jiang, M.E. McCann, S. Mock, S.A. Qureshi, R. Saperstein, X. Shen, X. Tong, L.M. Tota, M.J. Wright, X. Yang, S. Zheng, K.T. Chapman, B.B. Zhang, J.R. Tata, E.R. Parmee, Discovery of novel, potent, selective, and orally active human glucagon receptor antagonists containing a pyrazole core, *Bioorg. Med. Chem. Lett.* 21 (2011) 76–81. doi:10.1016/j.bmcl.2010.11.074.
- [9] P.D. Sauzem, G. da S. Sant'Anna, P. Machado, M.M.M.F. Duarte, J. Ferreira, C.F. Mello,

-
- P. Beck, H.G. Bonacorso, N. Zanatta, M.A.P. Martins, M.A. Rubin, Effect of 5-trifluoromethyl-4,5-dihydro-1H-pyrazoles on chronic inflammatory pain model in rats, *Eur. J. Pharmacol.* 616 (2009) 91–100. doi:10.1016/j.ejphar.2009.06.008.
- [10] X. Liu, X. Huang, W. Lin, D. Wang, Y. Diao, H. Li, X. Hui, Y. Wang, A. Xu, D. Wu, D. Ke, New aromatic substituted pyrazoles as selective inhibitors of human adipocyte fatty acid-binding protein, *Bioorganic Med. Chem. Lett.* 21 (2011) 2949–2952. doi:10.1016/j.bmcl.2011.03.063.
- [11] P. Aragade, M. Palkar, P. Ronad, D. Satyanarayana, Coumarinyl pyrazole derivatives of INH: Promising antimycobacterial agents, *Med. Chem. Res.* 22 (2013) 2279–2283. doi:10.1007/s00044-012-0222-8.
- [12] M. Pitucha, M. Woś, M. Miazga-Karska, K. Klimek, B. Mirosław, A. Pachuta-Stec, A. Gładysz, G. Ginalska, Synthesis, antibacterial and antiproliferative potential of some new 1-pyridinecarbonyl-4-substituted thiosemicarbazide derivatives, *Med. Chem. Res.* 25 (2016) 1666–1677. doi:10.1007/s00044-016-1599-6.
- [13] K. Alomar, V. Gaumet, M. Allain, G. Bouet, A. Landreau, Synthesis, crystal structure, characterisation, and antifungal activity of 3-thiophene aldehyde semicarbazone (3STCH), 2,3-thiophene dicarboxaldehyde bis(semicarbazone) (2,3BSTCH₂) and their nickel (II) complexes, *J. Inorg. Biochem.* 115 (2012) 36–43. doi:10.1016/j.jinorgbio.2012.04.022.
- [14] S.M.M. Ali, M.A.K. Azad, M. Jesmin, S. Ahsan, M.M. Rahman, J.A. Khanam, M.N. Islam, S.M.S. Shahriar, *In vivo* anticancer activity of vanillin semicarbazone, *Asian Pac. J. Trop. Biomed.* 2 (2012) 438–442. doi:10.1016/S2221-1691(12)60072-0.
- [15] M.J. Ahsan, Semicarbazone analogs as anticonvulsant agents: a review., *Cent. Nerv. Syst. Agents Med. Chem.* 13 (2013) 148–58. doi:10.2174/18715249113136660016.
- [16] D. Sriram, P. Yogeewari, R. Thirumurugan, Antituberculous activity of some aryl semicarbazone derivatives, *Bioorganic Med. Chem. Lett.* 14 (2004) 3923–3924. doi:10.1016/j.bmcl.2004.05.060.
- [17] G.A. Hampannavar, R. Karpoornath, M.B. Palkar, M.S. Shaikh, An appraisal on recent medicinal perspective of curcumin degradant: Dehydrozingerone (DZG), *Bioorg. Med. Chem.* 24 (2016) 501–520. doi:10.1016/j.bmc.2015.12.049.
- [18] A. Chilin, G. Marzaro, S. Zanatta, V. Barbieri, G. Pastorini, P. Manzini, A. Guiotto, A new access to quinazolines from simple anilines, *Tetrahedron.* 62 (2006) 12351–12356. doi:10.1016/j.tet.2006.09.103.
-

- [19] P.K. Sharma, N. Chandak, P. Kumar, C. Sharma, K.R. Aneja, Synthesis and biological evaluation of some 4-functionalized-pyrazoles as antimicrobial agents, *Eur. J. Med. Chem.* 46 (2011) 1425–1432. doi:10.1016/j.ejmech.2011.01.060.
- [20] C.M. Mann, J.L. Markham, A new method for determining the minimum inhibitory concentration of essential oils., *J. Appl. Microbiol.* 84 (1998) 538–544. doi:10.1046/j.1365-2672.1998.00379.x.
- [21] J. McFARLAND, The Nephelometer:an Instrument for Estimating the Number of Bacteria in Suspensions Used for Calculating the Opsonic Index and for Vaccines., *JAMA J. Am. Med. Assoc.* XLIX (1907) 1176. doi:10.1001/jama.1907.25320140022001f.
- [22] J.-C. Palomino, A. Martin, M. Camacho, H. Guerra, J. Swings, F. Portaels, Resazurin Microtiter Assay Plate: Simple and Inexpensive Method for Detection of Drug Resistance in *Mycobacterium tuberculosis*, *Antimicrob. Agents Chemother.* 46 (2002) 2720–2722. doi:10.1128/AAC.46.8.2720–2722.2002.

CHAPTER 6

1 SUMMARY AND CONCLUSION

Microbial and tubercular infections are nowadays become fatal owing to the development of resistance and co-infections. TB is the leading cause of mortality and morbidity worldwide. Emergence of several resistant forms and persistence of latent infections have intensified the need of effective treatment. Early detection of resistant strain, appropriate use of medicines, patient compliance, accelerated drug discovery and development programs, and identification of effective lead molecules, are crucial and are of rising concern in controlling TB and microbial infections.

The aim of this entire study was to identify a novel and potential antimicrobial and antimycobacterial leads that were encouraged from a natural compound, Dehydrozingerone (DZG). DZG was fused with various antimicrobial/antitubercular five membered heterocycles by molecular hybridisation approach to yield novel assorted DZG derivatives. Thus obtained 54 novel derivatives were well characterized by thin layer chromatography, infrared spectroscopy, nuclear magnetic resonance spectroscopy (^1H , ^{13}C and 2D), and high resolution mass spectrometry. Results on biological activity suggest that, thus designed compounds were explicitly active as antimicrobial and antitubercular agents. Hence, emphasizing the significance of considering natural compounds as a standpoint in drug discovery.

In chapter 2, we have comprehensively performed literature assessment of DZG for its various reported biological activities. During this literature investigation, it was evident that DZG was a versatile scaffold exploited extensively in building up of diverse chemical libraries. These libraries were evaluated for their diverse pharmacological actions namely antioxidant, anti-inflammatory, antioxidant, antidepressant, antifungal, antimalarial etc. Therefore, it was quite marked and impressive about the contributions made by the DZG structural core. Apparently, there were no investigations performed on DZG or its derivatives describing its antimycobacterial properties. This literature outcome enthused us to choose this structural framework (of DZG) for modifying further as antimycobacterial agent. The substantial outcome of this chapter has emerged as a review publication in **Bioorganic and medicinal chemistry** journal published in **2016**, **volume 24** and **page number 501** to **520**. (<http://www.sciencedirect.com/science/article/pii/S0968089615302157>)

In chapter 3, we hypothesized to fuse DZG with thiazole heterocycle, a distinguished antitubercular scaffold via hydrazine linker by molecular hybridisation approach. This strategic synthetic scheme was more pragmatic producing decent yields (51-74%) of final compounds. The

synthesis was achieved by Hantzsch cyclo-condensation reaction of compound **4**, (*E*)-2-((*E*)-4-(3,4-dimethoxyphenyl)but-3-en-2-ylidene)hydrazine-1-carbothioamide with various appropriately substituted 2-bromo-1-phenylethanones (**5a-o**) in presence of methanol as depicted in scheme 2 of chapter 3. Structures of synthesized compounds were characterized by spectral data (IR, ¹H NMR, ¹³C NMR, 2D NMR and HRMS). Antimycobacterial screening was performed in two levels, preliminary (for determining MIC for *Mycobacterium tuberculosis*, H₃₇Rv) and secondary (for determining broad spectrum efficiency against relevant drug resistant isolates of *Mycobacterium tuberculosis*) by National Institute of Allergy and Infectious Diseases (NIAID), Bethesda, MD, USA. Compound **6o**, outstood as potential lead with antimycobacterial activity under hypoxic (MIC = 46 μM) and normal oxygen (MIC = 0.28 μM) conditions along with antimycobacterial efficiency against isoniazid (MIC = 3.2 μM for INH-R1; 1.5 μM for INH-R2) and rifampicin (MIC = 2.2 μM for RIF-R1; 6.3 μM for RIF-R2) resistant strains of Mtb. SAR studies revealed correlations of structural variations with antimycobacterial activity as discussed above in chapter 3. This work was published in the journal *ACS Medicinal Chemistry Letters*, volume 7, issue 7, page 686 to 691 in 2016. (<http://pubs.acs.org/doi/abs/10.1021/acsmedchemlett.6b00088>)

In chapter 4, as a continued effort in synthesizing DZG inspired antimycobacterial compounds, DZG was fused with thiazolidin-4-one, a five membered heterocycle distinguished for its antimycobacterial properties through a hydrazine linker. Diverse novel compounds of substituted 2-((4-(3,4-dimethoxyphenyl)but-3-en-2-ylidene)hydrazono)thiazolidin-4-one derivatives (**7a-d**, **10a-l** and **13a-b**) were synthesized by efficient and adaptable synthetic routes (scheme I to IV) as described in chapter 4. These compounds were well characterized by IR, ¹H NMR, ¹³C NMR, 2D NMR, HRMS and x-ray crystallography. Thus obtained compounds were evaluated for their *in vitro* antimycobacterial activity against *Mycobacterium tuberculosis* H₃₇Rv strain at NIAID, Bethesda, MD, USA. From the tested series, compounds **7a** (MIC = 110 μM; IC₅₀ = 67 μM), **7c** (MIC = 120 μM; IC₅₀ = 66 μM) and **10g** (MIC = 100 μM; IC₅₀ = 100 μM) exhibited noteworthy antimycobacterial activity. Besides, these title compounds showed miniscule cytotoxic effect against a mammalian Vero cell line (MTT assay), suggesting for a good therapeutic index. This work has been communicated for publication in *RSC Advances*.

Finally, in chapter 5, as an ongoing endeavour in synthesizing DZG inspired antimycobacterial compounds, we have synthesized styryl fused pyrazolo carbazones. Compounds **8a-i**, **11a-h** and **14a-c** were synthesized having diverse structural variations with simple and effective synthetic routes as described in chapter 5. Several intermediate compounds (acid hydrazides **7a-i**, carbothioamides **10a-h**, and hydrazonocarboxamides **13a-c**) were efficiently synthesized and used further for synthesis of final derivatives. All the final compounds were well characterized

by IR, ^1H NMR, ^{13}C NMR, and HRMS thus conforming their formation. *In vitro* antibacterial, antifungal and antimycobacterial screening were performed at Department of Microbiology, National Health Laboratory Services (NHLS), Inkosi Albert Luthuli Central Hospital, Durban, South Africa. Obtained results suggest that compounds **8a**, **8c**, **8d**, **8g**, **8h**, **8i** and **11f** showed reasonable antibacterial activity (MIC = 50 $\mu\text{g}/\text{mL}$) against *B. subtilis*, compound **11a** demonstrated sensible activity towards *P. aeruginosa* (MIC = 25 $\mu\text{g}/\text{mL}$). Further compounds **8a**, **8d**, **8e**, **8f**, **8i**, and **11h** showed good to moderate antifungal activity ranging from 25 to 50 $\mu\text{g}/\text{mL}$ towards *C. neoformans* (MIC = 25 $\mu\text{g}/\text{mL}$) and *C. albicans* (MIC = 50 $\mu\text{g}/\text{mL}$). Besides, compound **8a**, comprising of isonicotinoyl hydrazide portion displayed remarkable antitubercular activity (MIC = 0.78 $\mu\text{g}/\text{mL}$) against H₃₇Rv. Substituted urea derivatives, **14a-c** and **11d** also exhibited encouraging activity (MIC = 12.5 and 25 $\mu\text{g}/\text{mL}$, respectively) whereas, derivative with carbothioamide portion **11a**, (MIC = 0.78 $\mu\text{g}/\text{mL}$) illustrated significant activity against H₃₇Rv. Moreover, some of the tested compounds showed reasonable activity against MDR (multi drug resistant) and MOTT (mycobacteria other than tuberculosis) strains. The overall findings suggest the significance of hybridisation to achieve styryl fused pyrazolo carbazones as effective antimicrobial and antimycobacterial agents. This work is in manuscript form and is ready to submit.

2 Future work

With the encouraging observations, data from all the synthesized compounds can be effectively utilized in further *in silico* optimization of the lead compounds by building up of 3D-QSAR (three dimensional quantitative structure activity relationship) and 3D-QSPR (three dimensional quantitative structure property relationship) models to attain potential ligands. These potential ligands can further be taken for their chemical synthesis to achieve drug-like compounds with better activity, bioavailability, and efficacy profiles.

In parallel, 3D-QSAR-based pharmacophore models could be generated from the available dataset molecules and validated using the test set ligands. Thus, ligand-based virtual screening of the best pharmacophore model against drug-like database (ZINC, Maybridge, Chembridge and NCI) can be performed to identify new set of antitubercular hits which can also be considered for chemical synthesis.

Further, molecular docking studies (structure-based drug design) will also offer comparatively enhanced solutions to the problem of identification and optimization of antitubercular leads. Additionally, in depth mechanistic studies would offer and reveal an understanding about the molecular mechanism of action of compounds into target proteins. With this data, suitable protein

target can be explored in protein data bank (PDB) for molecular docking studies and further lead identification followed by lead development.

Furthermore, many of the curcumin degradants (as discussed in chapter 2) are yet to be explored for their prospective biological potentials, which could certainly afford impending antimycobacterial leads. Thus, the presented work will contribute extensively to the advanced level of research in exploring and developing novel class of dehydrozingerone based antitubercular compounds as potential drug candidates.

APPENDIX - I

SUPPLEMENTARY INFORMATION

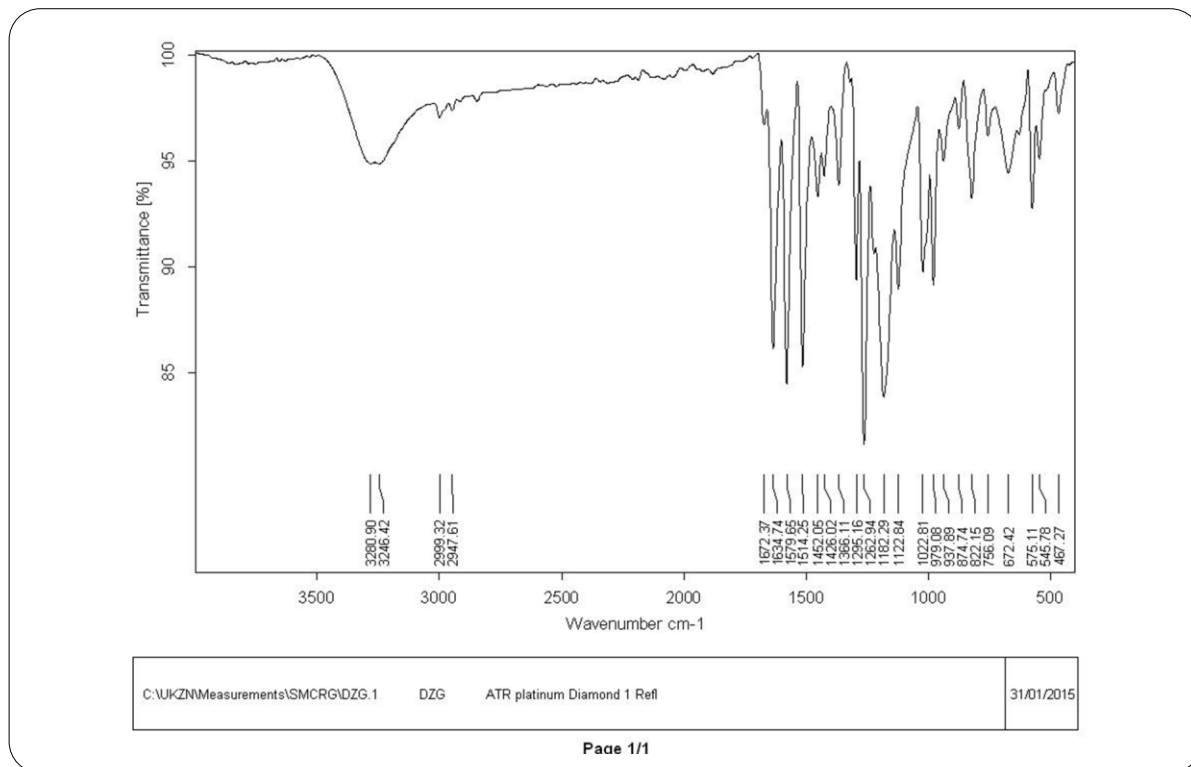
CHAPTER 3

Dehydrozingerone inspired styryl hydrazine thiazole hybrids as promising class of anti-mycobacterial agents.

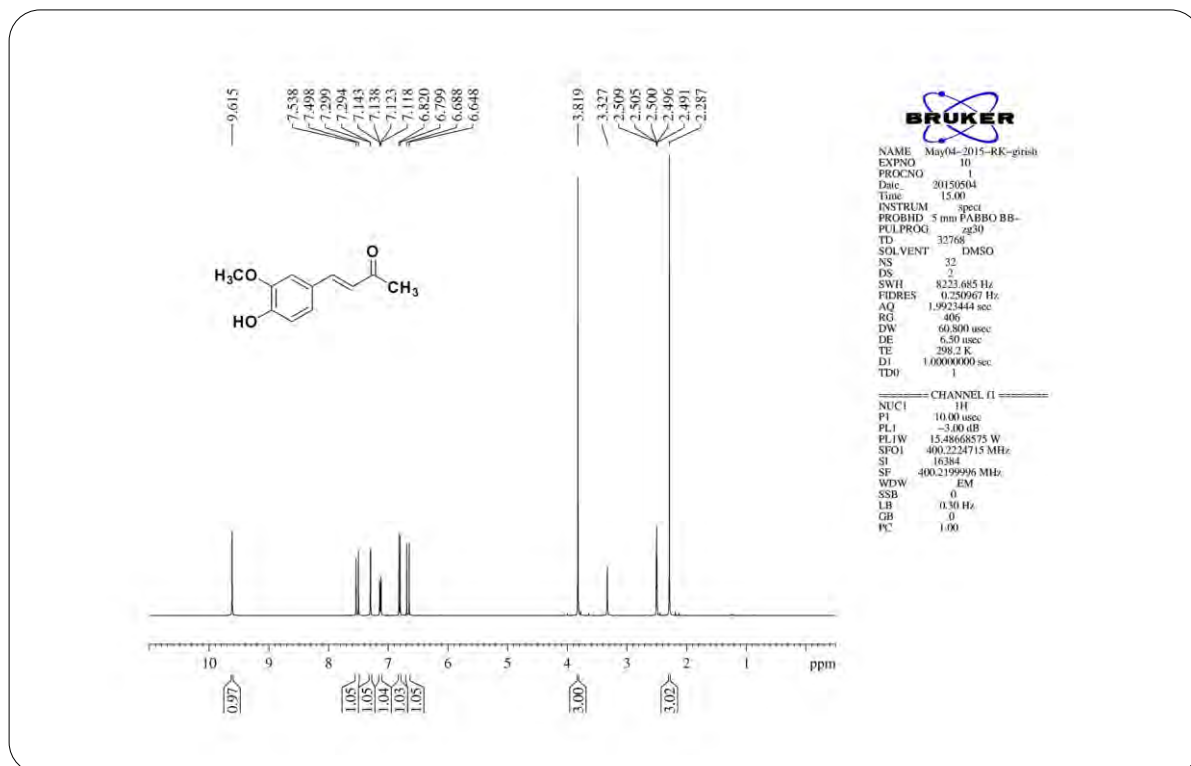
Girish A. Hampannavar,[†] Rajshekhar Karpoormath,^{*,†} Mahesh B. Palkar,^{§,†} Mahamadhanif S. Shaikh[†] and Balakumar Chandrasekaran[†]

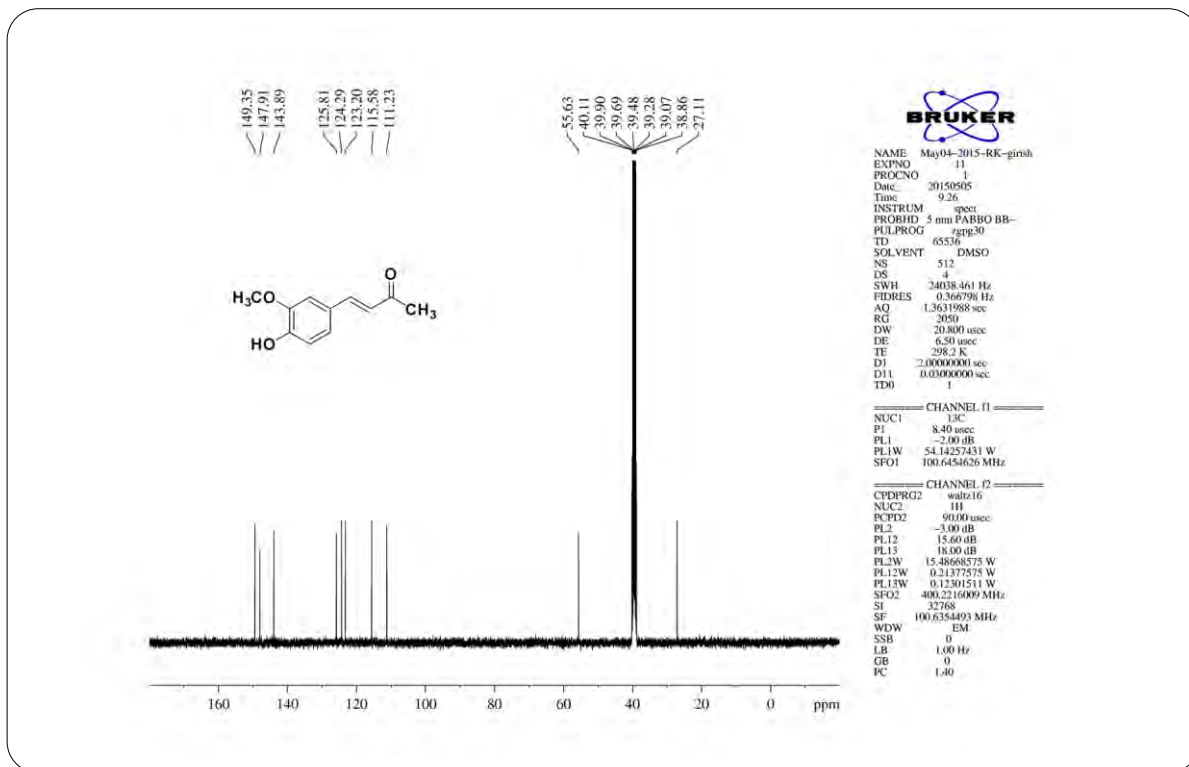
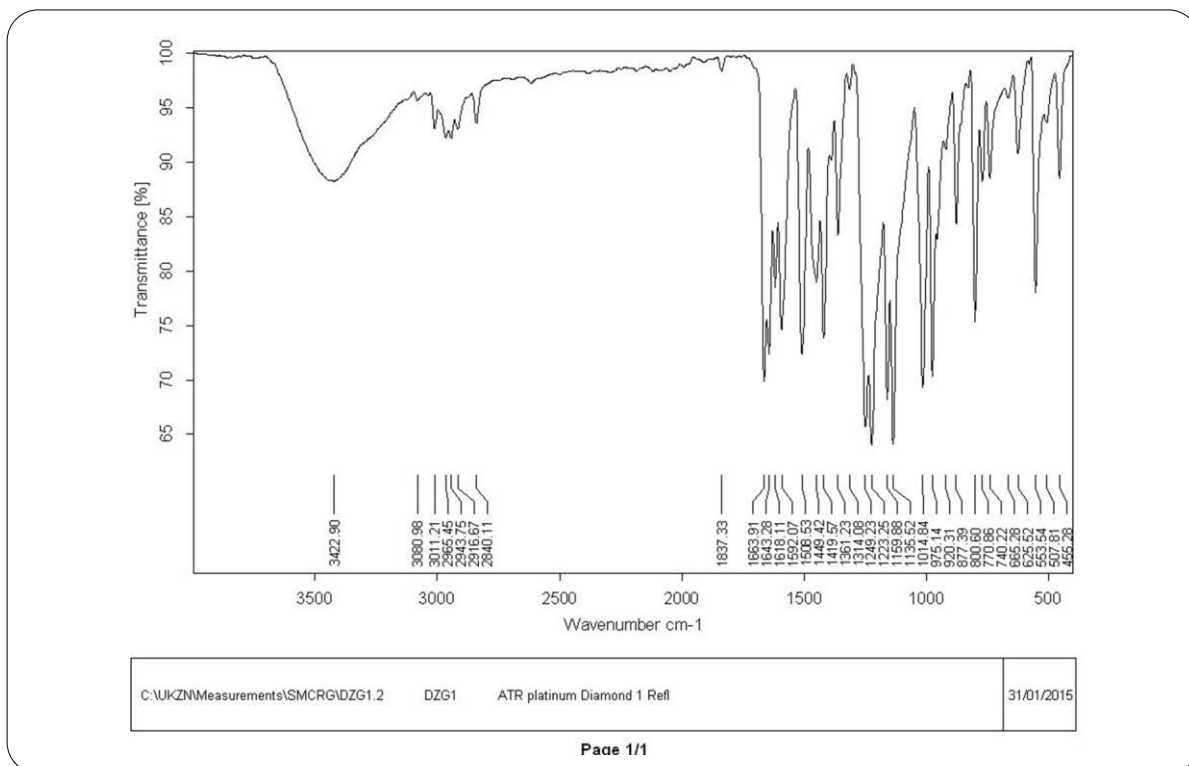
[†]Department of Pharmaceutical Chemistry, Discipline of Pharmaceutical Sciences, College of Health Sciences, University of KwaZulu-Natal, Westville Campus, Durban – 4000, South Africa

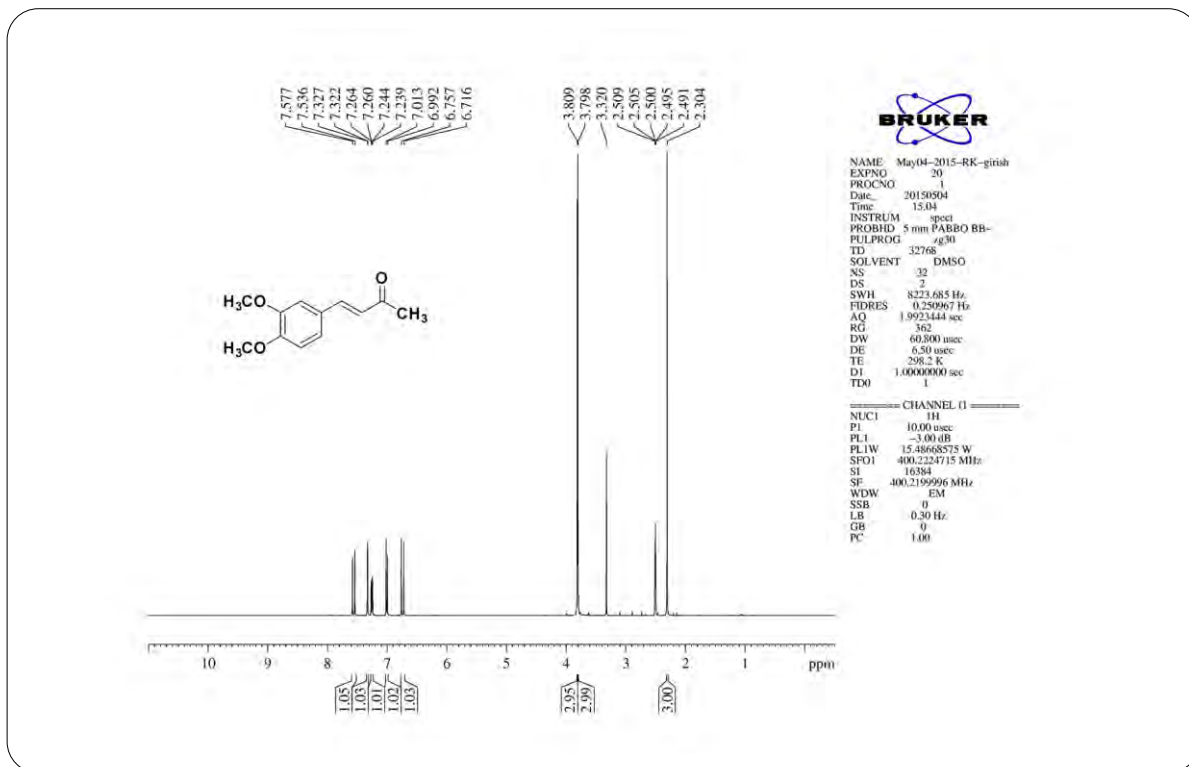
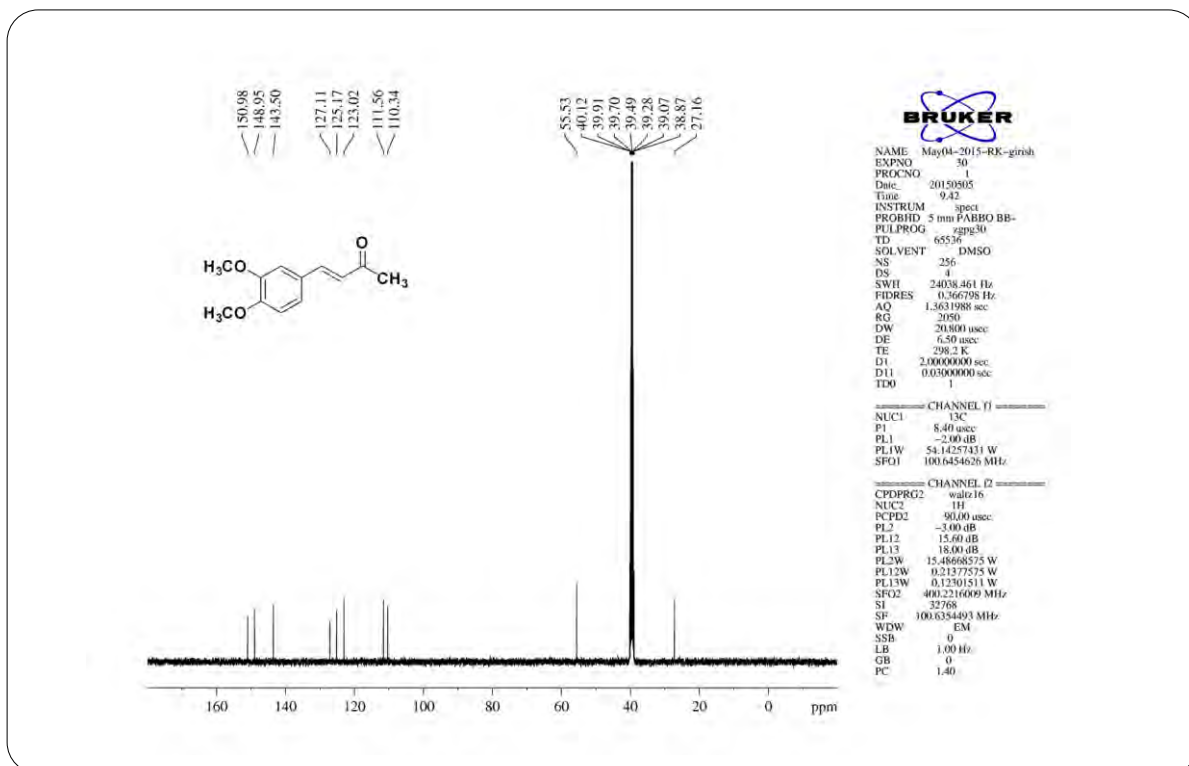
[§]Department of Pharmaceutical Chemistry, K.L.E. University College of Pharmacy, Vidyanagar, Hubballi – 580031, Karnataka, India

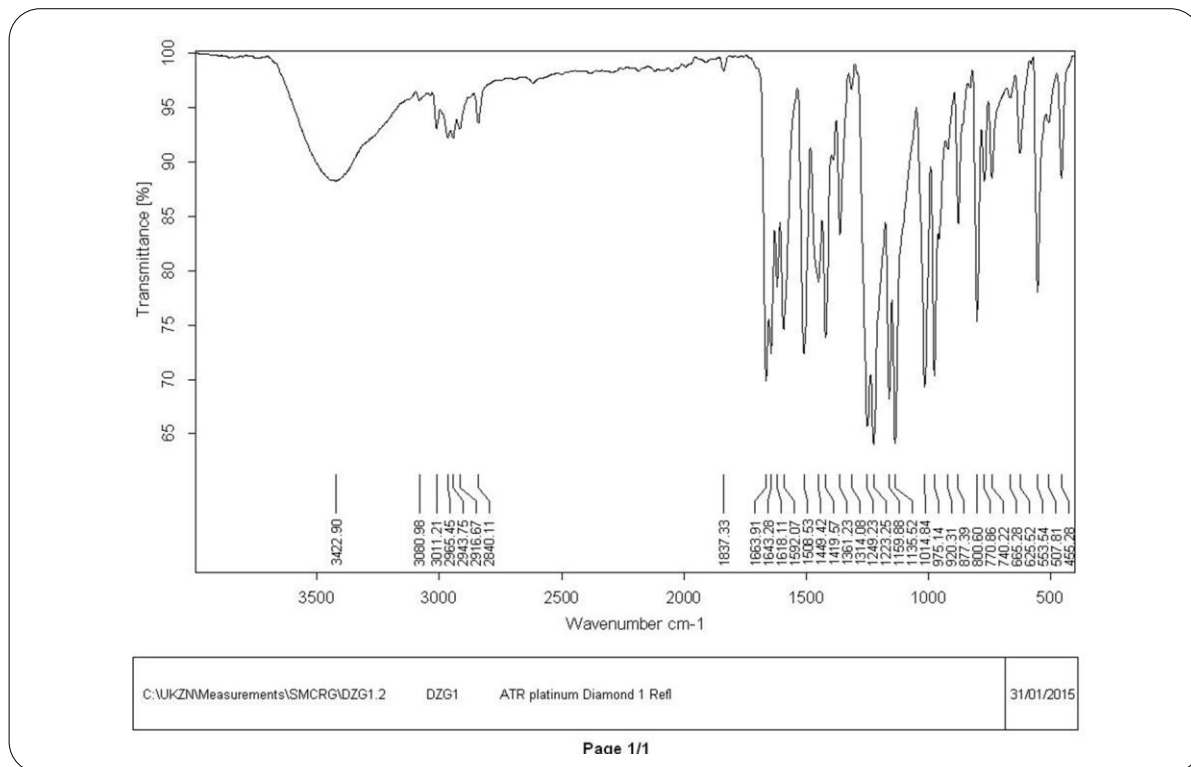


IR Spectrum of Compound 2 (chapter 3)

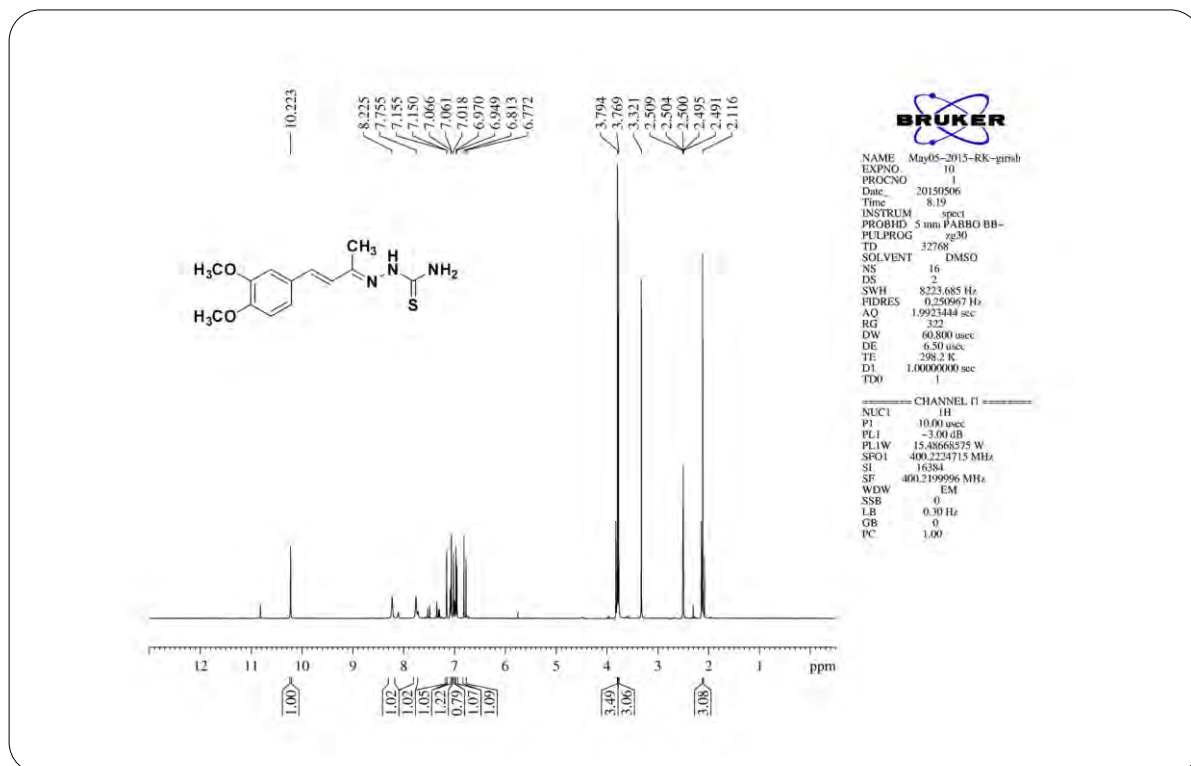
¹H NMR Spectrum of Compound 2 (chapter 3)

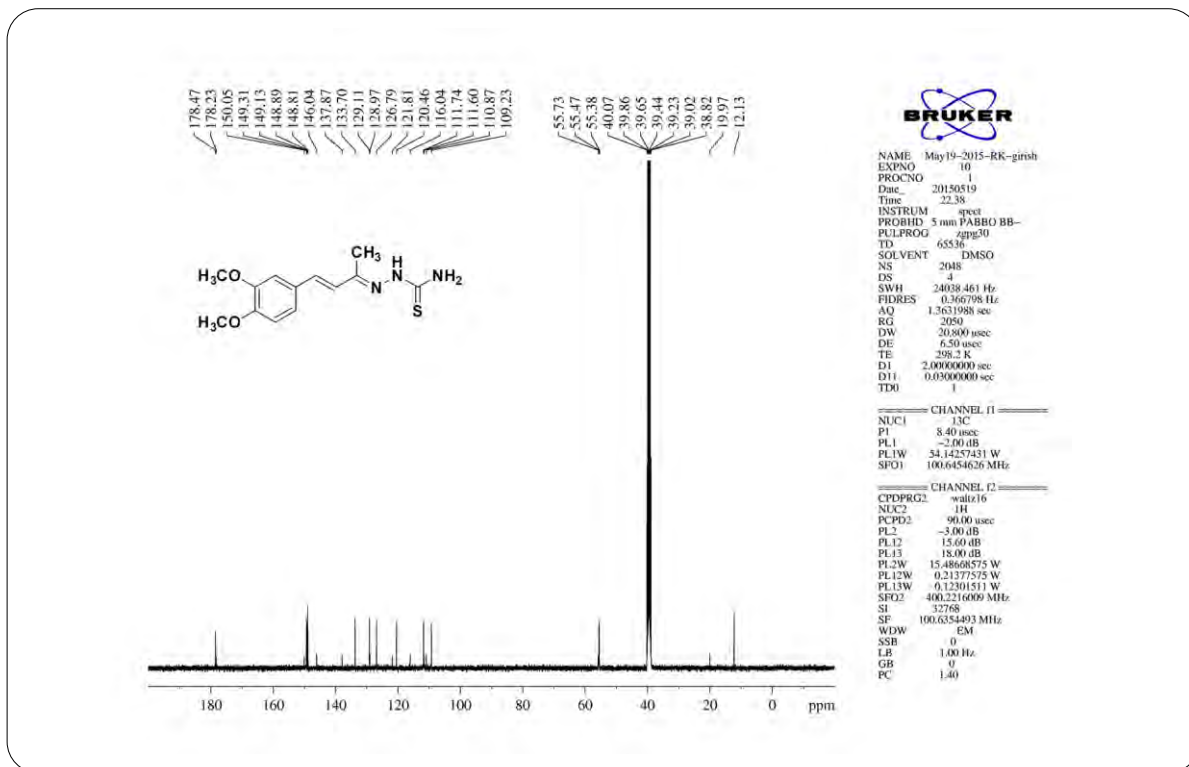
**¹³C NMR Spectrum of Compound 2 (chapter 3)****IR Spectrum of Compound 3 (chapter 3)**

**¹H NMR Spectrum of Compound 3 (chapter 3)****¹³C NMR Spectrum of Compound 3 (chapter 3)**



IR Spectrum of Compound 4 (chapter 3)

¹H NMR Spectrum of Compound 4 (chapter 3)

¹³C NMR Spectrum of Compound 4 (chapter 3)

Elemental Composition Report

Page 1

Single Mass Analysis

Tolerance = 5.0 PPM / DBE: min = -1.5, max = 100.0

Element prediction: Off

Number of isotope peaks used for i-FIT = 3

Monoisotopic Mass, Even Electron Ions

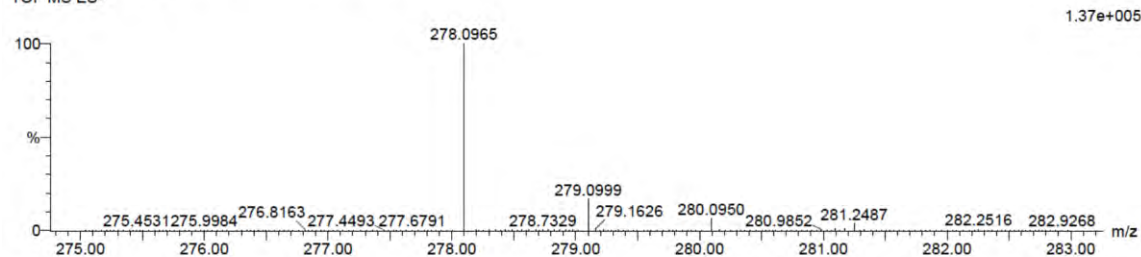
33 formula(e) evaluated with 1 results within limits (up to 20 closest results for each mass)

Elements Used:

C: 10-15 H: 15-20 N: 0-5 O: 0-5 S: 0-1

4 9 (0.270) Cm (1:61)

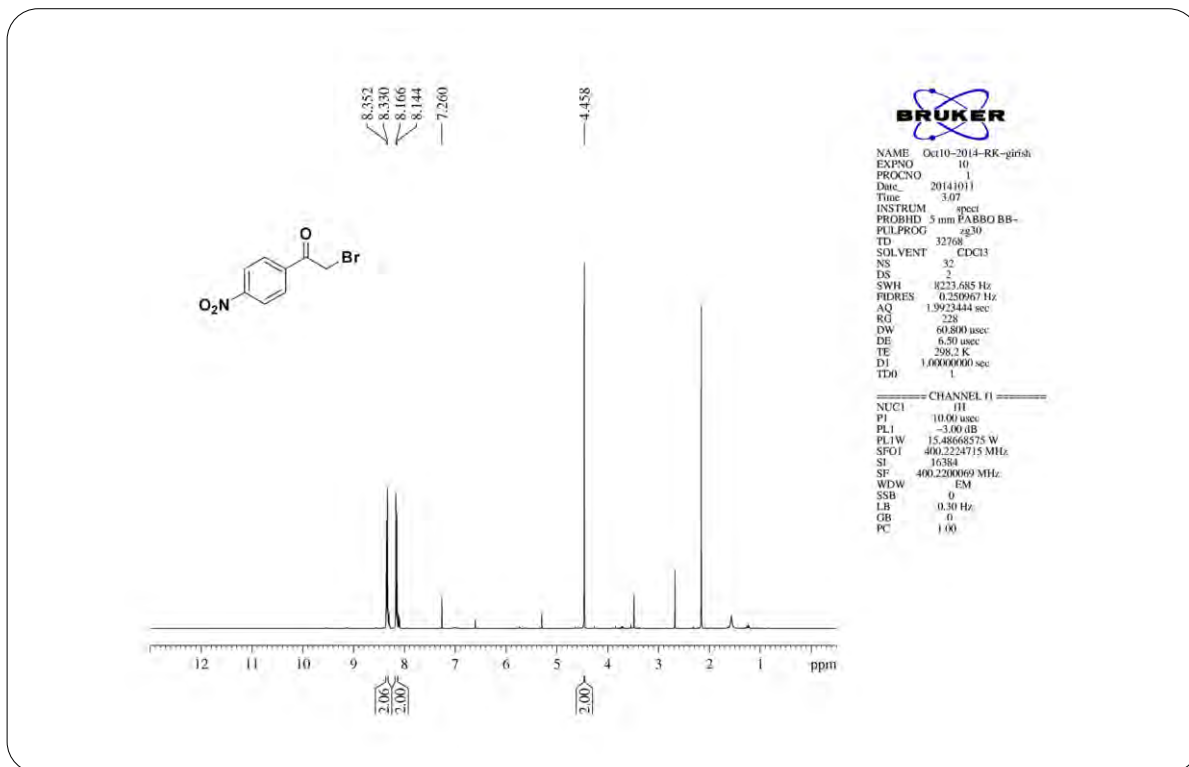
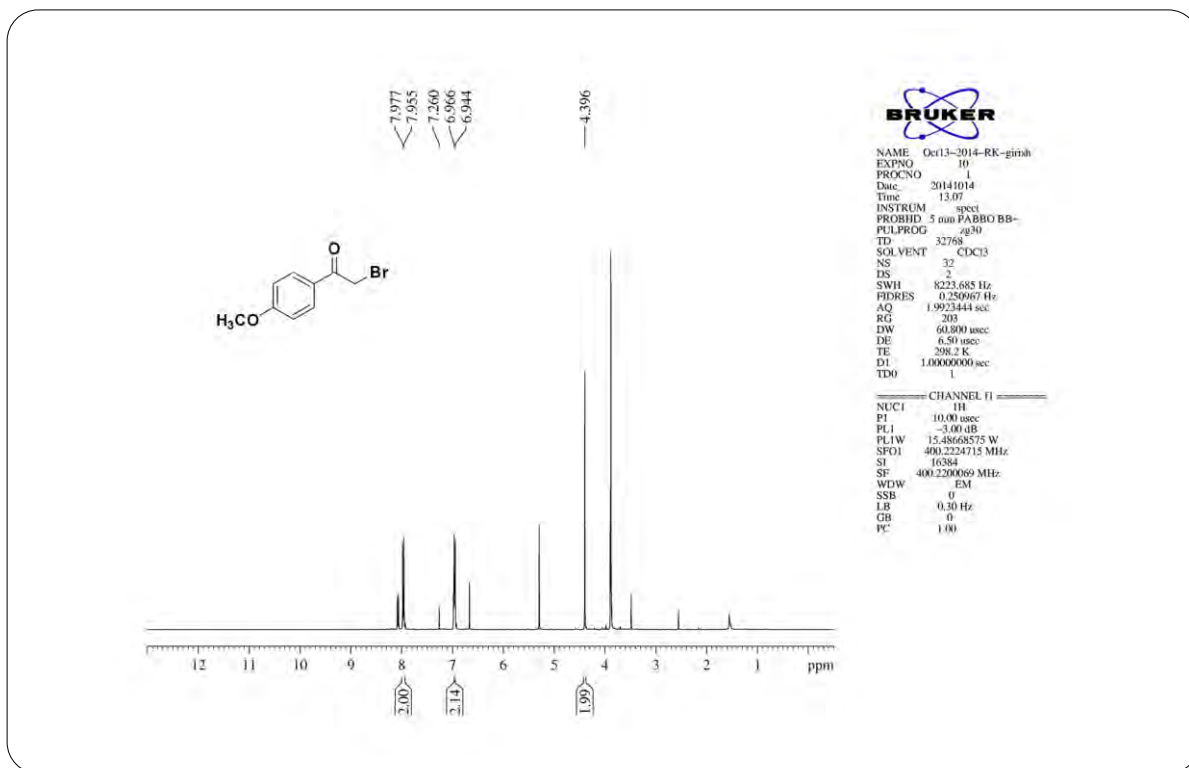
TOF MS ES-

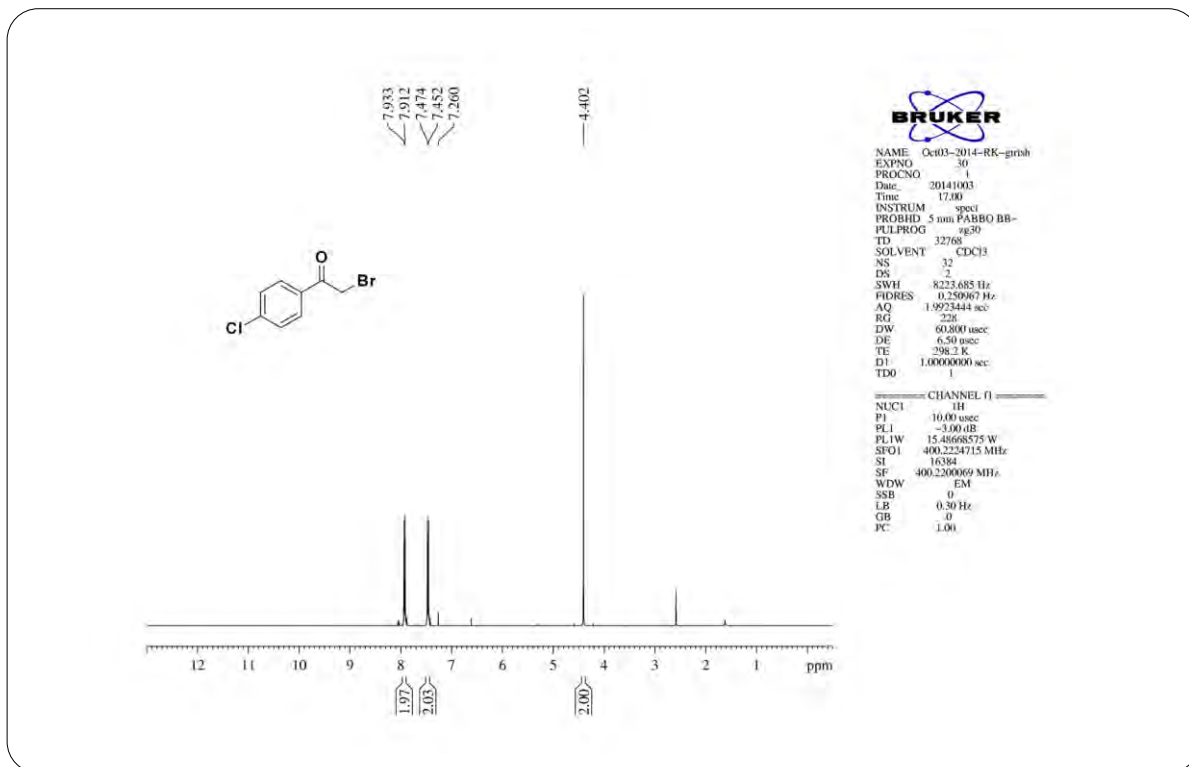
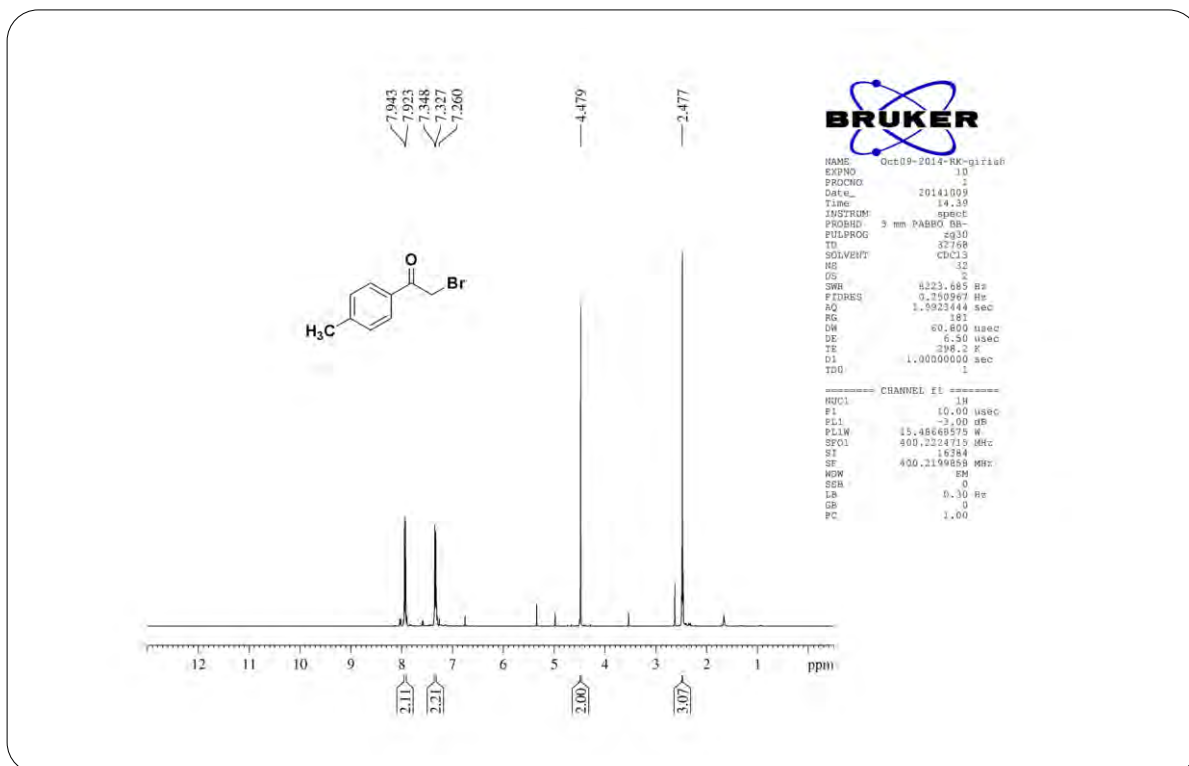


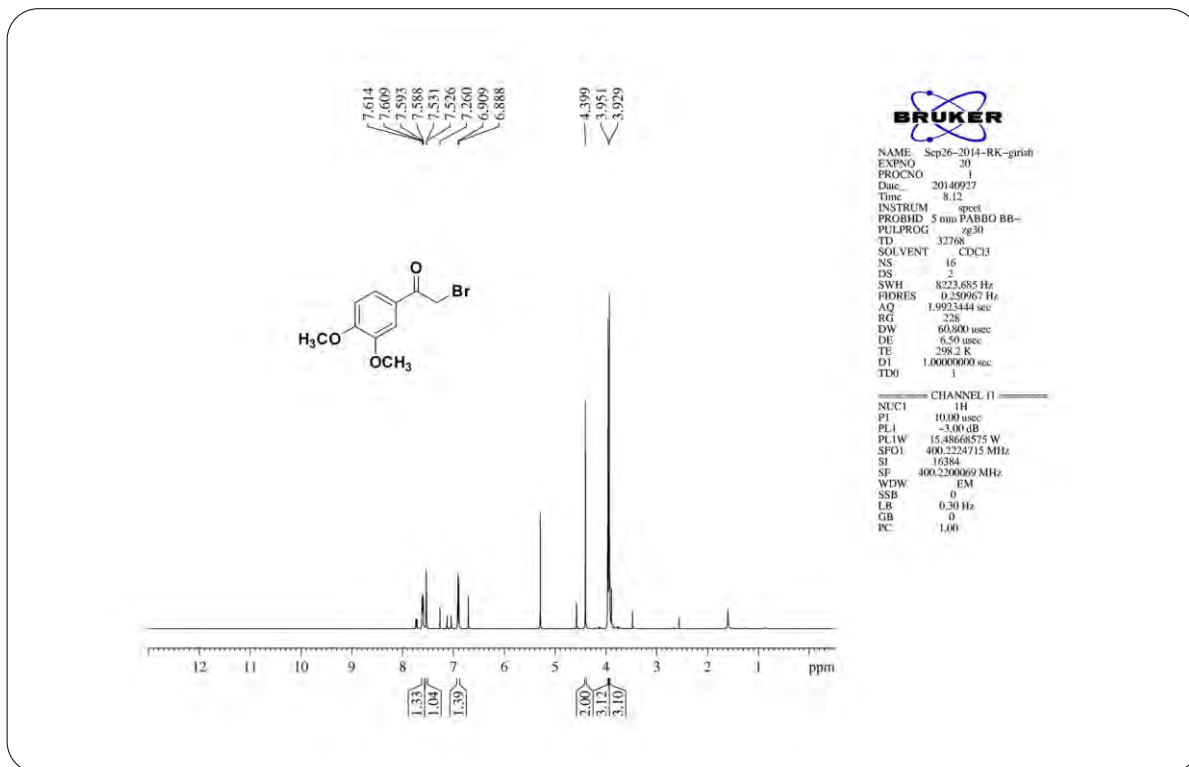
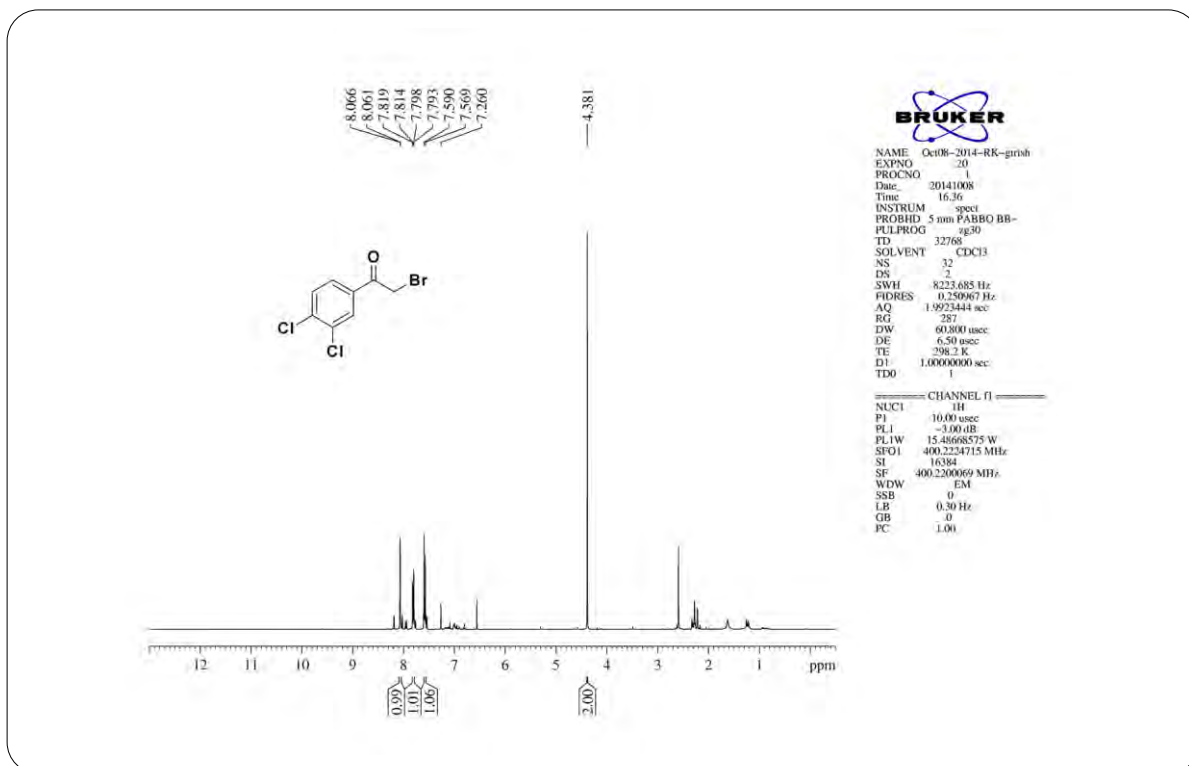
Minimum: -1.5
 Maximum: 5.0 5.0 100.0

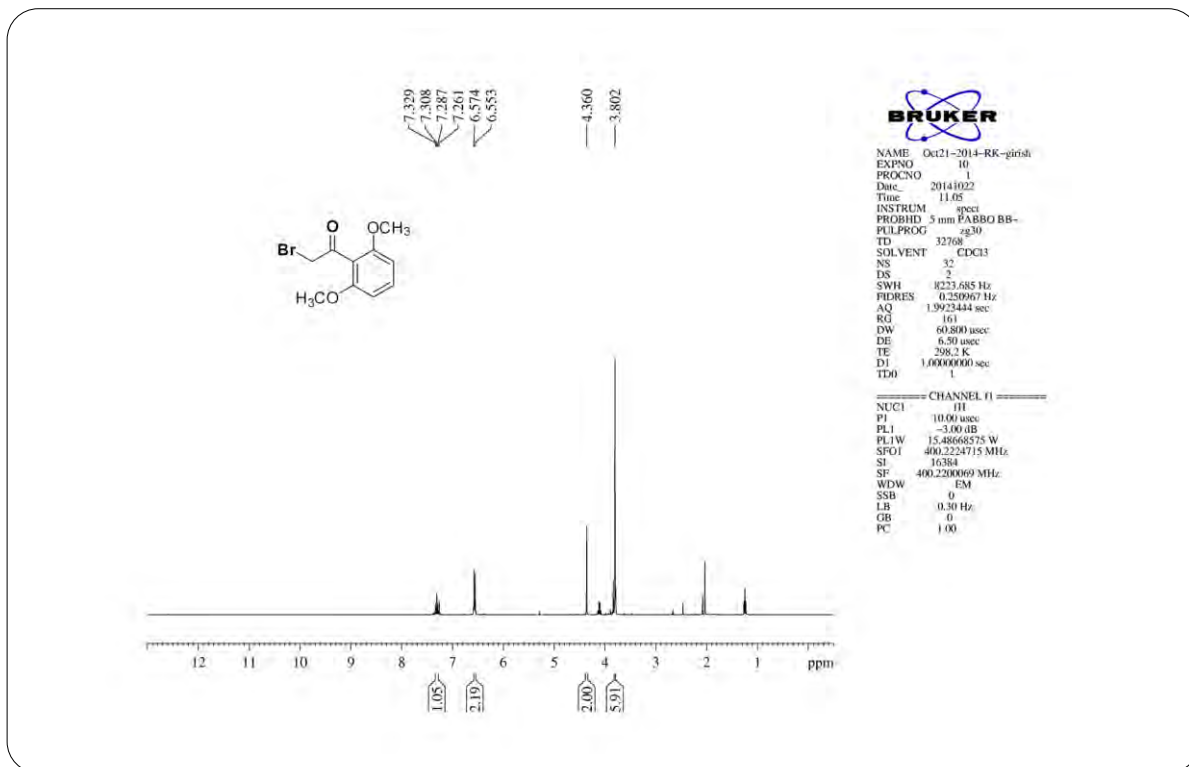
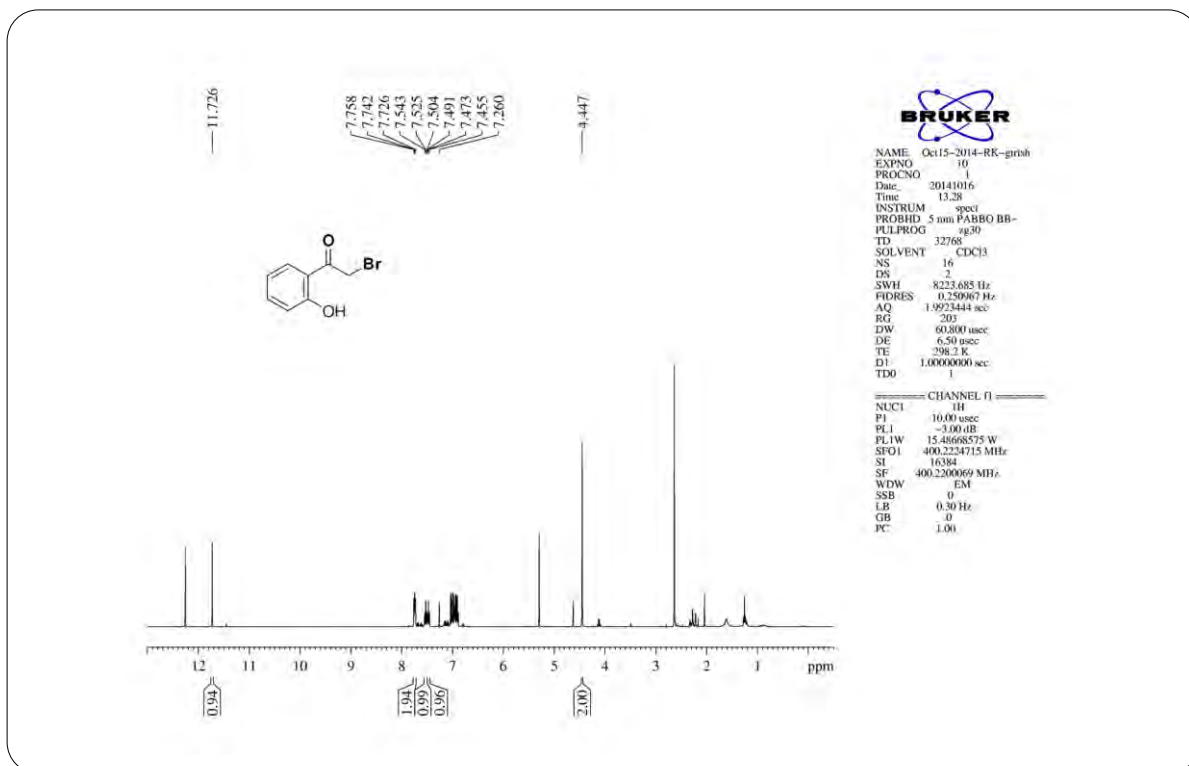
Mass	Calc. Mass	mDa	PPM	DBE	i-FIT	i-FIT (Norm)	Formula
278.0965	278.0963	0.2	0.7	7.5	593.8	0.0	C13 H16 N3 O2 S

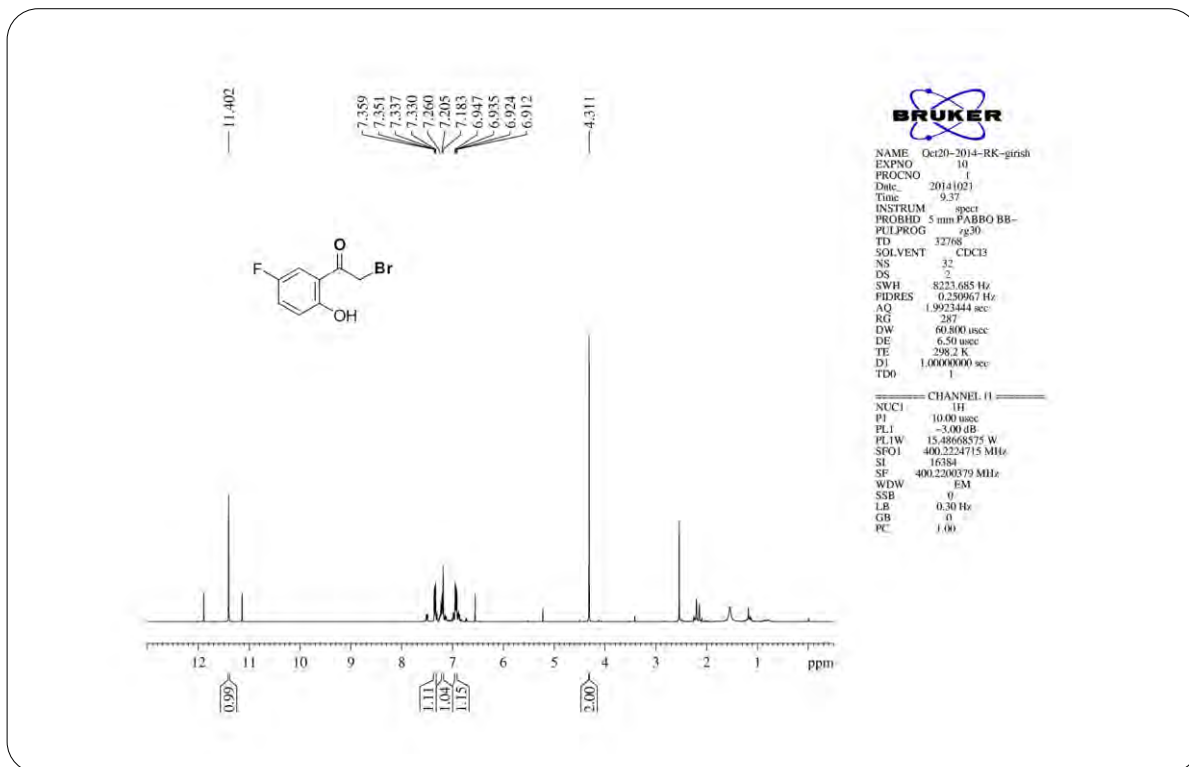
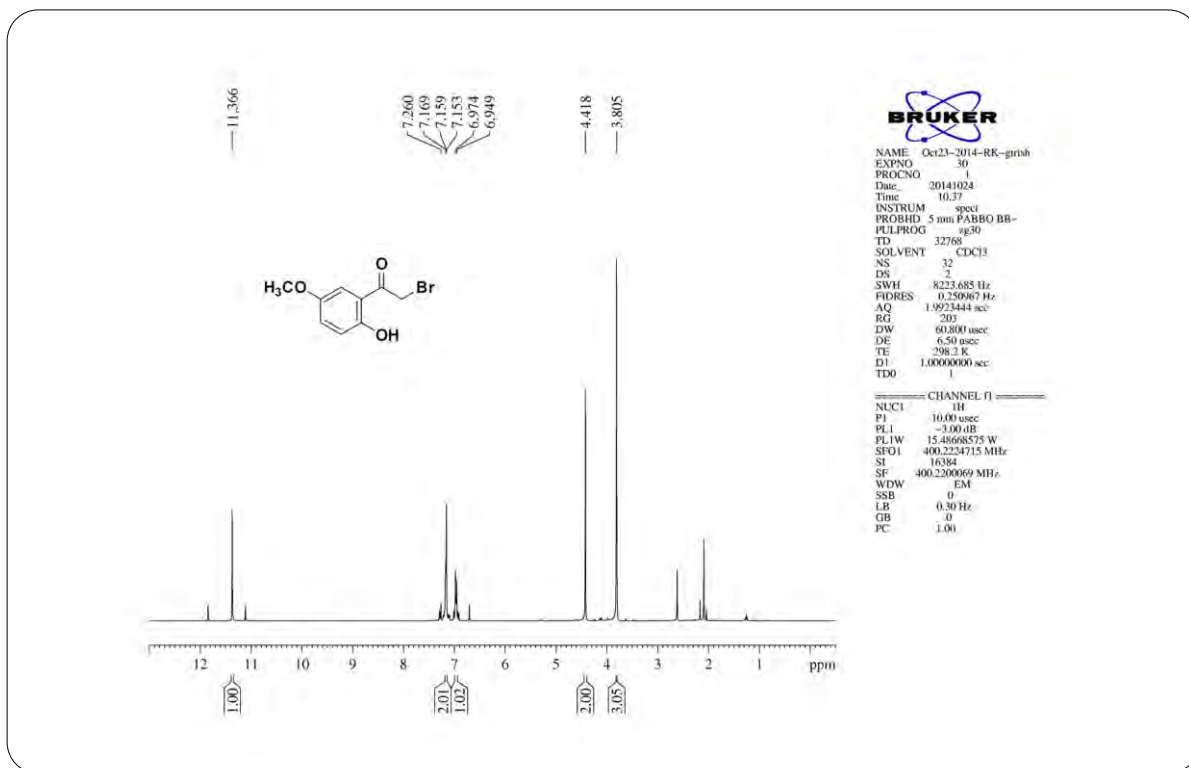
HRMS Spectrum of Compound 4 (chapter 3)

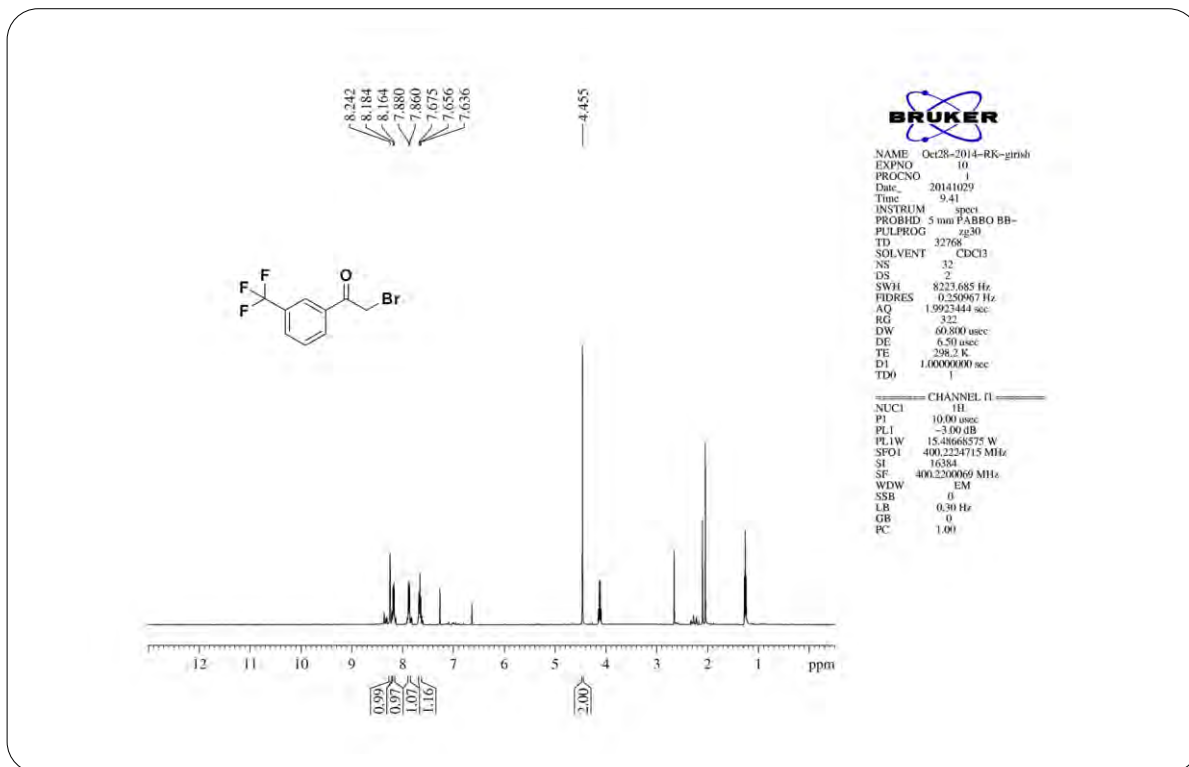
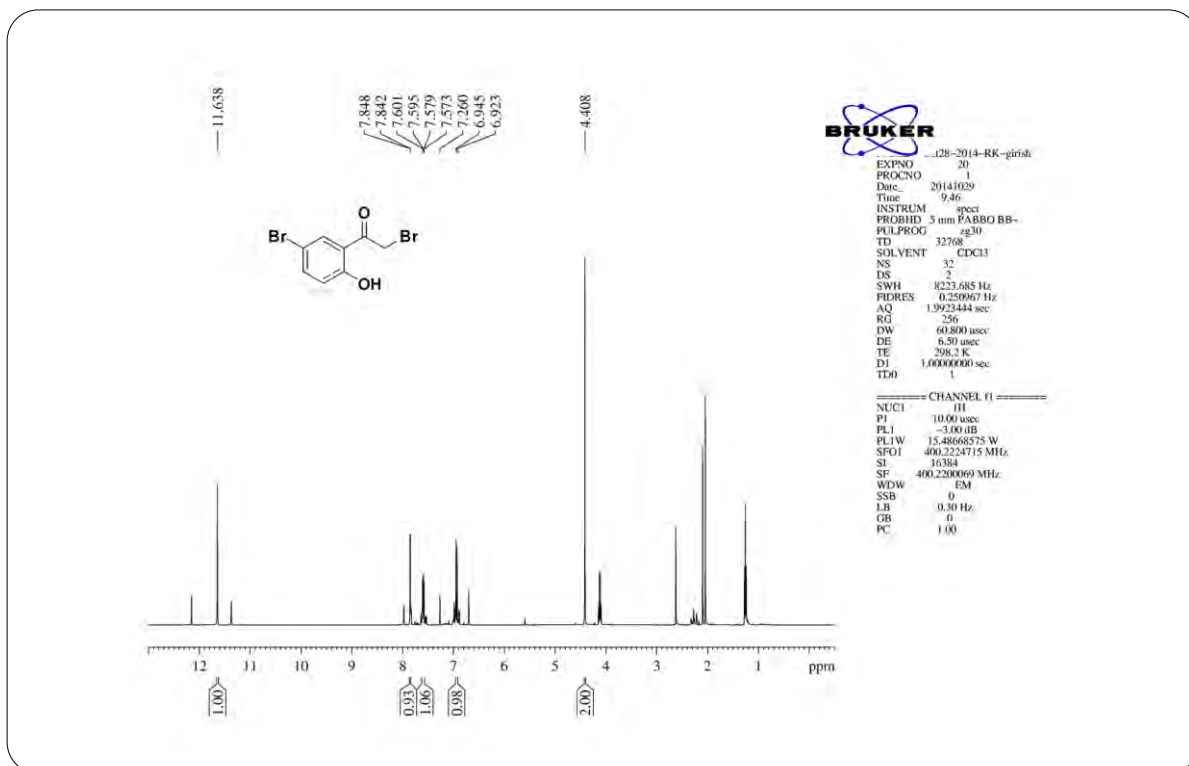
**¹H NMR Spectrum of Compound 5c (chapter 3)****¹H NMR Spectrum of Compound 5d (chapter 3)**

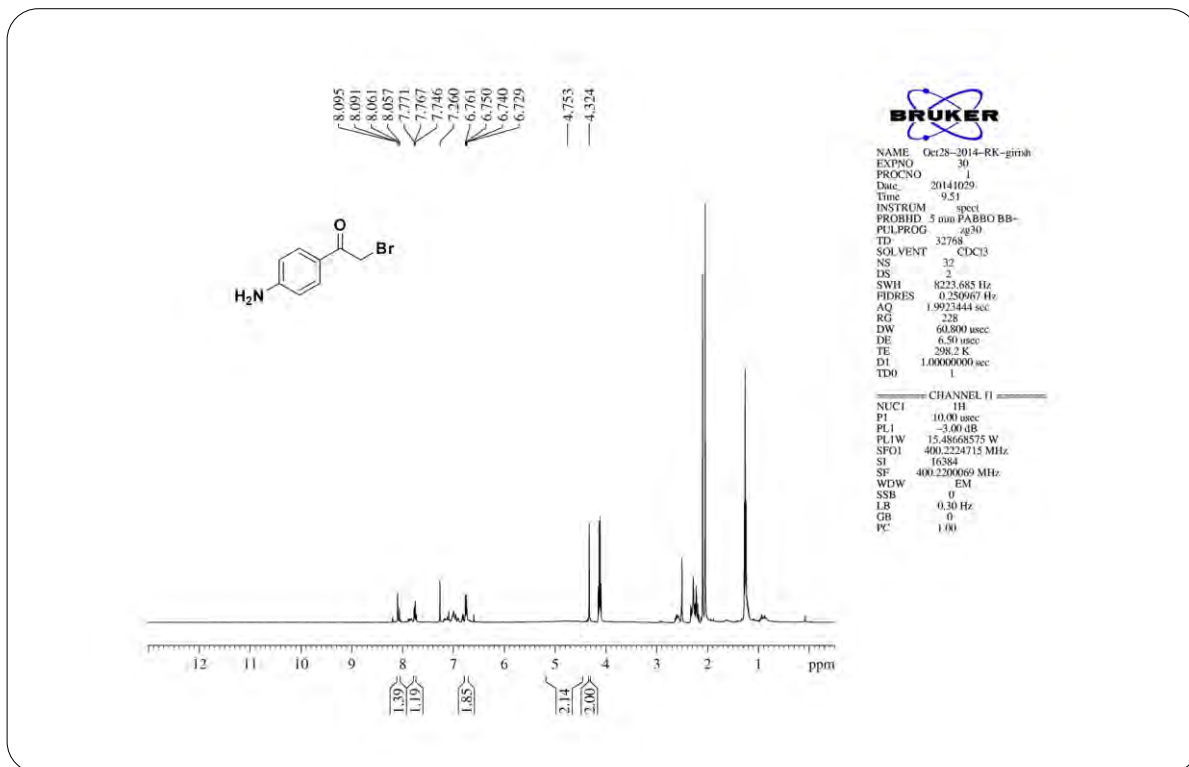
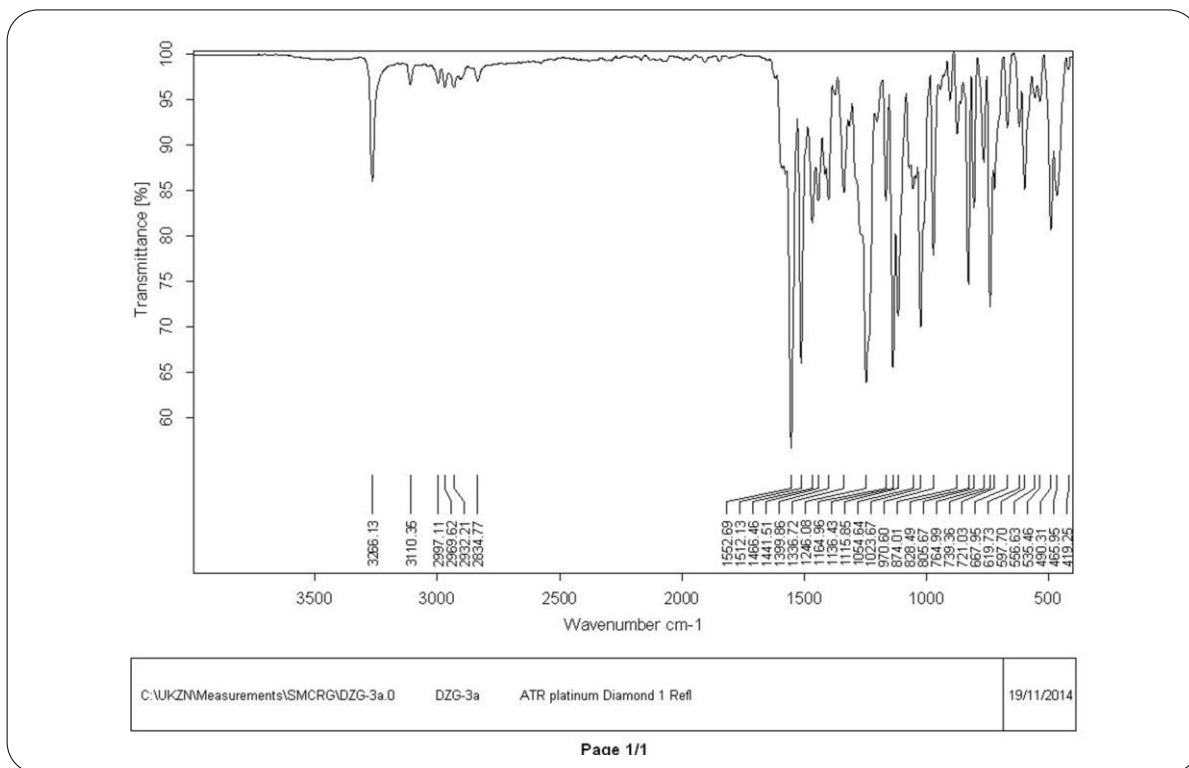
¹H NMR Spectrum of Compound 5e (chapter 3)¹H NMR Spectrum of Compound 5f (chapter 3)

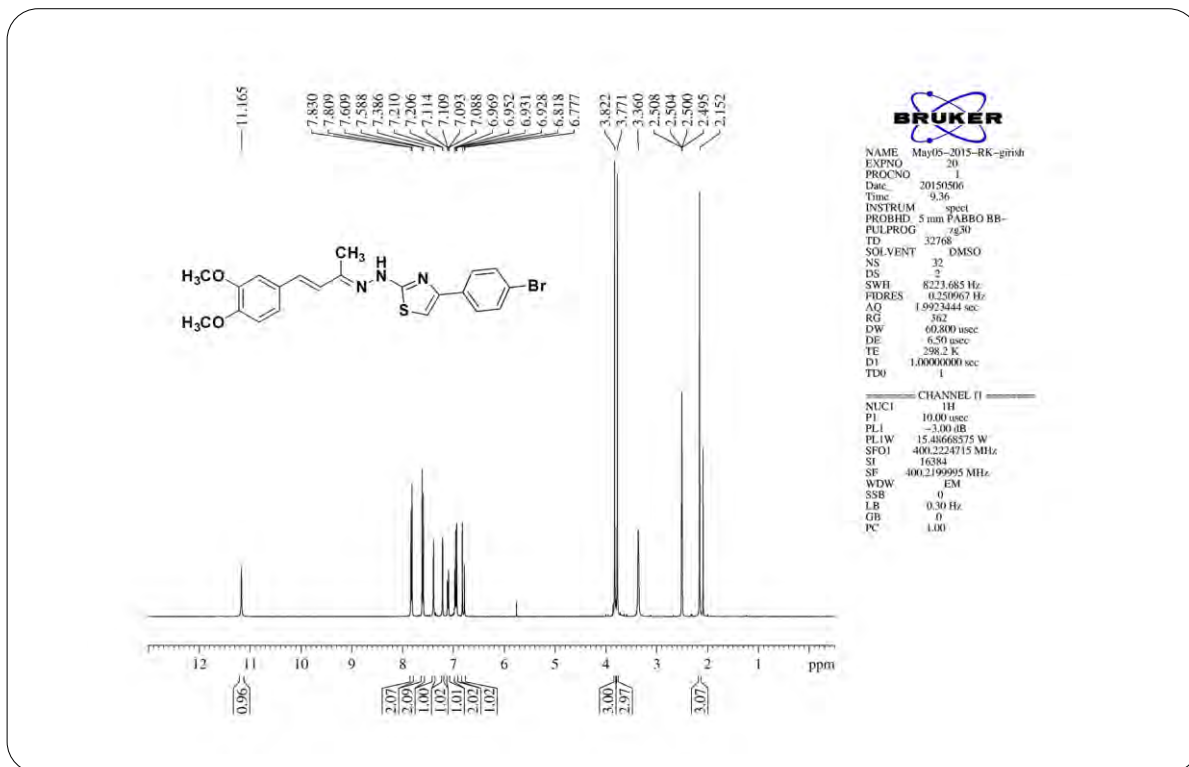
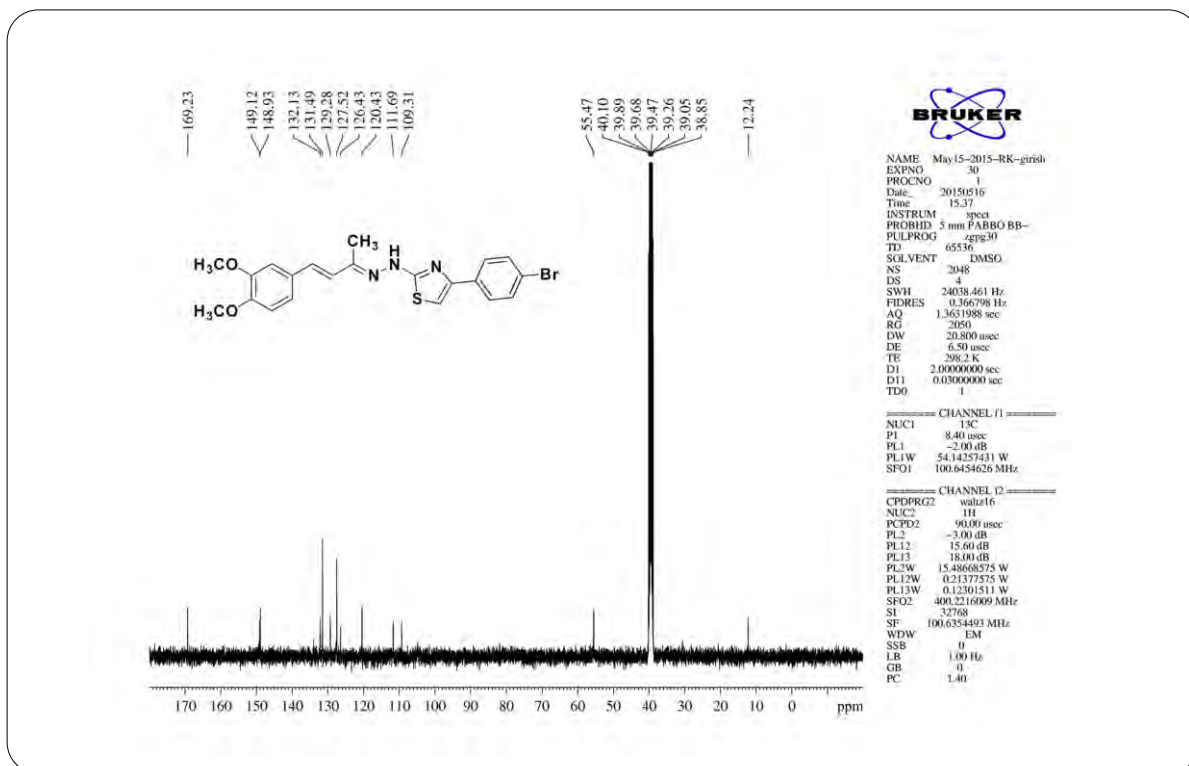
**¹H NMR Spectrum of Compound 5g (chapter 3)****¹H NMR Spectrum of Compound 5h (chapter 3)**

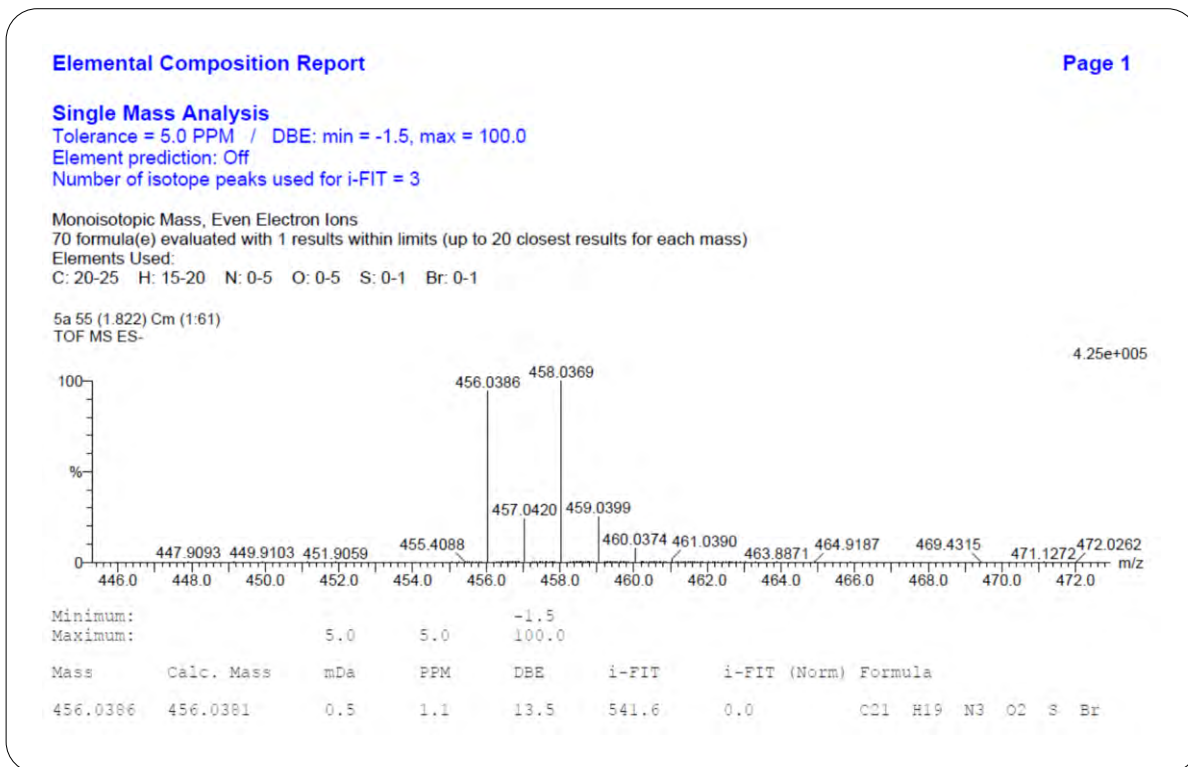
**¹H NMR Spectrum of Compound 5i (chapter 3)****¹H NMR Spectrum of Compound 5j (chapter 3)**

**¹H NMR Spectrum of Compound 5k (chapter 3)****¹H NMR Spectrum of Compound 5l (chapter 3)**

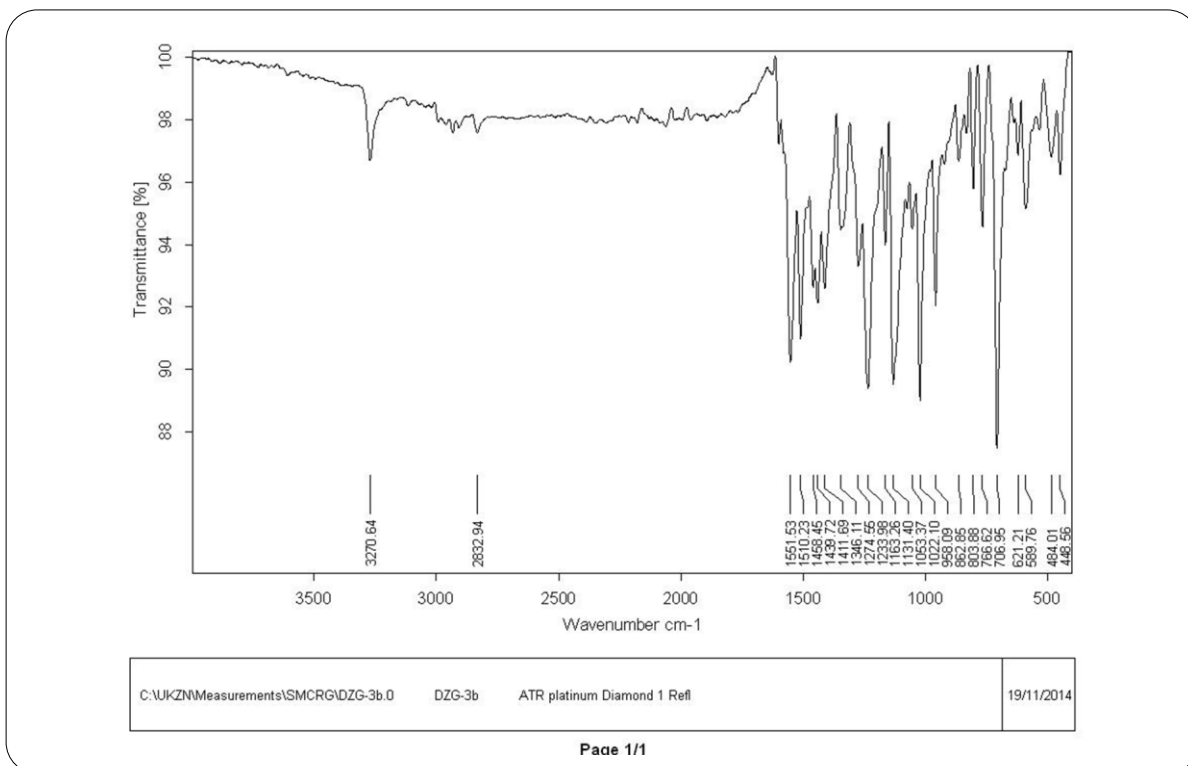
**¹H NMR Spectrum of Compound 5m (chapter 3)****¹H NMR Spectrum of Compound 5n (chapter 3)**

**¹H NMR Spectrum of Compound 5o (chapter 3)****IR Spectrum of Compound 6a (chapter 3)**

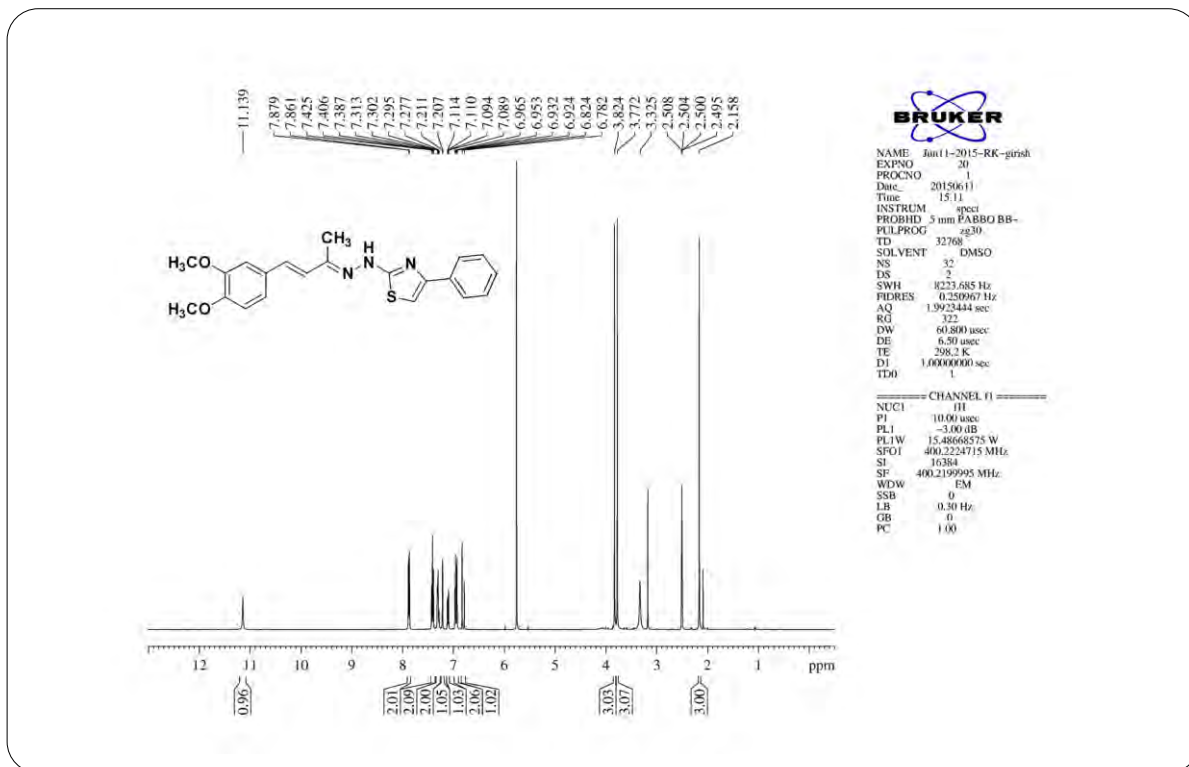
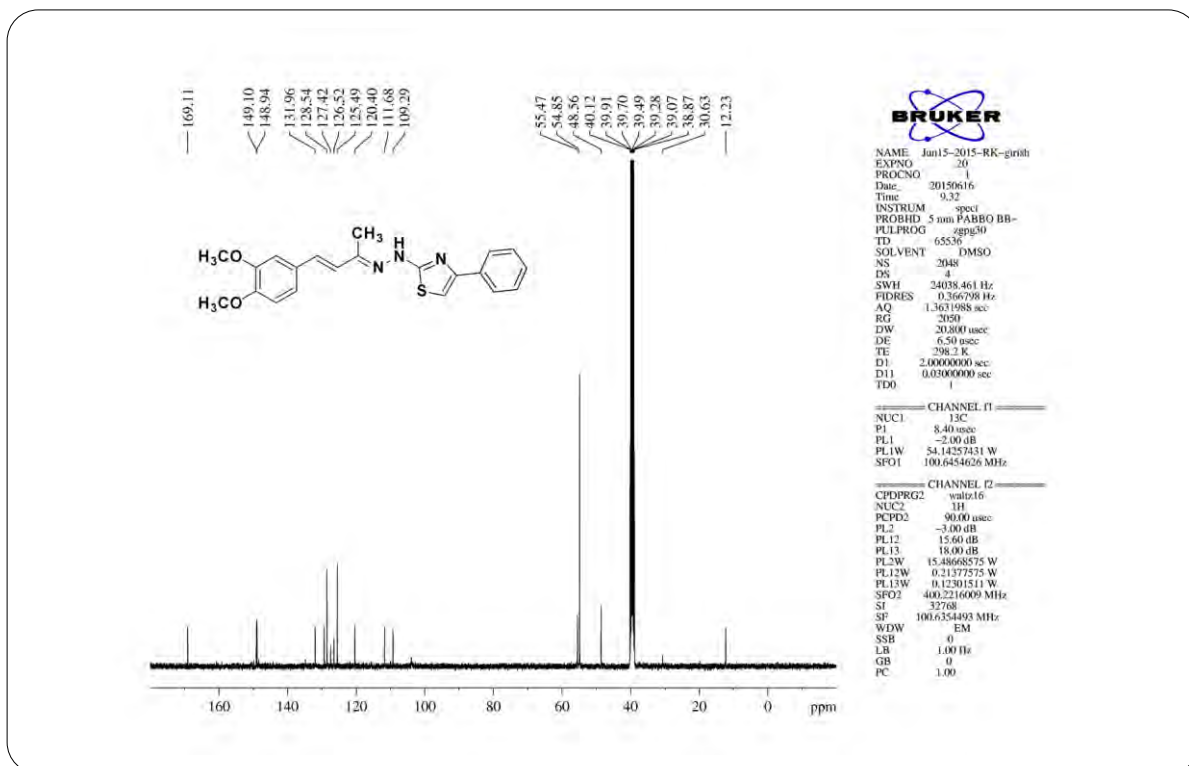
**¹H NMR Spectrum of Compound 6a (chapter 3)****¹³C NMR Spectrum of Compound 6a (chapter 3)**

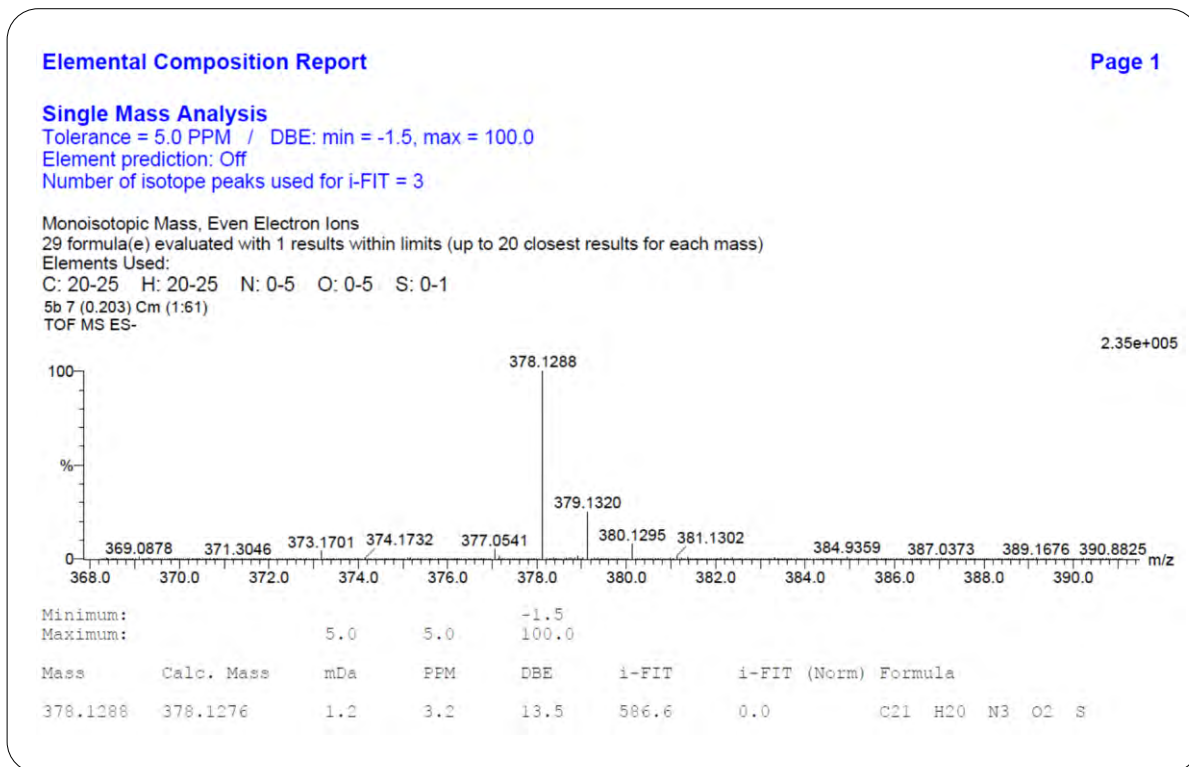


HRMS Spectrum of Compound 6a (chapter 3)

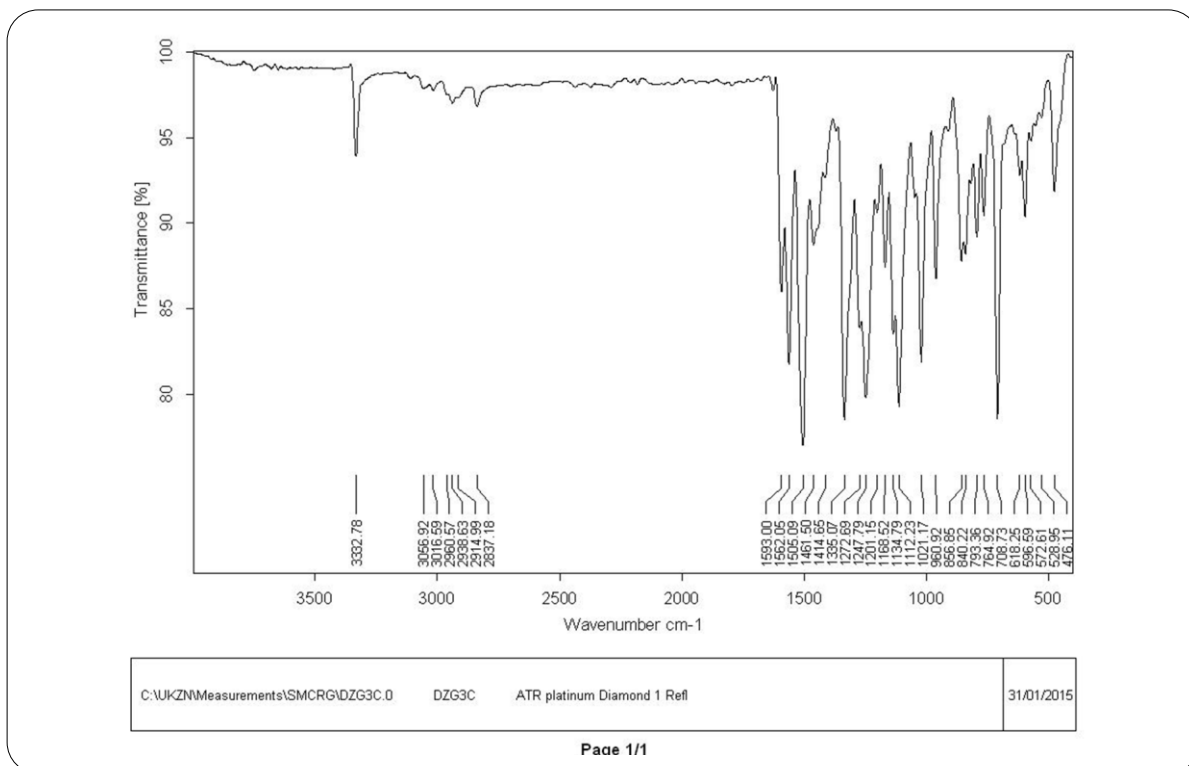


IR Spectrum of Compound 6b (chapter 3)

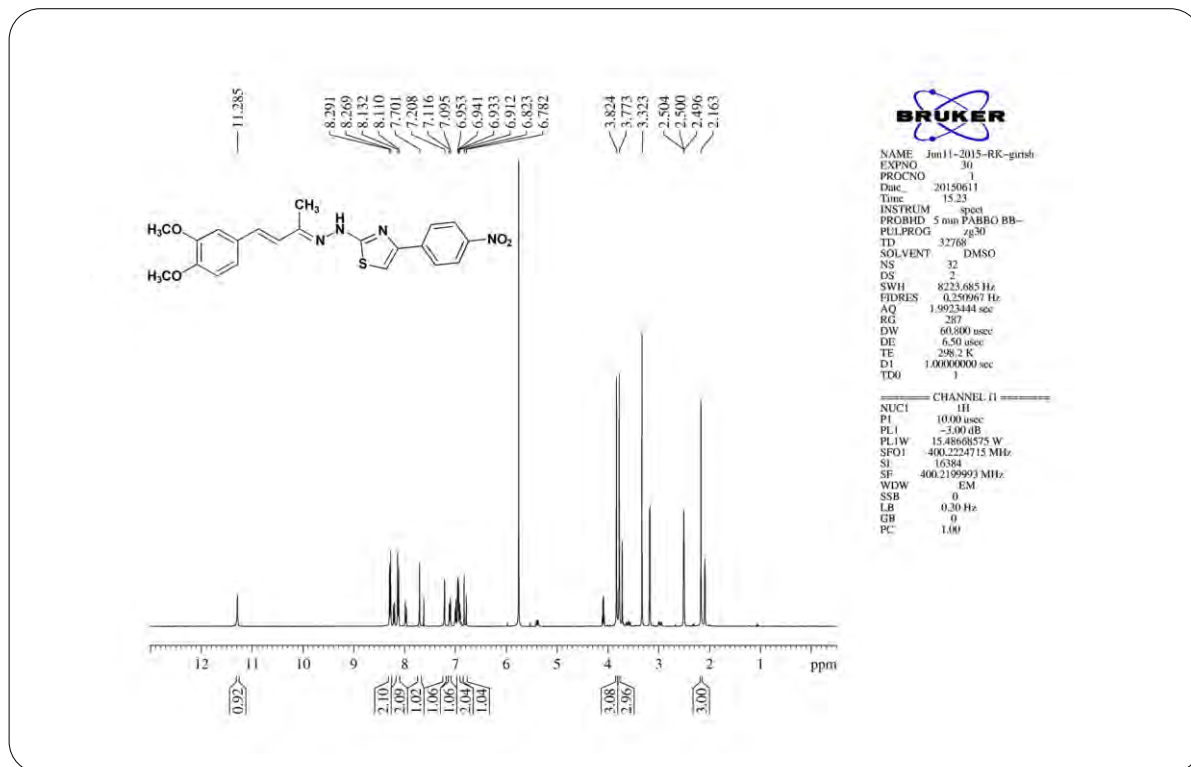
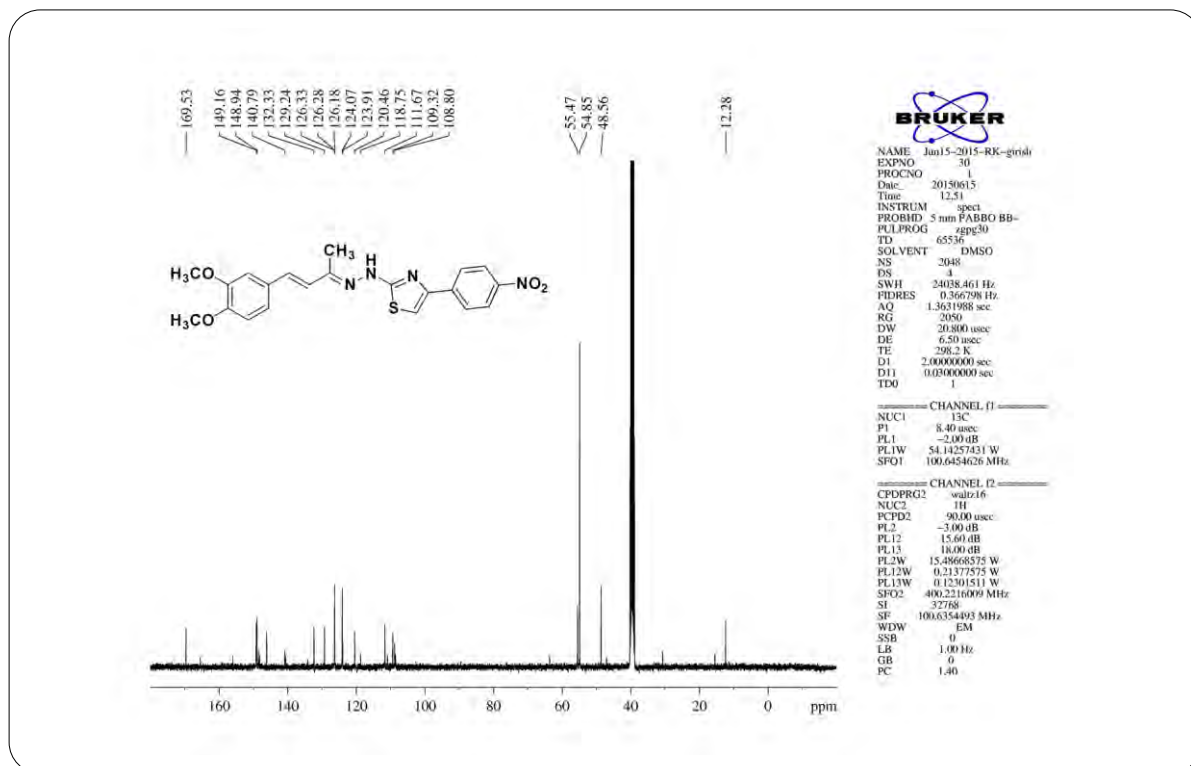
**¹H NMR Spectrum of Compound 6b (chapter 3)****¹³C NMR Spectrum of Compound 6b (chapter 3)**

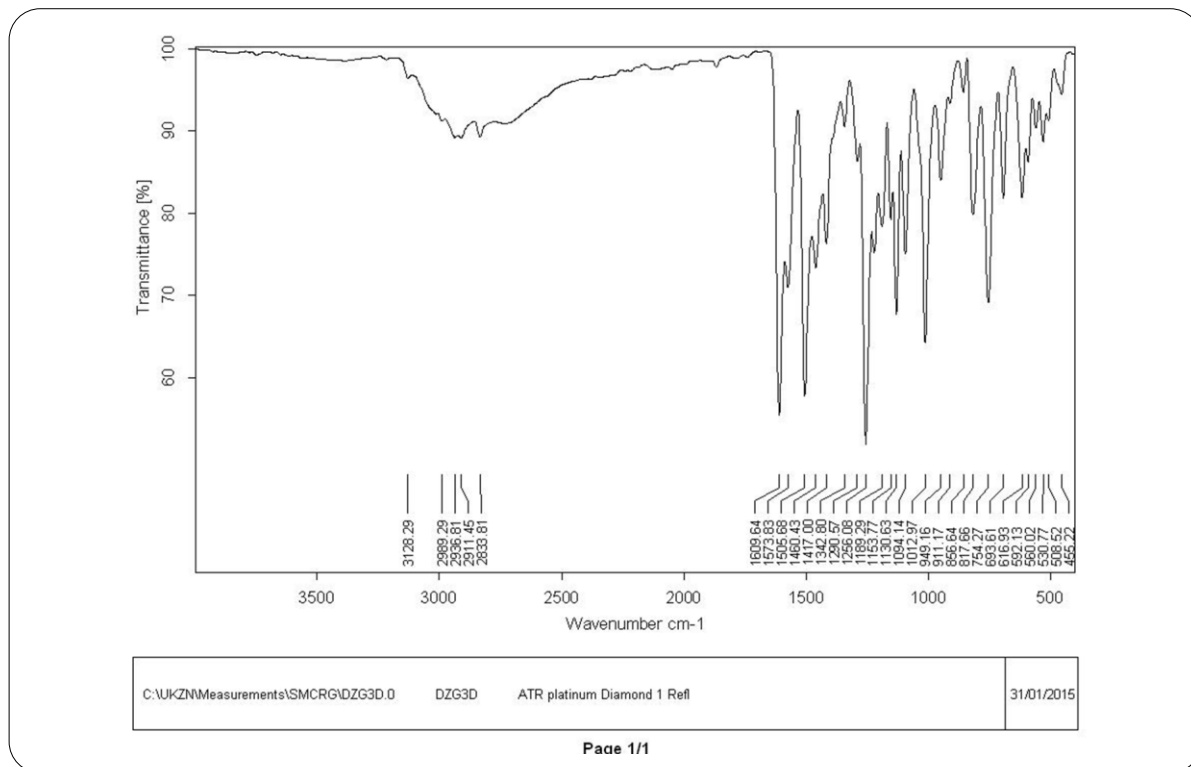


HRMS Spectrum of Compound 6b (chapter 3)

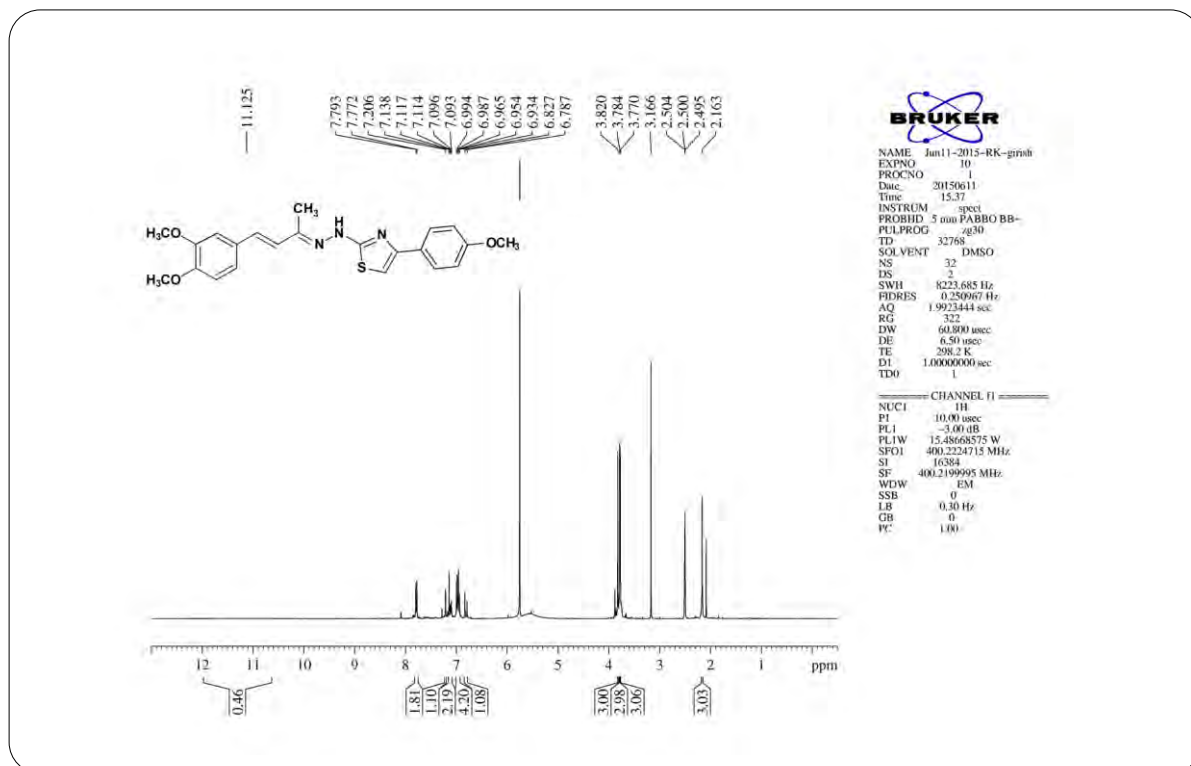


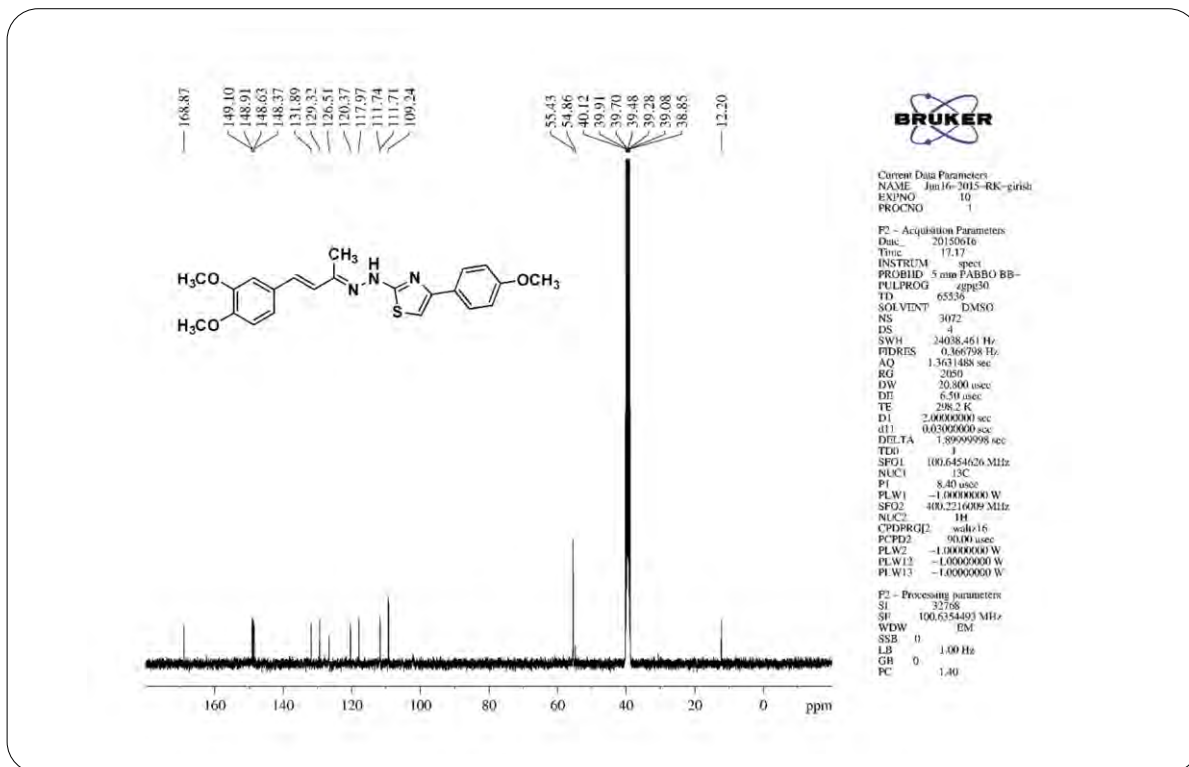
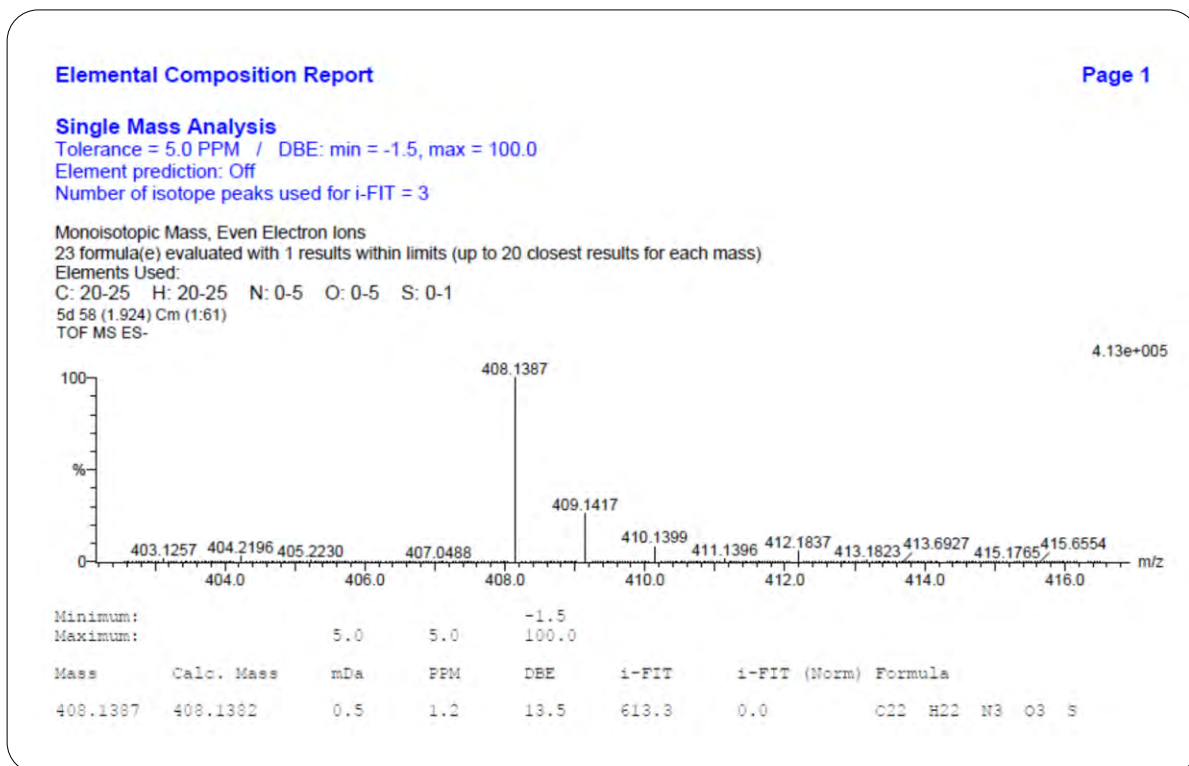
IR Spectrum of Compound 6c (chapter 3)

**¹H NMR Spectrum of Compound 6c (chapter 3)****¹³C NMR Spectrum of Compound 6c (chapter 3)**

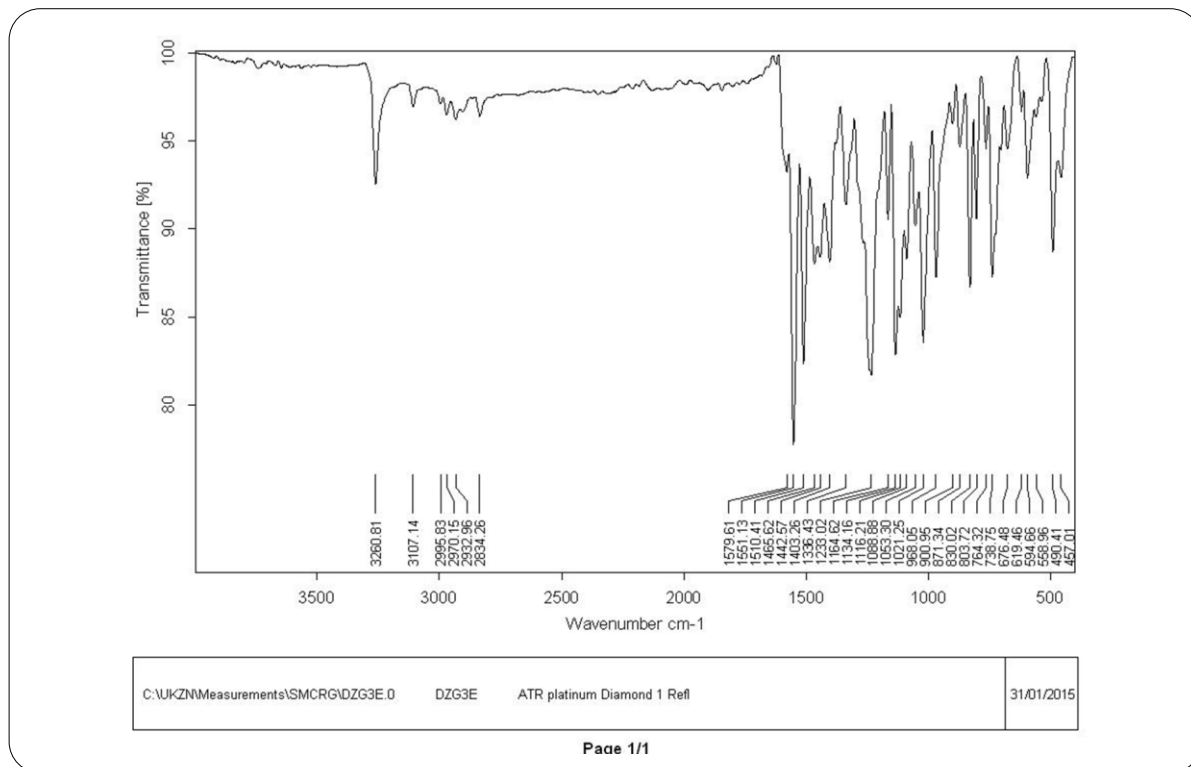


IR Spectrum of Compound 6d (chapter 3)

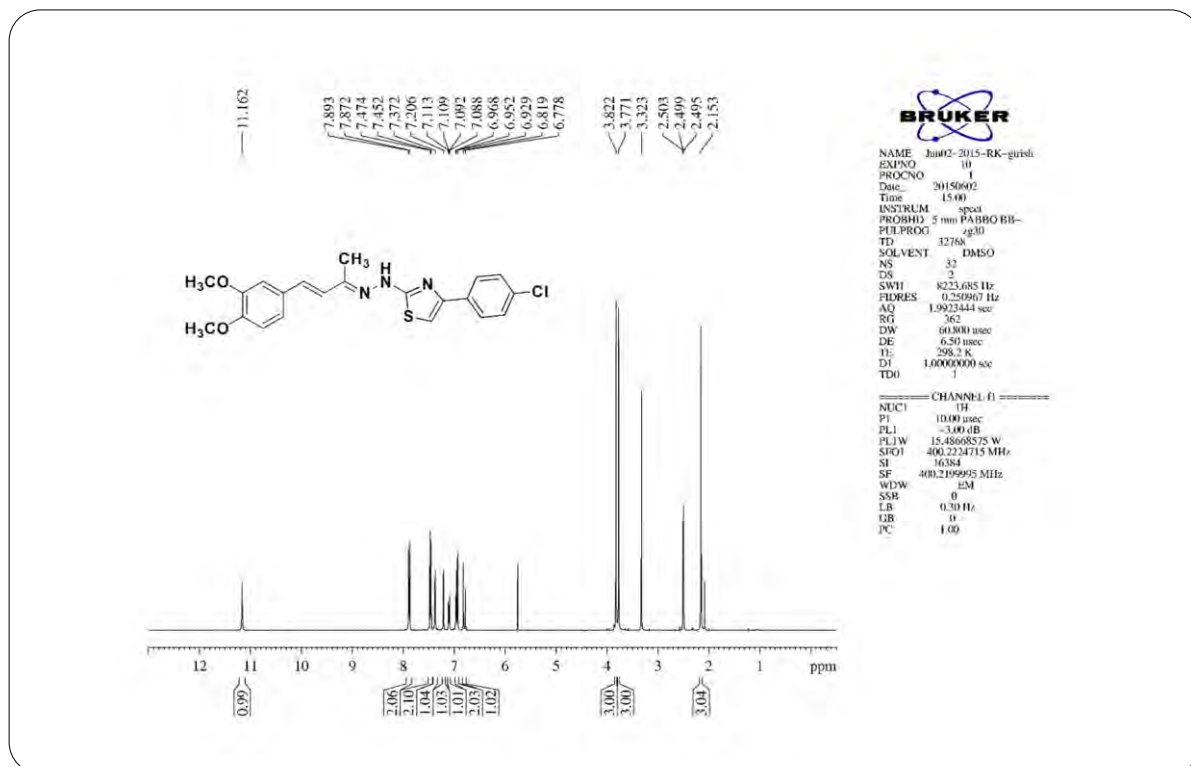
¹H NMR Spectrum of Compound 6d (chapter 3)

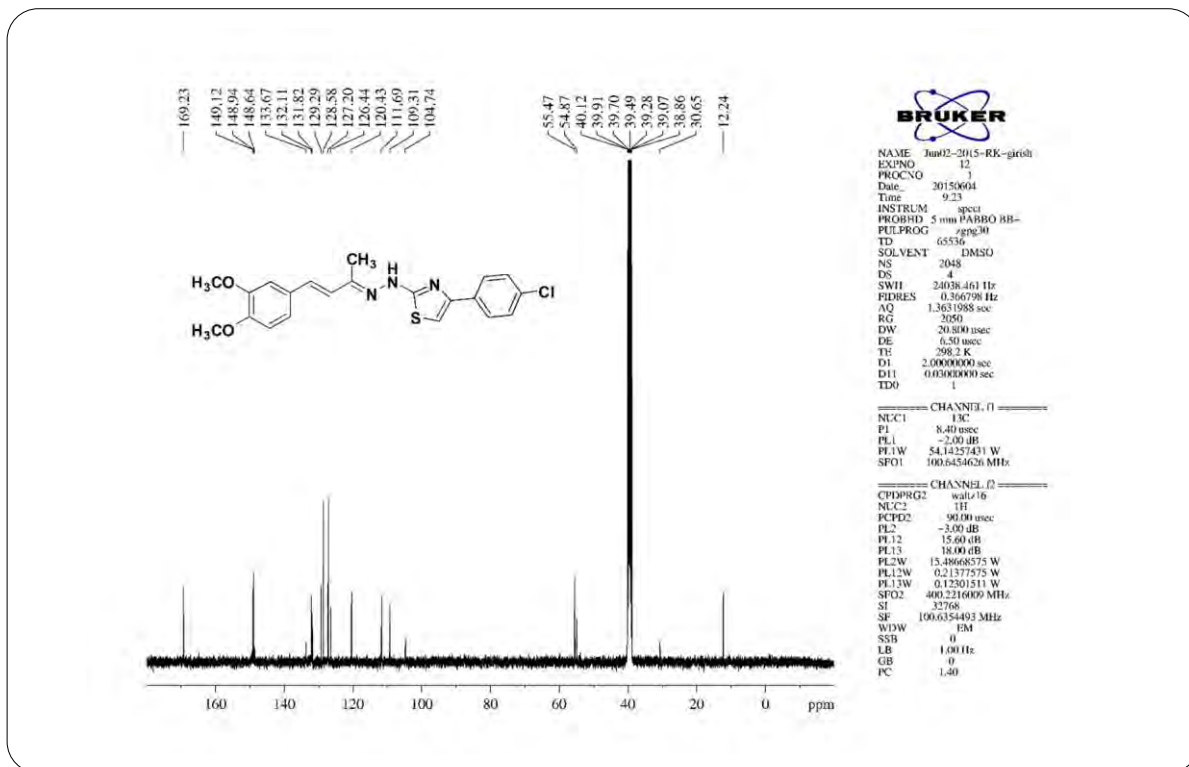
¹³C NMR Spectrum of Compound 6d (chapter 3)

HRMS Spectrum of Compound 6d (chapter 3)



IR Spectrum of Compound 6e (chapter 3)

¹H NMR Spectrum of Compound 6e (chapter 3)

**¹³C NMR Spectrum of Compound 6e (chapter 3)****Elemental Composition Report**

Page 1

Single Mass Analysis

Tolerance = 5.0 PPM / DBE: min = -1.5, max = 100.0

Element prediction: Off

Number of isotope peaks used for i-FIT = 3

Monoisotopic Mass, Even Electron Ions

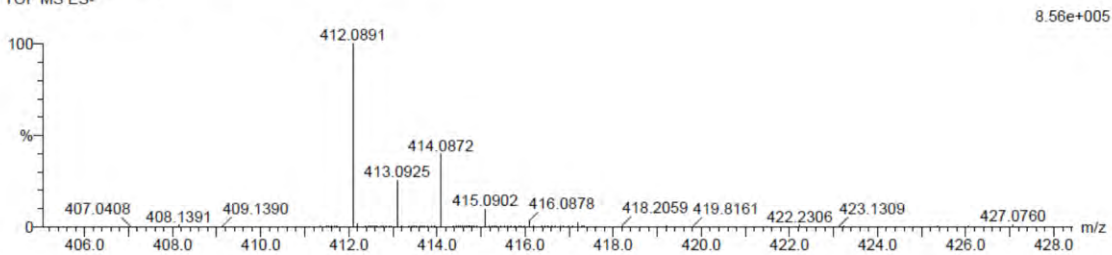
52 formula(e) evaluated with 1 results within limits (up to 20 closest results for each mass)

Elements Used:

C: 20-25 H: 15-25 N: 0-5 O: 0-5 S: 0-1 Cl: 1-1

5e 4 (0.101) Cm (1:61)

TOF MS ES-

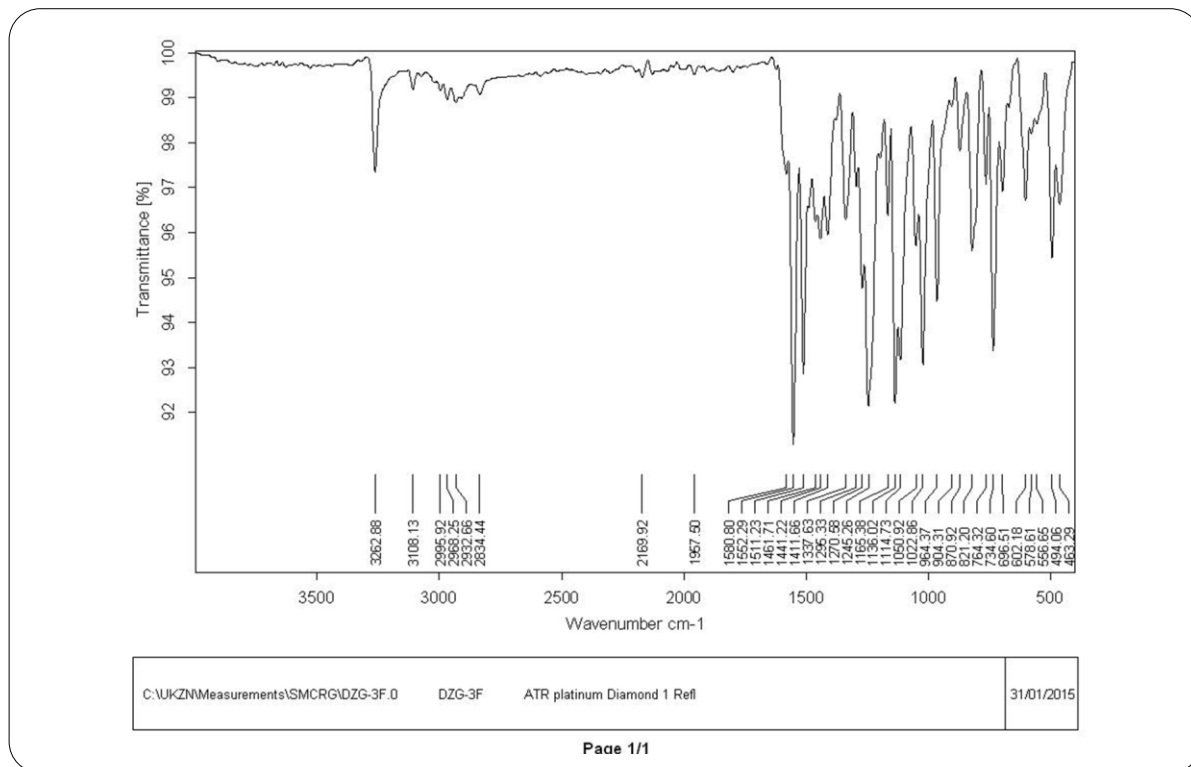


Minimum:

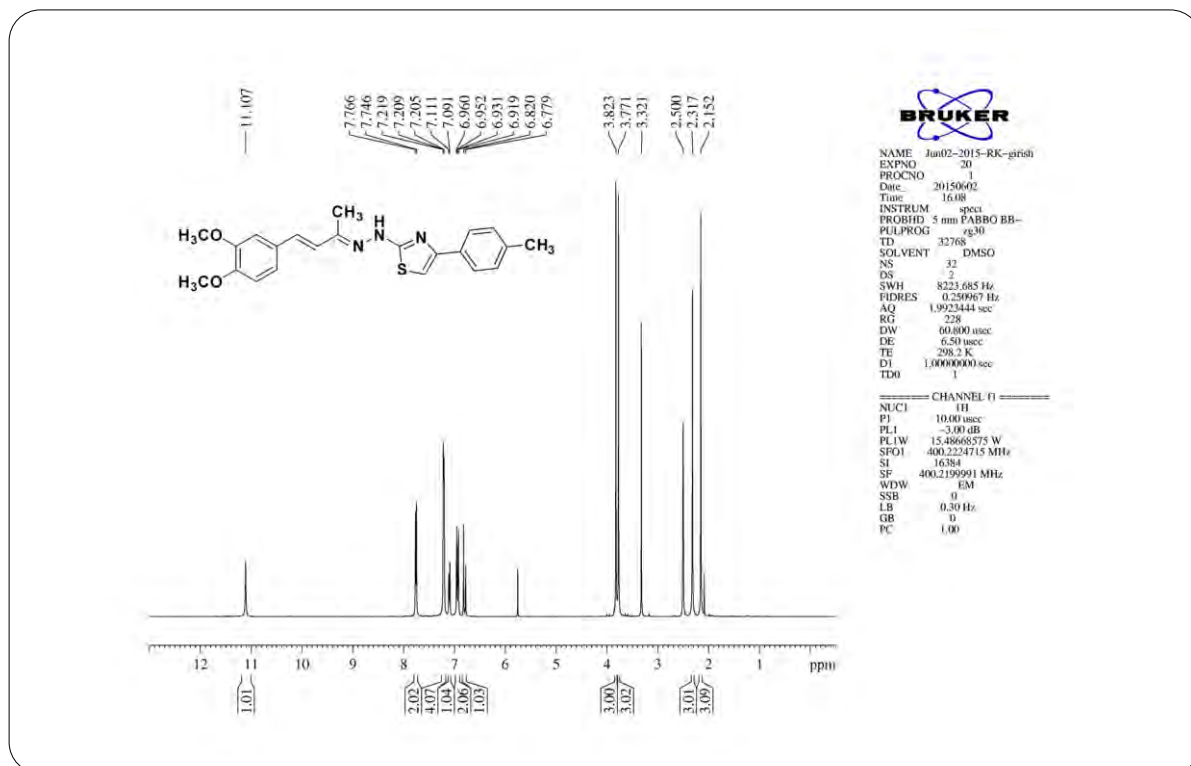
Maximum: 5.0 5.0 100.0

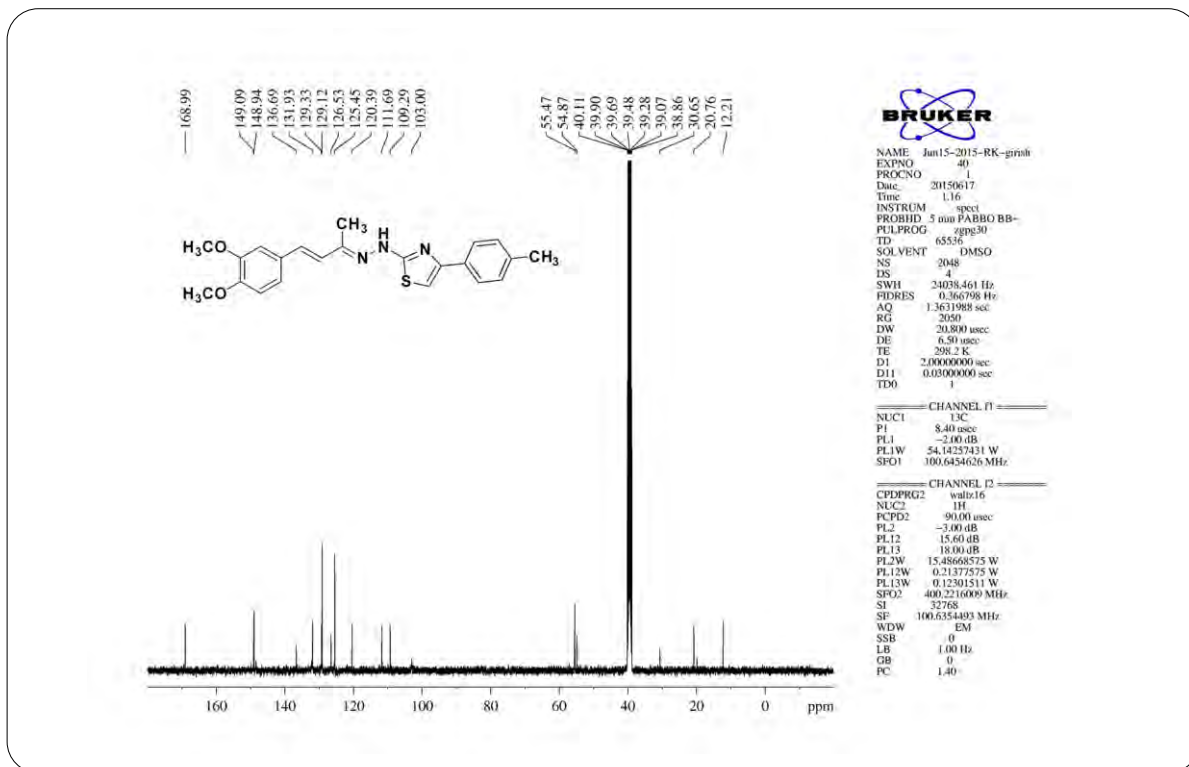
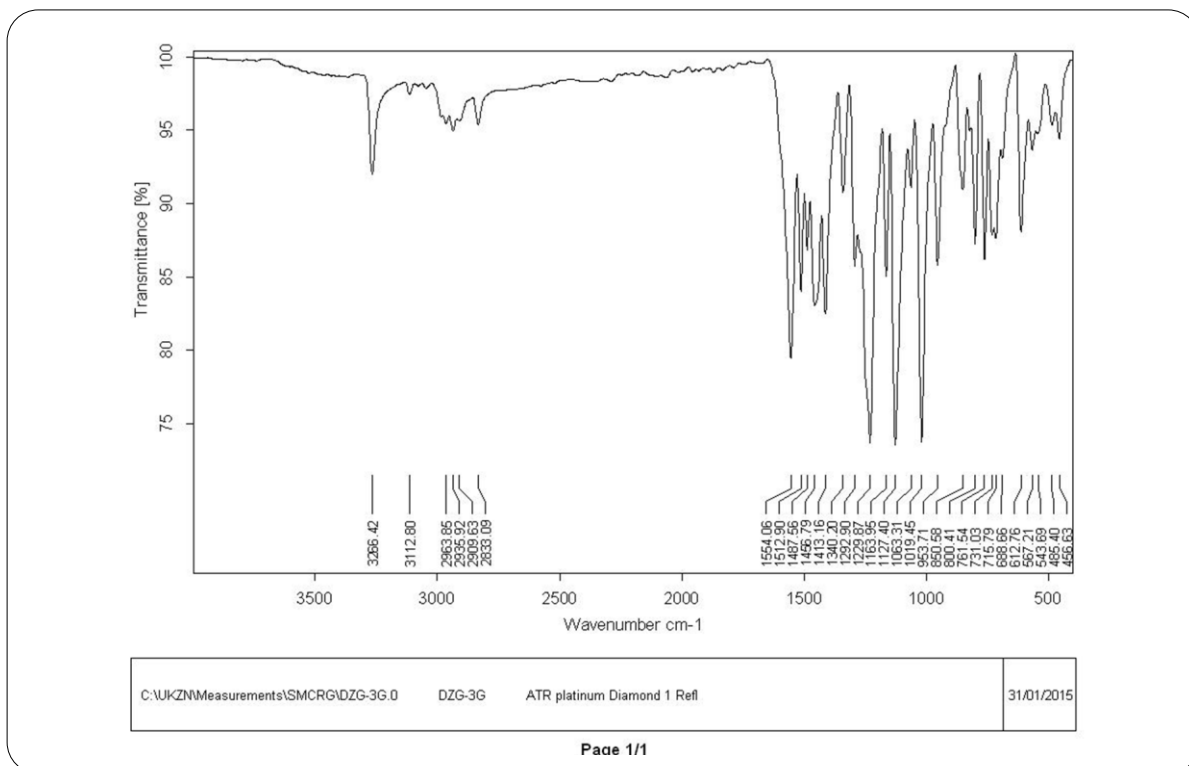
Mass	Calc. Mass	mDa	PPM	DBE	i-FIT	i-FIT (Norm)	Formula
412.0891	412.0887	0.4	1.0	13.5	623.4	0.0	C21 H19 N3 O2 S Cl

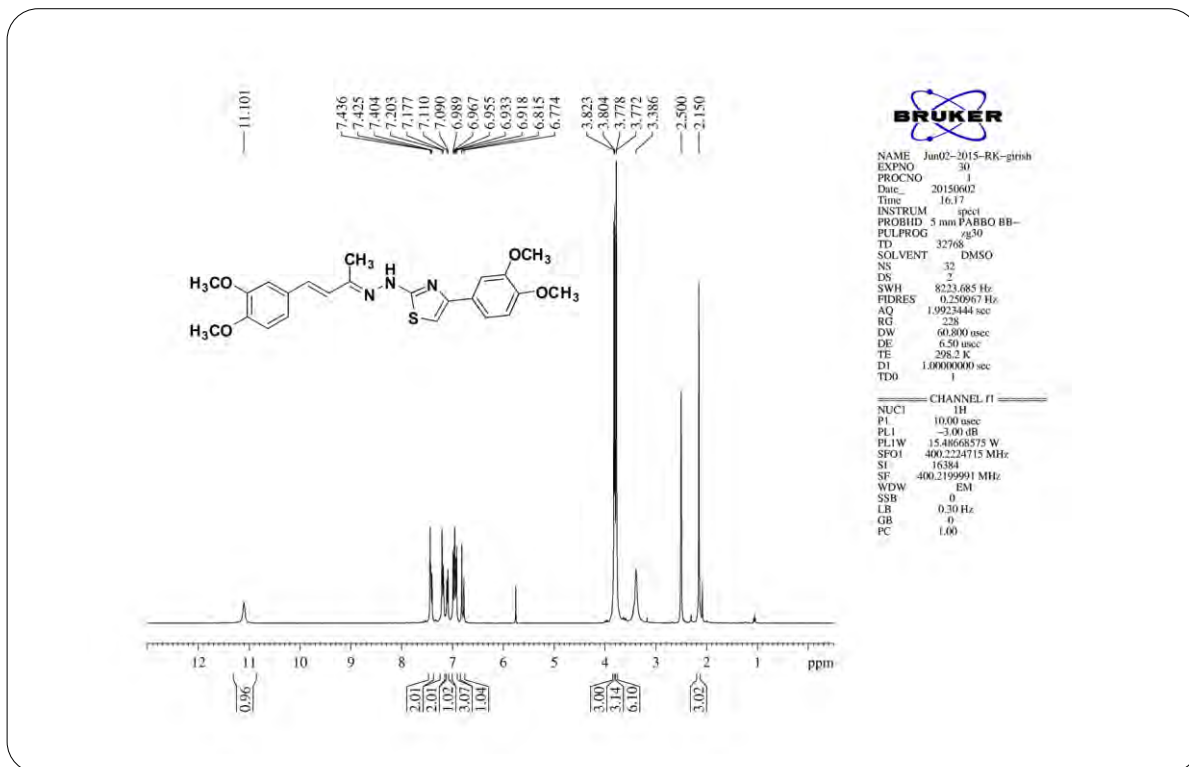
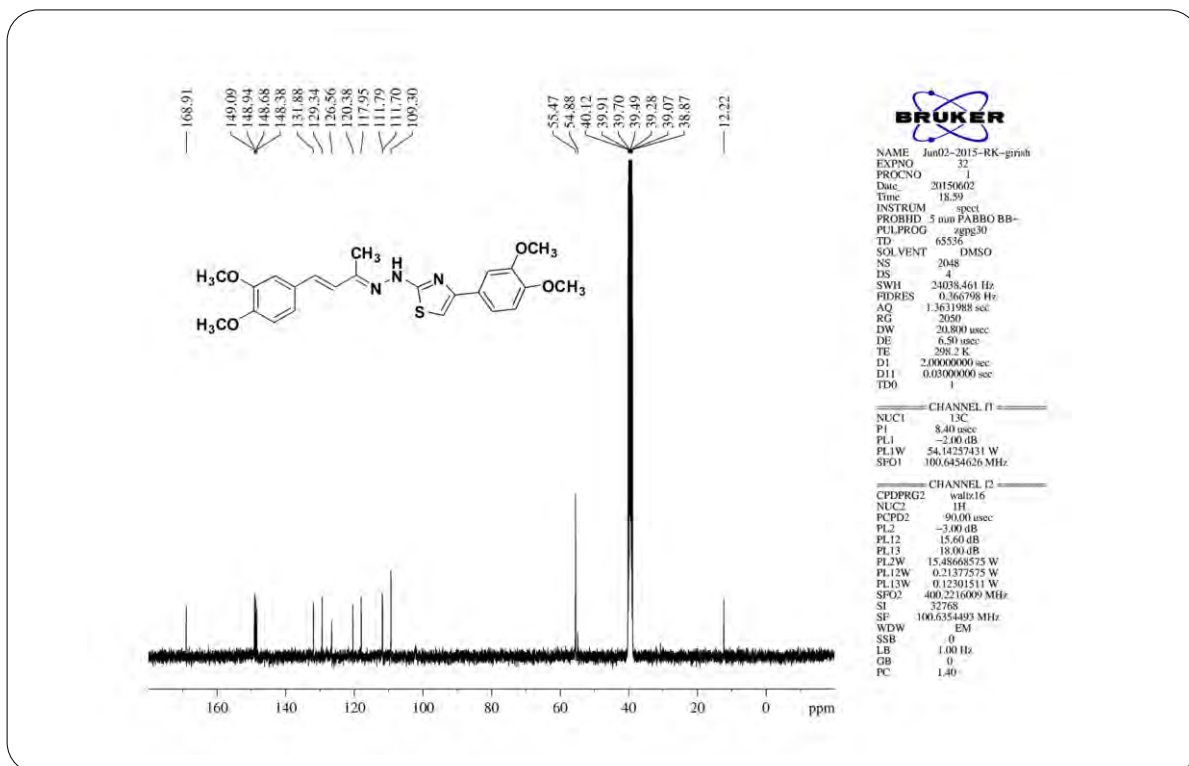
HRMS Spectrum of Compound 6e (chapter 3)

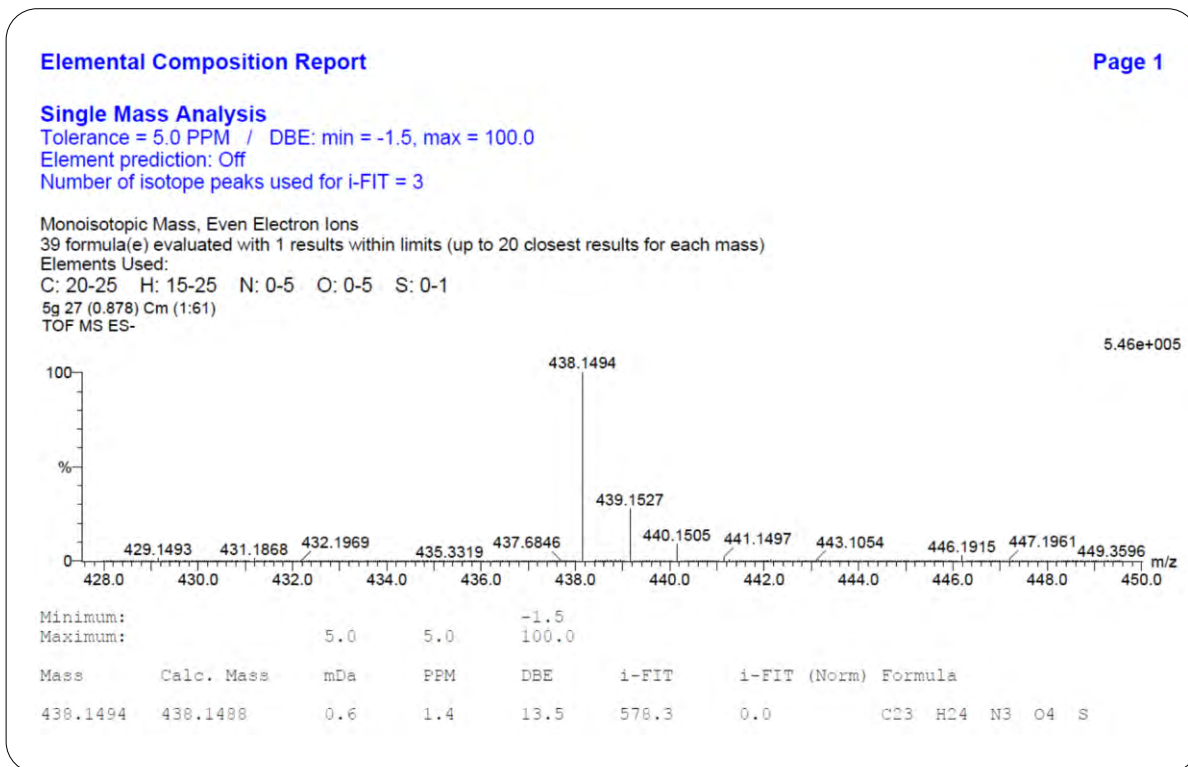


IR Spectrum of Compound 6f (chapter 3)

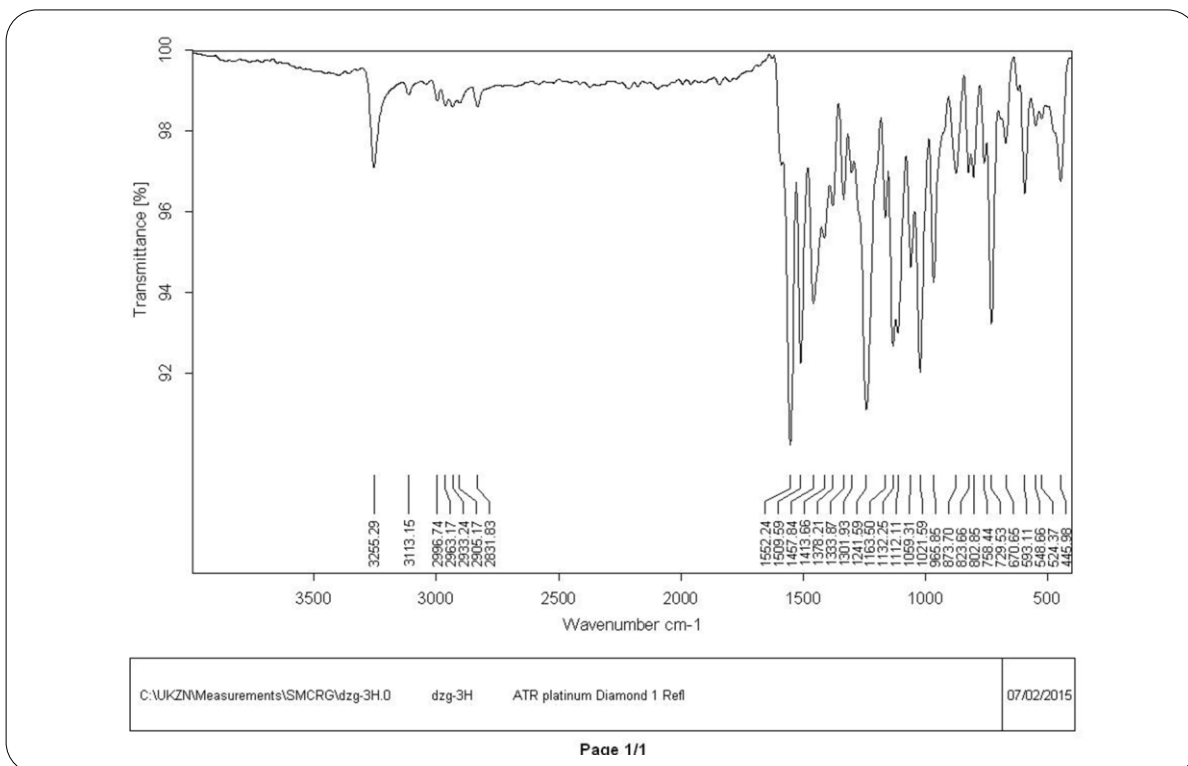


**¹³C NMR Spectrum of Compound 6f (chapter 3)****IR Spectrum of Compound 6g (chapter 3)**

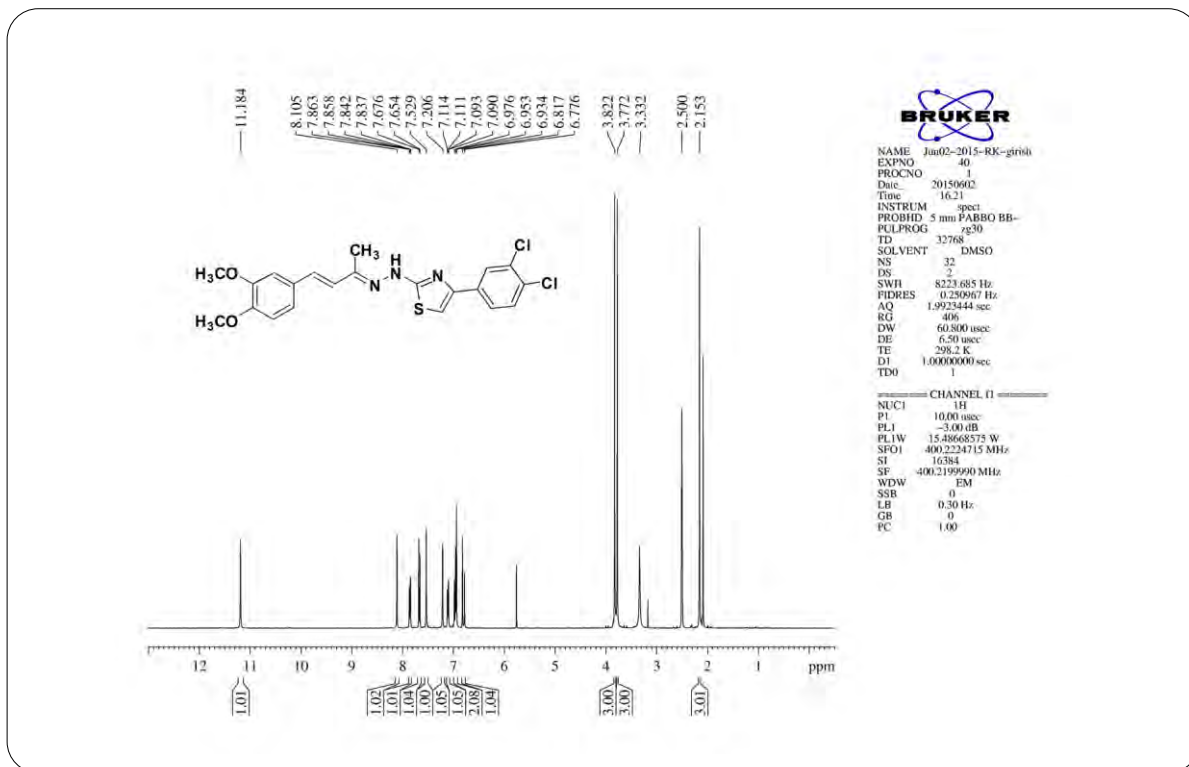
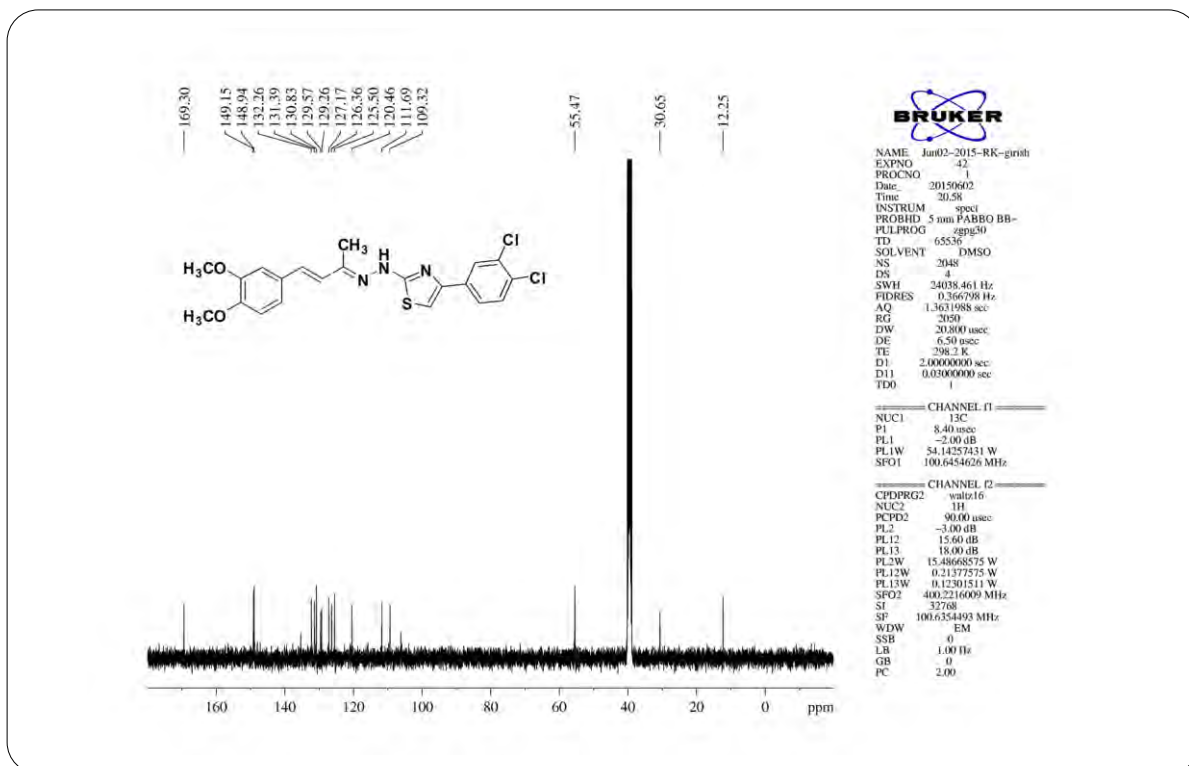
**¹H NMR Spectrum of Compound 6g (chapter 3)****¹³C NMR Spectrum of Compound 6g (chapter 3)**

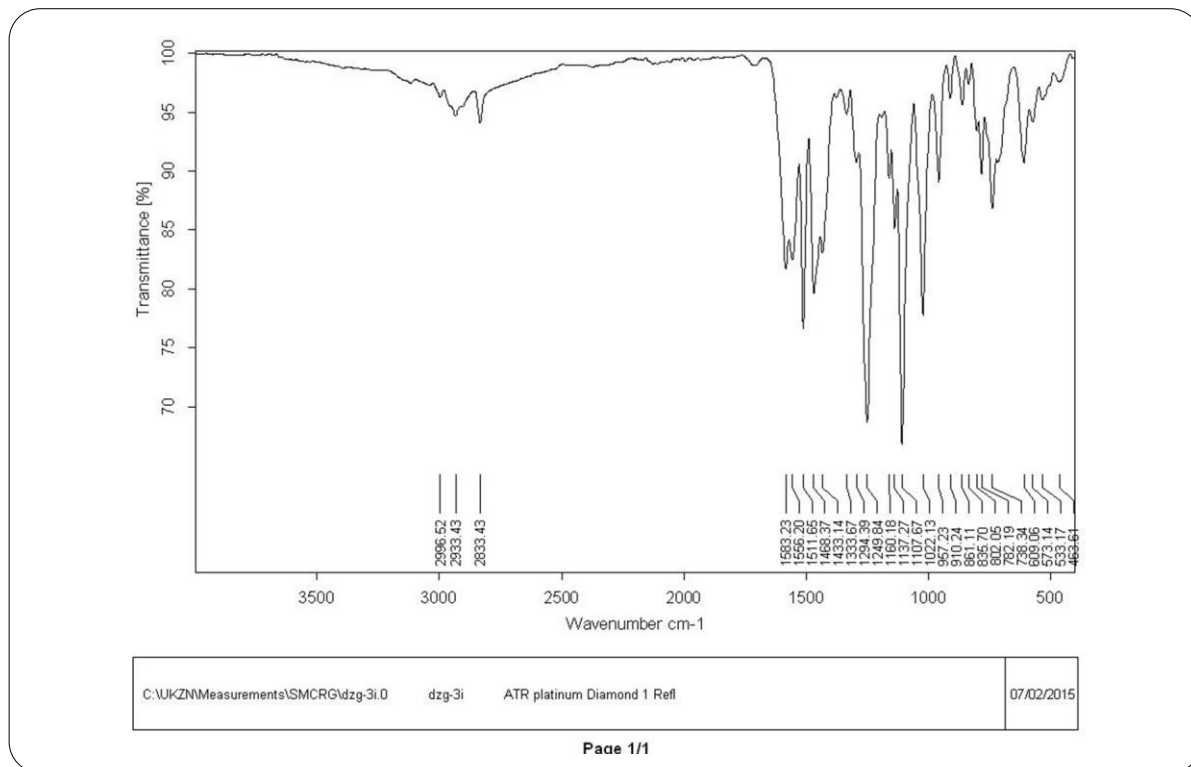


HRMS Spectrum of Compound 6g (chapter 3)

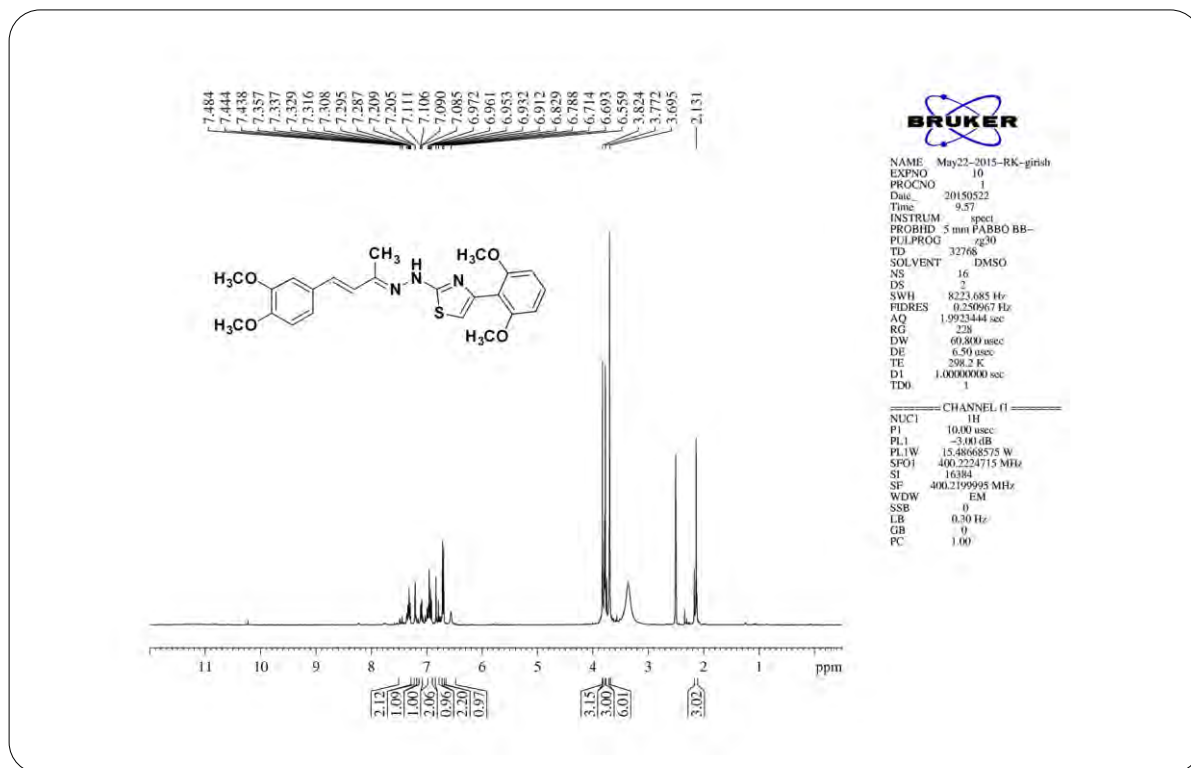


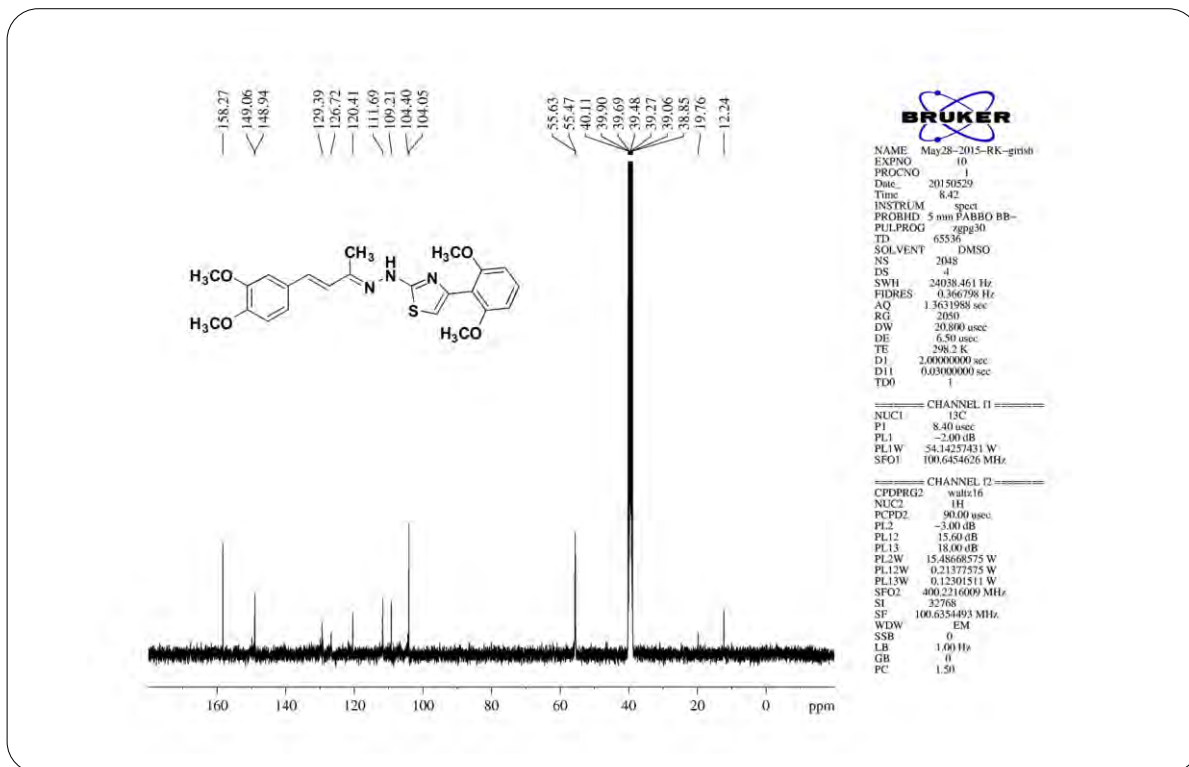
IR Spectrum of Compound 6h (chapter 3)

**¹H NMR Spectrum of Compound 6h (chapter 3)****¹³C NMR Spectrum of Compound 6h (chapter 3)**



IR Spectrum of Compound 6i (chapter 3)

¹H NMR Spectrum of Compound 6i (chapter 3)

**¹³C NMR Spectrum of Compound 6i (chapter 3)****Elemental Composition Report**

Page 1

Single Mass Analysis

Tolerance = 5.0 PPM / DBE: min = -1.5, max = 100.0

Element prediction: Off

Number of isotope peaks used for i-FIT = 3

Monoisotopic Mass, Even Electron Ions

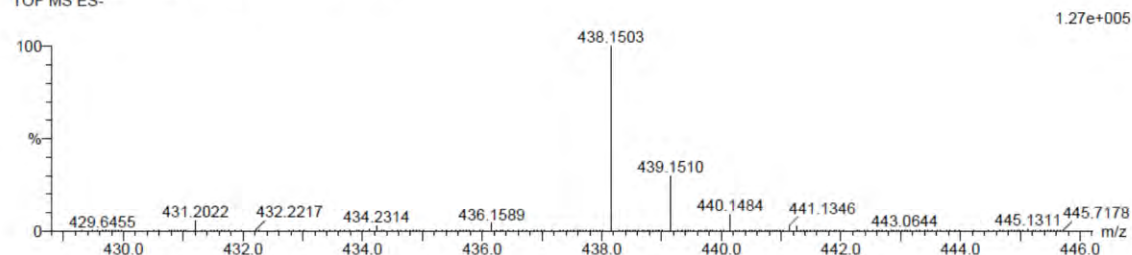
39 formula(e) evaluated with 1 results within limits (up to 20 closest results for each mass)

Elements Used:

C: 20-25 H: 15-25 N: 0-5 O: 0-5 S: 0-1

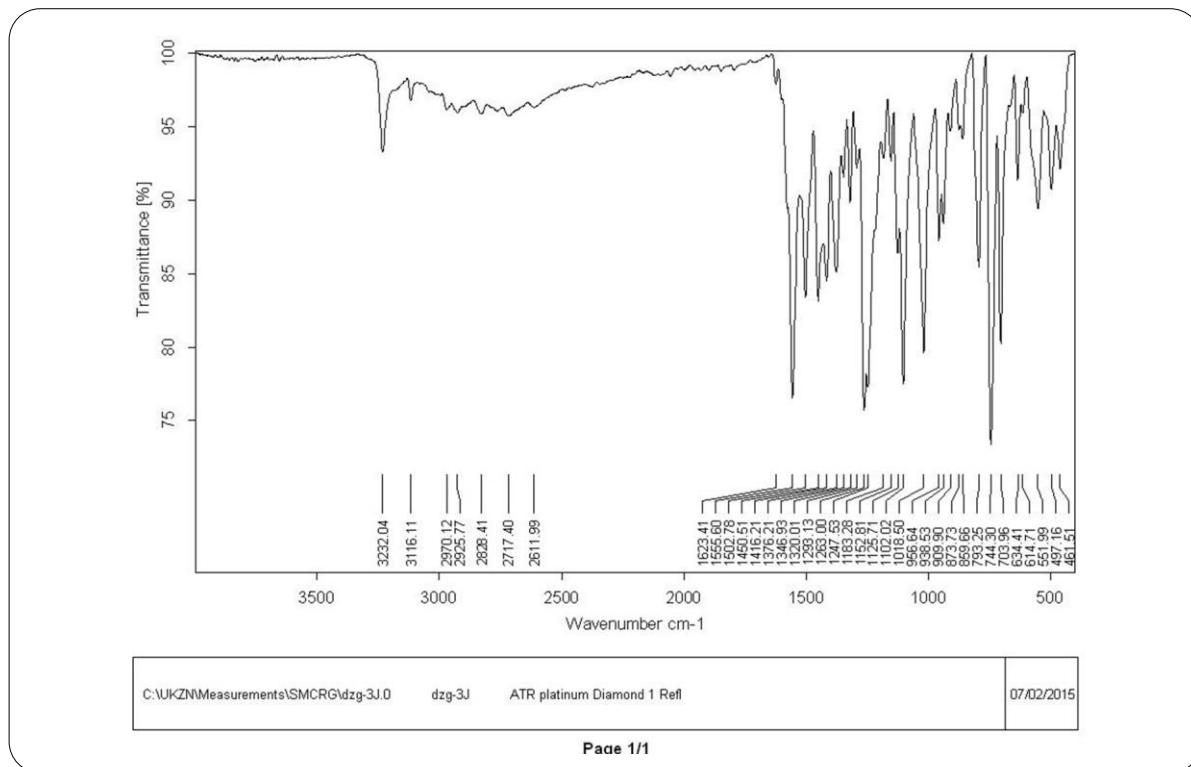
5i 55 (1.822) Cm (1.61)

TOF MS ES-



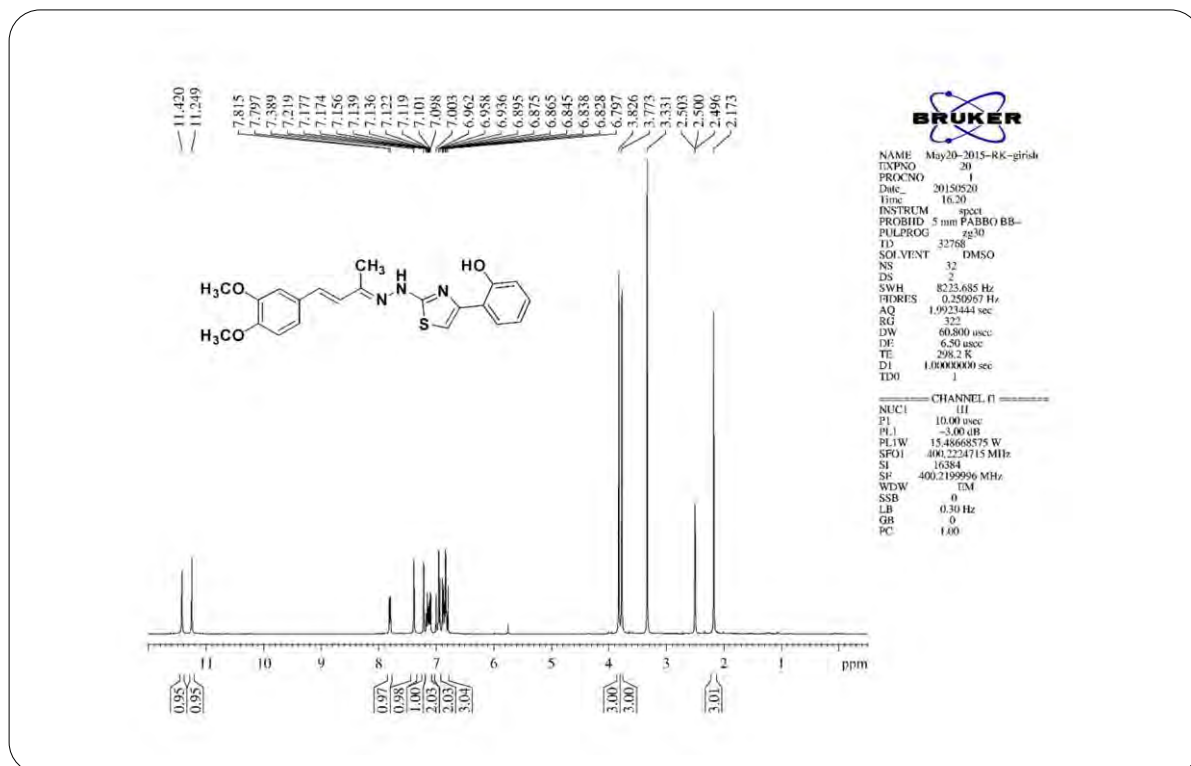
Mass	Calc. Mass	mDa	PPM	DBE	i-FIT	i-FIT (Norm)	Formula
438.1503	438.1488	1.5	3.4	13.5	536.1	0.0	C23 H24 N3 O4 S

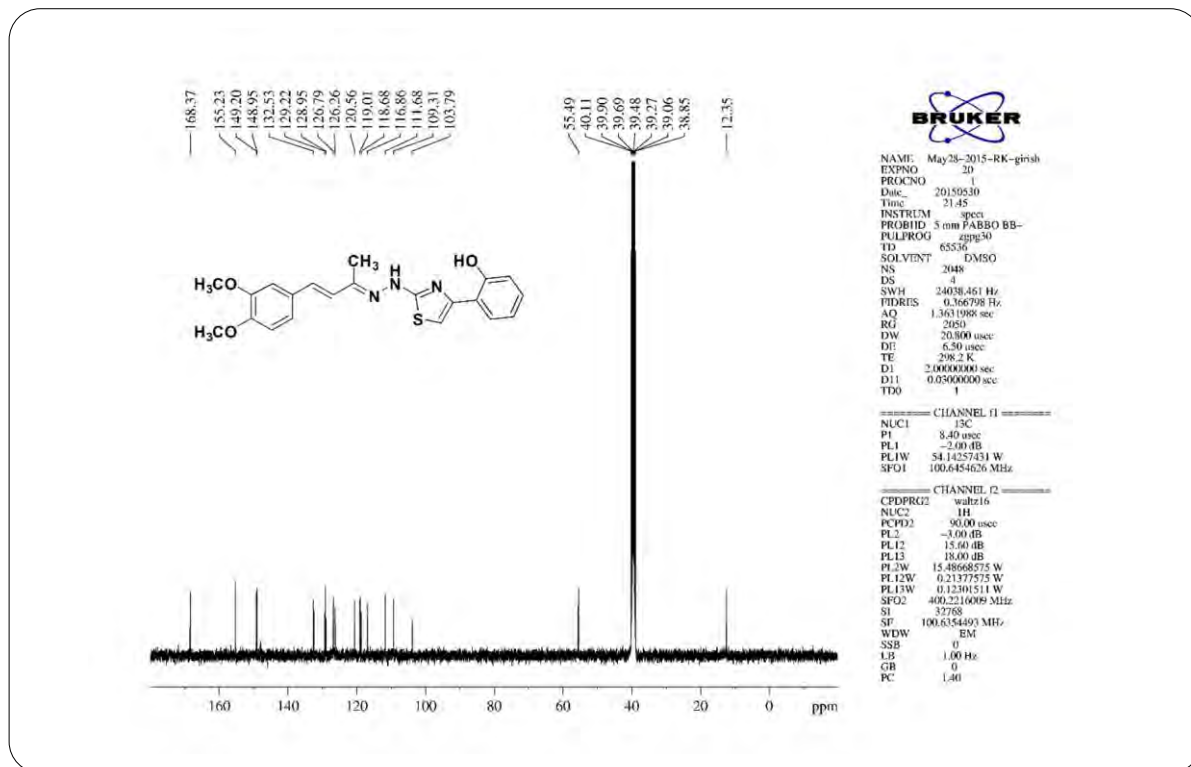
HRMS Spectrum of Compound 6i (chapter 3)



Page 1/1

IR Spectrum of Compound 6j (chapter 3)

¹H NMR Spectrum of Compound 6j (chapter 3)

**¹³C NMR Spectrum of Compound 6j (chapter 3)****Elemental Composition Report**

Page 1

Single Mass Analysis

Tolerance = 5.0 PPM / DBE: min = -1.5, max = 100.0

Element prediction: Off

Number of isotope peaks used for i-FIT = 3

Monoisotopic Mass, Even Electron Ions

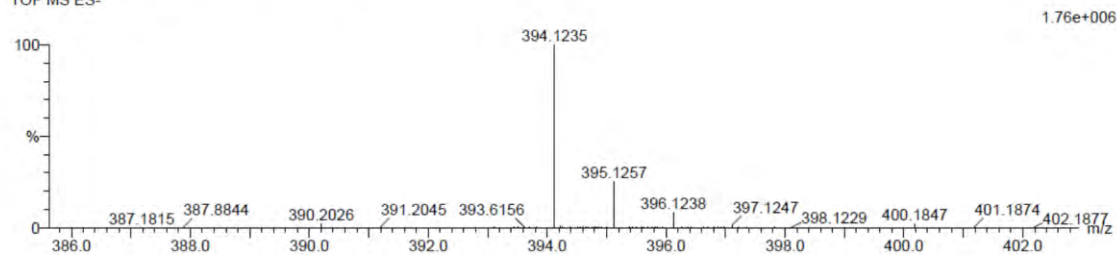
43 formula(e) evaluated with 1 results within limits (up to 20 closest results for each mass)

Elements Used:

C: 20-25 H: 15-25 N: 0-5 O: 0-5 S: 0-1

5j 11 (0.338) Cm (1.81)

TOF MS ES-

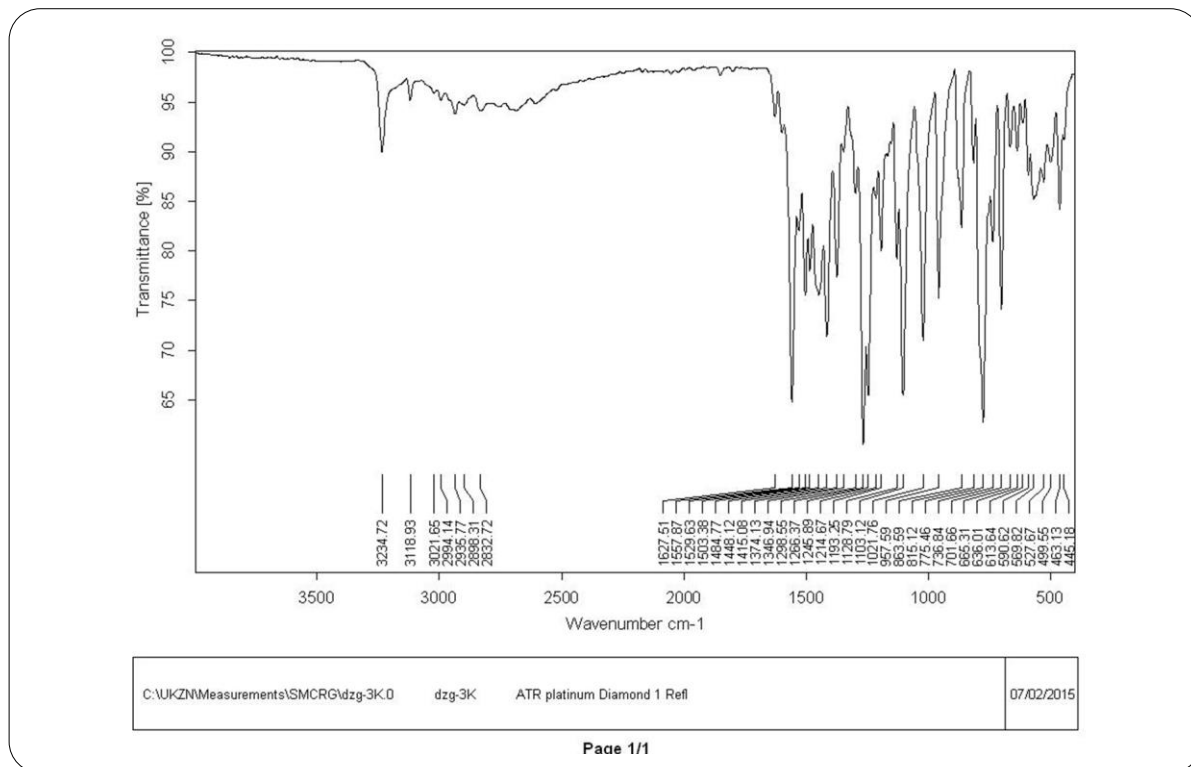


Minimum:

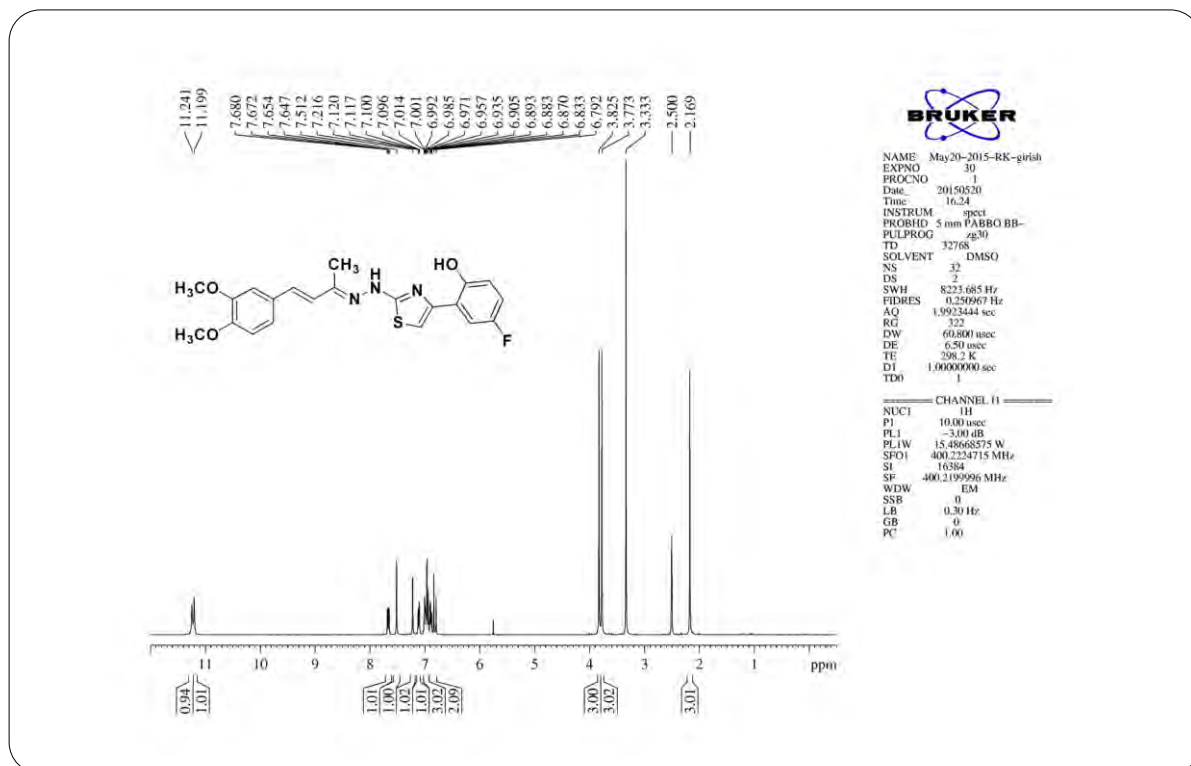
Maximum: 5.0 5.0 100.0

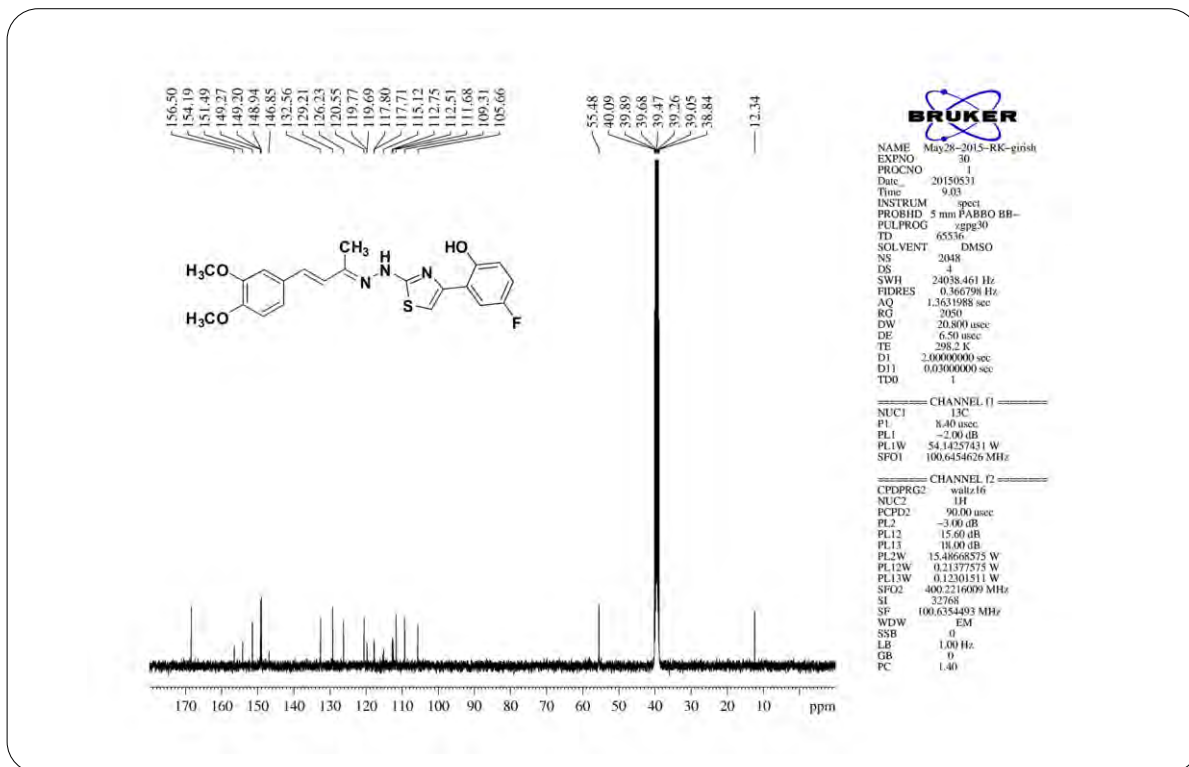
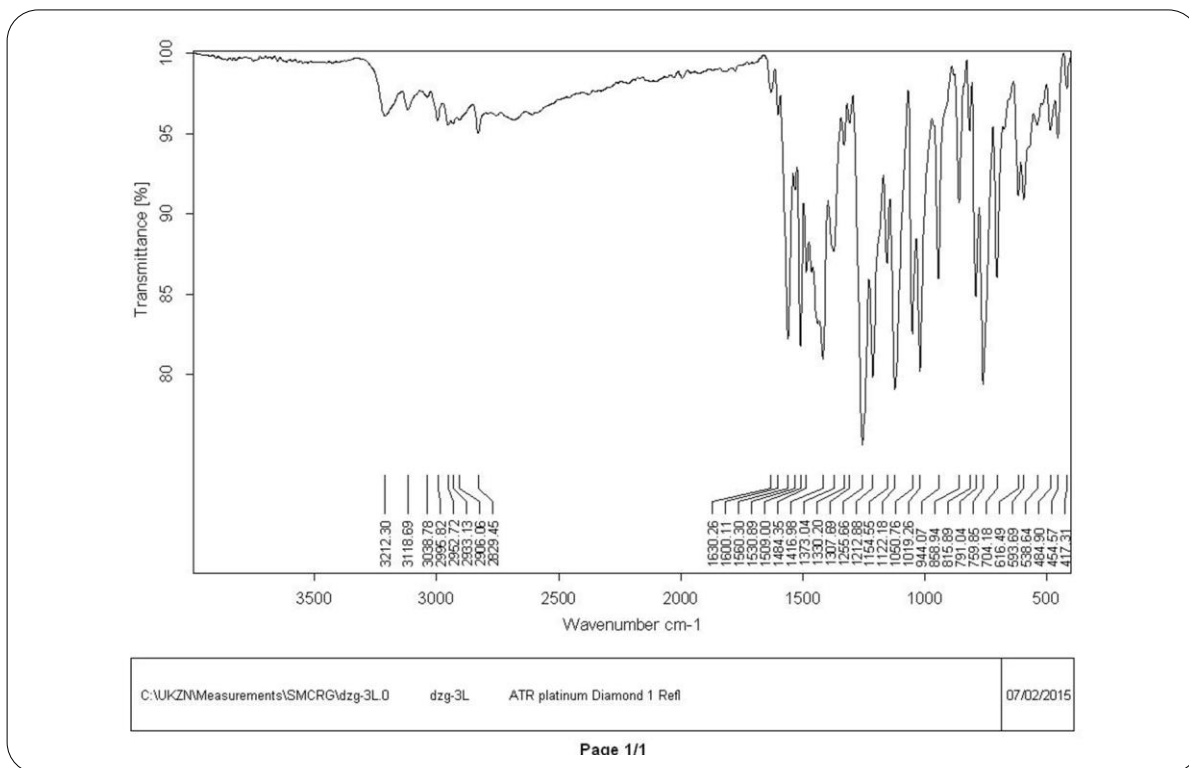
Mass	Calc. Mass	mDa	PPM	DBE	i-FIT	i-FIT (Norm)	Formula
394.1235	394.1225	1.0	2.5	13.5	665.7	0.0	C21 H20 N3 O3 S

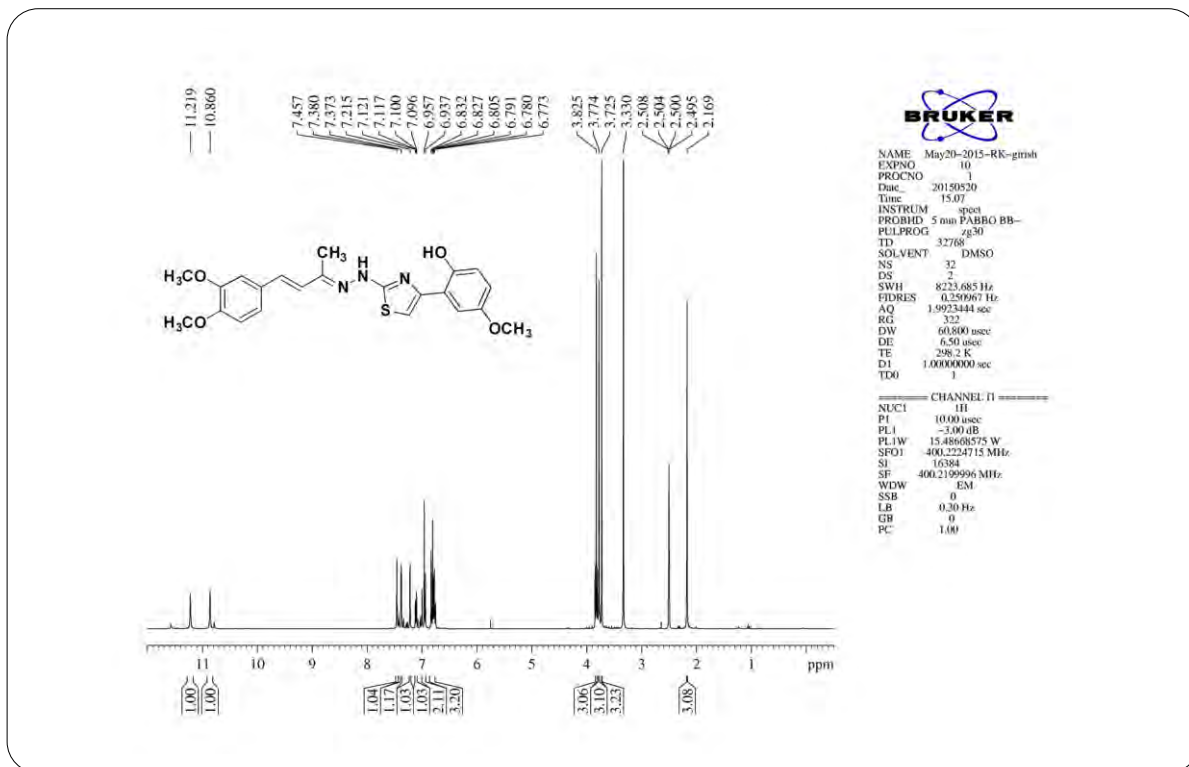
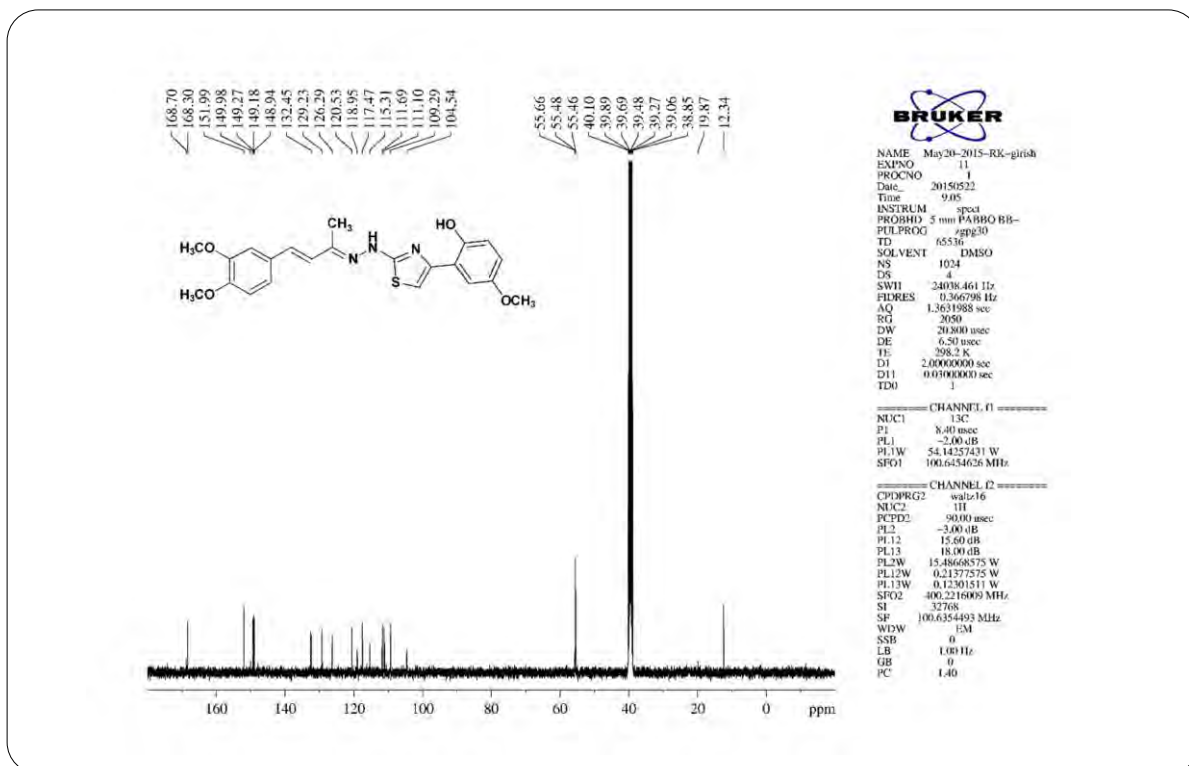
HRMS Spectrum of Compound 6j (chapter 3)

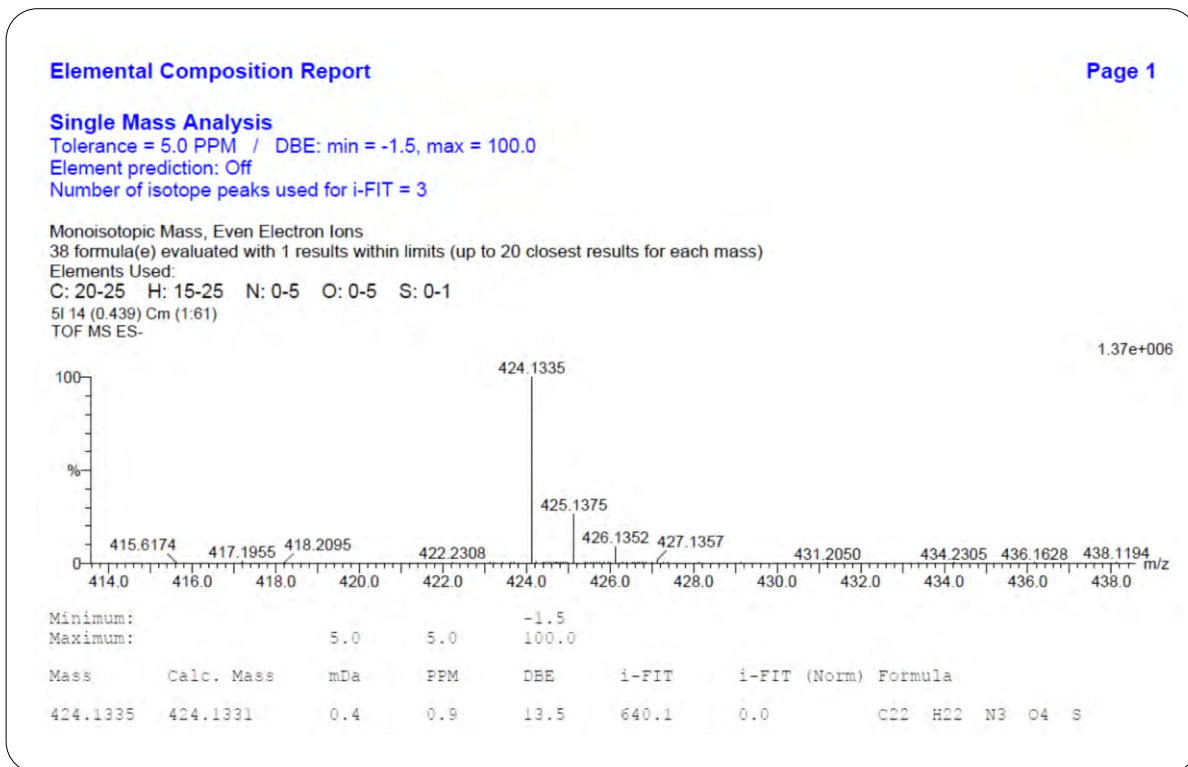


IR Spectrum of Compound 6k (chapter 3)

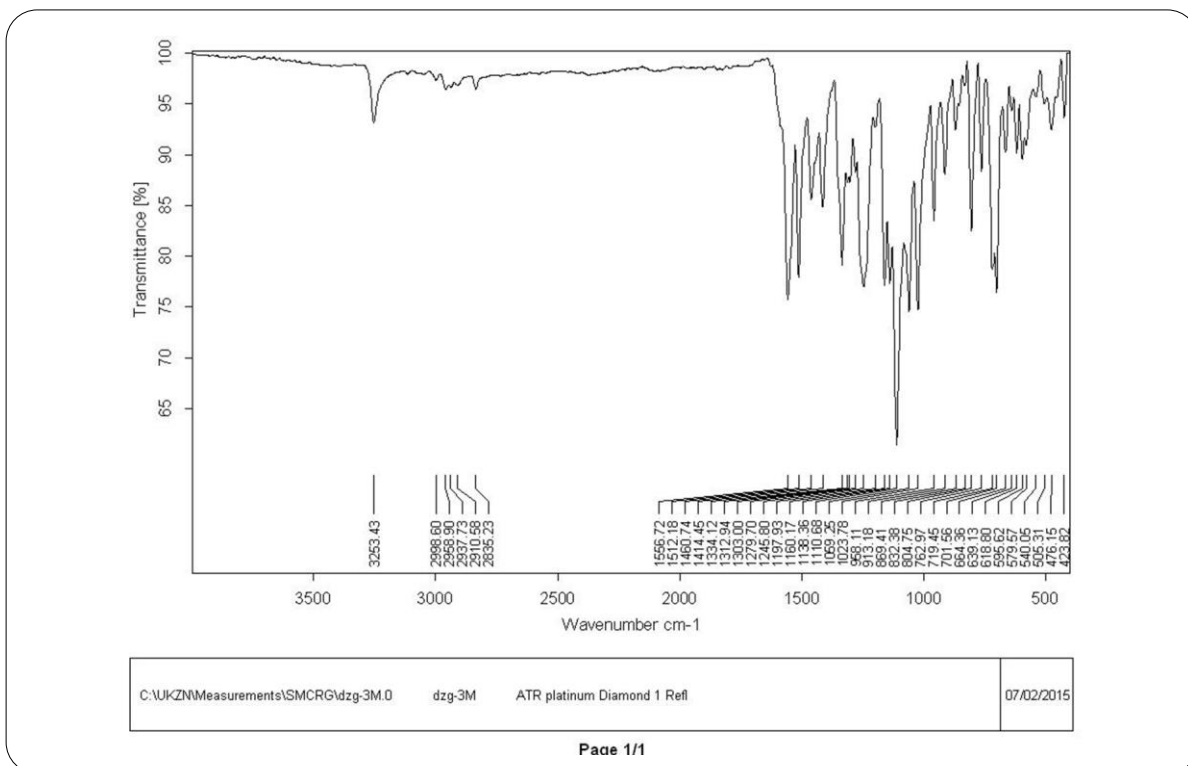
¹H NMR Spectrum of Compound 6k (chapter 3)

**¹³C NMR Spectrum of Compound 6k (chapter 3)****IR Spectrum of Compound 6l (chapter 3)**

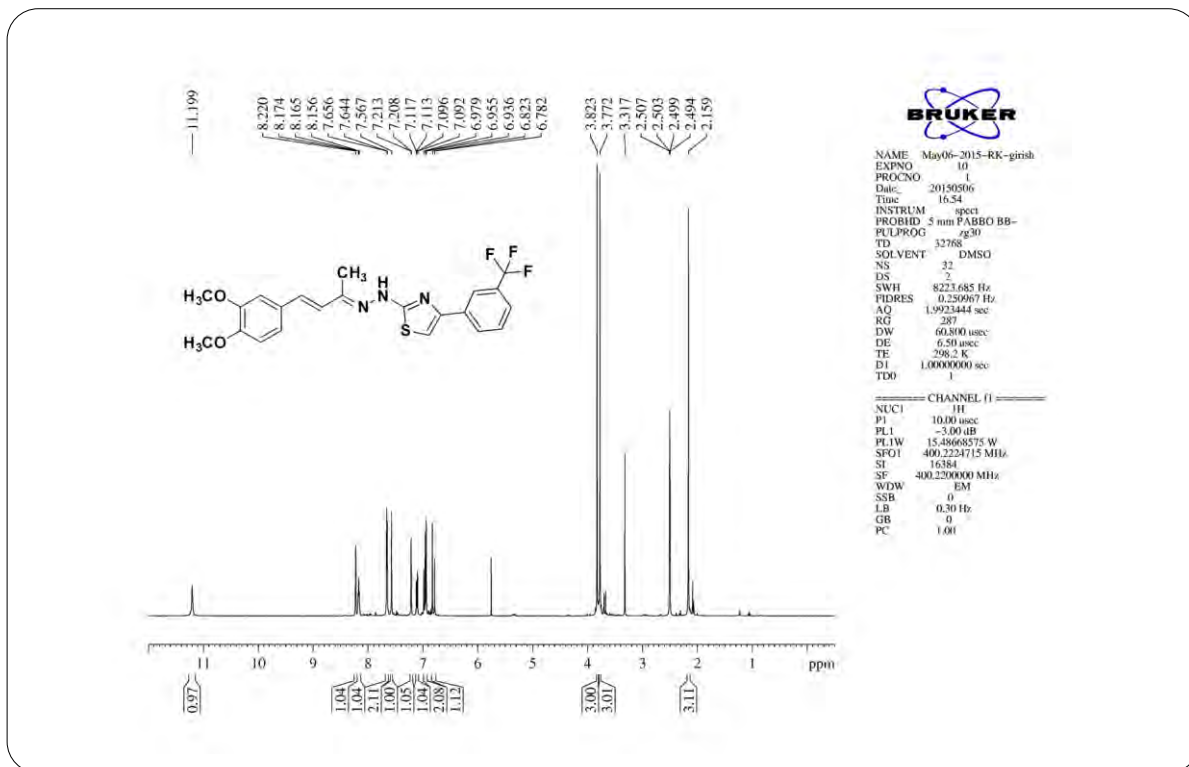
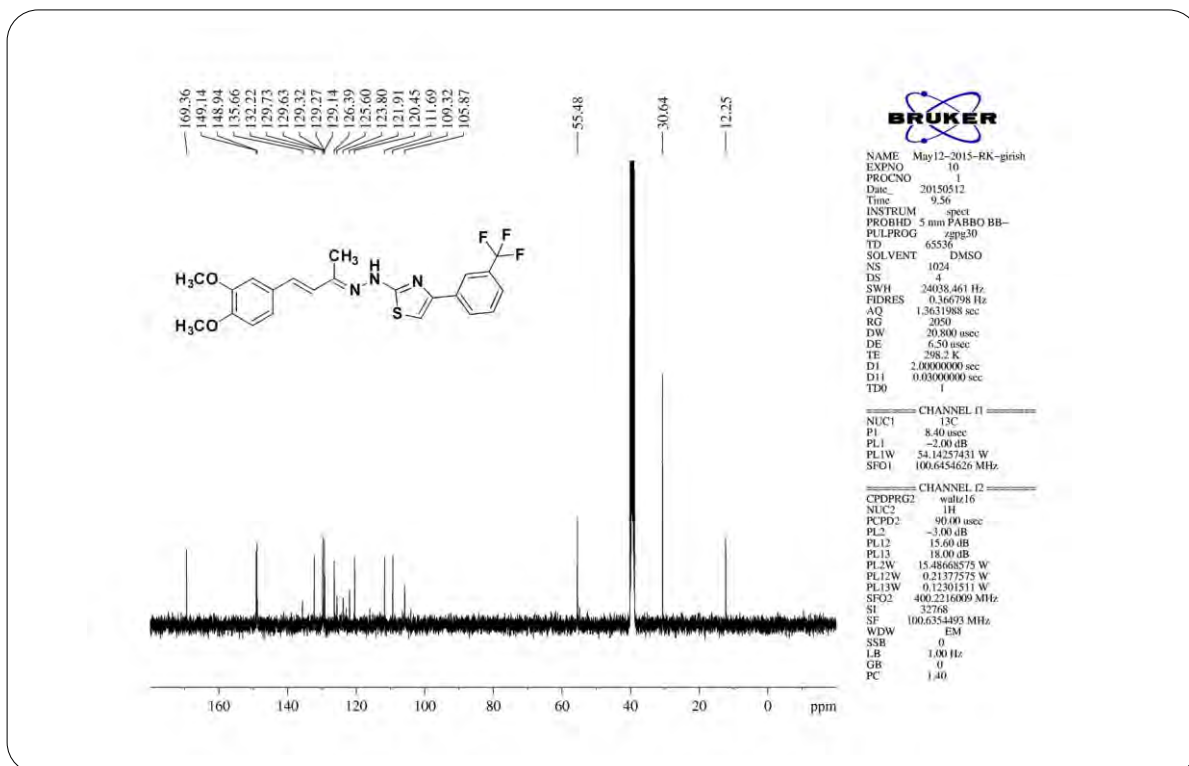
**¹H NMR Spectrum of Compound 6l (chapter 3)****¹³C NMR Spectrum of Compound 6l (chapter 3)**

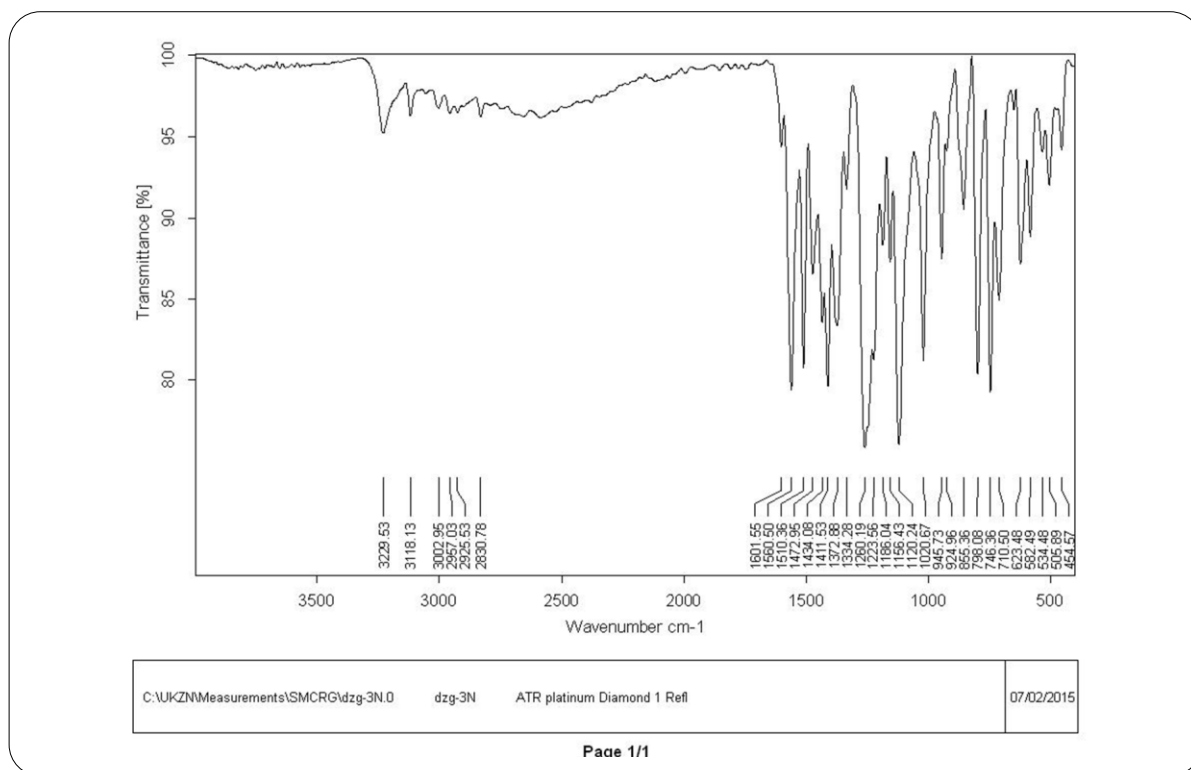


HRMS Spectrum of Compound 6l (chapter 3)

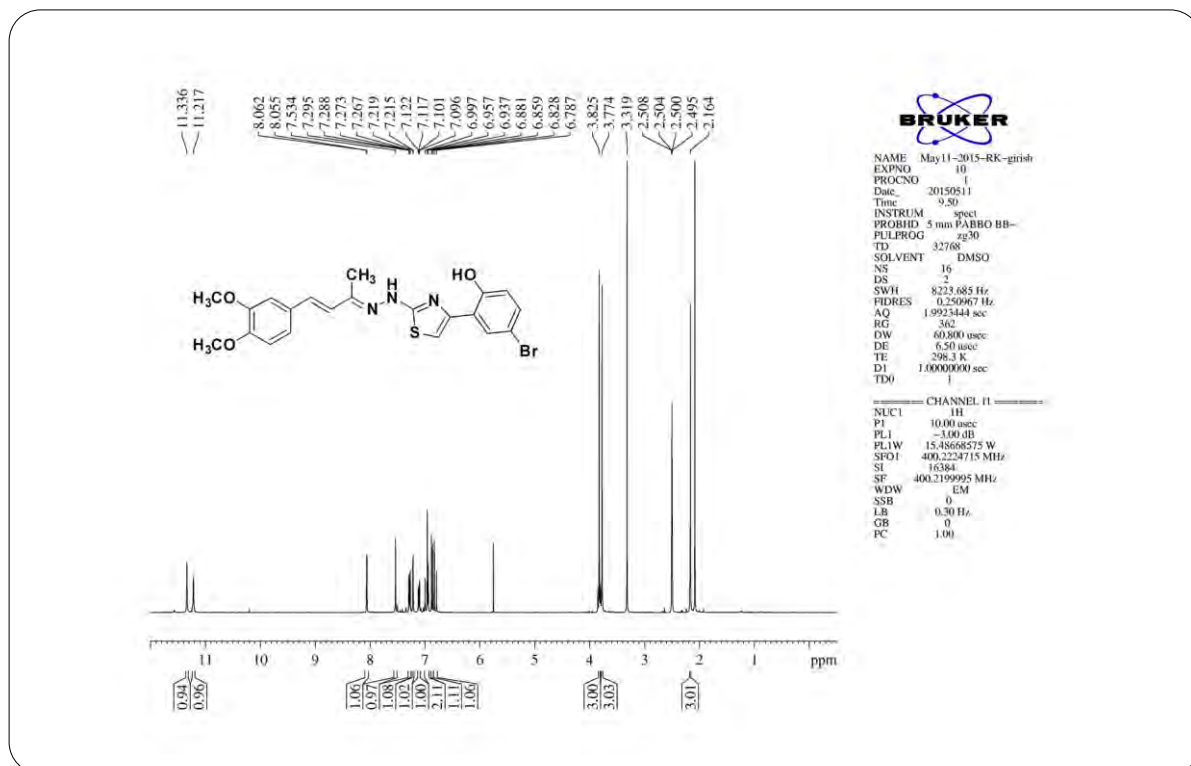


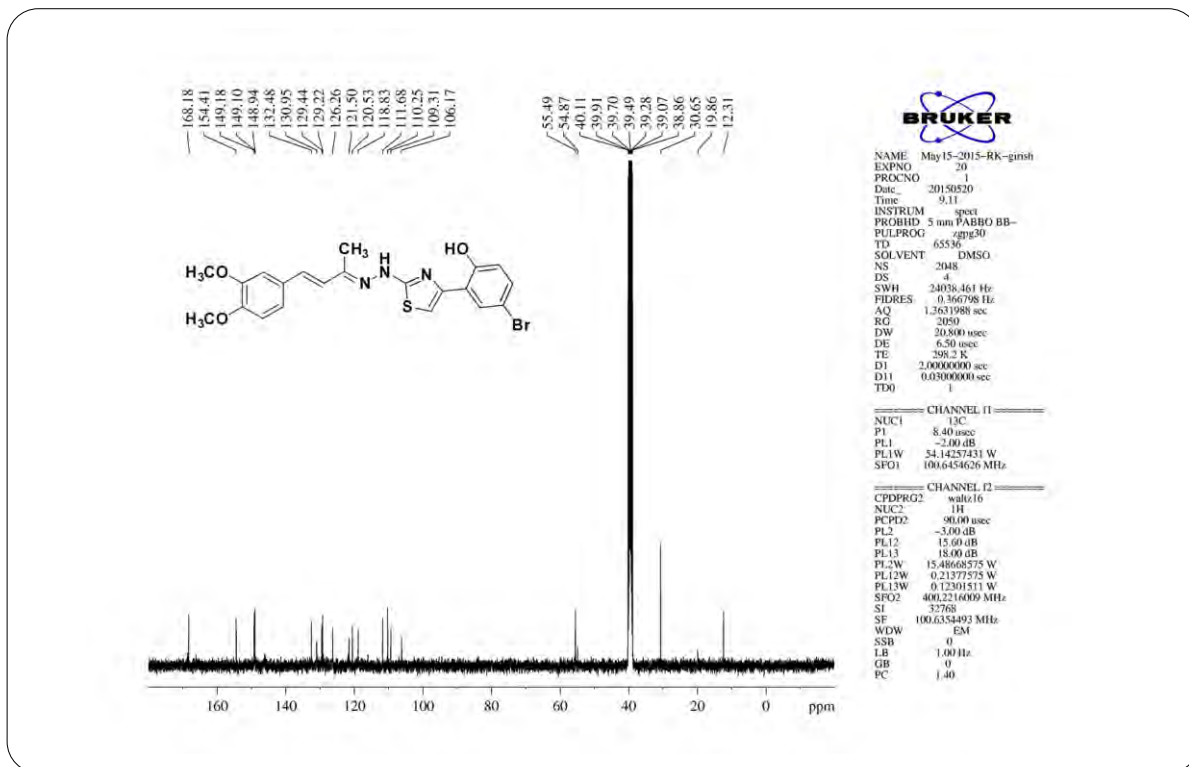
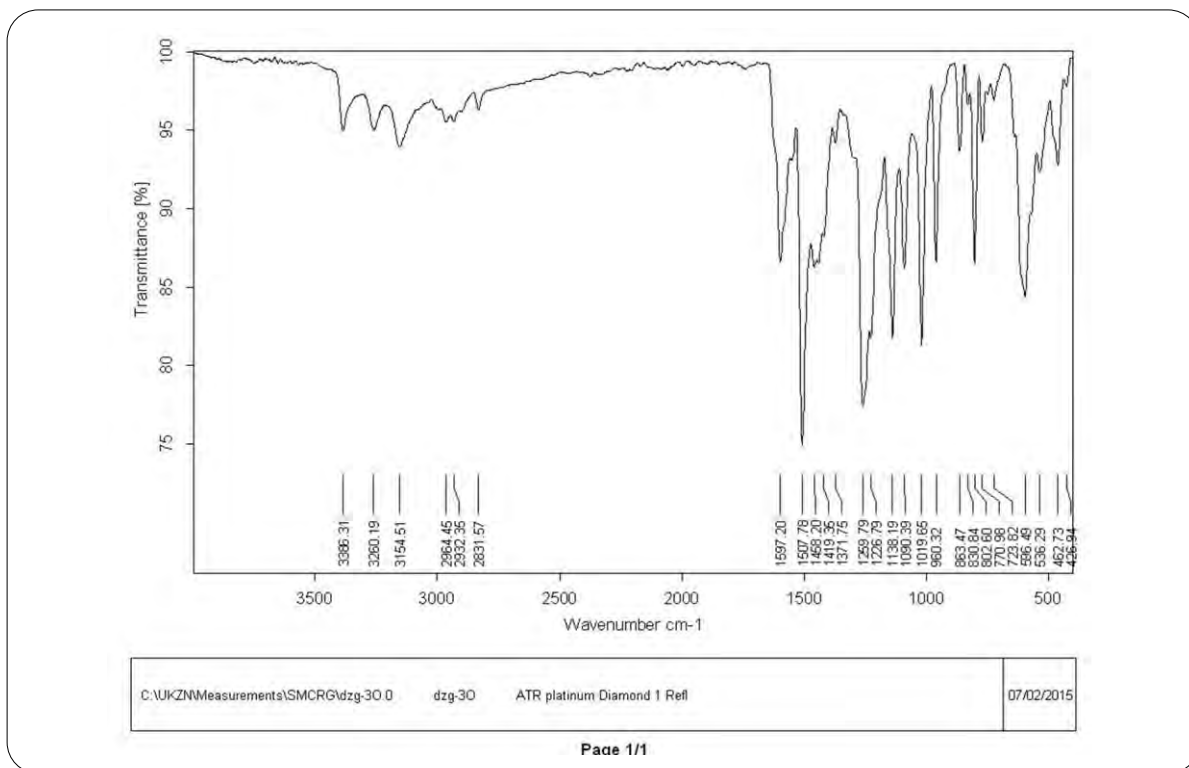
IR Spectrum of Compound 6m (chapter 3)

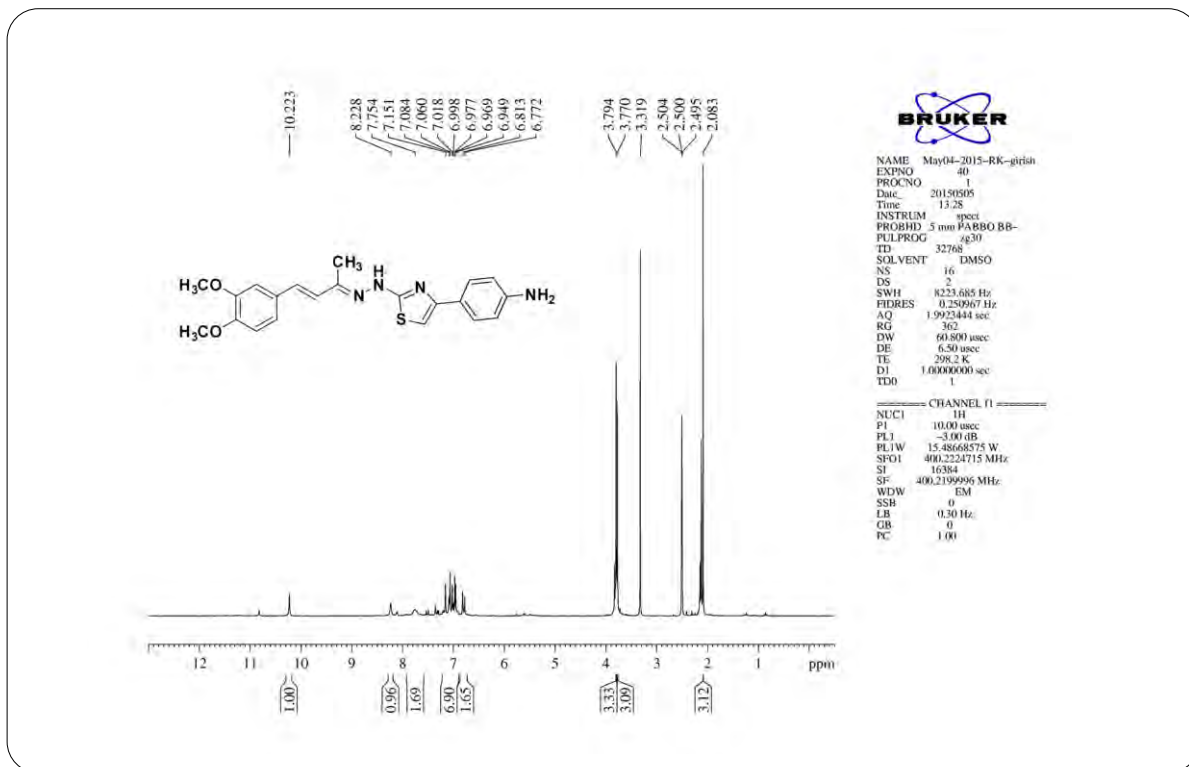
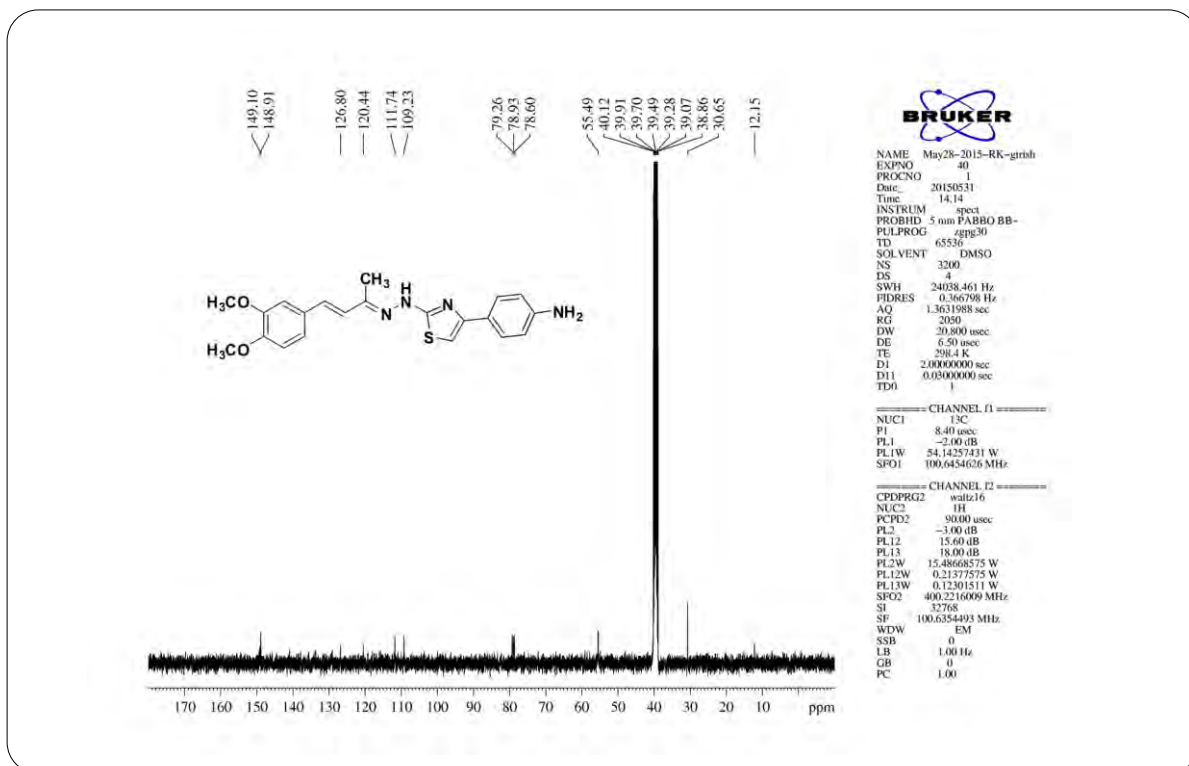
**¹H NMR Spectrum of Compound 6m (chapter 3)****¹³C NMR Spectrum of Compound 6m (chapter 3)**

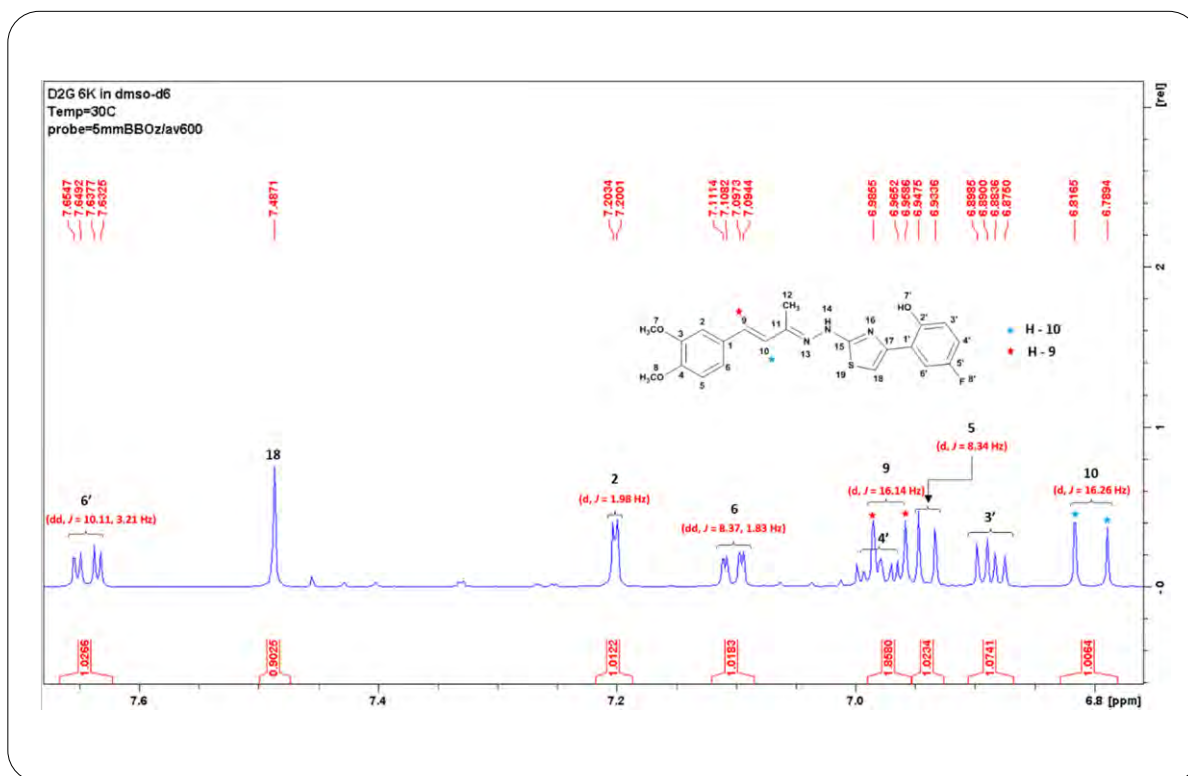


IR Spectrum of Compound 6n (chapter 3)

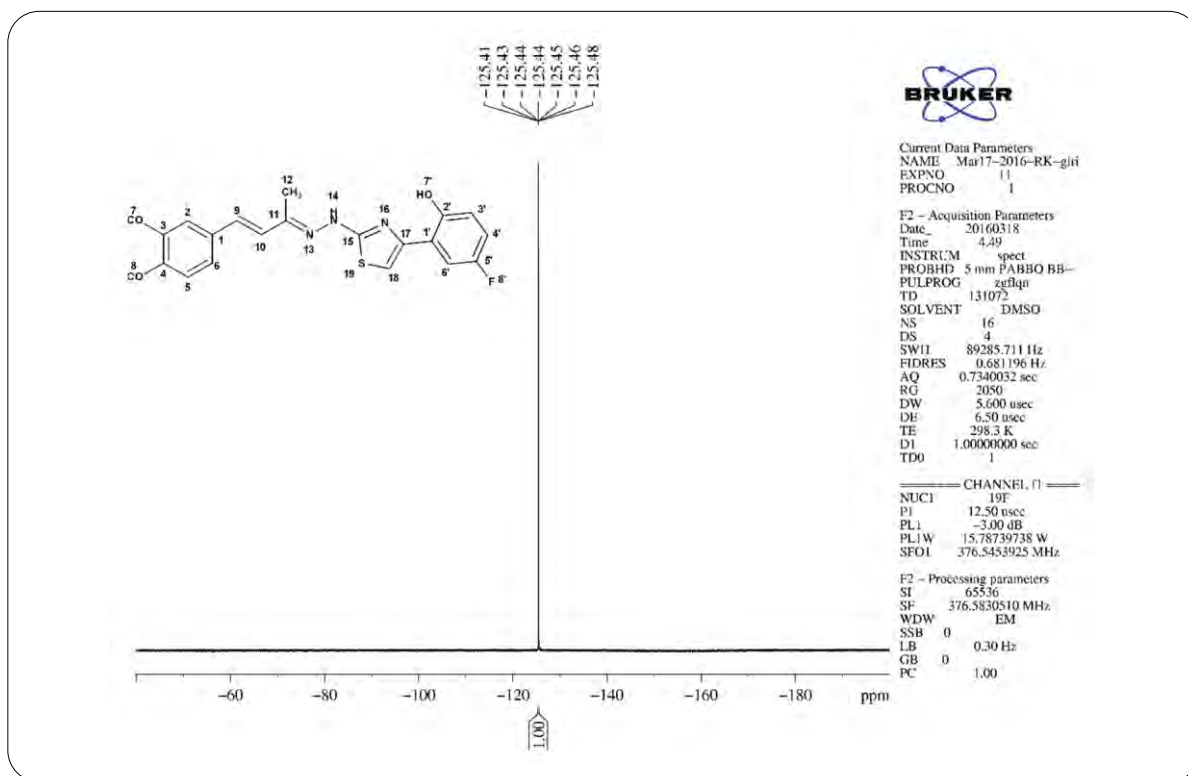
¹H NMR Spectrum of Compound 6n (chapter 3)

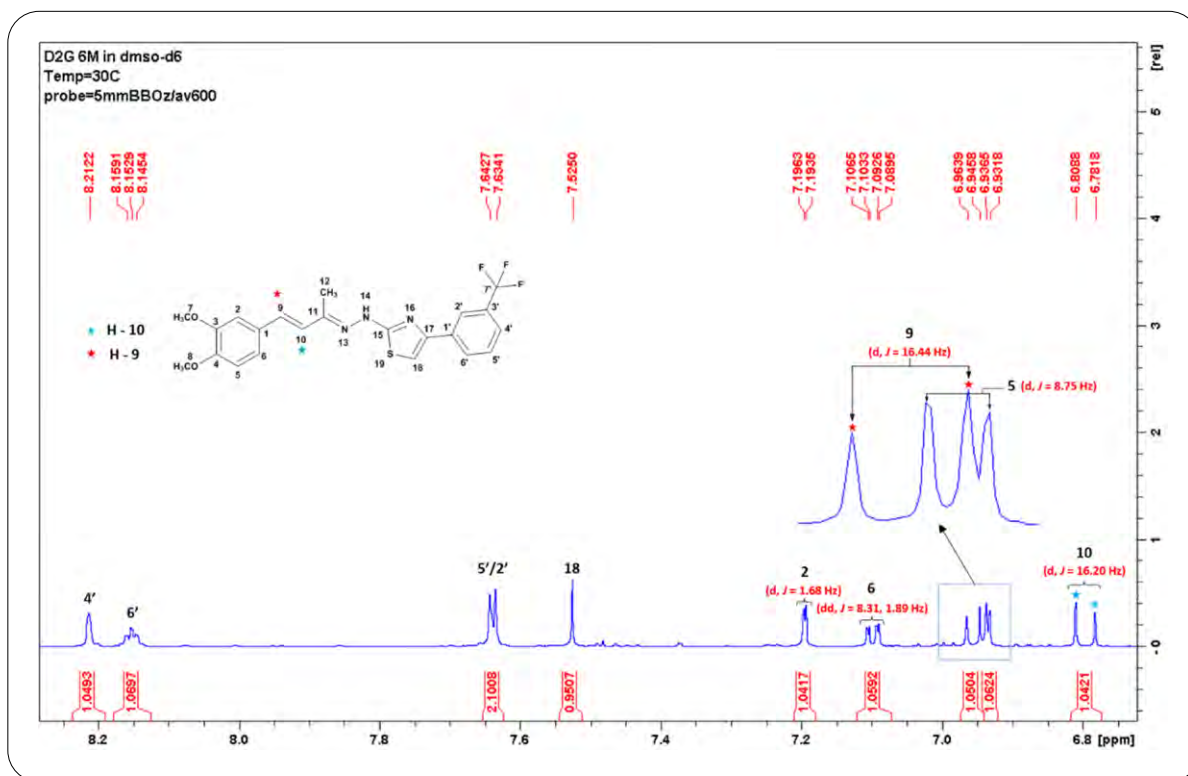
**¹³C NMR Spectrum of Compound 6n (chapter 3)****IR Spectrum of Compound 6n (chapter 3)**

**¹H NMR Spectrum of Compound 60 (chapter 3)****¹³C NMR Spectrum of Compound 60 (chapter 3)**

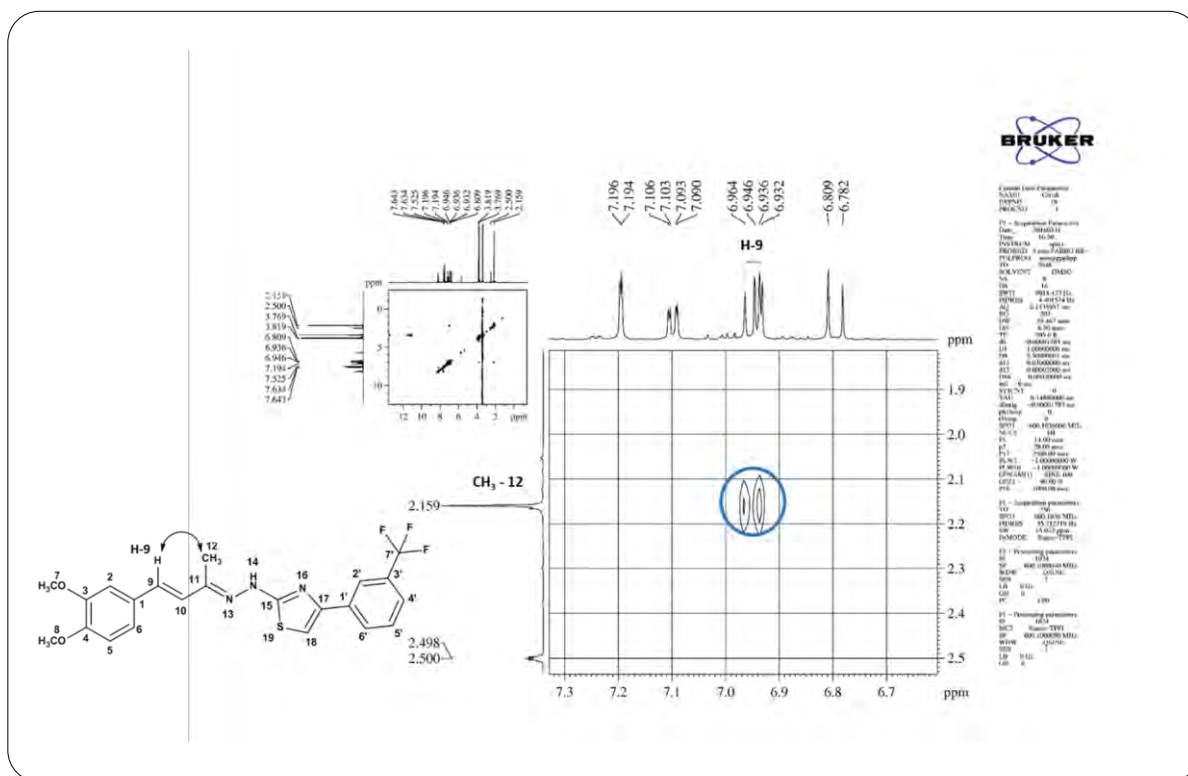


A section of the ^1H NMR spectrum (600 MHz) of compound 6k illustrating the merging of *trans* (*E*) olefinic proton (H-9) in aromatic region.

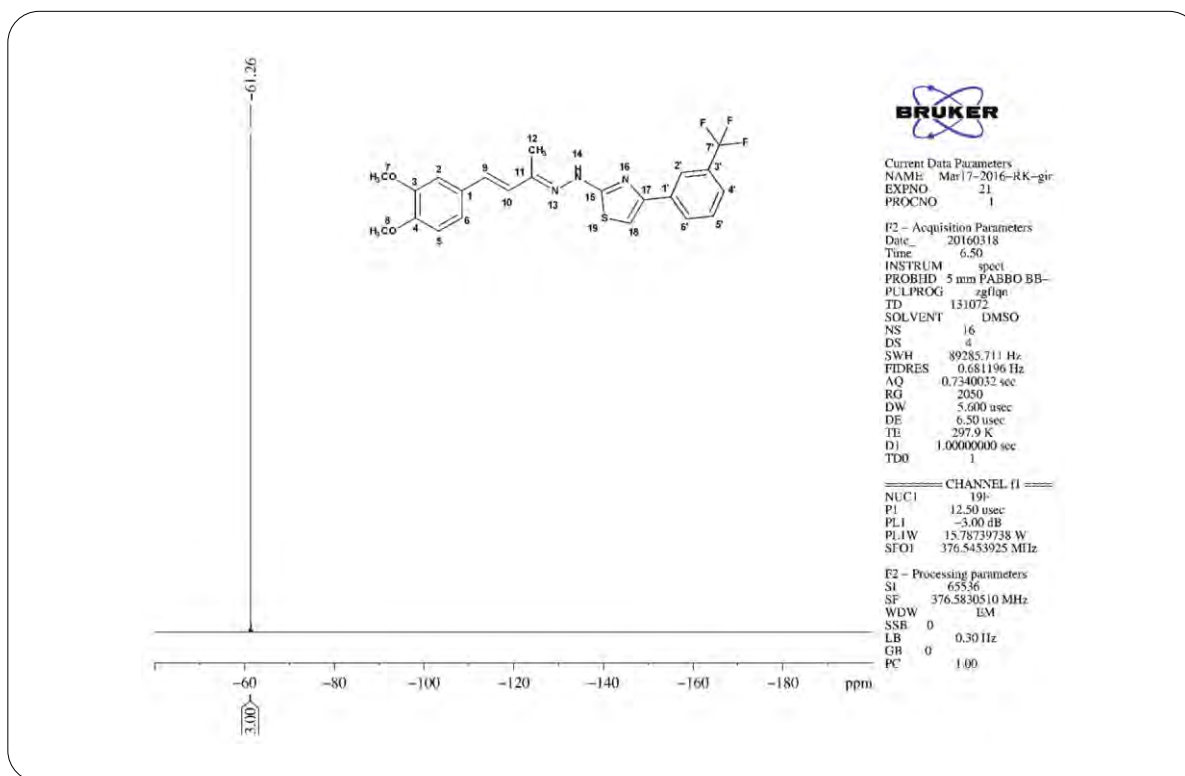
**¹⁹F NMR spectrum of compound 6k.**



A section of the ^1H NMR spectrum (600 MHz) of compound 6m illustrating the merging of *trans* (*E*) olefinic proton (H-9) in aromatic region.



NOESY correlation spectrum of compound 6m clarifying the *trans* (*E*) configuration of two olefinic protons (H-9 and H-10).

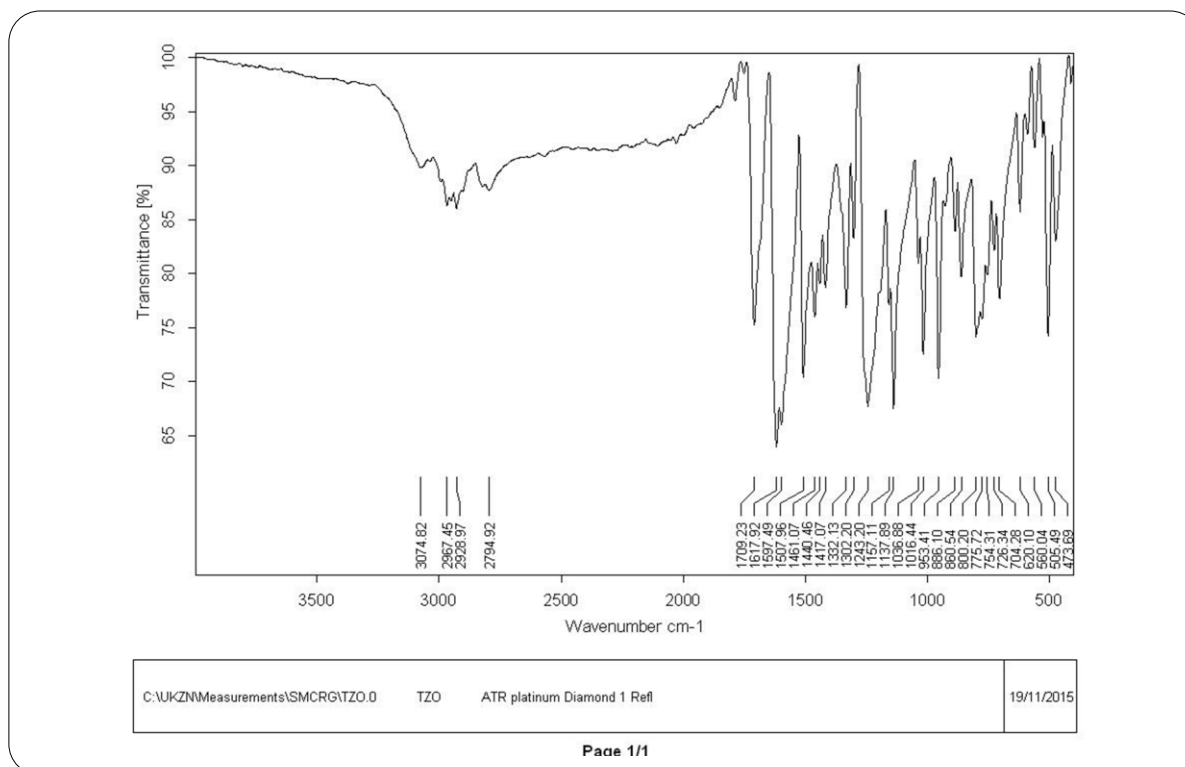
**¹⁹F NMR spectrum of compound 6m.**

APPENDIX - II**SUPPLEMENTARY INFORMATION****CHAPTER 4****Design and synthesis of novel styryl hydrazine thiazolidin-4-one hybrids impelled from Dehydrozingerone as potential antimycobacterial agents**

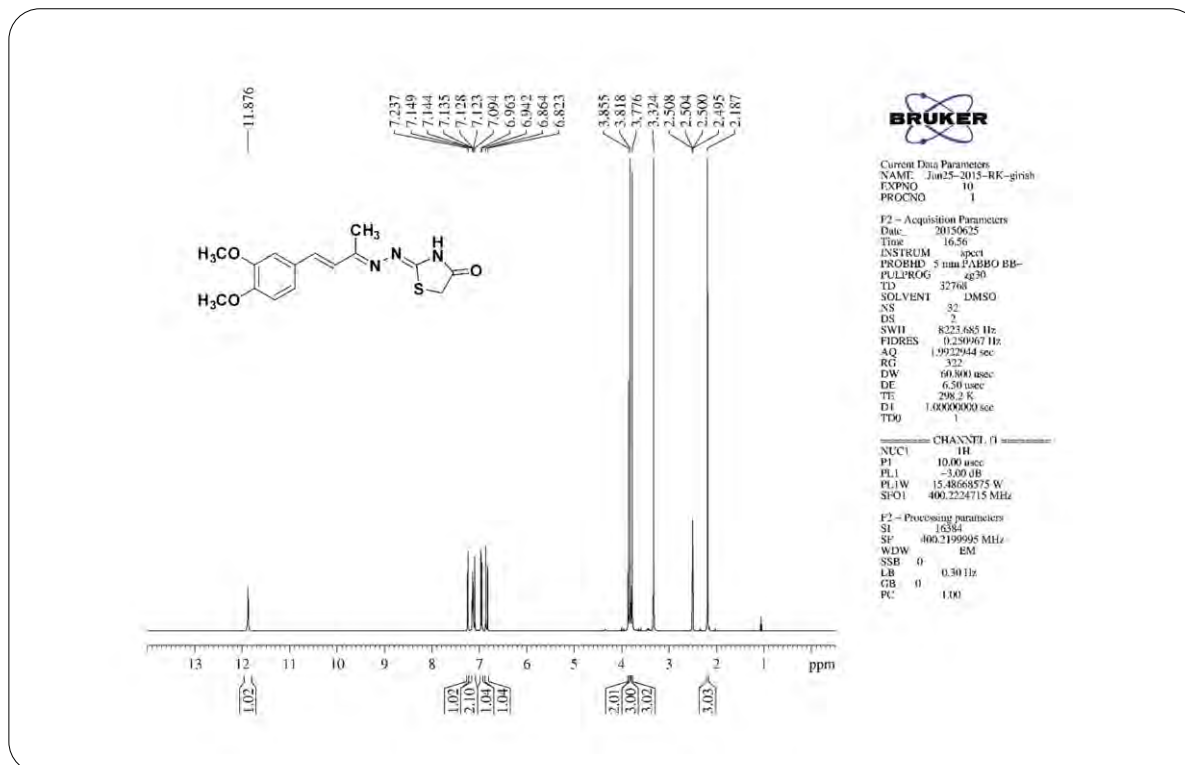
Girish A. Hampannavar^a, Mahesh B. Palkar^{b,a}, Mahamadhanif S. Shaikh^a, Srinivasulu Cherukupalli^a, Rajshekhar V. Karpoormath^{a*}

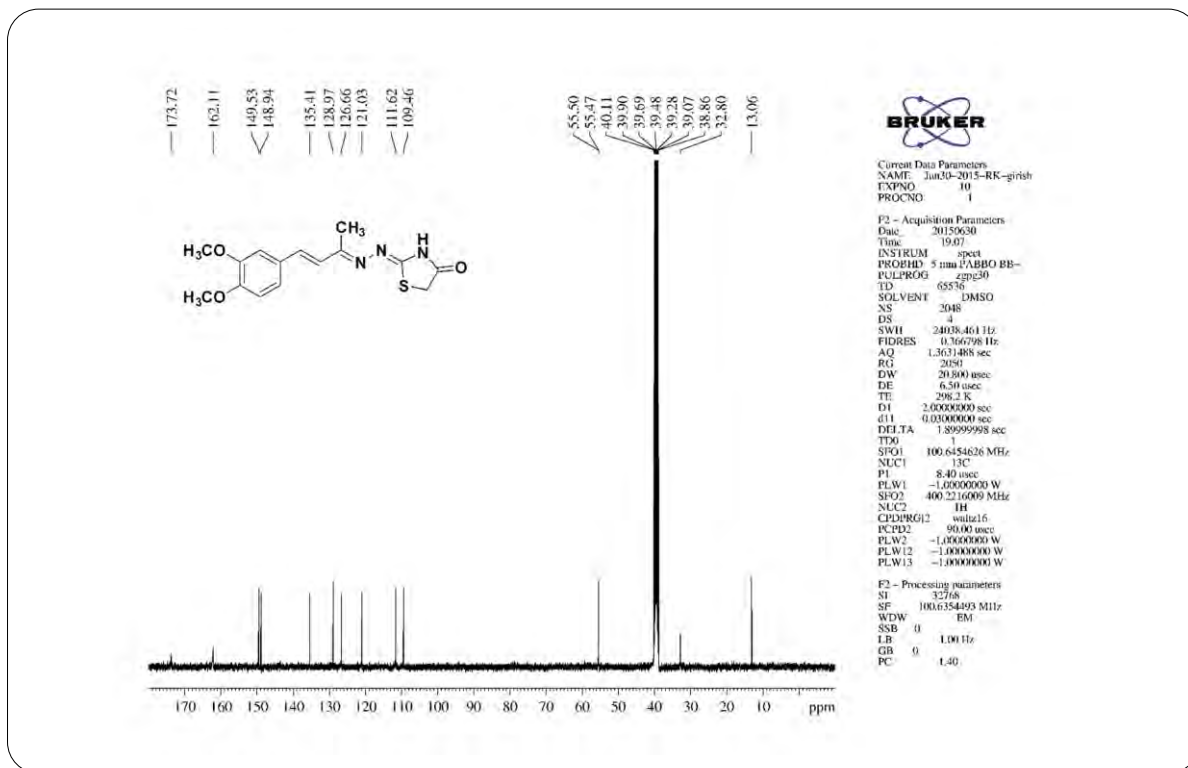
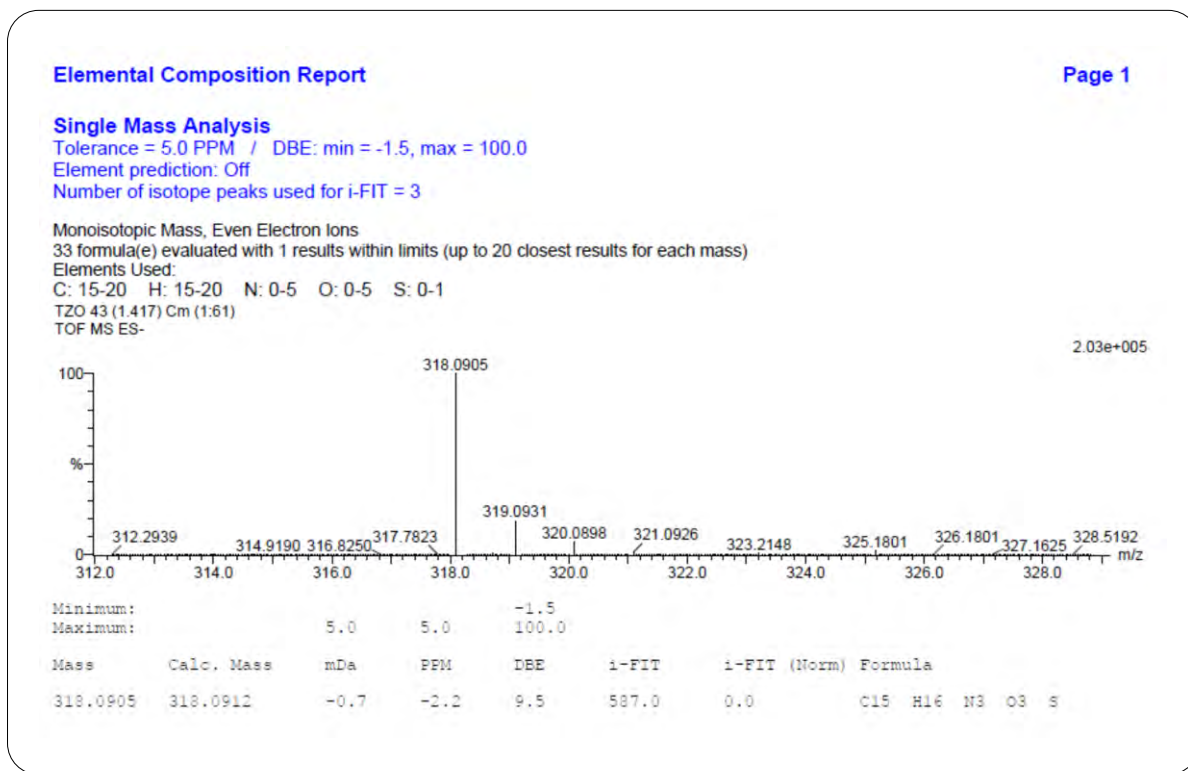
^a Department of Pharmaceutical Chemistry, Discipline of Pharmaceutical Sciences, College of Health Sciences, University of KwaZulu-Natal (Westville), Durban-4000, South Africa.

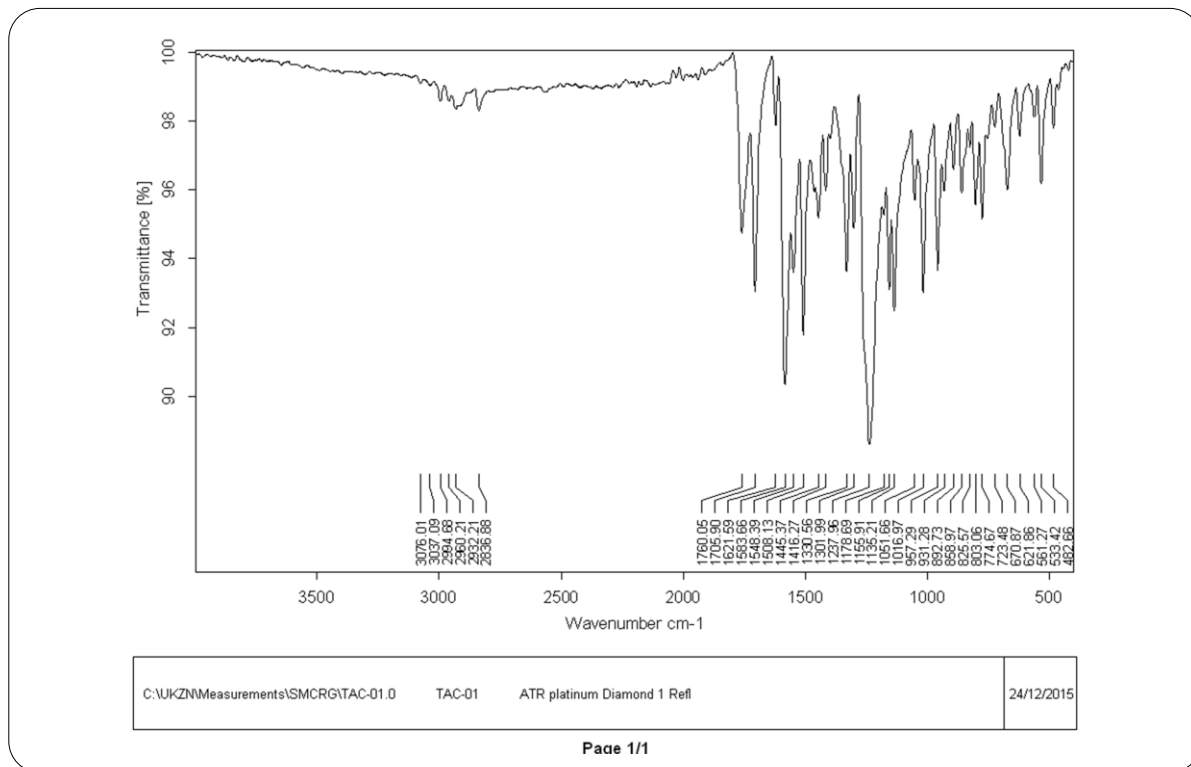
^b Department of Pharmaceutical Chemistry, K.L.E. University College of Pharmacy, Vidyanagar, Hubballi-580031, Karnataka, India.



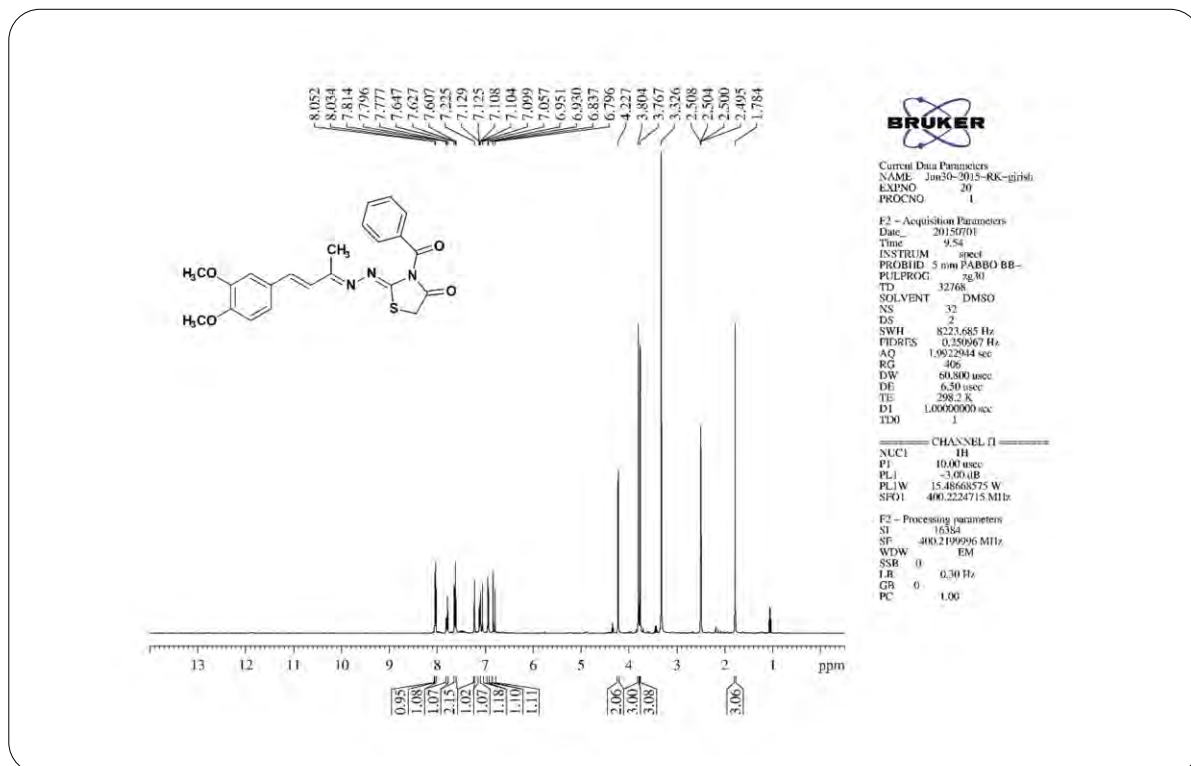
IR Spectrum of Compound 5 (chapter 4)

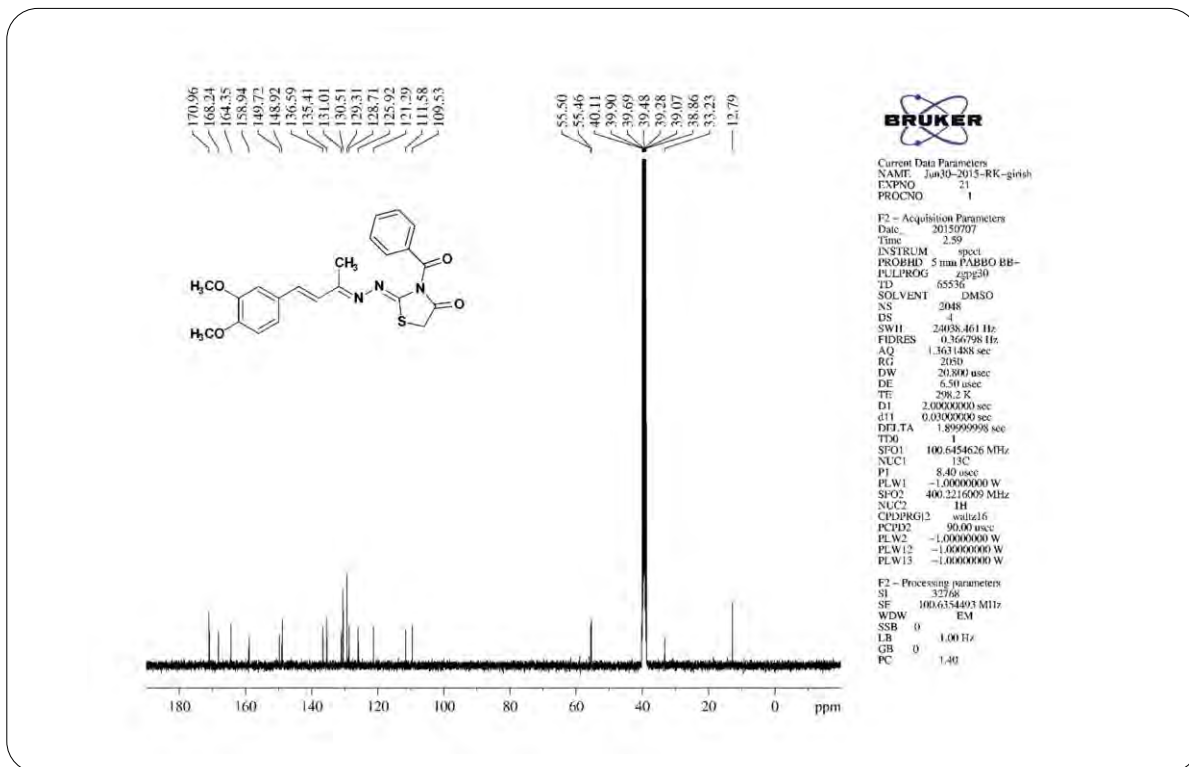
¹H NMR Spectrum of Compound 5 (chapter 4)

**¹³C NMR Spectrum of Compound 5 (chapter 4)****HRMS Spectrum of Compound 5 (chapter 4)**



IR Spectrum of Compound 7a (chapter 4)

¹H NMR Spectrum of Compound 7a (chapter 4)

**¹³C NMR Spectrum of Compound 7a (chapter 4)****Elemental Composition Report**

Page 1

Single Mass Analysis

Tolerance = 5.0 PPM / DBE: min = -1.5, max = 100.0

Element prediction: Off

Number of isotope peaks used for i-FIT = 3

Monoisotopic Mass, Even Electron Ions

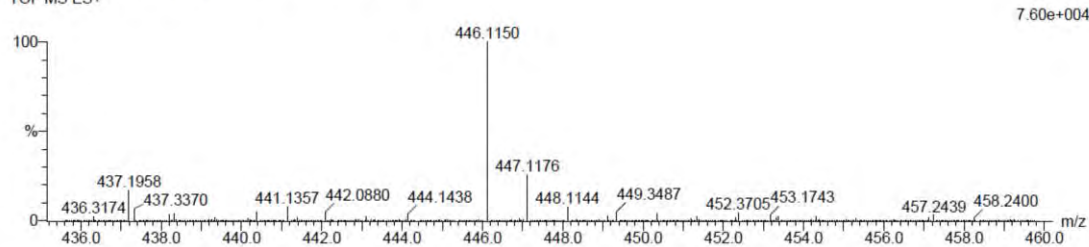
57 formula(e) evaluated with 1 results within limits (up to 20 closest results for each mass)

Elements Used:

C: 20-25 H: 20-25 N: 0-5 O: 0-5 Na: 0-1 S: 0-1

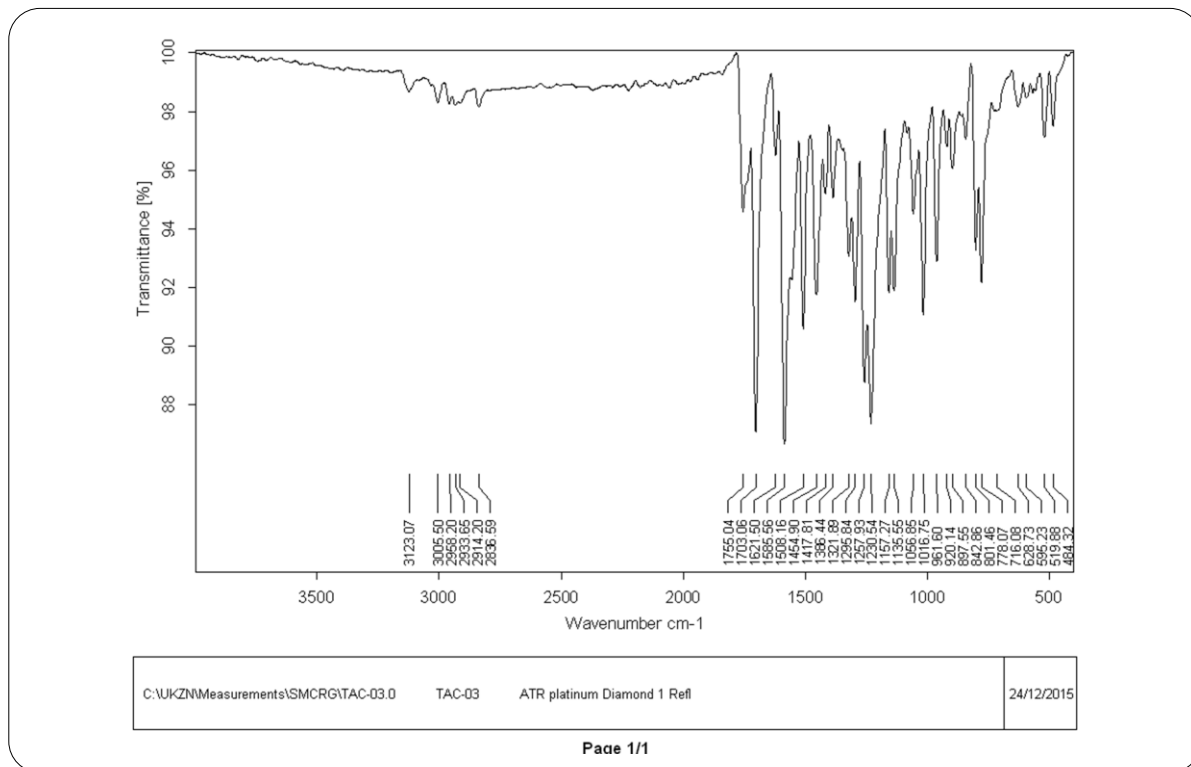
TAC-01 58 (1.956) Cm (1.60)

TOF MS ES+

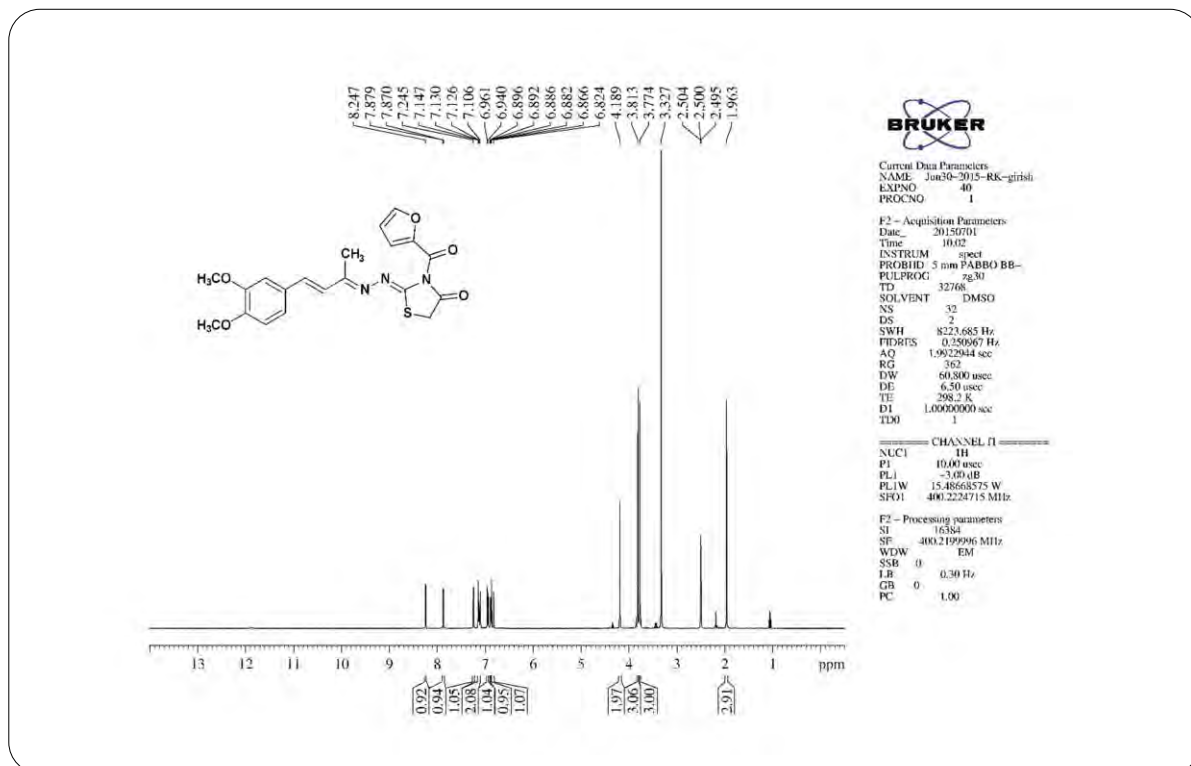


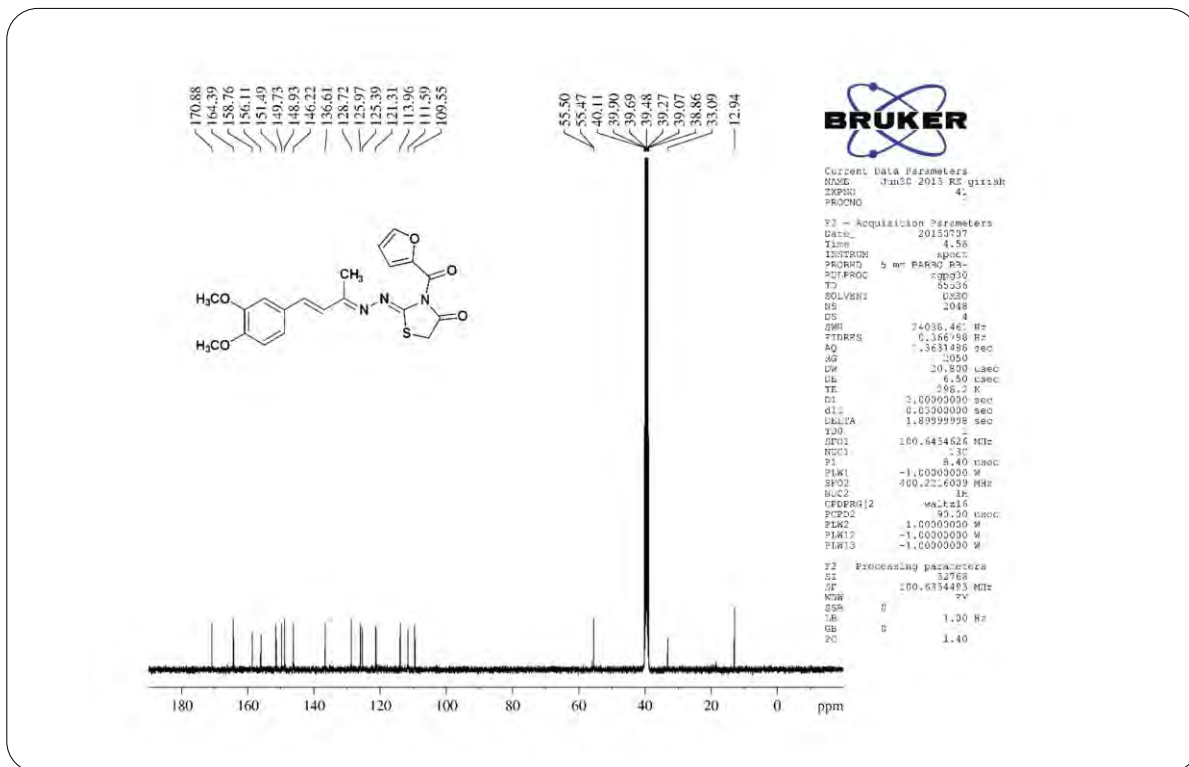
Mass	Calc. Mass	mDa	PPM	DBE	i-FIT	i-FIT (Norm)	Formula
446.1150	446.1150	0.0	0.0	13.5	468.5	0.0	C22 H21 N3 O4 Na S

HRMS Spectrum of Compound 7a (chapter 4)



IR Spectrum of Compound 7b (chapter 4)

¹H NMR Spectrum of Compound 7b (chapter 4)

**¹³C NMR Spectrum of Compound 7b (chapter 4)****Elemental Composition Report**

Page 1

Single Mass Analysis

Tolerance = 5.0 PPM / DBE: min = -1.5, max = 100.0

Element prediction: Off

Number of isotope peaks used for i-FIT = 3

Monoisotopic Mass, Even Electron Ions

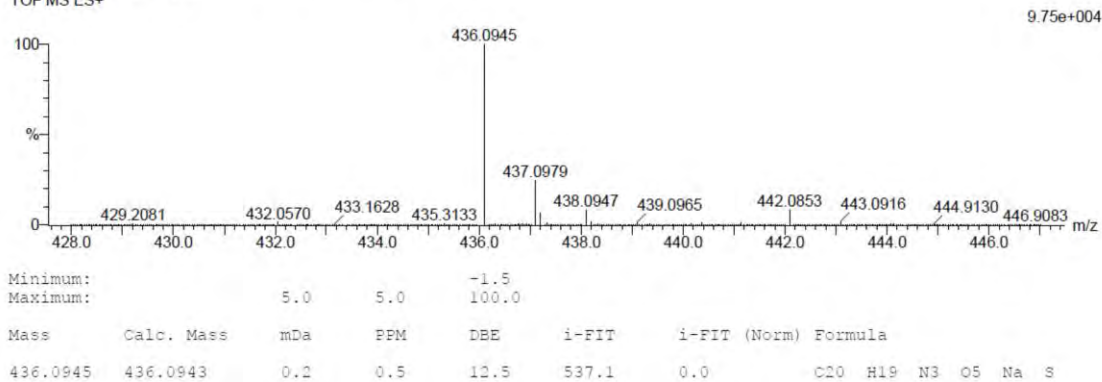
53 formula(e) evaluated with 1 results within limits (up to 20 closest results for each mass)

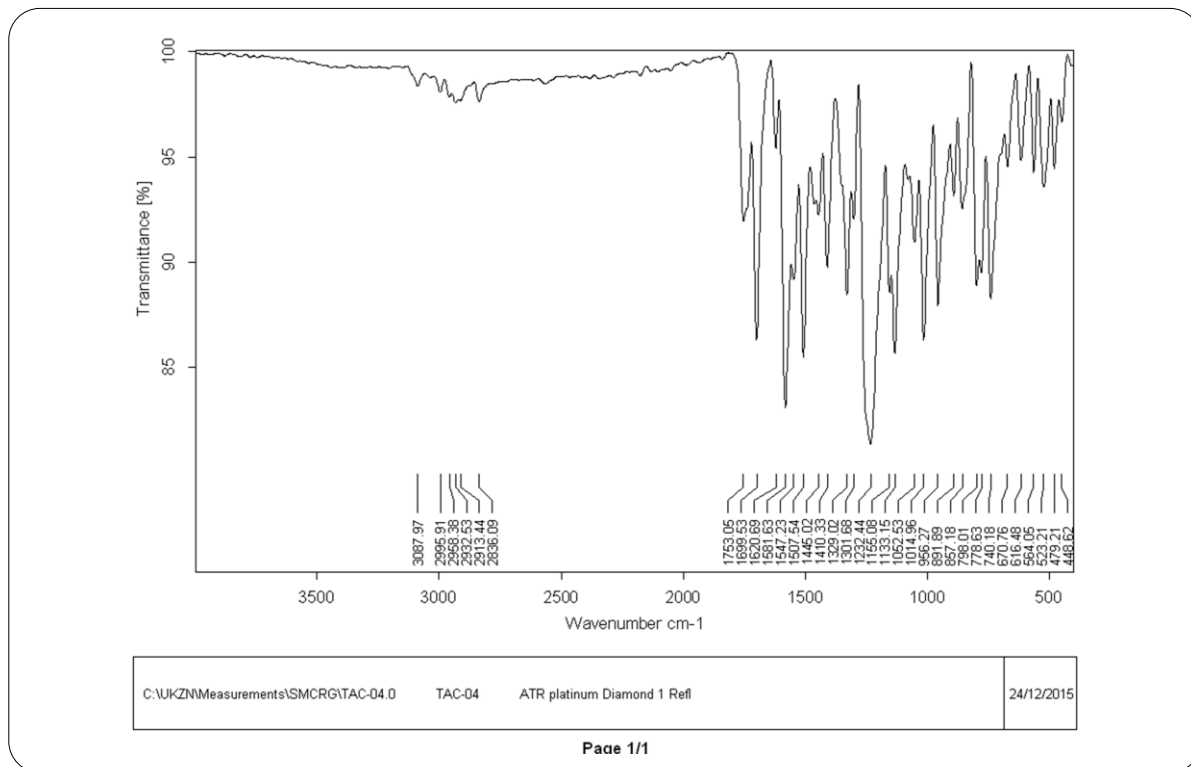
Elements Used:

C: 20-25 H: 15-20 N: 0-5 O: 0-5 Na: 0-1 S: 0-1

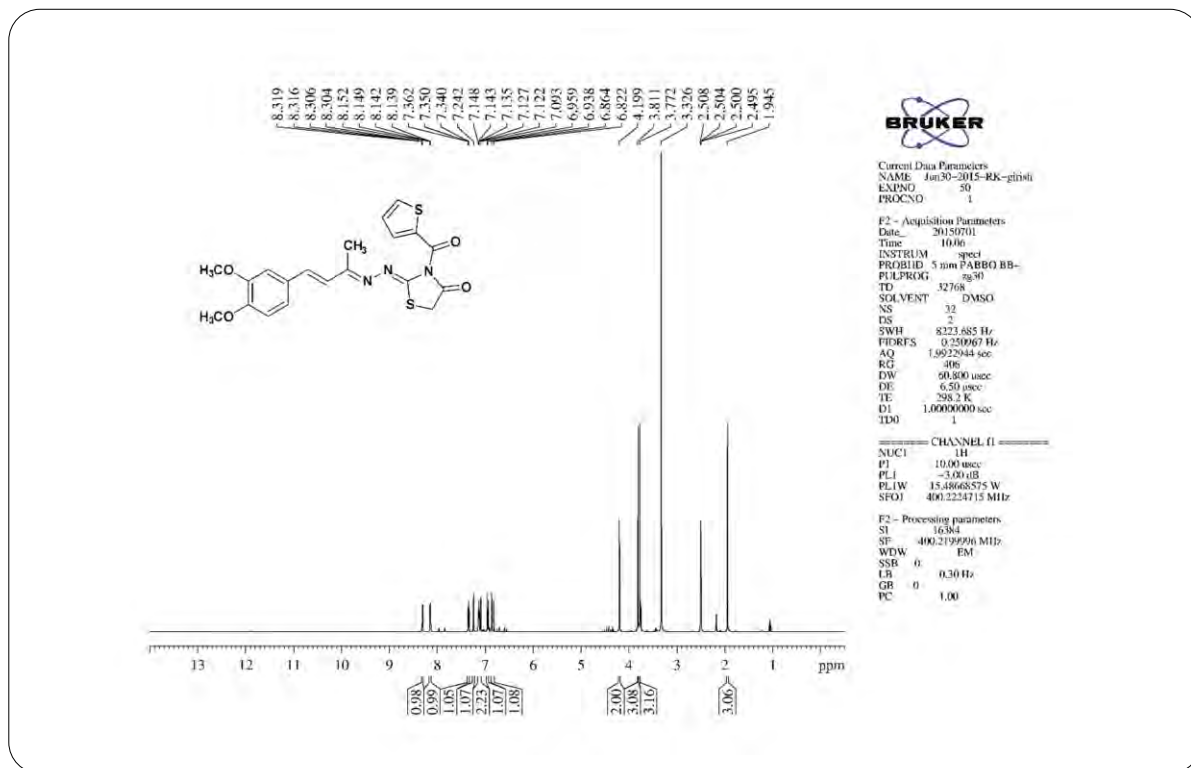
TAC-03 16 (0.506) Cm (1.61)

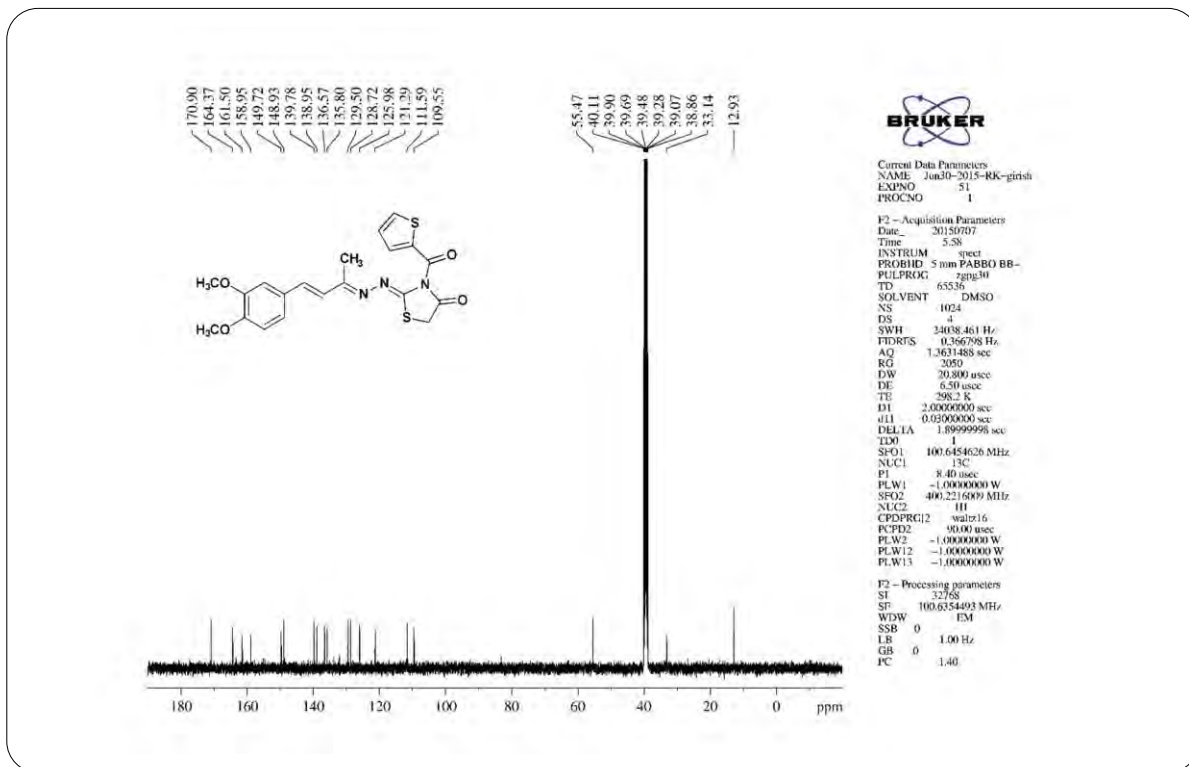
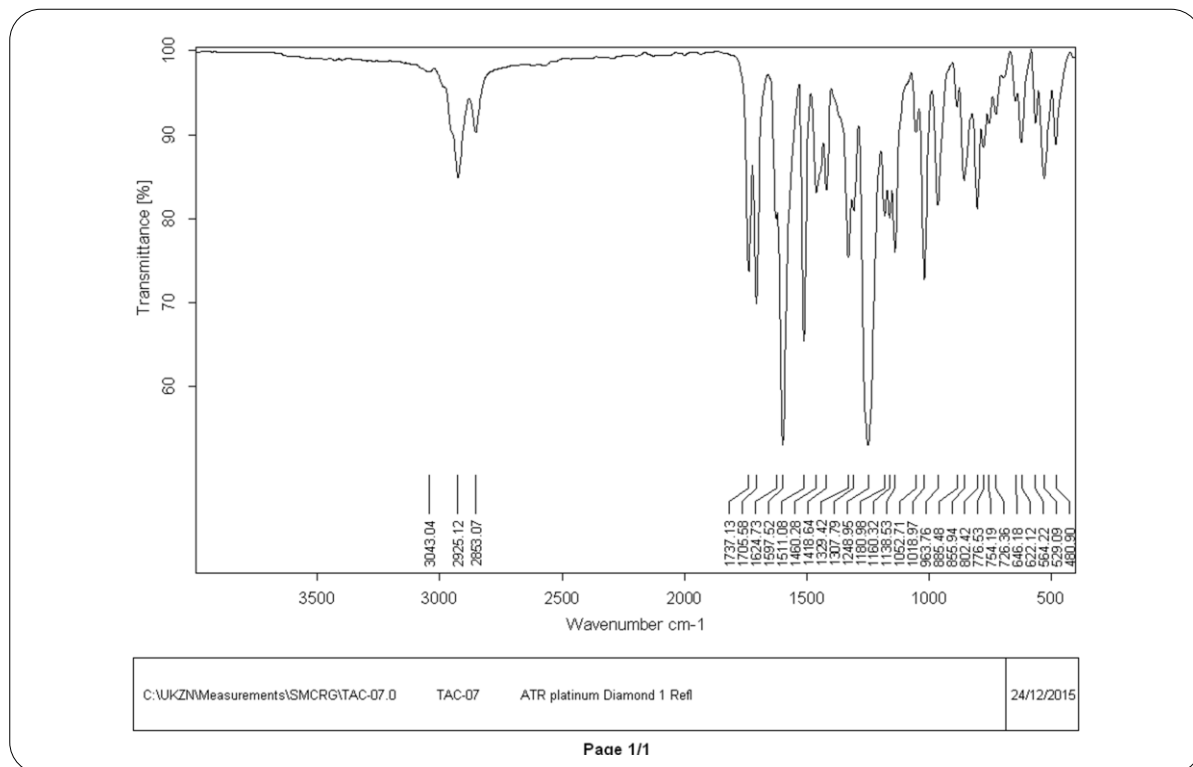
TOF MS ES+

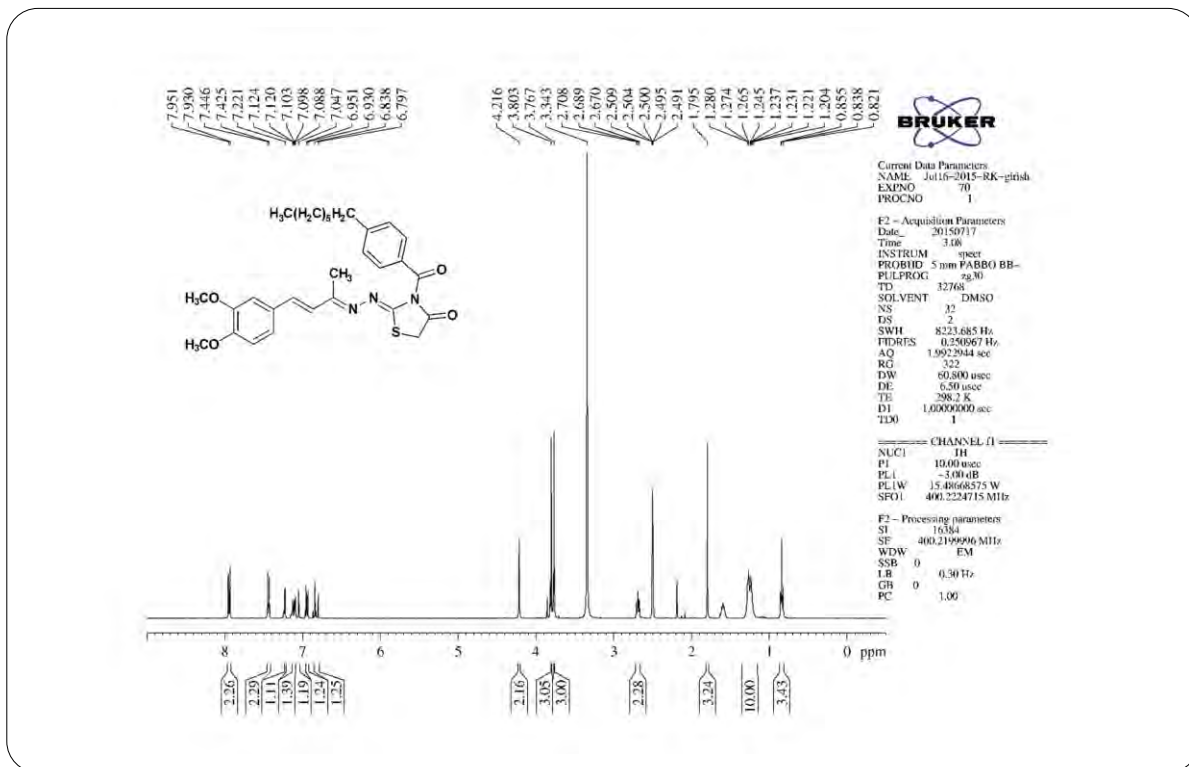
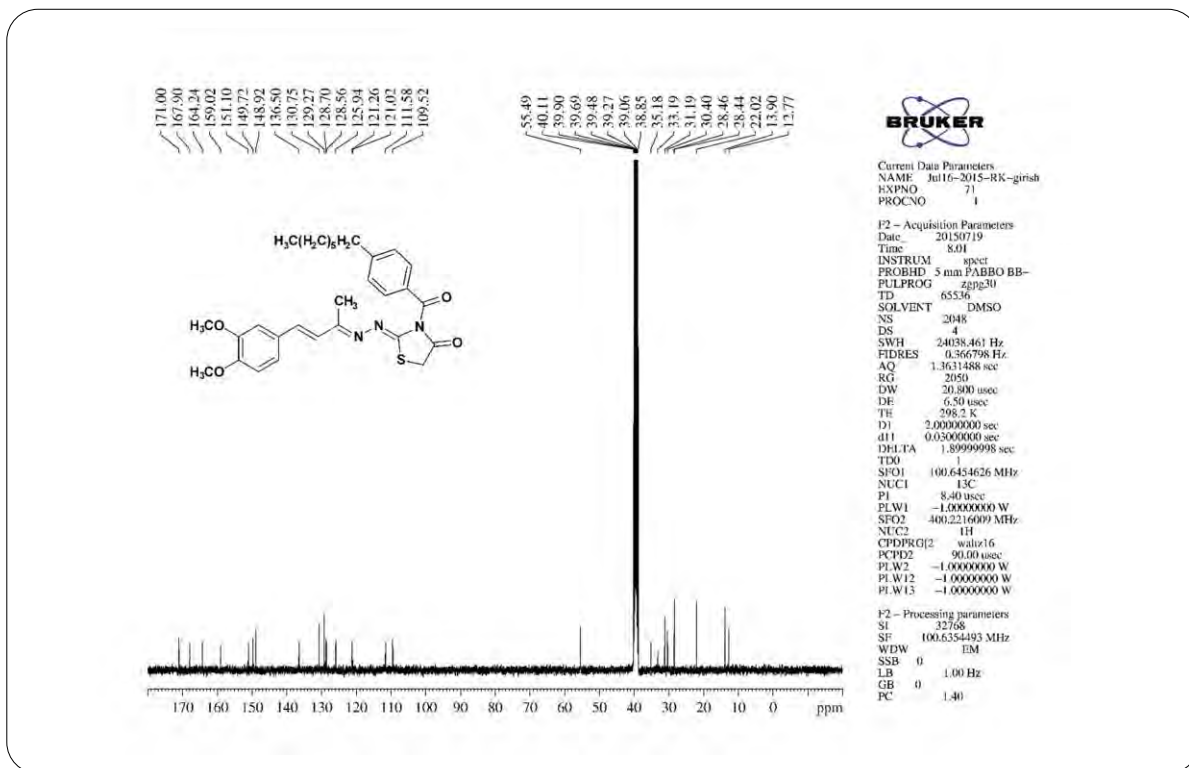
**HRMS Spectrum of Compound 7b (chapter 4)**

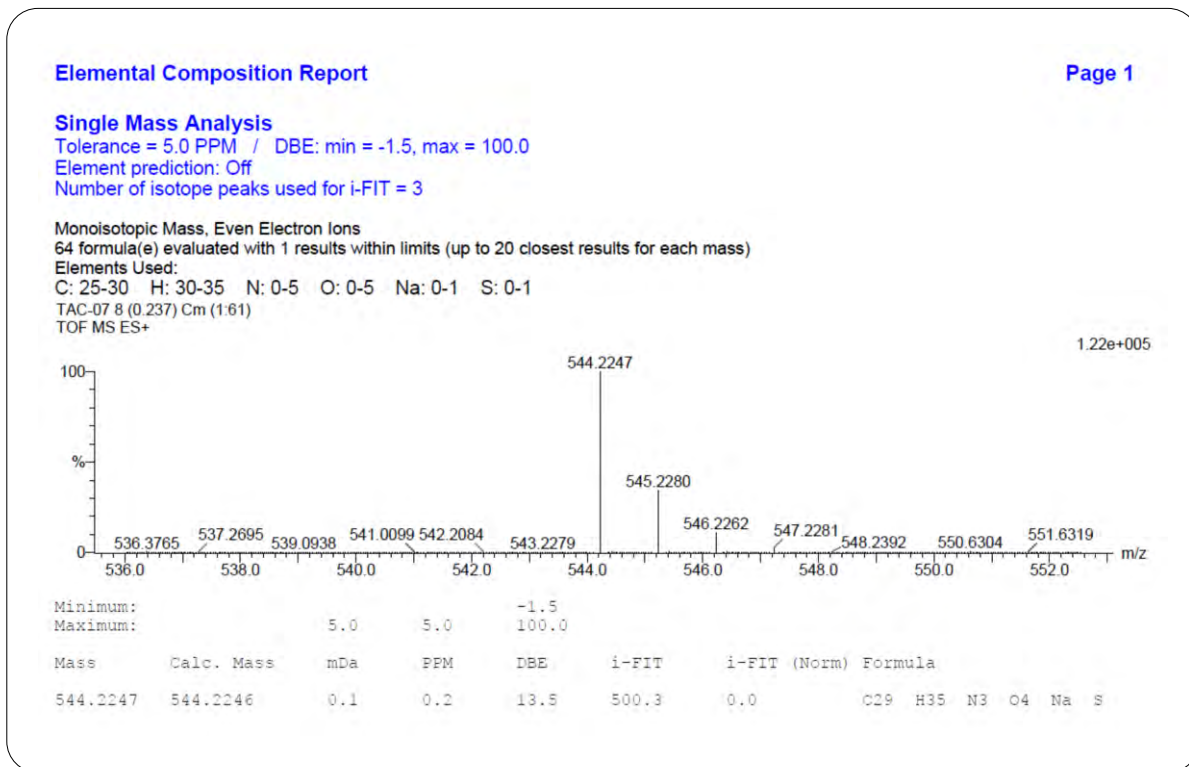


IR Spectrum of Compound 7c (chapter 4)

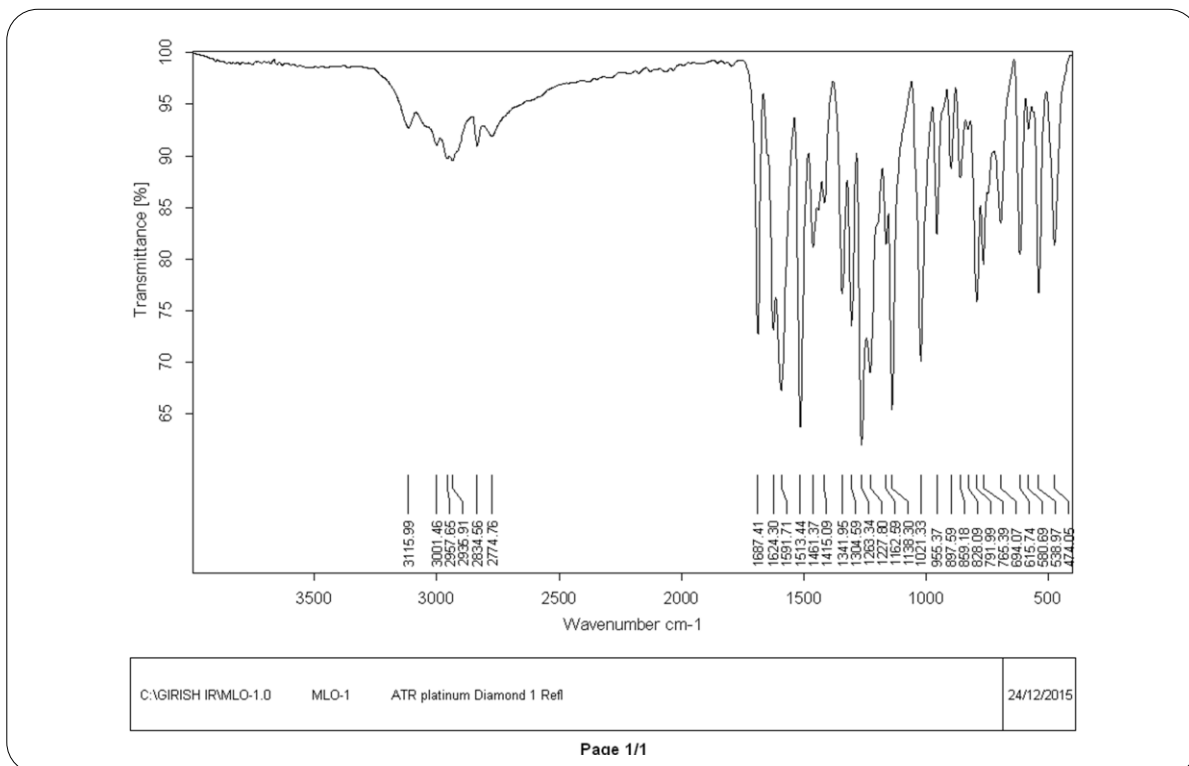
¹H NMR Spectrum of Compound 7c (chapter 4)

**¹³C NMR Spectrum of Compound 7c (chapter 4)****IR Spectrum of Compound 7d (chapter 4)**

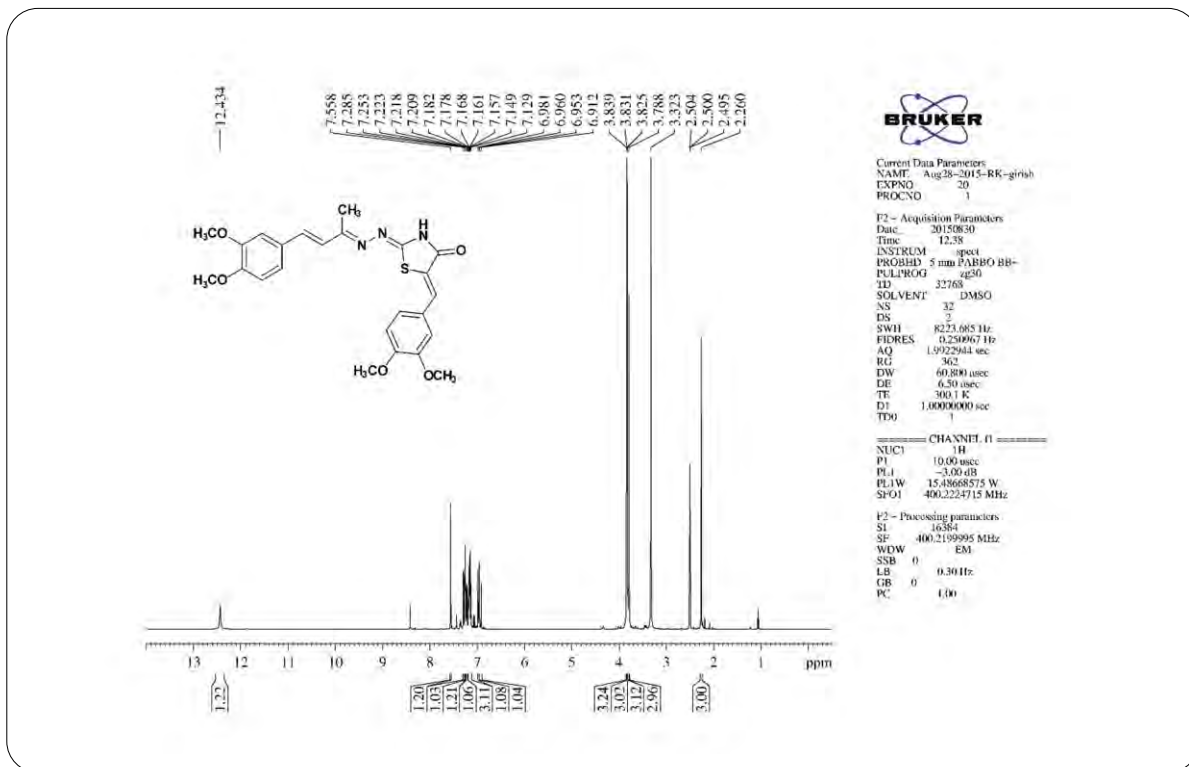
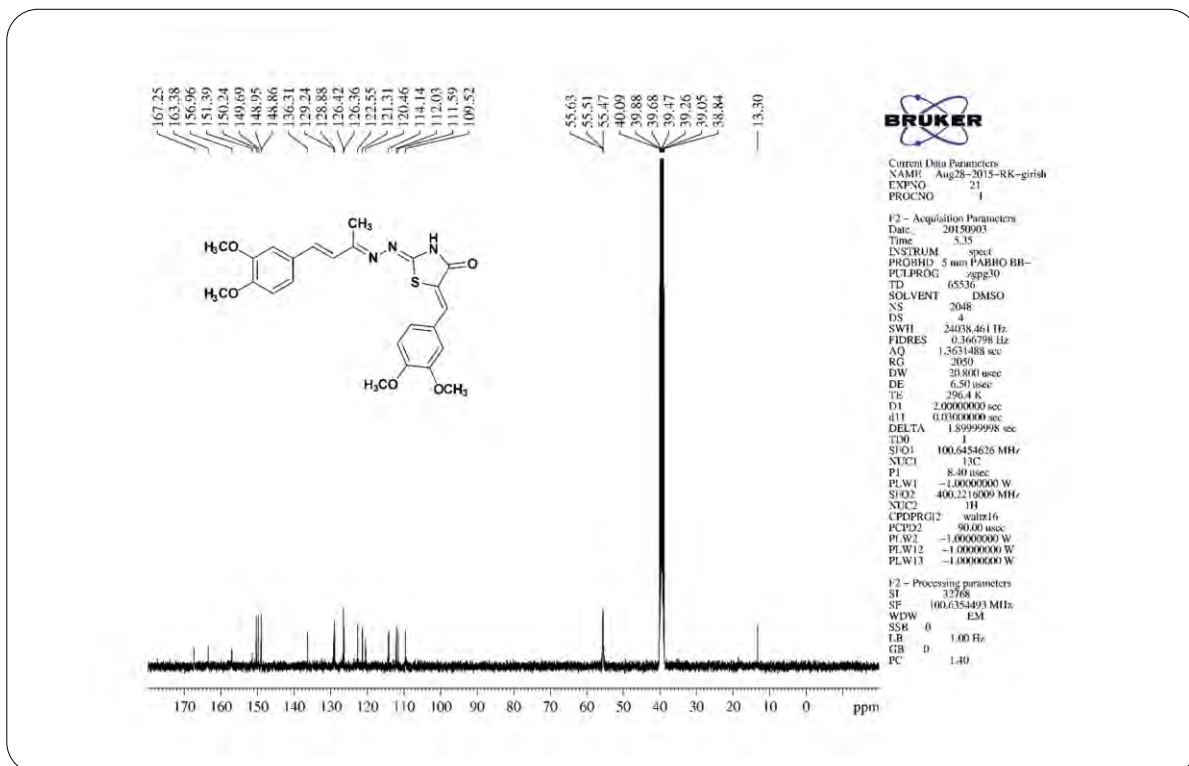
**¹H NMR Spectrum of Compound 7d (chapter 4)****¹³C NMR Spectrum of Compound 7d (chapter 4)**

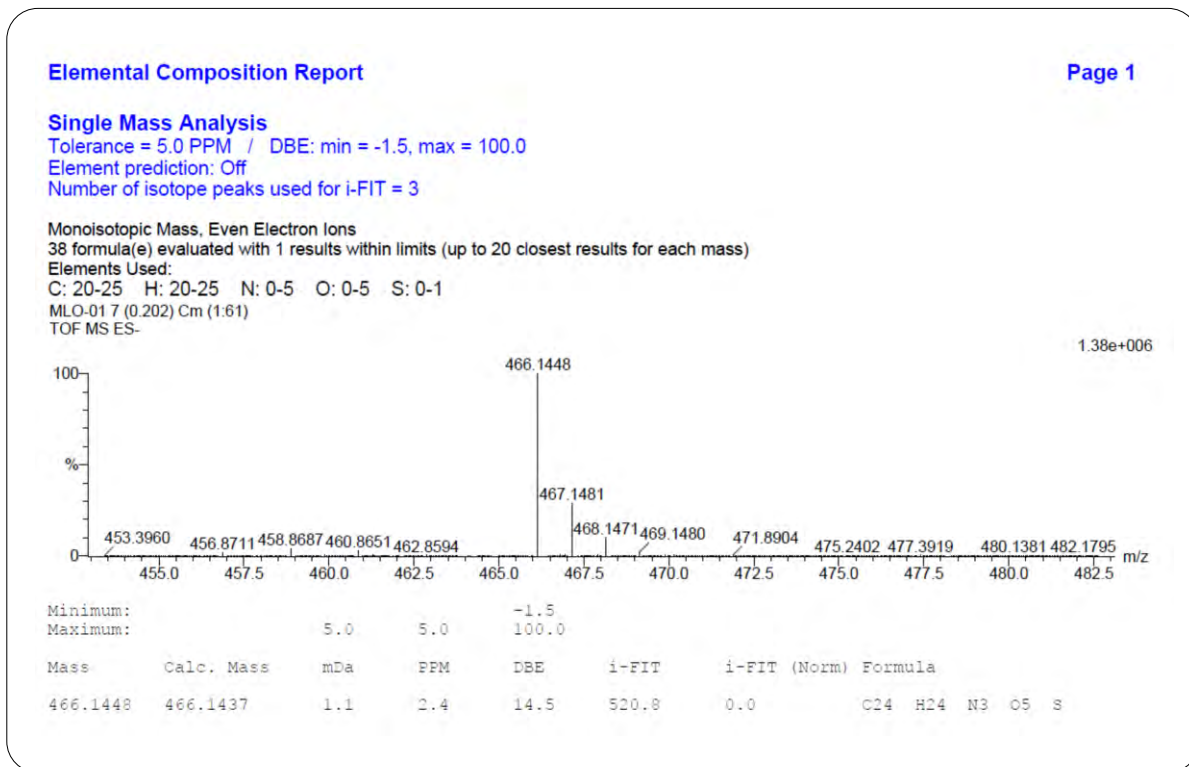


HRMS Spectrum of Compound 7d (chapter 4)

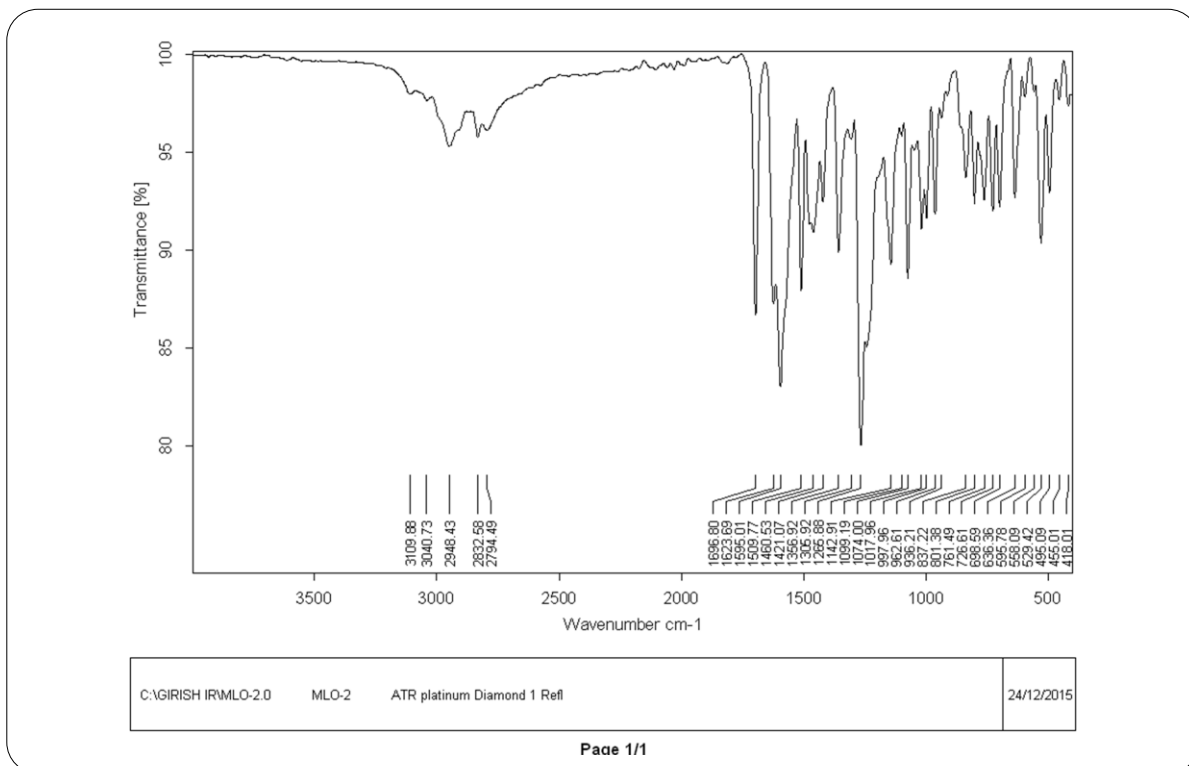


IR Spectrum of Compound 10a (chapter 4)

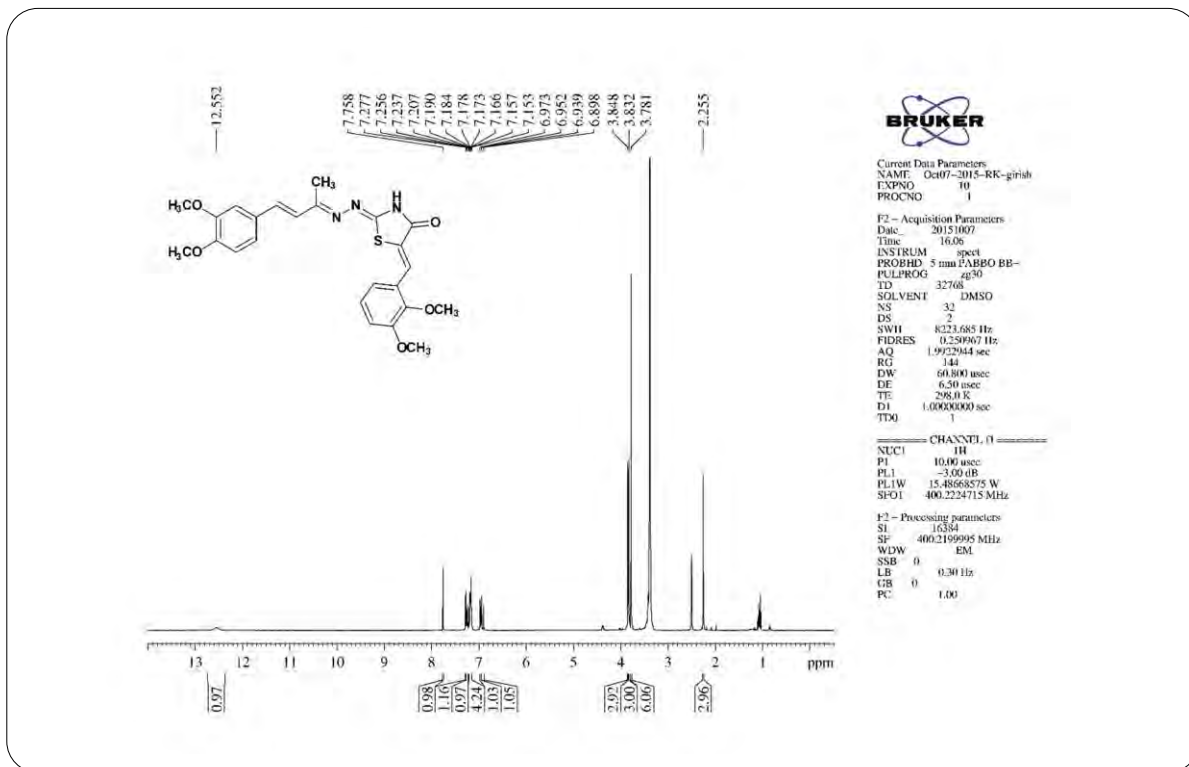
**¹H NMR Spectrum of Compound 10a (chapter 4)****¹³C NMR Spectrum of Compound 10a (chapter 4)**



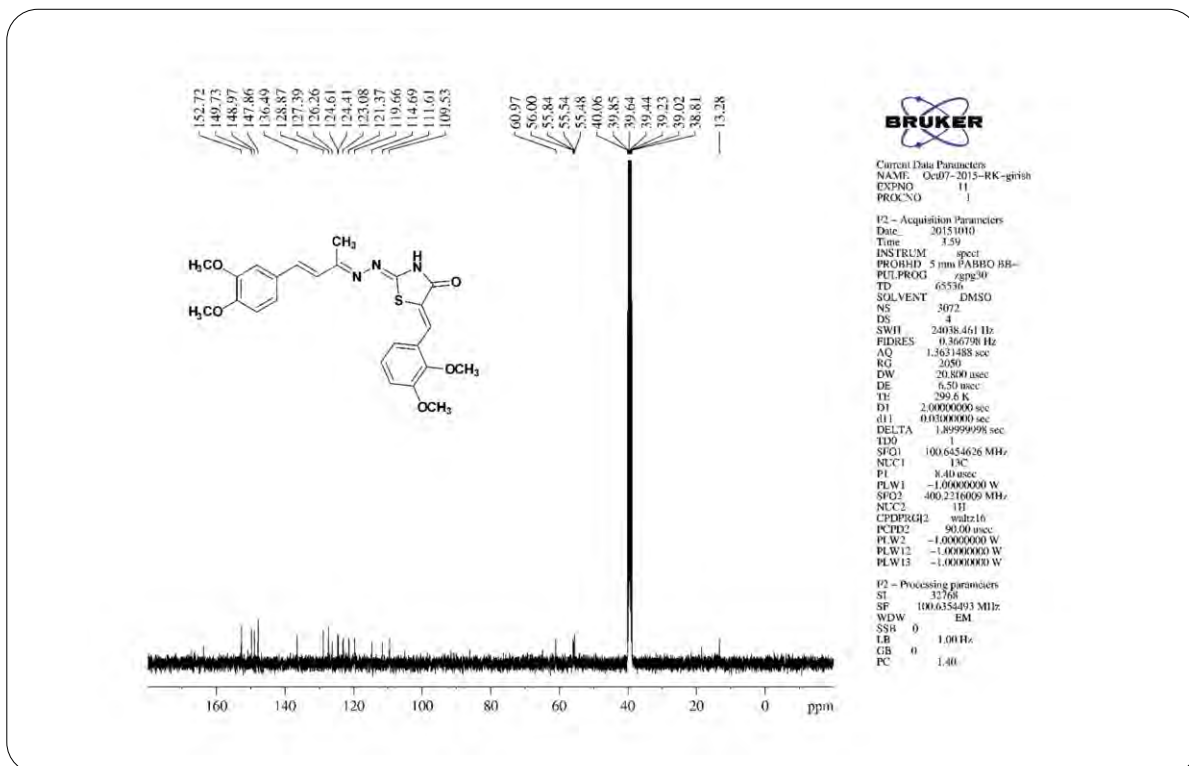
HRMS Spectrum of Compound 10a (chapter 4)



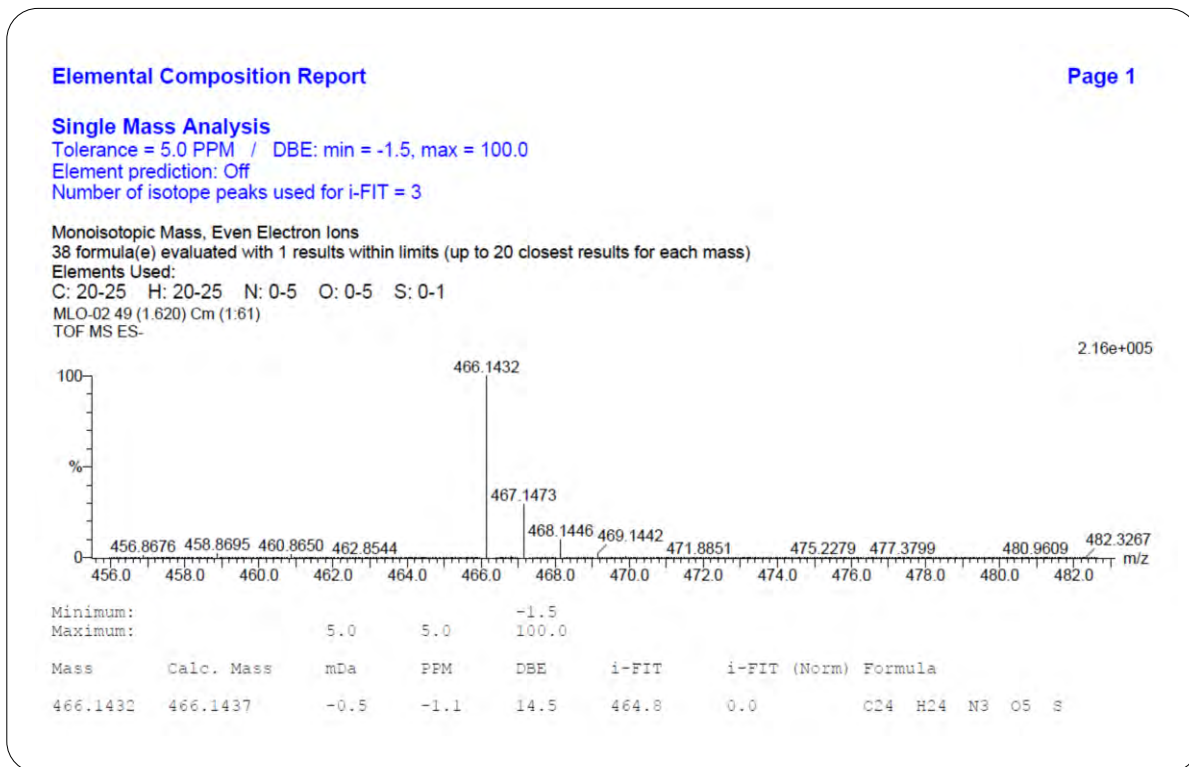
IR Spectrum of Compound 10b (chapter 4)



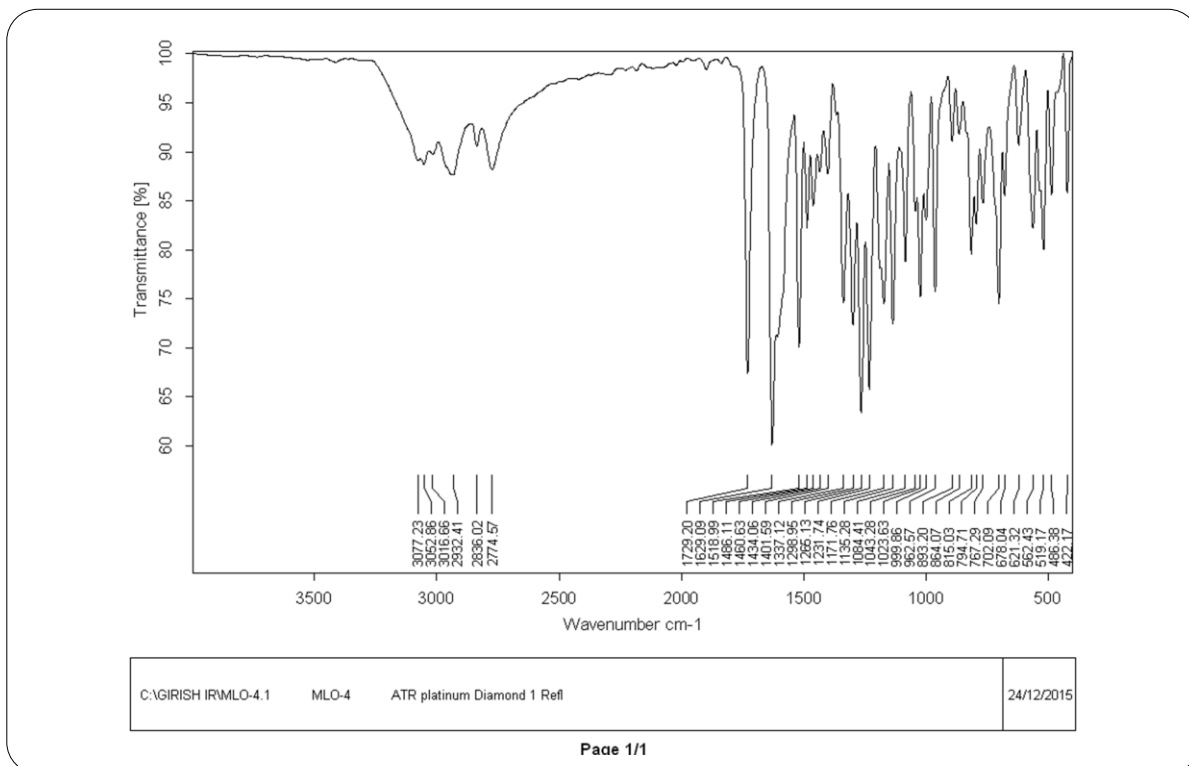
¹H NMR Spectrum of Compound 10b (chapter 4)



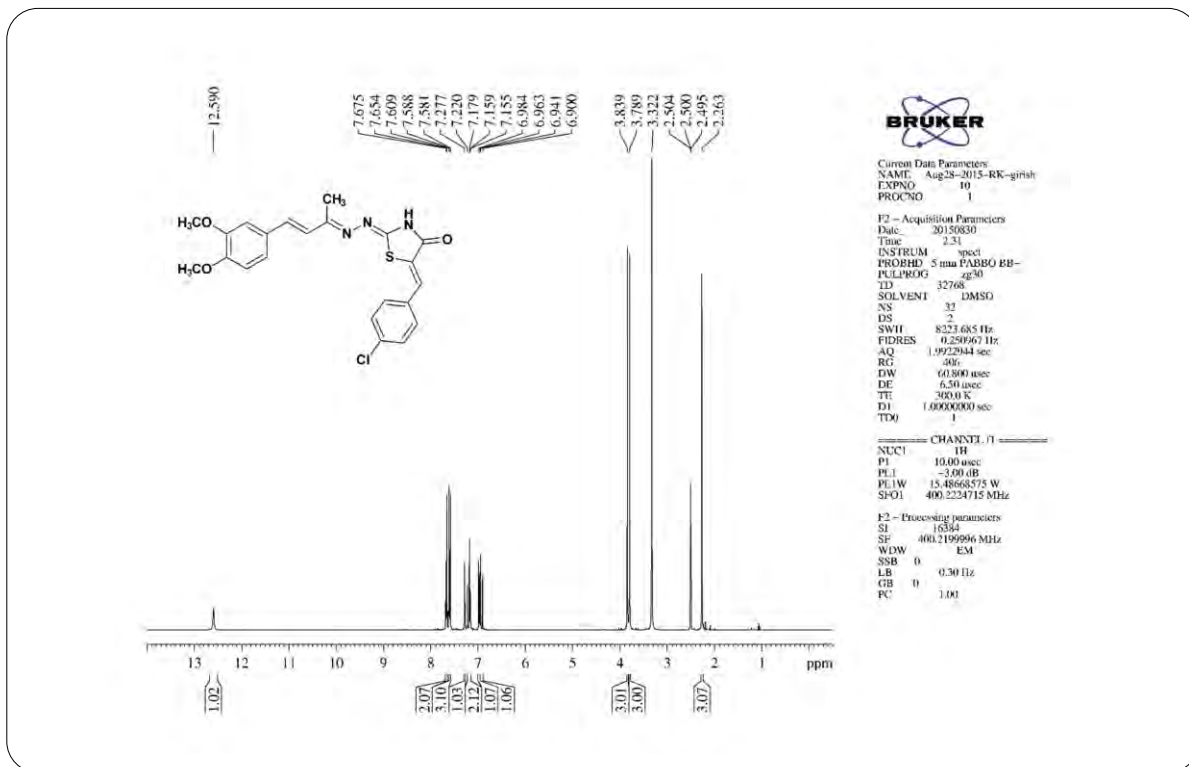
¹³C NMR Spectrum of Compound 10b (chapter 4)



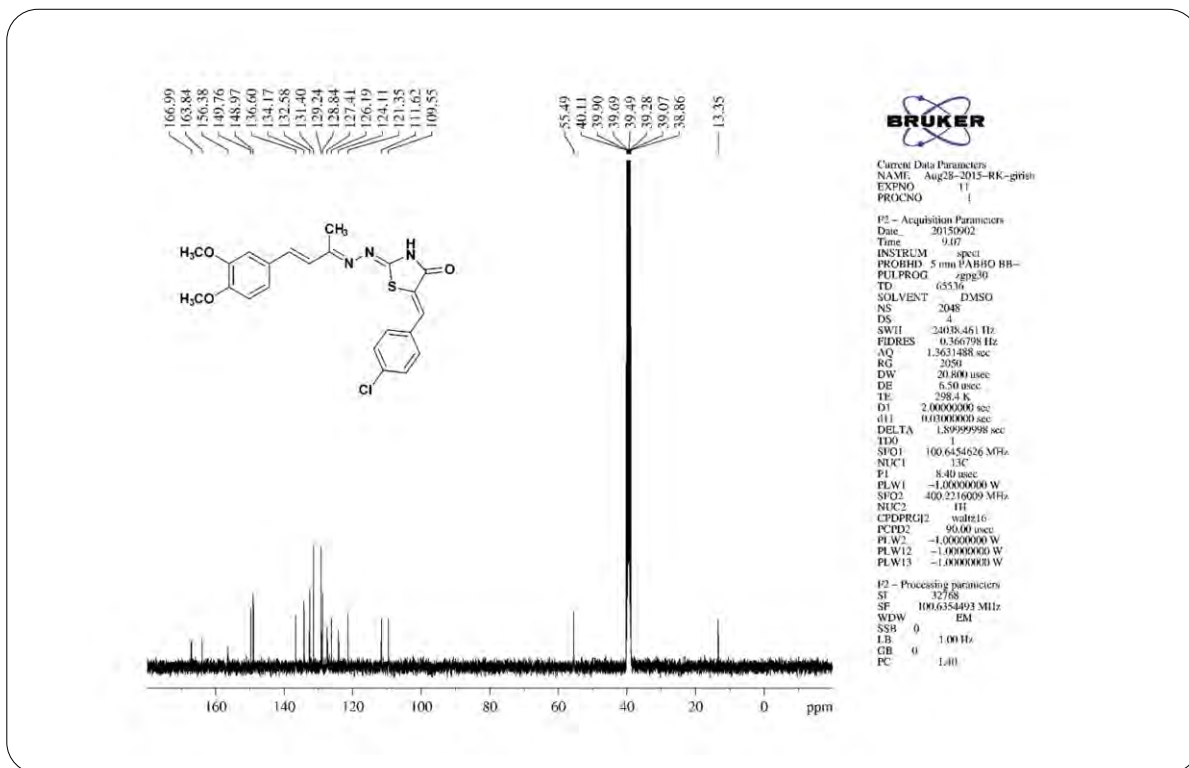
HRMS Spectrum of Compound 10b (chapter 4)



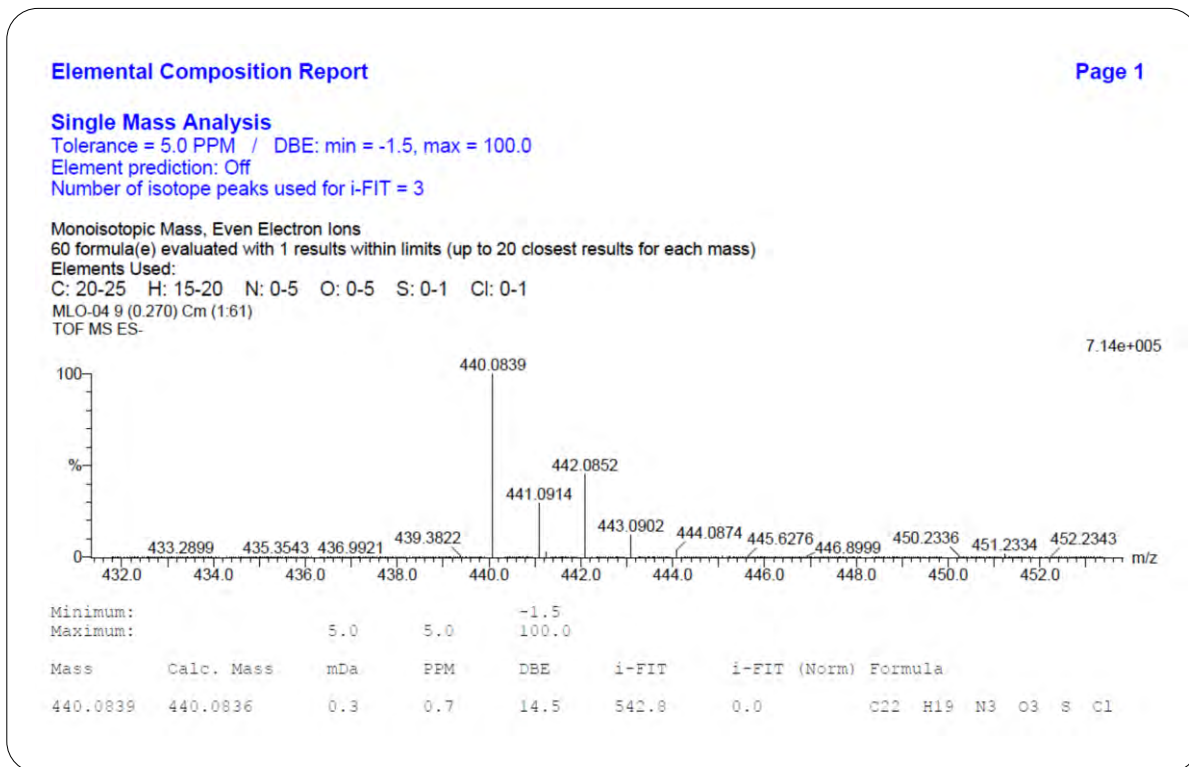
IR Spectrum of Compound 10c (chapter 4)



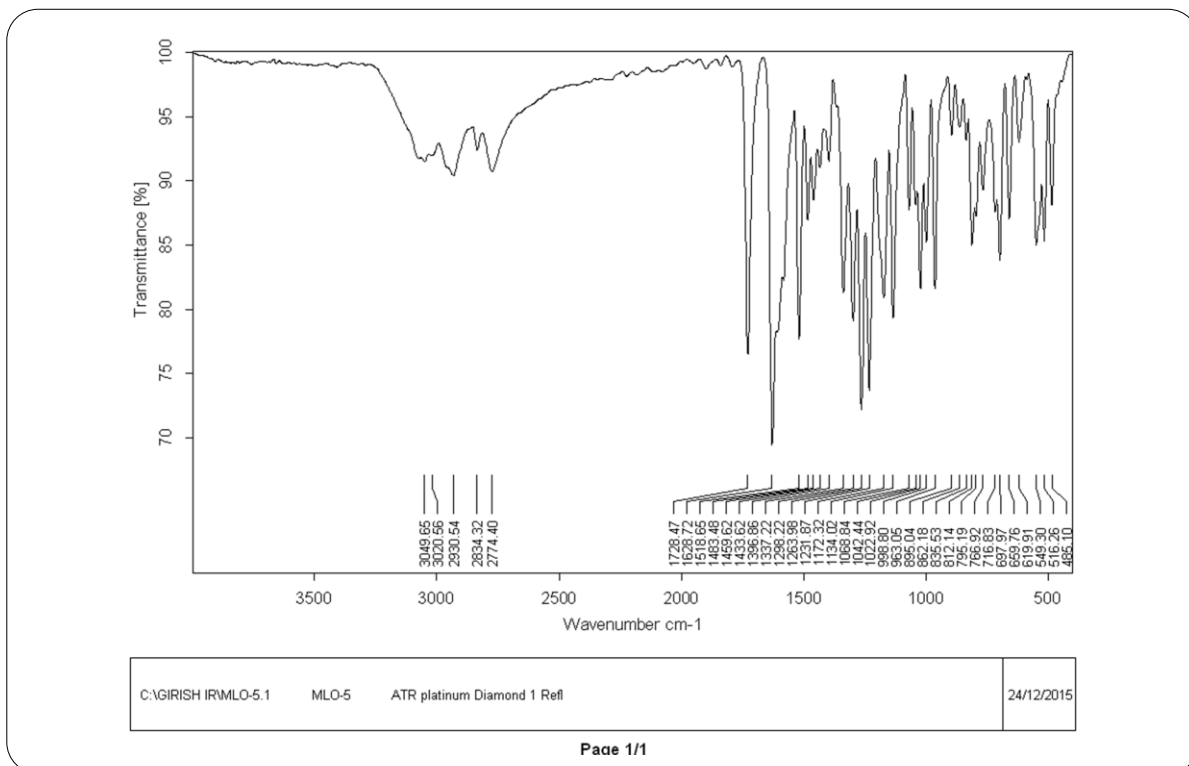
¹H NMR Spectrum of Compound 10c (chapter 4)



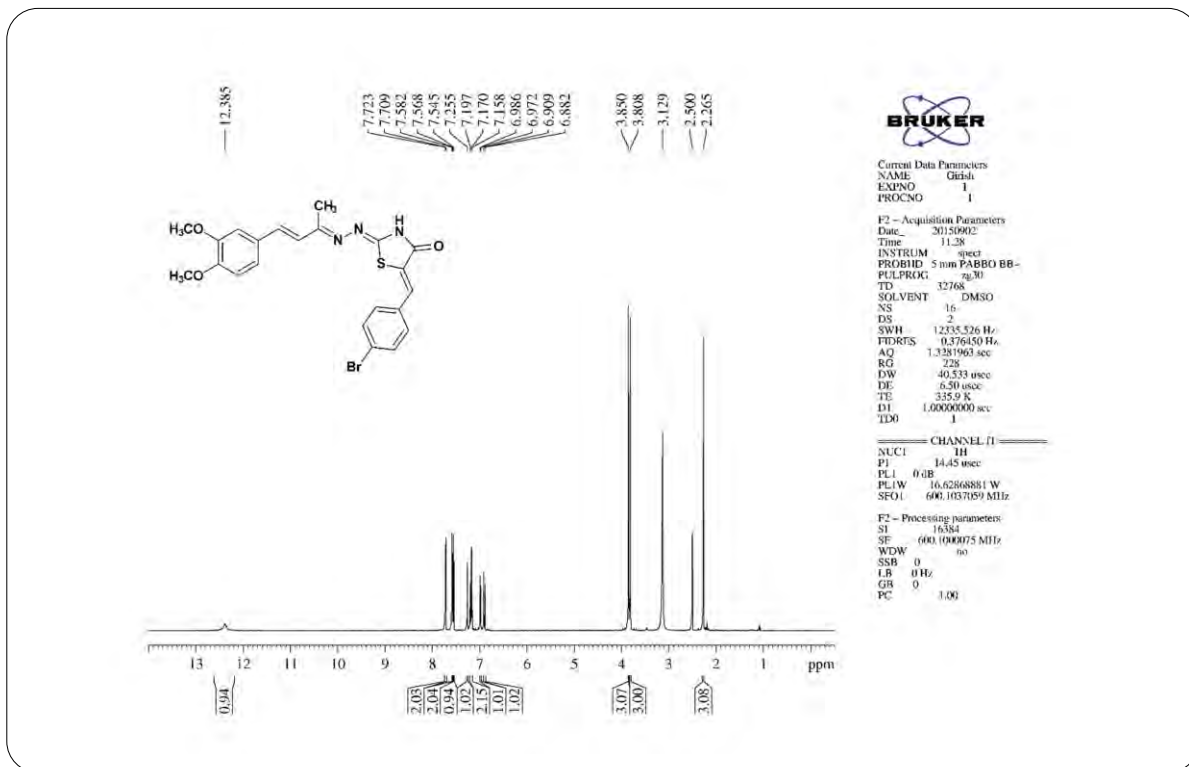
¹³C NMR Spectrum of Compound 10c (chapter 4)



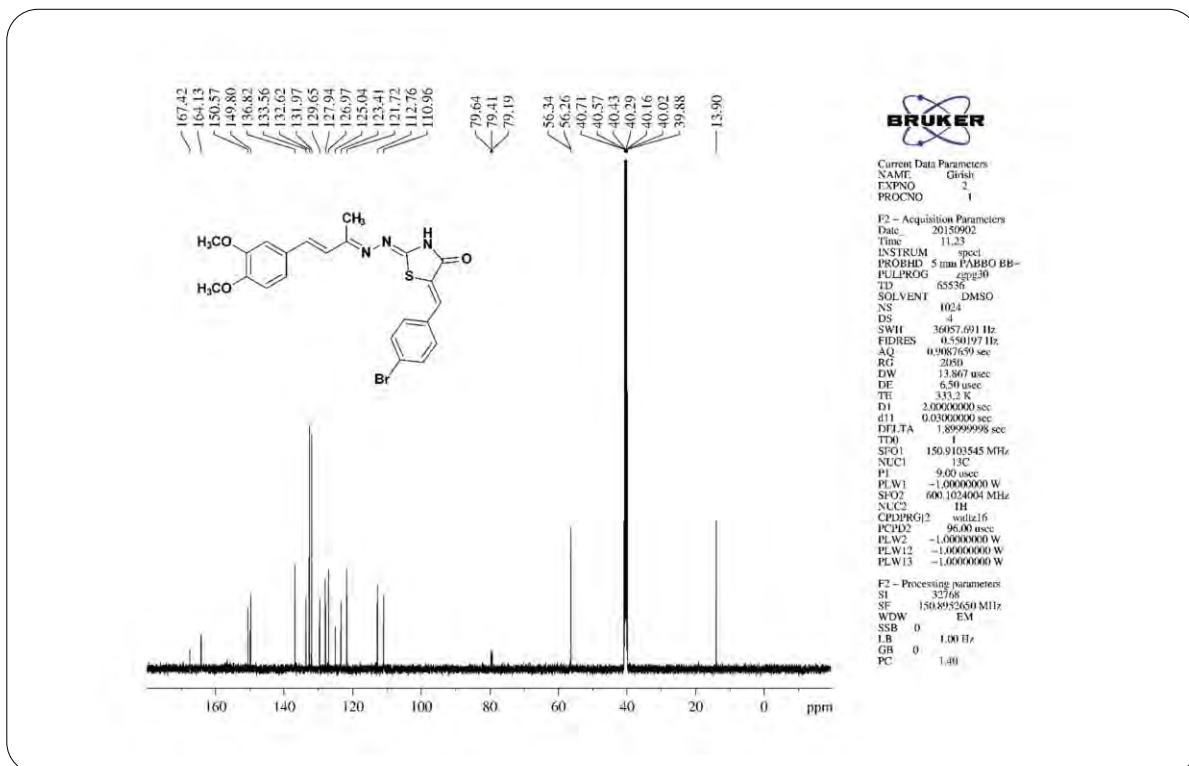
HRMS Spectrum of Compound 10c (chapter 4)



IR Spectrum of Compound 10d (chapter 4)



¹H NMR Spectrum of Compound 10d (chapter 4)



¹³C NMR Spectrum of Compound 10d (chapter 4)

Elemental Composition Report

Page 1

Single Mass Analysis

Tolerance = 5.0 PPM / DBE: min = -1.5, max = 100.0

Element prediction: Off

Number of isotope peaks used for i-FIT = 3

Monoisotopic Mass, Even Electron Ions

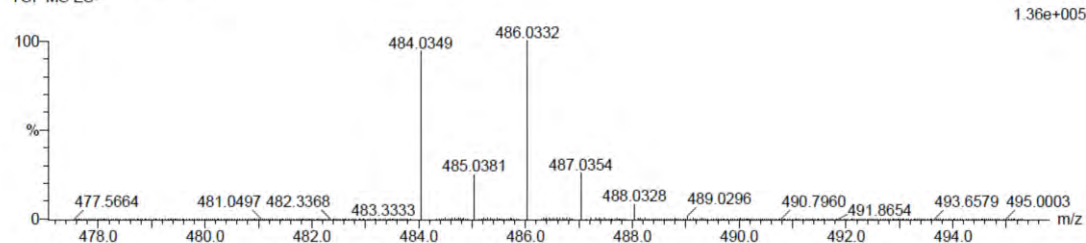
80 formula(e) evaluated with 1 results within limits (up to 20 closest results for each mass)

Elements Used:

C: 20-25 H: 15-20 N: 0-5 O: 0-5 S: 0-1 Br: 0-1

MLO-05 15 (0.473) Cm (1.61)

TOF MS ES-



Minimum:

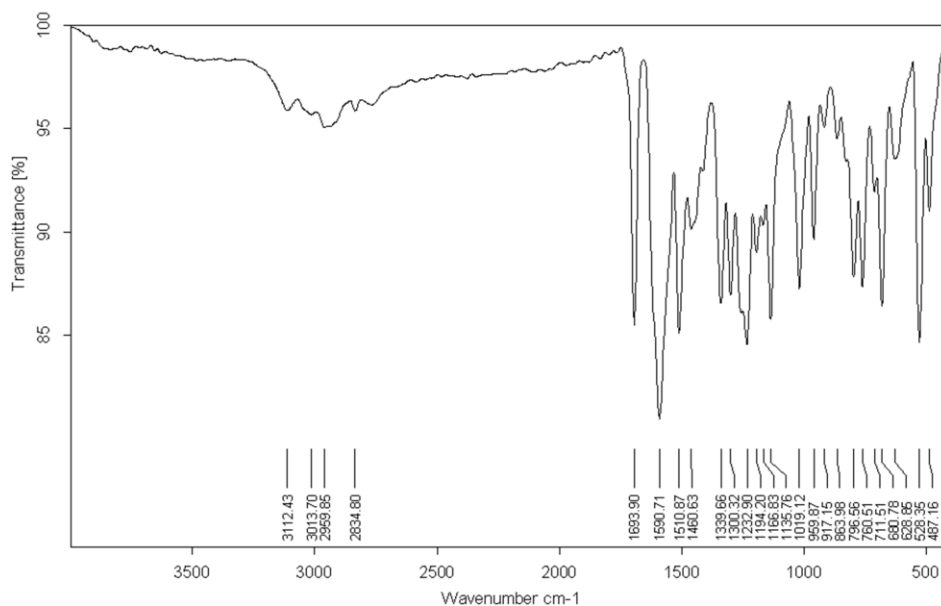
5.0 5.0 -1.5

Maximum:

5.0 5.0 100.0

Mass	Calc. Mass	mDa	PPM	DBE	i-FIT	i-FIT (Norm)	Formula
484.0349	484.0330	1.9	3.9	14.5	435.6	0.0	C22 H19 N3 O3 S Br

HRMS Spectrum of Compound 10d (chapter 4)

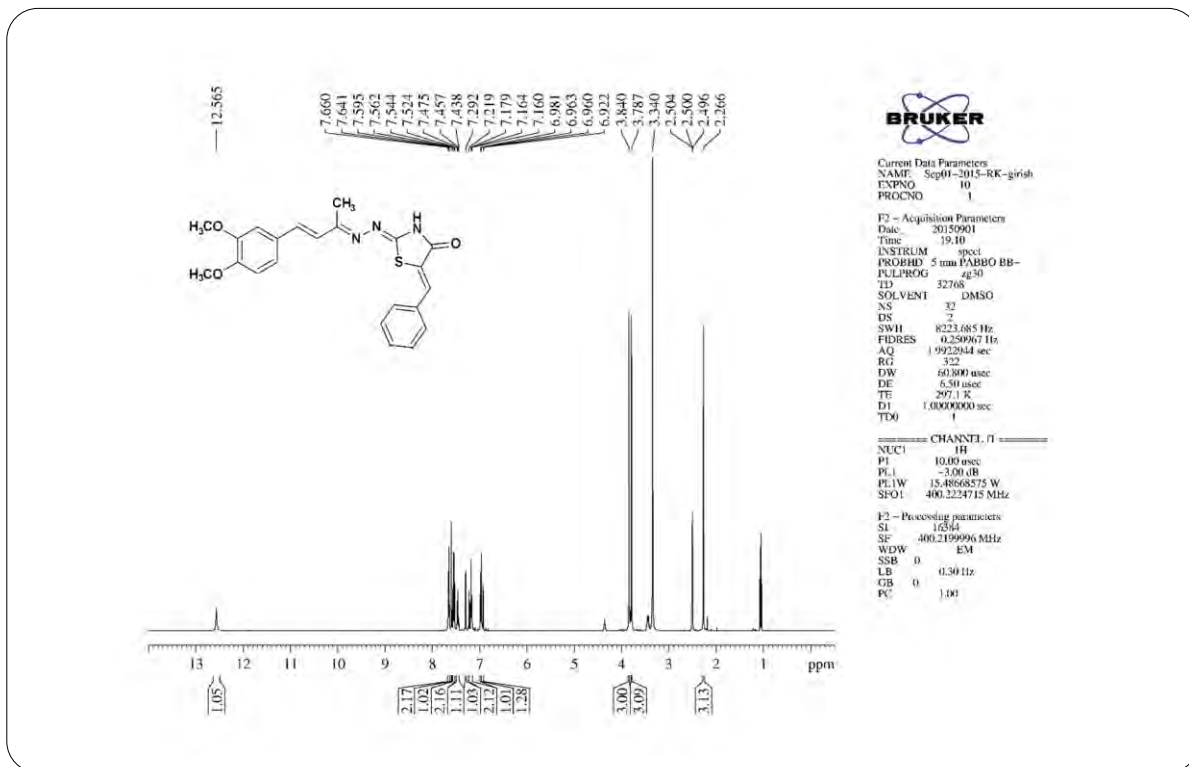
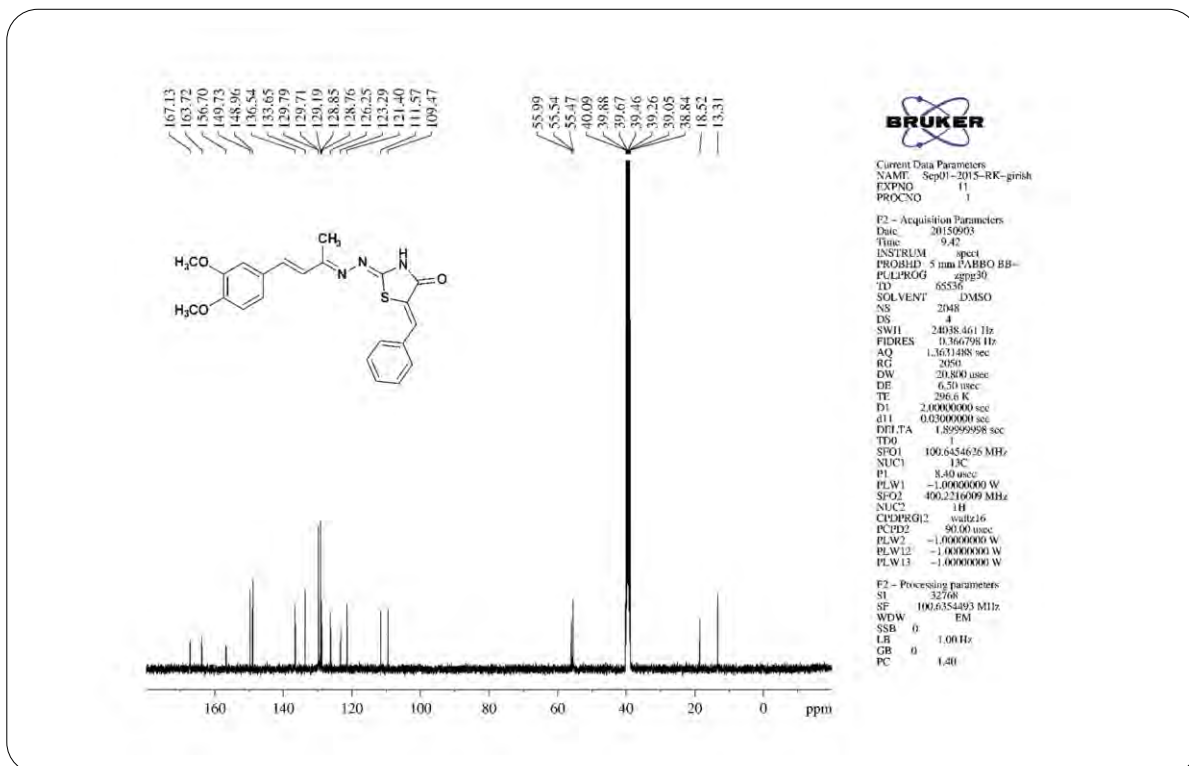


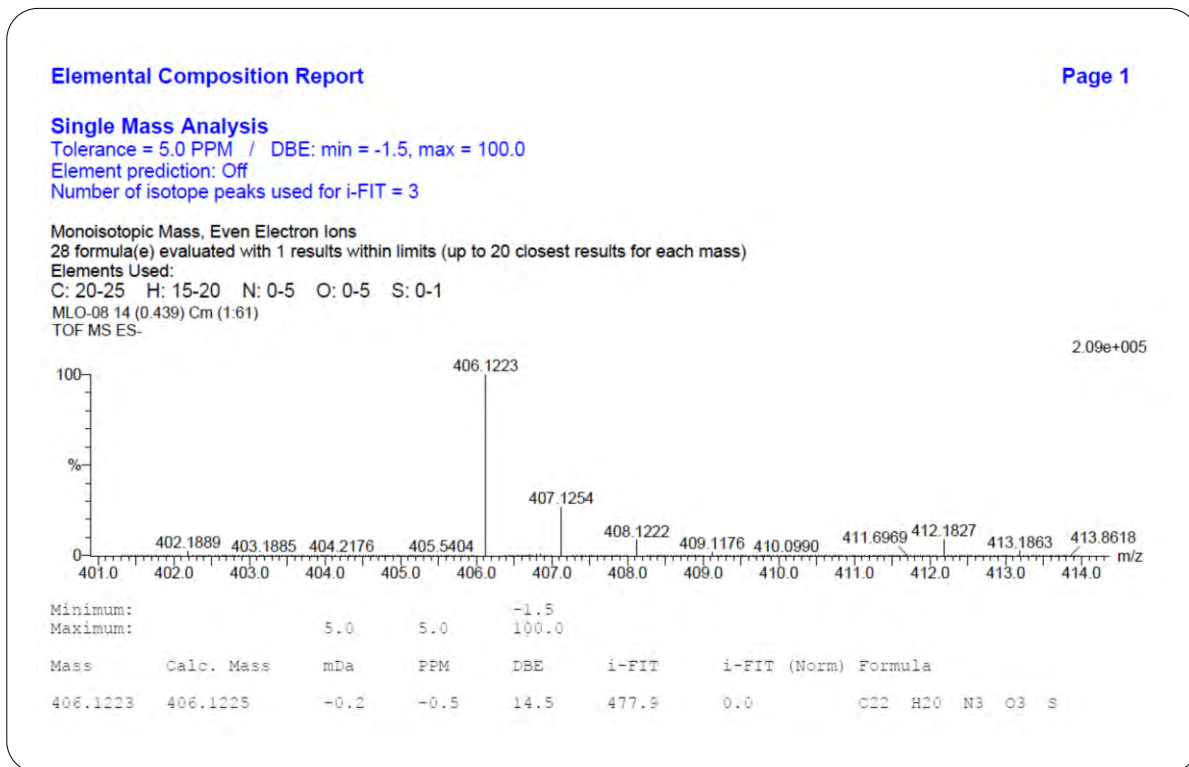
C:\GIRISH IR\MLO-8.0 MLO-8 ATR platinum Diamond 1 Ref

24/12/2015

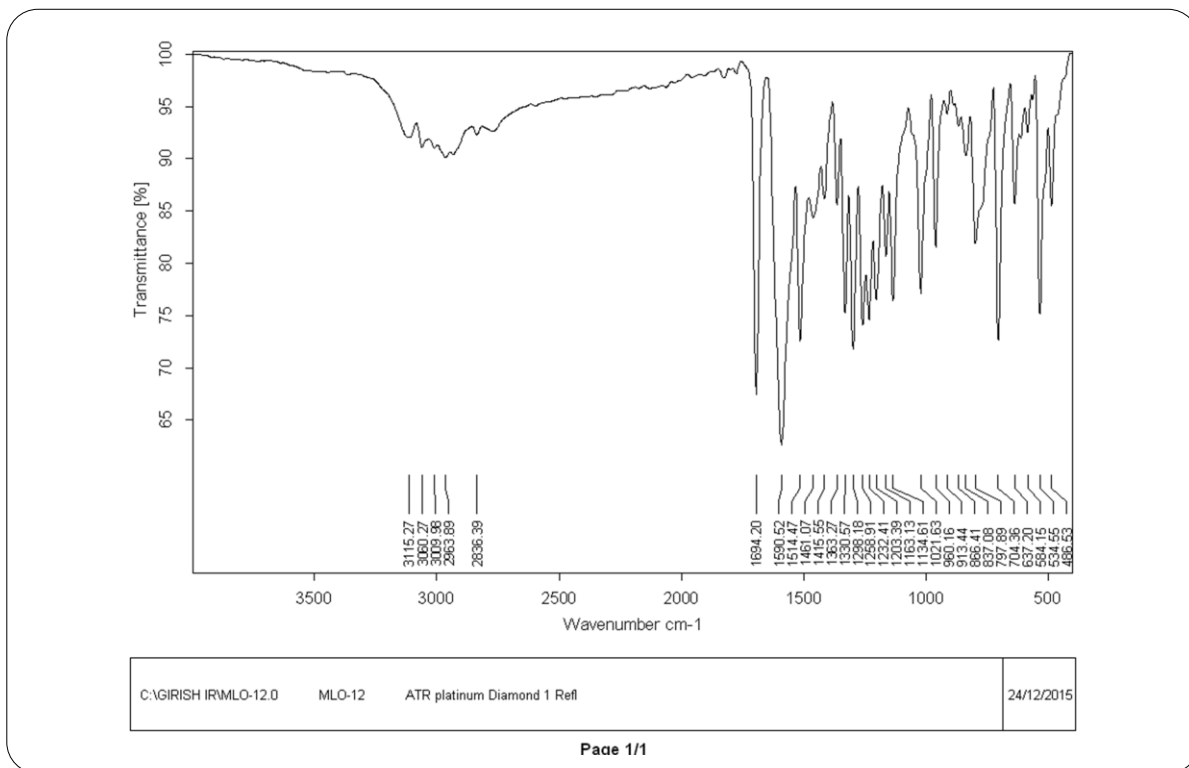
Page 1/1

IR Spectrum of Compound 10e (chapter 4)

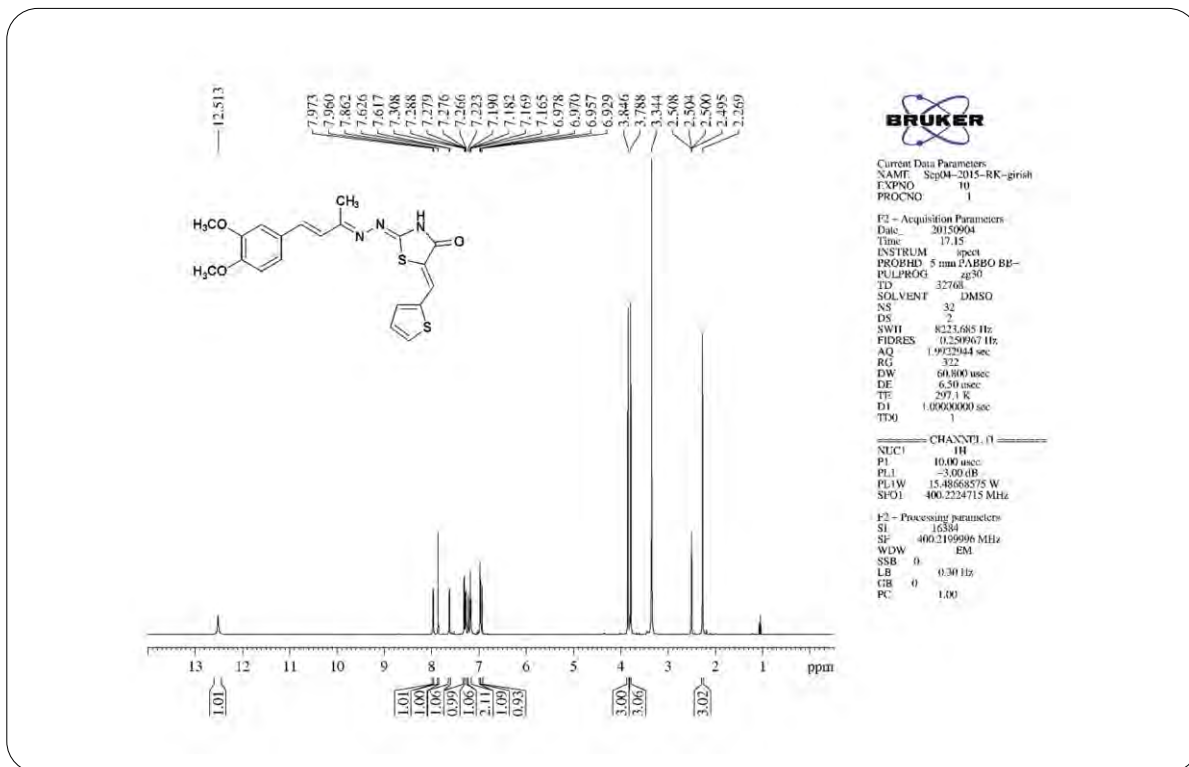
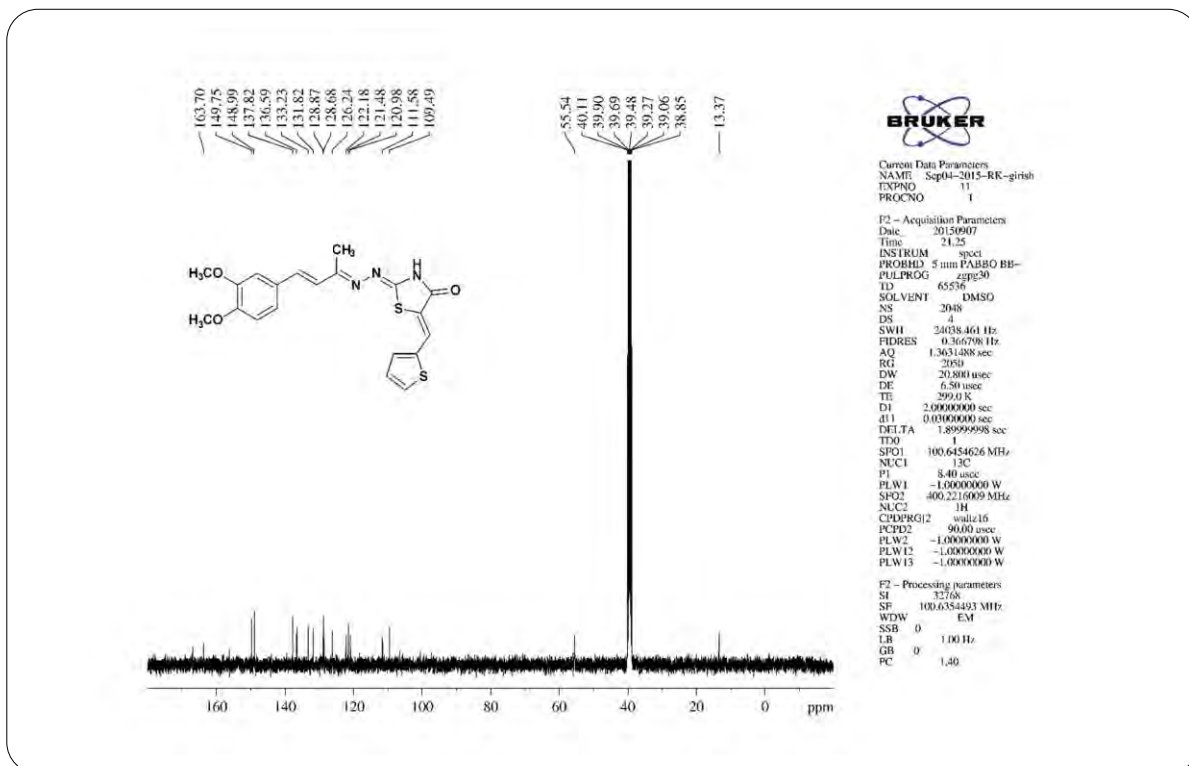
**¹H NMR Spectrum of Compound 10e (chapter 4)****¹³C NMR Spectrum of Compound 10e (chapter 4)**

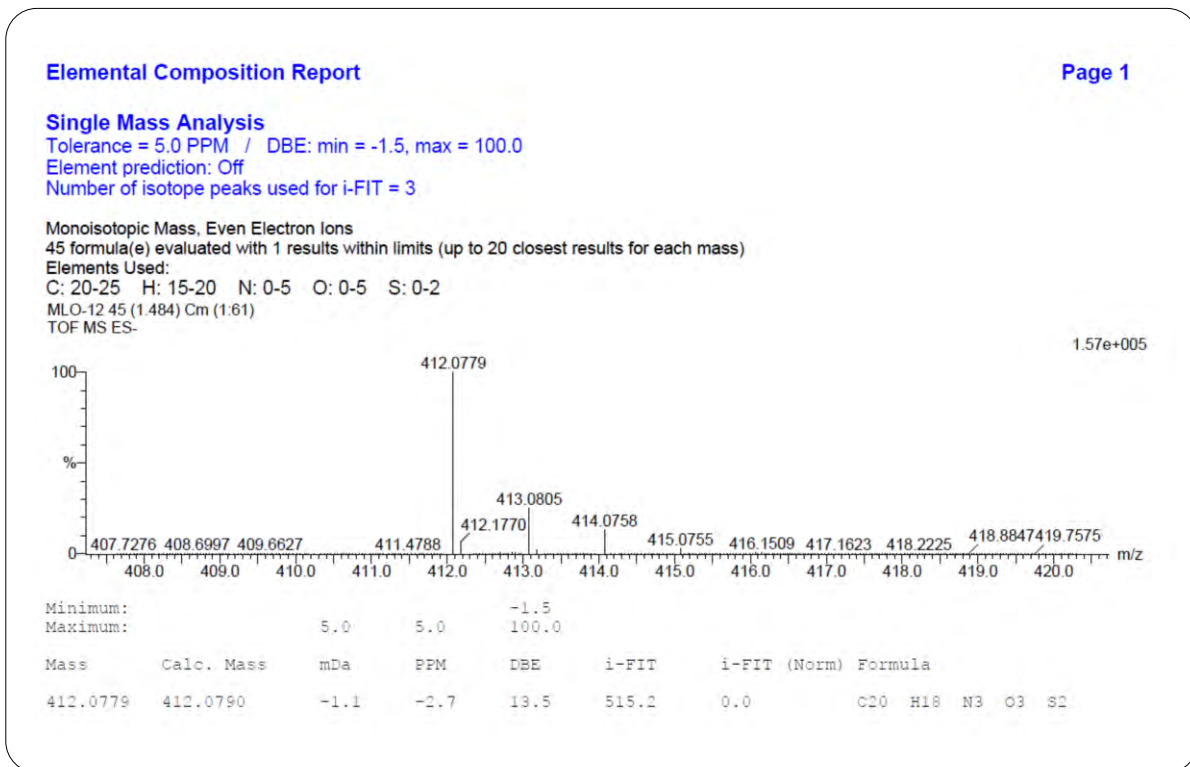


HRMS Spectrum of Compound 10e (chapter 4)

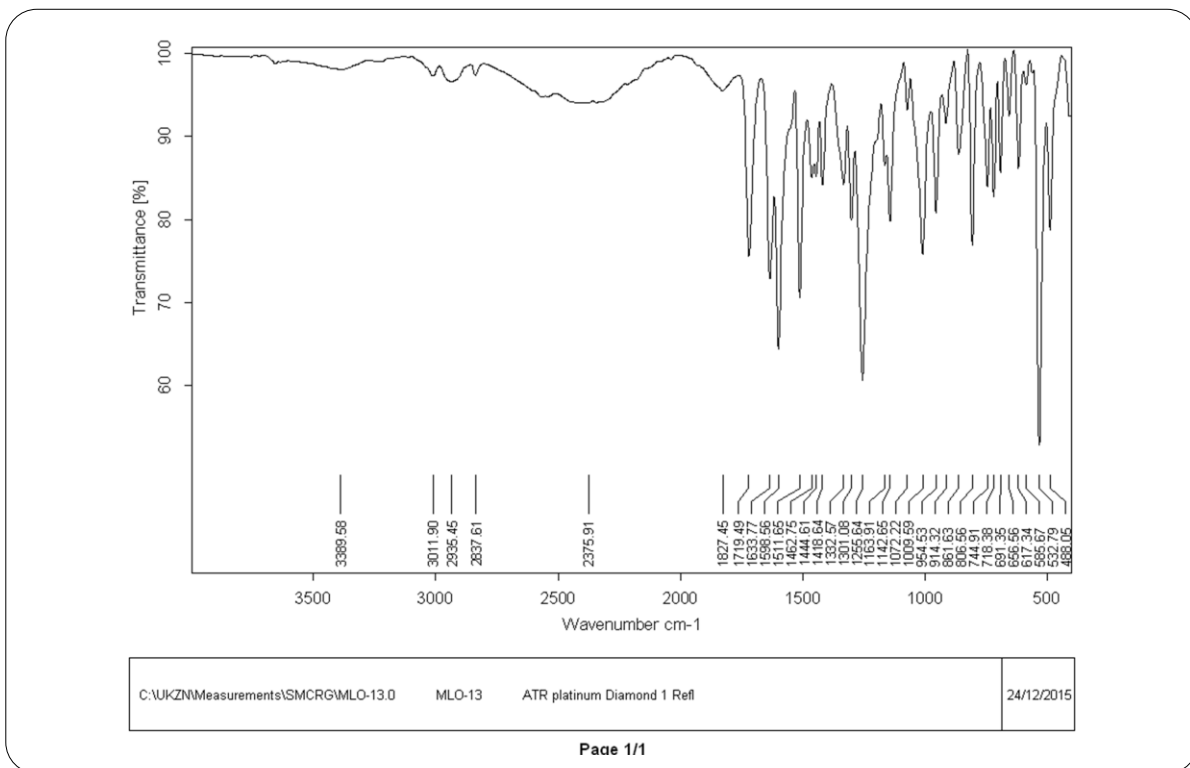


IR Spectrum of Compound 10f (chapter 4)

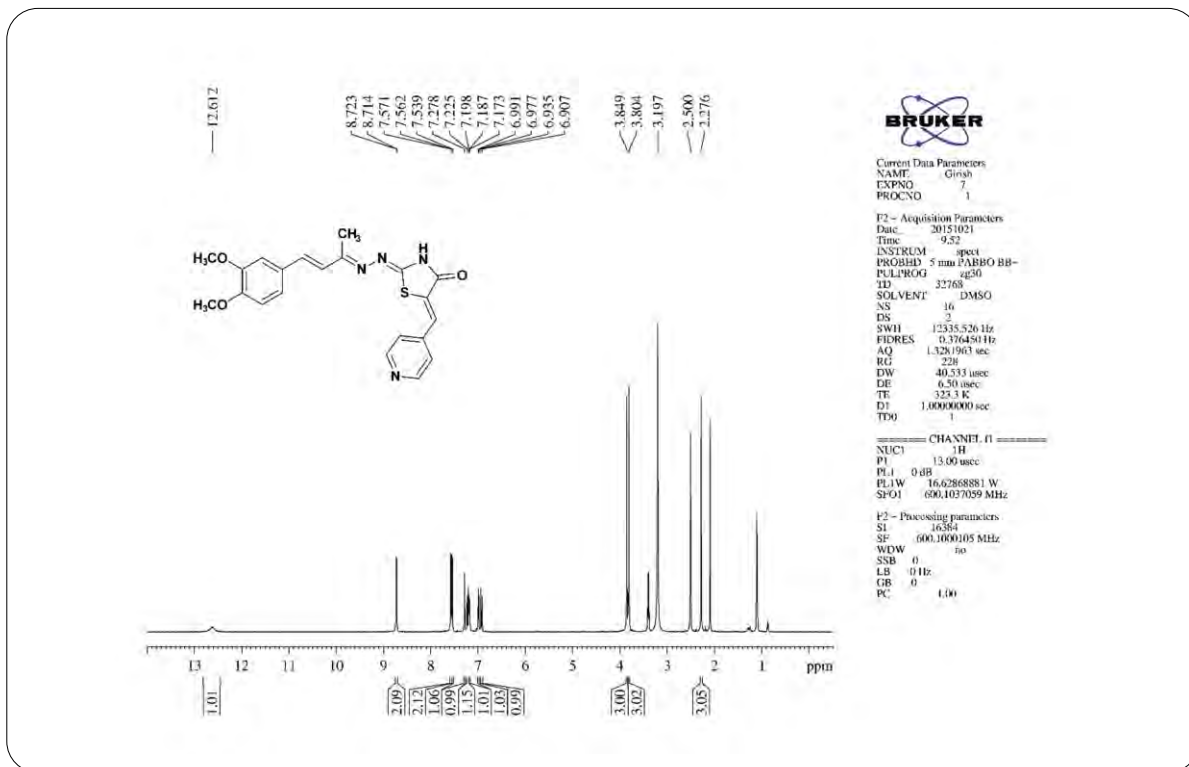
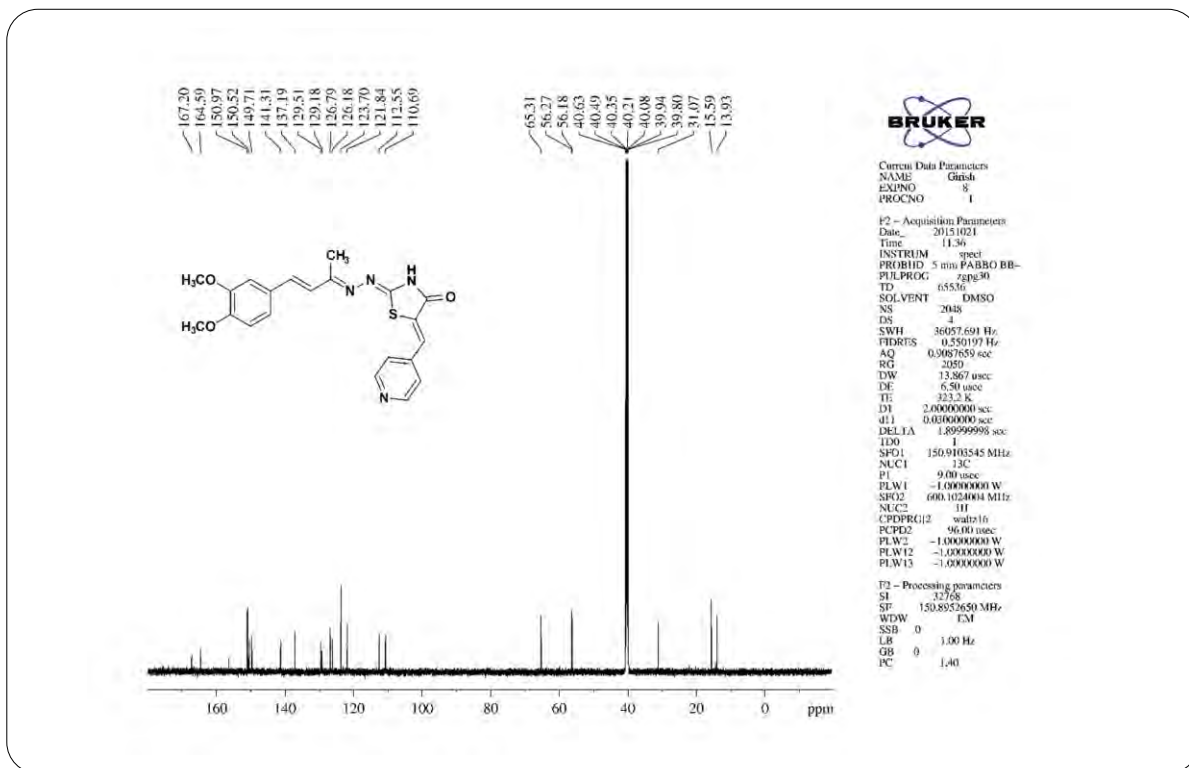
**¹H NMR Spectrum of Compound 10f (chapter 4)****¹³C NMR Spectrum of Compound 10f (chapter 4)**

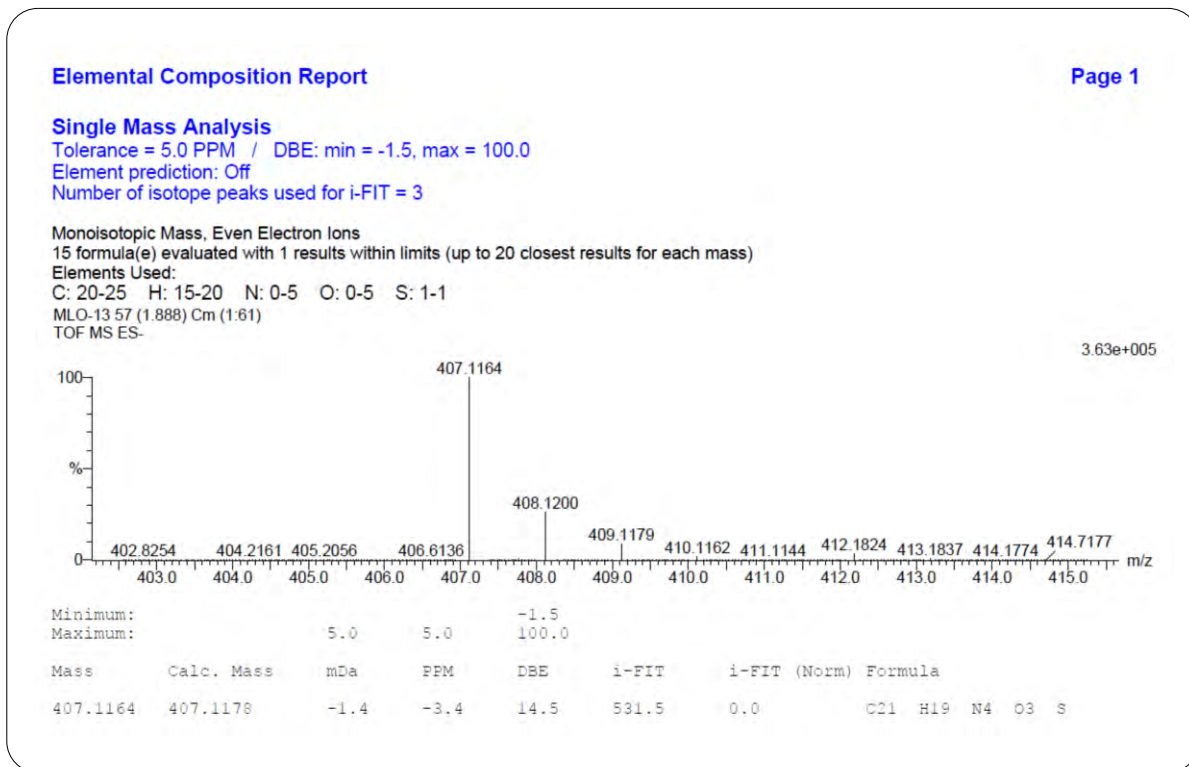


HRMS Spectrum of Compound 10f (chapter 4)

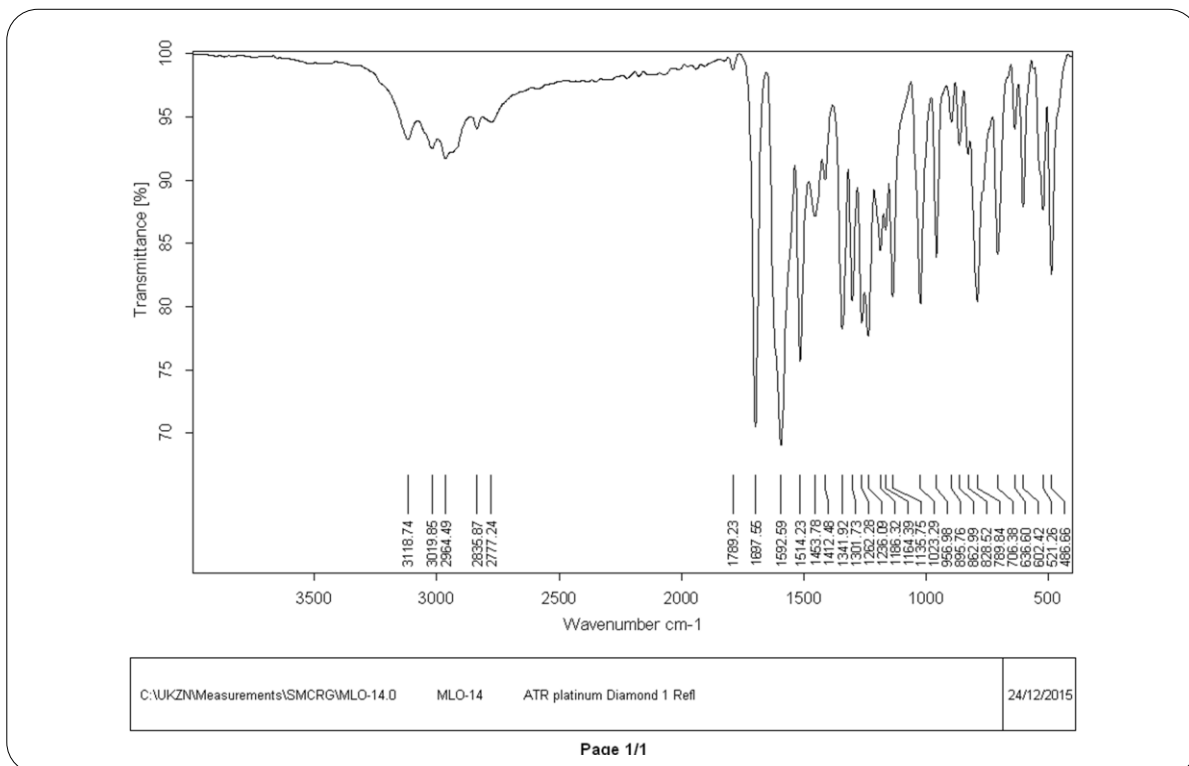


IR Spectrum of Compound 10g (chapter 4)

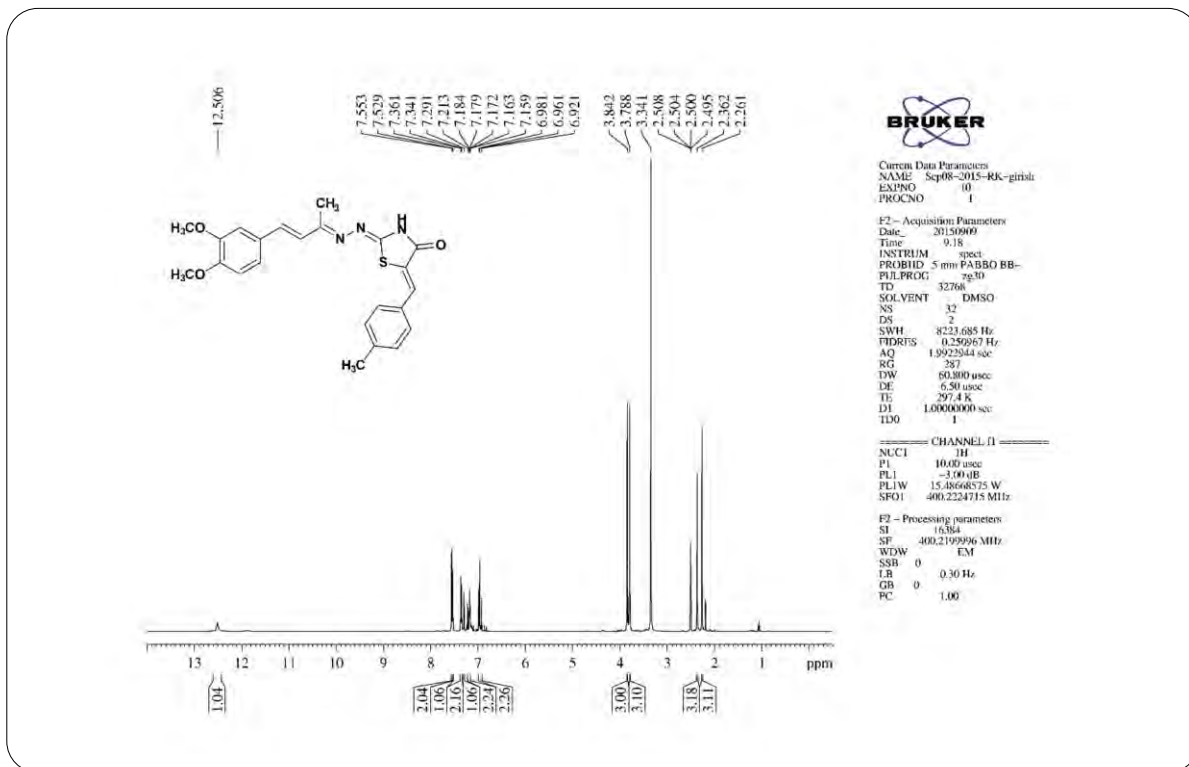
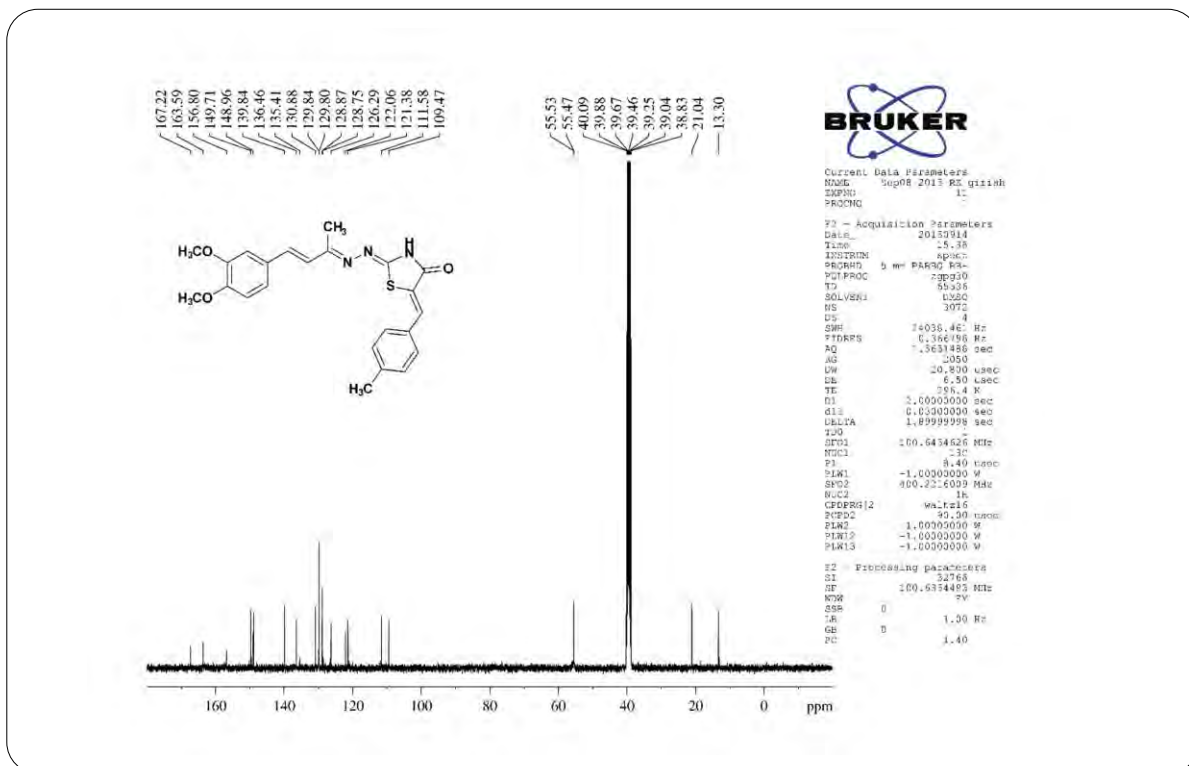
**¹H NMR Spectrum of Compound 10g (chapter 4)****¹³C NMR Spectrum of Compound 10g (chapter 4)**

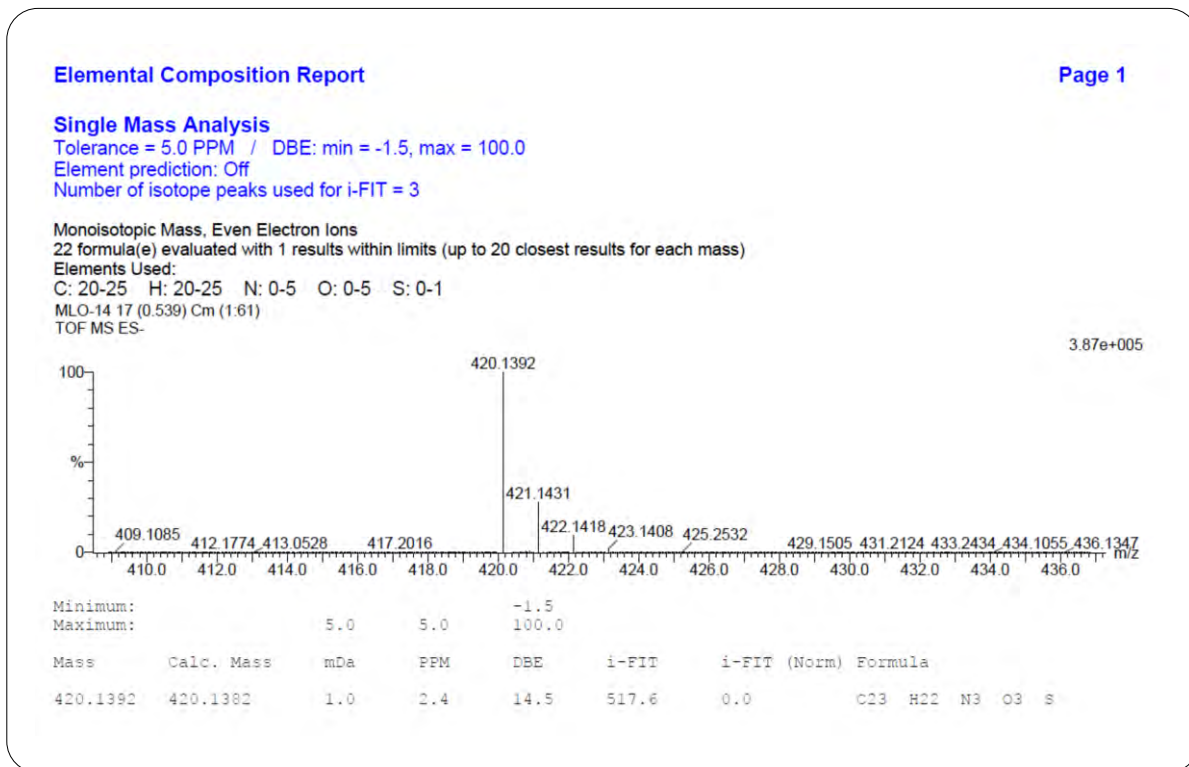


HRMS Spectrum of Compound 10g (chapter 4)

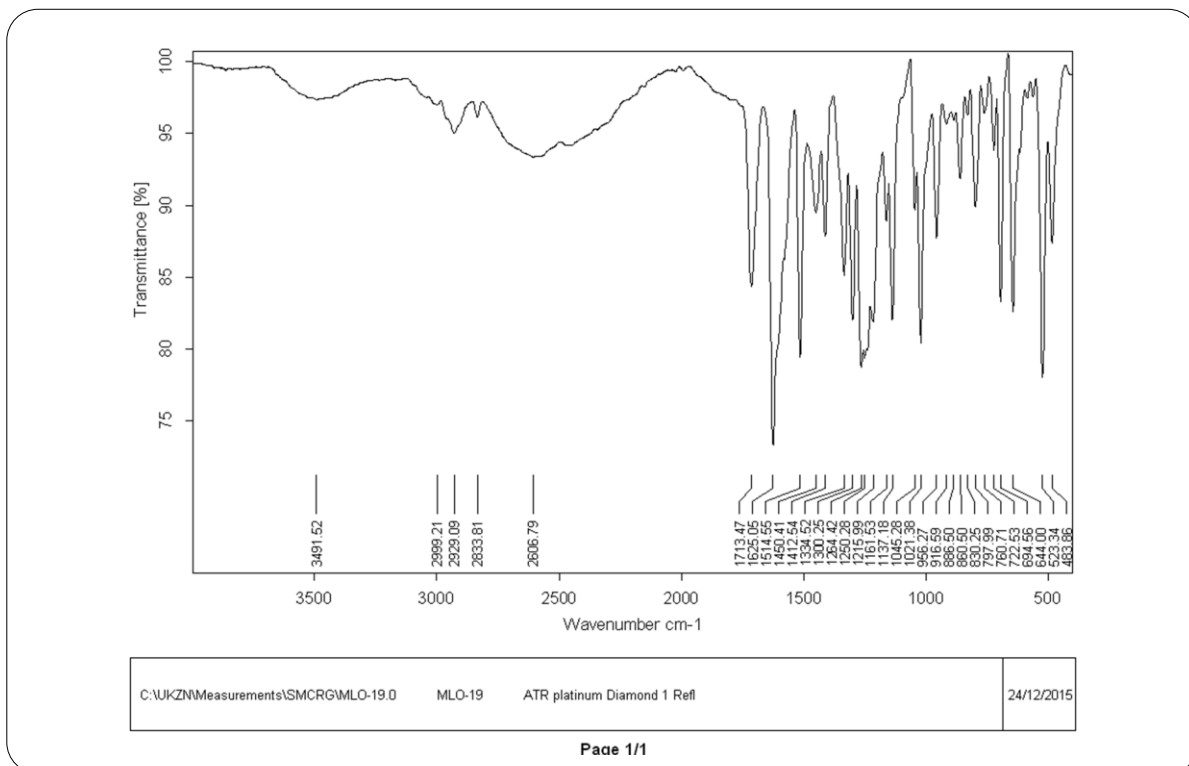


IR Spectrum of Compound 10h (chapter 4)

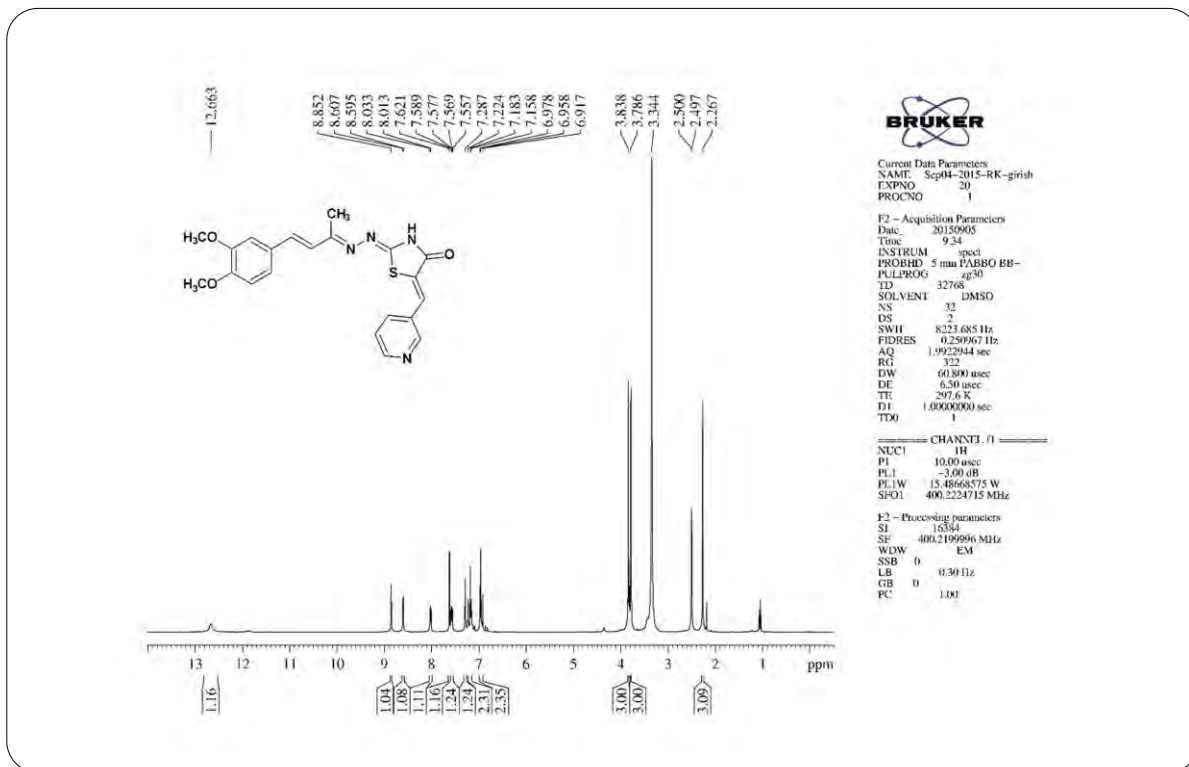
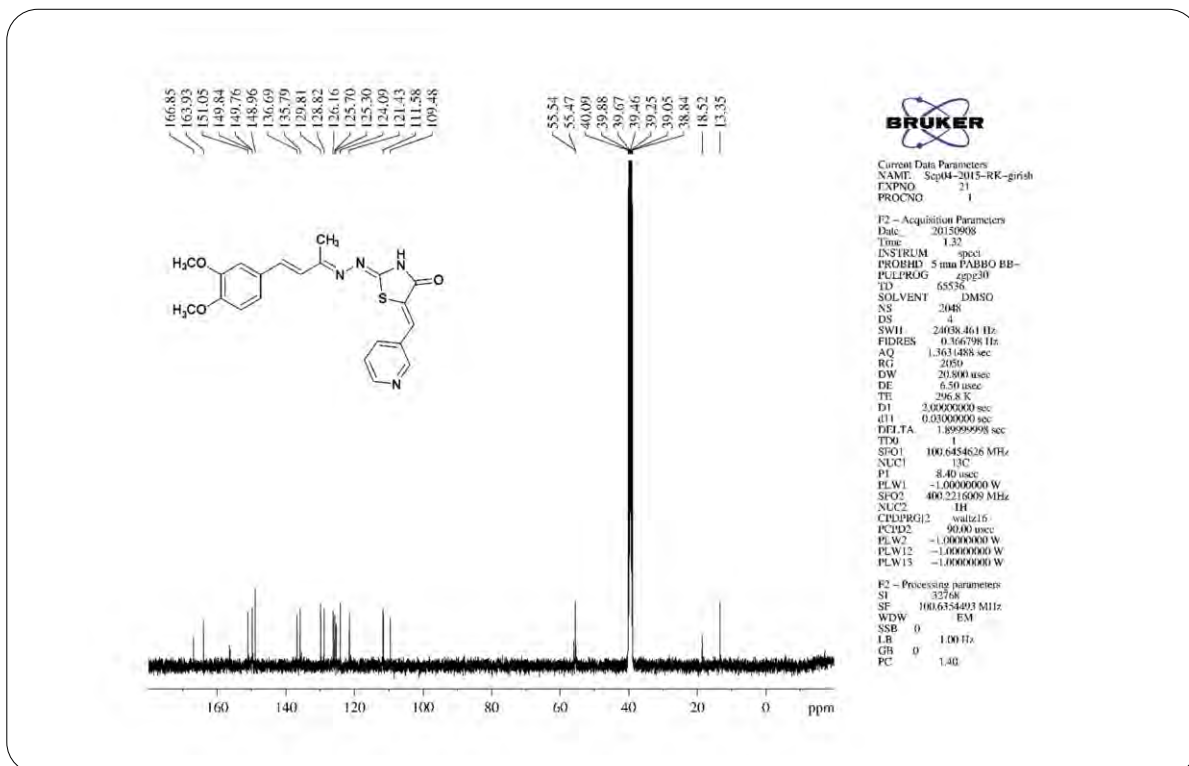
**¹H NMR Spectrum of Compound 10h (chapter 4)****¹³C NMR Spectrum of Compound 10h (chapter 4)**



HRMS Spectrum of Compound 10h (chapter 4)



IR Spectrum of Compound 10i (chapter 4)

**¹H NMR Spectrum of Compound 10i (chapter 4)****¹³C NMR Spectrum of Compound 10i (chapter 4)**

Elemental Composition Report

Page 1

Single Mass Analysis

Tolerance = 5.0 PPM / DBE: min = -1.5, max = 100.0

Element prediction: Off

Number of isotope peaks used for i-FIT = 3

Monoisotopic Mass, Even Electron Ions

28 formula(e) evaluated with 1 results within limits (up to 20 closest results for each mass)

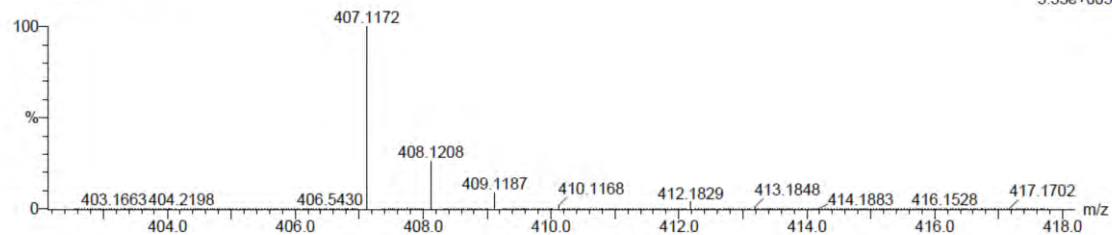
Elements Used:

C: 20-25 H: 15-20 N: 0-5 O: 0-5 S: 0-1

MLO-19 18 (0.573) Cm (1.61)

TOF MS ES-

3.33e+005

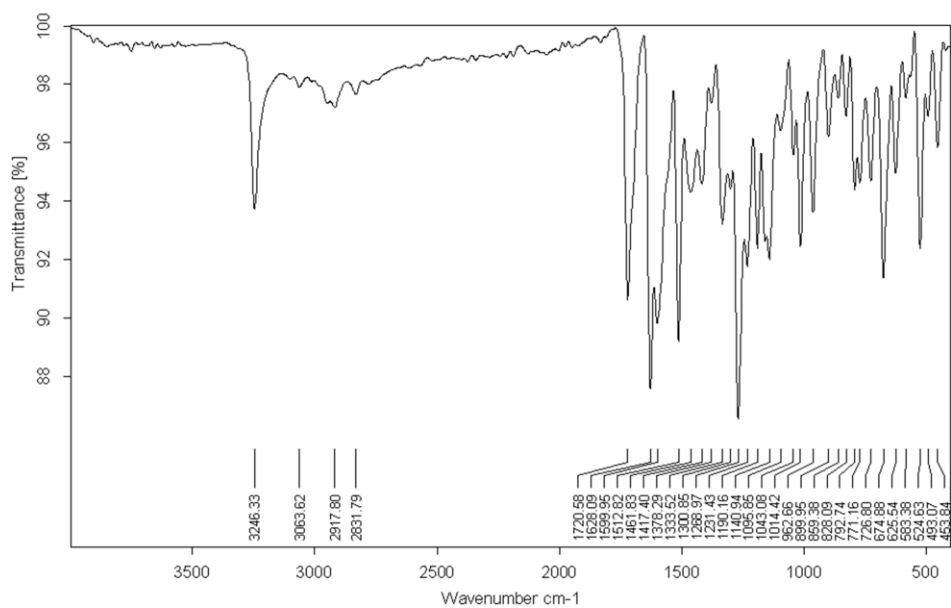


Minimum:

Maximum: 5.0 5.0 -1.5

Mass	Calc. Mass	mDa	PPM	DBE	i-FIT	i-FIT (Norm)	Formula
407.1172	407.1178	-0.6	-1.5	14.5	524.3	0.0	C21 H19 N4 O3 S

HRMS Spectrum of Compound 10i (chapter 4)

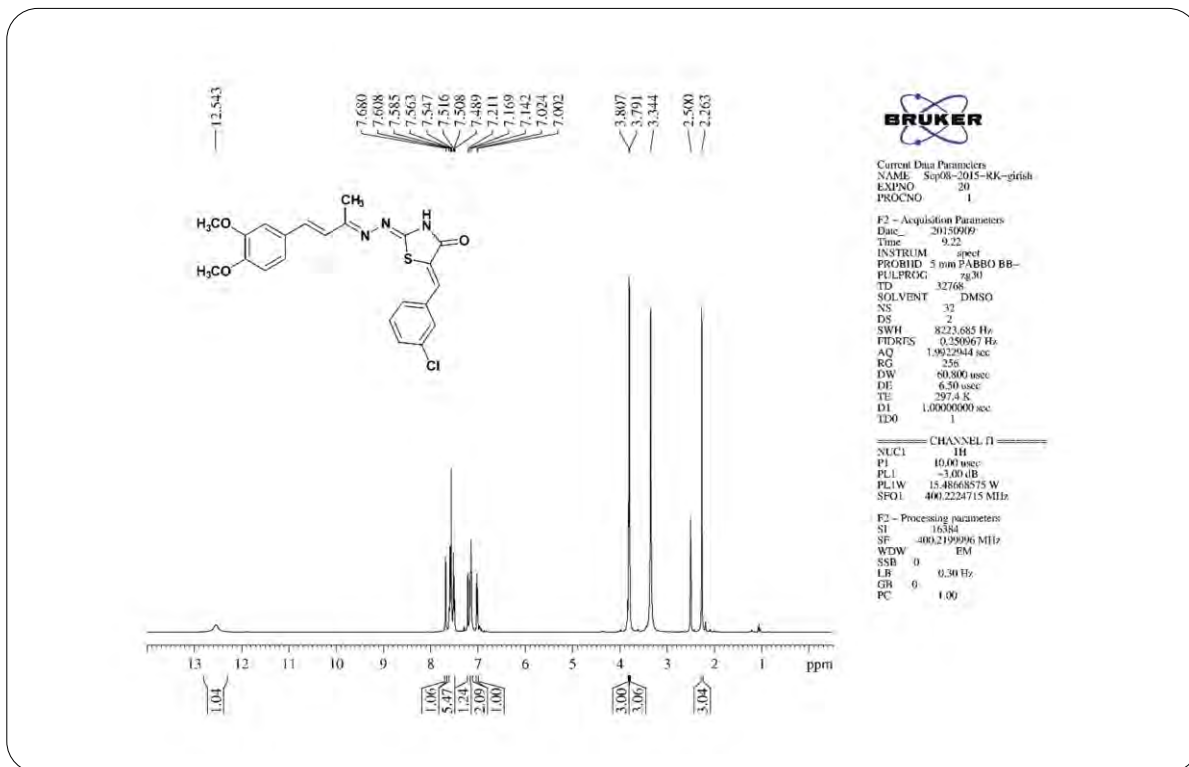
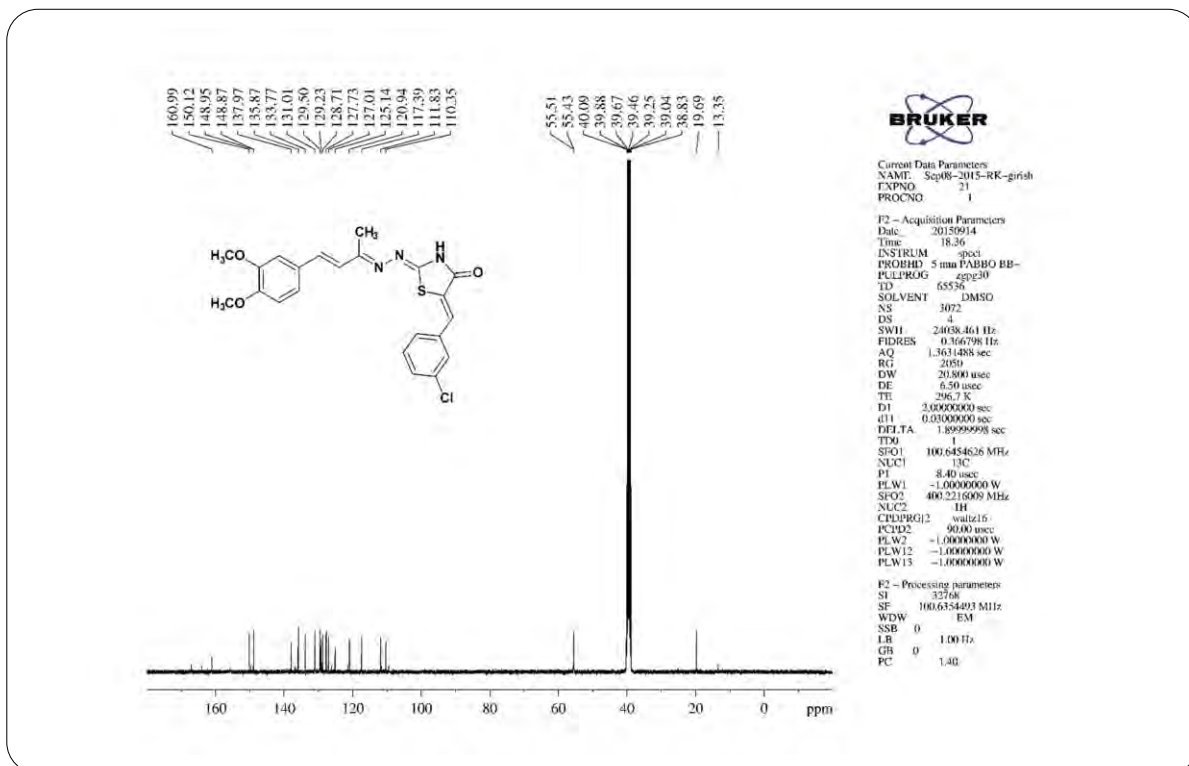


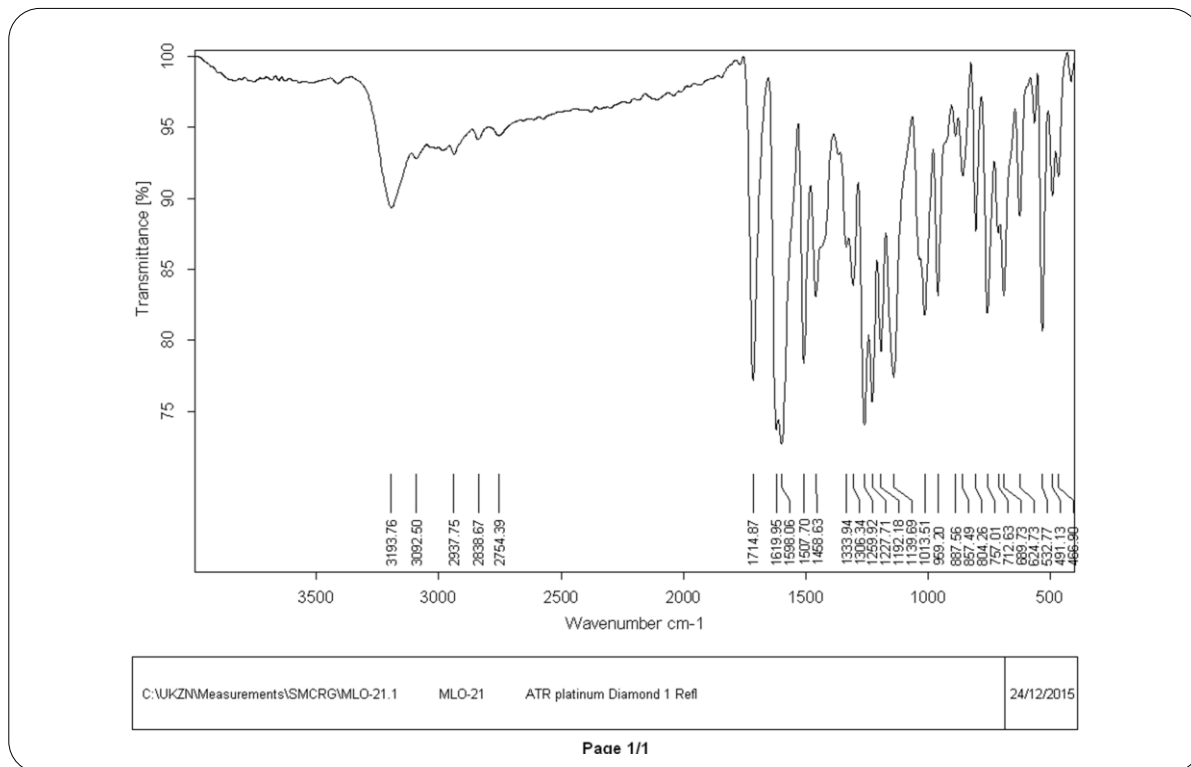
C:\UKZN\Measurements\SMCRG\MLO-20.0 MLO-20 ATR platinum Diamond 1 Ref

24/12/2015

Page 1/1

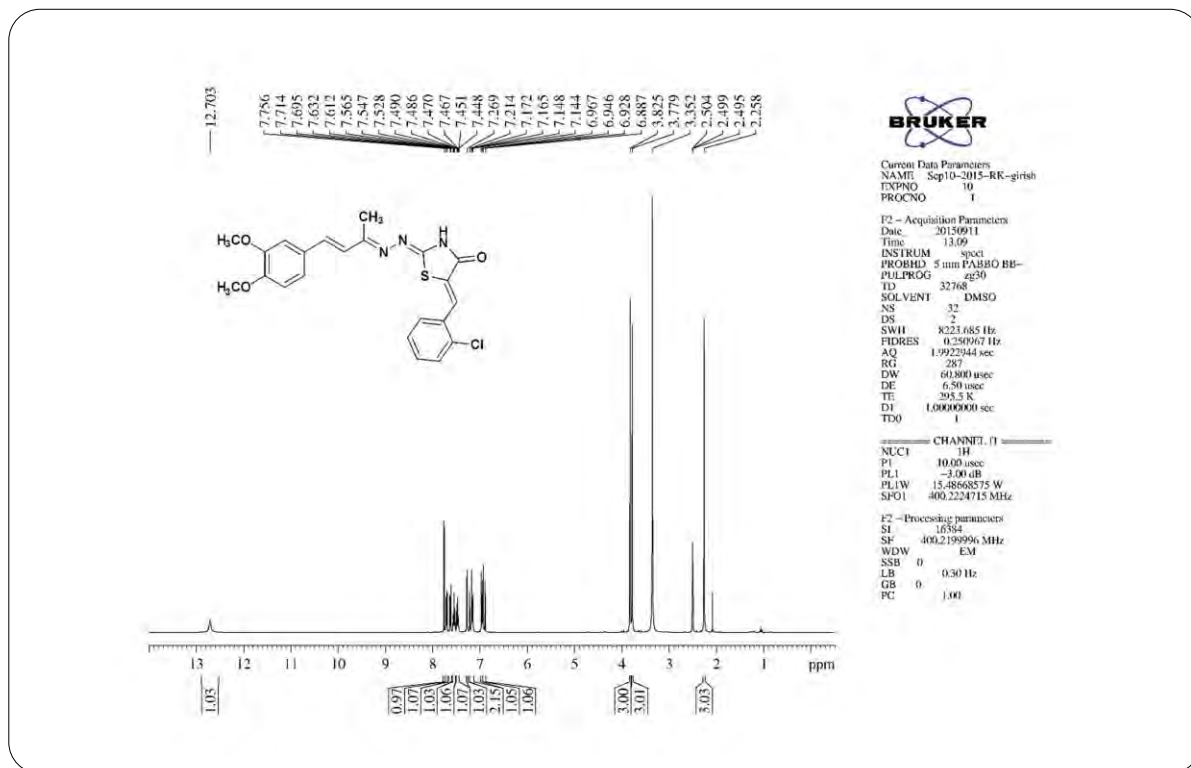
IR Spectrum of Compound 10j (chapter 4)

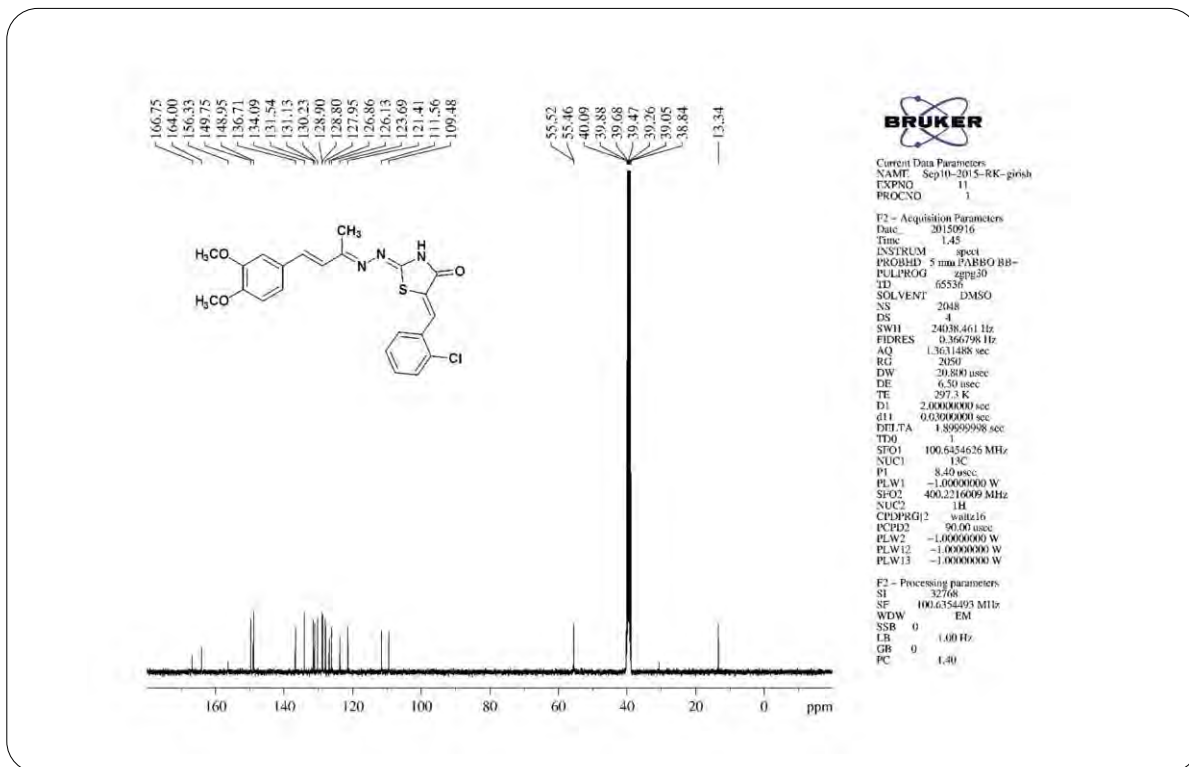
**¹H NMR Spectrum of Compound 10j (chapter 4)****¹³C NMR Spectrum of Compound 10j (chapter 4)**



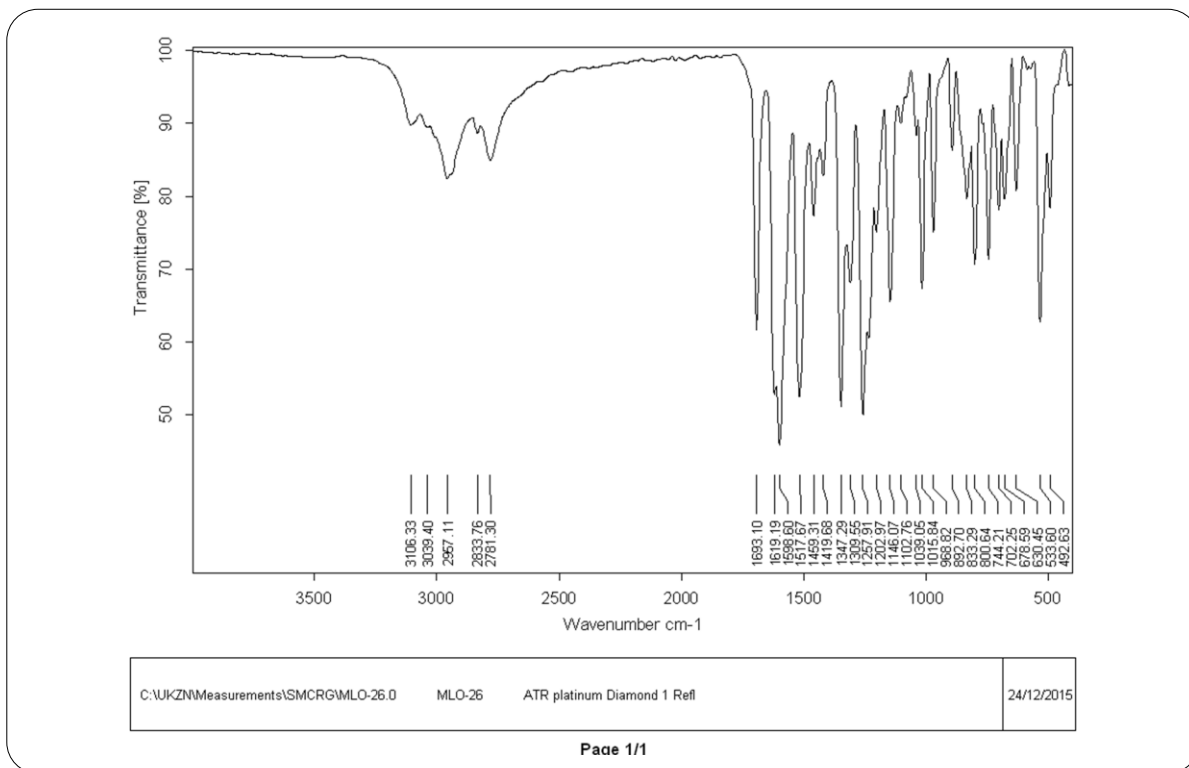
Page 1/1

IR Spectrum of Compound 10k (chapter 4)

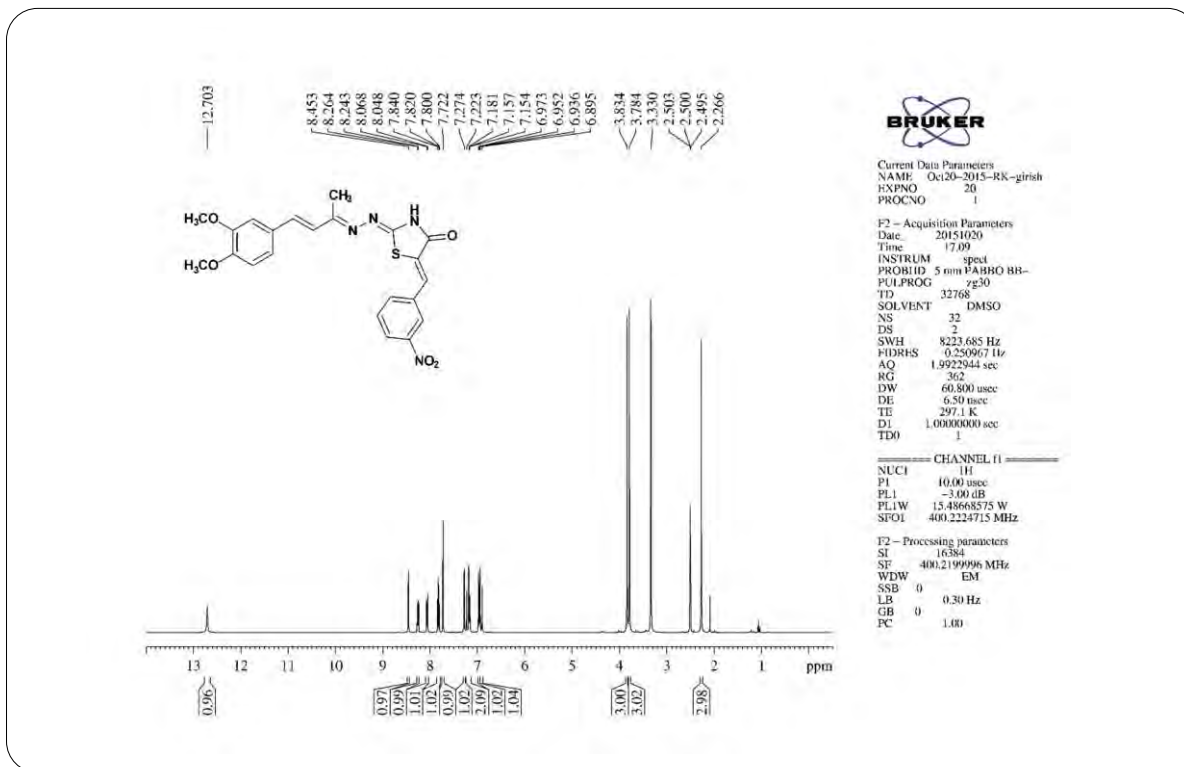
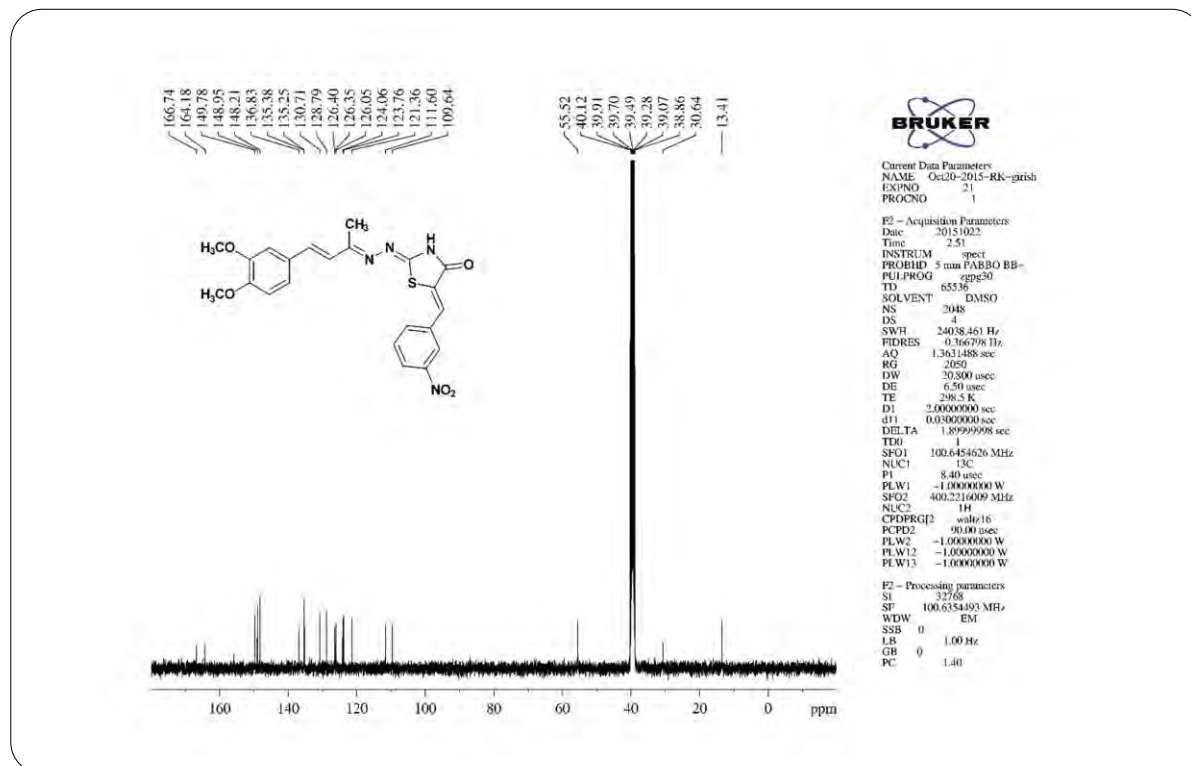
¹H NMR Spectrum of Compound 10k (chapter 4)

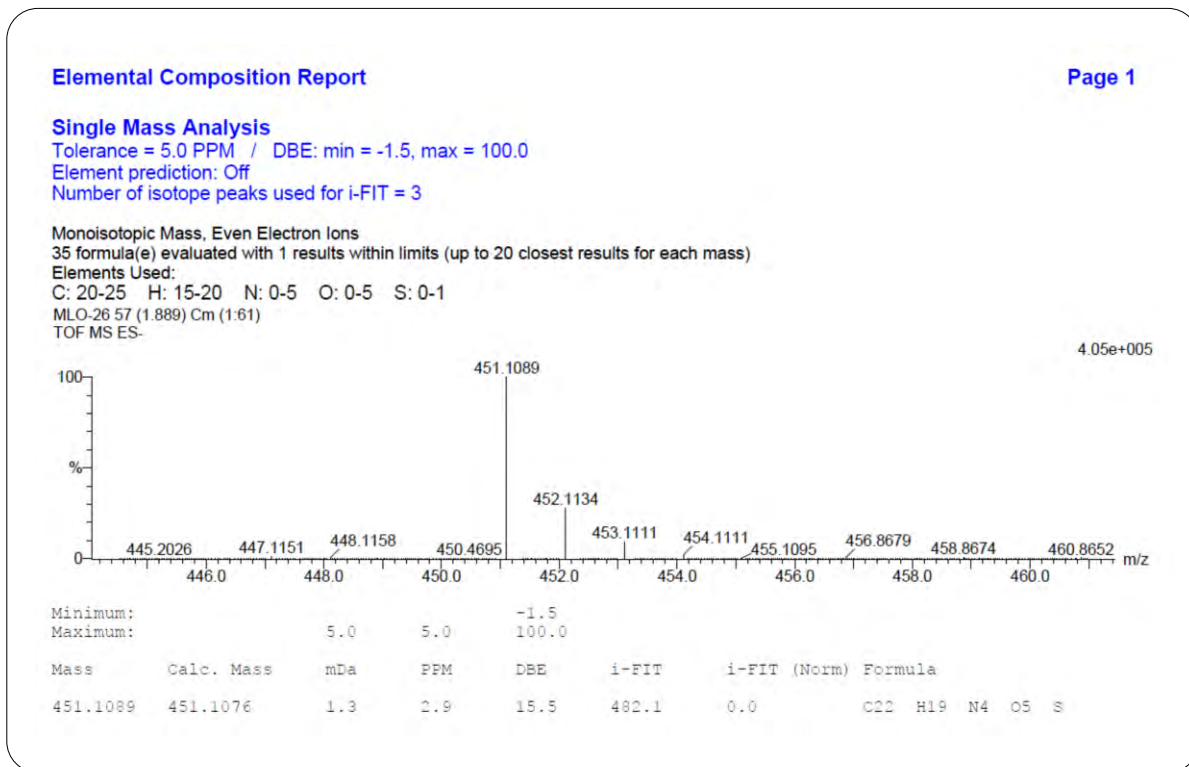


¹³C NMR Spectrum of Compound 10k (chapter 4)

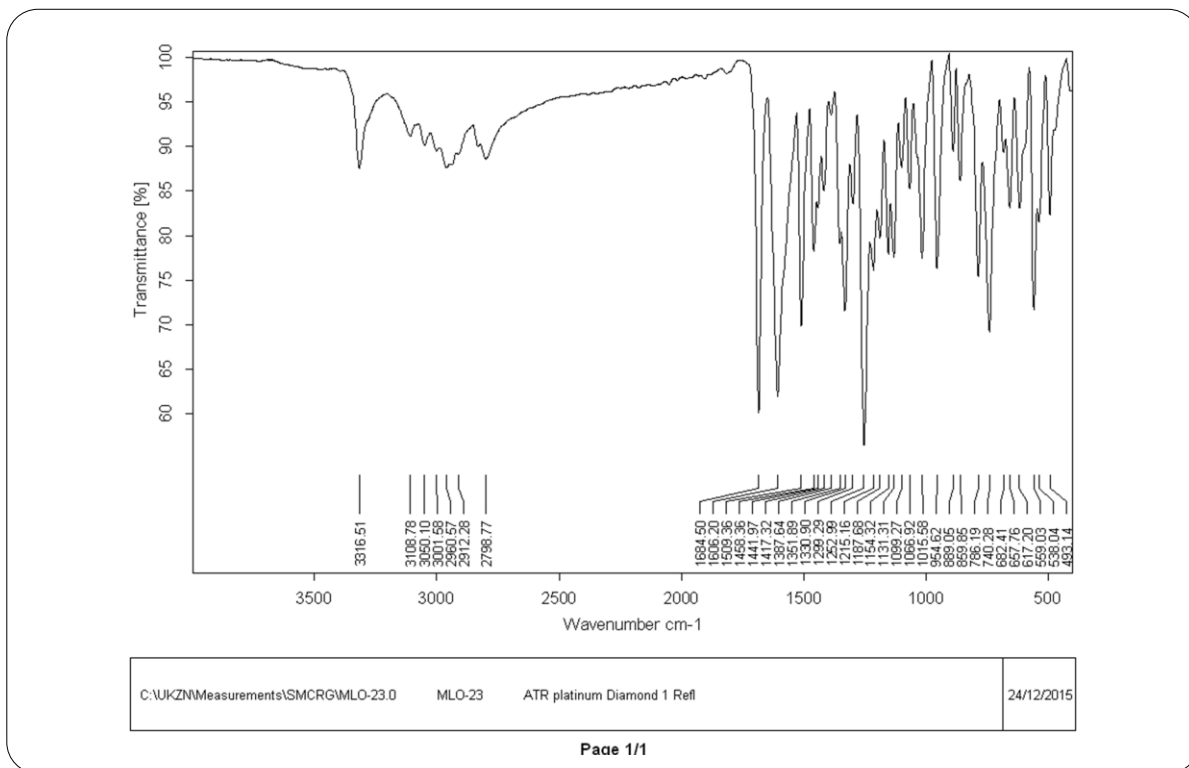


IR Spectrum of Compound 10l (chapter 4)

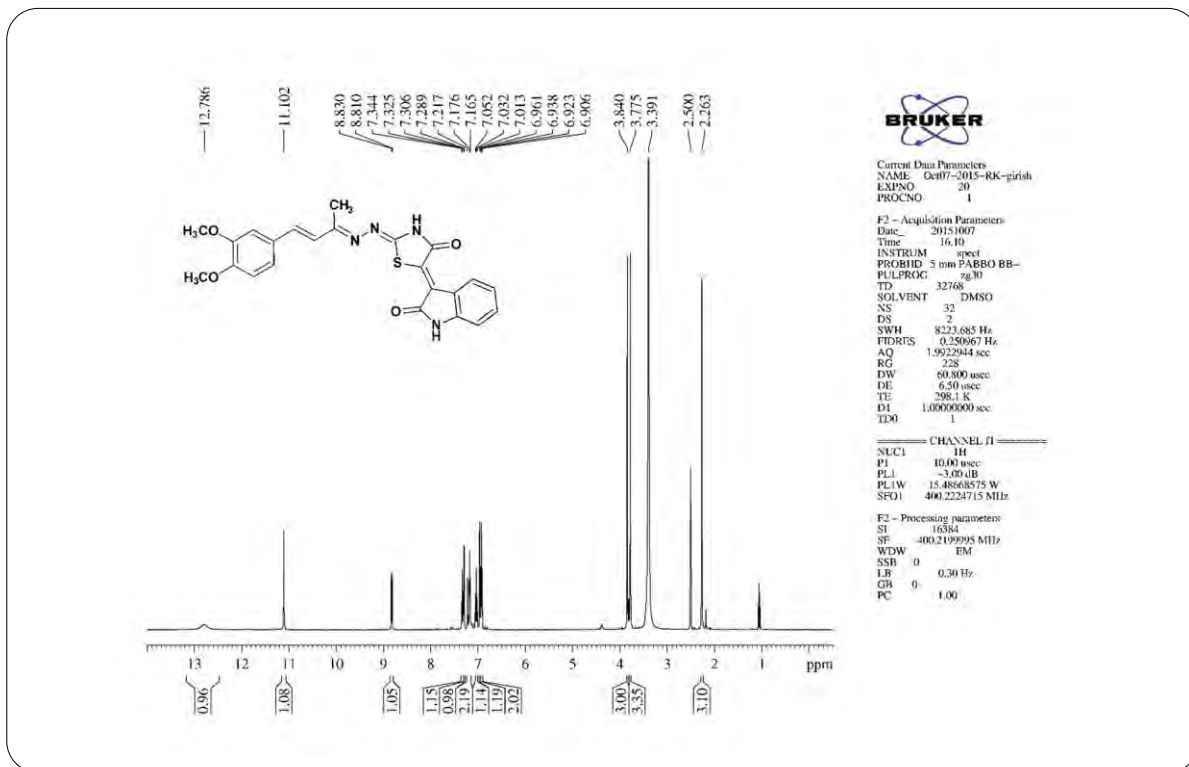
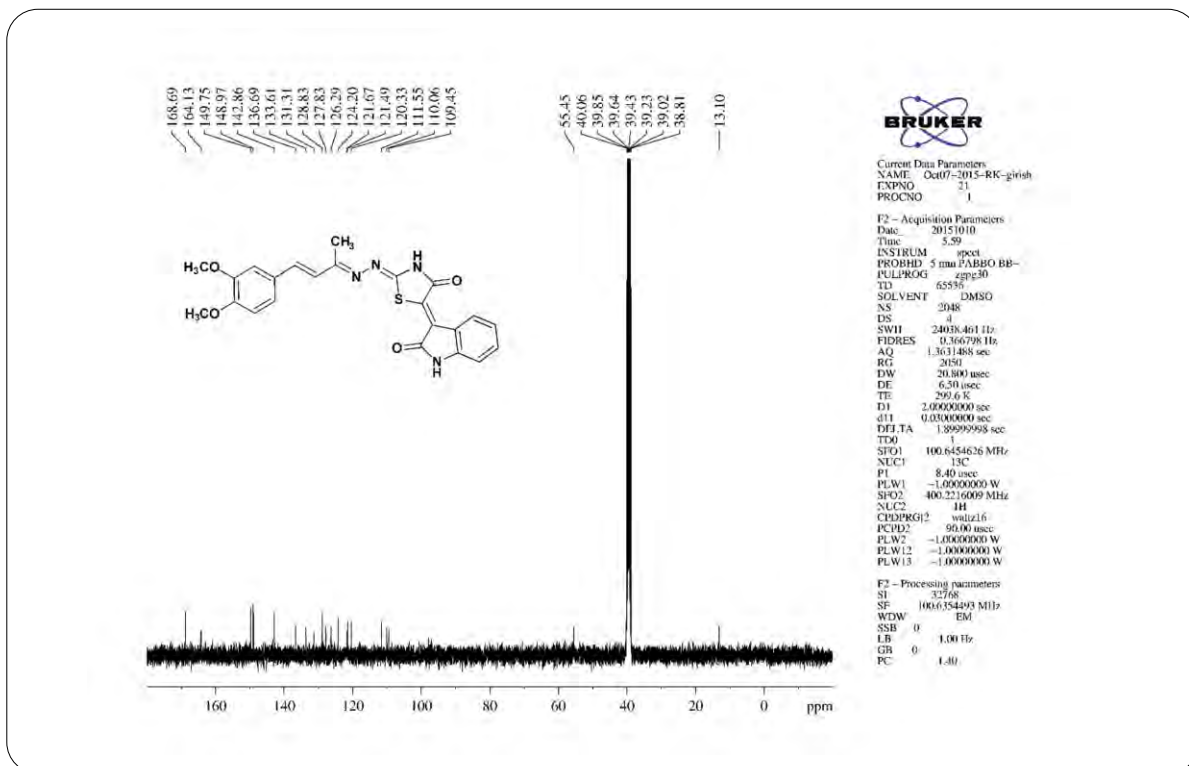
**¹H NMR Spectrum of Compound 10l (chapter 4)****¹³C NMR Spectrum of Compound 10l (chapter 4)**

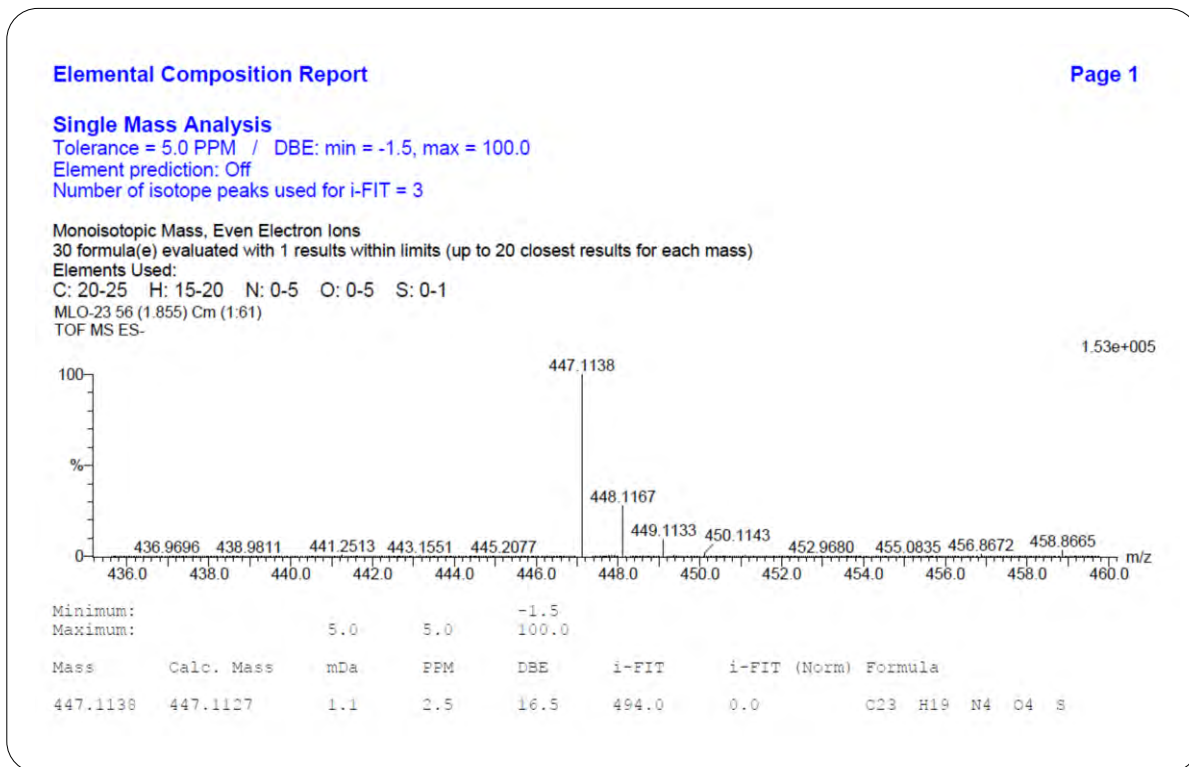


HRMS Spectrum of Compound 10l (chapter 4)

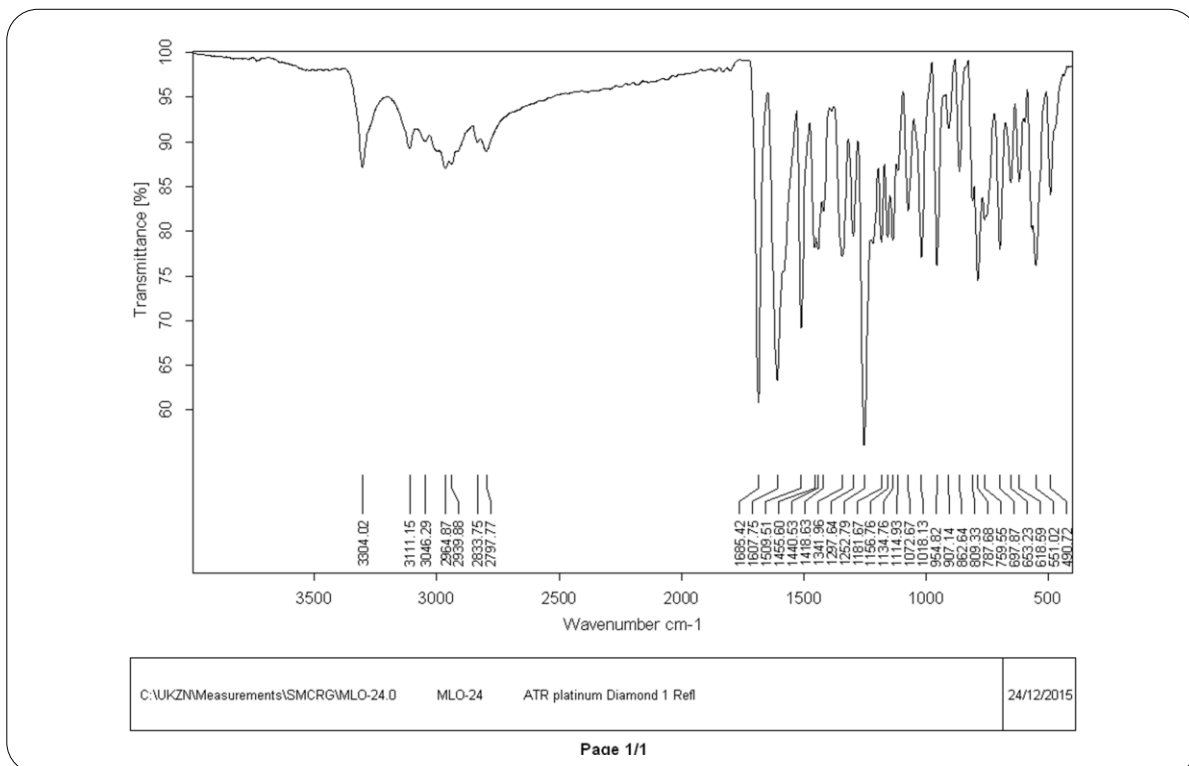


IR Spectrum of Compound 13a (chapter 4)

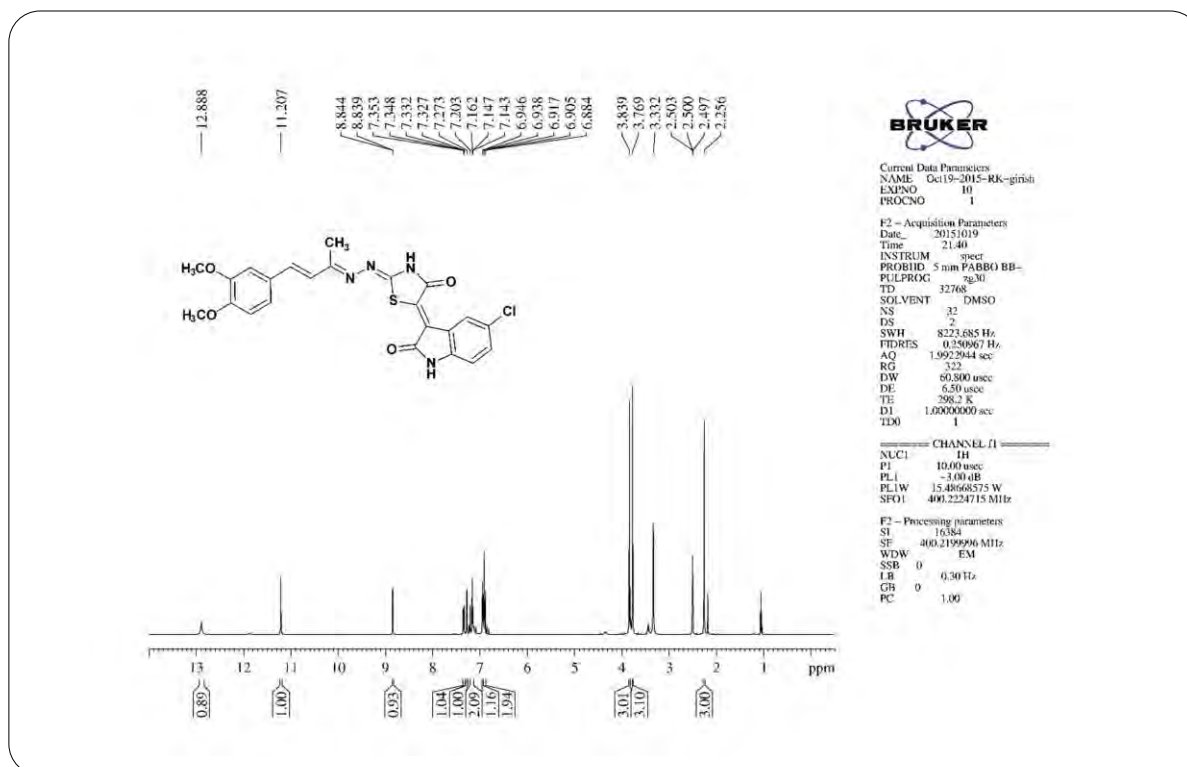
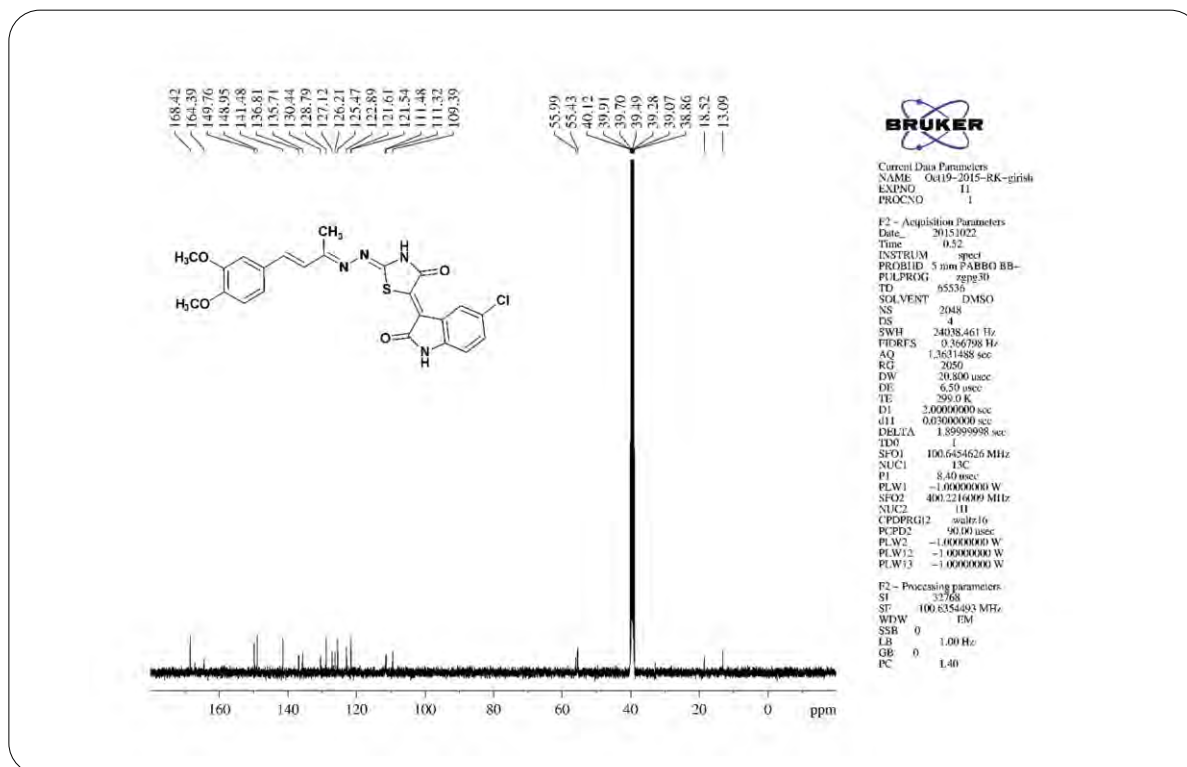
**¹H NMR Spectrum of Compound 13a (chapter 4)****¹³C NMR Spectrum of Compound 13a (chapter 4)**

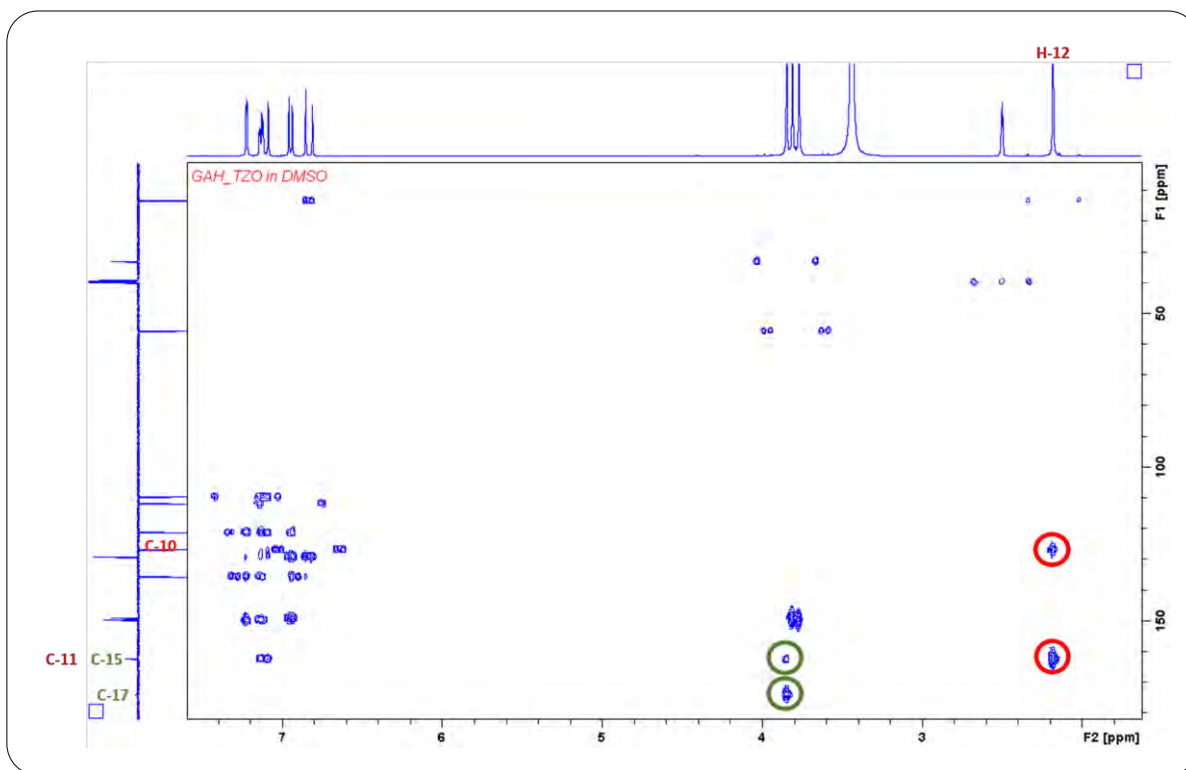


HRMS Spectrum of Compound 13a (chapter 4)

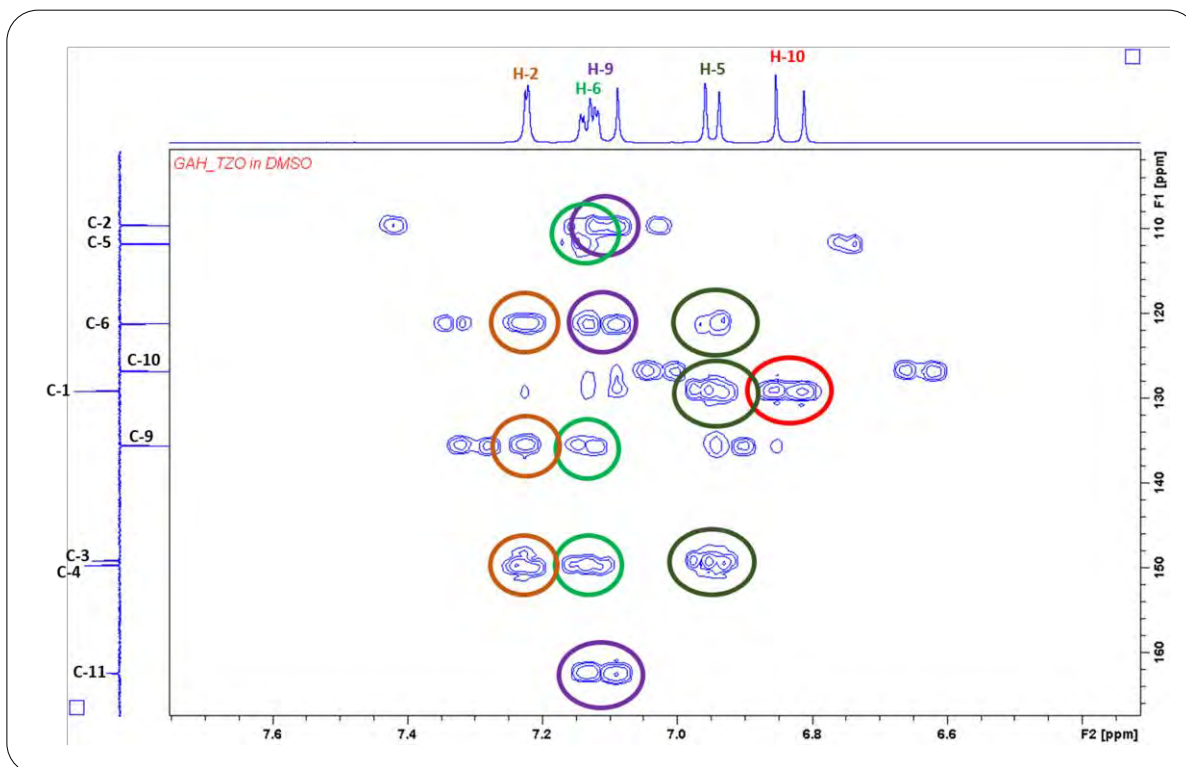


IR Spectrum of Compound 13b (chapter 4)

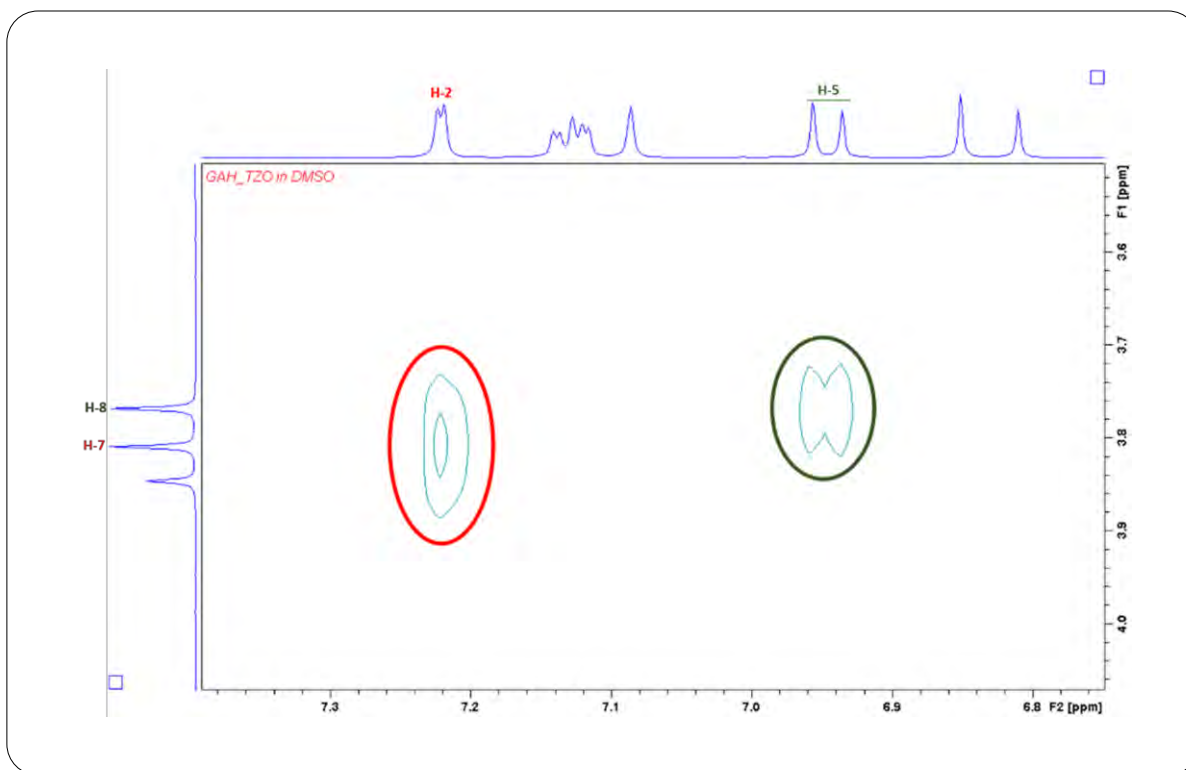
**¹H NMR Spectrum of Compound 13b (chapter 4)****¹³C NMR Spectrum of Compound 13b (chapter 4)**



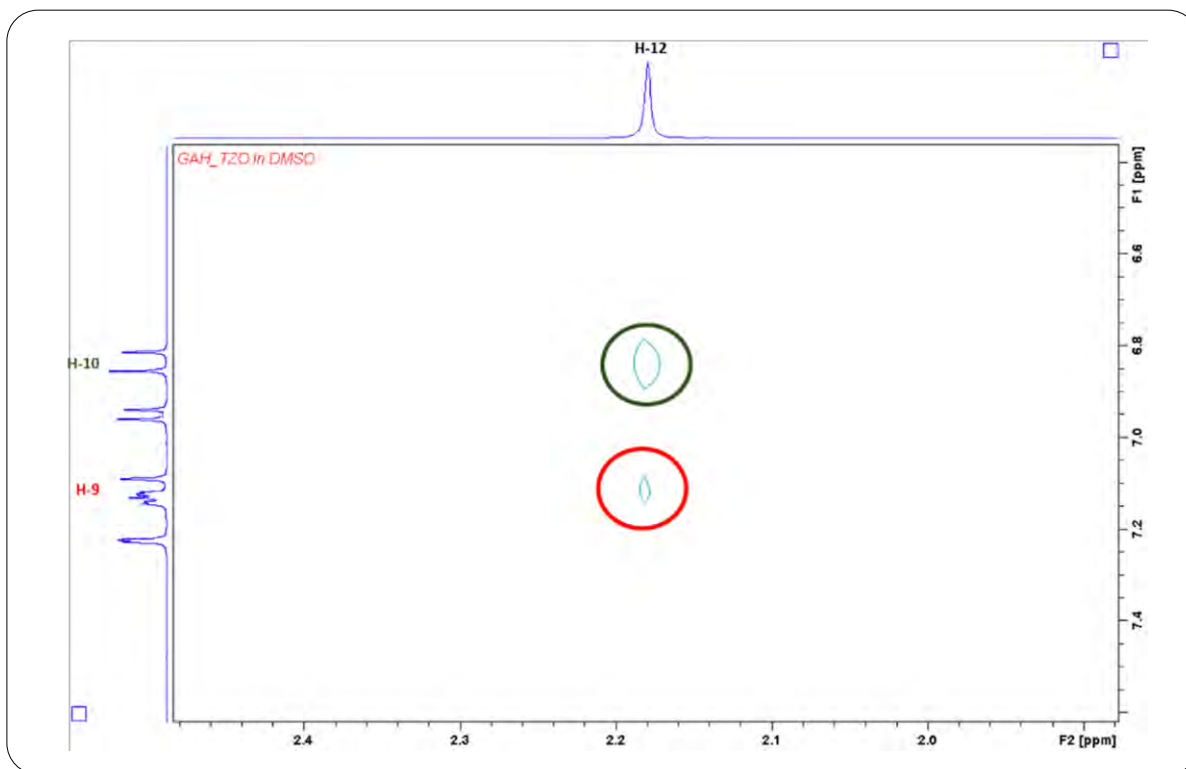
HMBC correlation Spectrum of Compound 5 (chapter 4)



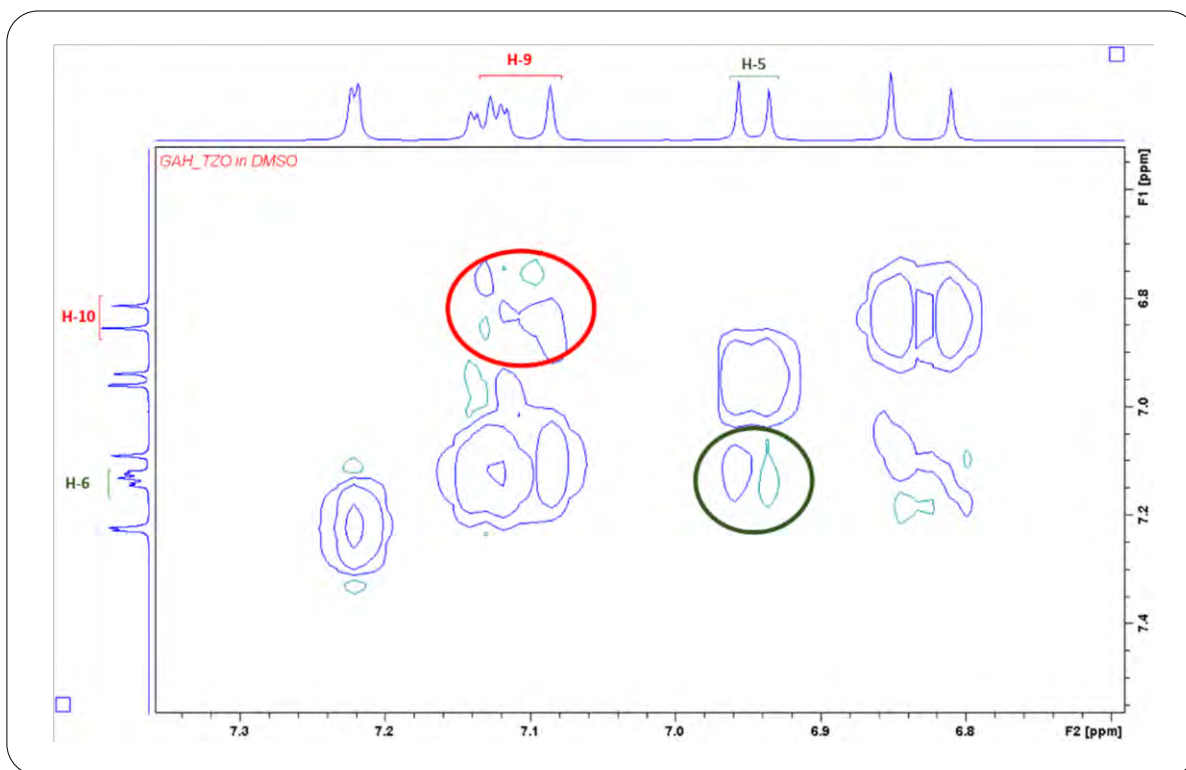
HMBC correlation Spectrum of Compound 5 (chapter 4)



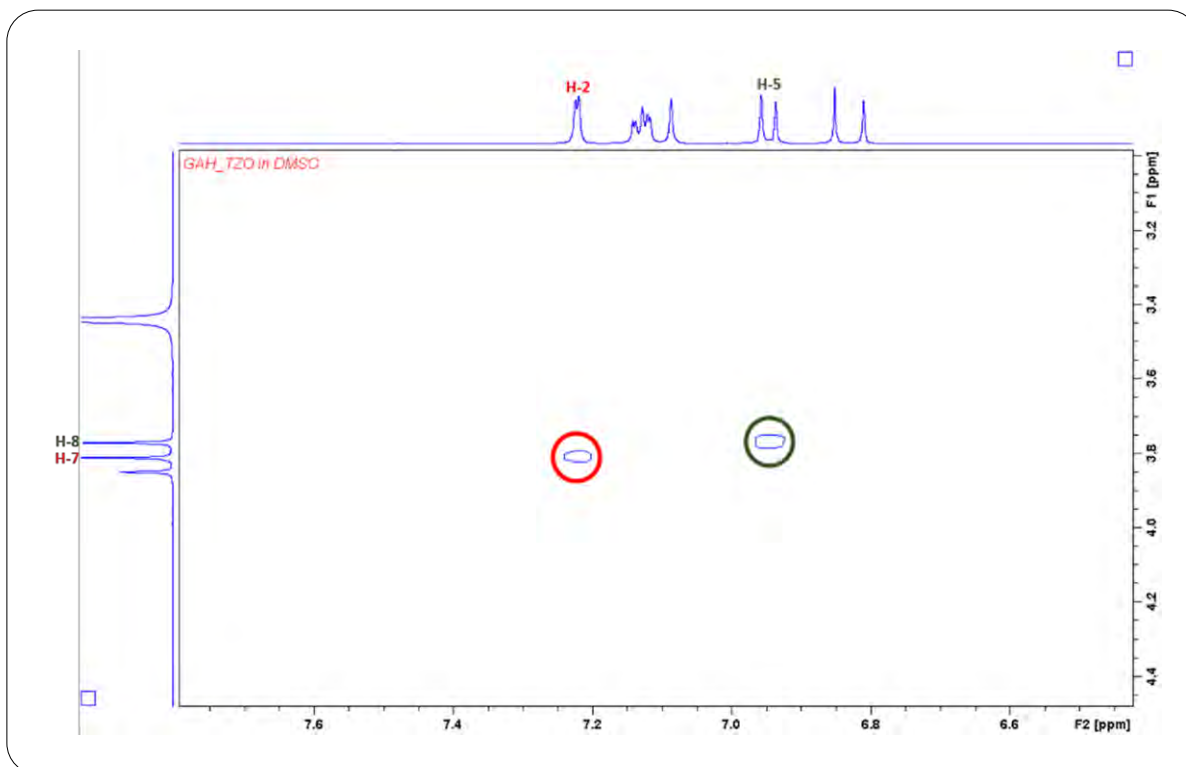
NOESY correlation Spectrum of Compound 5 (chapter 4)



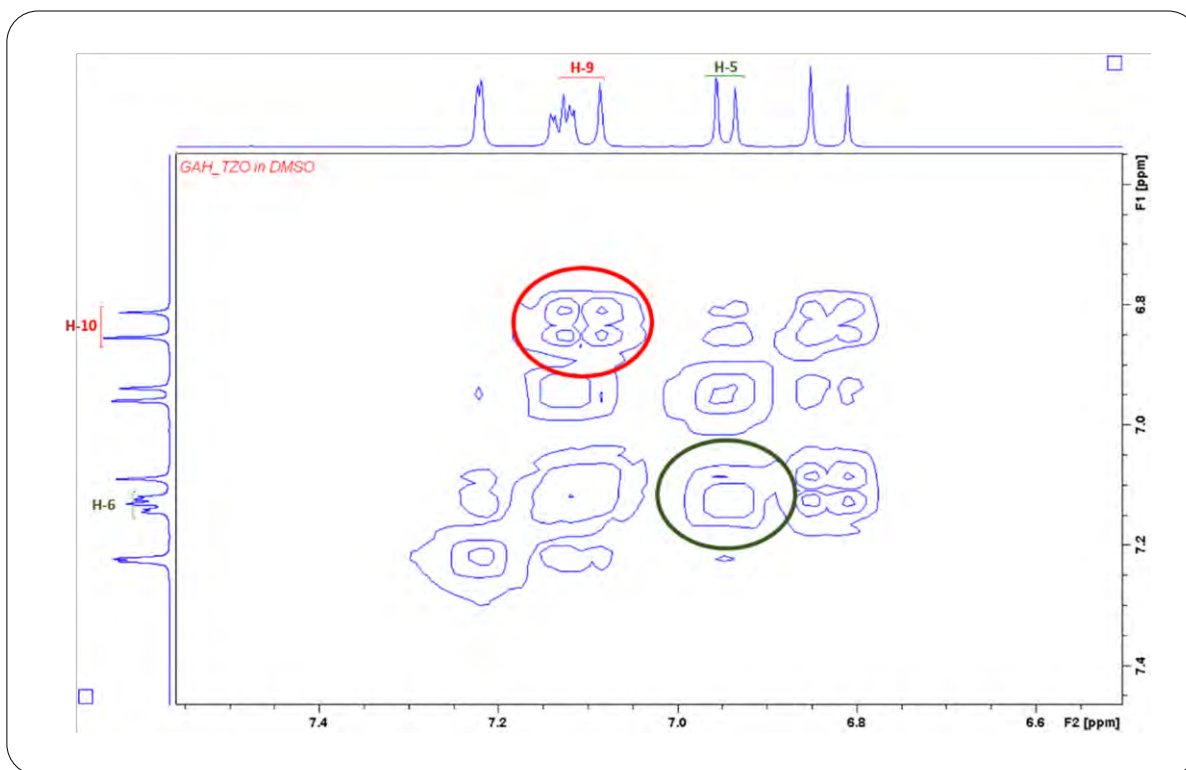
NOESY correlation Spectrum of Compound 5 (chapter 4)



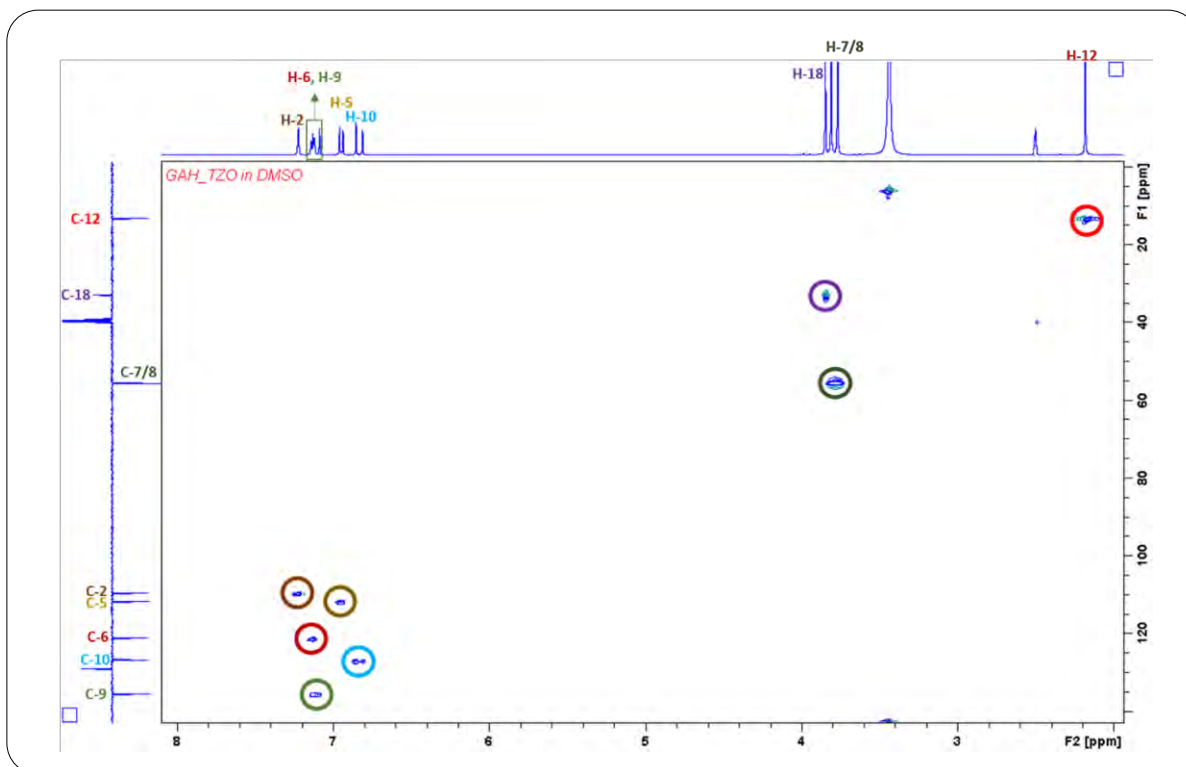
NOESY correlation Spectrum of Compound 5 (chapter 4)



COSY correlation Spectrum of Compound 5 (chapter 4)



COSY correlation Spectrum of Compound 5 (chapter 4)



HSQC correlation Spectrum of Compound 5 (chapter 4)

APPENDIX - III

SUPPLEMENTARY INFORMATION

CHAPTER 5

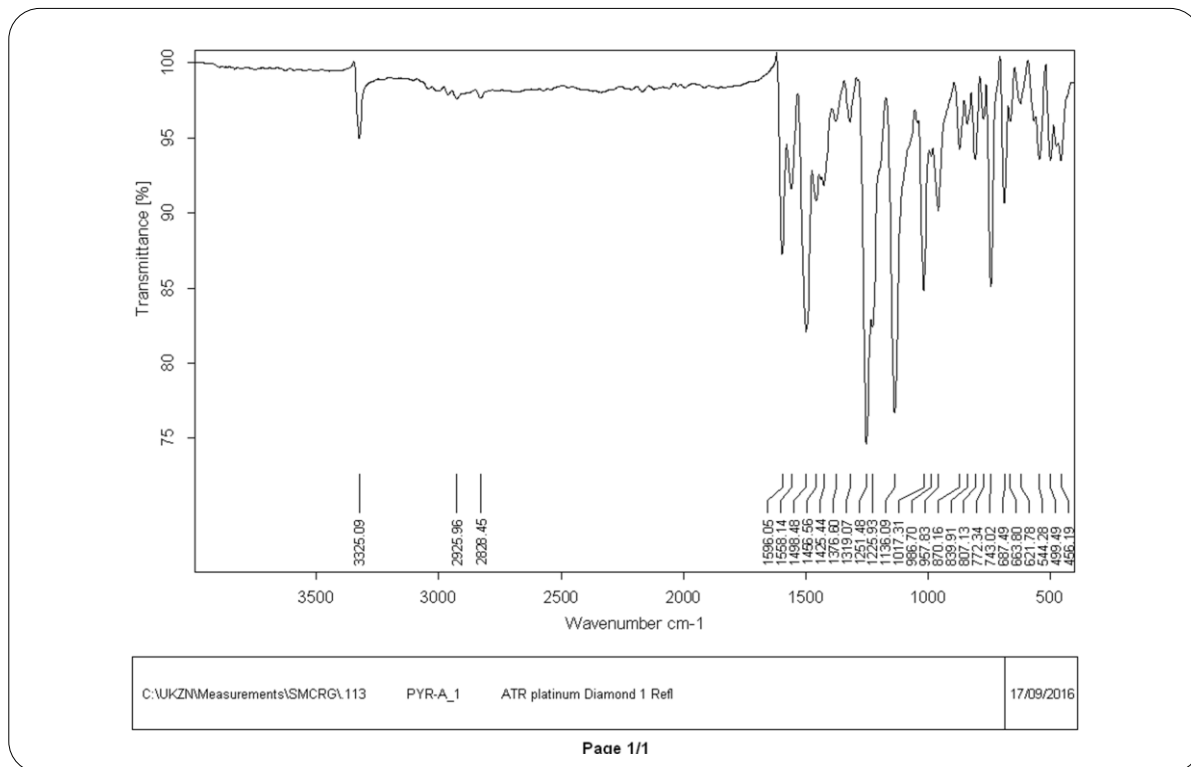
Dehydrozingerone encouraged novel styryl pyrazolo carbazone hybrids as potential antimicrobial and antimycobacterial agents

Girish A. Hampannavar^a, Mahesh B. Palkar^{b,a}, Afsana Kajee^a, Mahamadhanif S. Shaikh^a, Koleka P. Mlisana^c, Rajshekhar V. Karpoormath^{a*}

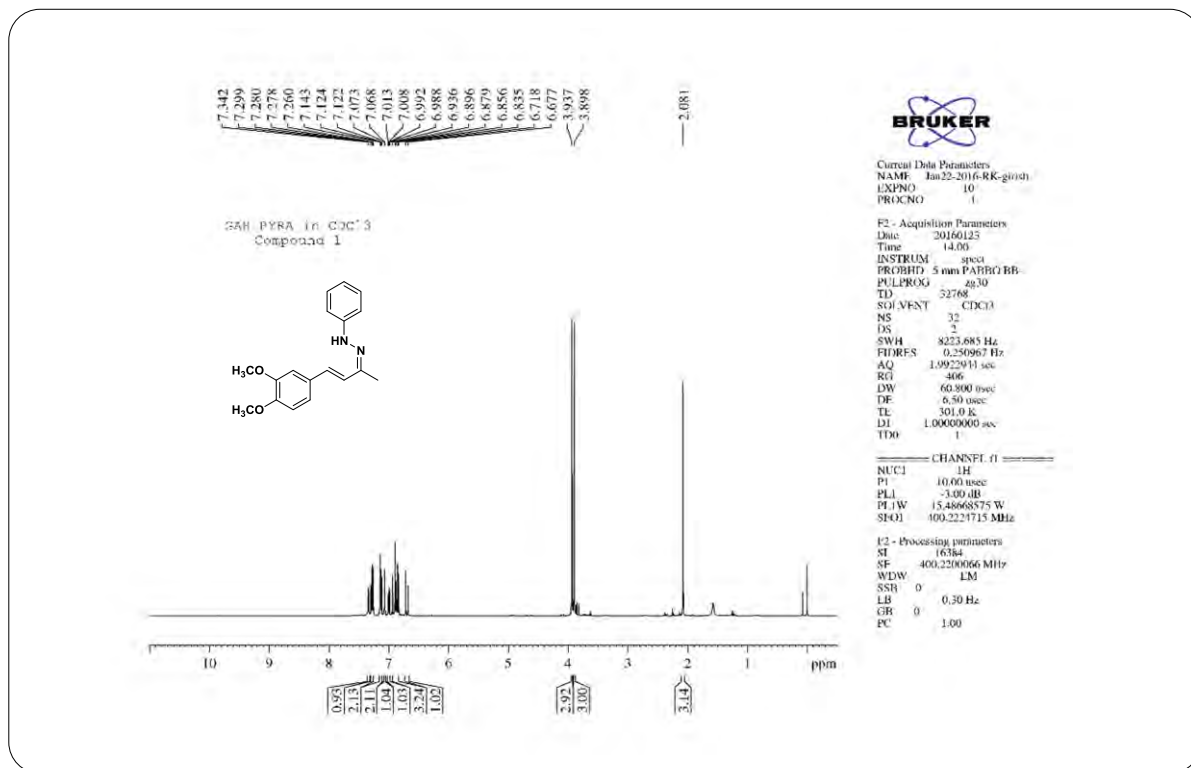
^a Department of Pharmaceutical Chemistry, Discipline of Pharmaceutical Sciences, College of Health Sciences, University of KwaZulu-Natal (Westville), Durban-4000, South Africa.

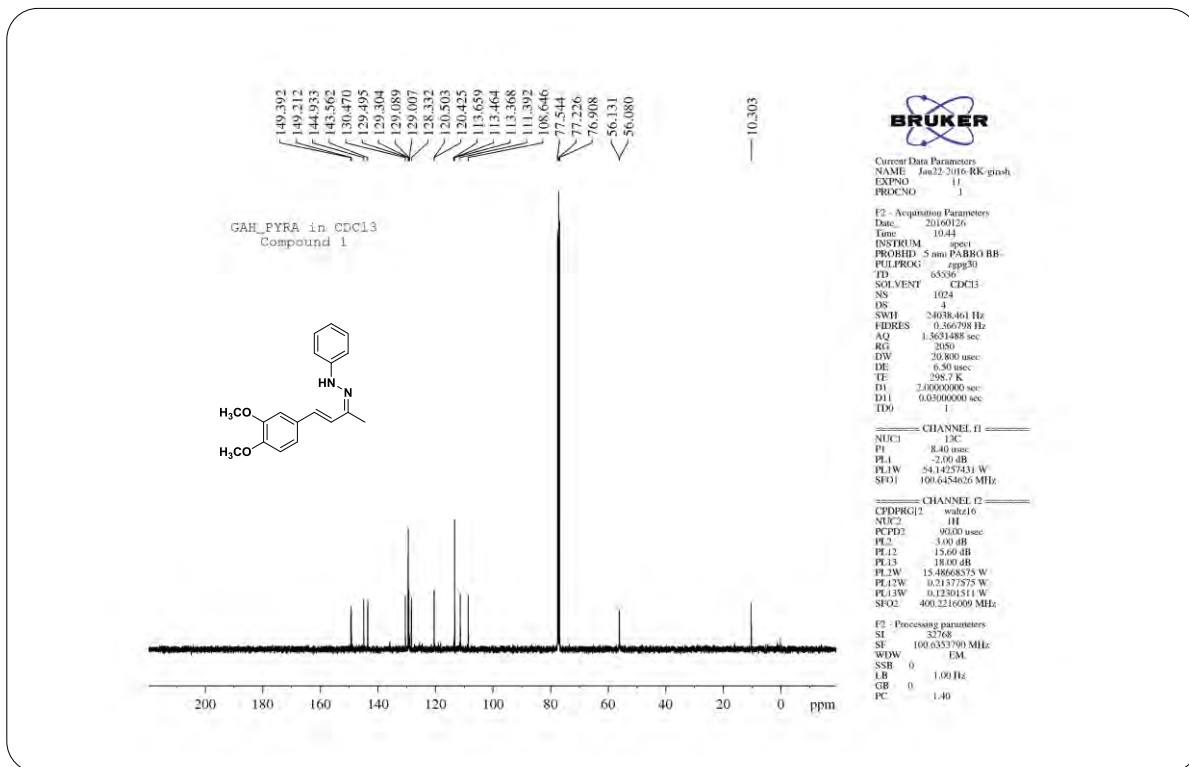
^b Department of Pharmaceutical Chemistry, K.L.E. University College of Pharmacy, Vidyanagar, Hubballi-580031, Karnataka, India.

^c Department of Microbiology, National Health Laboratory Services (NHLS), Inkosi Albert Luthuli Central Hospital, Durban, South Africa



IR Spectrum of Compound 4 (chapter 5)

¹H NMR Spectrum of Compound 4 (chapter 5)

**¹³C NMR Spectrum of Compound 4 (chapter 5)****Elemental Composition Report**

Page 1

Single Mass Analysis

Tolerance = 5.0 PPM / DBE: min = -1.5, max = 100.0

Element prediction: Off

Number of isotope peaks used for i-FIT = 3

Monoisotopic Mass, Even Electron Ions

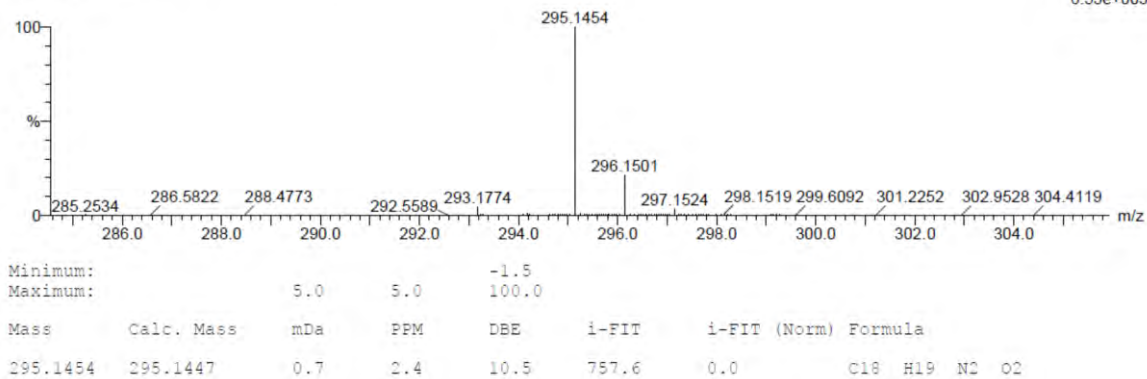
13 formula(e) evaluated with 1 results within limits (up to 20 closest results for each mass)

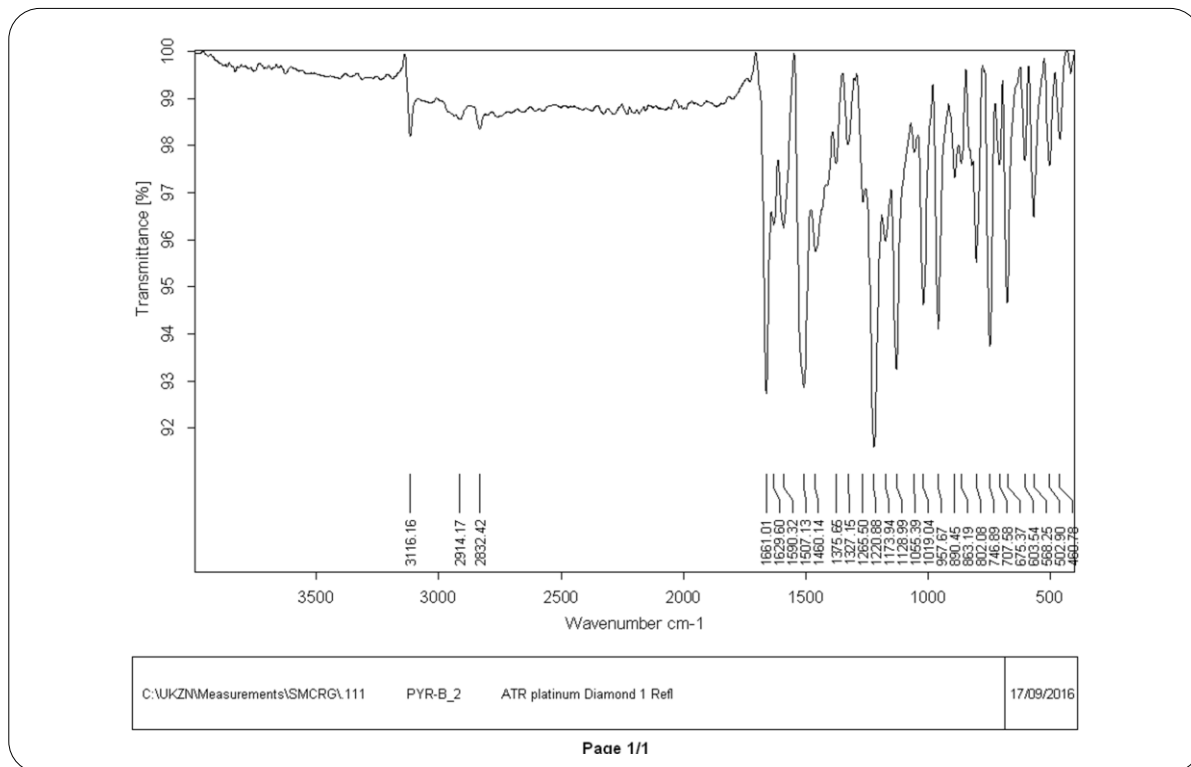
Elements Used:

C: 15-20 H: 15-20 N: 0-5 O: 0-5

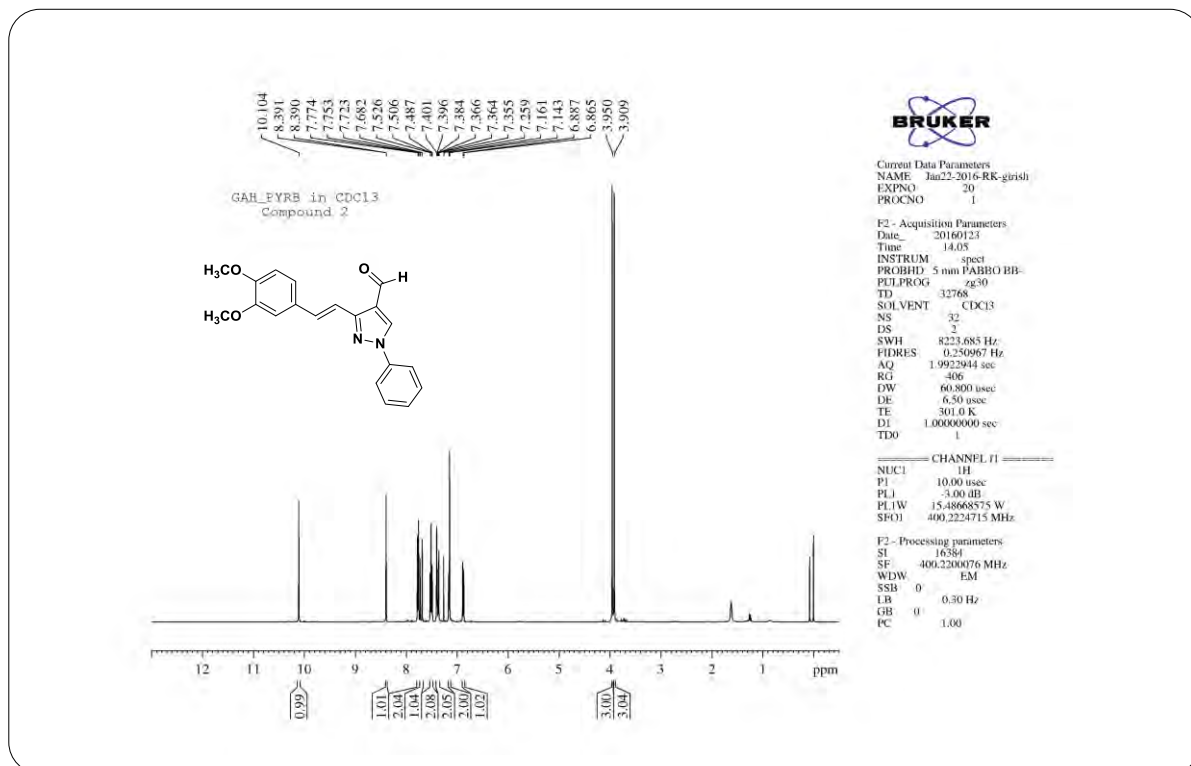
PYR-A 53 (1.753) Cm (1:61)

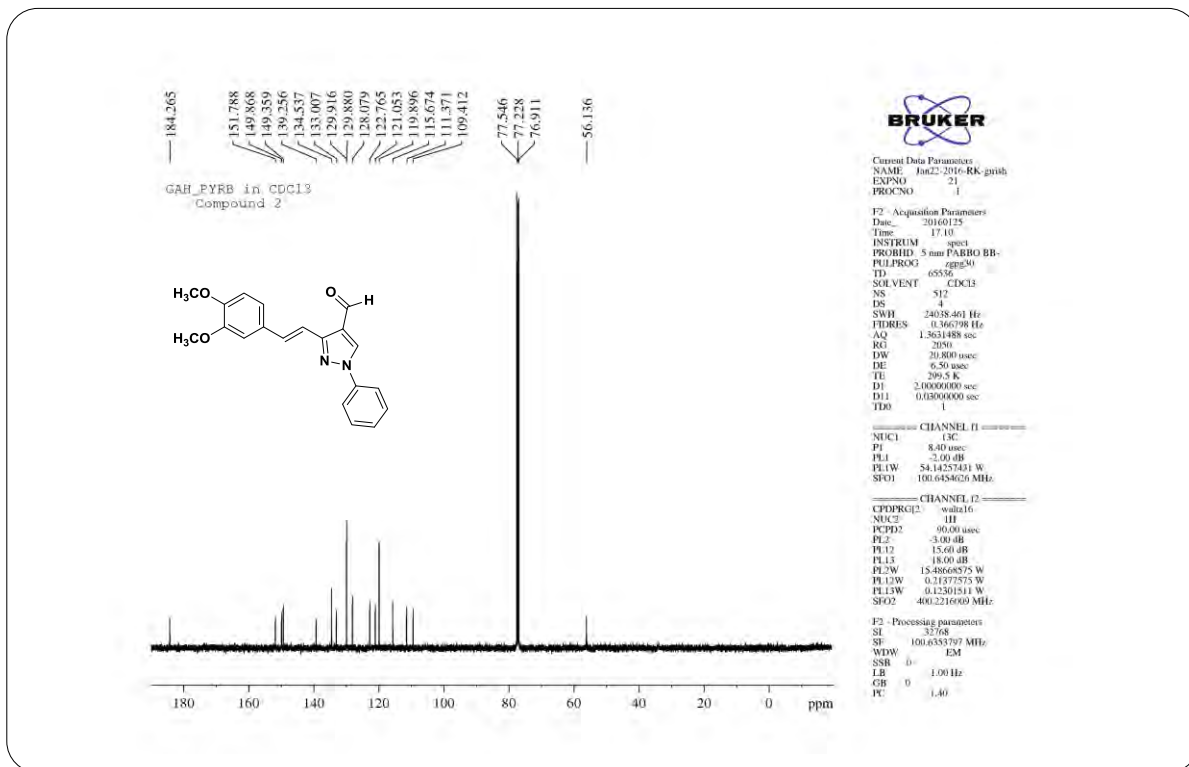
TOF MS ES-

**HRMS Spectrum of Compound 4 (chapter 5)**



IR Spectrum of Compound 5 (chapter 5)

¹H NMR Spectrum of Compound 5 (chapter 5)

**¹³C NMR Spectrum of Compound 5 (chapter 5)****Elemental Composition Report**

Page 1

Single Mass Analysis

Tolerance = 5.0 PPM / DBE: min = -1.5, max = 100.0

Element prediction: Off

Number of isotope peaks used for i-FIT = 3

Monoisotopic Mass, Even Electron Ions

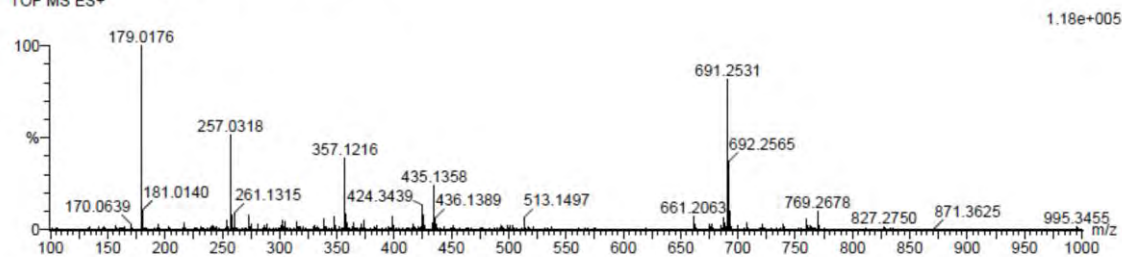
15 formula(e) evaluated with 1 results within limits (up to 20 closest results for each mass)

Elements Used:

C: 15-20 H: 15-20 N: 0-5 O: 0-5 Na: 1-1

PYR-B 2 (0.034) Cm (1:61)

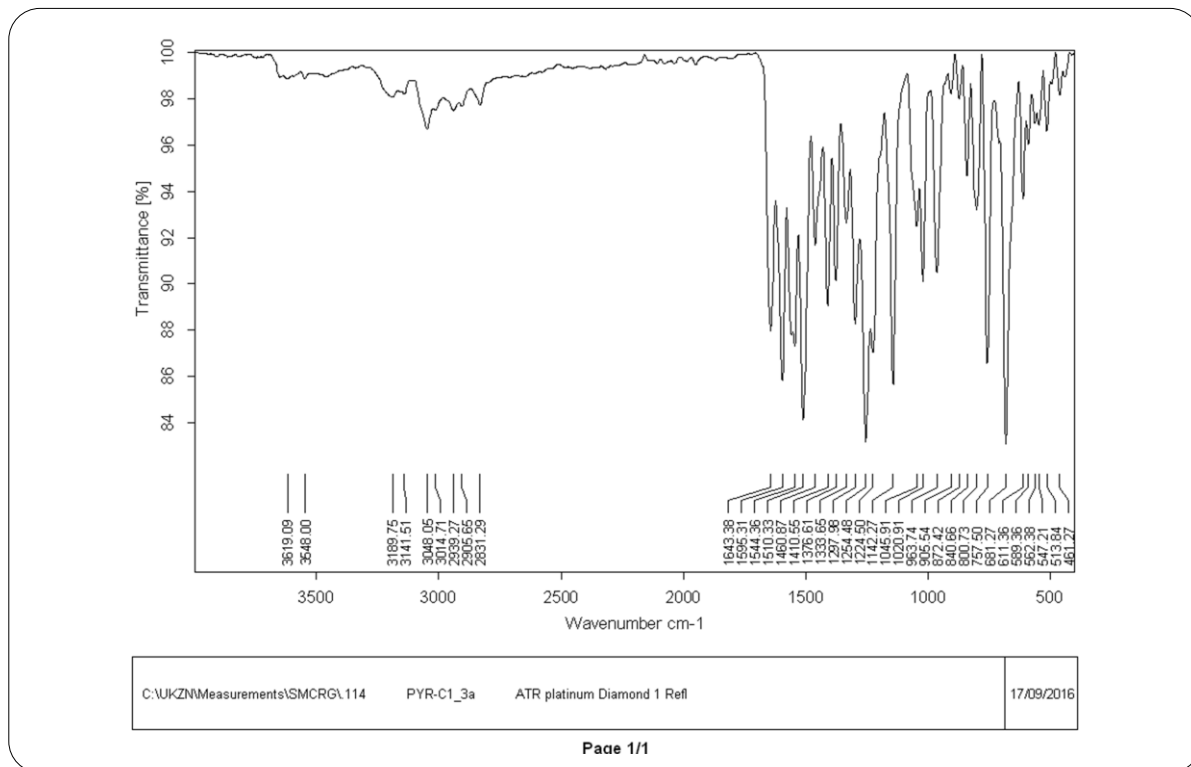
TOF MS ES+



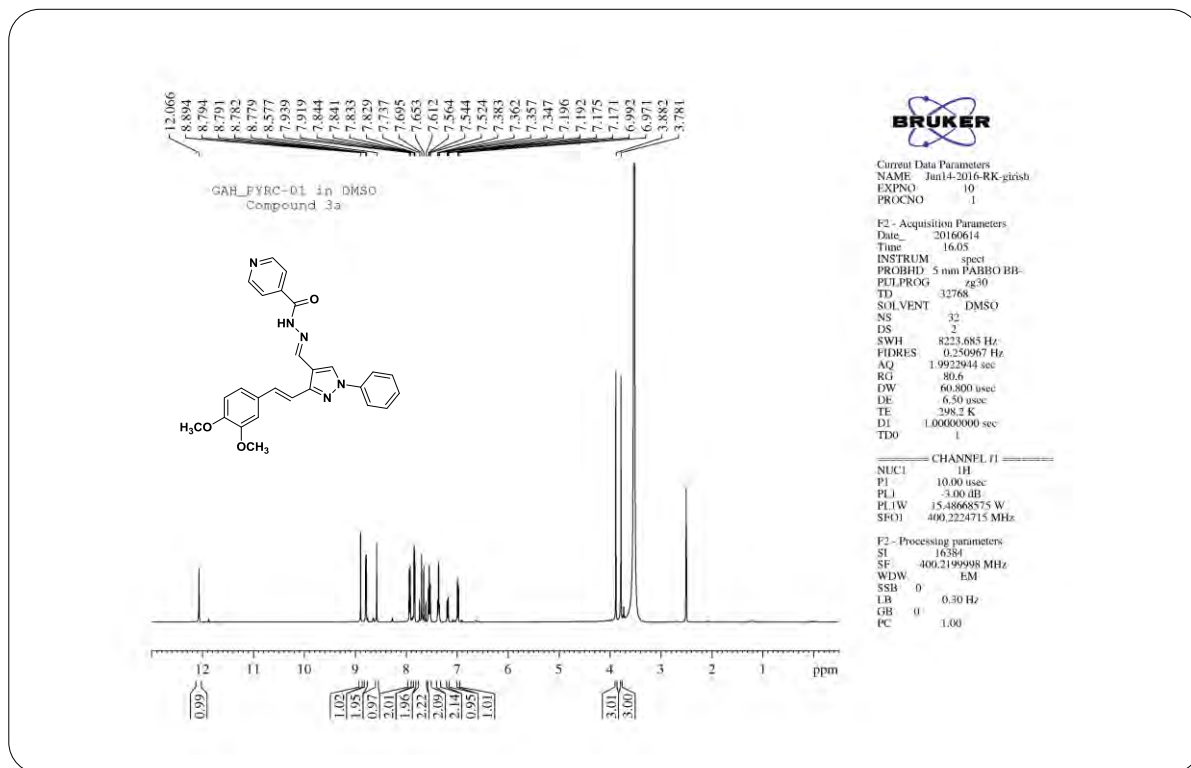
Minimum: -1.5
Maximum: 5.0 5.0 100.0

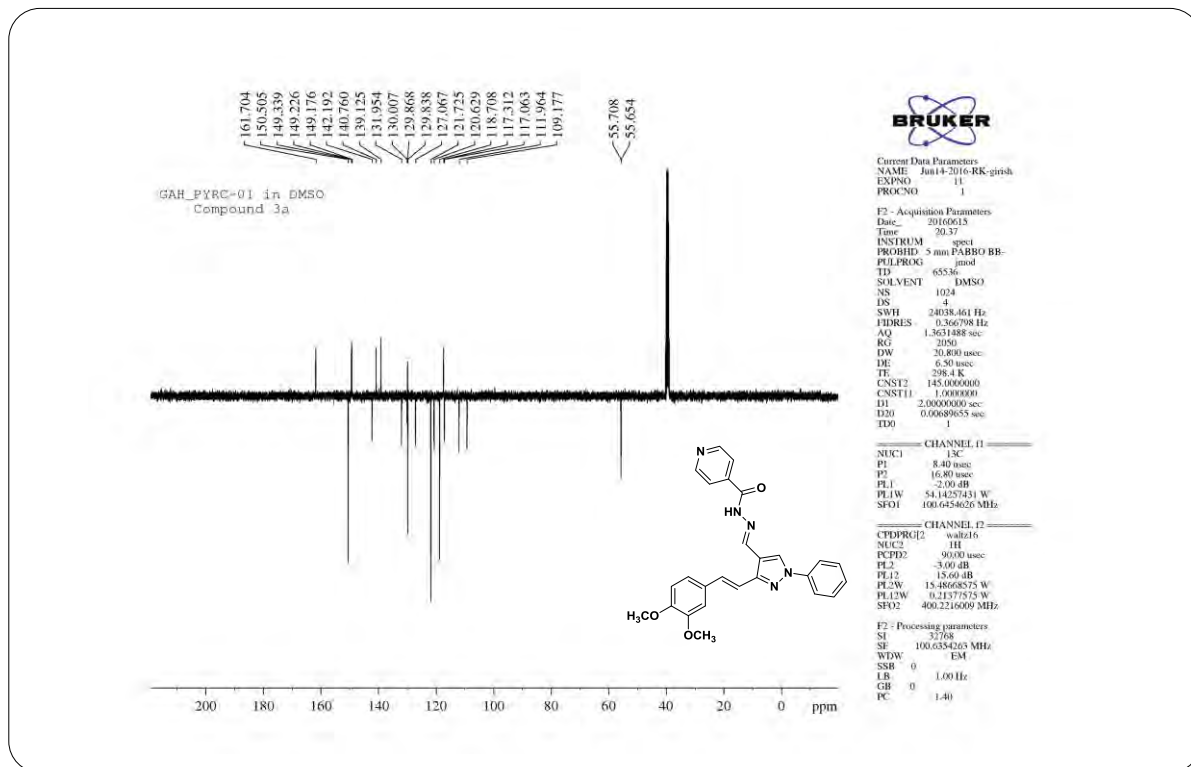
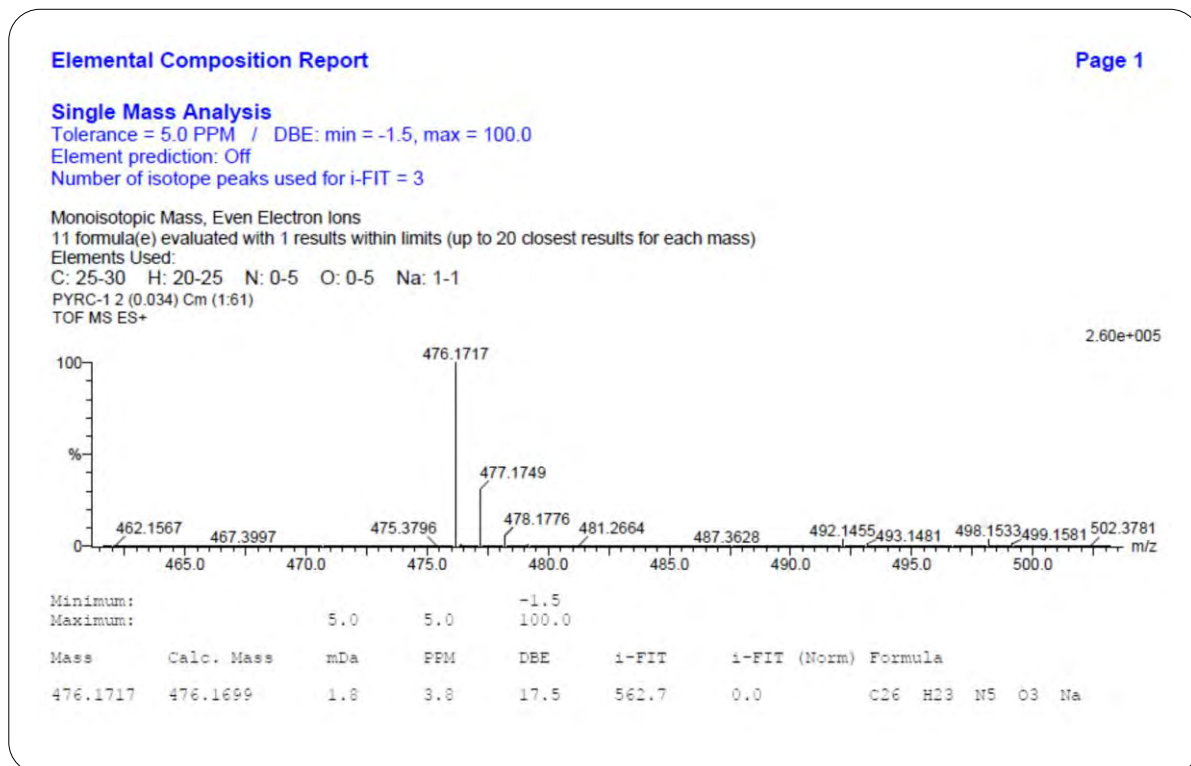
Mass	Calc. Mass	mDa	PPM	DBE	i-FIT	i-FIT (Norm)	Formula
357.1216	357.1215	0.1	0.3	12.5	506.7	0.0	C20 H18 N2 O3 Na

HRMS Spectrum of Compound 5 (chapter 5)

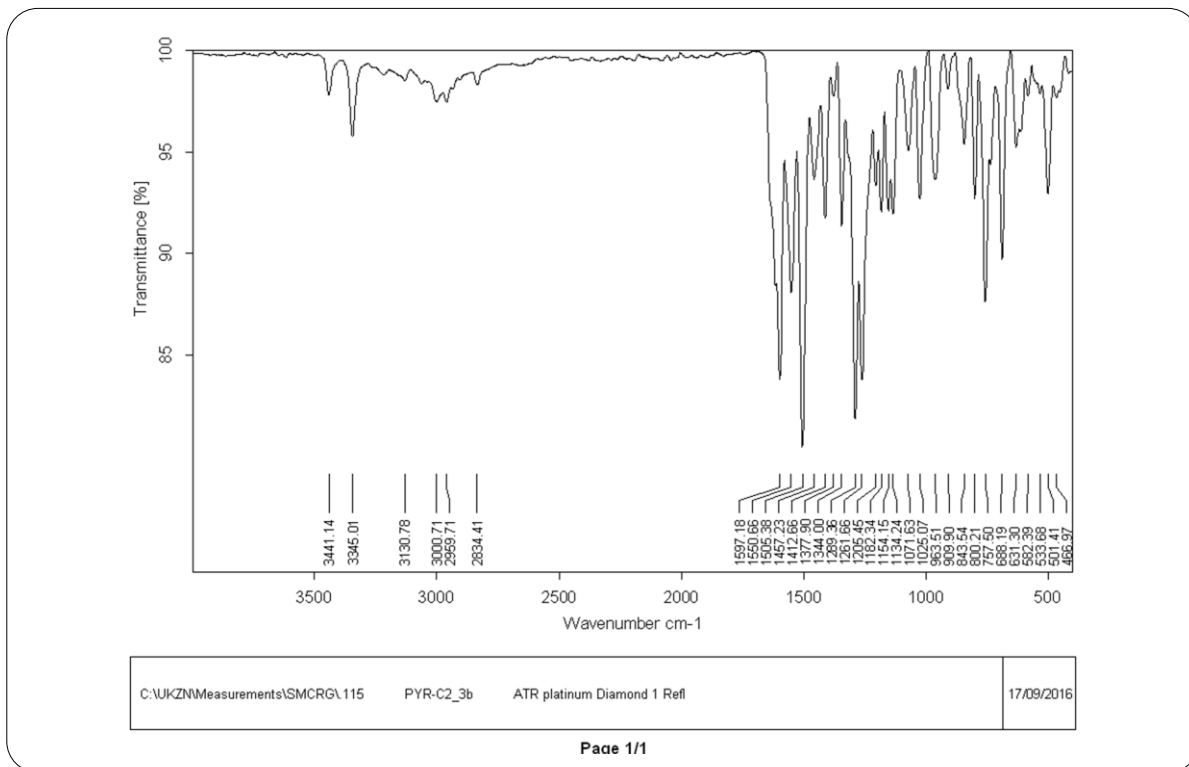


IR Spectrum of Compound 8a (chapter 5)

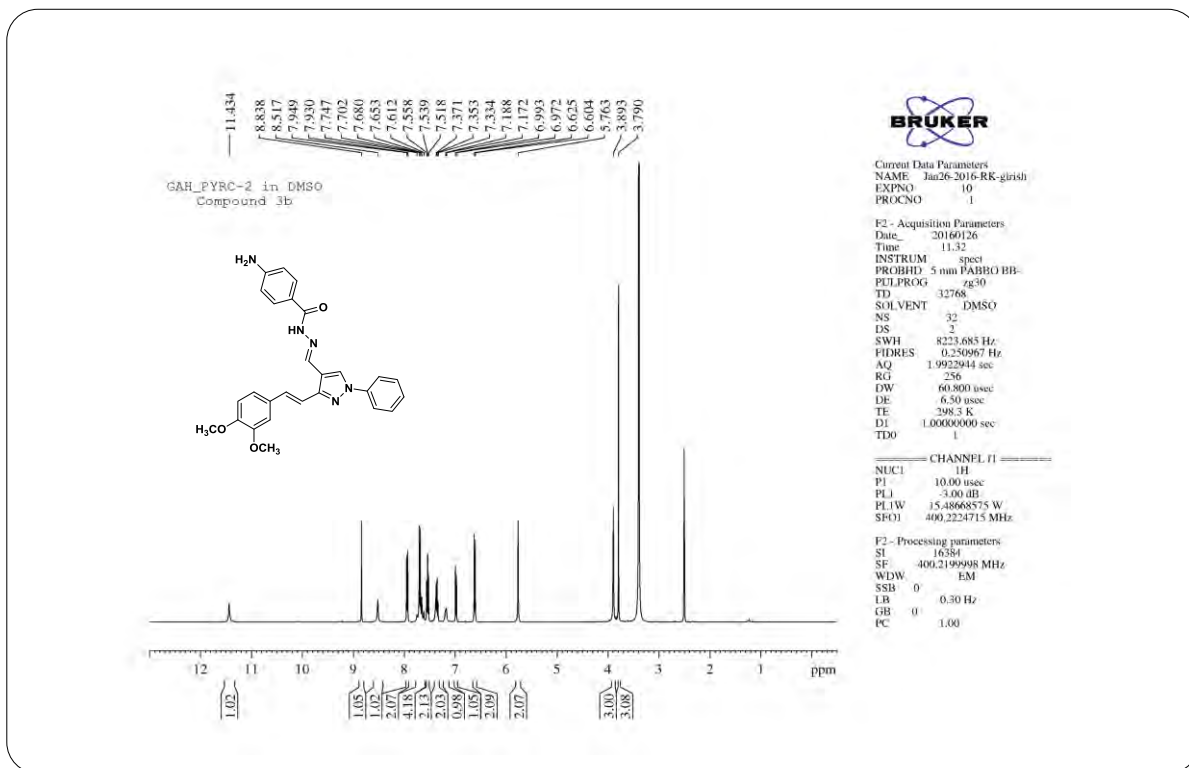
¹H NMR Spectrum of Compound 8a (chapter 5)

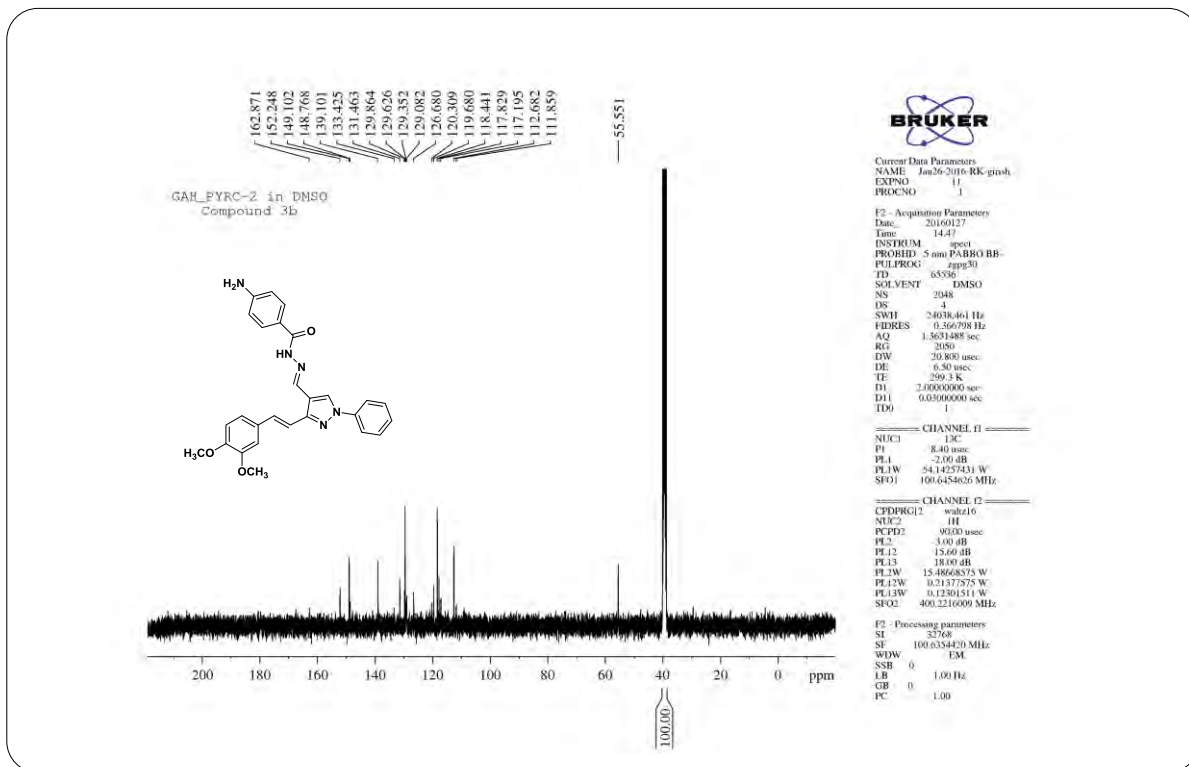
¹³C NMR Spectrum of Compound 8a (chapter 5)

HRMS Spectrum of Compound 8a (chapter 5)



IR Spectrum of Compound 8b (chapter 5)

¹H NMR Spectrum of Compound 8b (chapter 5)

**¹³C NMR Spectrum of Compound 8b (chapter 5)****Elemental Composition Report**

Page 1

Single Mass Analysis

Tolerance = 5.0 PPM / DBE: min = -1.5, max = 100.0

Element prediction: Off

Number of isotope peaks used for i-FIT = 3

Monoisotopic Mass, Even Electron Ions

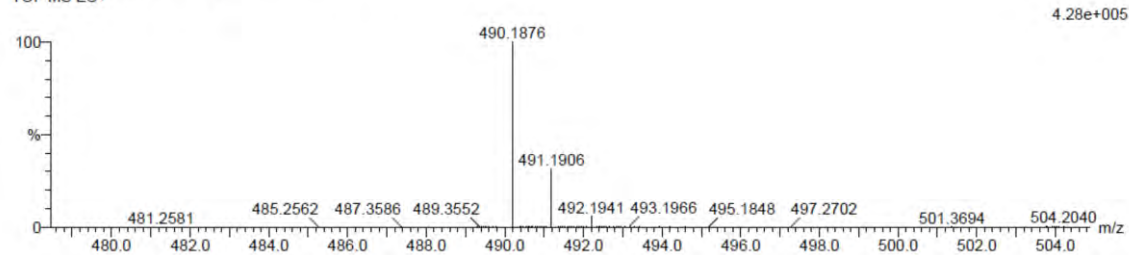
11 formula(e) evaluated with 1 results within limits (up to 20 closest results for each mass)

Elements Used:

C: 25-30 H: 20-25 N: 0-5 O: 0-5 Na: 1-1

PYRC-2 55 (1.822) Cm (1:61)

TOF MS ES+

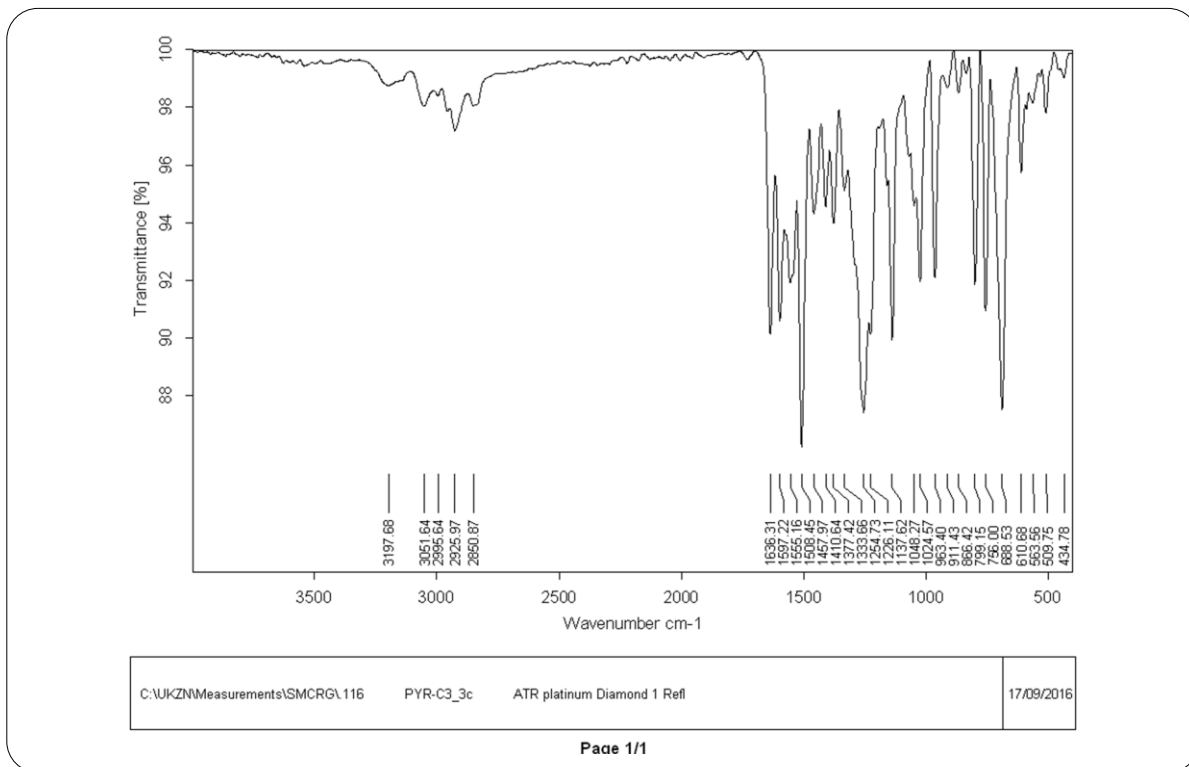


Minimum:

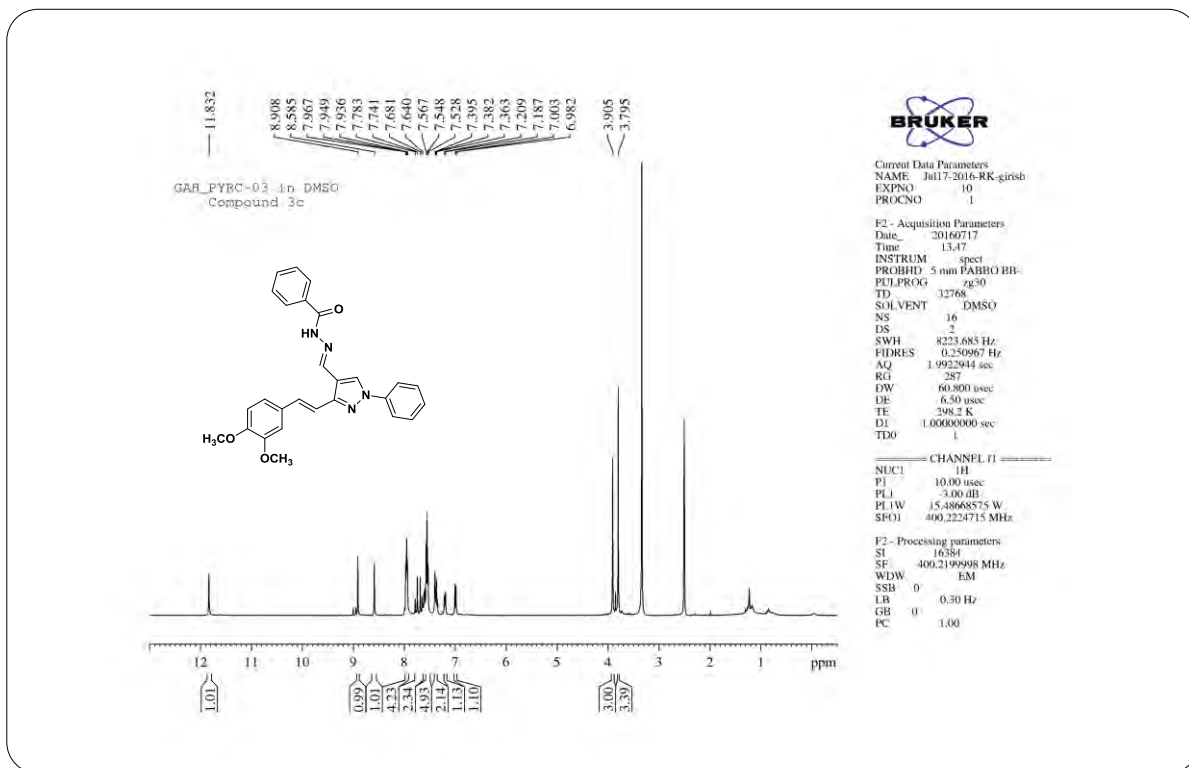
Maximum: 5.0 5.0 100.0

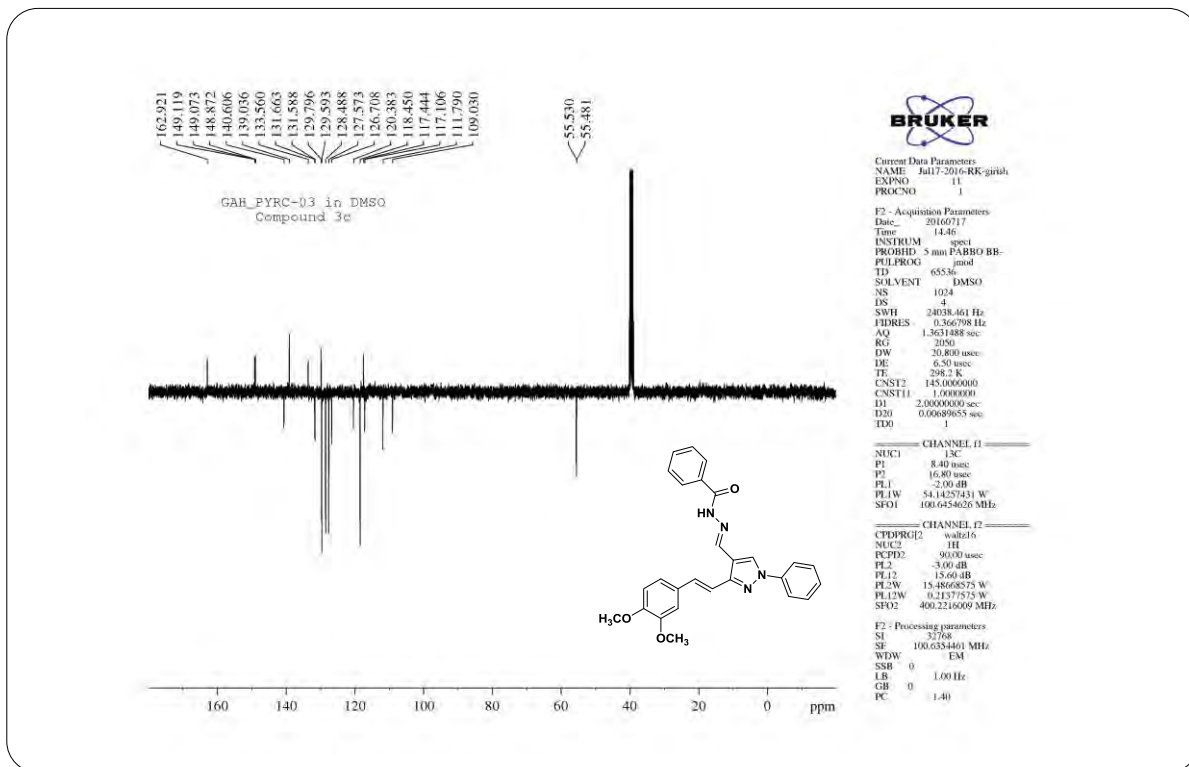
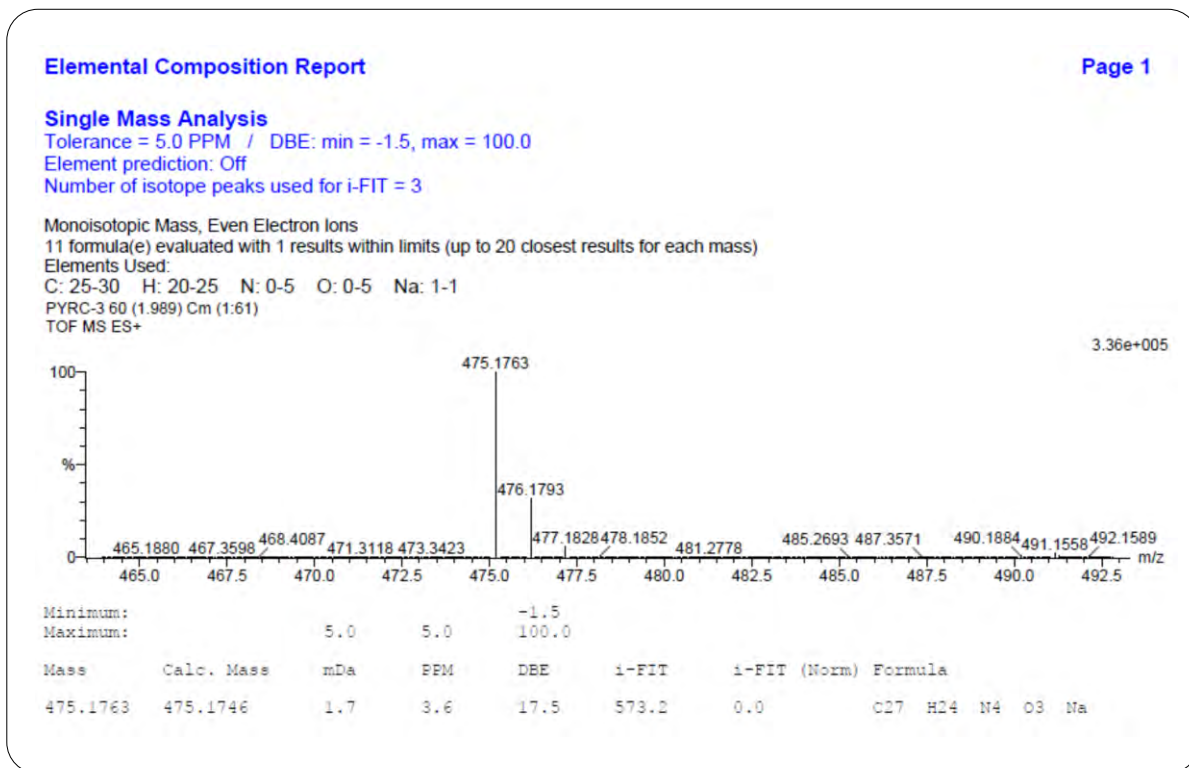
Mass	Calc. Mass	mDa	PPM	DBE	i-FIT	i-FIT (Norm)	Formula
490.1876	490.1855	2.1	4.3	17.5	606.2	0.0	C27 H25 N5 O3 Na

HRMS Spectrum of Compound 8b (chapter 5)

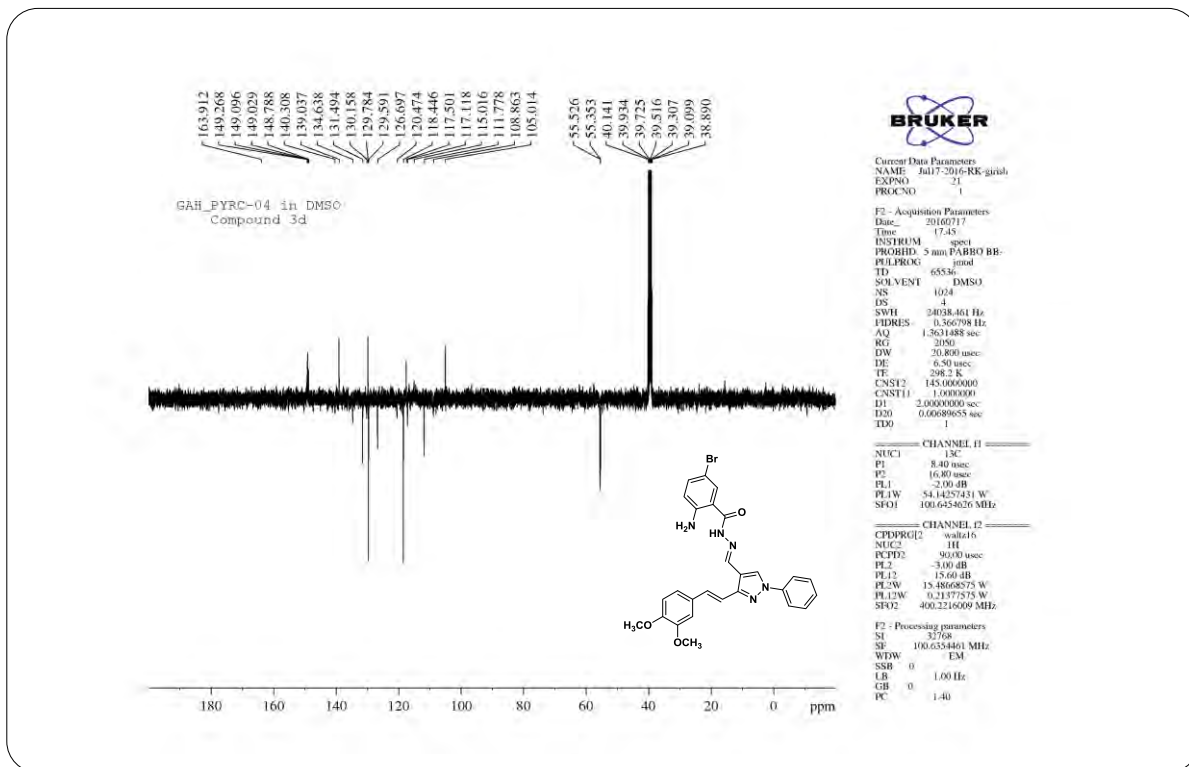
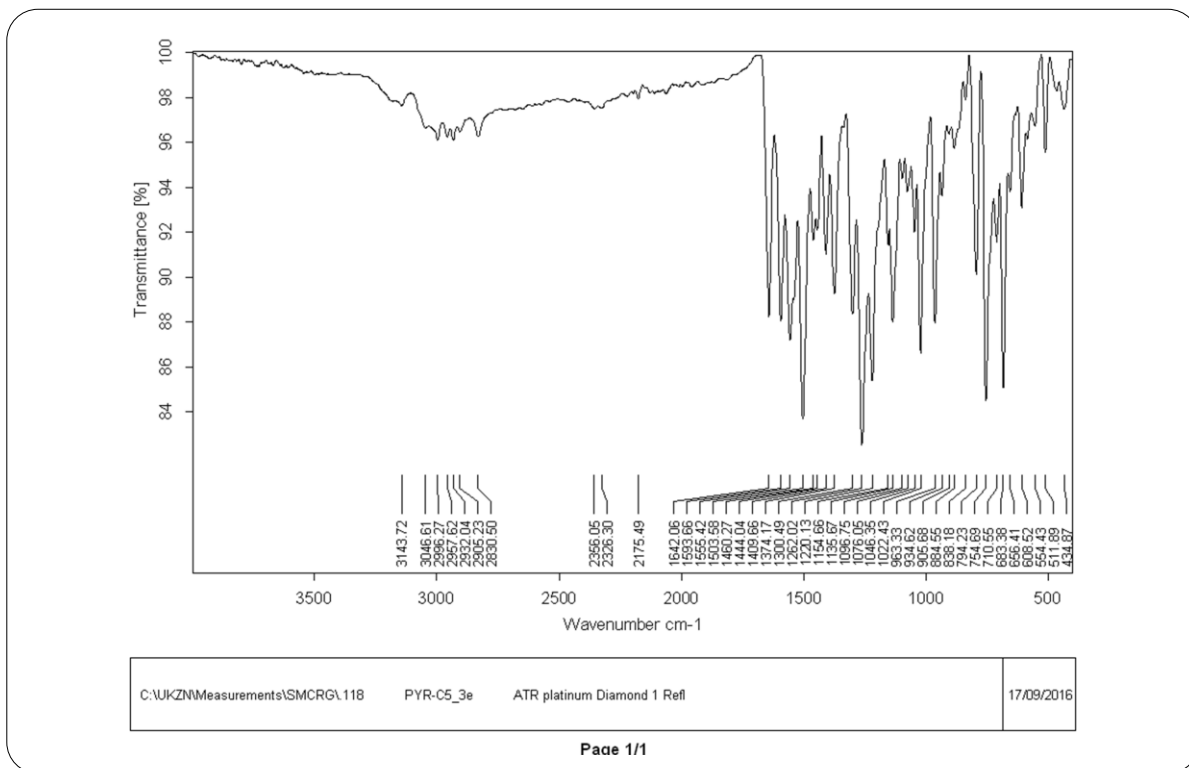


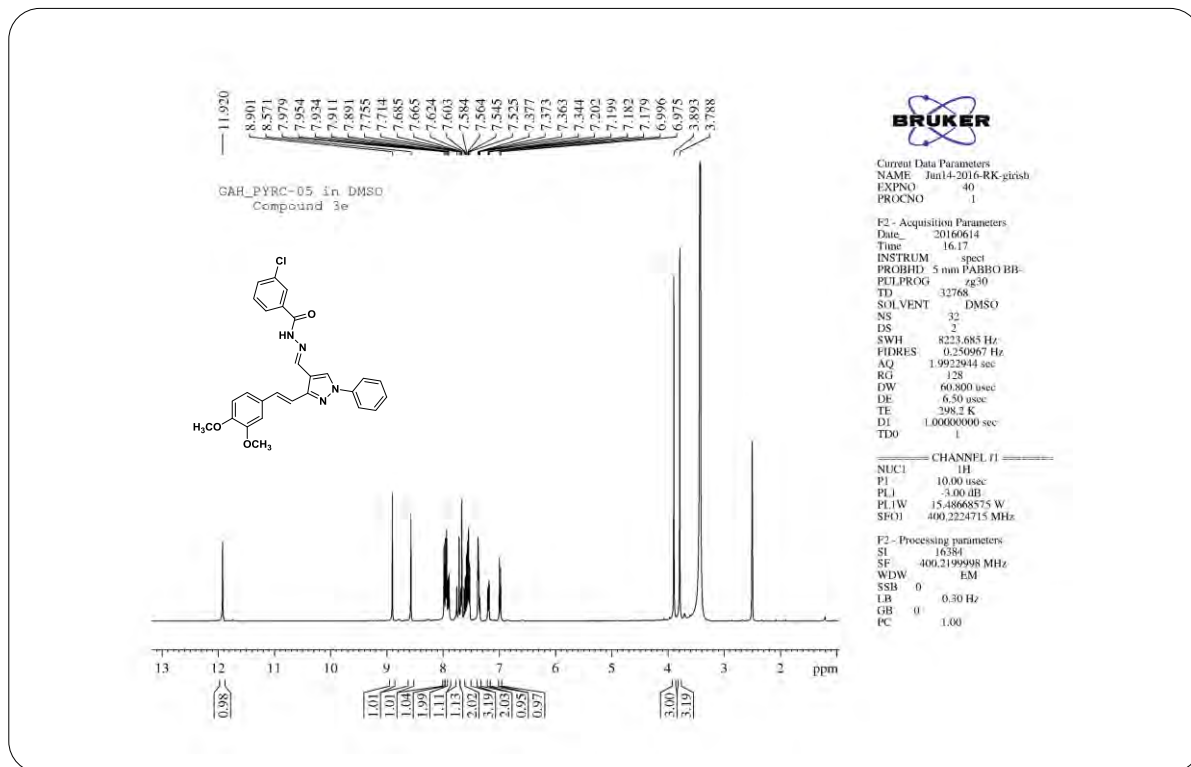
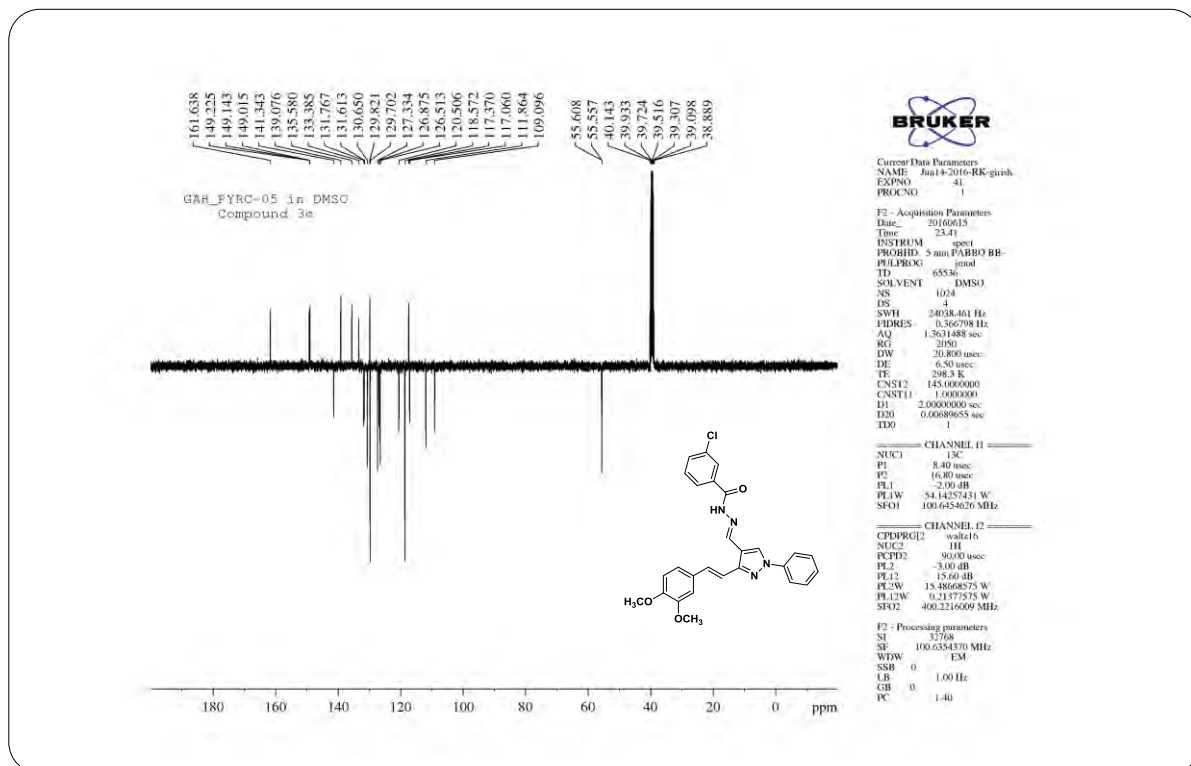
IR Spectrum of Compound 8c (chapter 5)

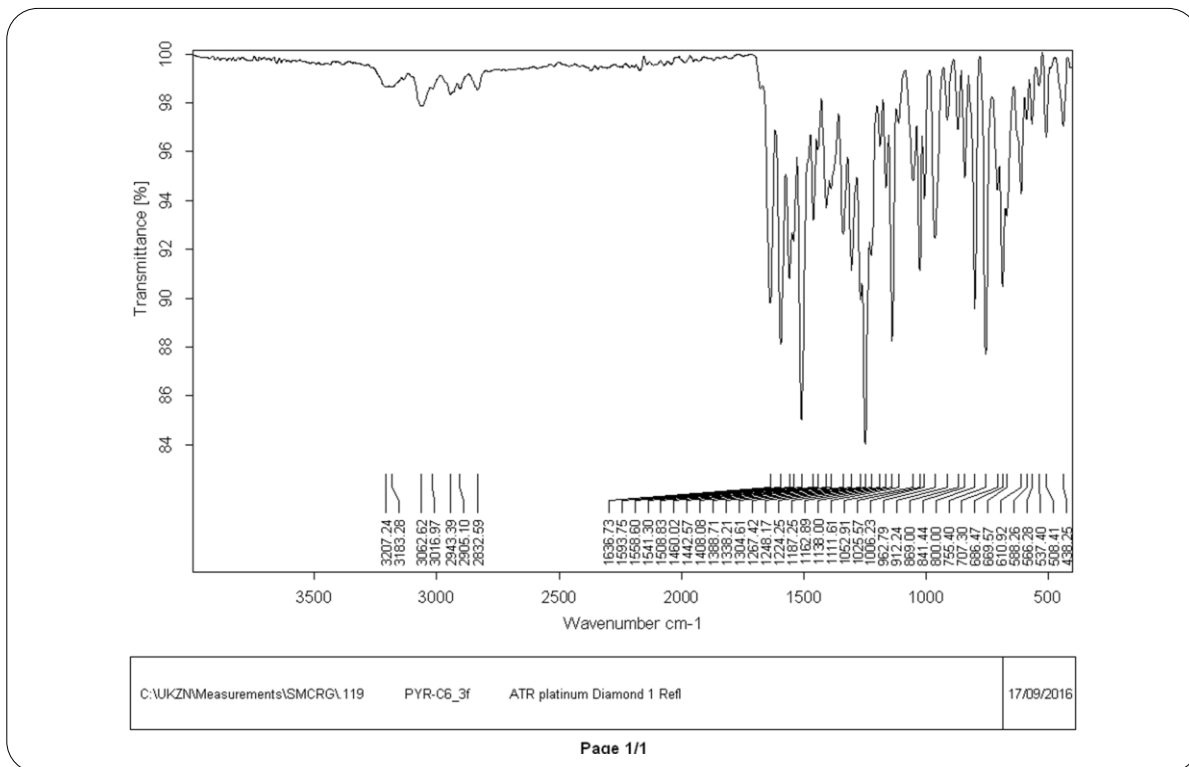
¹H NMR Spectrum of Compound 8c (chapter 5)

¹³C NMR Spectrum of Compound 8c (chapter 5)

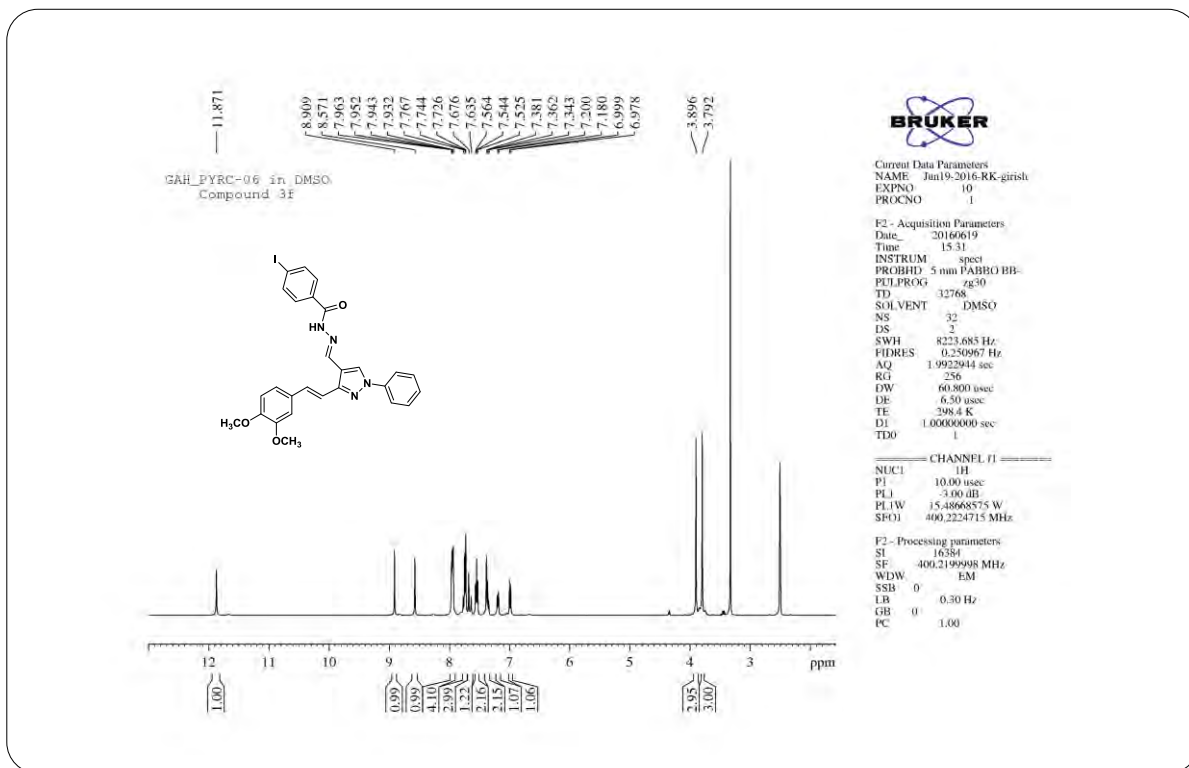
HRMS Spectrum of Compound 8c (chapter 5)

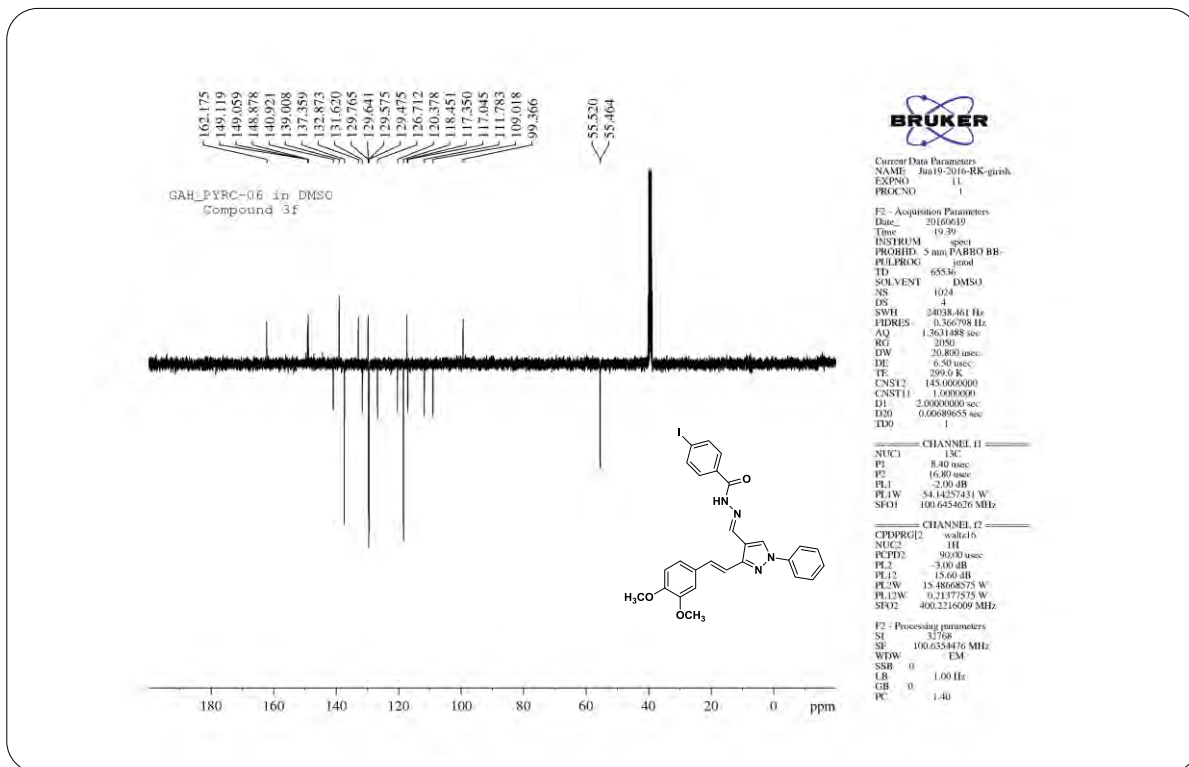
**¹³C NMR Spectrum of Compound 8d (chapter 5)****IR Spectrum of Compound 8e (chapter 5)**

¹H NMR Spectrum of Compound 8e (chapter 5)¹³C NMR Spectrum of Compound 8e (chapter 5)



IR Spectrum of Compound 8f (chapter 5)

¹H NMR Spectrum of Compound 8f (chapter 5)

**¹³C NMR Spectrum of Compound 8f (chapter 5)****Elemental Composition Report**

Page 1

Single Mass Analysis

Tolerance = 5.0 PPM / DBE: min = -1.5, max = 100.0

Element prediction: Off

Number of isotope peaks used for i-FIT = 3

Monoisotopic Mass, Even Electron Ions

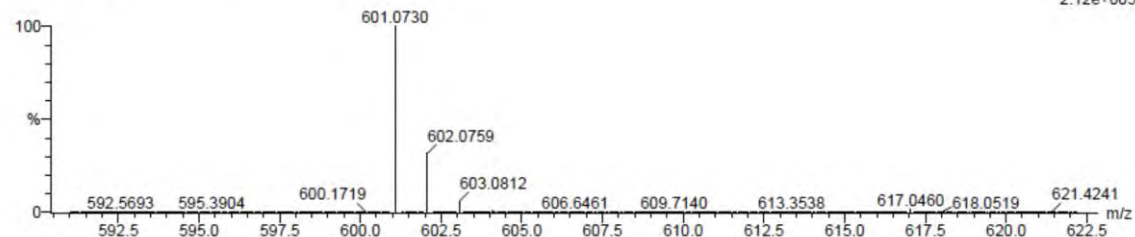
44 formula(e) evaluated with 1 results within limits (up to 20 closest results for each mass)

Elements Used:

C: 25-30 H: 20-25 N: 0-5 O: 0-5 Na: 1-1 I: 0-1

PYRC-6 34 (1.114) Cm (1:61)

TOF MS ES+



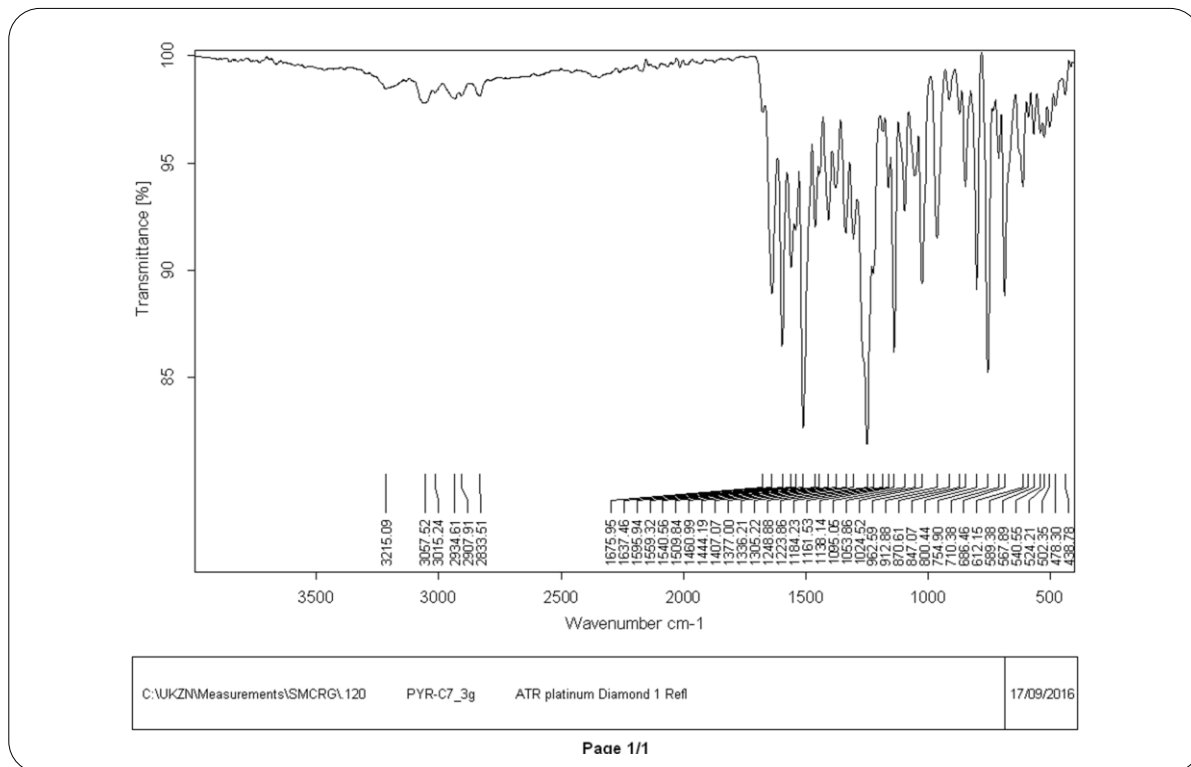
Minimum:

Maximum: 5.0 5.0 100.0

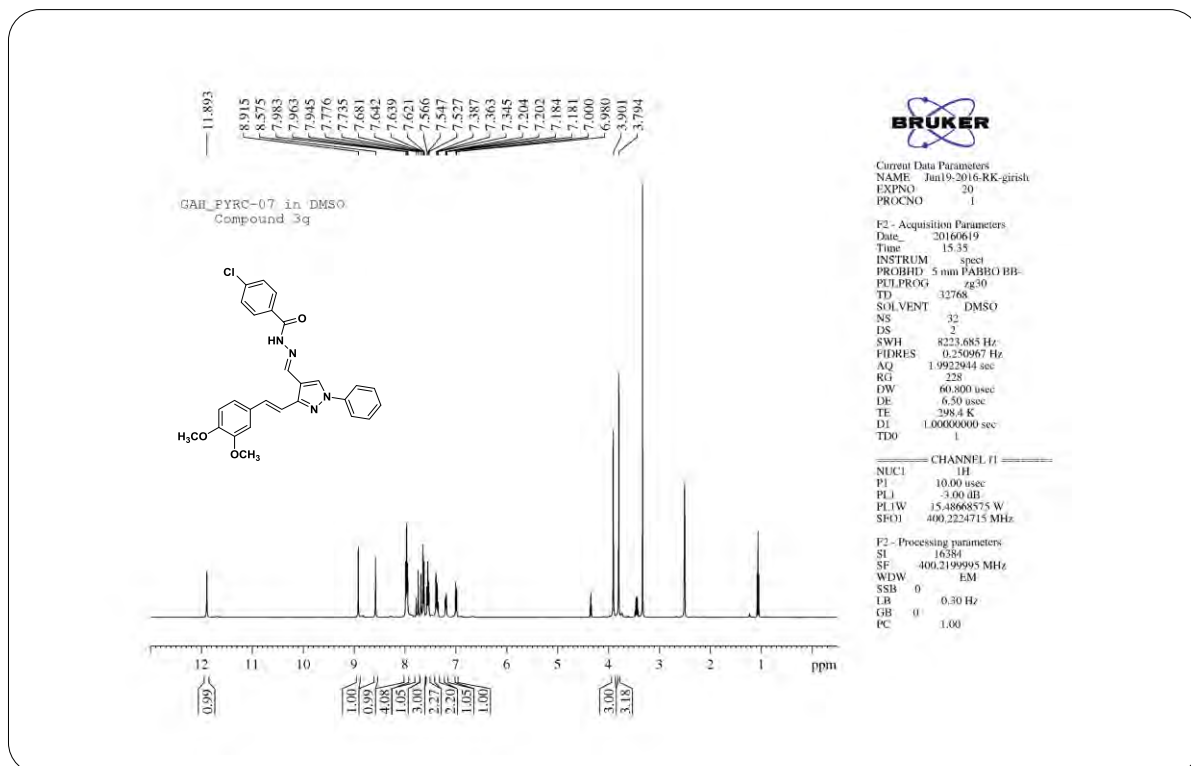
Mass Calc. Mass mDa PPM DBE i-FIT i-FIT (Norm) Formula

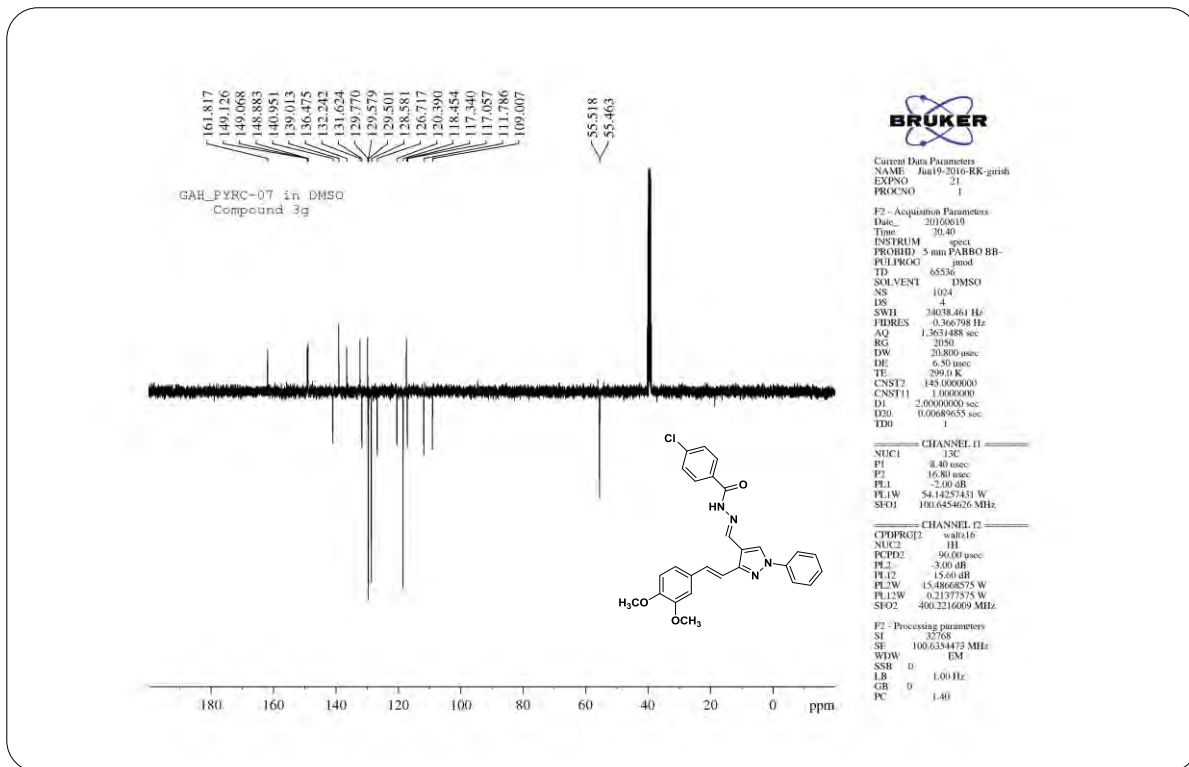
601.0730 601.0713 1.7 2.8 17.5 492.5 0.0 C27 H23 N4 O3 Na I

HRMS Spectrum of Compound 8f (chapter 5)



IR Spectrum of Compound 8g (chapter 5)

¹H NMR Spectrum of Compound 8g (chapter 5)

¹³C NMR Spectrum of Compound 8g (chapter 5)

Elemental Composition Report

Page 1

Single Mass Analysis

Tolerance = 5.0 PPM / DBE: min = -1.5, max = 100.0

Element prediction: Off

Number of isotope peaks used for i-FIT = 3

Monoisotopic Mass, Even Electron Ions

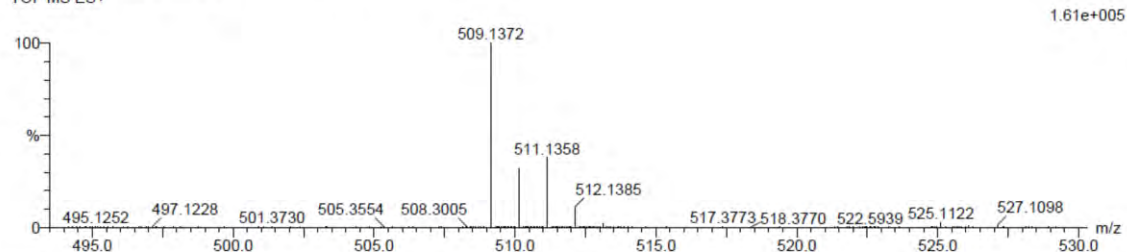
22 formula(e) evaluated with 1 results within limits (up to 20 closest results for each mass)

Elements Used:

C: 25-30 H: 20-25 N: 0-5 O: 0-5 Na: 1-1 Cl: 0-1

PYRC-7 58 (1.923) Cm (1:61)

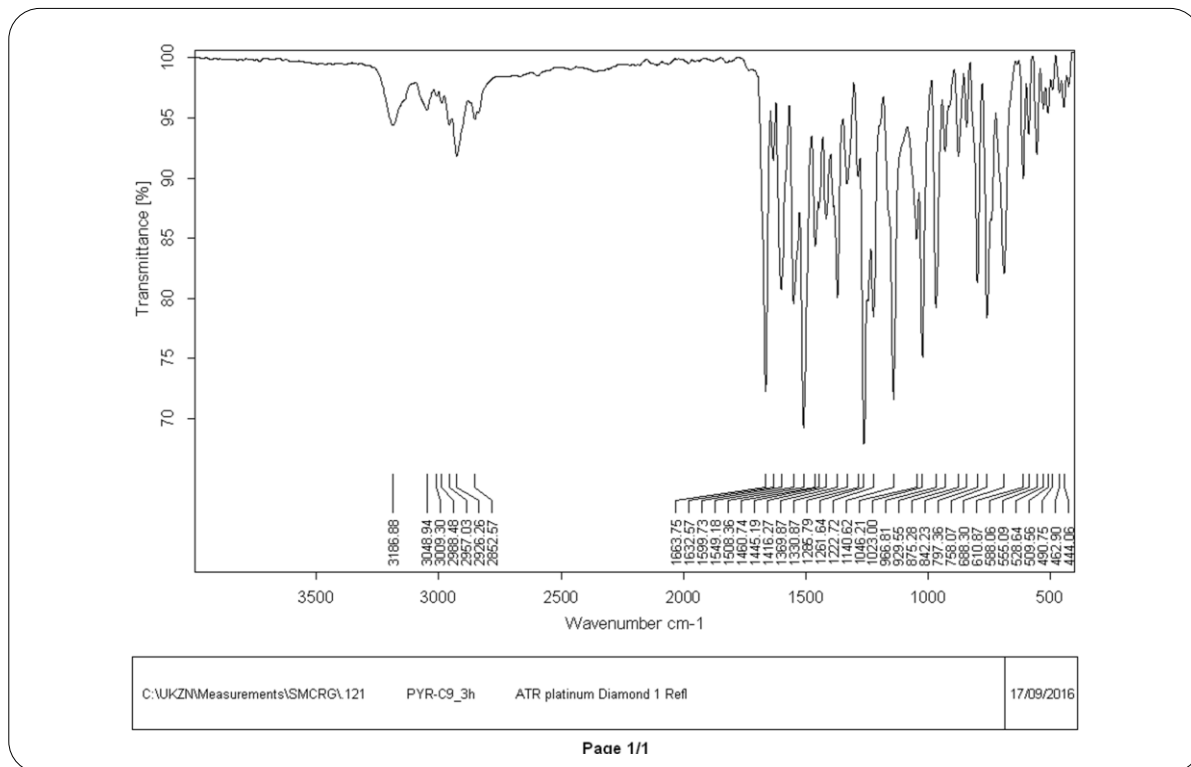
TOF MS ES+



Minimum: -1.5
 Maximum: 5.0 5.0 100.0

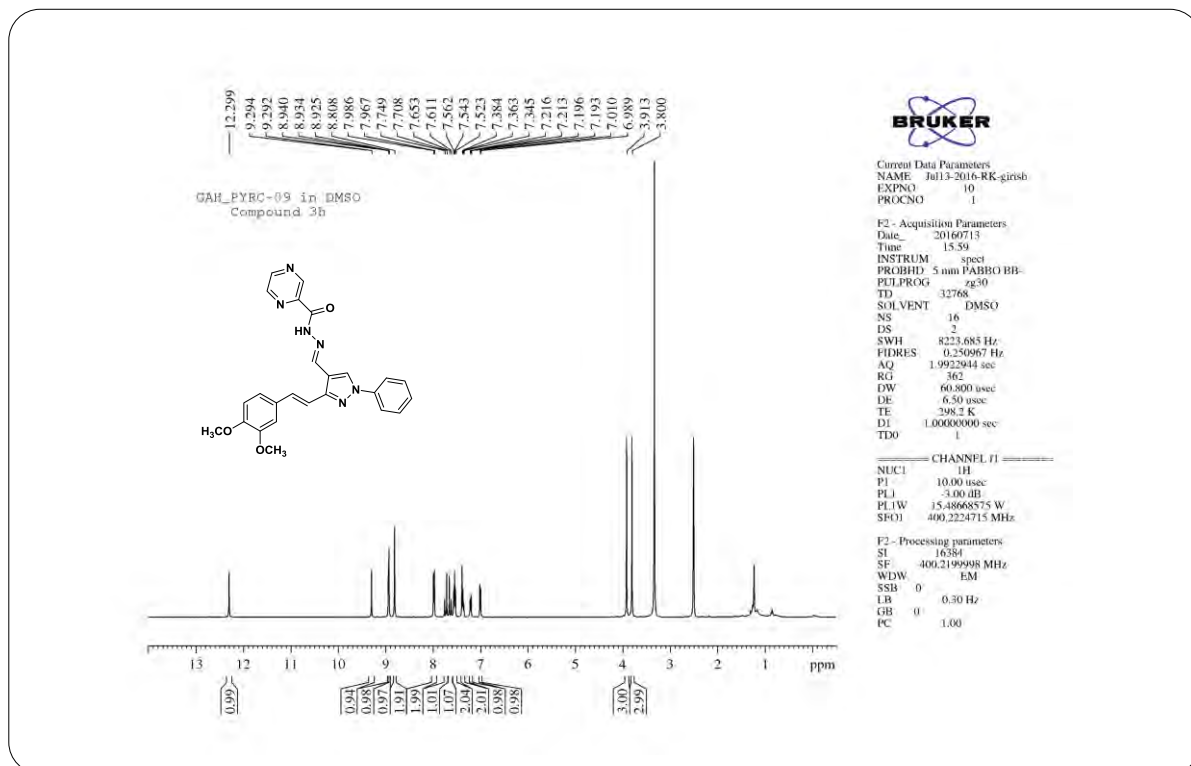
Mass	Calc. Mass	mDa	PPM	DBE	i-FIT	i-FIT (Norm)	Formula
509.1372	509.1356	1.6	3.1	17.5	512.6	0.0	C27 H23 N4 O3 Na Cl

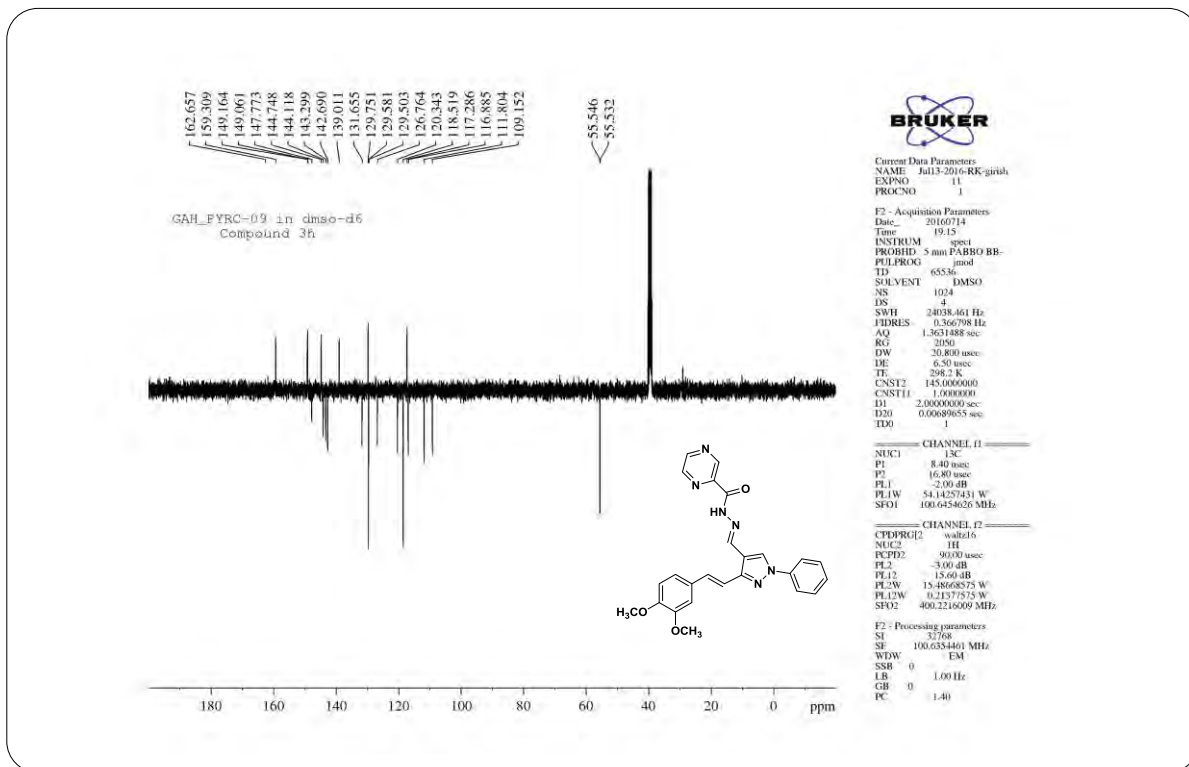
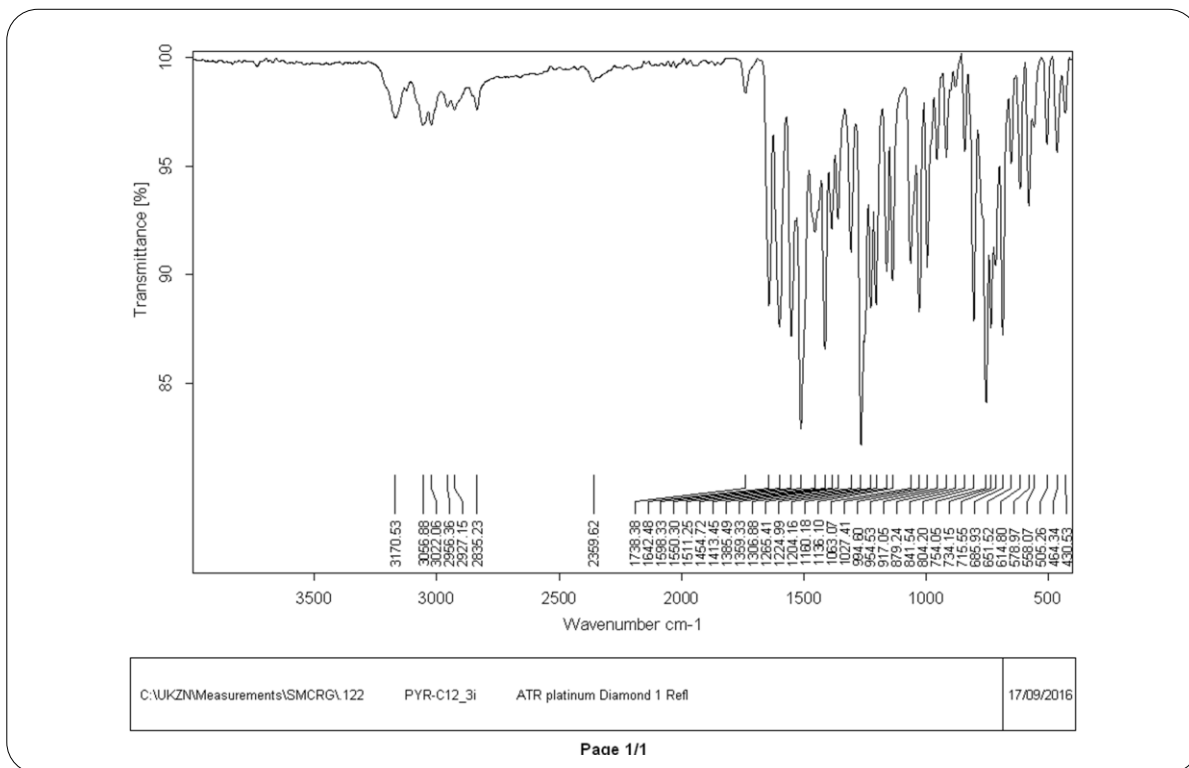
HRMS Spectrum of Compound 8g (chapter 5)

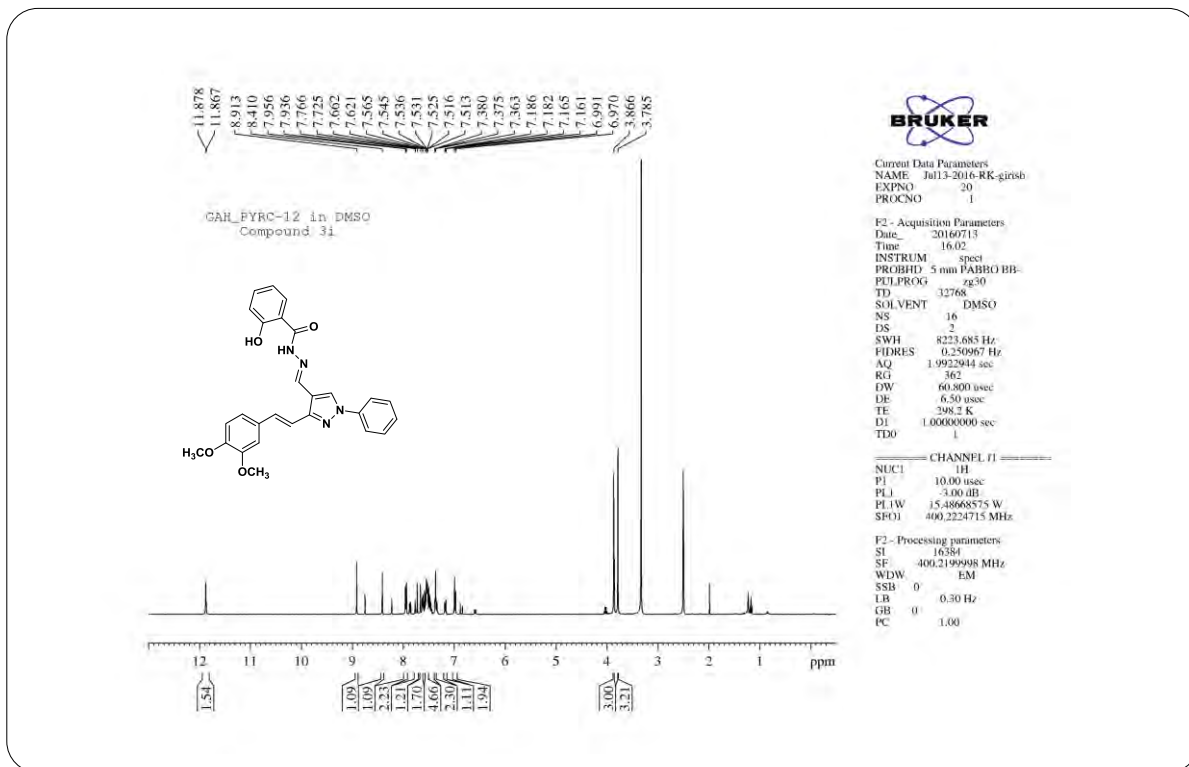
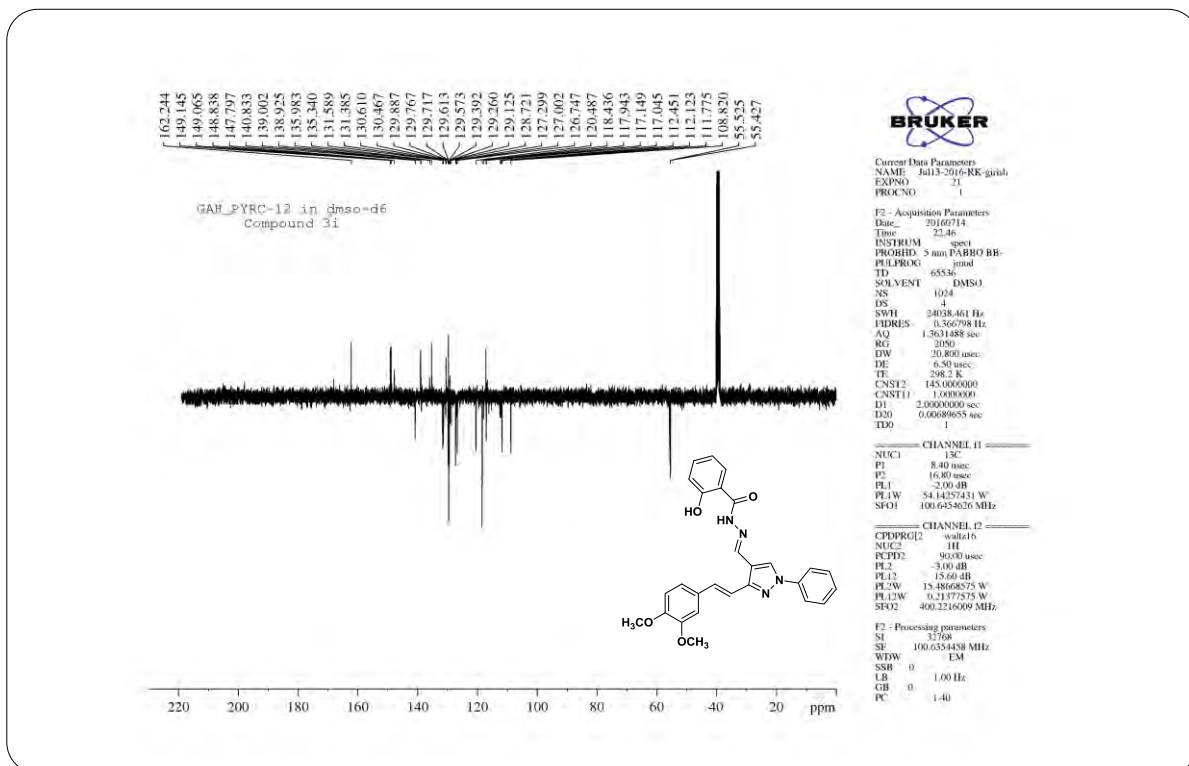


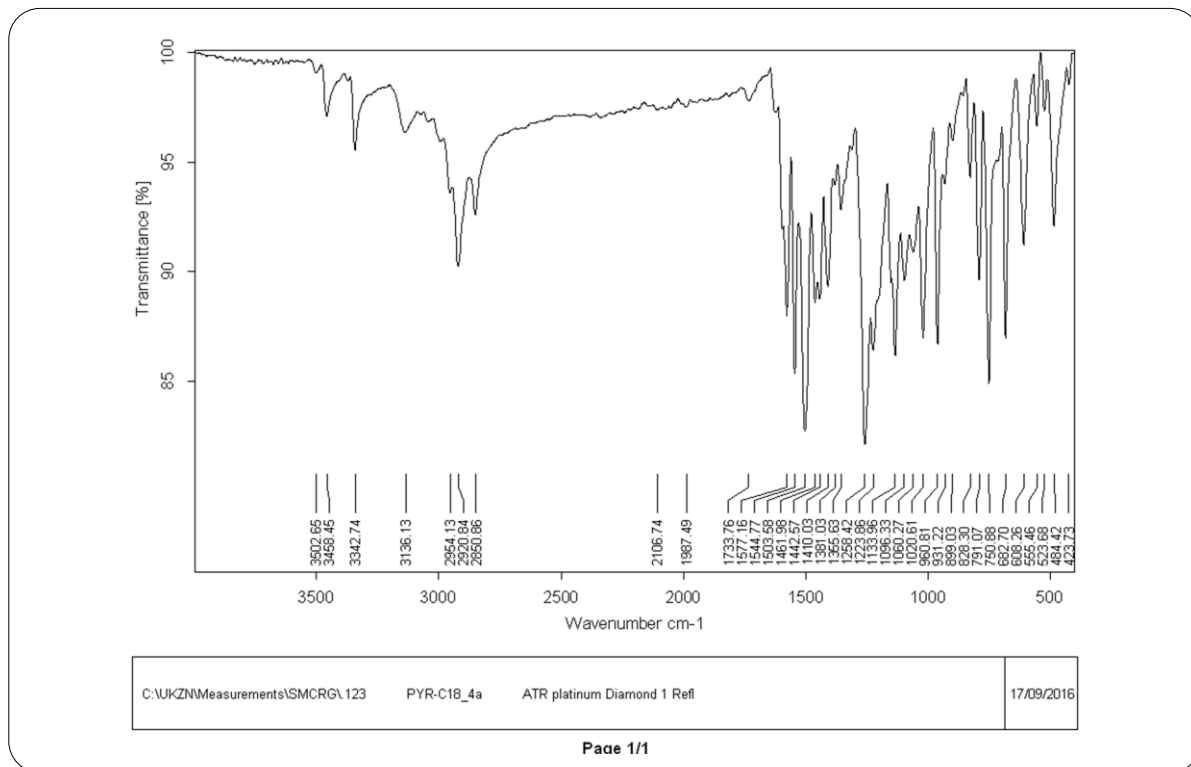
Page 1/1

IR Spectrum of Compound 8h (chapter 5)

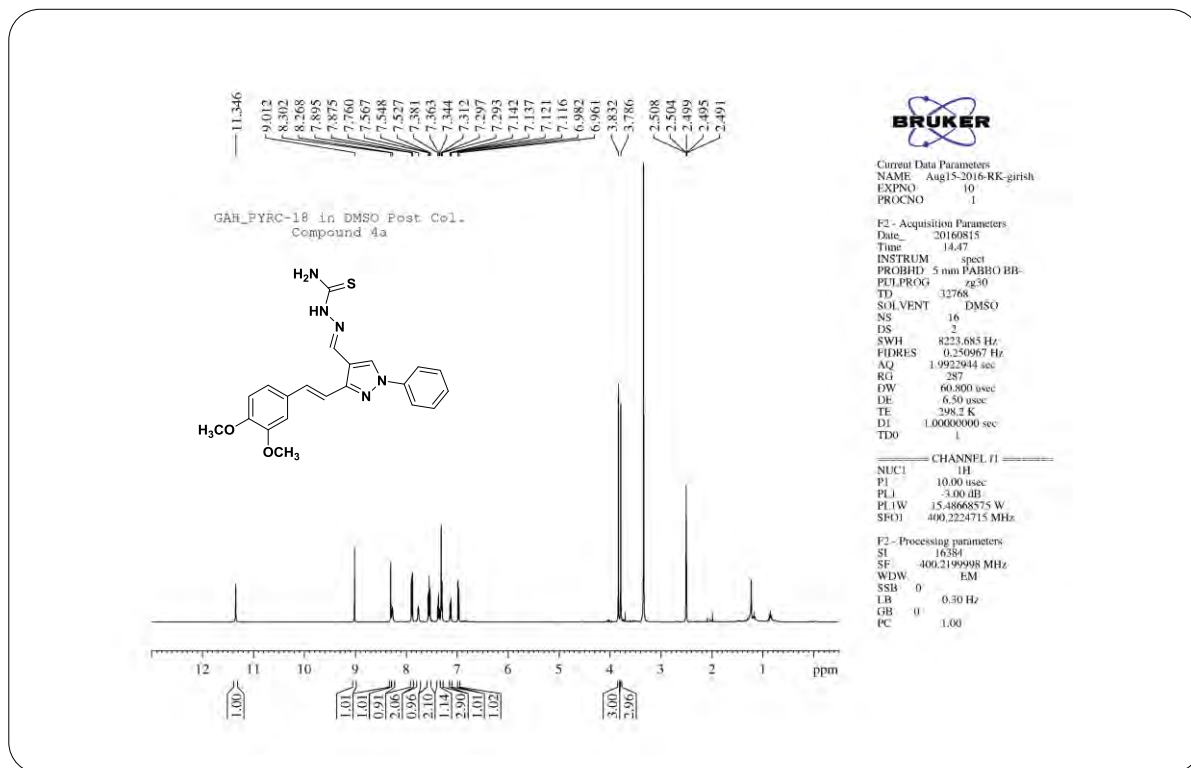
¹H NMR Spectrum of Compound 8h (chapter 5)

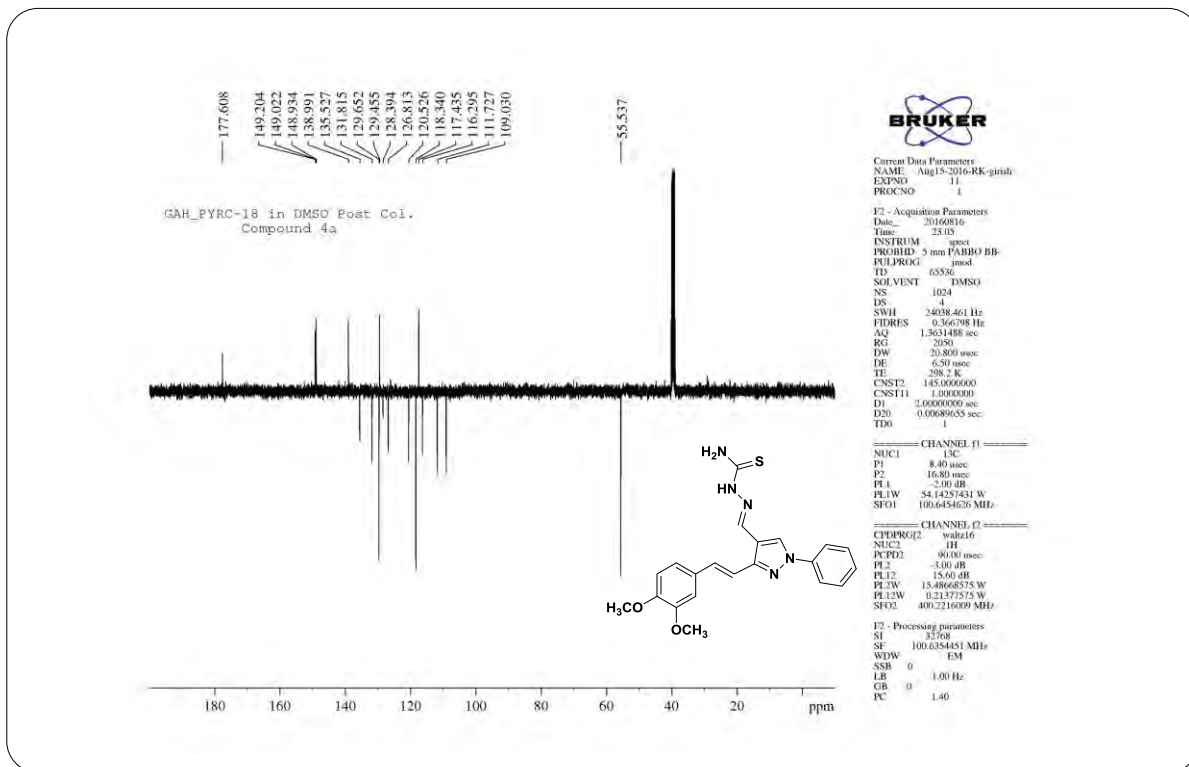
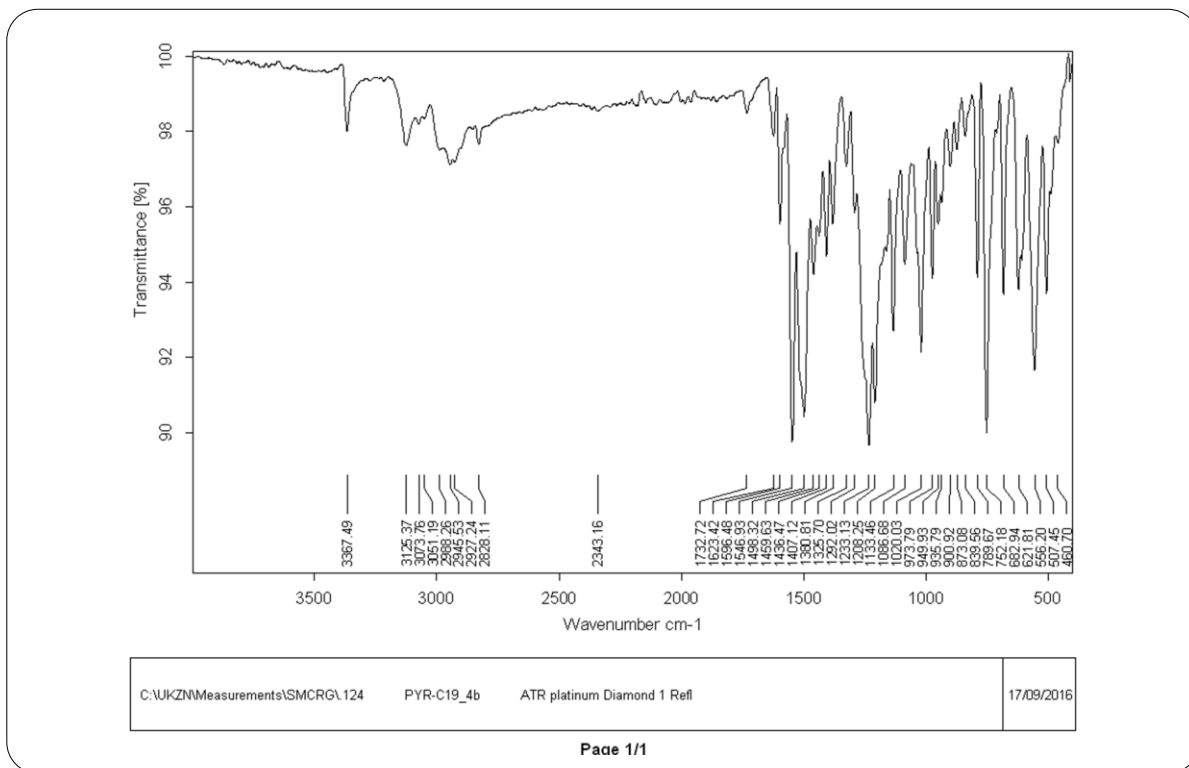
**¹³C NMR Spectrum of Compound 8h (chapter 5)****IR Spectrum of Compound 8i (chapter 5)**

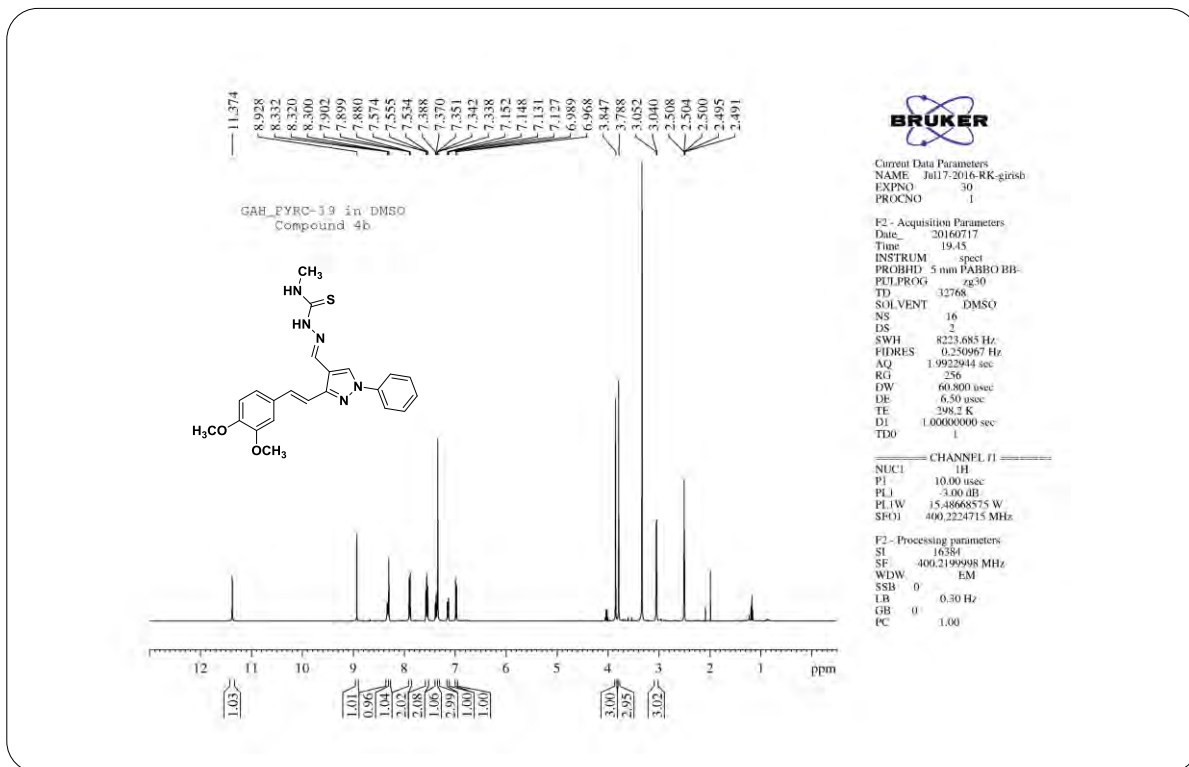
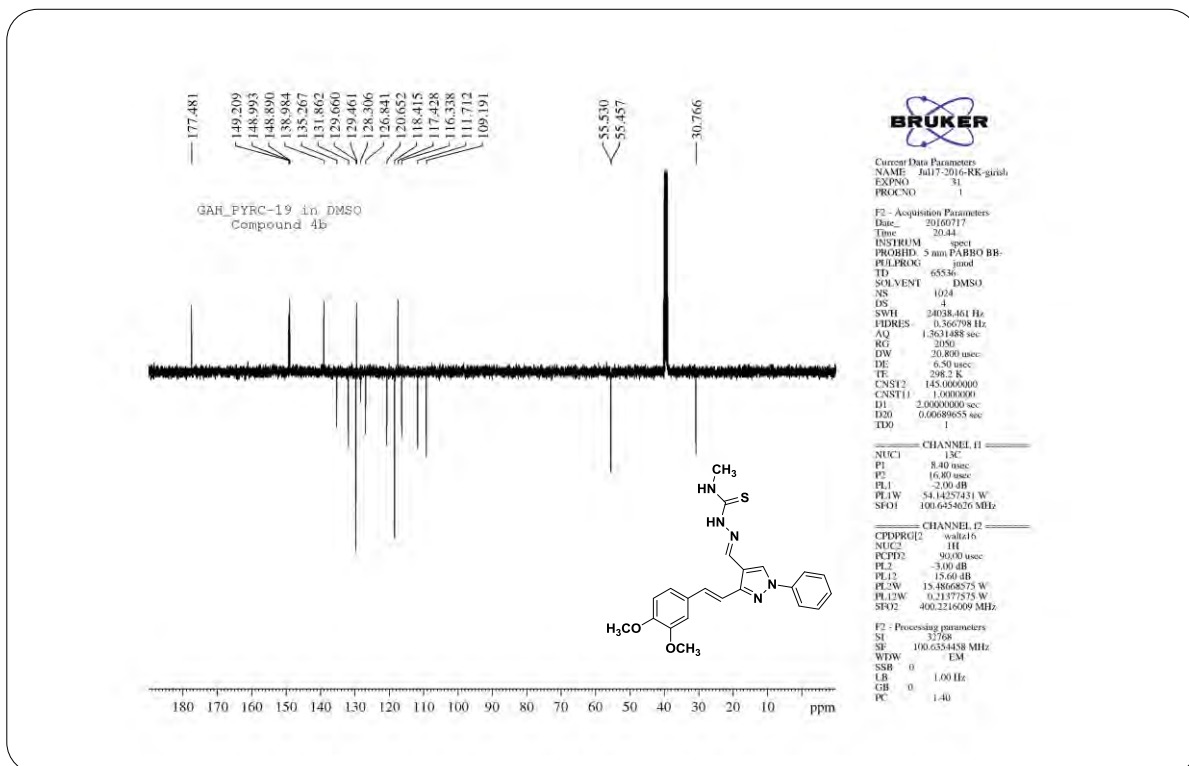
¹H NMR Spectrum of Compound 8i (chapter 5)¹³C NMR Spectrum of Compound 8i (chapter 5)

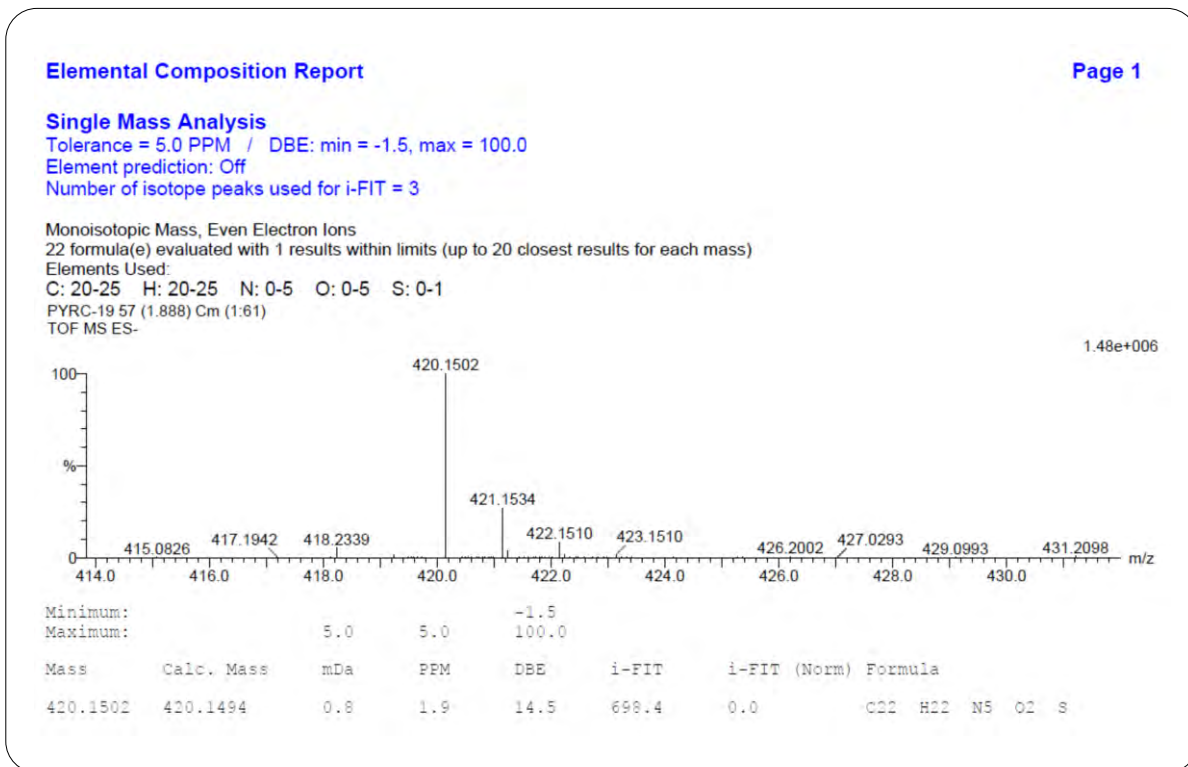


IR Spectrum of Compound 11a (chapter 5)

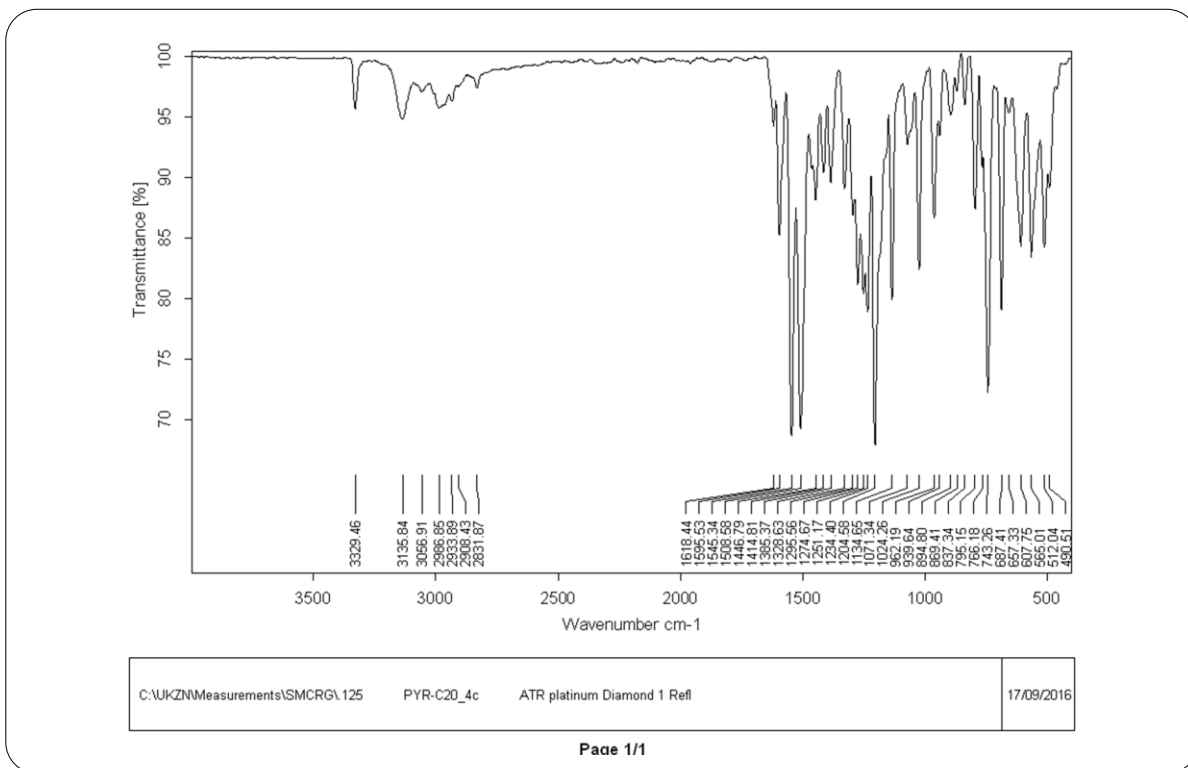
¹H NMR Spectrum of Compound 11a (chapter 5)

**¹³C NMR Spectrum of Compound 11a (chapter 5)****IR Spectrum of Compound 11b (chapter 5)**

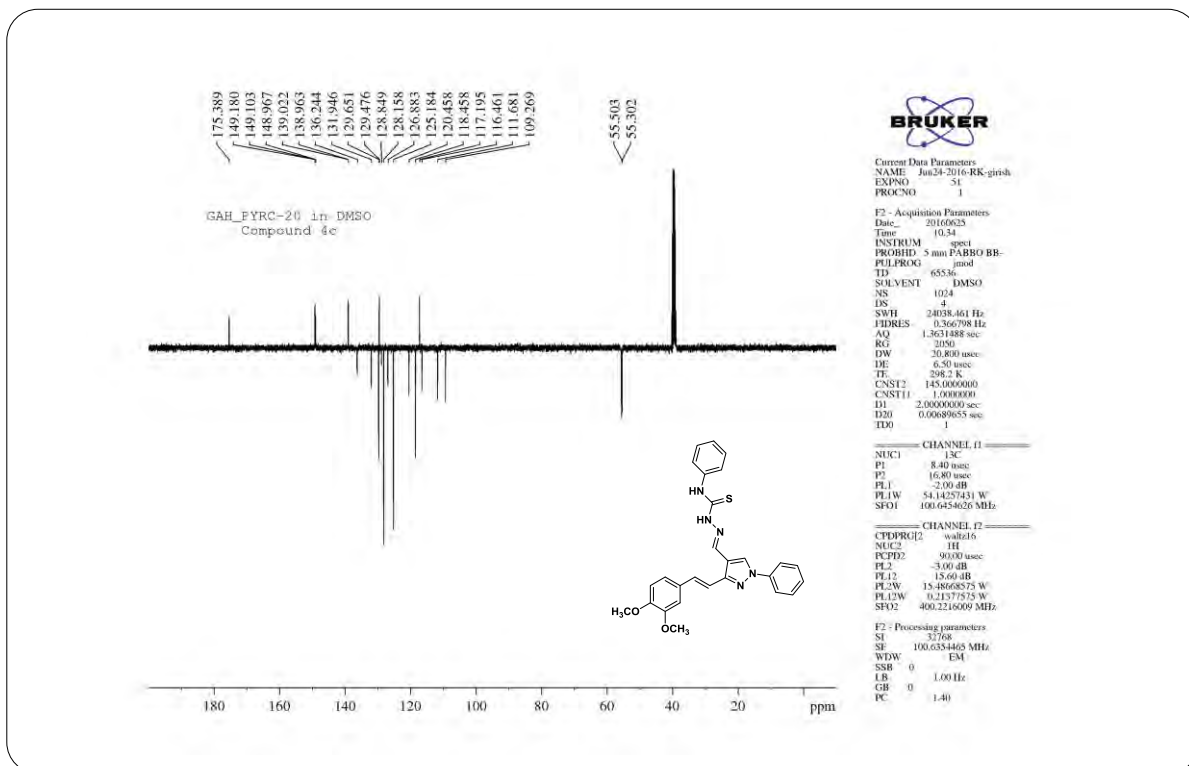
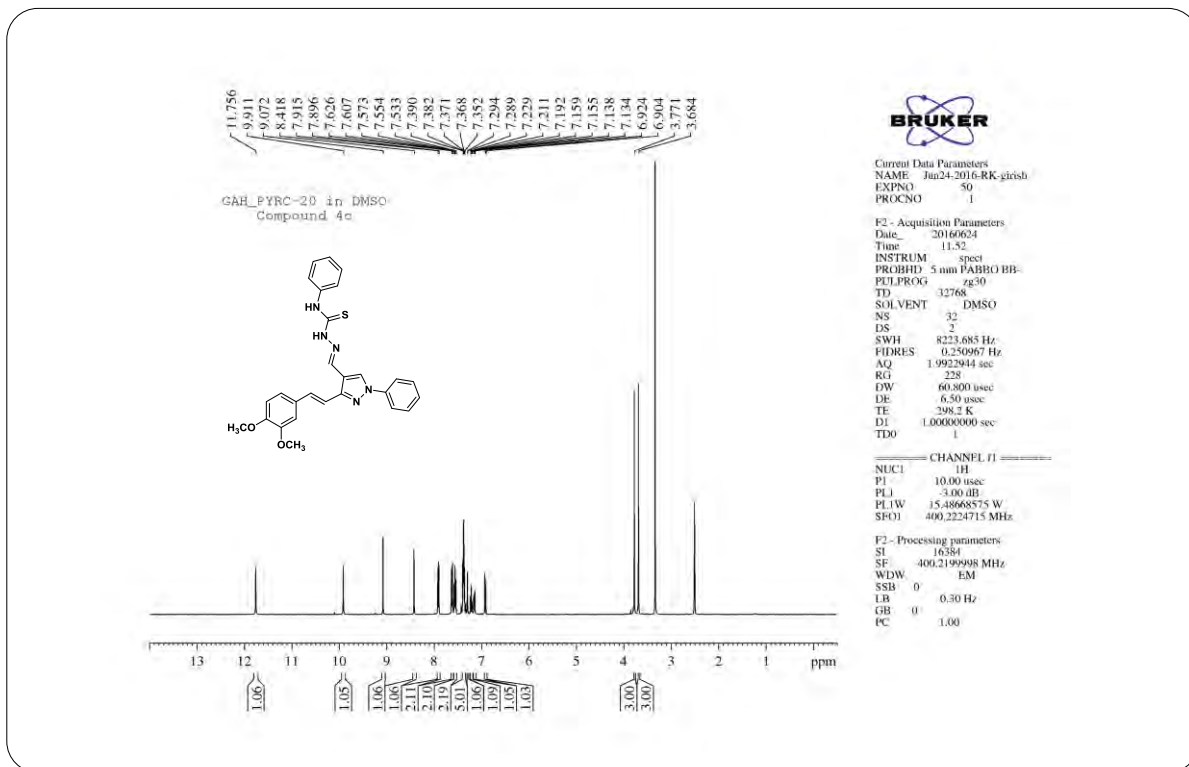
¹H NMR Spectrum of Compound 11b (chapter 5)¹³C NMR Spectrum of Compound 11b (chapter 5)

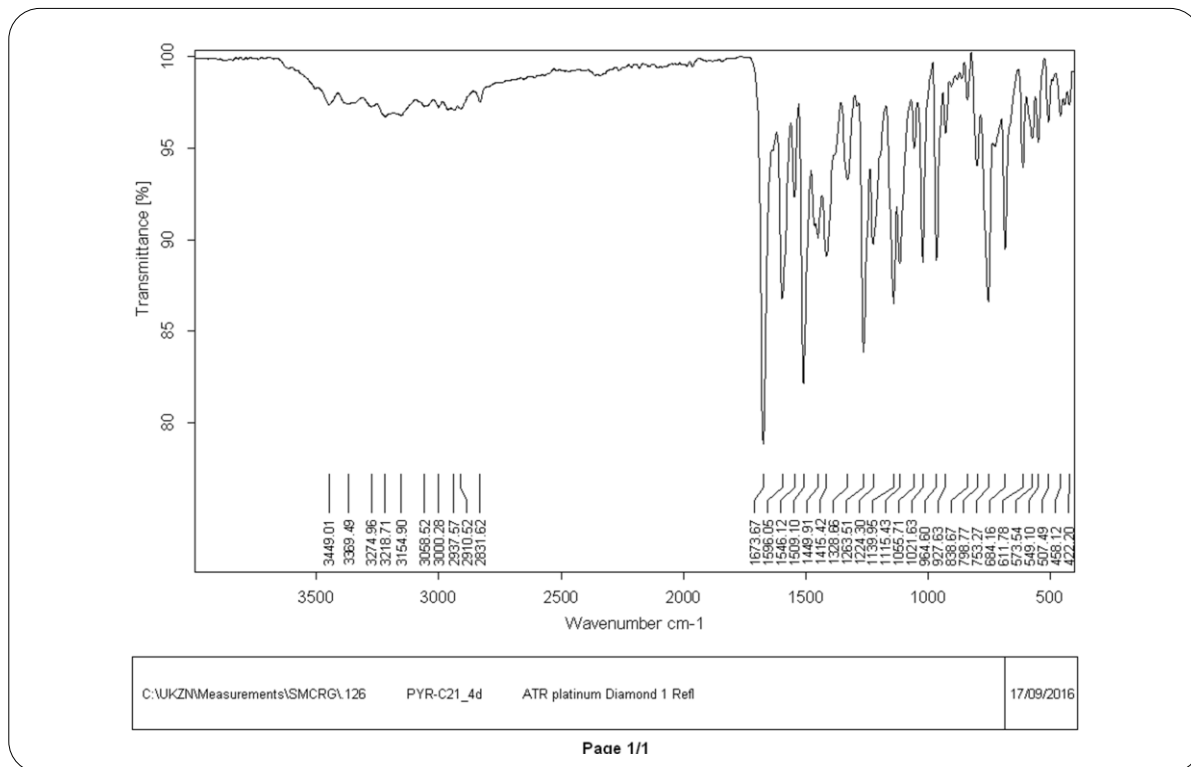


HRMS Spectrum of Compound 11b (chapter 5)

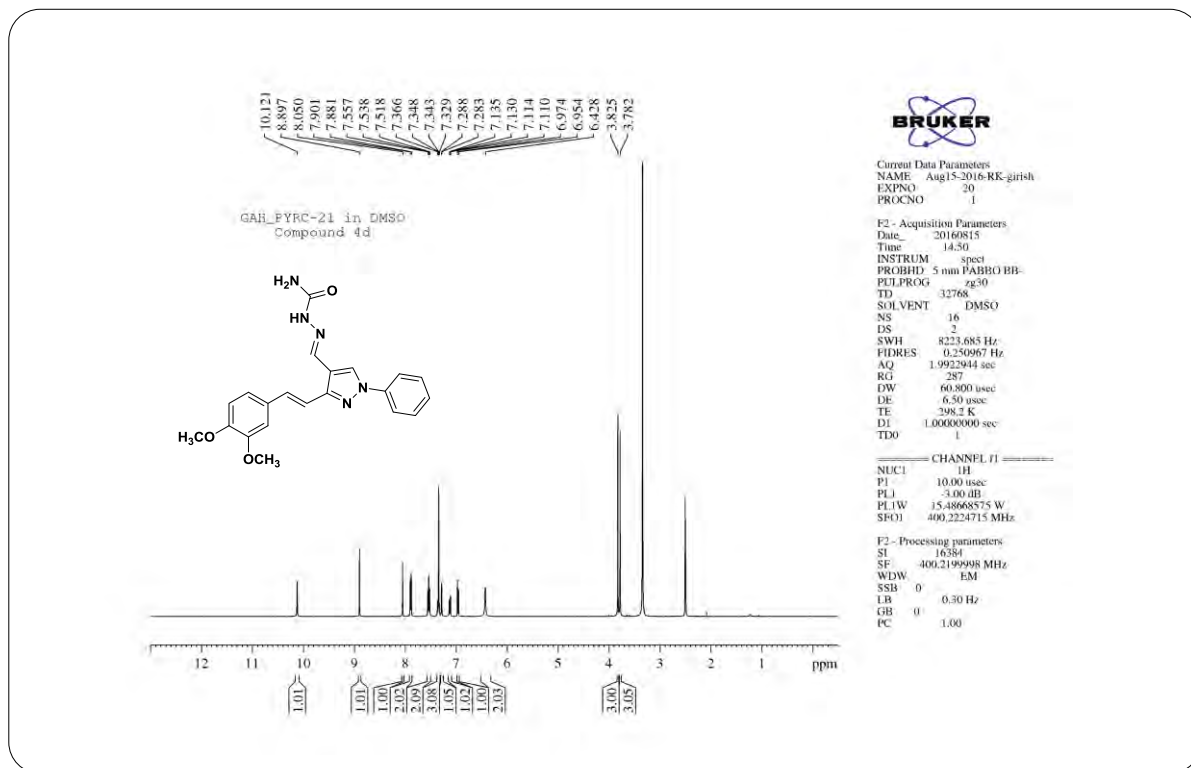


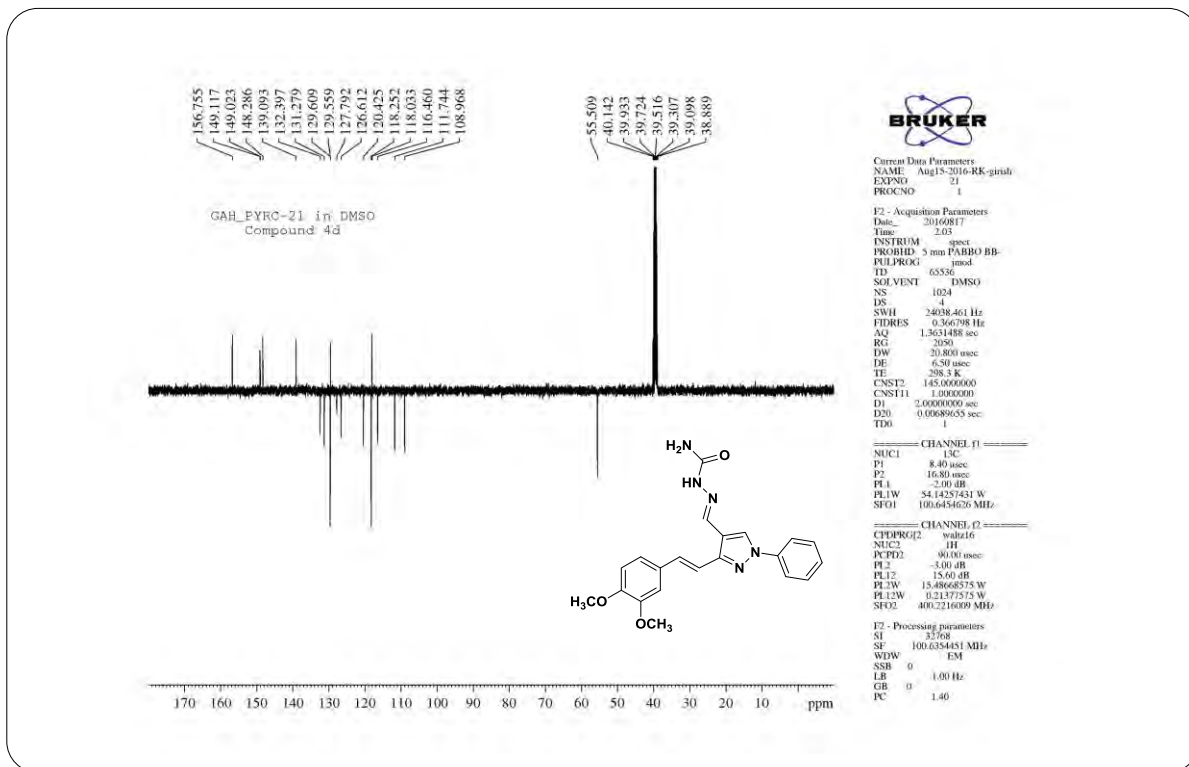
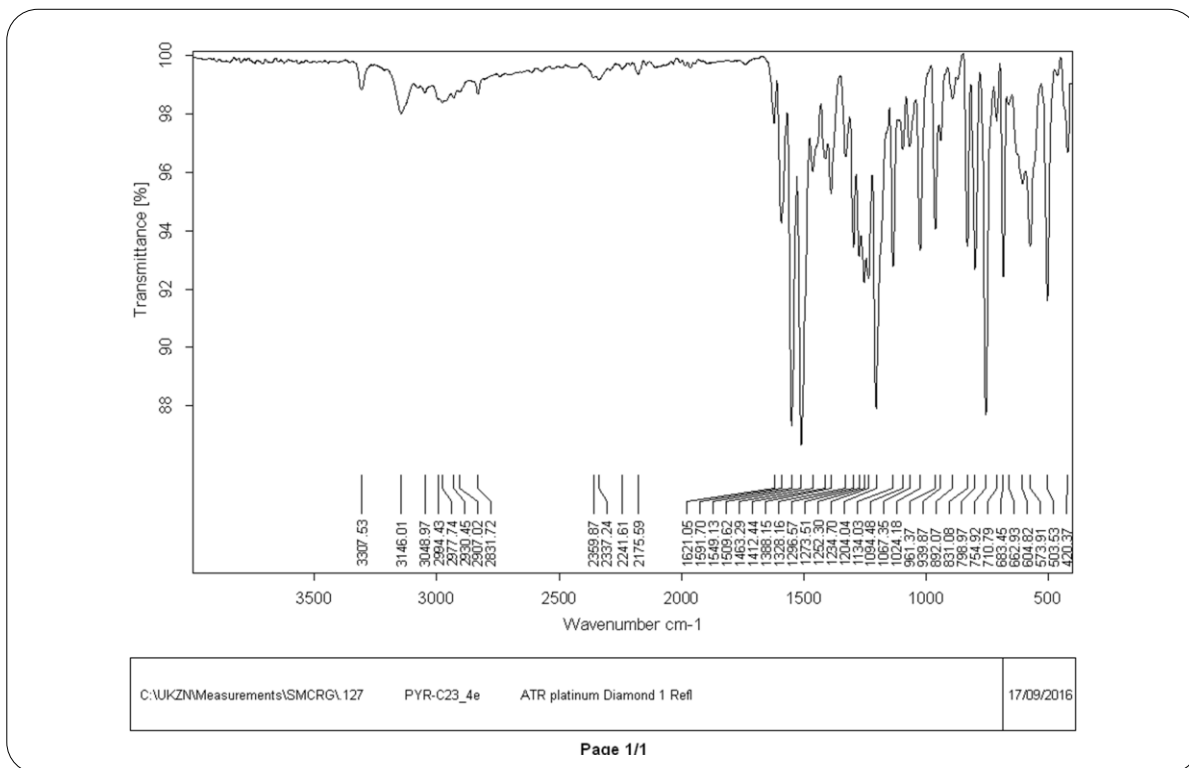
IR Spectrum of Compound 11c (chapter 5)

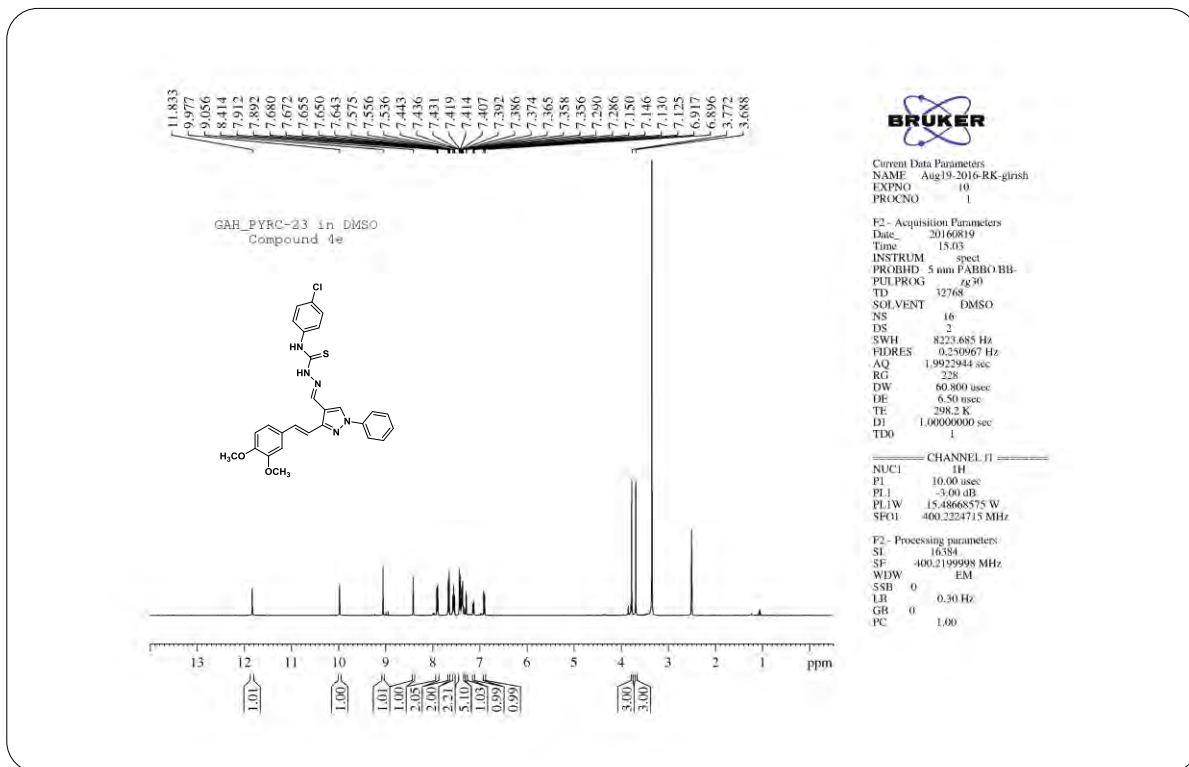
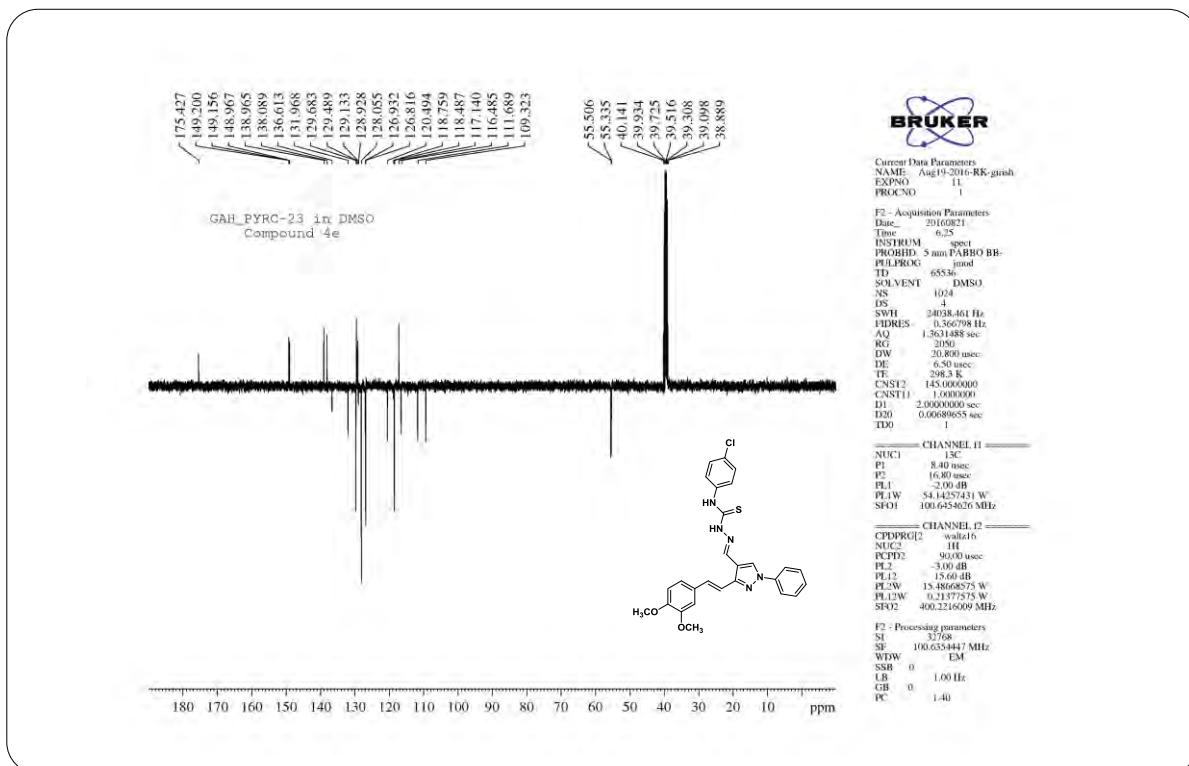


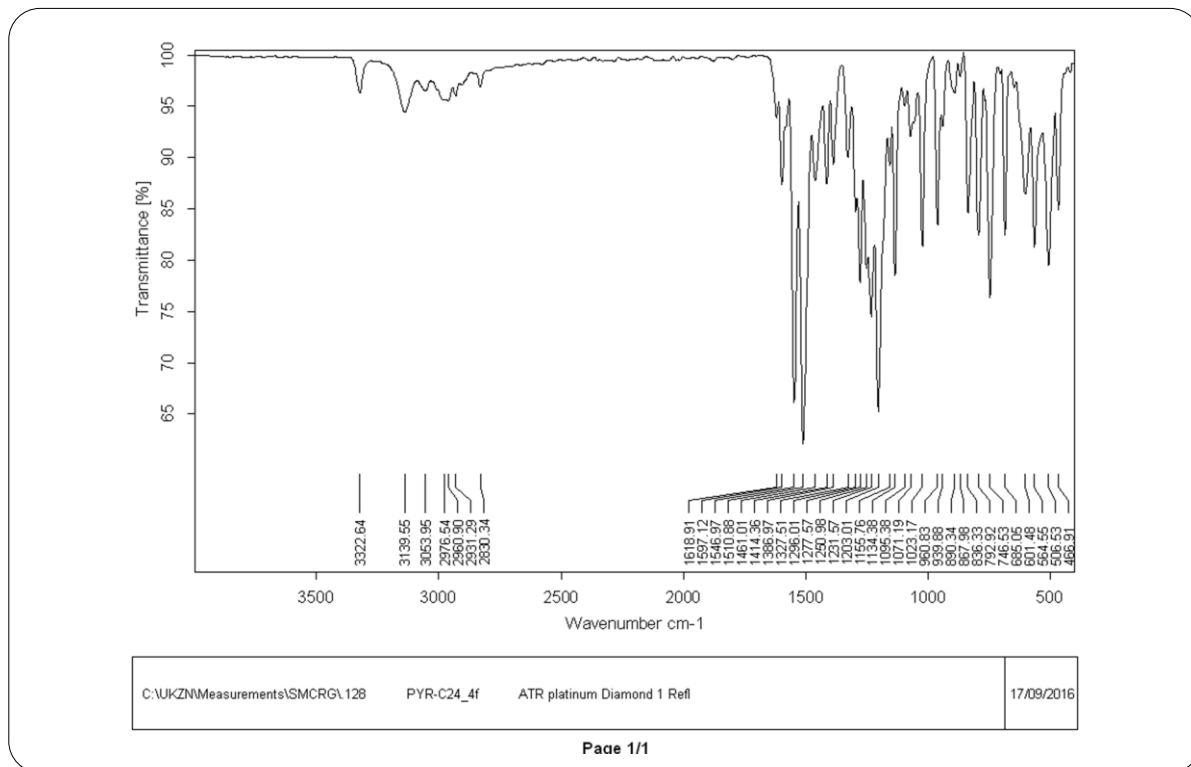


IR Spectrum of Compound 11d (chapter 5)

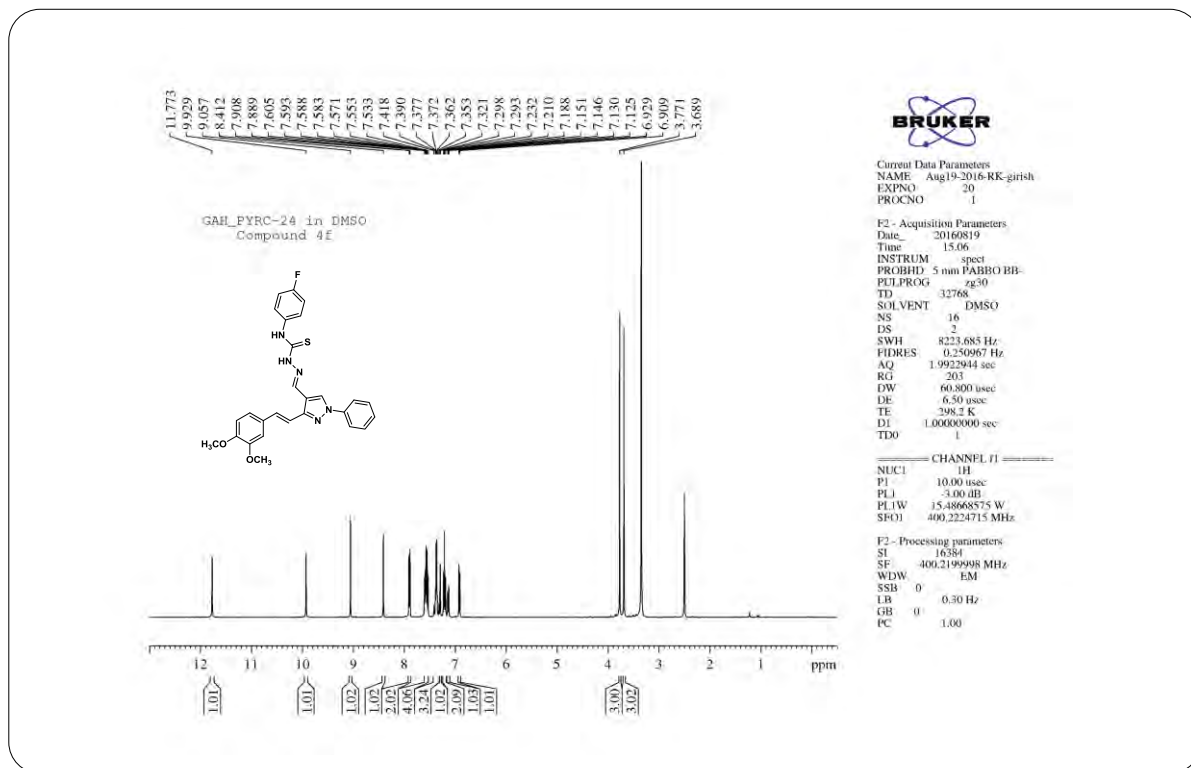
¹H NMR Spectrum of Compound 11d (chapter 5)

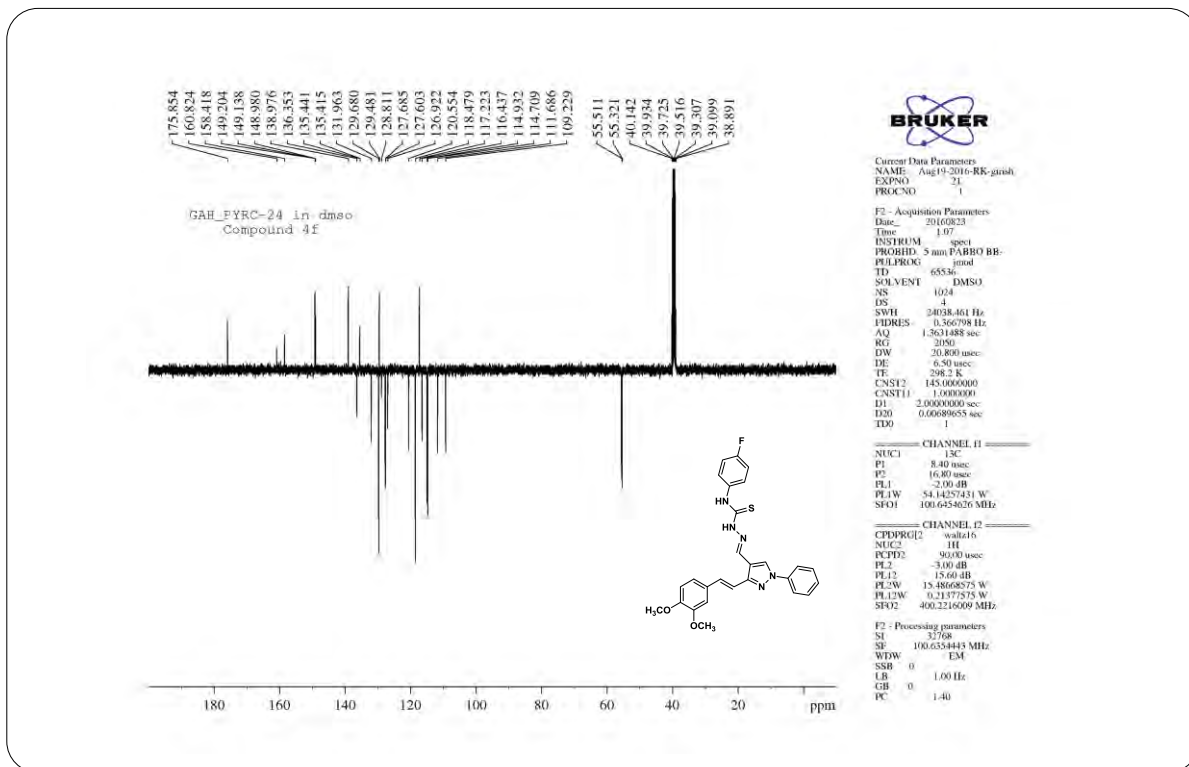
**¹³C NMR Spectrum of Compound 11d (chapter 5)****IR Spectrum of Compound 11e (chapter 5)**

**¹H NMR Spectrum of Compound 11e (chapter 5)****¹³C NMR Spectrum of Compound 11e (chapter 5)**



IR Spectrum of Compound 11f (chapter 5)

¹H NMR Spectrum of Compound 11f (chapter 5)

**¹³C NMR Spectrum of Compound 11f (chapter 5)****Elemental Composition Report**

Page 1

Single Mass Analysis

Tolerance = 5.0 PPM / DBE: min = -1.5, max = 100.0

Element prediction: Off

Number of isotope peaks used for i-FIT = 3

Monoisotopic Mass, Even Electron Ions

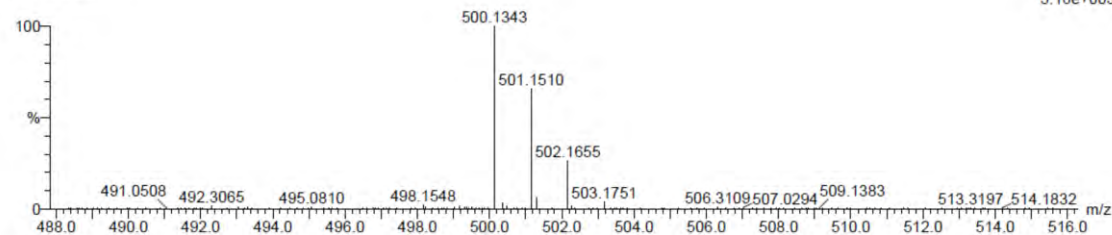
43 formula(e) evaluated with 1 results within limits (up to 20 closest results for each mass)

Elements Used:

C: 25-30 H: 20-25 N: 0-5 O: 0-5 S: 0-1 F: 0-1

PYRC-24 6 (0.169)

TOF MS ES-



Minimum:

-1.5

Maximum:

5.0

5.0

100.0

Mass

Calc. Mass

mDa

PPM

DBE

i-FIT

i-FIT (Norm)

Formula

500.1343

500.1332

1.1

2.2

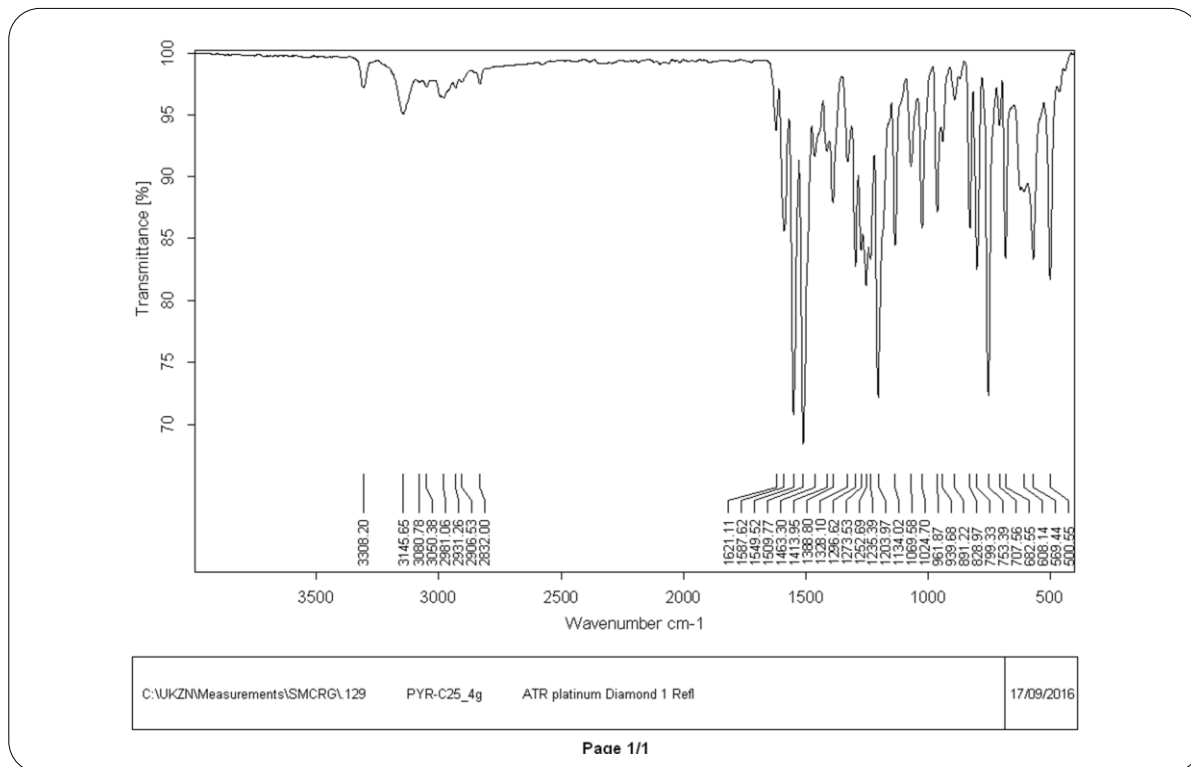
18.5

104.5

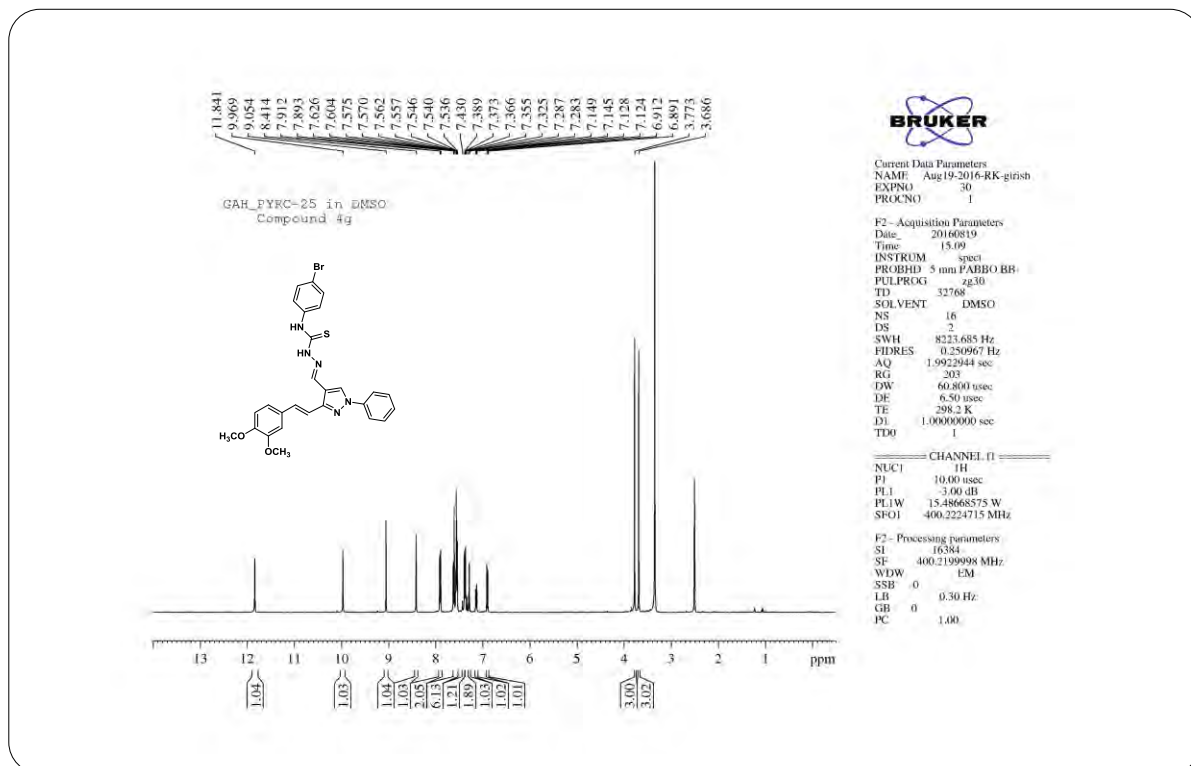
0.0

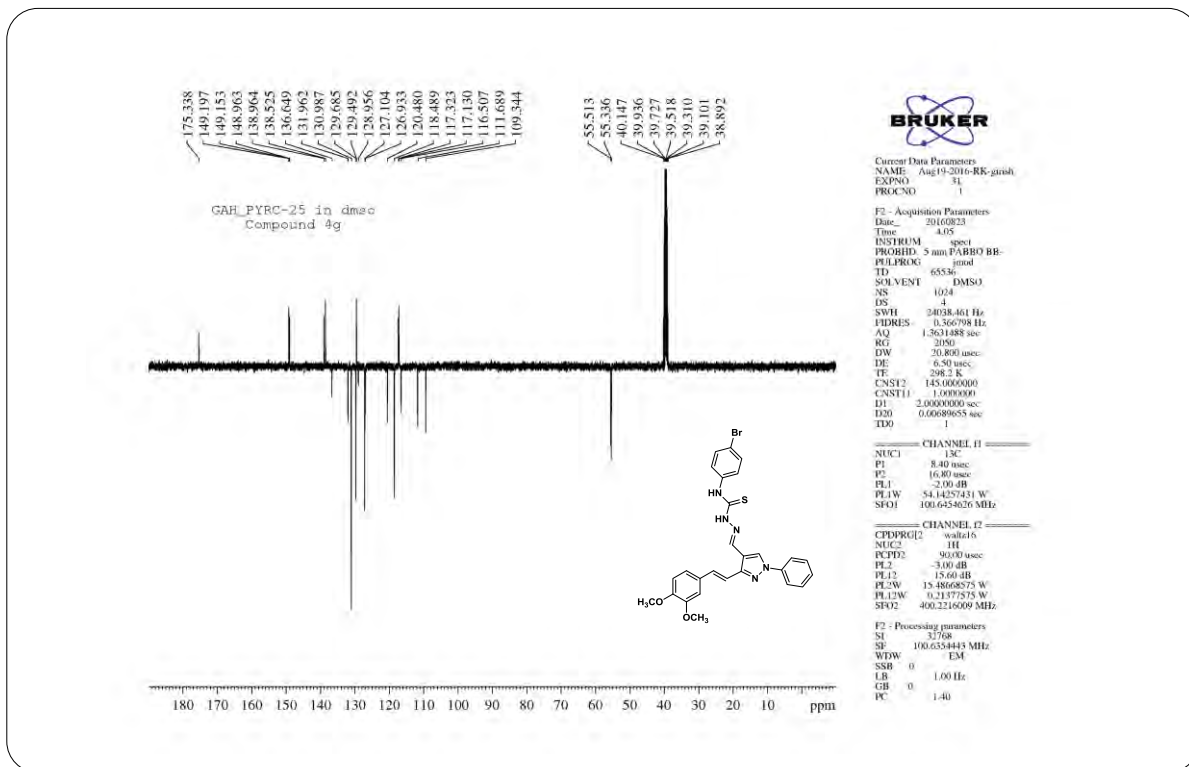
C29 H23 N O4 S F

HRMS Spectrum of Compound 11f (chapter 5)



IR Spectrum of Compound 11g (chapter 5)

¹H NMR Spectrum of Compound 11g (chapter 5)

¹³C NMR Spectrum of Compound 11g (chapter 5)

Elemental Composition Report

Page 1

Single Mass Analysis

Tolerance = 5.0 PPM / DBE: min = -1.5, max = 100.0

Element prediction: Off

Number of isotope peaks used for i-FIT = 3

Monoisotopic Mass, Even Electron Ions

72 formula(e) evaluated with 1 results within limits (up to 20 closest results for each mass)

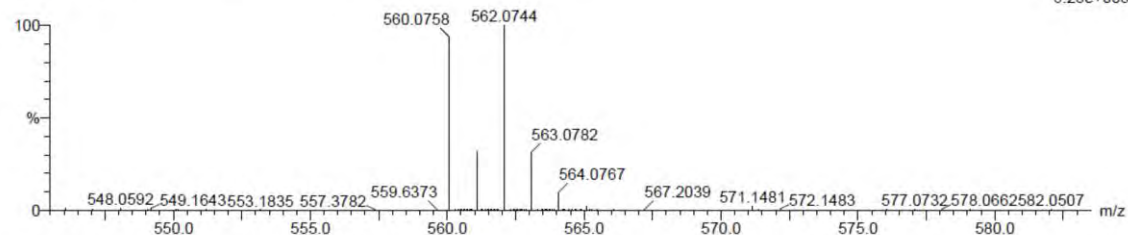
Elements Used:

C: 25-30 H: 20-25 N: 0-5 O: 0-5 S: 0-1 Br: 0-1

PYRC-25 2 (0.034) Cm (1:61)

TOF MS ES-

6.25e+005

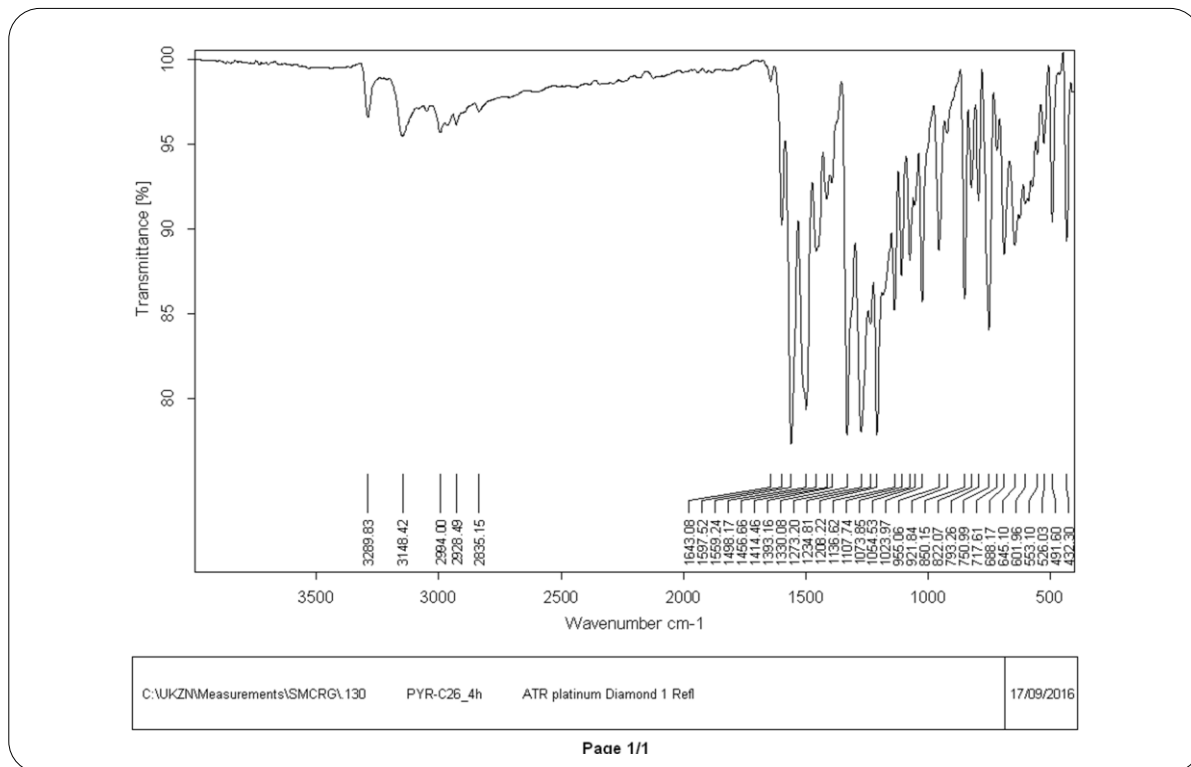


Minimum:

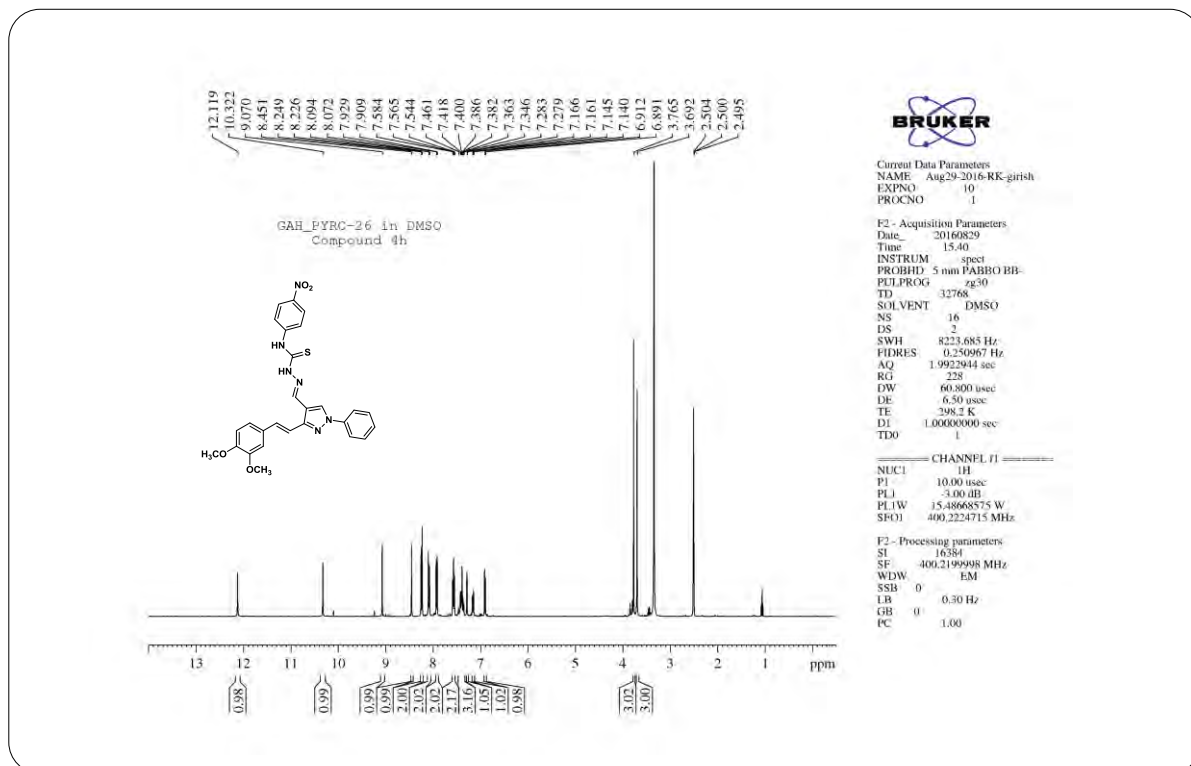
Maximum: 5.0 5.0 100.0

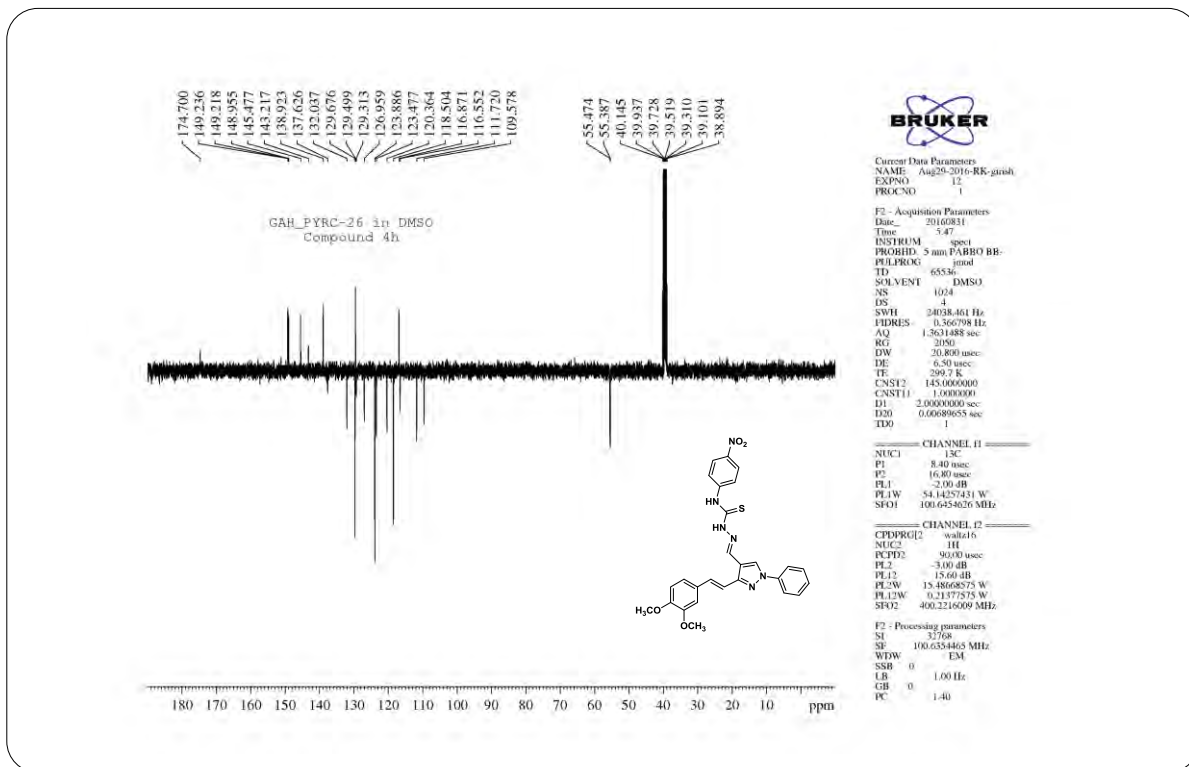
Mass	Calc. Mass	mDa	PPM	DBE	i-FIT	i-FIT (Norm)	Formula
560.0758	560.0756	0.2	0.4	18.5	504.9	0.0	C27 H23 N5 O2 S Br

HRMS Spectrum of Compound 11g (chapter 5)



IR Spectrum of Compound 11h (chapter 5)

¹H NMR Spectrum of Compound 11h (chapter 5)

¹³C NMR Spectrum of Compound 11h (chapter 5)

Elemental Composition Report

Page 1

Single Mass Analysis

Tolerance = 5.0 PPM / DBE: min = -1.5, max = 100.0

Element prediction: Off

Number of isotope peaks used for i-FIT = 3

Monoisotopic Mass, Even Electron Ions

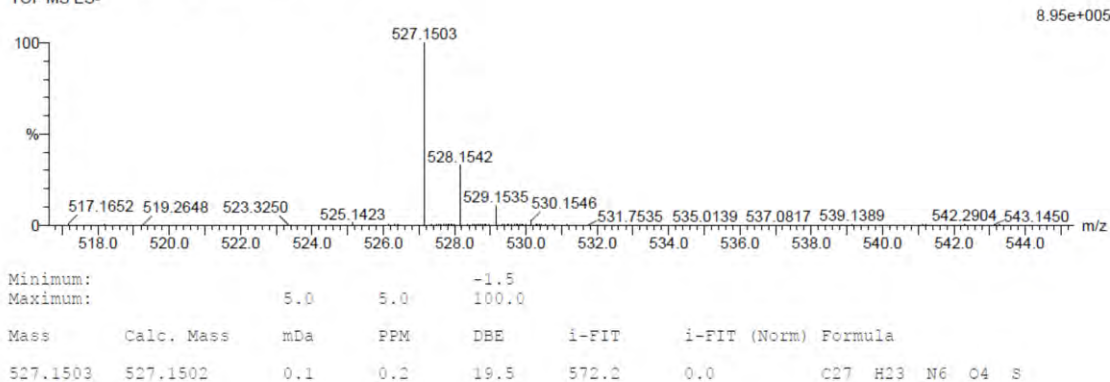
56 formula(e) evaluated with 1 results within limits (up to 20 closest results for each mass)

Elements Used:

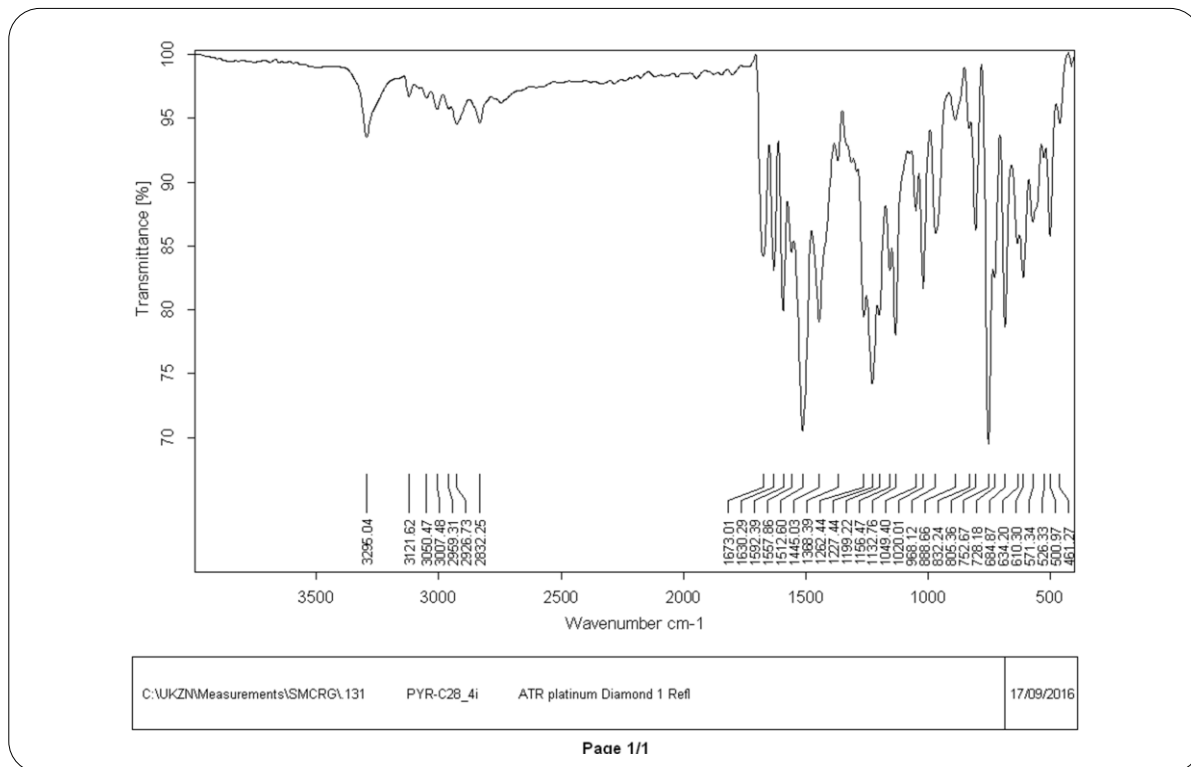
C: 25-30 H: 20-25 N: 0-10 O: 0-5 S: 0-1

PYRC-26 53 (1.754) Cm (1:61)

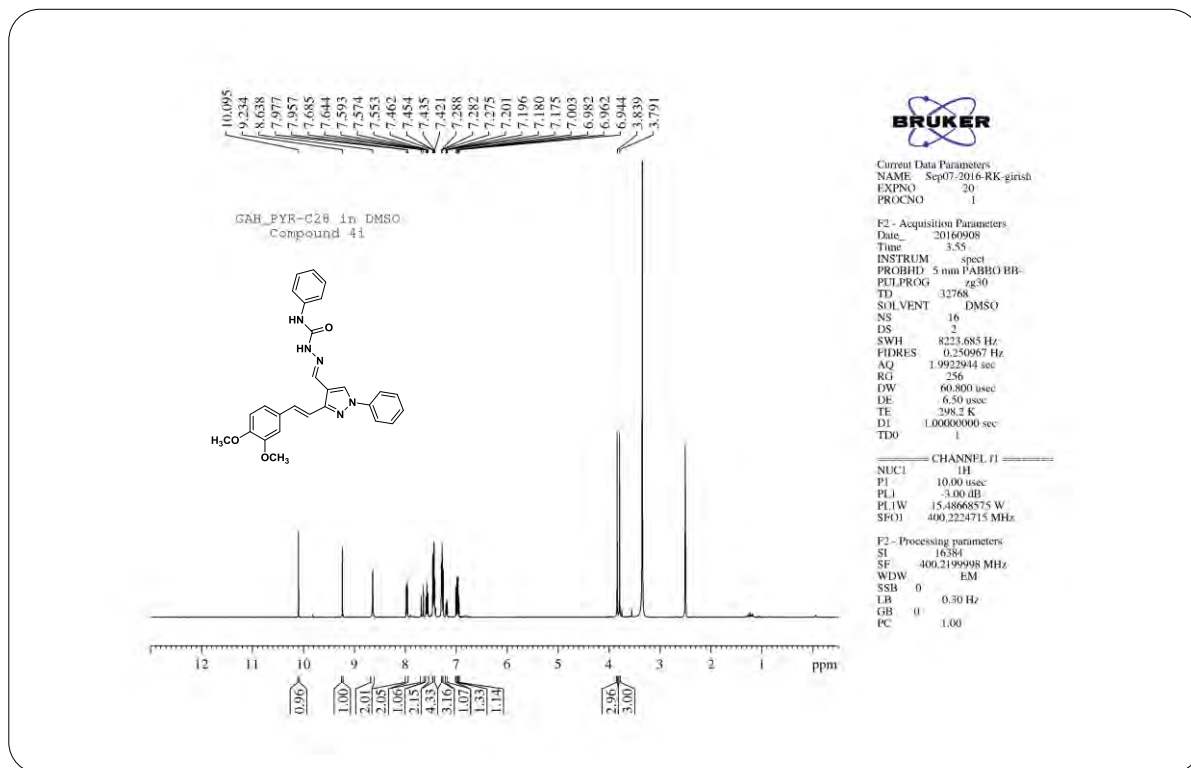
TOF MS ES-

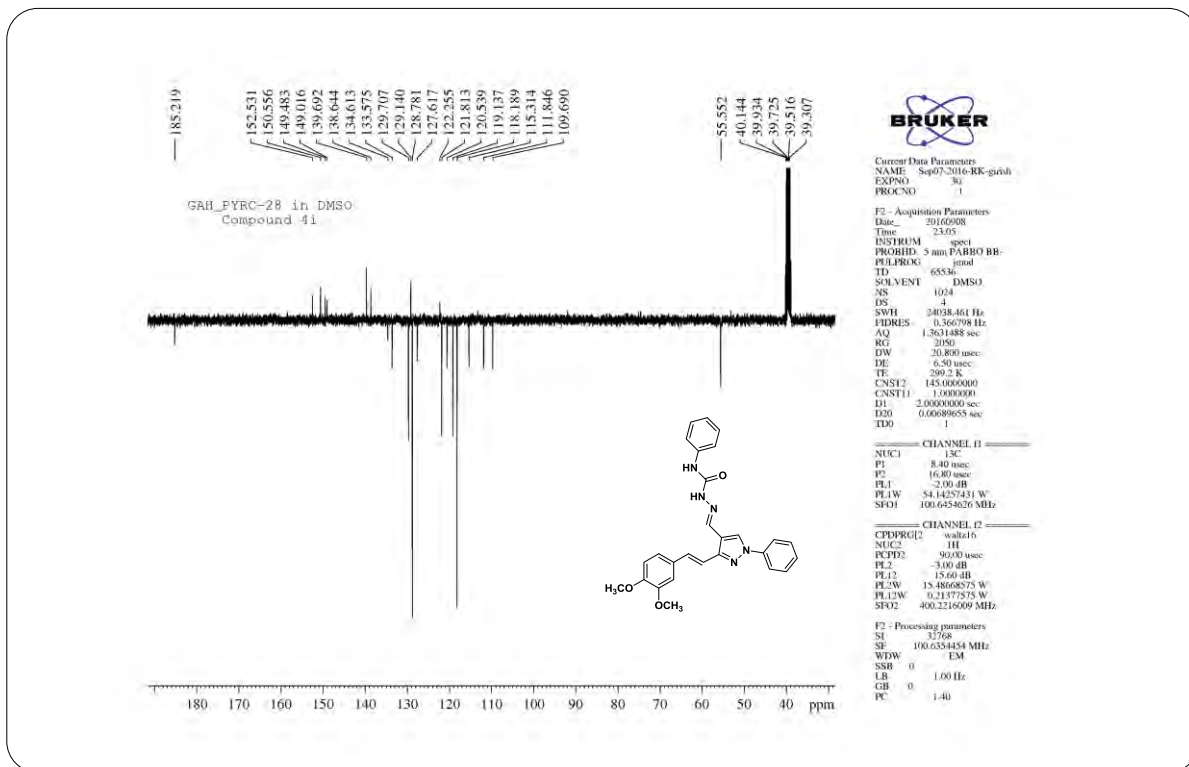
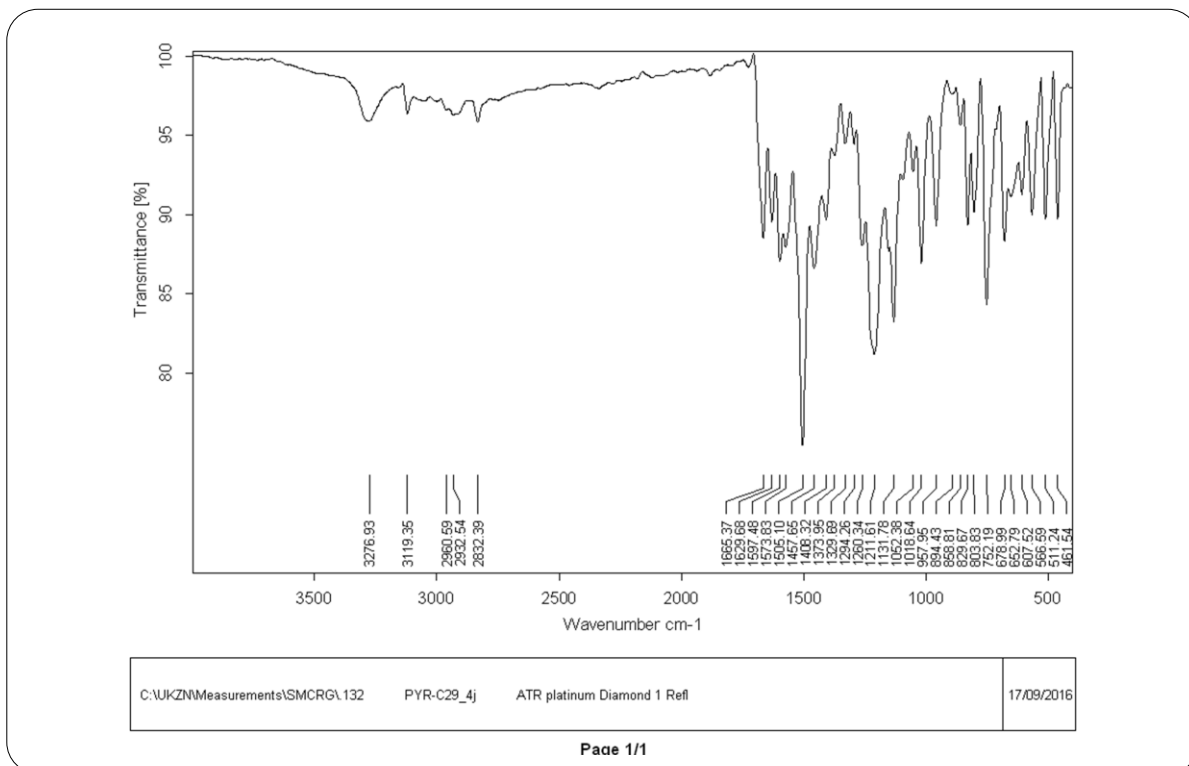


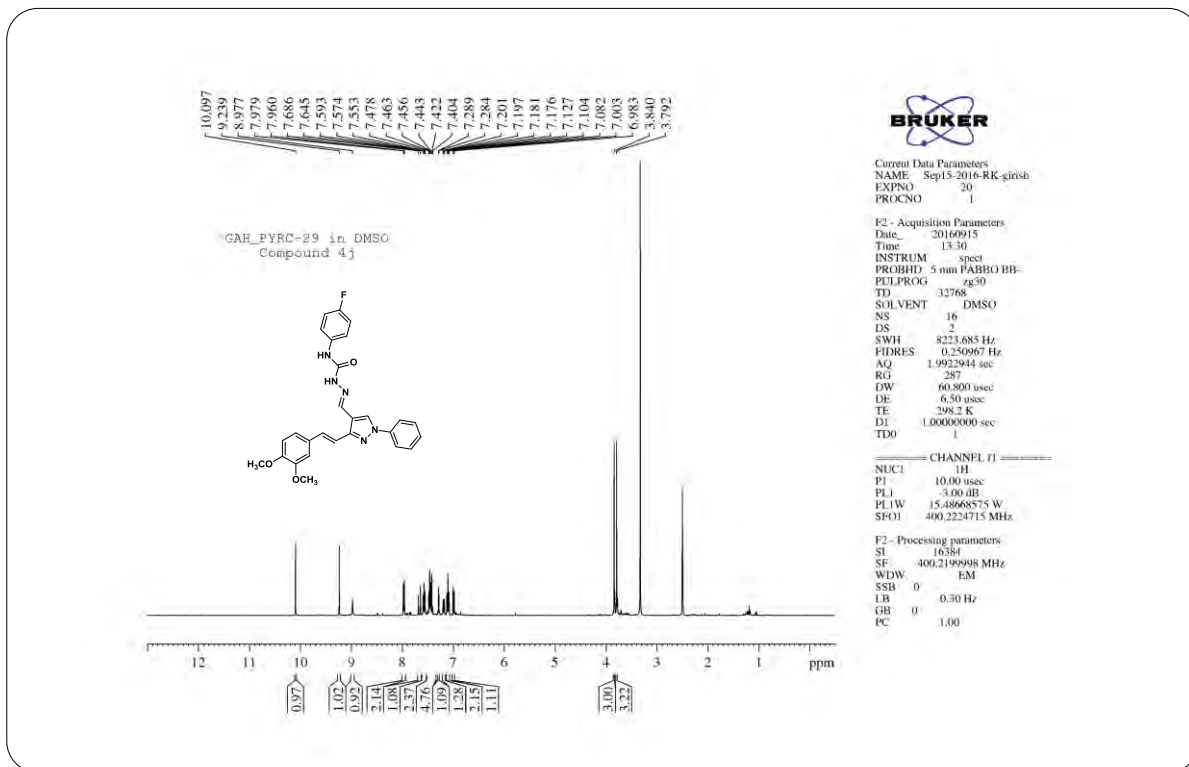
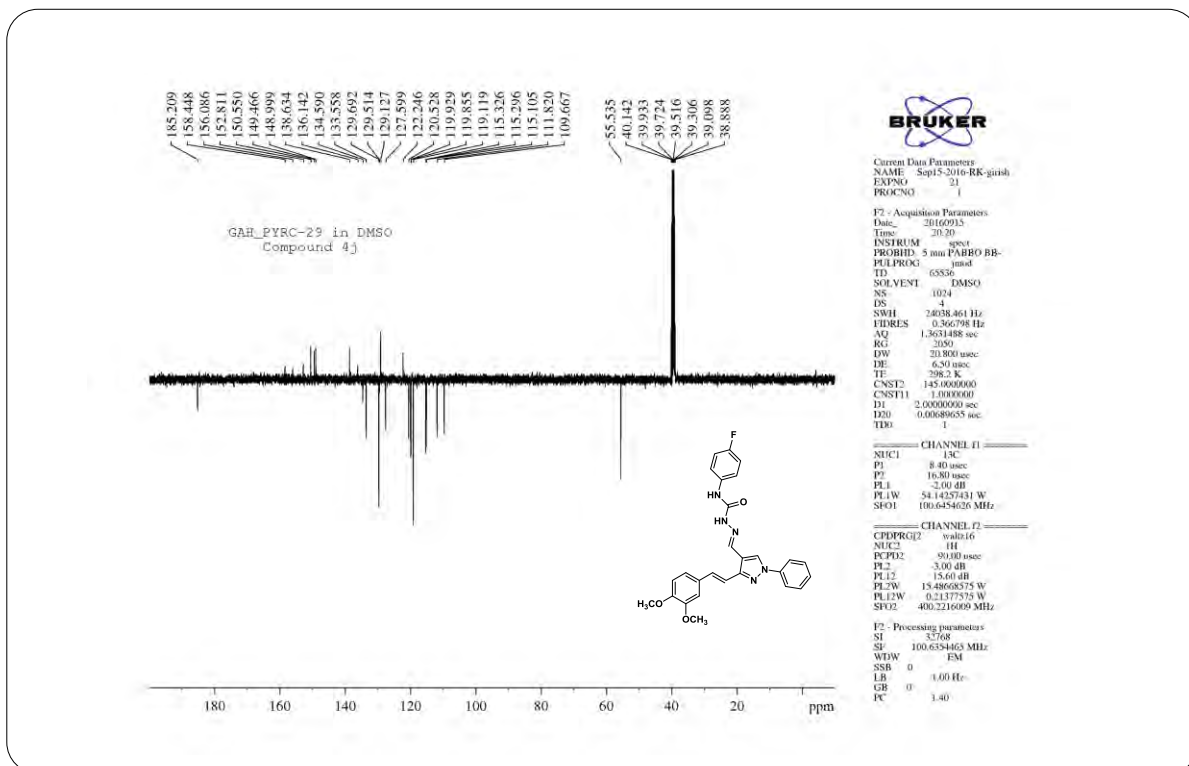
HRMS Spectrum of Compound 11h (chapter 5)

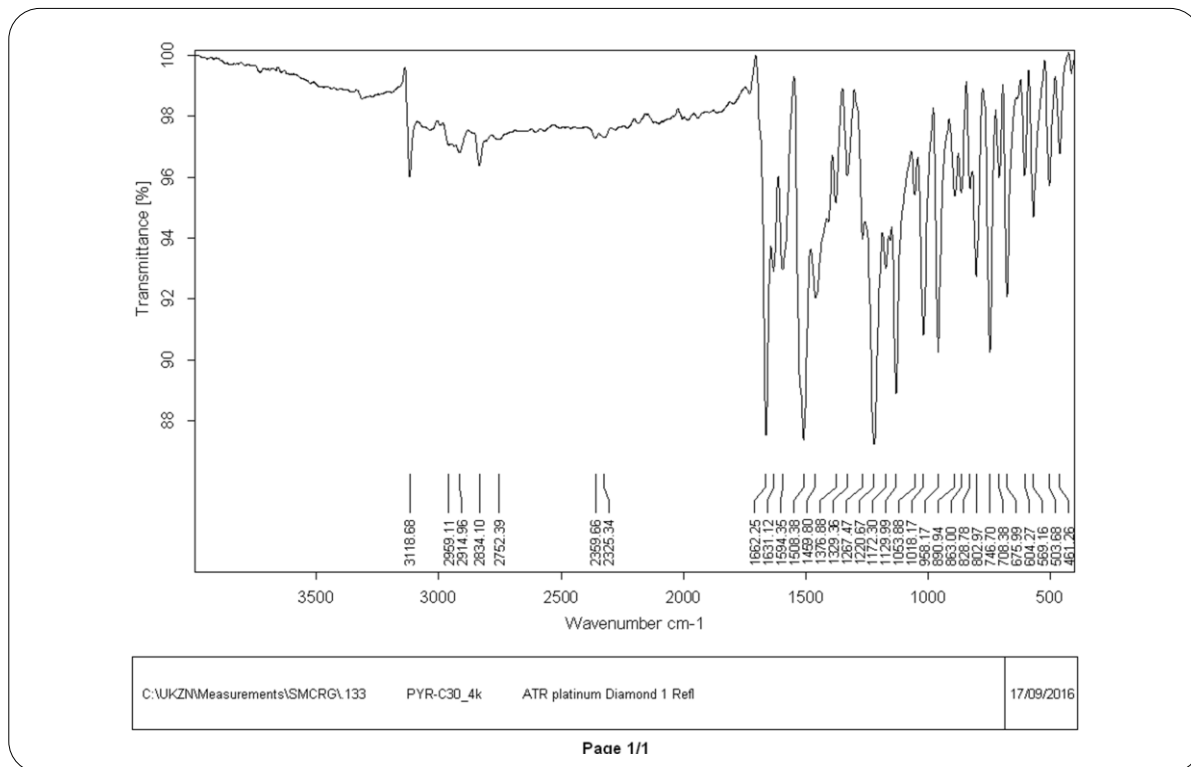


IR Spectrum of Compound 14a (chapter 5)

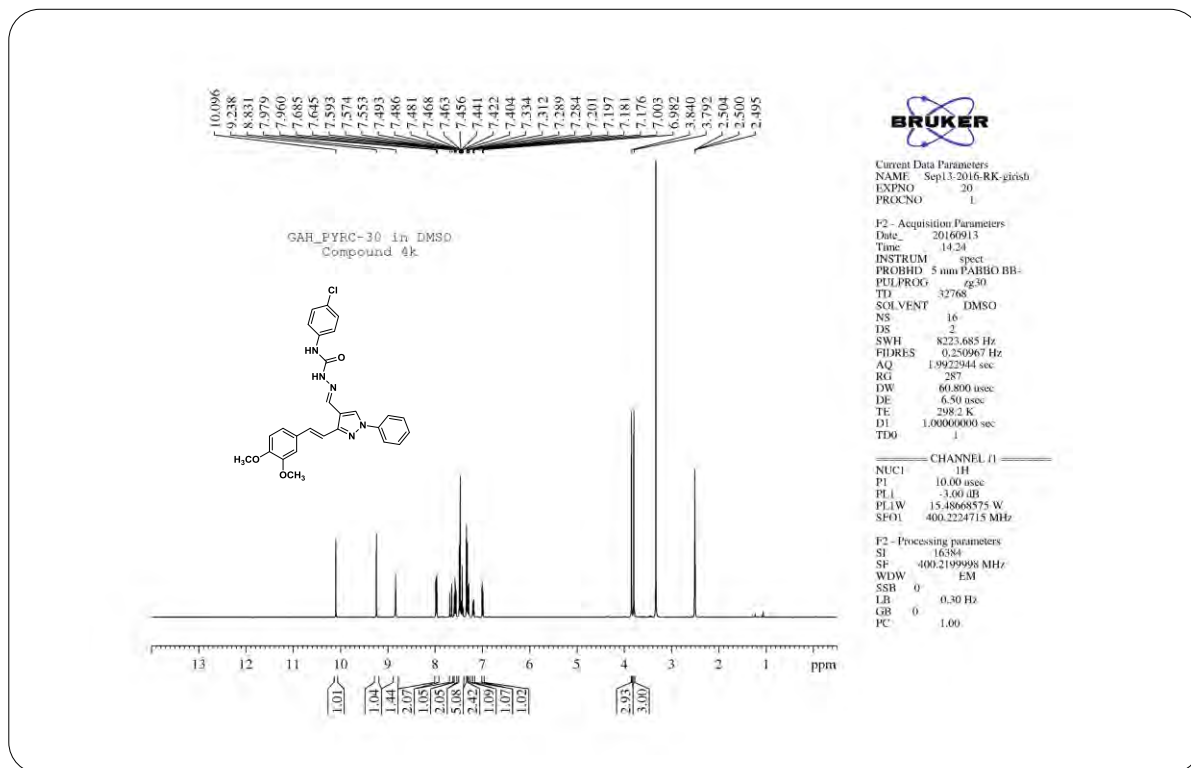
¹H NMR Spectrum of Compound 14a (chapter 5)

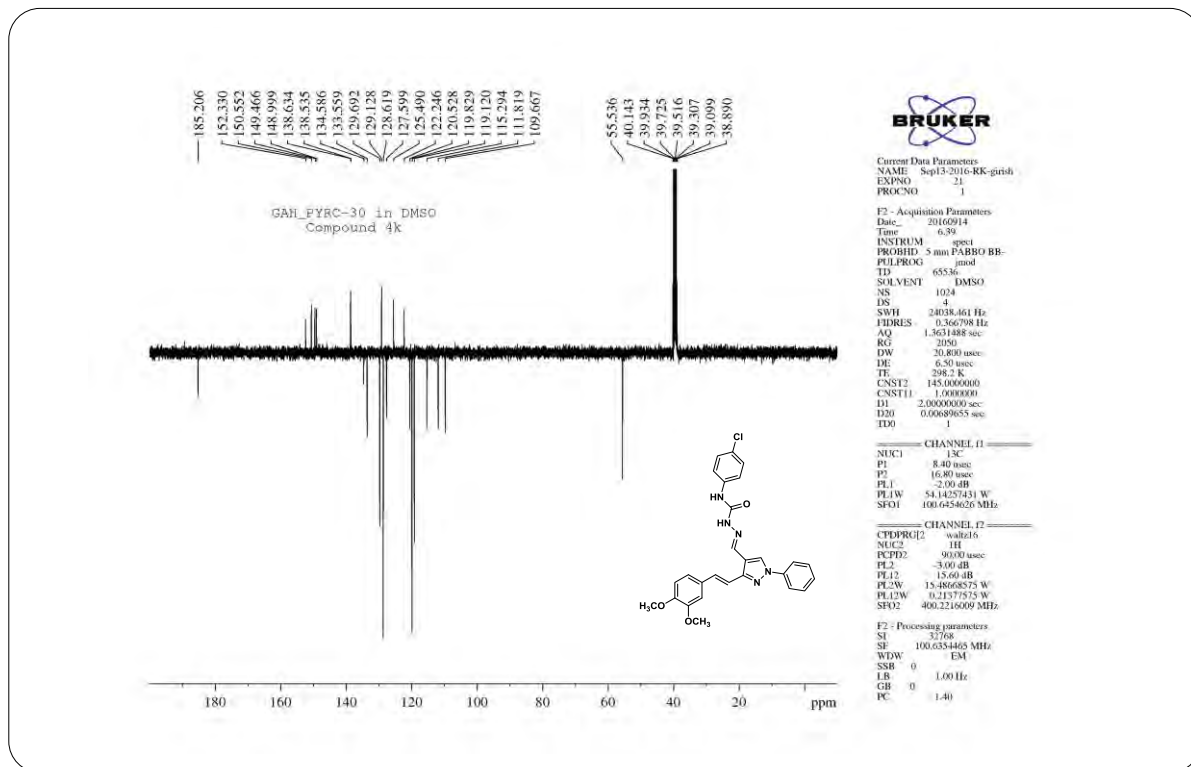
**¹³C NMR Spectrum of Compound 14a (chapter 5)****IR Spectrum of Compound 14b (chapter 5)**

¹H NMR Spectrum of Compound 14b (chapter 5)¹³C NMR Spectrum of Compound 14b (chapter 5)



IR Spectrum of Compound 14c (chapter 5)

¹H NMR Spectrum of Compound 14c (chapter 5)

**¹³C NMR Spectrum of Compound 14c (chapter 5)**

APPENDIX IV

APPENDIX - IV

PUBLISHED PAPERS



Review article

An appraisal on recent medicinal perspective of curcumin degradant: Dehydrozingerone (DZG)



Girish A. Hampannavar^a, Rajshekhar Karpoormath^{a,*}, Mahesh B. Palkar^{a,b}, Mahamadhanif S. Shaikh^a

^a Department of Pharmaceutical Chemistry, Discipline of Pharmaceutical Sciences, College of Health Sciences, University of KwaZulu-Natal, Westville Campus, Durban 4000, South Africa

^b Department of Pharmaceutical Chemistry, K.L.E. University College of Pharmacy, Vidyanagar, Hubballi 580031, Karnataka, India

ARTICLE INFO

Article history:

Received 20 October 2015

Revised 23 December 2015

Accepted 31 December 2015

Available online 2 January 2016

Keywords:

Review

Dehydrozingerone (DZG)

Zingiber officinale

Curcumin degradants

Feruloylmethane

ABSTRACT

Natural products serve as a key source for the design, discovery and development of potentially novel drug like candidates for life threatening diseases. Curcumin is one such medicinally important molecule reported for an array of biological activities. However, it has major drawbacks of very poor bioavailability and solubility. Alternatively, structural analogs and degradants of curcumin have been investigated, which have emerged as promising scaffolds with diverse biological activities. Dehydrozingerone (DZG) also known as feruloylmethane, is one such recognized degradant which is a half structural analog of curcumin. It exists as a natural phenolic compound obtained from rhizomes of *Zingiber officinale*, which has attracted much attention of medicinal chemists. DZG is known to have a broad range of biological activities like antioxidant, anticancer, anti-inflammatory, anti-depressant, anti-malarial, antifungal, anti-platelet and many others. DZG has also been studied in resolving issues pertaining to curcumin since it shares many structural similarities with curcumin. Considering this, in the present review we have put forward an effort to revise and systematically discuss the research involving DZG with its biological diversity. From literature, it is quite clear that DZG and its structural analogs have exhibited significant potential in facilitating design and development of novel medicinally active lead compounds with improved metabolic and pharmacokinetic profiles.

© 2016 Elsevier Ltd. All rights reserved.

Contents

1. Introduction	502
2. Dehydrozingerone identified for manifold pharmacological activities	503
2.1. Dehydrozingerone as antioxidant	503
2.2. Dehydrozingerone as antimutagen	507
2.3. Dehydrozingerone as anti-inflammatory	513
2.4. Dehydrozingerone as anti-depressant	514
2.5. Dehydrozingerone against Alzheimer's disease	514
2.6. Dehydrozingerone as anti-malarial	515
2.7. Dehydrozingerone as antifungal/antifeedant	517
2.8. Dehydrozingerone as antiplatelet	518
2.9. Dehydrozingerone as β -adrenoceptor antagonist	518
2.10. Dehydrozingerone: in silico studies	518
2.11. Dehydrozingerone reported for miscellaneous activities	519
3. Conclusion and future perspective	519
Acknowledgments	520
References and notes	520

* Corresponding author. Tel.: +27 (0)312607179, +27 721107207; fax: +27 (0)312607792.

E-mail addresses: karpoormath@ukzn.ac.za, rvk2006@gmail.com (R. Karpoormath).

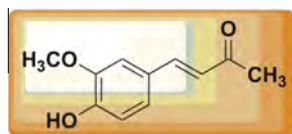


Figure 1. Structure of Dehydrozingerone (DZG).

1. Introduction

From time immemorial natural products sourced from plants, animals, marines and minerals have been the basis of treatment for variety of diseases. Plants in particular have been the basis of many traditional medicine systems throughout the world for thousands of years and they still continue to offer humankind with new remedies. The foundation of the modern pharmaceutical industry was primarily based on the techniques developed to identify and synthesize active ingredients from the traditional medicines obtained from natural sources. Plant-based medicines were initially dispensed as crude medicines such as tinctures, teas, poultices, powders and other herbal formulations,¹ which now serve as the basis of novel drug discovery. For example, plant based compounds like quinine, reserpine, curcumin, vincristine, vinblastine, pilocarpine, atropine, morphine, taxol, etc., have been investigated and exploited as important pharmaceutical drugs for the treatment of vital diseases or disorders. Hence, natural products have been proven templates for the development of new scaffolds for drugs.^{2–5}

Dehydrozingerone (DZG; Fig. 1) also known as feruloylmethane and vanillylidene acetone, isolated from rhizomes of ginger (*Zingiber officinale* Roscoe, family Zingiberaceae)^{6–8} and can be synthesized in laboratory by simple aldol condensation of vanillin and acetone.⁹ It is famously identified as a half structural analog of curcumin and is a classic example of a natural chalcone. DZG [(*E*)-4-(4-hydroxy-3-methoxyphenyl)but-3-en-2-one] is a remarkable scaffold comprising of a phenyl ring bearing methoxy group

ortho to the phenolic OH and an α,β -unsaturated carbonyl group with terminal methyl group. Besides, DZG is an unsaturated derivative of the natural product zingerone and resembles segment of curcumin as well as share many structural and pharmacological similarities with curcumin.

DZG and curcumin also claim mutual chemical resemblances as both bear styryl ketone moieties with similar substitutions on the phenyl ring.^{10,11} It is a recognized biosynthetic intermediate¹² and also an identified degradant of curcumin¹³ (Fig. 2).^{13–16} DZG is a known metabolic product of curcumin that has a larger biological half-life than curcumin itself.¹⁷ In spite of versatile applications of Curcumin (*diferuloylmethane*), a polyphenol extract of *Curcuma longa*,¹⁸ is still known to have weak bioavailability and suffers from premature degradation on oral administration that holds back its use as a successful therapeutic agent.¹⁹ These pharmacokinetic instabilities of curcumin may be due to following reasons,

- Liability of β -diketone moiety in the structure of curcumin (as substrates) to several aldo-keto reductases in vivo.^{20–22}
- Enzymatic cleavage at the benzylic position.²³
- Instability of reactive β -diketone moiety at neutral-basic pH conditions in vitro.^{13,24}
- Instability of active methylene group at a pH above 6.5.²⁵

However, the curcuminoids, degradants and biosynthetic intermediates of curcumin also exhibit many exceptional pharmacological effects. These emerging new class of compounds have been termed as mono-carbonyl analogs (MCA's) or mono-carbonyl enones or dienones.²⁶ These enone analogs emanate in 5, 3 and 7 carbon spacers (7 carbon spacers as in curcumin) and have explicable biological activities on comparison with curcumin.²⁷ Furthermore several studies involving MCA's have proven improved bioactivities and enhanced pharmacokinetic profiles compared to curcumin.^{28–30}

In recent times, scientists have shown enormous interest towards exploring the medicinal potentials especially for their

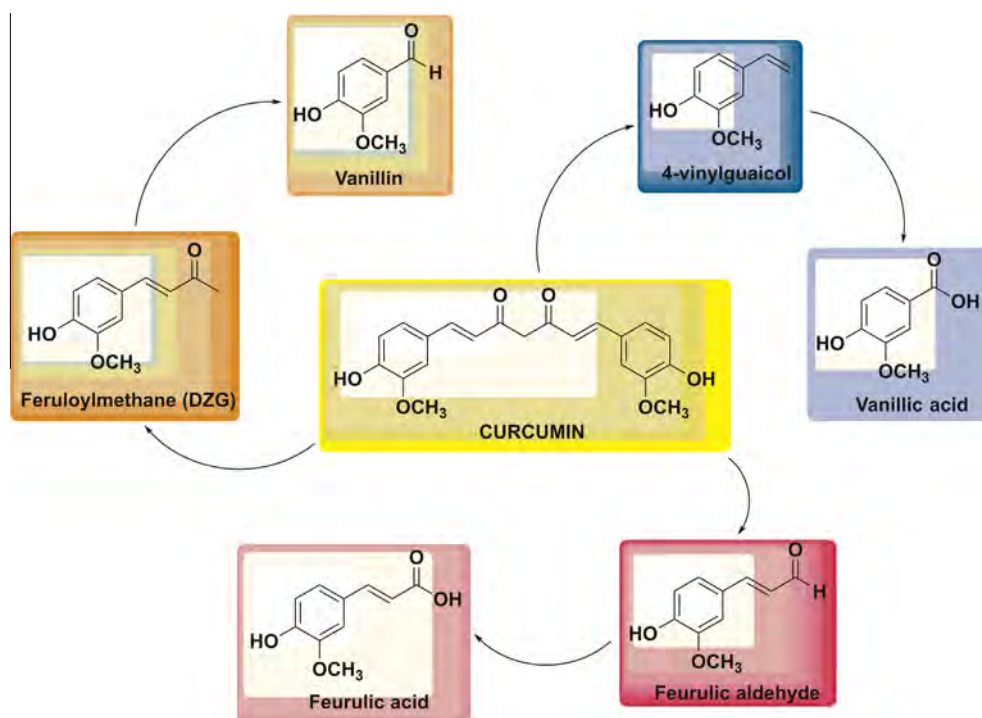


Figure 2. Degradation products of curcumin.

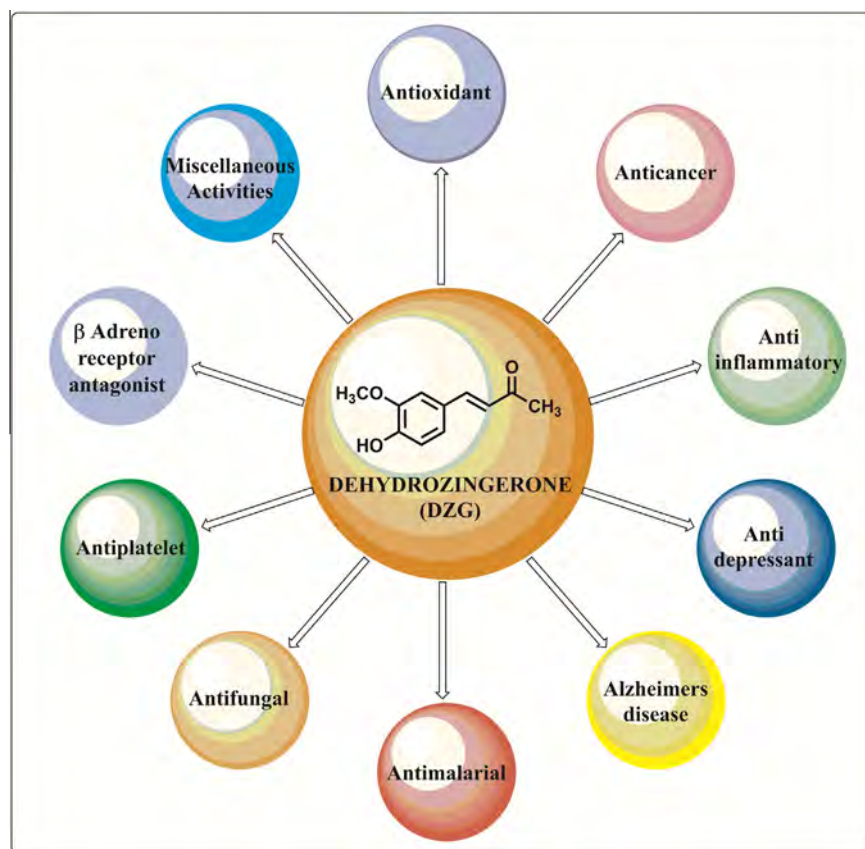


Figure 3. DZG as active scaffold with manifold pharmacological activities.

antioxidant and anticancer activity. The degradation products as well as curcuminoids have played a key role in understanding the mechanism of action of curcumin. Recent studies have shown that degradation products such as ferulic acid and vanillic acid as human metabolites of curcumin, have contributed towards the antioxidant effects of curcumin.³¹ Hence, the structural analogs or degradants have emerged as promising scaffolds that have contributed towards designing valuable impending drugs. With these distinguishing structural features DZG as an active scaffold has been exploited for diverse medicinal properties (Fig. 3) as discussed in this review.

The variations in the biological activity of DZG as a result of its structural manipulations are precisely highlighted in Figure 4. In this mini review we have recapitulated the progress of research involving DZG and its derivatives and discussed its diverse application in the field of medicinal chemistry emphasizing on their brief structure activity-relationships (SAR).

2. Dehydrozingerone identified for manifold pharmacological activities

2.1. Dehydrozingerone as antioxidant

Reactive oxygen species (ROS) are produced during aerobic respiration. Regardless of multiple preserved redox modulating systems, a part of ROS constantly flee from the mitochondrial respiratory sequence which is sufficient to damage cells in a variety of ways that include DNA mutations,³² lipid peroxidation,³³ ATP depletion,³⁴ and apoptosis.³⁵ Antioxidants are the key negotiators that prevent the reaction of ROS with biomolecules and have immense potential against pathophysiology of numerous diseases

including cancer, heart disease, aging and different neurological disorders. Ranges of naturally occurring antioxidants have been isolated from plants and have been further tailored structurally to give in newer derivatives. Some of the naturally occurring antioxidants usually phenols and poly phenols³⁶ have been depicted in the Figure 5.³⁷

Rajakumar et al., have reported the antioxidant properties of three structurally related compounds namely DZG, eugenol (**1**) and isoeugenol (**2**) by means of various experimental models. In this study compound **2** was found to be the highly active in restraining ferrous-ion, ferric-ion and cumene-hydroperoxide-induced lipid peroxidation in rat brain homogenates. All the tested compounds displayed considerable hydroxyl radical scavenging activity. Compound **2** was found as a powerful scavenging superoxide anion produced by the xanthine-xanthine oxidase system, whereas Compound **1** was observed to inhibit xanthine oxidase. The high antioxidant activity of **2** was due to the existence of a conjugated double bond, which augments the stability of the phenoxyl radical by electron delocalization. Such electron delocalization is not possible with **1**. In DZG, the stability was diminished by an electron withdrawing keto group at the para position to hydroxyl group. Over all, this study evidently demonstrated the essential structural features and the antioxidant potential of naturally occurring phenols, of which compound **2** emerged as a potential antioxidant as compared to DZG.¹⁰



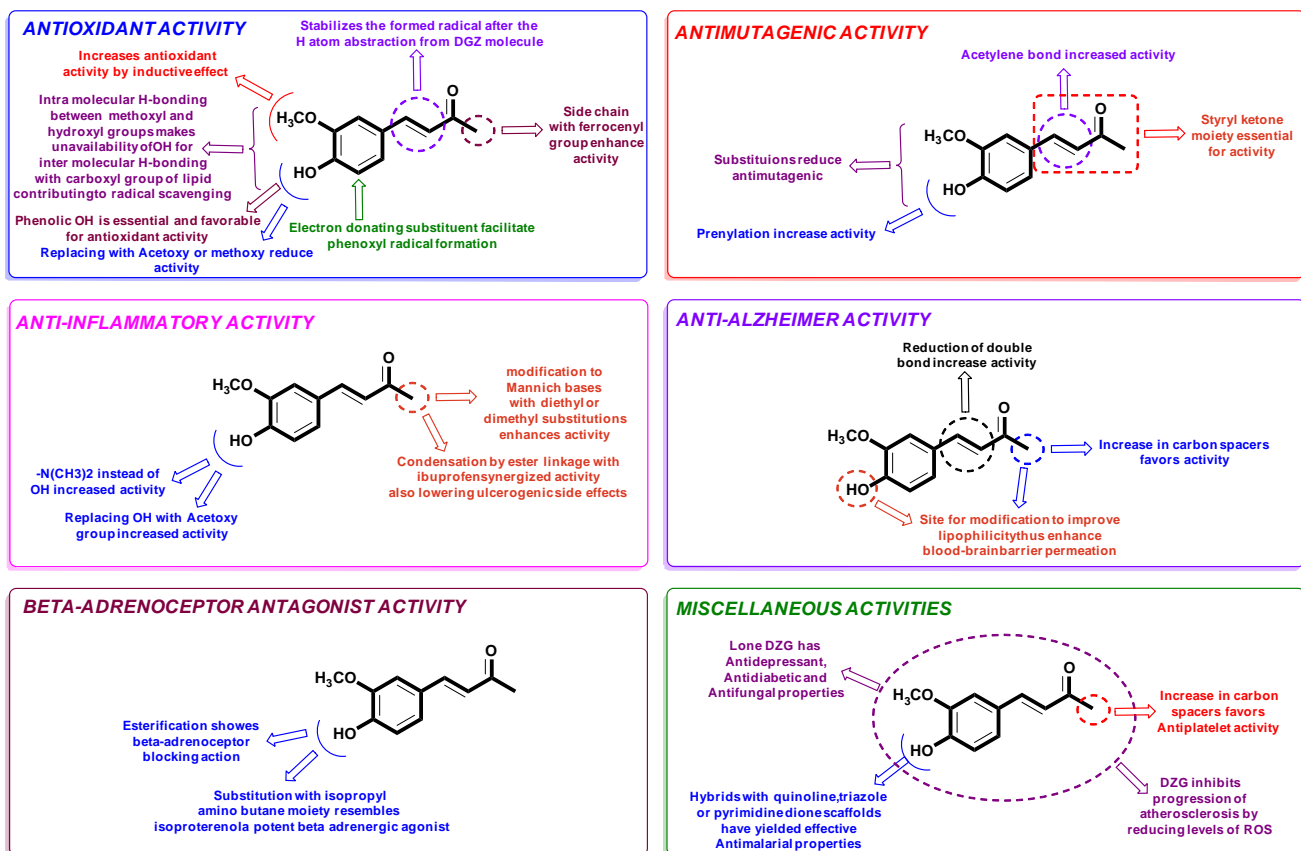


Figure 4. Imperative structural features of Dehydrozingerone (DZG) and effects of substitutions over various biological activities.

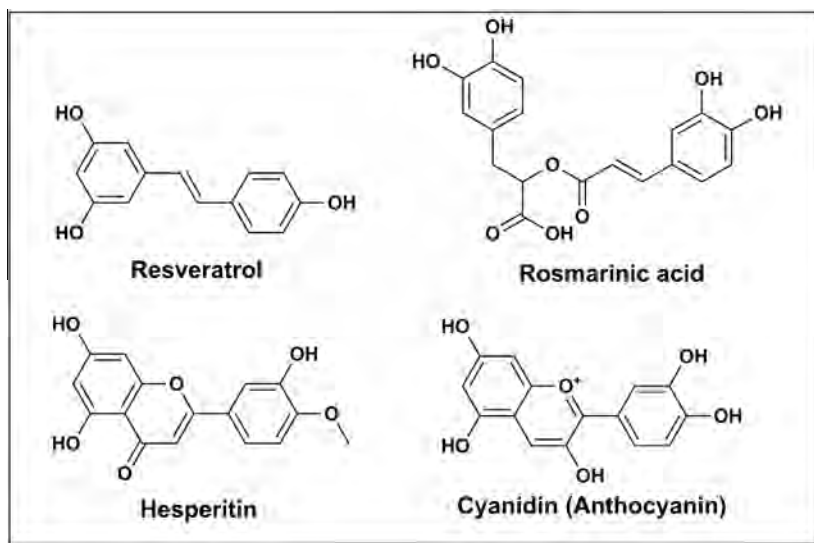


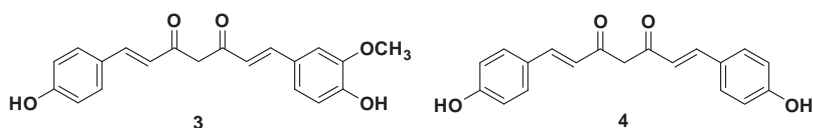
Figure 5. Naturally occurring antioxidants.

In order to understand the antioxidant properties of DZG and curcumin, Rajakumar et al., have reported the inhibition of lipid peroxidation by both DZG and curcumin in rat brain homogenates. Interestingly both compounds inhibited the formation of conjugated dienes and spontaneous lipid peroxidation. These two compounds also inhibited lipid peroxidation induced by ferrous ions, ferric-ascorbate and ferric-ADP-ascorbate. In each of these cases

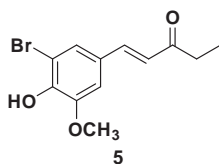
curcumin was found to be more active than DZG and α -tocopherol. This study established that 1,3-diketone structure was not necessary for inhibiting lipid peroxidation by curcumin because DZG, which is devoid of this system was also capable of inhibiting lipid peroxidation. The phenolic groups in both of these compounds were found to favor considerably for the antioxidant properties, since they react with free radicals to form phenoxyl radical.

Methoxy group at *ortho*-position to the phenolic group in both DZG and curcumin were known to increase the antioxidant activity due to inductive effect. This study demonstrated that DZG like curcumin inhibits lipid peroxidation although to a lesser extent and additionally the antioxidant activity of curcumin was refereed by its two phenolic groups, which accounts for its superior activity.¹¹

Subramanian et al., have reported the shielding potential of natural antioxidants against oxidative damage of DNA by excited species of oxygen that is, $^1\text{O}_2$, a singlet molecular oxygen, known to induce single strand breaks in plasmid DNA. Natural antioxidants namely curcumin, DZG besides two other desmethoxycurcumin (**3**) and bisdemethoxycurcumin (**4**) were examined in this study. The results showed that curcumin and its derivatives and to a smaller degree other natural antioxidants tender noteworthy protection to DNA against $^1\text{O}_2$. Curcumin was found to be most effective followed by DZG then **3** and **4**. At higher concentration DZG, **3** and **4** were found to be equally active. Thus this study fairly highlighted an explanation regarding probable mechanism of antimutagenic properties of these tested natural antioxidants.⁵



Priyadarsini et al., have reported structurally allied phenols namely DZG, bromopentenone (**5**), eugenol (**1**) and isoeugenol (**2**) for antioxidant properties by inhibiting lipid peroxidation in membrane models. Additionally, the physicochemical properties of the transient intermediates of these antioxidants produced by the scavenging of several oxidizing free radicals were computed using pulse radiolysis technique.³⁸



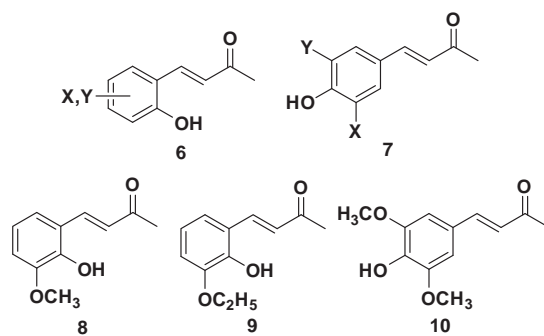
Jovanovic et al., have reported antioxidant mechanisms of curcumin by laser flash photolysis and pulse radiolysis. This study revealed that the apparent site of reaction is the central CH_2 group in the heptadienone link of curcumin, which has two labile hydrogens. This was supported by comparing the reaction patterns of curcumin and DZG. DZG did not react with the methyl radical, indicating that the presence of the labile hydrogens is crucial for the H-atom donating ability of curcumin. Thus the electron donating ability of curcumin is assessed from the measurements of one-electron-transfer equilibria of DZG radicals. The major conclusion of this study was that the H-atom transfer plays a crucial role in the antioxidant action of curcumin.³⁹

Priyadarsini et al., have reported the free radical reactions of DZG studied at different pH using a range of oxidants by means of nanosecond pulse radiolysis procedure. This study employed several free radicals both primary and secondary to access the antioxidant potential of DZG. Several specific free radicals were generated namely N_3^\cdot , Br^\cdot , Br_2^\cdot , and Ti(II) that were employed with DZG giving rise to the phenoxyl radical across the total pH range. Observations at pH 6 suggest that there is formation of OH-adduct which absorbs at 460 nm along with another small oxidation product confirmed by HPLC analysis. And at pH 10 there was only one oxidation product, that is, phenoxyl radical absorbing at 360 nm. This study demonstrated that the phenoxyl radical from DZG is

deficient to abstract hydrogen because of delocalization of the unpaired electron into an aromatic ring structure. The phenoxyl radical was recognized to have a lifetime of a few milliseconds. The thermodynamic parameter and one-electron reduction potential of DZG was considerably high thus not making DZG as a perfect candidate for an antioxidant property, but the rapid kinetic parameters might be accountable for its antioxidant activity. In lack of any other substrate, the phenoxyl radicals might vanish by several mechanisms, for example, radical–radical reactions with alkoxyl and peroxy radicals, thus averting the spread of the chain reaction of lipid peroxidation. These results put forward that DZG like many other phenolic antioxidants can counter both primary and secondary radicals.¹⁷

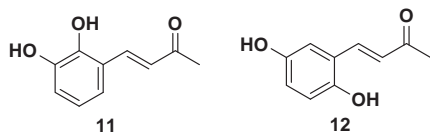
Yamagami et al., have reported antioxidant activities against lipid peroxidation induced by *tert*-butylhydroperoxide or γ -irradiation for a series of hydroxybenzalacetones derivatives **6** and **7**. Authors have also reported relationship between the structure and activity by using free-energy related substituent parameters. Further in order to interpret the resultant correlations, authors

have further measured DPPH free radical scavenging activities of synthesized compounds and later performed the QSAR analysis. In this study it was concluded that the inhibitory potencies were primarily due to the formation of phenoxy radicals as well as from the electron-donating substituents, which further contributed to ease phenoxy radical formations. Similarly the *ortho* substituents were effective in stabilizing the generated phenoxy radicals. The results indicated a remarkable enhancement of activity for compounds **8**, **9**, and **10**.⁴⁰

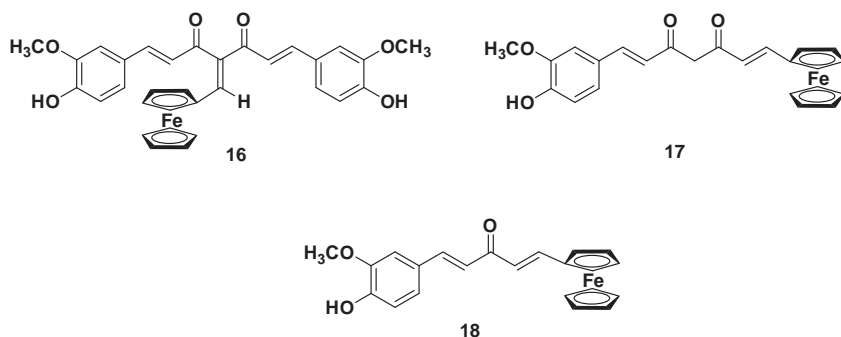


Kuo et al., have synthesized a novel series of DZG derivatives and evaluated them as potential antioxidants. Amongst the series, compound **11** displayed significant inhibition of Fe^{2+} -induced lipid peroxidation (to elucidate antioxidant activity) in rat brain homogenate with an IC_{50} of $6.3 \pm 0.4 \mu\text{M}$ as compared to the standard antioxidant, α -tocopherol (TOH) with $\text{IC}_{50} = 2.5 \pm 0.1 \mu\text{M}$. In addition, the tested compounds did not form complex with ferrous ion in the iron chelation study performed by authors as addition of ferrous ion did not source any spectral shift or absorbance variation. Thus the authors expected that the test compounds might have exerted their effects on lipid peroxidation primarily by scavenging free radicals rather than functioning as iron chelators. This belief was further supported by reassessing DPPH test that gave information about the reactivities of the tested compounds with

a stable free radical. In this test, free radical scavenging activity was expressed by $IC_{0.200}$. Thus compound **11** ($IC_{0.200} = 3.2 \mu\text{M}$) and **12** ($IC_{0.200} = 4.9 \mu\text{M}$) were found to be two and five fold more active than TOH ($IC_{0.200} = 8.3 \mu\text{M}$) and ascorbic acid ($IC_{0.200} = 23.7 \mu\text{M}$) respectively in DPPH assay model.⁸

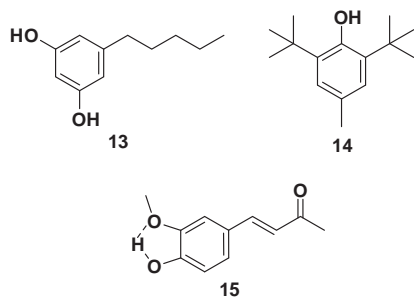


Parihar et al., have demonstrated the *in vitro* and *in vivo* antioxidant potential as well as *in vivo* radioprotective activity of DZG against whole body gamma irradiation in Swiss albino mice. DZG scavenged the $ABTS^{\bullet+}$ (2,2'-azobis (3-ethylbenzothiazoline-6-sulfonic acid) and DPPH free radicals at room temperature DZG



reduced Fe(III) to Fe(II) at pH 7.4 and scavenged the NADH/phenazine methosulfate generated superoxide radical in cell free system. DZG also scavenged the nitric oxide radical generated by sodium nitroprusside.⁴¹

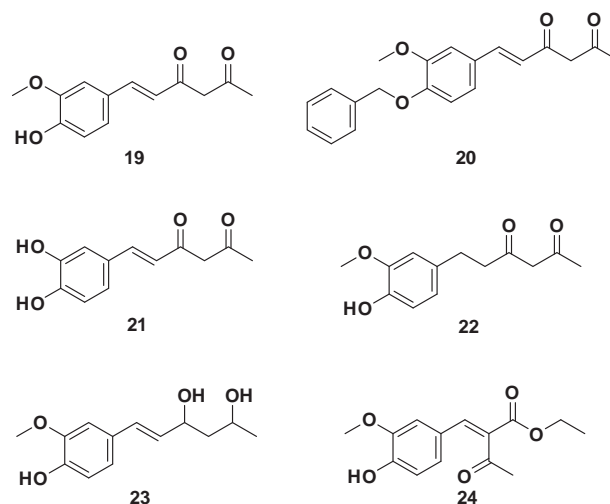
Musialik et al., have reported the antioxidant property of two natural compounds Olivetol (**13**) and DZG along with 2,6-di-*tert*-butyl-4-methylphenol (BHT) (**14**) by Ozawa–Flynn–Wall method for inhibition of non-isothermal autoxidation of linolenic acid. Inhibition of non-isothermal oxidation of linolenic acid (LNA) in bulk phase was monitored by differential scanning calorimetry. Among these compounds, DZG displayed best antioxidant properties in which phenolic hydroxyl group is internally hydrogen bonded to *ortho*-methoxyl group (**15**), thus making OH group, unavailable to form intermolecular hydrogen bond with carboxyl group of lipid, proving as efficient radical scavenger. Further, the presence of double bond conjugated to aromatic ring in DZG brings additional stabilization of the radical formed after the H atom abstraction from DGZ molecule.⁴²



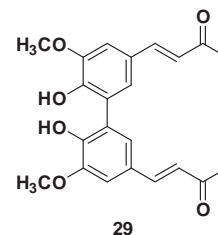
Li et al., have reported antioxidant properties for a new series of ferrocenyl-substituted curcumin derivatives (**16–18**). The ferrocenyl group was linked with the methylene in feruloylacetone to

produce ferrocenyl curcuminoids by using Knoevenagel condensation. Antioxidant activity of the synthesized compounds were evaluated in 2,2'-azobis(2-amidinopropane hydrochloride) (AAPH), Cu^{2+} /glutathione (GSH), hydroxyl radical ($\cdot\text{OH}$)-induced oxidation of DNA, and in trapping DPPH, $ABTS^{\bullet+}$ and galvinoxyl radicals. Results revealed that all compounds protected DNA against Cu^{2+} /GSH-induced oxidation, but promoted $\cdot\text{OH}$ -induced oxidation of DNA. Compounds **16**, **17** and **18** scavenged the radicals with *n* values (*n* is a stoichiometric factor that implies the number of radicals trapped by one molecule of the antioxidant and can be used as a quantitative index to express the antioxidant capacity) 9.5, 5.7 and 4.7, respectively, thus protecting DNA against AAPH-induced oxidation. Further compound **16** could trap more DPPH and $ABTS^{\bullet+}$ than compounds **17** and **18**. All the compounds could not react with galvinoxyl radical. This study conclude that phenolic hydroxyl groups and iron atom in ferrocenylidene curcumin derivatives play an important role for antioxidant activity.⁴³

In order to clarify the contribution of phenolic and enolic hydroxyl group to the antioxidant capacity of feruloylacetone Feng et al., have reported derivatives of DZG (**19–24**), which was taken as a model compound of half-curcumin. The synthesized compounds were evaluated for their antioxidant properties by trapping $ABTS^{\bullet+}$, DPPH and galvinoxyl radicals. The reductive capacities were also screened by quenching singlet oxygen and by inhibiting the oxidation of linoleic acid. Oxidation of DNA mediated by hydroxyl radical and AAPH were also studied with the synthesized compounds. In addition, compounds were applied to protect erythrocytes against AAPH and hemin-induced hemolysis. The results suggest that the antioxidant capacity of half-curcumin was derived from the phenolic-OH and the conjugated linkage between phenolic and enolic-OH. The enolic-OH itself could not trap radicals.⁴⁴

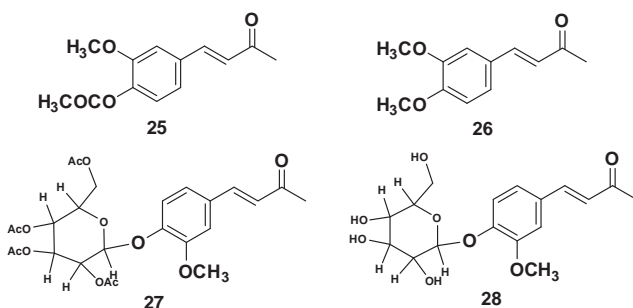


Kubra et al., have reported synthesis and antioxidant properties of DZG derivatives by scavenging the stable DPPH (1,1-diphenyl-2-picrylhydrazil) radical. The reduction capability of the DPPH radical was established by its absorbance decrease at 517 nm, as induced by natural antioxidants. The IC₅₀ value of DZG was found to be 0.3 mM comparable to Trolox (0.26 mM), whereas the IC₅₀ value of **25**, **26**, **27** and **28** were found to be 40, 20, 10 and 7.5 mM, respectively. Antioxidant activity assays of derivatives with varied substituents inferred that the existence of hydroxyl substituents on the phenyl nucleus enhanced activity, whereas substitutions like methoxyl and acetoxy groups reduced antioxidant activity remarkably. DZG, which hold an extended conjugated system was found to be active.⁴⁵



29

Li et al., have reported a new series of asymmetrical mono-carbonyl ferrocenylidene curcumin and their dihydropyrazole compounds from dehydrozingerone derivatives (**30–44**, Table 1) and investigated their antioxidant abilities in protecting DNA against AAPH induced oxidation and scavenging ABTS cationic radical. Compound **40** possessed the highest scavenging of ABTS⁺, whereas compound **33** had higher protecting property of DNA against AAPH induced oxidation. These results suggest that the antioxidant abilities of compounds would increase when the ferrocenyl group was introduced along with other substituent groups in the molecule.⁴⁷



2.2. Dehydrozingerone as antimutagen

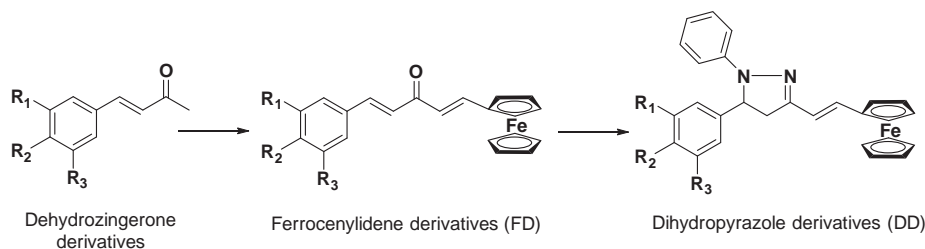
Kancheva et al., synthesized DZG and dimer of DZG **29** and screened their antioxidant activity by bulk lipid autoxidation method, which involved DZG and compound **29** as individual compounds (1 mM), as equimolar binary (1:1) and ternary (1:1:1) mixtures with TOH and/or ascorbyl palmitate (AscPH). The highest oxidation stability of lipid substrate in the presence of individual compounds was found for TOH, followed by **29** and DZG, which was established from the main kinetic parameters (antioxidant efficiency, reactivity and capacity). AscPH did not demonstrate any protective effect. Synergism was achieved for the binary mixtures of (TOH + AscPH) [42.4%], (DZG + TOH) [32.4%] and (DZG + AscPH) [35.6%] and for the ternary combination of (DZG + TOH + AscPH) [28.7%]. Unusual protective effects observed were explained on the basis (of results) of TOH regeneration and its content determined by HPLC.⁴⁶

The phyto-constituents are vital and important part of our routine diet providing protective effects from mutagens. Numerous phyto-constituents namely Coumarin, Xanthenes, Terpenoid, Pigments, Anthraquinone, Tannin, Phenolic, Cymopol, Halogenated Flavonoids, Dibenzate diterpenes, Organosulfur, Nitrogenous compounds and Curcuminoids from various plant species have been reported to have antimutagenic properties.⁴⁸

Synthetic curcuminoid derivatives have been reported to have Antimutagenic properties.^{49–52} Monocarbonyl analogs of curcumin are widely explored as they have better pharmacokinetic and pharmacodynamic properties than curcumin and are emerging as a new class of anticancer agents.^{53,54} Dehydrozingerone, isolated from ginger (*Zingiber officinale*) has the structure corresponding to half analog of curcumin and also monocarbonyl analog of curcumin have been reported to have antimutagenic properties. Following discussion reviews about DZG as an antimutagen.

Motohashi et al., have investigated antimutagenic activities of DZG and their synthetic analogs (**45–56**) against UV-induced

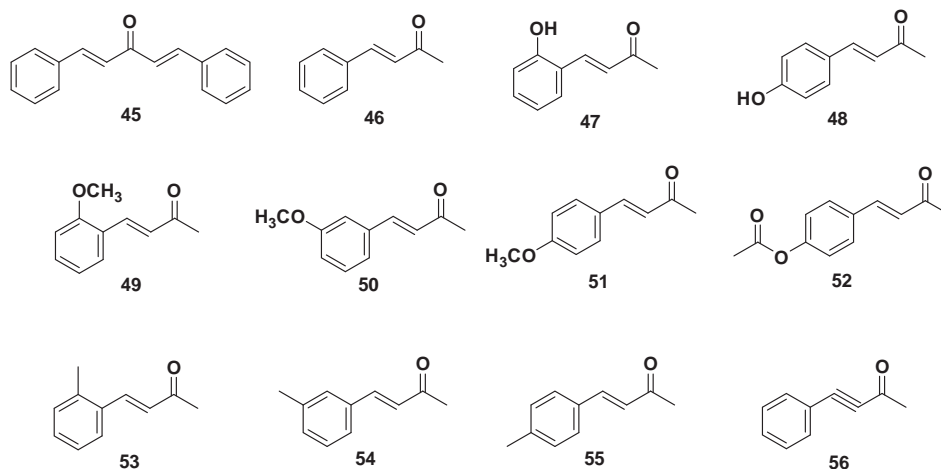
Table 1
Structures of asymmetrical mono-carbonyl ferrocenylidene curcumin and their dihydropyrazole compounds from dehydrozingerone derivatives



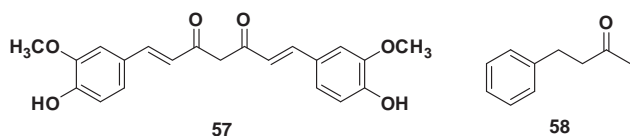
	Ferrocenylidene derivatives			Dihydropyrazole derivatives		
	R ₁	R ₂	R ₃	R ₁	R ₂	R ₃
30	H	H	H	38	H	H
31	H	OH	H	39	H	H
32	H	H	H	40	H	N(CH ₃) ₂
33	H	N(CH ₃) ₂	H	41	H	OH
34	H	OH	H	42	H	H
35	H	H	OH	43	H	OH
36	H	OH	OC ₂ H ₅	44	H	OH
37	NO ₂	OH	OCH ₃			OC ₂ H ₅

Note: It is phenyl instead of ferrocenyl for structures **30**, **31** and **38** only.

mutagenesis in *Escherichia coli*. Studies suggest that the effect of DZG against the UV-induced mutagenesis was poor, but benzalacetone (**46**), a dehydroxy-demethoxy product of DZG revealed the strongest antimutagenic activity among the ring-substituted analogs except for 2-hydroxybenzalacetone (**47**). Results also disclosed that the ring-substitution with a group such as 4-hydroxyl, methoxyl or methyl reduced the antimutagenic activity, while α,β -unsaturated (double bond) carbonyl functionality was essential for the antimutagenicity. Compounds **46**, **47** and **56** decreased both the UV- and γ -induced mutagenesis. This clearly suggests that ring-substitution was not effective and a double- or triple-bonded carbonyl system was required for the antimutagenic activity.⁷



Motohashi et al., have evaluated anti-tumor activity of DZG and its related compounds (**57**, **26**, **8**, **47**, **48**, **50**, **51**, **2**, **56**, **46** and **58**) by determining the inhibitory effect on Epstein–Barr virus early antigen (EBV-EA) activation induced by 12-*O*-tetradecanoylphorbol-13-acetate (TPA). The IC_{50} of DZG was found to be 95 mol ratio/TPA, which was almost similar to curcumin (**57**) 97 mol ratio/TPA. Isoeugenol (**2**) that lacks carbonyl group in the side chain, exhibited 50% inhibition with 38 mol ratio/TPA, thus accounting for one-third antioxidant activity of DZG. Compounds **26**, **8** and monosubstituted compounds were also tested for the EBV-EA activation. Compound **26**, IC_{50} = 107 mol ratio/TPA was less effective than DZG while compound **8** (IC_{50} = 50) exhibited more potent activity than DZG. Compounds **47**, **48** and **51** were found to be more active whereas compound **50** was less active as compared to DZG. The influence of the carbon–carbon bond attached to the benzene ring was also assessed with compound **56** having a triple bond, **46** with a double bond and **58** with a single bond. The inhibitory effect was significant and highest in **56** (IC_{50} = 48 mol ratio/TPA) followed by **46** (IC_{50} = 129 mol ratio/TPA) and then **58** (IC_{50} = 222 mol ratio/TPA).⁵⁵



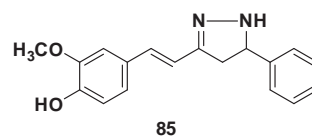
Rao et al., have reported the cyto-protective effects of DZG and two other structurally related phenolic compounds Eugenol (**1**)

and Isoeugenol (**2**) against cisplatin-induced toxicity in vero (African Green Monkey Kidney) cells by observing variation in percentage trypan blue exclusion (TBE), percentage release of lactate dehydrogenase (LDH), and glutathione (GSH) content. Cisplatin is known to cause cytotoxicity in kidney cells due to oxidative injury, involvement of hydrogen peroxide in outer medullary cortical tubule cells and peroxidation of cell membranes. Several literature reports reveal that various antioxidants are known to prevent cisplatin induced cytotoxicity. Among the tested series, compound **2** was the most active followed by **1** and then DZG in preventing cell death induced by cisplatin, while none of the compounds were able to prevent the reduction of the GSH content.⁵⁶

Motohashi et al., in conjunction with previous studies, have further reported the structure activity relationship of benzalacetone derivatives as potential anti-tumor agents by assaying in EBV-EA activation model. The results of benzalacetone derivatives were in agreement with the previous findings.⁵⁷

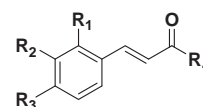
Tatsuzaki et al., have synthesized twenty-eight new compounds (summarized in Tables 2 and 3) related to DZG, isoeugenol and 2-hydroxychalcone, which were evaluated for their in vitro activity against a panel of human tumor cells viz. Human epidermoid carcinoma of the nasopharynx (KB), multidrug-resistant expression P-glycoprotein (KB-VCR) and human lung carcinoma (A549). From results it was clear that other than isoeugenol analogs **76–84**, most compounds exhibited moderate to strong cytotoxic activity against the cell lines tested. Particularly, compound **65** displayed significant cytotoxic activity against the A549 (IC_{50} = 0.6 μ g/mL), while compounds **9**, **66** and **67** showed comparable cytotoxic activity against both KB (IC_{50} = 2.0, 1.0, and 2.0 μ g /mL) and KB-VCR (IC_{50} = 1.9, 1.0, and 2.0 μ g/mL) respectively, suggesting that they are not substrates for the P-glycoprotein drug efflux pump.⁵⁸

In 2006, Ex-Elaxis INC reported pyrazole derivatives as tyrosine kinase modulators in treatment of cancer. This study reports anti-cancer potential of compound **85**, which is analogous to DGZ derivative.⁵⁹



Conjugation of two bioactive compounds/scaffolds has been effective strategy in designing pharmacophores as ligands, inhibitors and other class of drugs. Tatsuzaki et al., have synthesized some novel conjugates of DZG with triterpenoids as promising cytotoxic agents. In this work, triterpenoids namely glycyrrhetic acid (GA, **86**), oleanolic acid (OA, **87**) and ursolic acid (UA, **88**) were esterified with DGZ (**89–91**) to yield eleven different novel DZG analogs **92–102**. These synthesized compounds were screened for their in vitro anti-cancer activity against nine different human cancer cell lines as depicted in Table 4.

Compounds **92**, **93** and **94** exhibited significant cytotoxic activity against LN-Cap, 1A9, and KB cells lines with ED₅₀ values of 0.6, 0.8 and 0.9 μM, respectively. Conjugates of DZG and OA or UA were inactive, suggesting that the GA component was critical for activity. In general, this study unearths that GA and DZG as individual components were inactive whereas their conjugates GA–DZG displayed potent cytotoxic activity. Thus GA–DZG conjugates were established as new chemical entities in anti-cancer drug discovery and development.⁶⁰

Table 2Structures of DZG and chalcone analogs (**8**, **59**, **60**, **46**, **61**, **9**, **62**, **63**, **64**, **65**, **66** and **67**)

	R ₁	R ₂	R ₃	R ₄
DZG	H	OMe	OH	Me
8	OH	OMe	H	Me
59	H	OH	OMe	Me
60	OH	H	OMe	Me
46	H	H	H	Me
61	H	OEt	OH	Me
9	OH	OEt	H	Me
62	OH	F	H	Me
63	H	F	OMe	Me
64	H	OMe	OH	Ph
65	OH	OMe	H	Ph
66	H	OH	OMe	Ph
67	OH	H	OMe	Ph

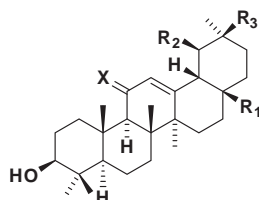
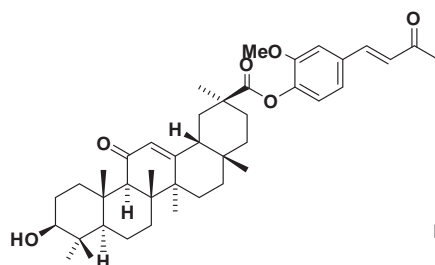
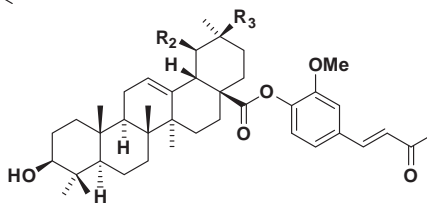
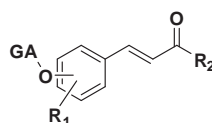
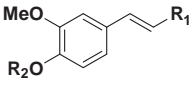
**86**: GA, X=O, R₁=Me, R₂=H, R₃=COOH**87**: OA, X=H, R₁=COOH, R₂=H, R₃=Me**88**: UA, X=H, R₁=COOH, R₂=Me, R₃=H**89**: GA-DZG**90**: OA-DZG, R₂=H, R₃=Me**91**: UA-DZG, R₂=Me, R₃=H**92**: 4-OGA, R₁=3-OMe, R₂=Me**93**: 2-OGA, R₁=3-OMe, R₂=Me**94**: 3-OGA, R₁=4-OMe, R₂=Me**95**: 2-OGA, R₁=4-OMe, R₂=Me**96**: 4-OGA, R₁=3-OEt, R₂=Me**97**: 2-OGA, R₁=3-OEt, R₂=Me**98**: 2-OGA, R₁=3-F, R₂=Me**99**: 4-OGA, R₁=3-OMe, R₂=Ph**100**: 2-OGA, R₁=3-OMe, R₂=Ph**101**: 3-OGA, R₁=4-OMe, R₂=Ph**102**: 2-OGA, R₁=4-OMe, R₂=Ph

Table 3
Structures of C-4¹-alkylated DZG (**26**, **68–75**) and Isoeugenol (**76–84**) analogs



DZG R ₁ = COMe	Isoeugenol R ₁ = Me	R ₂
68	76	
69	77	
70	78	
71	79	
72	80	
26	81	Me
73	82	
74	83	
75	84	

Nakagawa-Goto and co-others have reported newer conjugates of cytotoxic drug, paclitaxel (**103**) and various dietary antioxidants as new class of antitumor drugs. Dietary antioxidants namely retinol (**104**, Vitamin A), retinoic acid (**105**, Vitamin A acid), α -tocopherol (**106**, Vitamin E), 2,2,5,7,8-pentamethyl-6-chromanol (**107**, Vitamin E analog), curcumin (**57**), DZG and its analog (**8**). In addition, certain antioxidant flavonoids such as galangin (**108**) and coumarins, chrysin (**109**) and 4-methylumbelliferone (**110**) were also conjugated with paclitaxel through an ester linkage. All these novel conjugates were tested against various multi-drug resistant human cancer cell lines. These tested conjugates showed selective inhibition towards ovarian carcinoma (1A9) and nasopharynx carcinoma (KB) cells. However, little or no activity was observed against other tested cell lines. Paclitaxel conjugates with DZG (**111**) and 4-methylumbelliferone (**112**) were found to be highly active against 1A9 (ED_{50} = 0.005 μ g/mL) and KB (ED_{50} = 0.005 and 0.14 μ g/mL,) cells respectively. The glycinate ester salt of vitamin E **113**, conjugated with **103** showed strong inhibitory activity against human pancreatic cancer cell

(Panc-1) with less effect on the normal ovarian epithelial cell line (E6E7) and emerged as a promising lead candidate in anticancer drug discovery.⁶¹

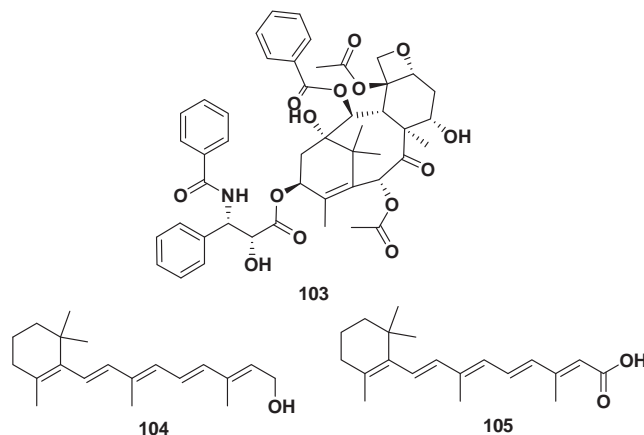
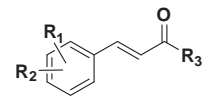


Table 5
Structures of DZG analogs (**8**, **9**, **46**, **59–67**)



	R ₁	R ₂	R ₃
DGZ	3-OMe	4-OH	Me
8	2-OH	3-OMe	Me
9	2-OH	3-OEt	Me
46	H	H	Me
59	3-OH	4-OMe	Me
60	2-OH	4-OMe	Me
61	3-OEt	4-OH	Me
62	2-OH	3-F	Me
63	3-F	4-OMe	Me
64	3-OMe	4-OH	Ph
65	2-OH	3-OMe	Ph
66	3-OH	4-OMe	Ph
67	2-OH	4-OMe	Ph

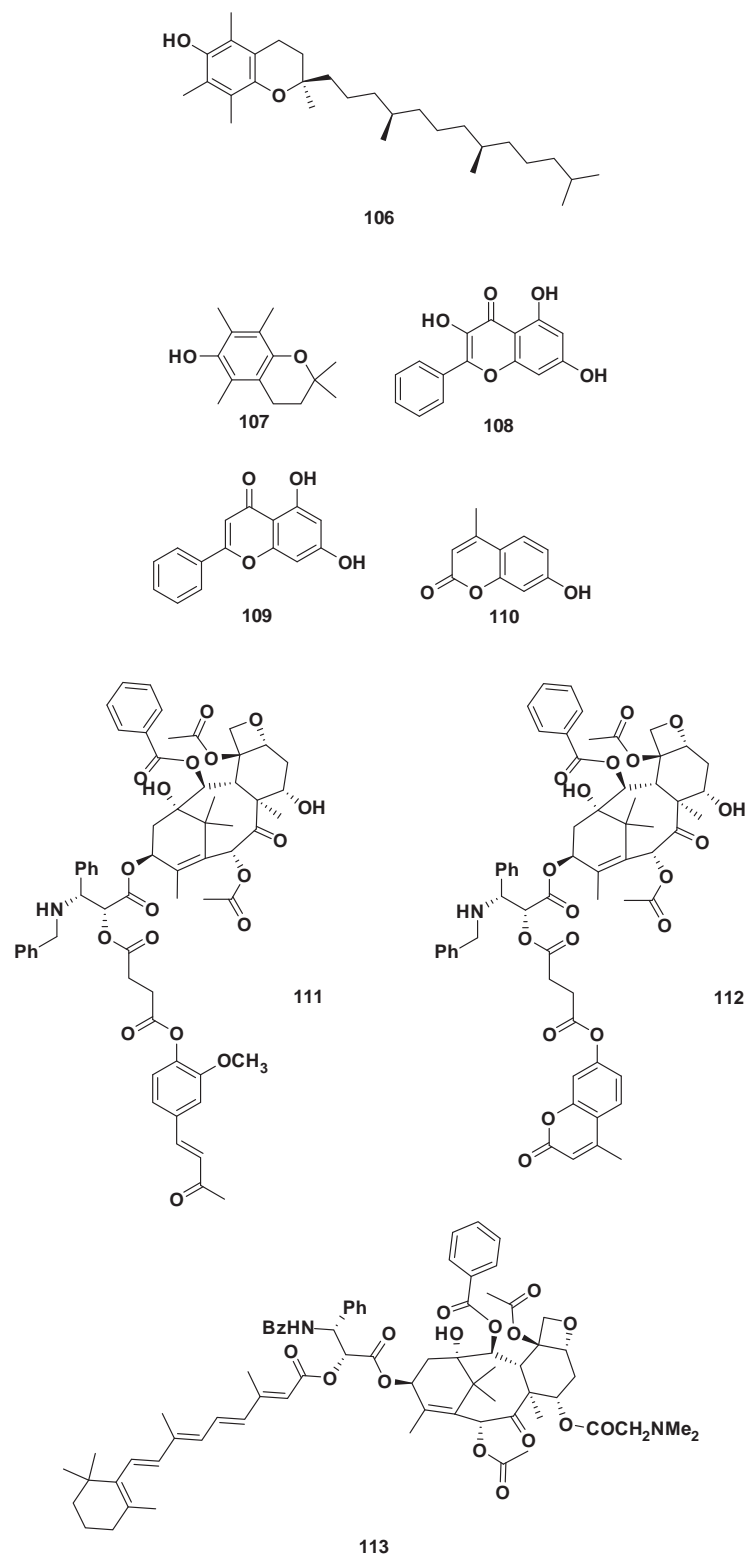
Table 4
Data for GA–DZG conjugates against human tumor cell replication

Compound	ED_{50} (μ M)/cell line ^a								
	KB	KB-VIN	A549	1A9	HCT-8	ZR-751	PC-3	DU-145	LN-Cap
92	1.6	2.5	2.0	0.9	1.7	2.8	1.4	3.1	0.6
93	0.8	2.8	2.2	0.8	1.9	3.0	1.1	3.6	2.8
94	0.9	1.9	2.8	1.6	2.0	1.9	2.8	9.9	6.5
95	6.2	>15	15.5	5.9	2.6	>15	7.4	>15	1.9
96	1.8	1.7	1.7	1.1	2.7	5.2	3.3	5.8	1.1
97	2.9	13.2	3.0	1.8	4.9	8.8	3.5	>15	6.8
98	3.0	8.7	3.2	1.3	2.2	2.7	1.6	2.7	4.4
99	NA ^b	NA	>14	>14	>14	NA	>14	>14	>14
100	9.9	NA	>14	13.3	>14	>14	14.1	>14	14.1
101	NA	NA	NA	>14	>14	NA	14.1	>14	14.1
102	>14	>14	NA	NA	>14	NA	>14	13.0	>14
GA, 86	>21	>21	NA	>21	19.5	NA	>21	>21	>21
DZG	NA	NA	>52	33.9	>52	>52	>52	>52	51.0
DOX ^c	0.1	4.97	0.18	0.02	1.20	0.04	0.26	0.15	0.04

^a Human epidermoid carcinoma of the lung (A549), ovarian (1A9), colon (HCT-8), breast (ZR-751), prostate (PC-3, DU-145, LN-Cap).

^b Not active.

^c Doxorubicin.



Tatsuzaki et al., have synthesized a series of forty new DZG analogs (Tables 5 and 6) and *in vitro* anticancer activity was evaluated against TPA-induced EBV-EA activation assay. Among the synthesized compounds, the prenylated analogs **114** and **123–125** exhibited the most significant and promising activity (100% inhibition of activation at 1×10^3 mol ratio/TPA and

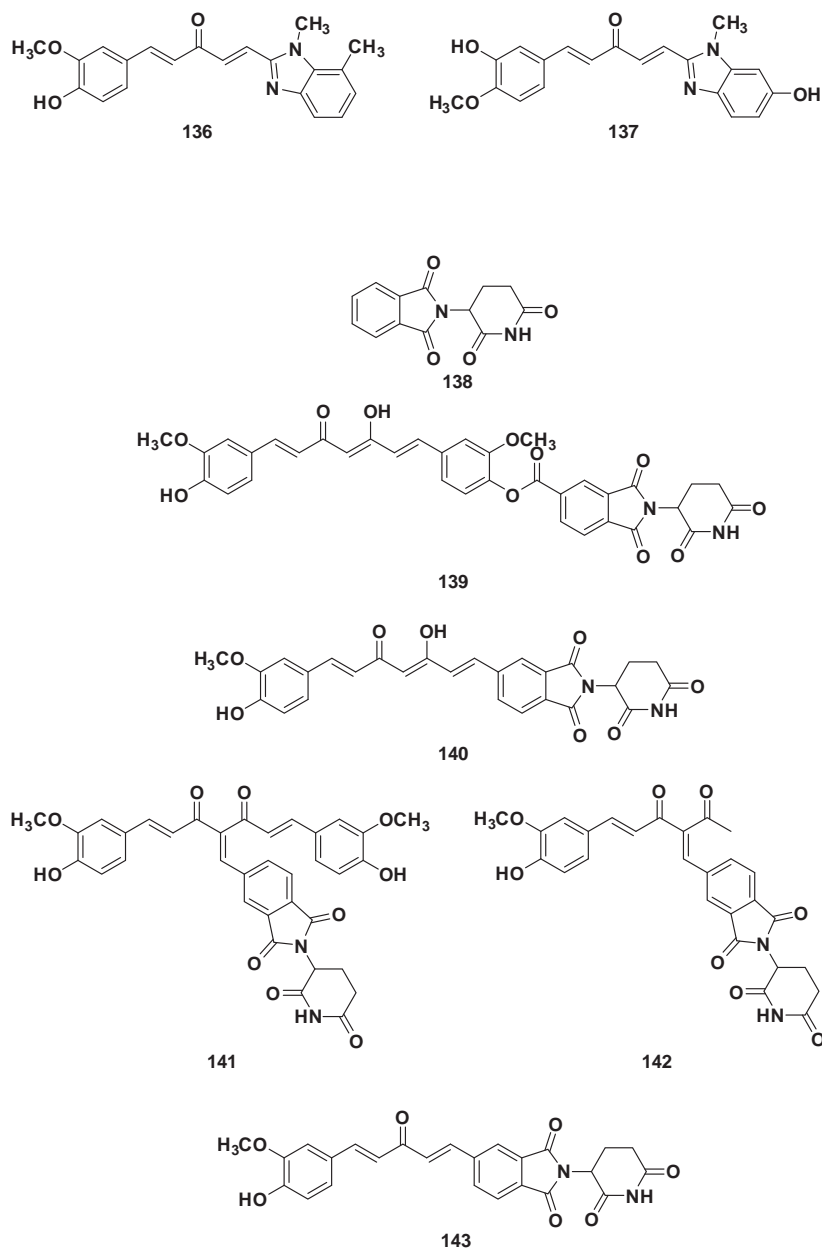
82–80%, 37–35% and 13–11% inhibition at 5×10^2 , 1×10^2 and 1×10 mol ratio/TPA, respectively).⁶²

Yogosawa et al., were the first to elucidate the growth-inhibitory mechanisms of DZG and its structural isomers (**8** and **59**) in human colon cancer cells (HT-29), thus providing some insights into the molecular mechanism of action of DZG. This study

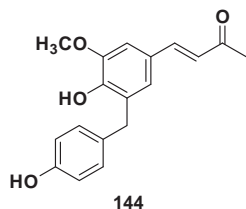
suggested that DZG inhibits the cell growth by inducing cell-cycle arrest at the G₂/M phase by up-regulation of p21 in a dose dependent manner. It is quite evident from this study that accumulation of ROS was interrelated with growth-inhibitory effects, thus suggesting DZG analogs as potential chemotherapeutic agents for colon cancer.⁶³

Woo et al., have reported the synthesis of a new library of some benzimidazolyl curcumin mimics by aldol condensation of DZG and DZG analogs with substituted benzimidazolyl-2-carbaldehyde. The *in vitro* anticancer activity was performed by colorimetrically using MTT (3-[4,5-dimethylthiazol-2-yl]-2,5-diphenyltetrazolium bromide) assay model against various human cancer cells viz. breast adenocarcinoma (MCF-7), neuroblastoma (SH-SY5Y), hepatocellular carcinoma (HEPG2) and Lung carcinoma (H460). Among the tested series, compound **136** (IC₅₀ = 1.0 and 1.9 μM) displayed most promising cytotoxicity against SH-SY5Y and Hep-G2 cells respectively, while compound **137** (IC₅₀ = 1.9 μM) presented significant activity against MCF-7 cancer cells.⁶⁴

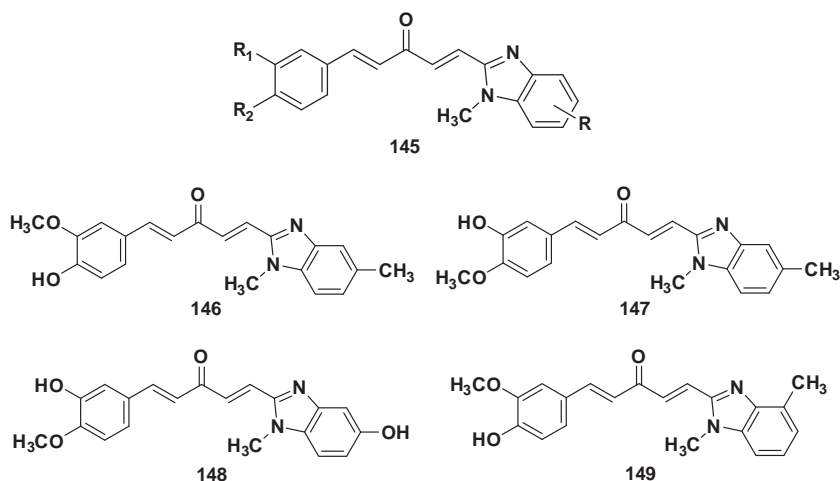
Liu et al., in an effort to develop agents for treating human multiple myeloma (MM), have reported the synthesis of a series of novel hybrid molecules of thalidomide (**138**) and curcumin (**139–142**) along with DZG (**143**). The anticancer activity of these synthesized hybrids was evaluated against various human multiple myeloma cells (MM1S, RPMI8226, U266) and human lung carcinoma cells (A549). Perusal of results, it was found that compound **141** (di-ketone) and **143** (mono-ketone) significantly inhibited the cell growth of all three cell lines by ≥90% at 10 μM, while compound **142** was inactive, thus suggesting that the 4-hydroxy-3-methoxy benzylidene moiety may be an essential scaffold for antiproliferative activity. Further, there was an attempt to study whether these active compounds produce cytotoxic effects through the modulation of ROS. Interestingly, compounds **141** and **143** increased the production of ROS in U266 cells at both 3 and 10 μM concentrations, leading to G1/S arrest, apoptosis and cell death. These findings suggest that the hybrid compounds could be a new leads against human multiple myeloma.⁶⁵



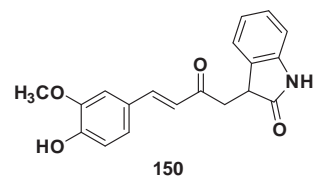
In 2013, Uha Mikakuto Co. Ltd., reported the synthesis of novel DZG derivative (**144**) having potent anticancer activity, particularly against oral cavity cancer than DZG.⁶⁶



Eom et al., have synthesized a library of curcumin derivatives mainly DZG mimics (**145**) having benzimidazole functionalities and evaluated them against multidrug resistant (MDR) ovarian cancer cell lines (NCI/ADR-RES). The cytotoxicity assay was carried out by MTT assay against both MDR strains with over-expressed P-glycoprotein (P-gp) and non-MDR strains (OVCAR-8) without P-gp. The cytotoxicity results against non-MDR cancer cells demonstrated reasonably strong to moderate potency suggesting comprehensive increase in activity after addition of the benzimidazole group to feruloyl structure. The inhibitory effect on MDR was found to be weaker in contrast to non-MDR cancer cells. However after taking into consideration the resistance factor (RF), that is, the ratio of the IC₅₀ values of MDR cells to that of non-MDR, the library illustrated a small RF values, which explains that the divergence of the inhibitory potency between MDR ovarian cancer cell (NCI/ADR-RES) and non-MDR ovarian cancer cell (OVCAR-8). Compounds **146**, **147** and **148** displayed strong cytotoxic effect on both type of cancer cells with the RF values 1.7, 1.7 and 1.4, respectively. Compound **149** showed inhibition with IC₅₀ value of 23.2 μM on MDR and 0.7 μM on non-MDR with high RF value of 33.1. This suggests the incapability of compound **149** to differentiate MDR cancer cells from non-MDR cells.⁶⁷



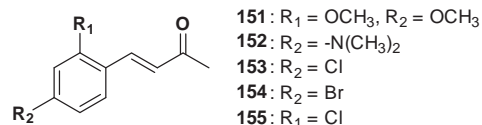
Bode et al., have disclosed the synthesis of novel DZG analog (**150**) and reported them for Aurora B kinase inhibition activity in cancer therapy.⁶⁸



2.3. Dehydrozingerone as anti-inflammatory

Curcuminoids have been reported as anti-inflammatory agents.⁶⁹ Many of the curcuminoids are synthetically tailored and studied for anti-inflammatory properties.^{70–72} Following discussion elaborates research employing DZG as anti-inflammatory agents.

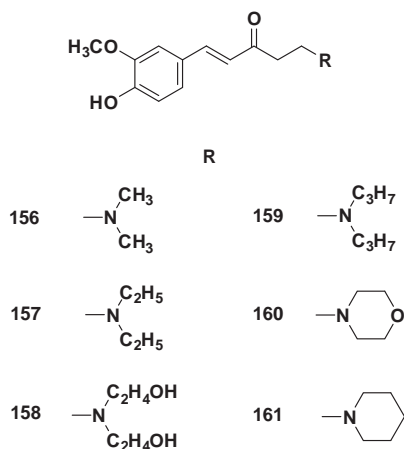
Elias et al., have reported the synthesis of a novel series of substituted 4-phenyl-3-buten-2-ones (**151–155**) and screened them for in vivo anti-inflammatory activity by carrageenan-induced paw edema in rats. Among the tested series, most of the compounds exhibited a comparable activity with DZG. In particular, compounds **25** and **152** displayed significant anti-inflammatory activity, while compounds **151** and **51** revealed little or no activity.⁹



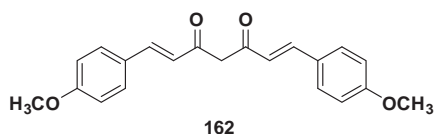
Jayasekhar et al., have reported the synthesis of DZG Mannich bases by two methods. The first method involved the treatment of DZG with secondary alkyl amine hydrochlorides and

paraformaldehydes, whereas the second method was direct aldol condensation of vanillin with 4-alkylaminobutan-2-one. All the synthesized compounds were evaluated for anti-inflammatory,

analgesic and antipyretic activities. Perusal of results it was found that most of the compounds showed superior anti-inflammatory activity compared to DZG. In particular, compounds **156**, **157** and **160** exhibited significant anti-inflammatory activity. Compounds **158** and **160** displayed the most promising analgesic activity whereas **156** and **158** presented excellent antipyretic activity.⁷³



Santhakumari et al., have reported novel method for synthesis of newer curcuminoids (**3**, **162** and **163**) by Claisen–Dieckmann condensation of α,β -unsaturated ketones (both DZG and 4-(4-methoxyphenyl)but-3-en-2-one) along with various esters in presence of sodium ethoxide and dimethyl sulphoxide. Further employing the same reaction procedure, authors have reported DGZ-Ibuprofen derivative (**163**) where the α,β -unsaturated moiety of DZG and the ester group of ibuprofen was condensed. The synthesized compound **163** was screened for analgesic activity by acetic acid-induced writhing in albino mice. Although compound **163** demonstrated analgesic activity (59% at 1.0 mmol/kg), it was less compared to Ibuprofen (69% at 1.0 mmol/kg). Compound **163** was also screened for anti-inflammatory activity for acute, sub acute and chronic models using reported methods. Results of this study suggested that **163** displayed significant activity (76%) compared to ibuprofen (73%) in equimole dose. Compound **163**, also showed predominant activity against formaldehyde induced arthritis at 0.5 mmol/kg dose level. However even the compound **163** did not induce gastrointestinal ulceration at dose level of 1 mmol/kg suggesting it to be a potent anti-inflammatory compound without any ulcerogenic side effects. These overall findings suggest that compound **163** emerged as the most promising anti-inflammatory agent with less gastrointestinal side effects.⁷⁴



2.4. Dehydrozingerone as anti-depressant

Various natural products have been explored as herbal medicines for treating depression.^{75–77} Numerous classes of phytoconstituents especially curcuminoids, flavonoids and poly

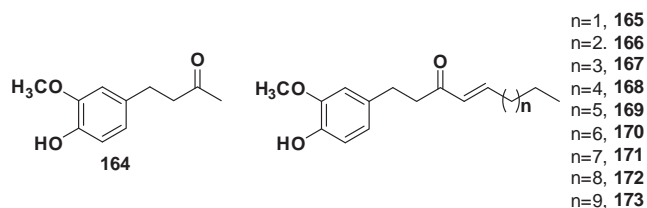
phenols have been reported to possess antidepressant properties.⁷⁸ A brief account from literature explains the use of DZG as antidepressant.

Martinez et al., have assessed the antidepressant property of DZG and the involvement of serotonergic and noradrenergic systems. Authors have also established the in vitro antioxidant activity of DZG by evaluating peroxidation in the hippocampus, cortex and cerebellum of mice. The participation of serotonergic and noradrenergic systems was verified by the tail suspension test (TST), forced swim test (FST) and yohimbine lethality test in mice models. DZG significantly reduced the period of immobility in the TST and FST, suggesting an antidepressant-like profile. Thus signifying that DZG could be a natural stand-in for development of antidepressants having little or no adverse effects.⁷⁹

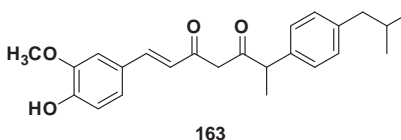
2.5. Dehydrozingerone against Alzheimer's disease

Alzheimer's disease (AD) is a neurodegenerative disorder and pathologically illustrated by gradual loss of memory, way of thinking and other cognitive functions along with dementia.

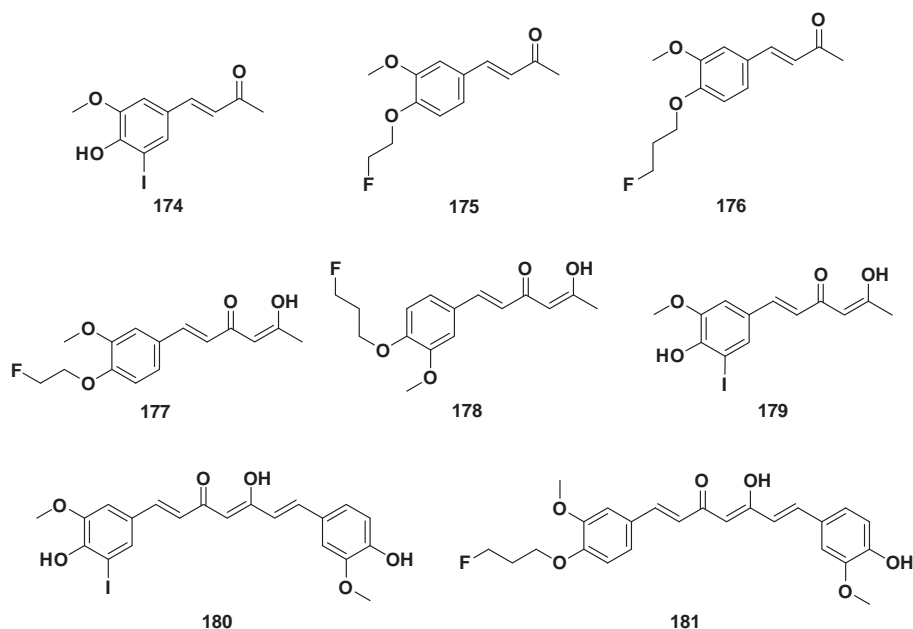
Kim et al., reported the synthesis of novel shogaols derivatives (**164–173**) prepared by the reduction of DZG. In this work authors evaluated the significance of the side-chain length connected to DZG in defending cells from β A insult using PC12 rat pheochromocytoma and IMR-32 human neuroblastoma cells. The cytoprotective property of synthesized compounds against β A insult was established using MTT assay. Results suggested that the efficacy of cell protection from β A insult increased with the increase in side chain. From this series compound (**173**) exhibited the best results.⁸⁰



AD is characterized by the buildup of amyloid plaques and neurofibrillary tangles in the brain and thus the in vivo imaging of plaques and tangles would be of great assistance for the early finding of AD. Ryu et al., reported the synthesis of a series of newer DZG (**174–179**) and curcumin (**180–181**) derivatives and evaluated them for in vitro and in vivo as β -amyloid (β A) plaque imaging probes by positron emission tomography (PET) or single photon emission computed tomography (SPECT). The curcumin analogs exhibited superior binding affinities for β A aggregates than DZG



derivatives. In particular, compound **181** was found to be most potent ligand having suitable lipophilicity, realistic initial brain uptake and metabolic firmness in the normal mouse brain. These outcome suggest that compound **181** was emerged as a potential candidate for β A plaque imaging.⁸¹

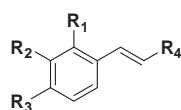


2.6. Dehydrozingerone as anti-malarial

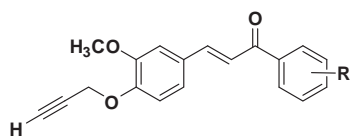
Molecular hybridization-based drug design approach⁸² has been exploited by many researchers in order to develop new hybrid chemical entities (NHCEs) as promising drug candidates. It is well known that more efficacious drug candidates with synergistic activity can be designed by joining two or more biologically

active pharmacophores or heterocyclic systems in a single molecular framework. Recently Guantai et al., have reported the synthesis of some series of novel DZG derived chalcones and dienone hybrid derivatives containing aminoquinoline and other nucleoside templates as potential antimalarial agents (**182–229**). Amongst all, compound **202** exhibited most promising antimalarial activity against three strains of *Plasmodium falciparum*.⁸³

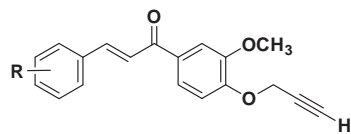
Table 6
Structures of DZG (**114–126**) and isoeugenol (**127–135**) analogs



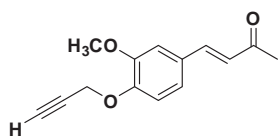
DZG R ₄ = COMe	R ₁	R ₂	R ₃	Isoeugenol R ₄ = Me
114	H	OMe		127
115	H	OMe		128
116	H	OMe		129
117	H	OMe		130
118	H	OMe		131
119	H	OMe		132
120	H	OMe		133
121	H	OMe		134
122	H	OMe		135
123		OMe	H	—
124	H			—
125		H		—
126		F	H	—



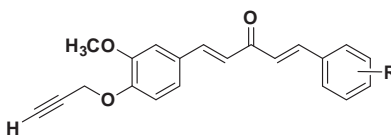
182: R= 4-OCH₃
 183: R= 2,4-OCH₃
 184: R=2,3,4-OCH₃



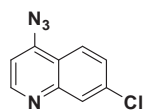
185: R=2,4-OCH₃
 186: R=2,3,4-OCH₃
 187: R=2,4-Cl
 188: R=4-F
 189: R=2,4-F



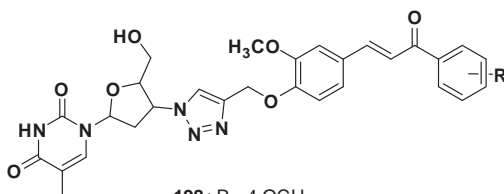
190



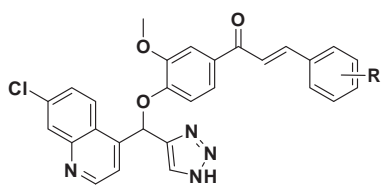
191: R= 4-OCH₃
 192: R= 2,4-OCH₃
 193: R=2,3,4-OCH₃
 194: R=2,4-Cl
 195: R=4-F
 196: R=2,4-F



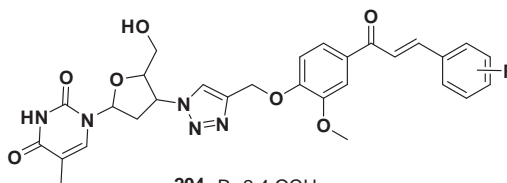
197



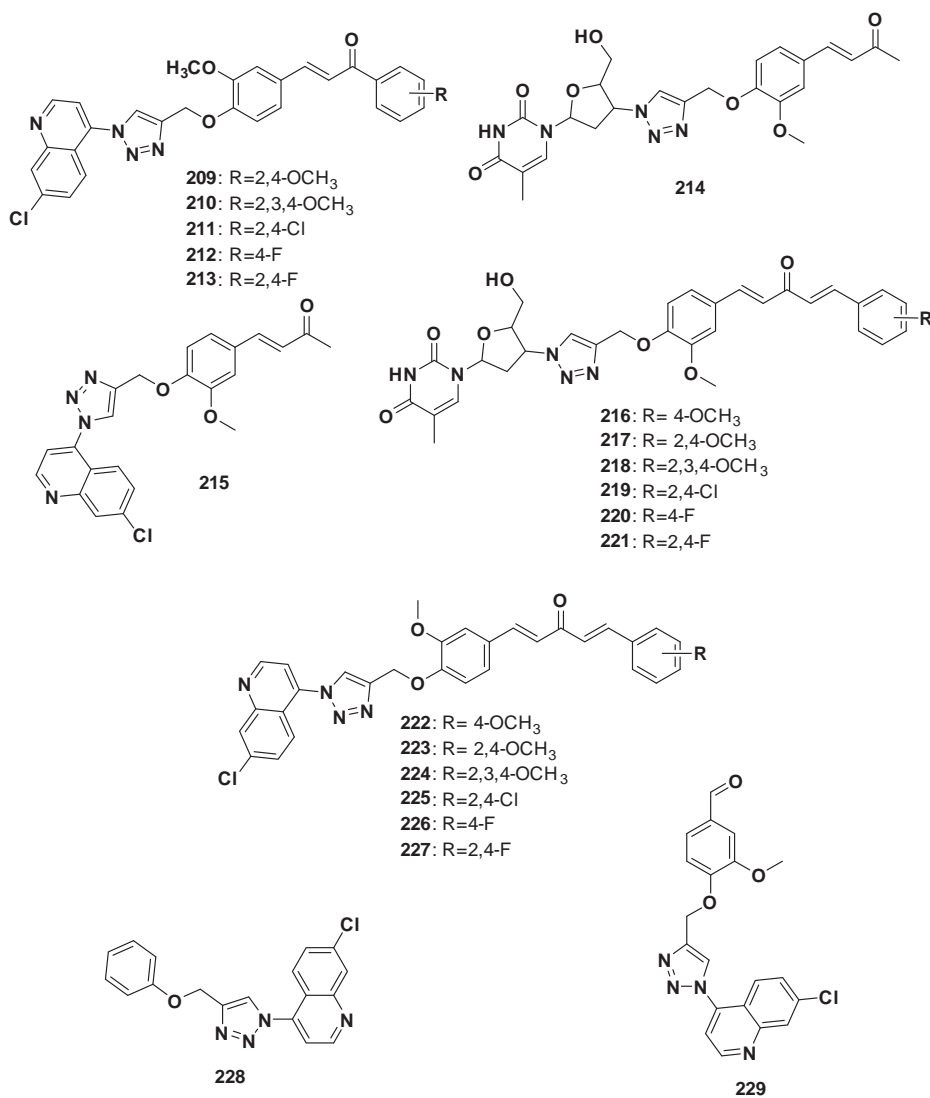
198: R= 4-OCH₃
 199: R= 2,4-OCH₃
 200: R=2,3,4-OCH₃



201: R= 4-OCH₃
 202: R= 2,4-OCH₃
 203: R=2,3,4-OCH₃



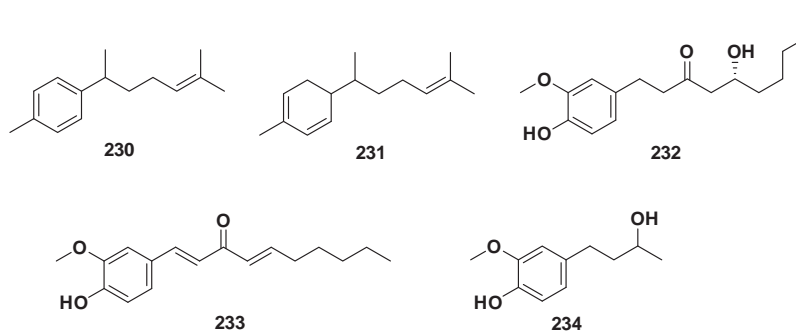
204: R=2,4-OCH₃
 205: R=2,3,4-OCH₃
 206: R=2,4-Cl
 207: R=4-F
 208: R=2,4-F



2.7. Dehydrozingerone as antifungal/antifeedant

Agarwal et al., have reported the isolation of various natural compounds like Curcumene (**230**), Zingerone (**231**) and 6-Gingerol (**232**, ginger oleoresin) from fresh rhizomes of *Zingiber*

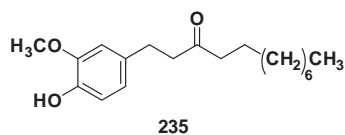
officinale. Authors have also reported the synthesis of DZG derivatives [6]-dehydroshogaol (**233**), Zingerone (**164**) and Dihydrozingerone (**234**). These tested compounds displayed modest insect growth regulatory (IGR) and antifeedant activity against *Spilosoma obliqua* and substantial antifungal activity against *Rhizoctonia solani*. Amongst the series tested, compound **233** exhibited maximum IGR activity ($EC_{50} = 3.55$ mg/ml) while its DZG portion has imparted maximum antifungal activity ($EC_{50} 86.49$ mg l⁻¹).⁸⁴



Kubra et al., have evaluated the antifungal effectiveness of DZG against *Aspergillus oryzae*, *Aspergillus flavus*, *Aspergillus niger*, *Aspergillus ochraceus*, *Fusarium oxysporum* and *Penicillium chrysogenum*. The MIC and fungicidal concentration was ranging from 755 to 911 μM and 880 to 1041 μM , respectively, which suggests that these fungal species were found vulnerable to DZG. Authors have also studied scanning electron microscopy to monitor morphological changes such as cell lysis, inhibition and morphological alterations in hyphae and sporulation in *A. ochraceus* on treatment with DZG. This study provides an insight for exploiting DZG as a potential antifungal scaffold with the presence of α,β -unsaturated carbonyl (C=O) group (conjugation system) on the aromatic ring with methoxyl and phenolic hydroxyl groups.⁸⁵

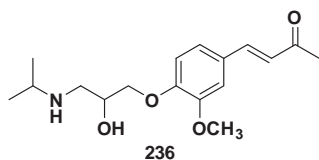
2.8. Dehydrozingerone as antiplatelet

Shih et al., have reported the synthesis of some novel DZG derivatives derived from shogaol and gingerol and evaluated them for anti-platelet aggregation activity. Amongst the synthesized compounds, [6]-paradol **235** displayed the most significant inhibition of platelet aggregation induced by arachidonic acid.⁸⁶



2.9. Dehydrozingerone as β -adrenoceptor antagonist

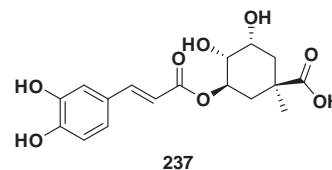
Wu et al., have reported the synthesis of a novel Dehydrozingeronolol (**236**) derived from DZG, and evaluated it for cardioselectivity, β -adrenoceptor antagonist and intrinsic sympathomimetic activity. Results suggested that compound **236** blocked (–) isoproterenol-induced tachycardia effects, thus signifying its bradycardia effect along with β -adrenoceptor blocking activities.⁸⁷



2.10. Dehydrozingerone: in silico studies

Singh et al., have reported in silico model to study the binding mode of curcumin and DZG with Human papilloma virus protein (HPV16 E6), a key protein dynamically participating in oral and cervical cancers and a model target for restoring the tumor suppressor role of p53. The binding interactions of the compounds have been studied by molecular docking using Autodock4. In this work, curcumin was found to have best binding interactions at the target site as compared to other curcuminoids, demethoxy and bis-demethoxy curcumin, which have lower but similar potential. Eighteen other naturally occurring congeners of curcumin were also docked in order to find the best candidate. However, only chlorogenic acid (**237**) was found to have considerable binding energy than curcumin itself (Table 7). This study has provided an

insight for the design and development of drugs against both oral and cervical cancers from natural origin.⁸⁸



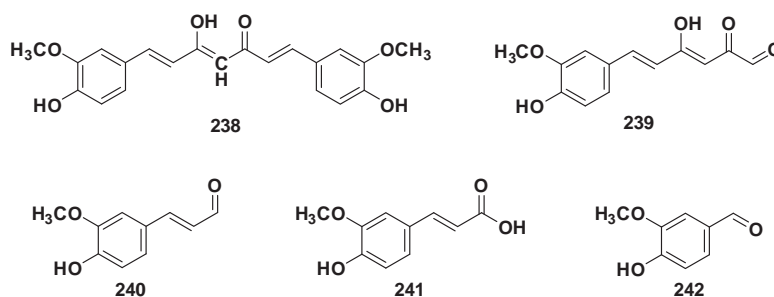
Shen et al., have reported the molecular docking simulation studies of curcumin (**57**) and tautomer of curcumin (**238**) and its degradation products (**239–242**) over Xanthine oxidase (XO), an enzyme capable of generating reactive oxygen species and having roles in pathogenesis of many diseases. As such curcumin did not display any inhibitory activity against XO because of its twisted steric bulkiness. However, degradation products of curcumin were found to fit efficiently into the binding pocket of XO, which was built by using salicylate as reference ligand. Two natural polyphenols, quercetin and luteolin known to possess high inhibitory activities against XO were chosen to validate the model. Quercetin displayed six binding interactions with amino acid residues namely Arg880, Arg912, Phe914, Phe1009, Thr1010 and Glu1261, while luteolin showed interactions with residues Asn768, Arg880, Phe914, Phe1009, Thr1010 and Ala1079 of XO. It was observed that both quercetin and luteolin have common binding region with four amino acid residues. Compound **239**, a major degradation product of curcumin, showed comparable binding affinity, that is, 4.57 μM with that of quercetin (1.12 μM) and luteolin (1.45 μM). DZG a minor degradation product was seen to bind with Phe914, Phe1009, Thr1010 and Ser876 residues of XO with a binding affinity of 91.2 μM . Thus this study highlighted the mechanisms underlying inhibition of XO.⁸⁹

Table 7
Automated docking analysis through Scigress Explorer 7.7.0.47

Ligands	PMF score dock flexible ligand in rigid active site (kcal/mol) through Scigress 7.7.0.47
Bis demethoxy curcumin	–51.503
Caffeic acid	–62.267
Capsaicin	–50.654
Chlorogenic acid	–99.782*
Cassumunin A	–44.556
Cassumunin B	–55.462
Curcumin	–85.699*
Curcumin dipiperoyl ester	–74.859
Cyclocurcumin	–54.515
Demethoxy curcumin	–78.974*
Dehydrozingerone	–41.759#
Diaryl pentanoids	–61.251
Diaryl pentanoids II	–54.224
Dihydro guarietic acid	–65.578
Eugenol	–37.275
Ferulic acid	–46.627
Piperic acid	–60.454
Quercetin	–67.679
Yakuchinone A	–45.20
Yakuchinone B	–53.811
Zingerone	–40.826

* Inhibitors showing significant binding affinities.

DZG.



2.11. Dehydrozingerone reported for miscellaneous activities

Transfer of vascular smooth muscle cells (VSMC) is known to be linked with development of atherosclerosis. Growth factors and ROS produced during vascular injury are considered to play a major role in pathogenesis of atherosclerosis. Therefore inhibition of growth factor or ROS-mediated signaling may signify a potential therapeutic approach for interference with the progression of atherosclerosis. Liu et al., have explored the effect of DZG on platelet-derived growth factor (PDGF) stimulated VSMC movement, proliferation, and collagen synthesis. In an effort to understand the mechanism, authors have studied the effect of DZG on hydrogen peroxide (H_2O_2)-stimulated PDGF receptor signaling. Further, growth factor-mediated cell proliferation is negatively regulated by protein tyrosine phosphatases (PTPs); therefore, authors have also assessed the effect of DZG on PTP activity in cells treated with H_2O_2 . In this study the efficacy of DZG with curcumin and isoeugenol (structural analogs of DZG) was compared in order to understand the structural necessities for activity and DZG emerged as an effective inhibitor of growth factor/ H_2O_2 -stimulated VSMC functions by inhibiting the oxidation of cellular phosphatases.⁹⁰

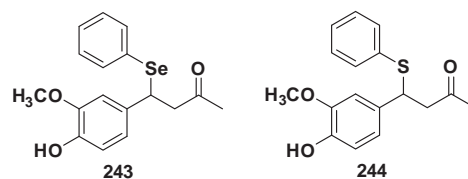
Oxidative stress is one of the interfering factors in wound healing course. This stress once triggered by the wound results in the production of ROS, thereby delaying usual wound repair. So reducing the level of ROS would be an important approach to improve healing process. Rao et al., have demonstrated the influence of DZG as a ROS scavenger on both normal and dexamethasone delayed wound healing in albino rats. It was found that DZG privileged the healing of re-sutured incision wounds as compared to control. Further, there was significant improvement in granulation breaking strength and the rise in the hydroxyproline (OHP) and lysyl oxidase (LO) levels in the granulation tissue was also observed clearly suggesting that the DZG was influential and supportive in hastening the healing process in both normal and dexamethasone-suppressed wounds in rat models.⁹¹

Soo et al., have reported the blood sugar lowering property of DZG. In this study authors have revealed that DZG increases phosphorylation or activation of AMP kinase to bring about a drop in blood sugar levels and boost insulin sensitivity as well as reduce body fat. Thus DZG could be an ideal molecule for drug discovery in the treatment of Type II diabetes mellitus and obesity.⁹²

Kim et al., have investigated the effects of DZG on metabolic profiles in mice. It was evidently found that DZG suppressed high-fat diet (HFD)-induced increase in glucose and cholesterol through a mechanism involving AMP-activated protein kinase (AMPK). This was due to increased phosphorylation of AMPK in skeletal muscles. Maximum AMPK activation by DZG was found at the concentration of 30 μM for 10 min. In addition, DZG was also found to activate p38 mitogen-activated protein kinase (MAPK) signaling in an AMPK-dependent manner and also increase in GLUT4 (major transporter for glucose uptake) expression in skeletal muscles. These all findings thus explain the possible molecular

mechanism of AMPK pathway activation in skeletal muscle by DZG.⁹³

Martinez et al., have synthesized two new organochalcogen-containing zingerone derivatives and evaluated for their antioxidant properties by ABTS⁺ assay. Novel compounds, **243** and **244** exhibited improved activity over DZG (IC_{50} 8.0 \pm 1.0 μM) with IC_{50} values of 8.0 \pm 1.0 μM and 6.5 \pm 0.5 μM , respectively, with two fold increase in activity as compared to phenolic antioxidants. The enhancement in activity was mainly attributed to a mechanism that eliminates phenylselenenyl or phenylthiyl radicals.⁹⁴



3. Conclusion and future perspective

A great deal of time has been taken to prove that the time-honored medicinal plants have the power to cure. Drugs derived from natural sources have always been precious precursors for modern medicines. Taking a step one day at a time, in the near future, the nature's enormity and diversity would provide us the solutions to fight even the most fearsome diseases. To overcome the problems associated with curcumin, curcuminoids and the degradants of curcumin have been looked upon for molecular variations in developing diverse scaffolds with least side effects and improved bioavailability. These curcuminoids and degradation products of curcumin have also helped towards improving its metabolic profile in humans as well as mechanism leading to pharmacological responses.^{15,95} Therefore, over the course of years several studies have come up with compounds or structural analogs of curcumin (mono-carbonyl analogs or mono-carbonyl enones) that have excluded β -diketone moiety to restrain stability and improve metabolic profiles. One such distinguished degradant of curcumin is DZG, which is endowed with a broad range of biological activities like antioxidant, anticancer, anti-inflammatory, anti-depressant, anti-malarial, antifungal, anti-platelet and many others. Therefore, in this review we have put forward an extensive effort to revise and systematically discuss the research involving DZG with its biological diversity. In conclusion, it is quite evident that DZG is an imperative scaffold and its numerous analogs have emerged as a promising leads in the design and development of some novel medicinally active compounds with improved metabolic, pharmacokinetic and pharmacological profiles, indicating that there is much scope for further investigation.

Acknowledgments

The authors are thankful to the College of Health Sciences, University of KwaZulu-Natal, Durban, South Africa for the facilities and financial support.

References and notes

- Samuelsson, G. *Drugs of Natural Origin: A Textbook of Pharmacognosy*, 5th Swedish Pharma Press, 5th ed.; Swedish Pharmaceutical Press, 2004.
- Newman, D. J.; Cragg, G. M.; Snader, K. M. *Nat. Prod. Rep.* **2000**, *17*, 215.
- Newman, D. J.; Cragg, G. M.; Snader, K. M. *J. Nat. Prod.* **2003**, *66*, 1022.
- Cragg, G. M.; Newman, D. J.; Snader, K. M. *J. Nat. Prod.* **1997**, *60*, 52.
- Subramanian, M.; Sreejayan, Rao, M. N. a.; Devasagayam, T. P. a.; Singh, B. B. *Fundam. Mol. Mech. Mutagen.* **1994**, *311*, 249.
- de Bernardi, M.; Vidari, G.; Vita-Finzi, P. *Phytochemistry* **1976**, *15*, 1785.
- Motohashi, N.; Ashihara, Y.; Yamagami, C.; Saito, Y. *Mutat. Res.—Fundam. Mol. Mech. Mutagen.* **1997**, *377*, 17.
- Kuo, P.-C.; Damu, A. G.; Cherng, C.-Y.; Jeng, J.-F.; Teng, C.-M.; Lee, E.-J.; Wu, T.-S. *Arch. Pharm. Res.* **2005**, *28*, 518.
- Elias, G.; Rao, M. N. a. *Eur. J. Med. Chem.* **1988**, *23*, 379.
- Rajakumar, D. V.; Rao, M. N. *Biochem. Pharmacol.* **1993**, *46*, 2067.
- Rajakumar, D. V.; Rao, M. N. a. *Mol. Cell. Biochem.* **1994**, *140*, 73.
- Roughley, P.; Whiting, D. J. *Chem. Soc.* **1973**, *20*, 2379.
- Wang, Y. J.; Pan, M. H.; Cheng, A. L.; Lin, L. I.; Ho, Y. S.; Hsieh, C. Y.; Lin, J. K. *J. Pharm. Biomed. Anal.* **1997**, *15*, 1867.
- Suresh, D.; Gurudutt, K. N.; Srinivasan, K. *Eur. Food Res. Technol.* **2009**, *228*, 807.
- Shen, L.; Ji, H.-F. *Trends Mol. Med.* **2012**, *18*, 138.
- Esatbeyoglu, T.; Ulbrich, K.; Rehberg, C.; Rohn, S.; Rimbach, G. *Food Funct.* **2015**, *6*, 887.
- Priyadarsini, K. I.; Devasagayam, T. P. a.; Rao, M. N. a.; Guha, S. N. *Radiat. Phys. Chem.* **1999**, *54*, 551.
- Anderson, A. M.; Mitchell, M. S.; Mohan, R. S. *J. Chem. Educ.* **2000**, *77*, 359.
- Anand, P.; Kunnumakkara, A. B.; Newman, R. a.; Aggarwal, B. B. *Mol. Pharm.* **2007**, *4*, 807.
- Rosemond, M. J. C.; St. John-Williams, L.; Yamaguchi, T.; Fujishita, T.; Walsh, J. S. *Chem. Biol. Interact.* **2004**, *147*, 129.
- Straganz, G. D.; Glieder, A.; Brecker, L.; Ribbons, D. W.; Steiner, W. *Biochem. J.* **2003**, *369*, 573.
- Grogan, G. *Biochem. J.* **2005**, *388*, 721.
- Nagpure, B. A. a. L.; Gupta, R. K. *Indian J. Chem., Sect. B Org. Med. Chem.* **2011**, *50*, 1119.
- Tomren, M. A.; Måsson, M.; Loftsson, T.; Tonnesen, H. H. *Int. J. Pharm.* **2007**, *338*, 27.
- Sardjiman, S.; Reksahadioprodo, M. *Eur. J. Med. Chem.* **1997**, *32*, 625.
- Mosley, C. A.; Liotta, D. C.; Snyder, J. P. In *The Molecular Targets and Therapeutic Uses of Curcumin in Health and Disease*, Springer Science+Business Media: New York, USA, 2007; Vol. 595, pp 77–103.
- Weber, W. M.; Hunsaker, L. a.; Roybal, C. N.; Bobrovnikova-Marjon, E. V.; Abcouwer, S. F.; Royer, R. E.; Deck, L. M.; Vander Jagt, D. L. *Bioorg. Med. Chem.* **2006**, *14*, 2450.
- Liang, G.; Shao, L.; Wang, Y.; Zhao, C.; Chu, Y.; Xiao, J.; Zhao, Y.; Li, X.; Yang, S. *Bioorg. Med. Chem.* **2009**, *17*, 2623.
- Zhao, C.; Liu, Z.; Liang, G. *Curr. Pharm. Des.* **2013**, *19*, 2114.
- Shetty, D.; Kim, Y.; Shim, H.; Snyder, J. *Molecules* **2014**, *20*, 249.
- Shen, L.; Ji, H.-F. *Trends Mol. Med.* **2012**, *18*, 363.
- Fuchs-Tarlovsky, V.; Calderon-Cuevas, J. *Nova Science; Publishers.*, 2014; pp 273–285.
- El-Beltagi, H. S.; Mohamed, H. I. *Not. Bot. Horti Agrobot. Cluj-Napoca* **2013**, *41*, 44.
- Jeong, J. I.; Lee, Y. W.; Kim, Y. K. *Neurochem. Res.* **2003**, *28*, 1201.
- Wang, X.; Zhang, P.; Zhao, L.; Tu, Y.; Dai, K. *Zhonghua Xueyexue Zazhi* **2014**, *35*, 511.
- Kelsey, N. a.; Wilkins, H. M.; Linseman, D. a. *Molecules* **2010**, *15*, 7792.
- Brewer, M. S. *Compr. Rev. Food Sci. Food Saf.* **2011**, *10*, 221.
- Priyadarsini, K. I.; Guha, S. N.; Rao, M. N. A. *Free Radical Biol. Med.* **1998**, *24*, 933.
- Jovanovic, S. V.; Steenken, S.; Boone, C. W.; Simic, M. G. *J. Am. Chem. Soc.* **1999**, *121*, 9677.
- Yamagami, C.; Motohashi, N.; Emoto, T.; Hamasaki, a.; Tanahashi, T.; Nagakura, N.; Takeuchi, Y. *Bioorg. Med. Chem. Lett.* **2004**, *14*, 5629.
- Parihar, V. K.; Dhawan, J.; Kumar, S.; Manjula, S. N.; Subramanian, G.; Unnikrishnan, M. K.; Rao, C. M. *Chem. Biol. Interact.* **2007**, *170*, 49.
- Musialik, M.; Litwinienko, G. *J. Therm. Anal. Calorim.* **2007**, *88*, 781.
- Li, P.-Z.; Liu, Z.-Q. *Eur. J. Med. Chem.* **2011**, *46*, 1821.
- Feng, J.-Y.; Liu, Z.-Q. *Eur. J. Med. Chem.* **2011**, *46*, 1198.
- Kubra, I. R.; Bettadaiah, B. K.; Murthy, P. S.; Rao, L. J. M. *J. Food Sci. Technol.* **2014**, *51*, 245.
- Kancheva, V.; Slavova-Kazakova, A.; Fabbri, D.; Dettori, M. A.; Delogu, G.; Janiak, M.; Amarowicz, R. *Food Chem.* **2014**, *157*, 263.
- Li, P.-Z.; Liu, Z.-Q. *Med. Chem. Res.* **2014**, *23*, 3478.
- Sangwan, N. S.; Shanker, S.; Sangwan, R. S.; Kumar, S. *Phyther. Res.* **1998**, *12*, 389.
- Anto, R. J.; George, J.; Dinesh Babu, K. V.; Rajasekharan, K. N.; Kuttan, R. *Mutat. Res.—Genet. Toxicol.* **1996**, *370*, 127.
- Anto, R. J.; Kuttan, G.; Babu, K. V. D.; Rajasekharan, K. N.; Kuttan, R. *Int. J. Pharm.* **1996**, *131*, 1.
- Ramsewak, R. S.; DeWitt, D. L.; Nair, M. G. *Phytomedicine* **2000**, *7*, 303.
- Ruby, a. J.; Kuttan, G.; Babu, K. D.; Rajasekharan, K. N.; Kuttan, R. *Cancer Lett.* **1995**, *94*, 79.
- Yin, S.; Zheng, X.; Yao, X.; Wang, Y.; Liao, D. *J. Cancer Ther.* **2013**, *04*, 113.
- Liu, Z.; Sun, Y.; Ren, L.; Huang, Y.; Cai, Y.; Weng, Q.; Shen, X.; Li, X.; Liang, G.; Wang, Y. *BMC Cancer* **2013**, *13*, 494.
- Motohashi, N.; Yamagami, C.; Tokuda, H.; Konoshima, T.; Okuda, Y.; Okuda, M.; Mukainaka, T.; Nishino, H.; Saito, Y. *Cancer Lett.* **1998**, *134*, 37.
- Rao, M. A. M.; Kumar, M. M.; Rao, M. A. M. *J. Biochem.* **1999**, *125*, 383.
- Motohashi, N.; Yamagami, C.; Tokuda, H.; Okuda, Y.; Ichiishi, E.; Mukainaka, T.; Nishino, H.; Saito, Y. *Mutat. Res.* **2000**, *464*, 247.
- Tatsuzaki, J.; Bastow, K. F.; Nakagawa-Goto, K.; Nakamura, S.; Itokawa, H.; Lee, K. H. *J. Nat. Prod.* **2006**, *69*, 1445.
- Exelixis, Inc., Patent WO2006033943(A2), 2006.
- Tatsuzaki, J.; Taniguchi, M.; Bastow, K. F.; Nakagawa-Goto, K.; Morris-Natschke, S. L.; Itokawa, H.; Baba, K.; Lee, K.-H. *Bioorg. Med. Chem.* **2007**, *15*, 6193.
- Nakagawa-Goto, K.; Yamada, K.; Nakamura, S.; Chen, T.-H.; Chiang, P.-C.; Bastow, K. F.; Wang, S.-C.; Spohn, B.; Hung, M.-C.; Lee, F.-Y.; Lee, F.-C.; Lee, K.-H. *Bioorg. Med. Chem. Lett.* **2007**, *17*, 5204.
- Tatsuzaki, J.; Nakagawa-Goto, K.; Tokuda, H.; Lee, K.-H. *J. Asian Nat. Prod. Res.* **2010**, *12*, 227.
- Yogosawa, S.; Yamada, Y.; Yasuda, S.; Sun, Q.; Takizawa, K.; Sakai, T. *J. Nat. Prod.* **2012**, *75*, 2088.
- Woo, H. B.; Eom, Y. W.; Park, K.-S.; Ham, J.; Ahn, C. M.; Lee, S. *Bioorg. Med. Chem. Lett.* **2012**, *22*, 933.
- Liu, K.; Zhang, D.; Chojnacki, J.; Du, Y.; Fu, H.; Grant, S.; Zhang, S. *Org. Biomol. Chem.* **2013**, *11*, 4757.
- Uha Mikakuto Company Limited. Patent JP2013010720A, 2013.
- Eom, Y. W.; Oh, S.; Woo, B.; Ham, J.; Ahn, C. M.; Lee, S. *Bull. Korean Chem. Soc.* **2013**, *34*, 1272.
- University of Minnesota. Patent WO2014066840A1, 2014.
- Bagad, A. S.; Joseph, J. A.; Bhaskaran, N.; Agarwal, A. *Adv. Pharmacol. Sci.* **2013**, *2013*, 538.
- Liu, Z.; Tang, L.; Zou, P.; Zhang, Y.; Wang, Z.; Fang, Q.; Jiang, L.; Chen, G.; Xu, Z.; Zhang, H.; Liang, G. *Eur. J. Med. Chem.* **2014**, *74*, 671.
- Claramunt, R. M.; Bouissane, L.; Cabildo, M. P.; Cornago, M. P.; Elguero, J.; Radziwon, a.; Medina, C. *Bioorg. Med. Chem.* **2009**, *17*, 1290.
- Wu, J.; Zhang, Y.; Cai, Y.; Wang, J.; Weng, B.; Tang, Q.; Chen, X.; Pan, Z.; Liang, G.; Yang, S. *Bioorg. Med. Chem.* **2013**, *21*, 3058.
- Jayasekhar, P.; Rao, S. B.; Santhakumari, G. *Indian J. Pharm. Sci.* **1998**, *60*, 191.
- Santhakumari, G.; Jayasekhar, P.; Rao, S. B. *Indian J. Pharm. Sci.* **2002**, *64*, 82.
- Abbas, G.; Rauf, K.; Mahmood, W. *Nat. Prod. Res.* **2014**, *29*, 302.
- Fajemiroye, J. O.; Galdino, P. M.; Marciano De Paula, J. A.; Rocha, F. F.; Akanmu, M. a.; Vanderlinde, F. A.; Zjawiony, J. K.; Costa, E. A. *Food Funct.* **2014**, *5*, 1819.
- Liao, J.-C.; Tsai, J.-C.; Liu, C.-Y.; Huang, H.-C.; Wu, L.-Y.; Peng, W.-H. *BMC Complement. Altern. Med.* **2013**, *13*, 299.
- Bhutani, M. K.; Bishnoi, M.; Kulkarni, S. K. *Pharmacol. Biochem. Behav.* **2009**, *92*, 39.
- Martinez, D. M.; Barcellos, A.; Casaril, A. M.; Savegnago, L.; Lernardão, E. J. *Pharmacol. Biochem. Behav.* **2014**, *127*, 111.
- Kim, D. S. H.; Kim, J. Y. *Bioorg. Med. Chem. Lett.* **2004**, *14*, 1287.
- Ryu, E. K.; Choe, Y. S.; Lee, K.-H.; Choi, Y.; Kim, B.-T. *J. Med. Chem.* **2006**, *49*, 6111.
- Claudio Viegas-Junior, B. S. P.; Amanda Danuello, B. S. P.; Vanderlan da Silva Bolzani, B. S. P.; Eliezer, J.; Barreiro, B. S. P.; Carlos Alberto Manssour Fraga, B. S. P. *Curr. Med. Chem.* **2007**, *14*, 1829.
- Guantai, E. M.; Ncozazi, K.; Egan, T. J.; Gut, J.; Rosenthal, P. J.; Smith, P. J.; Chibale, K. *Bioorg. Med. Chem.* **2010**, *18*, 8243.
- Agarwal, M.; Walia, S.; Dhingra, S.; Khambay, B. P. *Pest Manag. Sci.* **2001**, *57*, 289.
- Kubra, I. R.; Murthy, P. S.; Rao, L. J. M. *J. Food Sci.* **2013**, *78*, M64.
- Shih, H.-C.; Chern, C.-Y.; Kuo, P.-C.; Wu, Y.-C.; Chan, Y.-Y.; Liao, Y.-R.; Teng, C.-M.; Wu, T.-S. *Int. J. Mol. Sci.* **2014**, *15*, 3926.
- Wu, B.-N.; Yang, C.-R.; Yang, J.-M.; Chen, I.-J. *Gen. Pharmacol. Vasc. Syst.* **1994**, *25*, 651.
- Singh, A. K.; Misra, K. *Interdiscip. Sci. Comput. Life Sci.* **2013**, *5*, 112.
- Shen, L.; Ji, H.-F. *Bioorg. Med. Chem. Lett.* **2009**, *19*, 5990.
- Liu, Y.; Dolence, J.; Ren, J.; Rao, M.; Sreejayan, N. *J. Cardiovasc. Pharmacol.* **2008**, *52*, 422.
- Rao, M. C.; Sudheendra, A. T.; Nayak, P. G.; Paul, P.; Kutty, G. N.; Shenoy, R. R. *Mol. Cell. Biochem.* **2011**, *355*, 249.
- Korea University Research and Business Foundation. Patent WO2014112763A1, 2014.
- Kim, S. J.; Kim, H. M.; Lee, E. S.; Kim, N.; Lee, J. O.; Lee, H. J.; Park, N. Y.; Jo, J. Y.; Ham, B. Y.; Han, S. H.; Park, S. H.; Chung, C. H.; Kim, H. S. *J. Cell. Mol. Med.* **2015**, *19*, 620.
- Martinez, D. M.; Barcellos, A. M.; Casaril, A. M.; Savegnago, L.; Perin, G.; Schiesser, C. H.; Callaghan, K. L.; Lenardão, E. J. *Tetrahedron Lett.* **2015**, *56*, 2243.
- Agarwal, B. B.; Sung, B. *Trends Pharmacol. Sci.* **2009**, *30*, 85.

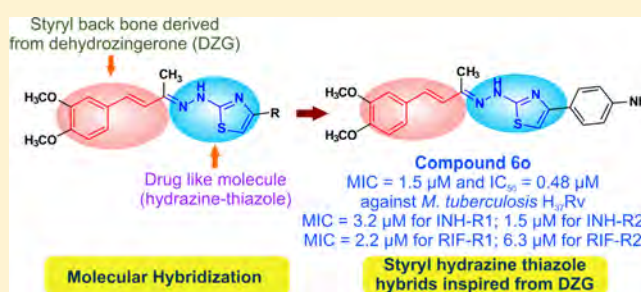
Dehydrozingerone Inspired Styryl Hydrazine Thiazole Hybrids as Promising Class of Antimycobacterial Agents

Girish A. Hampannavar,[†] Rajshekhar Karpoormath,^{*,†} Mahesh B. Palkar,^{§,†} Mahamadhanif S. Shaikh,[†] and Balakumar Chandrasekaran[†][†]Department of Pharmaceutical Chemistry, Discipline of Pharmaceutical Sciences, College of Health Sciences, University of KwaZulu-Natal, Westville Campus, Durban 4000, South Africa[§]Department of Pharmaceutical Chemistry, K.L.E. University College of Pharmacy, Vidyanagar, Hubballi 580031, Karnataka, India

S Supporting Information

ABSTRACT: Series of styryl hydrazine thiazole hybrids inspired from dehydrozingerone (DZG) scaffold were designed and synthesized by molecular hybridization approach. *In vitro* antimycobacterial activity of synthesized compounds was evaluated against *Mycobacterium tuberculosis* H₃₇Rv strain. Among the series, compound **60** exhibited significant activity (MIC = 1.5 μM; IC₅₀ = 0.48 μM) along with bactericidal (MBC = 12 μM) and intracellular antimycobacterial activities (IC₅₀ = <0.098 μM). Furthermore, **60** displayed prominent antimycobacterial activity under hypoxic (MIC = 46 μM) and normal oxygen (MIC = 0.28 μM) conditions along with antimycobacterial efficiency against isoniazid (MIC = 3.2 μM for INH-R1; 1.5 μM for INH-R2) and rifampicin (MIC = 2.2 μM for RIF-R1; 6.3 μM for RIF-R2) resistant strains of Mtb. Presence of electron donating groups on the phenyl ring of thiazole moiety had positive correlation for biological activity, suggesting the importance of molecular hybridization approach for the development of newer DZG clubbed hydrazine thiazole hybrids as potential antimycobacterial agents.

KEYWORDS: Antimycobacterial activity, bactericidal, dehydrozingerone, NIAID, thiazole



Tuberculosis (TB) is a chronic necrotizing bacterial infection caused by *Mycobacterium tuberculosis* (Mtb), which has been a bane of humanity for thousands of years and remains as one of the rampant health problems in the world. TB is an ancient enemy, and current threat that has been ranked among the foremost killers of the 21st century.¹ According to a World Health Organization (WHO) report, around 9 million people were found infected and around 1.5 million casualties occurred because of TB. Besides, the life threatening strains of MDR-TB (Multi Drug Resistance Tuberculosis) are appearing, some of which can lead to high mortality rate (e.g., 72–89%) with death occurring in short period (4–16 weeks).² In 2013 around 480,000 affirmative cases of MDR-TB were witnessed.³ India, China, the Russian Federation, and South Africa have almost 60% of the world's cases of MDR-TB. In addition, the risk becomes even greater if the person is coinfecting with the HIV (human immunodeficiency virus).⁴ The global resurgence of TB and development of drug resistance necessitates for an imperative attention of medicinal chemists to develop innovative antimycobacterial agents as no new classes of anti-TB agents have been developed since the introduction of rifampin in to clinical practice in 1960s.

It is well-known fact that *trans*-cinnamic acid analogues have recently drawn back the intentness of medicinal chemists due to their admirable pharmacological properties like antioxidant,⁵

antibacterial,⁶ and antitumor.⁷ Rastogi et al. have demonstrated the synergistic activity of *trans*-cinnamic acid in amalgamation with INH, rifampicin, and other recognized antimicrobial agents against Mtb.⁸ Further, Reddy et al. have reported the superior intracellular and *in vivo* activity of a cinnamoyl–rifampicin derivative (Figure 1) in contrast with rifampicin when tested against susceptible and MDR strains of Mtb along with *M. avium* complex (MAC).⁹ Several compounds resembling cinnamic acid and bearing styryl group or α,β -unsaturated

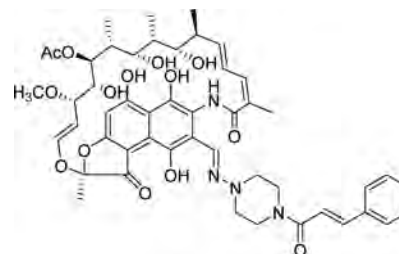


Figure 1. Cinnamoyl–rifampicin derivative.

Received: February 27, 2016

Accepted: May 13, 2016

Published: May 13, 2016

carbonyl groups are reported for antimycobacterial activities (Figure 2).¹⁰

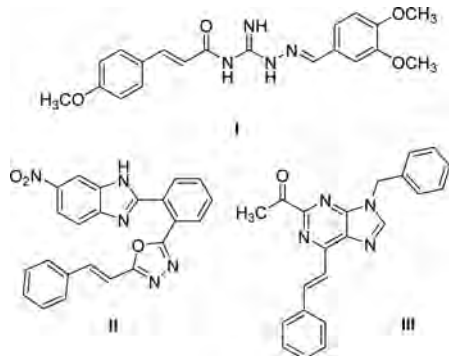


Figure 2. Compounds with styryl portion reported against *M. tuberculosis* H₃₇Rv: (I, MIC 6.49 μ M);¹¹ (II, MIC 12.5 μ g/mL);¹² (III, MIC 6.25 μ M).¹³

From the literature, it was also found that derivatives resulting by combining cinnamoyl portion with various chemical classes of compounds have been reported to possess promising antimycobacterial activity.^{14–16} Besides, various drug-like heterocycles, namely, benzimidazoles¹⁷ and quinazolinones,¹⁸ integrated with cinnamoyl or aryl styryl groups have also been reported to augment the antimycobacterial properties.

Dehydrozingerone (DZG), also known as feruloylmethane, a half structural analogue of curcumin, is isolated from *Curcuma longa*. Chemically DZG is (*E*)-4-(4-hydroxy-3-methoxyphenyl)but-3-en-2-one and possess an α,β -unsaturated carbonyl (styryl ketone) group that resembles the *trans*-cinnamic acid structure. DZG analogues have been reported to possess a broad range of biological activities like antioxidant, anticancer, anti-inflammatory, antidepressant, antimalarial, antifungal, etc.¹⁹

The thiazole nucleus is a common motif presently found in several FDA-approved drugs, such as the nonsteroidal anti-inflammatory drug meloxicam²⁰ and the tyrosine kinase inhibitor dasatinib.²¹ Recently, Meissner et al. have demonstrated the structure–activity relationships (SAR) of novel series of 2-aminothiazole analogues as effective antimycobacterial agents,²² and Carradori et al. have reported microwave-assisted method for the synthesis of substituted-thiazolyl hydrazines.²³ Therefore, thiazole is an essential scaffold in drug discovery since its derivatives known to possess wide spectrum of activities such as antihypertensive, anti-inflammatory, anti-HIV, antibacterial, and antimycobacterial,^{24,25} which have tremendously captivated attention of medicinal chemists. Figure 3 highlights the molecular manipulation of DZG–thiazole moiety and their resultant antimycobacterial activities.

In view of the above facts and in continuation of our research program on the design and development of new antimycobacterial agents,^{19,24,29} it was foreseen to amalgamate two biologically active pharmacophores (styryl portion of DZG and thiazole) in one molecular platform to engender a new scaffold for antimycobacterial evaluation. As shown in Figure 3, the designed hybrid analogues possess both DZG (comprising styryl) and thiazole motifs connected with each other via a hydrazine linker. These unifications were suggested as an effort to explore the possible synergistic influence of such structural hybridizations on the anticipated activity, hoping to discover a

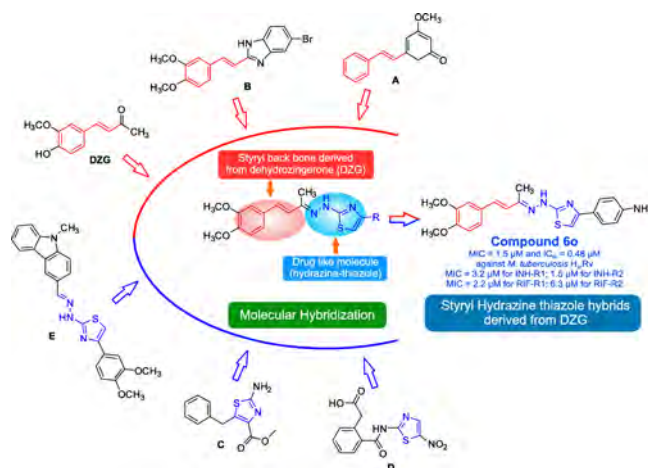
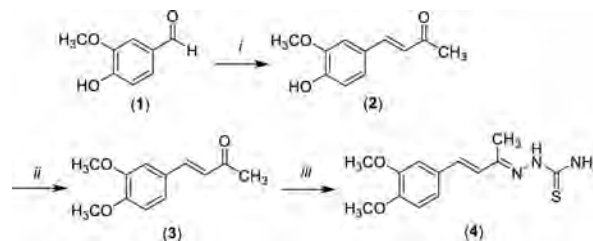


Figure 3. Literature reported derivatives containing styryl and thiazole moieties and their antimycobacterial activities along with the designed compounds. Compound **60** exhibited most promising antimycobacterial activity among the synthesized compounds. (A) (*E*)-3-methoxy-5-styrylcyclohexa-2,4-dien-1-one (MIC against H₃₇Rv = 32 μ g/mL);²⁶ (B) (*E*)-5-bromo-2-(3,4-dimethoxystyryl)-1*H*-benzo[*d*]imidazole (MIC against H₃₇Rv = >7.25 μ g/mL);¹⁷ (C) 2-amino-5-benzylthiazole-4-carboxylate (MIC against H₃₇Rv = 0.06 μ g/mL);²⁷ (D) nitazoxanide (MIC against H₃₇Rv = 16 μ g/mL);²⁸ (E) carbazolothiazole analogue (MIC against H₃₇Rv = 21 μ M).²⁴

new lead structure that would have a promising antimycobacterial activity.

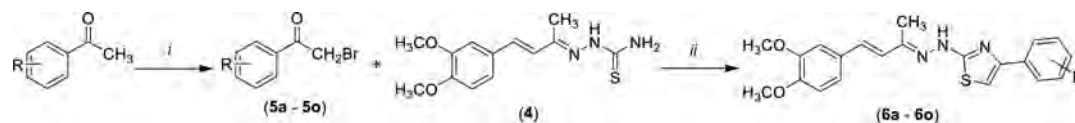
The synthesis of a novel series of styryl hydrazine thiazole hybrids derived from DZG (**6a–6o**) was achieved through efficient and versatile synthetic routes. The starting material DZG (**2**) was prepared by using commercially available vanillin (**1**) by simple aldol condensation with acetone in the presence of base. Methylation of **2** was done with methyl iodide in the presence of potassium carbonate in *N,N*-dimethylformamide to yield (*E*)-4-(3,4-dimethoxyphenyl)but-3-en-2-one (**3**). Further, Schiff base of compound **3** was formed with thiosemicarbazide to yield **4** (Scheme 1). The various appropriately substituted 2-

Scheme 1^a



^aReaction conditions: (i) acetone, NaOH; (ii) CH₃I, K₂CO₃, DMF, reflux, 1.5 h; (iii) thiosemicarbazide, AcOH, CH₃OH, reflux, 3 h.

bromo-1-phenylethanones (**5c–5o**) were synthesized from their respective acetophenones. Compound (**4**) was then condensed with various freshly synthesized 2-bromo-1-(substituted phenyl)-ethanones (**5a–5o**) to yield corresponding final compounds, i.e., 2-(2-((2*E*,3*E*)-4-(3,4-dimethoxyphenyl)but-3-en-2-ylidene)hydrazinyl)-4-(substituted phenyl)thiazoles (**6a–6o**; Scheme 2). The anticipated structures of the final compounds were in agreement with the spectral (IR, ¹H NMR, and ¹³C NMR) data obtained and were further substantiated by

Scheme 2^a

^aReaction conditions: (i) Br₂, ether, 0–5 °C for 5c; Br₂, CHCl₃, reflux, 3 h for 5d and 5g; Br₂, CHCl₃, 0–5 °C for 5e and 5f; CuBr₂, EtOAc, CHCl₃, reflux, 12 h for 5h–5o; (ii) methanol, reflux, 3 h.

Table 1. Antimycobacterial Activity Data of Newly Synthesized Compounds (4, 6d, 6g, 6i, and 6o) against Five Drug-Resistant Isolates of *M. tuberculosis* H₃₇Rv

compd	INH-R1 ^a			INH-R2 ^b			RIF-R1 ^c			RIF-R2 ^d			FQ-R1 ^e		
	MIC (μM)	IC ₅₀ (μM)	IC ₉₀ (μM)	MIC (μM)	IC ₅₀ (μM)	IC ₉₀ (μM)	MIC (μM)	IC ₅₀ (μM)	IC ₉₀ (μM)	MIC (μM)	IC ₅₀ (μM)	IC ₉₀ (μM)	MIC (μM)	IC ₅₀ (μM)	IC ₉₀ (μM)
4	5.3	1.3	6.6	2.5	0.79	2.9	4	1.1	4.6	4.8	1.2	5.9	17	2.8	16
6d	15	12	>50	12	8	>50	25	11	>50	31	8.7	>50	22	23	>50
6g	24	12	>200	13	7.1	12	28	9.2	27	46	19	>200	30	18	>200
6i	32	9.1	>25	19	5.6	>25	17	7	19	41	10	>25	33	13	>25
6o	3.2	0.68	3.8	1.5	0.38	1.7	2.2	0.54	2.6	6.3	0.76	9.2	21	2.3	33
rifampicin	0.018	0.0084	0.022	0.0065	0.0047	0.012	2	1.2	2.3	>50	>50	>50	0.027	0.013	0.039
isoniazid	>200	>200	>200	>200	>200	>200	0.17	0.15	0.21	0.62	0.54	0.6	0.35	0.36	0.47
levofloxacin	1.2	0.64	1.4	1.4	0.84	1.4	0.76	0.59	0.91	1.1	0.6	1.2	20	12	22

^aINH-R1 was derived from H₃₇Rv and is a *katG* mutant (Y155* = truncation). ^bINH-R2 is strain ATCC35822. ^cRIF-R1 was derived from H₃₇Rv and is a *nrpB* mutant (S522L). ^dRIF-R2 is strain ATCC35828. ^eFQ-R1 is a fluoroquinolone-resistant strain derived from H₃₇Rv and is a *gyrB* mutant (D94N). INH, isoniazid; RIF, rifampicin; FQ, Fluoroquinolone.

HRMS data, which is summarized in the [Supporting Information](#).

The ¹H NMR spectrum of compound 4 exhibited the presence of distinctive singlet signals at around δ 10.22, 8.22–7.76, 7.154–7.150, 3.79–3.76, and 2.11 for the N–H proton, NH₂ proton, second proton of phenyl ring, methoxyl (OCH₃) protons, and methyl (CH₃) protons indicating its formation by a process of simple carbon–nitrogen bond creation with thiosemicarbazide in the presence of acetic acid as catalyst. In addition, the appearance of most informative doublet signals around δ 6.81–6.77 ppm (*J* = 16.53 Hz) and 7.06–7.01 (*J* = 16.84 Hz) confirms the presence of olefinic protons.

The ¹H NMR spectrum (400 and 600 MHz, DMSO-*d*₆) of the final compounds (6a–6o) displayed some distinctive singlet signals at around δ 11.42–10.22 ppm for N–H proton, δ 7.21–7.20 for second and δ 7.12–7.08 for sixth aromatic protons of DZG scaffold, and δ 2.17–2.08 ppm for methyl (N=C–CH₃) protons, respectively. In addition, the most informative singlet signal resonated around δ 7.70–7.31 ppm, which was attributed to the aromatic proton at H-5 of thiazole ring, thus indicating its formation through cyclo-condensation process. Whereas most characteristic doublet signals around δ 6.83–6.64 ppm (*J* = 16.52–16.24 Hz, Ph–HC=CH–) and δ 7.57–6.91 ppm (*J* = 16.52–14.76 Hz, Ph–HC=CH–) evidently indicated the presence of olefinic protons. This observation was found in consistence with previously reported similar type of compounds.³⁰ Further, the unique singlet signals resonating around δ 3.82–3.77 ppm indicated the presence of methoxyl protons (OCH₃) on the third and fourth position of the DZG scaffold, while the hydroxyl (OH) protons on aromatic ring resonated as singlet signals around δ 11.24–10.86 ppm. The various signals appearing as either doublets or multiplets around δ 8.29–6.77 ppm accounted for aromatic protons. The *E*-configuration was ascertained for all final derivatives on the basis of 2D NMR studies. These findings were further corroborated from their respective ¹³C NMR

spectra of the title compounds. The characteristic signals resonating at around δ 169.53–156.50 and 108.52–102.10 ppm were assigned to carbons C-2 and C-5 of thiazole ring. The most prominent carbon signals observed around δ 149.27–148.91 and 132.56–126.23 ppm accounted for aromatic carbons having methoxyl groups and olefinic (Ph–HC=CH–) carbons, respectively. Further, the characteristic carbon signals appearing around δ 55.49–55.47 and 12.35–12.15 ppm indicated the presence of methoxyl and methyl groups in the title compounds, while the various aromatic carbons resonated around δ 140.78–108.03 ppm. Further, the fluorine containing compounds 6k and 6m have been discussed, which results in a very characteristic NMR spectra and the *J*_{CF} values are represented in Tables S1 and S2 ([Supporting Information](#)).

Both level I and II (*in vitro*) characterizations of antimycobacterial activity of newly synthesized title compounds (4, 6a–6o) were carried out at Infectious Disease Research Institute (IDRI) within the National Institute of Allergy and Infectious Diseases (NIAID) screening program, Bethesda, MD, USA. In the initial studies (level I), minimum inhibitory concentration (MIC) was established against Mtb strain H₃₇Rv grown under aerobic conditions by using a dual read-out (OD₅₉₀ and fluorescence) assay procedure. All the synthesized compounds exhibited interesting and noteworthy activity profiles with MIC ranging from 1.5 to >200 μM against the tested mycobacterial strain (Table S3, [Supporting Information](#)).

Interestingly, it was observed that compound 4 (MIC = 2.1 μM) having a thiourea group (without thiazole moiety) displayed encouraging antimycobacterial activity with an IC₅₀ value of 0.98 μM. This evidently indicated that the DZG structural core has greatly contributed for antimycobacterial activity. This finding instigated us to explore brief SAR investigations in order to study the biological effects of various substituents on the aromatic ring at the fourth position of the thiazole moiety, which was in turn attached to DZG scaffold

through a hydrazine linkage. Among tested series, compound **6o** (MIC = 1.5 μM) with *p*-amino (NH_2) group on phenyl ring at fourth position of thiazole moiety exhibited excellent antimycobacterial activity with IC_{50} value of 0.48 μM , whereas compounds **6d** (MIC = 15 μM), **6g** (MIC = 16 μM), and **6i** (MIC = 28 μM) substituted with one or two methoxyl (OCH_3) groups on thiazolylphenyl ring exhibited good inhibitory activity with IC_{50} value of 8.4, 7.4, and 6.6 μM , respectively. In the case of compounds **6j** (MIC = 40 μM) and **6l** (MIC = 88 μM) with a hydroxyl (OH) group on the phenyl ring displayed considerable antimycobacterial activity with IC_{50} value of 24 and 23 μM , respectively. These findings demonstrate that the thiazole core contributed to enhanced activity and played a significant role in the action against Mtb. The activity was also considerably affected by the nature of the substituent on the phenyl ring at the fourth position of the thiazole nucleus. Consistent with our prior report,²⁴ we found that the presence of electron donating (NH_2 , OCH_3 , and OH) groups on phenyl ring have greatly influenced and conferred good antimycobacterial activity, while the electron withdrawing (CF_3 , NO_2 , F and Br) substituents have caused a decrease in activity. Thus, compounds **6a**, **6c**, **6h**, and **6m**, having either nitro or halogen groups on the phenyl ring, were found to exhibit poor activity with MIC value $>200 \mu\text{M}$. (Figure S1, Supporting Information). Compounds with promising antimycobacterial activity profile were further subjected for level II screening in order to evaluate their broad spectrum efficiency under assorted conditions against relevant drug resistant isolates of Mtb and other disease causing mycobacterial species.

The MIC of test compounds (**4**, **6d**, **6g**, **6i**, and **6o**) was assessed against five drug resistant isolates (INH-R1, INH-R2, RIF-R1, RIF-R2, and FQ-R1) of Mtb strains under aerobic conditions. The antimycobacterial activity results are summarized in Table 1. From perusal of the data, we observed that all tested compounds showed excellent antimycobacterial activity against INH-R1 and INH-R2, while two compounds (**4** and **6o**) exhibited the most promising antimycobacterial activity against the tested organisms. In particular, both resistant strains (R1 and R2) of INH and RIF were found to be extremely susceptible to compounds **4** and **6o**, while these two compounds had an almost comparable activity with that of Levofloxacin against FQ-R1. As compared to reference drug INH (MIC = $>200 \mu\text{M}$; IC_{50} = $>200 \mu\text{M}$), compounds **4** (MIC = 5.3 and 2.5 μM ; IC_{50} = 1.3 and 0.79 μM) and **6o** (MIC = 3.2 and 1.5 μM ; IC_{50} = 0.68 and 0.38 μM) displayed highest antimycobacterial activity against INH-R1 and INH-R2, respectively. In the case of RIF-R1 and RIF-R2, compound **6o** (MIC = 2.2 and 6.3 μM ; IC_{50} = 0.54 and 0.76 μM) exhibited significant antibacterial activity, whereas compounds **4** (MIC = 4 and 4.8 μM ; IC_{50} = 1.1 and 1.2 μM) showed moderate activity when compared to reference drug RIF (MIC = 2 and $>50 \mu\text{M}$; IC_{50} = $>50 \mu\text{M}$). Nevertheless, the fluoroquinolone-resistant strain (FQ-R1) was found to be less susceptible to these compounds.

In addition, these five promising compounds (**4**, **6d**, **6g**, **6i**, and **6o**) were systematically assessed against Mtb H₃₇Rv grown under varied conditions. The antimicrobial activity of these compounds under hypoxic conditions was assessed using the low oxygen recovery assay (LORA). Further, the bactericidal (MBC: Minimum Bactericidal Concentration) activity of these compounds was assessed against Mtb H₃₇Rv grown in aerobic conditions in 7H9-Tw-OADC medium. The cytotoxicity and intracellular antimycobacterial activity of compounds was also

determined using the THP-1 human monocytic cell line, and THP1 cells infected with Mtb, respectively. The results of all these investigations are represented in Table S4 (Supporting Information). A systematic analysis of the data revealed that compounds **4** and **6o** exhibited an interesting and potent antimycobacterial activity profile as depicted in Figure 4. All the

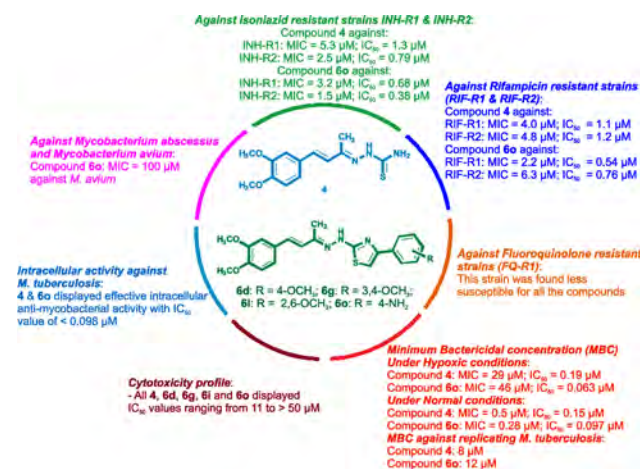


Figure 4. Anti-TB activity profile of most active compounds: **6d**, R = 4-OCH₃; **6g**, R = 3,4-OCH₃; **6i**, R = 2,6-OCH₃; **6o**, R = 4-NH₂.

five title compounds displayed an interesting cytotoxicity profile with IC_{50} values ranging from 11 to $>50 \mu\text{M}$. Among the series tested, compounds **6o** (IC_{50} = 11 μM) and **6g** (IC_{50} = 38 μM) showed moderate cytotoxicity, while other compounds did not show cytotoxic effect up to concentrations $>50 \mu\text{M}$. The existence of virulent intracellular Mtb in primary human macrophages compromise its functioning and arrest phagosome maturation, thus coping up with various host threats. The aptitude of the bacteria to assault and survive inside cells may be implicated for the persistence of TB. Therefore, it is of greater corollary for an effective tuberculosis management that these compounds should also be capable of killing intracellular TB in human macrophages, apart from their *in vitro* activity against TB strains. Accordingly, two compounds (**4** and **6o**) also displayed effective intracellular antimycobacterial activity with IC_{50} value of $<0.098 \mu\text{M}$. However, oxygen restriction also affects adaptive immune responses and triggers antimicrobial effector mechanisms in macrophages and restricts growth of intracellular Mtb.

The title compounds (**4**, **6d**, **6g**, **6i**, and **6o**) were also evaluated for their *in vitro* antimycobacterial activity against other disease-relevant Mycobacterial species like *Mycobacterium abscessus* and *Mycobacterium avium* by using MABA method (Table S5, Supporting Information). The results reveal that compound **6o** (MIC = 100 μM) demonstrated a moderate activity especially against *M. avium* as compared to the reference drug RIF (MIC = 0.1 μM), while compound **6i** displayed a MIC of $>100 \mu\text{M}$ against *M. abscessus* and *M. avium*. However, the remaining compounds showed little or poor activity (MIC = $>200 \mu\text{M}$) against tested organisms.

In summary, in this work we established the synthesis of a series of styryl hydrazine thiazole hybrids derived from dehydrozingerone and their *in vitro* anti-TB activity. The ease, simply obtainable reactants and reagents, and practically good yields (51–74%) make this synthetic method more attractive and efficient. Moreover, compound **6o** emerged as most promising antimycobacterial agent since it has demon-

strated most prominent activity under hypoxic condition along with its potential efficiency against drug resistant isolates of Mtb strains and displayed significant bactericidal and intracellular antimycobacterial activity. These findings suggest that the designed compounds highlighted the benefit of incorporating a hydrazine linkage to combine the styryl portion of DZG and the thiazole core, thus providing a good starting point for further lead optimization. The possible enhancement in the antimycobacterial activity can be further accomplished by slender variation in the ring substituents and/or extensive additional functionalization, which warrants further investigation.

■ ASSOCIATED CONTENT

Supporting Information

The Supporting Information is available free of charge on the ACS Publications website at DOI: [10.1021/acsmedchemlett.6b00088](https://doi.org/10.1021/acsmedchemlett.6b00088).

Synthetic procedures, spectral data, and protocols of bioassay (PDF)

■ AUTHOR INFORMATION

Corresponding Author

*Phone: +27 31 260 7179. Fax: +27 (0) 31 260 7792. E-mail: karpoomath@ukzn.ac.za.

Author Contributions

The manuscript was written through contributions of all authors.

Funding

This work was supported by funds from the University of KwaZulu-Natal (UKZN), Westville Campus, Durban, South Africa.

Notes

The authors declare no competing financial interest.

■ ACKNOWLEDGMENTS

Authors sincerely thank National Institutes of Health and the National Institute of Allergy and Infectious Diseases (NIAID; Contract No.: HHSN272201100009I/HHSN27200002 A14), Bethesda, MD (USA), for *in vitro* antimycobacterial activity characterization. Authors are also grateful to Mr. Dilip Jagjivan and Dr. Caryl Janse Van Rensburg (UKZN, South Africa) for their assistance in the NMR and HRMS experiments.

■ REFERENCES

- (1) Herzog, H. History of Tuberculosis. *Respiration* **1998**, *65* (1), 5–15.
- (2) Collins, F. M. Mycobacterial Pathogenesis: A Historical Perspective. *Front. Biosci., Landmark Ed.* **1998**, *3*, e123–e132.
- (3) World Health Organization. *Global Tuberculosis Report 2014 (WHO/HTM/TB/2014.08)*; 2014.
- (4) Bloom, B. R., Ed. *Tuberculosis: Pathogenesis, Protection, and Control*; ASM Press, 1994.
- (5) Chung, H. S.; Shin, J. C. Characterization of Antioxidant Alkaloids and Phenolic Acids from Anthocyanin-Pigmented Rice (*Oryza Sativa* Cv. *Heuginjubyeo*). *Food Chem.* **2007**, *104* (4), 1670–1677.
- (6) Guzman, J. Natural Cinnamic Acids, Synthetic Derivatives and Hybrids with Antimicrobial Activity. *Molecules* **2014**, *19* (12), 19292–19349.
- (7) Bezerra, D. P.; Castro, F. O.; Alves, a. P. N. N.; Pessoa, C.; Moraes, M. O.; Silveira, E. R.; Lima, M. a S.; Elmiro, F. J. M.; Costa-Lotufo, L. V. *In vivo* Growth-Inhibition of Sarcoma 180 by Piplartine

and Piperine, Two Alkaloid Amides from Piper. *Braz. J. Med. Biol. Res.* **2006**, *39* (6), 801–807.

- (8) Rastogi, N.; Goh, K. S.; Wright, E. L.; Barrow, W. W. Potential Drug Targets for *Mycobacterium Avium* Defined by Radiometric Drug-Inhibitor Combination Techniques. *Antimicrob. Agents Chemother.* **1994**, *38* (10), 2287–2295.

- (9) Reddy, V. M.; Nadadhur, G.; Daneluzzi, D.; Dimova, V.; Gangadharam, P. R. Antimycobacterial Activity of a New Rifamycin Derivative, 3-(4-Cinnamylpiperazinyl Iminomethyl) Rifamycin SV (T9). *Antimicrob. Agents Chemother.* **1995**, *39* (10), 2320–2324.

- (10) De, P.; Veau, D.; Bedos-Belval, F.; Chassaing, S.; Baltas, M. In *Cinnamic Derivatives in Tuberculosis, Understanding Tuberculosis - New Approaches to Fighting Against Drug Resistance*; Cardona, P.-J., Ed.; InTech, 2012.

- (11) Bairwa, R.; Kakwani, M.; Tawari, N. R.; Lalchandani, J.; Ray, M. K.; Rajan, M. G. R.; Degani, M. S. Novel Molecular Hybrids of Cinnamic Acids and Guanyldiazones as Potential Antitubercular Agents. *Bioorg. Med. Chem. Lett.* **2010**, *20* (5), 1623–1625.

- (12) Joshi, D. G.; Oza, H. B.; Parekh, H. H. Synthesis of Some Novel 1,3,4-Oxadiazoles and 5-Oxo-Imidazolines as Potent Biologically Active Agents. *Heterocycl. Commun.* **1997**, *3* (2), 169–174.

- (13) Bakkestuen, A. K.; Gundersen, L.-L.; Langli, G.; Liu, F.; Nolsøe, J. M. 9-Benzylpurines with Inhibitory Activity against *Mycobacterium Tuberculosis*. *Bioorg. Med. Chem. Lett.* **2000**, *10* (11), 1207–1210.

- (14) Carvalho, S. A.; da Silva, E. F.; de Souza, M. V. N.; Lourenço, M. C. S.; Vicente, F. R. Synthesis and Antimycobacterial Evaluation of New Trans-Cinnamic Acid Hydrazide Derivatives. *Bioorg. Med. Chem. Lett.* **2008**, *18* (2), 538–541.

- (15) De, P.; Koumba Yoya, G.; Constant, P.; Bedos-Belval, F.; Duran, H.; Saffon, N.; Daffé, M.; Baltas, M. Design, Synthesis, and Biological Evaluation of New Cinnamic Derivatives as Antituberculosis Agents. *J. Med. Chem.* **2011**, *54* (5), 1449–1461.

- (16) Rastogi, N.; Goh, K. S.; Horgen, L.; Barrow, W. W. Synergistic Activities of Antituberculous Drugs with Cerulenin and Trans-Cinnamic Acid against *Mycobacterium Tuberculosis*. *FEMS Immunol. Med. Microbiol.* **1998**, *21* (2), 149–157.

- (17) Shingalapur, R. V.; Hosamani, K. M.; Keri, R. S. Synthesis and Evaluation of *in vitro* Anti-Microbial and Anti-Tubercular Activity of 2-Styryl Benzimidazoles. *Eur. J. Med. Chem.* **2009**, *44* (10), 4244–4248.

- (18) Babu, R. R.; Naresh, K.; Ravi, A.; Madhava Reddy, B.; Harinadha Babu, V. Synthesis of Novel Isoniazid Incorporated Styryl Quinazolinones as Anti-Tubercular Agents against INH Sensitive and MDR M. Tuberculosis Strains. *Med. Chem. Res.* **2014**, *23* (10), 4414–4419.

- (19) Hampannavar, G. A.; Karpoomath, R.; Palkar, M. B.; Shaikh, M. S. An Appraisal on Recent Medicinal Perspective of Curcumin Degradant: Dehydrozingerone (DZG). *Bioorg. Med. Chem.* **2016**, *24* (4), 501–520.

- (20) Luger, P.; Daneck, K.; Engel, W.; Trummelitz, G.; Wagner, K. Structure and Physicochemical Properties of Meloxicam, a New NSAID. *Eur. J. Pharm. Sci.* **1996**, *4*, 175–187.

- (21) Das, J.; Chen, P.; Norris, D.; Padmanabha, R.; Lin, J.; Moquin, R. V.; Shen, Z.; Cook, L. S.; Doweiko, A. M.; Pitt, S.; Pang, S.; Shen, D. R.; Fang, Q.; De Fex, H. F.; McIntyre, K. W.; Shuster, D. J.; Gillooly, K. M.; Behnia, K.; Schieven, G. L.; Wityak, J.; Barrish, J. C. 2-Aminothiazole as a Novel Kinase Inhibitor Template. Structure-Activity Relationship Studies toward the Discovery of N-(2-Chloro-6-Methylphenyl)-2-[[6-[4-(2-Hydroxyethyl)-1-Piperazinyl]-2-Methyl-4-Pyrimidinyl]amino]-1, 3-Thiazole-5-Carboxamide (Dasatinib, BMS-354825) as a Potent *pan*-Src Kinase Inhibitor. *J. Med. Chem.* **2006**, *49* (23), 6819–6832.

- (22) Meissner, A.; Boshoff, H. I.; Vasani, M.; Duckworth, B. P.; Barry, C. E.; Aldrich, C. C. Structure-Activity Relationships of 2-Aminothiazoles Effective against *Mycobacterium Tuberculosis*. *Bioorg. Med. Chem.* **2013**, *21* (21), 6385–6397.

- (23) Carradori, S.; Secci, D.; D'Ascenzio, M.; Chimenti, P.; Bolasco, A. Microwave and Ultrasound-Assisted Synthesis of Thiosemicarbazones and Their Corresponding (4,5-Substituted-Thiazol-2-Yl)-hydrazines. *J. Heterocycl. Chem.* **2014**, *51* (6), 1856–1861.

(24) Shaikh, M. S.; Palkar, M. B.; Patel, H. M.; Rane, R. A.; Alwan, W. S.; Shaikh, M. M.; Shaikh, I. M.; Hampannavar, G. A.; Karpoomath, R. Design and Synthesis of Novel Carbazolo-thiazoles as Potential Anti-Mycobacterial Agents Using a Molecular Hybridization Approach. *RSC Adv.* **2014**, *4* (107), 62308–62320.

(25) Villemagne, B.; Flipo, M.; Blondiaux, N.; Crauste, C.; Malaquin, S.; Leroux, F.; Piveteau, C.; Villeret, V.; Brodin, P.; Villoutreix, B. O.; Sperandio, O.; Soror, S. H.; Wohlkönig, A.; Wintjens, R.; Deprez, B.; Baulard, A. R.; Willand, N. Ligand Efficiency Driven Design of New Inhibitors of *Mycobacterium Tuberculosis* Transcriptional Repressor EthR Using Fragment Growing, Merging, and Linking Approaches. *J. Med. Chem.* **2014**, *57* (11), 4876–4888.

(26) Mata, R.; Morales, I.; Pérez, O.; Rivero-Cruz, I.; Acevedo, L.; Enriquez-Mendoza, I.; Bye, R.; Franzblau, S.; Timmermann, B. Antimycobacterial Compounds from *Piper S Anctum*. *J. Nat. Prod.* **2004**, *67* (12), 1961–1968.

(27) Al-Balas, Q.; Anthony, N. G.; Al-Jaidi, B.; Alnimr, A.; Abbott, G.; Brown, A. K.; Taylor, R. C.; Besra, G. S.; McHugh, T. D.; Gillespie, S. H.; Johnston, B. F.; Mackay, S. P.; Coxon, G. D. Identification of 2-Aminothiazole-4-Carboxylate Derivatives Active against *Mycobacterium Tuberculosis* H₃₇Rv and the β -Ketoacyl-ACP Synthase mtFabH. *PLoS One* **2009**, *4* (5), e5617.

(28) de Carvalho, L. P. S.; Lin, G.; Jiang, X.; Nathan, C. Nitazoxanide Kills Replicating and Nonreplicating *Mycobacterium Tuberculosis* and Evades Resistance. *J. Med. Chem.* **2009**, *52* (19), 5789–5792.

(29) Palkar, M. B.; Noolvi, M. N.; Maddi, V. S.; Ghatole, M.; Nargund, L. G. Synthesis, Spectral Studies and Biological Evaluation of a Novel Series of 2-Substituted-5,6-Diarylsubstituted imidazo(2,1-B)-1,3,4-Thiadiazole Derivatives as Possible Anti-Tubercular Agents. *Med. Chem. Res.* **2012**, *21* (7), 1313–1321.

(30) Kubra, I. R.; Bettadaiah, B. K.; Murthy, P. S.; Rao, L. J. M. Structure-Function Activity of Dehydrozingerone and Its Derivatives as Antioxidant and Antimicrobial Compounds. *J. Food Sci. Technol.* **2014**, *51* (2), 245–255.